IMPERIAL INSTITUTE
OF
AGRICULTURAL RESEARCH, PUSA.

PROCEEDINGS

OF THE

ROYAL SOCIETY OF LONDON

SERIES A

CONTAINING PAPERS OF A MATHEMATICAL AND
PHYSICAL CHARACTER

VOL CXX

314735
IARI

LONDON

PRINTED FOR THE ROYAL SOCIETY AND SOLD BY
HARRISON AND SONS, LTD, ST MARTINS LANE,
PRINTERS IN ORDINARY TO HIS MAJESTY

OCTOBER, 1928

LONDON:
HARRISON AND SONS, LTD., PRINTERS IN ORDINARY TO HIS MAJESTY,
ST. MARTIN'S LANE.

CONTENTS.

SERIES A. VOL. CXX.

No 784—August 1, 1928

PAGE

On the Potential of Electromagnetic Phenomena in a Gravitational Field By E T Whittaker, F R.S 1

The Energy of a Body moving in an Infinite Fluid, with an Application to Airships. By G I. Taylor, F R S 13

The Absorption Spectra of Solutions of Cobalt Chloride, Cobalt Bromide, and Cobalt Iodide in Concentrated Hydrochloric, Hydrobromic, and Hydriodic Acids. By W. R Brode and R. A Morton Communicated by E C. C Baly, F R S. (Plates 1 and 2)....... 21

The Characteristics of a Karman Vortex Street in a Channel of Finite Breadth By H Glauert Communicated by G I. Taylor, F R S. 34

Photoelectric Effect of Soft X-Rays By G B Bandopadhyaya Communicated by O. W Richardson, F.R.S. 46

The Electrolytic Behaviour of Thin Films Part I. Hydrogen By F. P Bowden and E K Rideal Communicated by T M Lowry, F R.S. 59

On the Electrolytic Behaviour of Thin Films. Part II.—The Areas of Catalytically Active Surfaces. By F. P. Bowden and E K Rideal Communicated by T. M. Lowry, F R.S....... 80

The Detonation-Wave in Gaseous Mixtures and the Pre Detonation Period. By W. Payman Communicated by H. B Dixon, F R S (Plates 3-7) 90

The Zeeman Effect in the Band Spectrum of Helium By W. E Curtis and W Jevons. Communicated by H. C. Plummer, F R S. 110

Studies in the Infra-Red Region of the Spectrum Part I.—Description of Prism Spectrometer and Apparatus. By Sir Robert Robertson, F R S., and J. J. Fox 128

Studies in the Infra-Red Region of the Spectrum. Part II —Calibration of Prism Spectrometer, General Procedure, and Preparation of Pure Ammonia, Phosphine and Arsine. By Sir Robert Robertson, F.R.S., J. J. Fox and E. S Hiscocks 149

Studies in the Infra-Red Region of the Spectrum. Part III.—Infra-Red Absorption Spectra of Ammonia, Phosphine and Arsine. By Sir Robert Robertson, F.R.S., and J. J. Fox....... 161

PAGE

Studies in the Infra-Red Region of the Spectrum. Part IV.—Discussion of Absorption Bands of Ammonia, Phosphine and Arsine. By Sir Robert Robertson, F.R.S., and J. J. Fox 189

The Kinetics of the Decomposition of Calcium Carbonate Hexahydrate. By B. Topley and J. Hume. Communicated by Sir Harold Hartley, F.R.S. 211

The Band Spectrum of Water Vapour.—III. By D. Jack. Communicated by O. W. Richardson, F.R.S. 222

The Electrical Condition of Hot Surfaces during the Adsorption of Gases. Part II.—A Nickel Surface at Temperatures up to 850° C. By G. I. Finch and J. C. Stimson. Communicated by W. A. Bone, F.R.S 235

No. 785—September 1, 1928.

Chemical Equilibrium in the Vapour of a Mixture of Paraffins and Unsaturated Hydrocarbons. By H. A. Wilson, F.R.S. 247

Observations of the Height of the Ozone in the Upper Atmosphere. By F. W. P. Götz and G. M. B. Dobson, F.R.S. 251

The Forces on a Body placed in a Curved or Converging Stream of Fluid. By G. I. Taylor, F.R.S. 260

On the Decomposition of Ammonia by High-Speed Electrons. By J. C. McLennan, F.R.S., and G. Greenwood 283

An Investigation of the Absorption Spectra of Water and Ice, with Reference to the Spectra of the Major Planets. By J. C. McLennan, F.R.S., R. Ruedy, and A. C. Burton. (Plates 8–10) 296

On the Luminescence of Solid Nitrogen under Cathode Ray Bombardment. By J. C. McLennan, F.R.S., H. J. C. Ireton and E. W. Samson. (Plate 11) 303

Further Investigations of the Spectrum of Singly-Ionised Carbon (C II). By A. Fowler, F.R.S., and E. W. H. Selwyn 312

Bakerian Lecture.—The Aurora and its Spectrum. By J. C. McLennan, F.R.S. (Plates 12–17) 327

A Series of Bessel Functions connected with the Lattice-Points of an n-Dimensional Ellipsoid. By J. R. Wilton. Communicated by G. H. Hardy, F.R.S. 358

The Chemical Reactions of Carbon Monoxide and Hydrogen after Collision with Electrons. By A. Caress and E. K. Rideal. Communicated by T. M. Lowry, F.R.S. 370

The Velocity Distribution of Photoelectrons produced by Soft X-Rays. By E. Rudberg. Communicated by O. W. Richardson, F.R.S. 385

The Action of Strong Electric Fields on the Current from a Thermionic Cathode. By N. A. de Bruyne. Communicated by Sir Ernest Rutherford, P.R.S. 423

PAGE

A Further X-Ray Investigation of Long Chain Compounds (n-Hydrocarbon). By A. Müller. Communicated by Sir William Bragg, F.R.S. (Plates 18–19)... 437

Steam Tables and Equations, extended by Direct Experiment to 4,000 lb./sq. in and 400° C. By H. L. Callendar, F.R.S.. 460

The Structure of Thin Films. Part XII —Cholesterol and its Effect in Admixture with other Substances. By N K. Adam and G. Jessop. Communicated by J. B. Leathes, F.R.S................ 473

No. 786—October 1, 1928.

The "Action" of an Electromagnetic Field. By S. R Milner, F.R.S. 483

The Zeeman Effect for the Spectrum of Tantalum By J. C. McLennan, F.R.S., and A. M. I. A. W. Durnford. (Plates 20–23) 502

Motion of Electrons in Gases. By J. S Townsend, F R.S.... 511

Researches on the Chemistry of Coal. Part V.—The Maturing of Coal considered from the Standpoint of its Benzene-Pressure-Extraction By W. A. Bone, F R.S., L. Horton, and L. J. Tei... 523

Gaseous Combustion at High Pressures Part XI —Further Experiments on the Influences of Hydrogen and Steam on the Explosion of Carbonic Oxide-Air, etc., Mixtures. By W. A. Bone, F.R S, D. T A Townend and G. A. Scott 546

Gaseous Combustion at High Pressures. Part XII.—The Influences of Steam and Temperature, respectively, upon the "Explosion Limits" of Carbonic Oxide-Air Mixtures. By W. A. Bone, F.R.S., D M Newitt and C M. Smith 563

A Theory of Partial Osmotic Pressures and Membrane Equilibria, with Special Reference to the Application of Dalton's Law to Hæmoglobin Solutions in the Presence of Salts. By G. S. Adair. Communicated by Sir William Hardy, F.R.S.. 573

Photographic Study of Detonation in Solid Explosives Part I.—The Development of a Photographic Method for measuring Rates of Detonation By E. Jones. Communicated by J. F. Thorpe, F.R.S. (Plates 24–26)......... 603

On the Magnetic Moment of the Electron. By C. G. Darwin, F.R.S..... 621

On the Diffraction of the Magnetic Electron. By C. G. Darwin, F.R.S. 631

The First Spark Spectrum of Krypton. By P. K. Kichlu. Communicated by M N. Saha, F.R.S. 643

The Absorption Spectrum of Cæsium. By I. M. Mathews. Communicated by S. R. Milner, F.R.S. (Plate 27) 650

The Effect of Ozone on the Temperature of the Upper Atmosphere. By E. H. Gowan. Communicated by F. A. Lindemann, F.R.S. 655

The Steady Motion and Stability of a Helical Vortex. By H. Levy and A. G. Forsdyke. Communicated by S. Chapman, F.R.S....... 670

PAGE

Flow in a Pipe of Rectangular Cross-Section. By R. J. Cornish. Communicated by E. A. Milne, F.R.S. 691

The Velocity Distribution of β-particles after passing through Thin Foils. By P. White and G. Millington. Communicated by Sir Ernest Rutherford, P.R.S. (Plate 28) 701

The Distribution of Electrons in a Metal. By J. E. Lennard-Jones and H. J. Woods. Communicated by R. H. Fowler, F.R.S. 727

Index 736

PROCEEDINGS OF
THE ROYAL SOCIETY.

SECTION A.—MATHEMATICAL AND PHYSICAL SCIENCES.

On the Potential of Electromagnetic Phenomena in a Gravitational Field.

By E. T. WHITTAKER, F.R.S.

(Received June 11, 1928.)

§ 1. *Introduction.*

In classical electromagnetic theory, the electromagnetic field due to any number of electrons moving in any manner is determined by a theorem which expresses the scalar and vector potentials of the field in terms of the positions and velocities of the electrons. The theorem* may be stated thus. Denoting by $\bar{t}$ the instant at which radiation was emitted from an electron e so as to reach a point P (x, y, z) at the instant t, by $(\bar{x}', \bar{y}', \bar{z}')$ the co-ordinates of the electron at the instant $\bar{t}$, by $\bar{r}$ the distance between the points $(\bar{x}', \bar{y}', \bar{z}')$ and (x, y, z), and by (v_x, v_y, v_z) the components of velocity of the electron at the instant $\bar{t}$, then the four-vector of the electromagnetic potential at P, due to the electron e, is

$$(\phi_0, \phi_1, \phi_2, \phi_3) = (e/s, -ev_x/s, -ev_y/s, -ev_z/s), \tag{1}$$

where

$$s = \bar{r} + \{(\bar{x}' - x)\,v_x + (\bar{y}' - y)\,v_y + (\bar{z}' - z)\,v_z\}/c.$$

The object of the present paper is to study the extension of this theorem to electromagnetic fields which contain gravitating masses, so that the metric of space-time is no longer Galilean. It is obvious at the outset that there will be difficulty in making such an extension, because the quantities occurring in formula (1) cannot readily be generalised to non-Galilean space-time; the quantities $\bar{r}$ and s, in fact, belong essentially to action-at-a-distance theories, and therefore if a formula exists which expresses the electromagnetic potential in a gravitational field in terms of the electric charges and their motions, it must be altogether different in type from the formula (1) above.

---

* It was discovered in 1900 by E. Wiechert, 'Arch. Neerl.,' vol. 5, p. 549.

The formula which we are seeking must, of course, be a tensor formula and must involve only physical quantities which are invariant. Now when a point P (x, y, z) is in the electric field generated by a moving electron e, there is (in the most general kind of space-time) only one physical invariant of the situation, namely, the proper-time τ of the electron at the instant when it was emitting the radiation which reaches P at the instant t; or, as we may say, the proper-time of the electron at the world-point where its world-line intersects the null-cone of P. The formula which we are seeking must therefore express the electric potential at P by means of tensor-operations performed on τ, when the field is generated by a single electron. When the field is generated by more than one electron, we must, of course, add together the potentials due to them separately.

The first step towards a solution of the electric potential-problem in general gravitational fields must therefore be to replace formula (1) in Galilean fields by a formula of a purely tensorial character, involving only the fundamental tensor and the covariant derivatives of τ. This is done in § 2 of the present paper, the resulting formula being as follows:—

Let an electron e be moving in any manner, and let τ *be its proper-time at the point where its world-line intersects the null-cone of any point* P. *Then the electromagnetic potential-vector at* P, *due to the electron e, is*

$$\left.\begin{aligned} \phi_p &= \frac{e}{c} \sum_{q,r} g^{qr} \sigma_{pqr}, \\ \text{where} \qquad & \\ \sigma_p &= \tau_p / \sum_{l,m} g^{lm} \tau_{lm} \end{aligned}\right\}, \qquad (2)$$

and where the subscripts p, q, r, l, m, on the right-hand side represent covariant differentiations.

It is remarkable that formula (2) should be so completely different in appearance from formula (1).

The question now arises whether the formula (2) is valid also in fields of a more general character, where gravitation is present. A complete answer to this question has not been found, but some indication may be obtained from § 5, in which it is proved that, although the first derivatives of τ involve the components of velocity of the electron, and the second derivatives of τ involve the components of acceleration, yet the combination $\tau_p / \sum_{l,m} g^{lm} \tau_{lm}$ or σ_p does not involve either the velocities or the accelerations, and that this result is true *in any metric whatever*. It seems unlikely (though it is not proved to be impossible) that such a remarkable analytical property could be possessed by any other simple vector formed covariantively from τ; and if this conjecture is correct, then the electric potential in the most general gravitational field must be some combination of covariant derivatives of σ_p, though it may not be the expression $\sum_{p,q} g^{pq}\sigma_{pqr}$ which is given in (2).

In any case, the formula (2) is valid in the "quasi-uniform" gravitational field, and in § 3 this fact is used in order to obtain the potentials due to the motion of an electron in a quasi-uniform field, while in § 4 it is shown that when the electron is at rest, the formulæ thus obtained agree with those found by direct solution of the partial differential equations for the electrostatic potential in a quasi-uniform gravitational field.

§ 2. *Comparison with Classical Electrodynamics.*

We shall now show that when there is no gravitational field, *i.e.*, when the ordinary Maxwell's equations of the electromagnetic field are valid, the formula (2) gives the ordinary classical theory of the electromagnetic effects produced by a moving electron.

Suppose the electric field at the point P(x, y, z) at the instant t is due to an electron of charge e, whose co-ordinates at the instant t are (x', y', z'); let $\bar{t}$ denote the instant at which the electron emits the radiation which reaches (x, y, z) at time t, and let $x'(\bar{t})$, $y'(\bar{t})$, $z'(\bar{t})$ (that is to say, the co-ordinates of the moving electron at the instant when it emits the radiation) be denoted by $(\bar{x}', \bar{y}', \bar{z}')$. Let

$$\bar{r}^2 = (\bar{x}' - x)^2 + (\bar{y}' - y)^2 + (\bar{z}' - z)^2$$

so

$$\bar{t} = t - \bar{r}/c.$$

Let τ denote the proper-time of the electron at the instant $\bar{t}$, and let

$$v_0 = \frac{d\bar{t}}{d\tau}, \qquad v_1 = \frac{d\bar{x}'}{d\tau}, \qquad v_2 = \frac{d\bar{y}'}{d\tau}, \qquad v_3 = \frac{d\bar{z}'}{d\tau},$$

so (v_0, v_1, v_2, v_3) is the absolute velocity (*i.e.*, referred to the proper-time as independent variable) of the electron at the instant when it emits the radiation in question. Then the above equations give

$$0 = -c^2(\bar{t} - t)^2 + (\bar{x}' - x)^2 + (\bar{y}' - y)^2 + (\bar{z}' - z)^2.$$

Differentiating this equation with respect to t we have

$$0 = c^2(\bar{t} - t) + \mu \frac{\partial \tau}{\partial t},$$

where

$$\mu = -c^2(t - t)\,v_0 + (\bar{x}' - x)\,v_1 + (\bar{y}' - y)\,v_2 + (\bar{z}' - z)\,v_3,$$

and therefore

$$\frac{\partial \tau}{\partial t} = -\frac{c^2(\bar{t} - t)}{\mu},$$

and similarly

$$\frac{\partial \tau}{\partial x} = \frac{\bar{x}' - x}{\mu}, \qquad \frac{\partial \tau}{\partial y} = \frac{\bar{y}' - y}{\mu}, \qquad \frac{\partial \tau}{\partial z} = \frac{\bar{z}' - z}{\mu}.$$

Differentiating again, we have

$$\frac{\partial^2 \tau}{\partial t^2} = \frac{c^2}{\mu} + \frac{2c^4 v_0(\bar{t} - t)}{\mu^2} - \frac{c^4(\bar{t} - t)^2}{\mu^3}\frac{d\mu}{d\tau},$$

$$\frac{\partial^2 \tau}{\partial x^2} = -\frac{1}{\mu} + \frac{2(\bar{x}' - x)\,v_1}{\mu^2} - \frac{(\bar{x} - x)^2}{\mu^3}\frac{d\mu}{d\tau},$$

and similar equations for $\partial^2\tau/\partial y^2$ and $\partial^2\tau/\partial z^2$.

Therefore

$$\sum_{l,m} g^{lm}\tau_{lm} = \frac{\partial^2 \tau}{\partial t^2} - c^2\left(\frac{\partial^2 \tau}{\partial x^2} + \frac{\partial^2 \tau}{\partial y^2} + \frac{\partial^2 \tau}{\partial z^2}\right) = \frac{2c^2}{\mu}.$$

Thus if we write $\sigma_p = \tau_p / \sum\limits_{l,m} g^{lm}\tau_{lm}$, we have

$$(\sigma_0, \sigma_1, \sigma_2, \sigma_3) = \left(-\tfrac{1}{2}(\bar{t} - t),\ \ \tfrac{1}{2}(\bar{x}' - x)/c^2,\ \ \tfrac{1}{2}(\bar{y}' - y)/c^2,\ \ \tfrac{1}{2}(\bar{z}' - z)/c^2\right),$$

and therefore

$$\begin{aligned}\sum_{q,r} g^{qr}(\sigma_0)_{qr} &= \sigma_{000} - c^2(\sigma_{011} + \sigma_{022} + \sigma_{033}) \\ &= -\tfrac{1}{2}\left(\frac{\partial^2 \bar{t}}{\partial t^2} - c^2\frac{\partial^2 \bar{t}}{\partial x^2} - c^2\frac{\partial^2 \bar{t}}{\partial y^2} - c^2\frac{\partial^2 \bar{t}}{\partial z^2}\right) \\ &= -\tfrac{1}{2}\frac{dt}{d\tau}\left(\frac{\partial^2 \tau}{\partial t^2} - c^2\frac{\partial^2 \tau}{\partial x^2} - c^2\frac{\partial^2 \tau}{\partial y^2} - c^2\frac{\partial^2 \tau}{\partial z^2}\right) \\ &\qquad - \tfrac{1}{2}\frac{d^2\bar{t}}{d\tau^2}\left\{\left(\frac{\partial \tau}{\partial t}\right)^2 - c^2\left(\frac{\partial \tau}{\partial x}\right)^2 - c^2\left(\frac{\partial \tau}{\partial y}\right)^2 - c^2\left(\frac{\partial \tau}{\partial z}\right)^2\right\} \\ &= -\tfrac{1}{2}\frac{d\bar{t}}{d\tau}\frac{2c^2}{\mu} = -\frac{c^2}{c\bar{r} + (\bar{x}' - x)\,v_x + (\bar{y}' - y)\,v_y + (\bar{z}' - z)\,v_z},\end{aligned}$$

where

$$v_x = \frac{d\bar{x}'}{d\bar{t}} = \frac{v_1}{v_0},\ \text{etc.},$$

so formula (2) gives*

$$\phi_0 = -e\Big/\Big[\bar{r} + \frac{1}{c}\{(\bar{x}' - x)v_x + (\bar{y}' - y)v_y + (\bar{z}' - z)x_z\}\Big],$$

and similarly

$$\phi_1 = ev_x/[c^2\bar{r} + c\{(\bar{x}' - x)v_x + (\bar{y}' - y)v_y + (\bar{z}' - z)v_z\}],$$

with similar formulæ for ϕ_2 and ϕ_3; that is, we have obtained the equations (1) above. Thus, *in a field free from gravitation, formula* (2) *gives the classical expressions for the vector potential of an electron moving in any way.*

§ 3. *The Motion of Electrons in a Quasi-Uniform Gravitational Field.*

As an application of the formula (2), we shall now obtain the electromagnetic vector potential due to the motion of electrons in the kind of gravitational field called† *quasi-uniform*, that is, a field whose metric is specified by the equation

$$ds^2 = \left(1 + \frac{2gx}{c^2}\right)dt^2 - \frac{1}{c^2}\left\{\frac{dx^2}{1 + 2gx/c^2} + dy^2 + dz^2\right\}. \tag{3}$$

This is the simplest possible type of gravitational field, being, near the origin a "uniform field of gravitational attraction parallel to the axis of x" in the sense of the older physics. Its Riemann tensor is null, and, therefore, formula (2), being a tensor formula already proved to be valid for Galilean fields, must certainly be valid for this field also.

Denoting (as always) by τ the proper-time of the electron at the instant when it emitted the radiation which reaches (x, y, z) at the instant t, the first step is to find the equation which gives τ as a function of (t, x, y, z). This amounts to finding the "null-cone" of an arbitrary world-point E, *i.e.*, the assemblage of null geodesics through E, or (to put it physically) the locus of the world-points which can receive radiation from the world-point E.

Now in the quasi-uniform gravitational field, whose metric is given by (3),

---

* The theorem that in classical electrodynamics the vector potential can be obtained by performing the operation

$$\left(\frac{\partial^2}{\partial t^2} - c^2\frac{\partial^2}{\partial x^2} - c^2\frac{\partial^2}{\partial y^2} - c^2\frac{\partial^2}{\partial z^2}\right)$$

on the vector $(\bar{t}, \bar{x}, \bar{y}, \bar{z})$ was discovered by Mr. R. Hargreaves, 'Mess. of Maths.,' vol. 52, p. 34 (1922).

† 'Roy. Soc. Proc.,' vol. 116, p. 722 (1927).

it is found without difficulty that any one of the ∞^5 null geodesics is given by the three equations

$$\frac{c^2}{g}\left(1+\frac{2gx}{c^2}\right)^{\frac{1}{2}}\cosh\left(\frac{gt}{c}+\lambda\right)=\alpha,$$

$$y+\frac{c^2}{g}\left(1+\frac{2gx}{c^2}\right)^{\frac{1}{2}}\sin\mu\sinh\left(\frac{gt}{c}+\lambda\right)=\beta,$$

$$z+\frac{c^2}{g}\left(1+\frac{2gx}{c^2}\right)^{\frac{1}{2}}\cos\mu\sinh\left(\frac{gt}{c}+\lambda\right)=\gamma,$$

where α, β, γ, λ, μ are the five arbitrary constants.

Writing down the conditions that this null geodesic passes through the two world-points (t, x, y, z) and $(\bar{t}, \bar{x}', \bar{y}', \bar{z}')$, and eliminating α, β, γ, λ, μ from the six equations thereby obtained, we have

$$\left(1+\frac{2gx}{c^2}\right)^{\frac{1}{2}}\left(1+\frac{2g\bar{x}'}{c^2}\right)^{\frac{1}{2}}\cosh\left\{\frac{g}{c}(\bar{t}-t)\right\}=1+\frac{gx}{c^2}+\frac{g\bar{x}'}{c^2}+\frac{g^2}{2c^4}\{(\bar{y}'-y)^2+(\bar{z}'-z)^2\}.$$

Thus, *in the quasi-uniform gravitational field, the equation of the null-cone of the world-point* $(\bar{t}, \bar{x}', \bar{y}', \bar{z}')$ *is* $\Omega=0$, *where*

$$\Omega=1+\frac{gx}{c^2}+\frac{g\bar{x}'}{c^2}+\frac{g^2}{2c^4}\{(\bar{y}'-y)^2+(\bar{z}'-z)^2\}$$
$$-\left(1+\frac{2gx}{c^2}\right)^{\frac{1}{2}}\left(1+\frac{2g\bar{x}'}{c^2}\right)^{\frac{1}{2}}\cosh\left\{\frac{g}{c}(\bar{t}-t)\right\}. \qquad (4)$$

The values of $\frac{\partial\tau}{\partial t}, \frac{\partial\tau}{\partial x}, \frac{\partial\tau}{\partial y}, \frac{\partial\tau}{\partial z}$ are obtained by differentiating the equation $\Omega=0$ with respect to t, x, y, z, respectively, thus, differentiating with respect to t, and writing

$$\frac{d\bar{t}}{d\tau}=v_0,\qquad \frac{d\bar{x}'}{d\tau}=v_1,\qquad \frac{d\bar{y}'}{d\tau}=v_2,\qquad \frac{d\bar{z}'}{d\tau}=v_3,$$

we have

$$\frac{g}{c}\left(1+\frac{2gx}{c^2}\right)^{\frac{1}{2}}\left(1+\frac{2g\bar{x}'}{c^2}\right)^{\frac{1}{2}}\sinh\left\{\frac{g}{c}(\bar{t}-t)\right\}+\mu\frac{\partial\tau}{\partial t}=0,$$

where

$$\mu=\frac{\partial\Omega}{\partial\bar{t}}v_0+\frac{\partial\Omega}{\partial\bar{x}'}v_1+\frac{\partial\Omega}{\partial\bar{y}'}v_2+\frac{\partial\Omega}{\partial\bar{z}'}v_3.$$

Let us now evaluate the quantity $\sum_{l,m} g^{lm}\tau_{lm}$. Remembering that

$$g^{00}=\frac{c^2}{c^2+2gx},\quad g^{11}=-c^2\left(1+\frac{2gx}{c^2}\right),\quad g^{22}=-c^2,\quad g^{33}=-c^2,$$

and using the ordinary formula for covariant differentiation, we have

$$\sum_{l,m} g^{lm}\tau_{lm} = \frac{c^2}{c^2+2gx}\frac{\partial^2\tau}{\partial t^2} - 2g\frac{\partial\tau}{\partial x} - c^2\left(1+\frac{2gx}{c^2}\right)\frac{\partial^2\tau}{\partial x^2} - c^2\frac{\partial^2\tau}{\partial y^2} - c^2\frac{\partial^2\tau}{\partial z^2}. \quad (5)$$

Now

$$\frac{\partial\tau}{\partial t} = -\frac{1}{\mu}\frac{\partial\Omega}{\partial t},$$

so

$$\frac{\partial^2\tau}{\partial t^2} = -\frac{1}{\mu}\frac{\partial^2\Omega}{\partial t^2} + \frac{2}{\mu^2}\left(\frac{\partial^2\Omega}{\partial t\,\partial\bar{t}}v_0 + \frac{\partial^2\Omega}{\partial t\,\partial\bar{x}'}v_1\right.$$

$$\left. + \frac{\partial^2\Omega}{\partial t\,\partial\bar{y}'}v_2 + \frac{\partial^2\Omega}{\partial t\,\partial\bar{z}'}v_3\right)\frac{\partial\Omega}{\partial t} - \frac{1}{\mu^3}\,\mathrm{U}\left(\frac{\partial\Omega}{\partial t}\right)^2,$$

where

$$\mathrm{U} = \frac{\partial^2\Omega}{\partial\bar{t}^2}v_0^2 + \frac{\partial^2\Omega}{\partial\bar{x}'^2}v_1^2 + \frac{\partial^2\Omega}{\partial\bar{y}'^2}v_2^2 + \frac{\partial^2\Omega}{\partial\bar{z}'^2}v_3^2$$

$$+ 2\frac{\partial^2\Omega}{\partial\bar{t}\,\partial\bar{x}'}v_0v_1 + 2\frac{\partial^2\Omega}{\partial\bar{t}\,\partial\bar{y}'}v_0v_2 + 2\frac{\partial^2\Omega}{\partial\bar{t}\,\partial\bar{z}'}v_0v_3$$

$$+ 2\frac{\partial^2\Omega}{\partial\bar{x}'\,\partial\bar{y}'}v_1v_2 + 2\frac{\partial^2\Omega}{\partial\bar{x}'\,\partial\bar{z}'}v_1v_3 + 2\frac{\partial^2\Omega}{\partial\bar{y}'\,\partial\bar{z}'}v_2v_3 + \frac{\partial\Omega}{\partial\bar{t}}w_0$$

$$+ \frac{\partial\Omega}{\partial\bar{x}'}w_1 + \frac{\partial\Omega}{\partial\bar{y}'}w_2 + \frac{\partial\Omega}{\partial\bar{z}'}w_3,$$

(the w's denoting the second derivatives of $\bar{t}$, $\bar{x}'$, $\bar{y}'$, $\bar{z}'$, with respect to τ), with similar expressions for $\partial^2\tau/\partial x^2$, etc. Substituting in (5), we obtain

$$\sum_{l,m} g^{lm}\tau_{lm} = -\frac{1}{\mu}\left\{\frac{c^2}{c^2+2gx}\frac{\partial^2\Omega}{\partial t^2} - 2g\frac{\partial\Omega}{\partial x}\right.$$

$$\left. - (c^2+2gx)\frac{\partial^2\Omega}{\partial x^2} - c^2\frac{\partial^2\Omega}{\partial y^2} - c^2\frac{\partial^2\Omega}{\partial z^2}\right\},$$

the other terms vanishing in consequence of the equation

$$\sum_{p,q} g^{pq}\frac{\partial\Omega}{\partial x^p}\frac{\partial\Omega}{\partial x^q} = 0;$$

and on substituting for the derivatives of Ω from (4) we have

$$\sum_{l,m} g^{lm}\tau_{lm} = 4g^2/c^2\mu.$$

Thus, if

$$\sigma_p = \tau_p \Big/ \sum_{l,m} g^{lm}\tau_{lm},$$

we have

$$\left.\begin{aligned}
\sigma_0 &= -\frac{c}{2g}\left(1+\frac{2gx}{c^2}\right)^{\frac{1}{2}}\left(1+\frac{2g\bar{x}'}{c^2}\right)^{\frac{1}{2}}\sinh\frac{g(\bar{t}-t)}{c}\\
\sigma_1 &= -\frac{1}{2g}+\frac{1}{2g}\left(1+\frac{2gx}{c^2}\right)^{-\frac{1}{2}}\left(1+\frac{2g\bar{x}'}{c^2}\right)^{\frac{1}{2}}\cosh\frac{g(\bar{t}-t)}{c}\\
\sigma_2 &= \frac{\bar{y}'-y}{2c^2}\\
\sigma_3 &= \frac{\bar{z}'-z}{2c^2}
\end{aligned}\right\}. \tag{6}$$

Now by (2), the vector potential of the electromagnetic field produced by the moving electron is

$$\phi_p = \frac{e}{c}\sum_{q,r} g^{qr}\sigma_{pqr} = \frac{e}{c}\left\{\left(1+\frac{2gx}{c^2}\right)^{-1}\sigma_{p00} - c^2\left(1+\frac{2gx}{c^2}\right)\sigma_{p11} - c^2\sigma_{p22} - c^2\sigma_{p33}\right\}, \tag{7}$$

and the formula for covariant differentiation is

$$\sigma_{pqq} = \frac{\partial^2\sigma_p}{\partial(x^q)^2} - 2\sum_t \left\{\begin{matrix} qp \\ t \end{matrix}\right\}\frac{\partial\sigma_t}{\partial x^q} - \sum_t \left\{\begin{matrix} qq \\ t \end{matrix}\right\}\frac{\partial\sigma_p}{\partial x^t} - \sum_s \frac{\partial}{\partial x^q}\left\{\begin{matrix} pq \\ s \end{matrix}\right\}\sigma_s$$
$$+ \sum_{t,s}\left\{\begin{matrix} qq \\ t \end{matrix}\right\}\left\{\begin{matrix} tp \\ s \end{matrix}\right\}\sigma_s + \sum_{s,t}\left\{\begin{matrix} qp \\ t \end{matrix}\right\}\left\{\begin{matrix} qt \\ s \end{matrix}\right\}\sigma_s. \tag{8}$$

Substituting from (8) in (7), we find that *the vector potential of the electromagnetic field due to an electron e moving in any manner in a quasi-uniform gravitational field is* (ϕ_0, ϕ, ϕ_2, ϕ_3), *where*

$$\left.\begin{aligned}
\phi_0 = \frac{e}{c}\Bigg\{&\left(1+\frac{2gx}{c^2}\right)^{-1}\frac{\partial^2\sigma_0}{\partial t^2} - c^2\left(1-\frac{2gx}{c^2}\right)\frac{\partial^2\sigma_0}{\partial x^2}\\
&- c^2\frac{\partial^2\sigma_0}{\partial y^2} - c^2\frac{\partial^2\sigma_0}{\partial z^2} - 2g\frac{\partial\sigma_1}{\partial t}\Bigg\}\\
\phi_1 = \frac{e}{c}\Bigg\{&\left(1+\frac{2gx}{c^2}\right)^{-1}\frac{\partial^2\sigma_1}{\partial t^2} - c^2\left(1+\frac{2gx}{c^2}\right)\frac{\partial^2\sigma_1}{\partial x^2}\\
&- c^2\frac{\partial^2\sigma_1}{\partial y^2} - c^2\frac{\partial^2\sigma_1}{\partial z^2} - \frac{2g}{c^2}\left(1+\frac{2gx}{c^2}\right)^{-2}\frac{\partial\sigma_0}{\partial t} - 4g\frac{\partial\sigma_1}{\partial x}\Bigg\}\\
\phi_2 = \frac{e}{c}\Bigg\{&\left(1+\frac{2gx}{c^2}\right)^{-1}\frac{\partial^2\sigma_2}{\partial t^2} - c^2\left(1+\frac{2gx}{c^2}\right)\frac{\partial^2\sigma_2}{\partial x^2}\\
&- c^2\frac{\partial^2\sigma_2}{\partial y^2} - c^2\frac{\partial^2\sigma_2}{\partial z^2} - 2g\frac{\partial\sigma_2}{\partial x}\Bigg\}\\
\phi_3 = \frac{e}{c}\Bigg\{&\left(1+\frac{2gx}{c^2}\right)^{-1}\frac{\partial^2\sigma_3}{\partial t^2} - c^2\left(1+\frac{2gx}{c^2}\right)\frac{\partial^2\sigma_3}{\partial x^2}\\
&- c^2\frac{\partial^2\sigma_3}{\partial y^2} - c^2\frac{\partial^2\sigma_3}{\partial z^2} - 2g\frac{\partial\sigma_3}{\partial x}\Bigg\}
\end{aligned}\right\}, \tag{9}$$

and where $(\sigma_0, \sigma_1, \sigma_2, \sigma_3)$ ***have the values given in*** (6), it being understood that in the differentiations $(\bar{t}, \bar{x}', \bar{y}, \bar{z}')$ are to be regarded as functions of (t, x, y, z); they are ***known*** functions, since the motion of the electron is supposed given, and the null-cone of any point in this metric is given by equation (4).

The problem of determining the electromagnetic field due to any given motion of electrons in a quasi-uniform gravitational field is thus reduced to the mere performance of differentiations.

§ 4. *An Électrostatic Distribution in a Quasi-Uniform Gravitational Field.*

As a particular case of the formulæ of the last article, let us suppose that the electric charges are all at rest, so that the field is electrostatic; for simplicity, let us suppose that there is a single electron, which is at the origin of co-ordinates, so

$$\bar{x}' = 0, \qquad \bar{y}' = 0, \qquad \bar{z}' = 0,$$

and equation (4) becomes

$$\Omega = 1 + \frac{gx}{c^2} + \frac{g^2}{2c^4}(y^2 + z^2) - \left(1 + \frac{2gx}{c^2}\right)^{\frac{1}{2}} \cosh \frac{g(\bar{t} - t)}{c},$$

while equations (6) become

$$\left.\begin{aligned} \sigma_0 &= -\frac{c}{2g}\left(1 + \frac{2gx}{c^2}\right)^{\frac{1}{2}} \sinh \frac{g(\bar{t} - t)}{c} \\ \sigma_1 &= -\frac{1}{2g} + \frac{1}{2g}\left(1 + \frac{2gx}{c^2}\right)^{-\frac{1}{2}} \cosh \frac{g(\bar{t} - t)}{c} \\ \sigma_2 &= -\frac{y}{2c^2} \\ \sigma_3 &= -\frac{z}{2c^2} \end{aligned}\right\}, \tag{10}$$

or, replacing $(\bar{t} - t)$ in (10) by its value obtained from the equation $\Omega = 0$,

$$\left.\begin{aligned} \sigma_0 &= -\frac{1}{2c}\left\{x^2 + y^2 + z^2 + \frac{gx}{c^2}(y^2 + z^2) + \frac{g^2}{4c^4}(y^2 + z^2)^2\right\}^{\frac{1}{2}} \\ \sigma_1 &= -\frac{x - \frac{g}{2c^2}(y^2 + z^2)}{2(c^2 + 2gx)} \\ \sigma_2 &= -\frac{y}{2c^2} \\ \sigma_3 &= -\frac{z}{2c^2} \end{aligned}\right\}. \tag{11}$$

Equations (9) now reduce to

$$\left.\begin{aligned}\phi_0 &= \frac{e}{c}\left\{-(c^2+2gx)\frac{\partial^2\sigma_0}{\partial x^2} - c^2\frac{\partial^2\sigma_0}{\partial y^2} - c^2\frac{\partial^2\sigma_0}{\partial z^2}\right\}\\ \phi_1 &= \frac{e}{c}\left\{-(c^2+2gx)\frac{\partial^2\sigma_1}{\partial x^2} - 4g\frac{\partial\sigma_1}{\partial x} - c^2\frac{\partial^2\sigma_1}{\partial y^2} - c^2\frac{\partial^2\sigma_1}{\partial z^2}\right\}\\ \phi_2 &= 0\\ \phi_3 &= 0\end{aligned}\right\}, \qquad (12)$$

and substituting from (11) in (12) we find

$$\left.\begin{aligned}\phi_0 &= e\,.\left\{1+\frac{gx}{e^2}+\frac{g^2}{2c^4}(y^2+z^2)\right\}\left\{(x^2+y^2+z^2)+\frac{gx}{c^2}(y^2+z^2)\right.\\ &\qquad\qquad\qquad\qquad\qquad\qquad\left.+\frac{g^2}{4c^4}(y^2+z^2)\right\}^{-\frac{1}{2}}\\ \phi_1 &= -\frac{e}{c}\cdot\frac{g}{c^2+2gx}\\ \phi_2 &= 0\\ \phi_3 &= 0\end{aligned}\right\},$$

which agrees with the solution found earlier* by the present writer for the electric potential due to an electron at rest at the origin in a quasi-uniform gravitational field. The method of the present paper is, of course, immensely more powerful than that of the earlier paper, since our formula (2) enables us to find the vector potential of any distribution of moving electrons, provided we can integrate the equations of the null geodesics.

§ 5. *Remarks on some Features of the Analysis.*

The co-ordinates $(\bar{t}, \bar{x}', \bar{y}', \bar{z}')$ of the moving electron at the instant when it emits the radiation which reaches (x, y, z) at the instant t, are, as we have seen, functions of (t, x, y, z); the first derivatives of $(\bar{t}, \bar{x}', \bar{y}', \bar{z}')$ with respect to (t, x, y, z) involve the components of velocity of the electron, while second derivatives such as $\partial^2\bar{x}'/\partial t^2$ involve the components of acceleration of the electron, and so on. Since the right-hand side of the formula (2) involves *fourth* derivatives of τ, it would therefore seem at first sight as if the vector potential ϕ_ν would involve the co-ordinates of the electron, the components of its velocity, the components of its acceleration, and two still higher deriva-

---

[*] 'Roy. Soc. Proc.,' vol. 116, p. 726 (1927).

tives; whereas, as we know, the vector potential due to an electron depends on the co-ordinates and components of velocity of the electron, but *not* on its components of acceleration or on any higher derivatives. It is therefore of interest to examine how the accelerations and the higher derivatives disappear. This can be seen in the following way :—

For convenience write $(\chi^0, \chi^1, \chi^2, \chi^3)$ for the co-ordinates of the electron, which we have previously denoted by $(\bar{t}, \bar{x}', \bar{y}', \bar{z}')$. Let the equation of the null-cone belonging to a world-point $(\chi^0, \chi^1, \chi^2, \chi^3)$ be

$$\Omega\,(\chi^0, \chi^1, \chi^2, \chi^3\,;\; x^0, x^1, x^2, x^3) = 0.$$

This equation depends solely on the metric of space-time. In it we regard (x^0, x^1, x^2, x^3) as the co-ordinates in space-time of the world-point at which we are investigating the electric field, while $(\chi^0, \chi^1, \chi^2, \chi^3)$ are the co-ordinates of the electron which generates the field, and are functions of the proper-time τ of the electron, so the equation may be written

$$\Omega\,\{\chi^0(\tau), \chi^1(\tau), \chi^2(\tau), \chi^3(\tau)\,;\; x^0, x^1, x^2, x^3\} = 0,$$

and this equation expresses τ as a function of (x^0, x^1, x^2, x^3).

Differentiating this equation partially with respect to x^p, we have

$$\frac{\partial\Omega}{\partial x^p} + \sum_r \frac{\partial\Omega}{\partial\chi^r}\frac{d\chi^r(\tau)}{d\tau}\frac{\partial\tau}{\partial x^p} = 0,$$

so

$$\frac{\partial\tau}{\partial x^p} = -\frac{1}{\mu}\frac{\partial\Omega}{\partial x^p},$$

where

$$\mu = \sum_r \frac{\partial\Omega}{\partial\chi^r}v_r, \quad \text{and } v_r = \frac{d\chi^r}{d\tau}.$$

Thus

$$\begin{aligned}\sum_{l,m} g^{lm}\tau_{lm} &= -\sum_{l,m} g^{lm}\left(\frac{1}{\mu}\frac{\partial\Omega}{\partial x^l}\right)_m \\ &= -\frac{1}{\mu}\sum_{l,m} g^{lm}\left[\frac{\partial_1}{\partial_1 x^m}\left(\frac{\partial\Omega}{\partial x^l}\right) - \sum_r \begin{Bmatrix} lm \\ r \end{Bmatrix}\frac{\partial\Omega}{\partial x^r}\right] + \sum_{l,m} g^{lm}\frac{1}{\mu^2}\frac{\partial\Omega}{\partial x^l}\frac{\partial_1\mu}{\partial_1 x^m},\end{aligned}$$

where the suffix $(\;\;)_1$ denotes that we are differentiating with respect to x^m not merely in so far as it is contained explicitly, but also in so far as it is involved in $\chi^0, \chi^1, \chi^2, \chi^3, v_0, v_1, v_2, v_3$, by reason of the dependence of τ on (x^0, x^1, x^2, x^3).

We have, therefore,

$$\frac{\partial_1 \mu}{\partial_1 x^m} = \frac{\partial \mu}{\partial x^m} + \left(\frac{\partial \mu}{\partial \chi^0} v_0 + \frac{\partial \mu}{\partial \chi^1} v_1 + \frac{\partial \mu}{\partial \chi^2} v_2 + \frac{\partial \mu}{\partial \chi^3} v_3 + \frac{\partial \mu}{\partial v_0} w_0 \right.$$
$$\left. + \frac{\partial \mu}{\partial v_1} w_1 + \frac{\partial \mu}{\partial v_2} w_2 + \frac{\partial \mu}{\partial v_3} w_3 \right) \frac{\partial \tau}{\partial x^m},$$

where w_r stands for $\dfrac{dv_r}{d\tau}$,

or

$$\frac{\partial_1 \mu}{\partial_1 x^m} = \sum_r \frac{\partial^2 \Omega}{\partial \chi^r \, \partial x^m} v_r - \frac{\mathrm{U}}{\mu} \frac{\partial \Omega}{\partial x^m},$$

where

$$\mathrm{U} = \sum_{p,\,q} \frac{\partial^2 \Omega}{\partial \chi^p \, \partial \chi^q} v_p v \ + \sum_p \frac{\partial \Omega}{\partial \chi^p} w_p .$$

Also

$$\frac{\partial_1}{\partial_1 x^m}\left(\frac{\partial \Omega}{\partial x^l}\right) = \frac{\partial^2 \Omega}{\partial x^l \partial x^m} + \sum_r \frac{\partial^2 \Omega}{\partial x^l \, \partial \chi^r} v_r \frac{\partial \tau}{\partial x^m} = \frac{\partial^2 \Omega}{\partial x^l \, \partial x^m} - \frac{1}{\mu} \sum_r v_r \frac{\partial^2 \Omega}{\partial x^l \, \partial \chi^r} \frac{\partial \Omega}{\partial x^m}.$$

Therefore

$$\sum_{l,m} g^{lm} \tau_{lm} = -\frac{1}{\mu} \sum_{l,m} g^{lm} \left[\frac{\partial^2 \Omega}{\partial x^l \partial x^m} - \sum_r \begin{Bmatrix} lm \\ r \end{Bmatrix} \frac{\partial \Omega}{\partial x^r}\right]$$
$$+ \frac{2}{\mu^2} \sum_{l,m,r} g^{lm} v_r \frac{\partial \Omega}{\partial x^l} \frac{\partial^2 \Omega}{\partial \chi^r \, \partial x^m} - \frac{\mathrm{U}}{\mu^3} \sum_{l,m} g^{lm} \frac{\partial \Omega}{\partial x^l} \frac{\partial \Omega}{\partial x^m}. \qquad (13)$$

Now the partial differential equation of all the hypersurfaces which touch the null-cone at every point is

$$\sum_{l,m} g^{lm} \frac{\partial f}{\partial x^l} \frac{\partial f}{\partial x^m} = 0,$$

and this is satisfied in particular by the equation of the null-cone itself, so we have

$$\sum_{l,m} g^{lm} \frac{\partial \Omega}{\partial x^l} \frac{\partial \Omega}{\partial x^m} = 0,$$

and by differentiating this equation with respect to χ^r, we have

$$\sum_{l,m} g^{lm} \frac{\partial \Omega}{\partial x^l} \frac{\partial^2 \Omega}{\partial x^m \partial \chi^r} = 0.$$

Thus equation (13) becomes

$$\sum_{l\,m} g^{lm} \tau_{lm} = -\frac{1}{\mu} \sum_{l,m} g^{lm} \left\{\frac{\partial^2 \Omega}{\partial x^l \partial x^m} - \sum_r \begin{Bmatrix} lm \\ r \end{Bmatrix} \frac{\partial \Omega}{\partial x^r}\right\},$$

and therefore *our general formula* (2) *becomes*

$$\phi_p = \frac{e}{c} \sum_{q,r} g^{qr} \sigma_{pqr},$$

where

$$\sigma_p = \frac{\partial\Omega}{\partial x^p} \Big/ \left[\sum_{l,m} g^{lm} \left\{ \frac{\partial^2\Omega}{\partial x^l \partial x^m} - \sum_r \left\{ \begin{matrix} lm \\ r \end{matrix} \right\} \frac{\partial\Omega}{\partial x^r} \right\} \right]$$

and $\Omega = 0$ *is the equation of the null-cone.* The differentiations in the last equation are true partial differentiations, *i.e.*, they take account only of the explicit occurrence of (x^0, x^1, x^2, x^3) in Ω, ignoring the dependence of $(\chi^0, \chi^1, \chi^2, \chi^3)$ on (x^0, x^1, x^2, x^3), through their dependence on τ. Therefore σ_p *does not involve the components of velocity or acceleration of the electron, and this is true in any gravitational field whatever.*

The Energy of a Body moving in an Infinite Fluid, with an Application to Airships.

By G. I. Taylor, F.R.S.

(Received May 23, 1928.)

When a rigid body moves without rotation in an infinite fluid it sets up a flow in the fluid the velocity potential of which may be represented by a series of spherical harmonics in the form

$$\phi = (ax + by + cz) r^{-3} + r^{-3} s_2 + r^{-4} s_3 + \ldots r^{-m-1} s_m + \ldots, \qquad (1)$$

where s_m is a surface spherical harmonic of degree m and the origin is chosen at some point inside the body. The energy of the flow, T, may be expressed in the form

$$2\mathrm{T}/\rho = \mathrm{A}u^2 + \mathrm{B}v^2 + \mathrm{C}w^2 + 2\mathrm{A}'vw + 2\mathrm{B}'wu + 2\mathrm{C}'uv, \qquad (2)$$

where u, v, w are the components of velocity of the body and the six constants A, B, C, A′, B′, C′ depend only on the shape of the body. It is proposed to show that T depends only on the harmonic terms of the first degree in the expansion (1) (namely, on $(ax + by + cz) r^{-3}$) and on the volume V of the body, the other terms in (1) making no contribution to T.

T may be expressed in the form of the surface integral

$$2\mathrm{T}/\rho = -\iint_i \phi \frac{\partial \phi}{\partial n} ds, \tag{3}$$

where the suffix i indicates that the integration is carried out over the surface of the body.

At the surface of the body $-\dfrac{\partial \phi}{\partial n} = lu + mv + nw$, where l, m, n are the direction cosines of the outward-drawn normal, so that

$$2\mathrm{T}/\rho = \iint_i (lu + mv + nw)\, \phi\, ds. \tag{4}$$

Now apply Green's theorem to the volume contained between the body and a closed surface which completely surrounds it. Using the suffix 0 to represent integration over the outer surface.

$$\iint_i \phi l\, ds = \iint_0 \phi l\, ds - \iiint \frac{\partial \phi}{\partial x}\, dx\, dy\, dz, \tag{5}$$

where the volume integral extends through the space included between the body and the outer surface. Another application of Green's theorem gives

$$\iiint \frac{\partial \phi}{\partial x}\, dx\, dy\, dz = \iint_0 x \frac{\partial \phi}{\partial x} l ds - \iint_i x \frac{\partial \phi}{\partial x} l ds - \iiint x \frac{\partial^2 \phi}{\partial x^2}\, dx\, dy\, dz, \tag{6}$$

and

$$\begin{aligned}\iiint x \frac{\partial^2 \phi}{\partial x^2}\, dx\, dy\, dz &= -\iiint x \left(\frac{\partial^2 \phi}{\partial y^2} + \frac{\partial^2 \phi}{\partial z^2}\right) dx\, dy\, dz \\ &= -\iint_0 x \frac{\partial \phi}{\partial y} m\, ds + \iint_i x \frac{\partial \phi}{\partial y} m\, ds - \iint_0 x \frac{\partial \phi}{\partial z} n\, ds + \iint_0 x \frac{\partial \phi}{\partial z} n\, ds. \end{aligned} \tag{7}$$

Hence from (5), (6) and (7)

$$\begin{aligned}\iint_i \phi l\, ds = \iint_0 \phi l\, ds &- \iint_0 x \left(l \frac{\partial \phi}{\partial x} + m \frac{\partial \phi}{\partial y} + n \frac{\partial \phi}{\partial z}\right) ds \\ &+ \iint_i x \left(l \frac{\partial \phi}{\partial x} + m \frac{\partial \phi}{\partial y} + n \frac{\partial \phi}{\partial z}\right) ds. \end{aligned} \tag{8}$$

But at the surface of the body

$$l \frac{\partial \phi}{\partial x} + m \frac{\partial \phi}{\partial y} + n \frac{\partial \phi}{\partial z} = \frac{\partial \phi}{\partial n} = -(lu + mv + nw).$$

Hence

$$\iint_i x\left(l\frac{\partial\phi}{\partial x}+m\frac{\partial\phi}{\partial y}+n\frac{\partial\phi}{\partial z}\right)ds=-\iint_i x\,(lu+mv+nw)\,ds$$

$$=-u\iint_i xl\,ds-v\iint_i xm\,ds-w\iint_i xn\,ds.$$

Of these integrals

$$\iint_i xl\,ds=\mathrm{V},$$

where V is the volume of the solid, and

$$\iint_i xm\,ds=\iint_i xn\,ds=0$$

because the integral is taken over a closed surface.

Now take the outer surface as a sphere of radius R. In that case

$$l=x/\mathrm{R},\qquad m=y/\mathrm{R},\qquad n=z/\mathrm{R},$$

so that

$$-\iint_0 x\left(l\frac{\partial\phi}{\partial x}+m\frac{\partial\phi}{\partial y}+n\frac{\partial\phi}{\partial z}\right)ds=-\iint_0 x\frac{\partial\phi}{\partial r}\,ds.$$

Collecting results (4) becomes

$$\begin{aligned}2\mathrm{T}/\rho=u&\left[\iint_0\frac{x\phi}{\mathrm{R}}\,ds-\iint_0 x\frac{\partial\phi}{\partial r}ds-u\mathrm{V}\right]\\&+v\left[\iint_0\frac{y\phi}{\mathrm{R}}\,ds-\iint_0 y\frac{\partial\phi}{\partial r}ds-v\mathrm{V}\right]\\&+w\left[\iint_0\frac{z\phi}{\mathrm{R}}\,ds-\iint_s z\frac{\partial\phi}{\partial r}ds-w\mathrm{V}\right]\end{aligned}\tag{9}$$

Inserting in each term the expansion (1) for ϕ in spherical harmonics, it will be seen that

$$\iint_0\frac{x\phi}{\mathrm{R}}\,ds=\frac{a}{\mathrm{R}^4}\iint_0 x^2\,ds=\tfrac{4}{3}\pi a,$$

all the other terms involving b, c, s_1, s_2, ... vanishing because they involve integrals of products of conjugate spherical harmonics over a spherical surface. Similarly

$$\iint_0 x\frac{\partial\phi}{\partial r}\,ds=-\frac{2a}{\mathrm{R}^4}\iint_0 x^2\,ds=-\tfrac{8}{3}\pi a.$$

Hence from (9)

$$2\mathrm{T}/\rho=4\pi\,(au+bv+cw)-\mathrm{V}\,(u^2+v^2+w^2).\tag{10}$$

The energy therefore only involves the volume V of the solid and the coefficients of the harmonics of the first degree in the expansion of the velocity potential.

It is of interest to notice why the term in V is necessary. Compare, for instance, the energy in the fluid in the case (*a*) of a solid S, fig. 1A, and (*b*) of the body S′ shown in fig 1B, which has the same external form as S except for a small opening which communicates with a hollow of volume V′ inside the body S′. Suppose now that each of these bodies moves without rotation with velocity components u, v, w. The motion of the fluid at great distances from the body must be identical in the two cases, and since at great distances the motion contributed by the terms in the expansion for the velocity potential of degree higher than the first becomes negligible compared with that due to the terms of the first degree, the part of the total energy contributed by the first term in (10), namely,

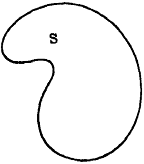

FIG. 1A.

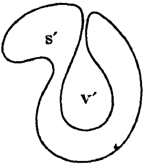

FIG. 1B.

$$2\pi\rho\,(au + bv + cw),$$

is the same in the two cases. The volume of the body S′ is less than that of S by an amount V′. Hence from (10) it will be seen that the total energy of the flow in case (*b*) exceeds that in case (*a*) by an amount $\frac{1}{2}\rho V'(u^2 + v^2 + w^2)$. This is evidently true if the fluid in the hollow is carried bodily along with solid and the energy of the flow external to the bodies is identical in the two cases.

We have seen that the energy in a fluid due to the translation of a rigid body in any direction is known if the terms of the first degree only in the expansion of the velocity potential are known. It remains to solve the converse problem, namely, to show that the terms in the first degree in the expansion of the velocity potential can be found if the six coefficients A, B, C, A′, B′, C′

in the expression (2) are known. Evidently a, b, c are linear functions of u, v, w and can therefore be expressed in the form

$$\left.\begin{aligned} a &= a_1 u + a_2 v + a_3 w \\ b &= b_1 u + b_2 v = b_3 w \\ c &= c_1 u + c_2 v + c_3 w \end{aligned}\right\}, \tag{11}$$

where the quantities $a_1, a_2, \ldots c_3$ depend only on the external surface of the body.

Inserting these values in (10) and comparing coefficients of u^2, v^2, w^2, uv, vw, wu with those in (2), the following six equations are obtained:—

$$\left.\begin{aligned} \mathrm{A} &= 4\pi a_1 - \mathrm{V} \\ \mathrm{B} &= 4\pi b_2 - \mathrm{V} \\ \mathrm{C} &= 4\pi c_3 - \mathrm{V} \end{aligned}\right\}, \tag{12}$$

$$\left.\begin{aligned} 2\mathrm{A}' &= 4\pi\,(b_3 + c_2) \\ 2\mathrm{B}' &= 4\pi\,(c_1 + a_3) \\ 2\mathrm{C}' &= 4\pi\,(a_2 + b_1) \end{aligned}\right\}. \tag{13}$$

Hence a_1, b_2 and c_3 are determined in terms of A, B, C, but three more equations are required before we can determine the other six. These are provided by certain reciprocal relationships first given by Kirchoff.*

If

$$\phi = u\phi_1 + v\phi_2 + w\phi_3, \tag{14}$$

then ϕ_1, ϕ_2, ϕ_3 are functions of x, y, z which depend only on the shape of the body. The coefficient A′ in (2) is

$$\mathrm{A}' = -\tfrac{1}{2}\iint_s \left(\phi_2 \frac{\partial \phi_3}{\partial n} + \phi_3 \frac{\partial \phi_2}{\partial n}\right) ds.$$

Hence by Green's theorem, since ϕ_2 and ϕ_3 are two different velocity potentials,

$$\mathrm{A}' = -\iint_s \phi_2 \frac{\partial \phi_3}{\partial n}\, ds = -\iint_s \phi_3 \frac{\partial \phi_2}{\partial n}\, ds.$$

At the surface of the body

$$\frac{\partial \phi_3}{\partial n} = -n \quad \text{and} \quad \frac{\partial \phi_2}{\partial n} = -m,$$

so that

$$\mathrm{A}' = \iint_s n\phi_2\, ds = \iint_s m\phi_3\, ds. \tag{15}$$

---

* "Ueber die bewegung eines Rotationkörpers in einer Flüssigkeit," 'Crelle,' vol. 71 (1869).

These integrals are each particular case of equations (8) and can be transformed into the form

$$\iint_i n\phi_2 ds = \iint_0 n\phi_2 ds + \iint_i z\frac{\partial\phi_2}{\partial n}ds - \iint_0 z\frac{\partial\phi_2}{\partial n}ds,$$

at the inner surface

$$\frac{\partial\phi_2}{\partial n} = -m \quad \text{and also} \quad \iint_i zm\,ds = 0,$$

so that

$$\iint_i z\frac{\partial\phi_2}{\partial n}ds = 0.$$

Hence

$$\iint_i n\phi_2 ds = \iint_0 \left(n\phi_2 - z\frac{\partial\phi_2}{\partial n}\right)ds, \tag{16}$$

and when the outer surface O is a sphere of radius R,

$$\iint_i n\phi_2 ds = \iint_0 \left(\frac{z\phi_2}{\mathrm{R}} - z\frac{\partial\phi_2}{\partial r}\right)ds.$$

To evaluate this integral notice that

$$\phi_2 = (a_2x + b_2y + c_2z)r^{-3} + \text{(harmonics of degree higher than the first).} \tag{17}$$

When this expression for ϕ_2 is substituted in (16) all the terms vanish except those involving c_2, so that

$$\iint_i n\phi_2 ds = \tfrac{4}{3}\pi c_2 + \tfrac{8}{3}\pi c_2 = 4\pi c_2.$$

Similarly

$$\iint_i m\phi_3 ds = 4\pi b_3.$$

Hence from (15) $b_3 = c_2$ and similarly $a_3 = c_1$ and $b_1 = a_2$.

When, therefore, the expression for the energy due to a translational velocity uvw is known in the form

$$2\mathrm{T}/\rho = \mathrm{A}u^2 + \mathrm{B}v^2 + \mathrm{C}w^2 + 2\mathrm{A}'vw + 2\mathrm{B}'wu + 2\mathrm{C}'uv,$$

the terms of the first degree in the expansion of the velocity potential in spherical harmonics are given by

$$4\pi\phi = [(\mathrm{A}+\mathrm{V})u + \mathrm{C}'v + \mathrm{B}'w]\,xr^{-3} + [\mathrm{C}'u + (\mathrm{B}+\mathrm{V})v + \mathrm{A}'w]\,yr^{-3} + [\mathrm{B}'u + \mathrm{A}'v + (\mathrm{C}+\mathrm{V})w]\,zr^{-3}. \tag{18}$$

Application to determine the "Virtual Mass" of an Airship in Accelerated Motion.

It is well known that if a number of sources and an equal number of sinks are arranged along a line parallel to the direction of a uniform stream of air, the flow outside a certain surface of revolution is the same as though this surface were the outer surface of a solid of revolution. A number of such surfaces have been constructed by Fuhrmann* from various distributions of sources and sinks. Suppose that the sources are distributed with line density mU along an axis in air moving with velocity U, and that the corresponding airship shape or surface of revolution has been found by the method of Fuhrmann. Let its volume be V.

If m is known as a function of x, the distance along the axis from some origin, then the contribution of an element $mU\,dx$ to the velocity potential is

$$\frac{mU\,dx}{4\pi r}\left(1 + \frac{x}{r}P_1 + \dots + \left(\frac{x}{r}\right)^s P_s + \dots\right),$$

where P_s is the zonal harmonic of degree s.

If the whole distribution of sources and sinks is contained within the length $x = x_1$ to $x = x_2$, the terms of degree 0 and 1 in the velocity potential are therefore

$$\frac{U}{4\pi r}\int_{x_1}^{x_2} m\,dx \quad \text{and} \quad \frac{UP_1}{4\pi r^2}\int_{x_1}^{x_2} mx\,dx. \tag{19}$$

But $\int_{x_1}^{x_2} m\,dx = 0$, for there is no flow through the surface of the solid.

Comparing (18) with (19) and remembering that $P_1 r^{-2} = xr^{-3}$, it will be seen that

$$A + V = \int_{x_1}^{x_2} mx\,dx, \tag{20}$$

so that the "virtual mass" of the airship in accelerated motion parallel to its axis is

$$\rho A = \rho\int_{x_1}^{x_2} mx\,dx - \rho V. \tag{21}$$

As a simple example we may recover the well-known result that the virtual addition to mass of a sphere in accelerated motion is half the mass of the fluid displaced. If R is the radius of the sphere, the appropriate distribution of sources and sinks forms a doublet of strength $2\pi Va^3$, so that

$$\int_{x_1}^{x_2} mx\,dx = 2\pi a^3.$$

---

* E. Fuhrmann, 'Theoretische u. Experimentelle Untersuchungen an Ballonmodellen Jahrb. der Motorluftschiff Studiengesellschaft.'

Hence from (21)

$$\rho A = \rho\left(\tfrac{3}{2}V - V\right) = \tfrac{1}{2}\rho V.$$

As an example of the use of formula (21) the virtual mass of the airship whose shape is shown in fig 2 has been found. This shape is one of a series

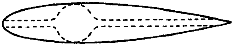

FIG 2.

which were worked out by Fuhrmann.* It is No. 4 of that series. It is derived from the following distribution of sources and sinks spread over a length $3l$ and placed in a stream of velocity U.

From $x = 0$ to $x = l$ the strength of the source per unit length is $\dfrac{4\pi U}{30}(l - x)$

From $x = l$ to $x = 2l$ it is $-\dfrac{4\pi U}{60}(x - l)$. From $x = 2l$ to $x = 3l$ it is $-\dfrac{4\pi U}{60}(3l - x)$.

Hence

$$\int_{x_1}^{x_2} mx\,dx = \frac{4\pi}{60}\left[2\int_0^l (l - x)\,dx - \int_l^{2l} (x - l)\,dx - \int_{2l}^{3l} (3l - x)\,dx\right] = \frac{\pi l^3}{9}.$$

Hence from (20), $\frac{1}{9}\pi l^3 = V + A = V(1 + \alpha)$.

Fuhrmann has determined by graphical integration the volume of this shape and finds it $V = 0{\cdot}3318 l^3$, so that

$$1 + \alpha = \pi/9 \times 0{\cdot}3318 = 1{\cdot}051,$$

and $\alpha = 0{\cdot}051$, or the virtual mass is $\cdot 051\rho V$. (22)

This may be compared with the virtual addition to mass of a prolate spheroid of the same ratio of length to breadth, namely, 6·09, moving parallel to its axis, which is

$$0{\cdot}044\rho V. \qquad (23)$$

Comparing (22) and (23) it will be seen that the ratio of virtual mass to mass of displaced fluid for the airship shape is greater than that of the corresponding spheroid with the same " fineness ratio " 6·09. At first sight this seems a little surprising, but it can easily be seen that if a model with a given fineness ratio is cut away and made finer at the nose or tail without altering its length or maximum diameter, the ratio α will increase. Suppose, for instance, that the model shown in fig. 2 were cut away till it consisted of a spherical centre together with narrow pencil-like projections in front and behind, as shown in the dotted lines of fig. 2. For this body α has, in the limit when the projections are narrow enough, the value appropriate to a sphere, namely, 0·5. The operation of fining down the nose and tail therefore increases α so that it is to be expected that the value of α appropriate to Fuhrmann's shape shown in fig. 2, which is pointed at the tail, will be greater than the value of α for a spheroid of the same length and breadth.

---

* *Ibid.*, p. 92.

The expression (21) for the virtual mass of a body in accelerated motion parallel to the axis of x is valid for any body, not necessarily a body of revolution, provided that the appropriate distribution of sources and units is known.

The Absorption Spectra of Solutions of Cobalt Chloride, Cobalt Bromide, and Cobalt Iodide in Concentrated Hydrochloric, Hydrobromic, and Hydriodic Acids.

By WALLACE R. BRODE and R. A. MORTON, Liverpool University.

(Communicated by E. C. C. Baly, F.R S.—Received March 27, 1928)

[PLATES 1 AND 2.]

In a recent paper by one of us (W. R. B.)* the selective absorption in the region of 600 to 710 $m\mu$ of cobalt chloride dissolved in concentrated hydrochloric acid was shown to consist of a number of superimposed, similarly shaped absorption bands. The frequency values at which these component bands exhibited a maximum of absorption corresponded with integral multiples of a common or fundamental frequency. The analysis of the observed absorption curve has now been extended into the blue so as to cover the whole of the selective absorption occurring in the visible portion of the spectrum. Similar analyses have also been obtained for the absorption shown by cobalt bromide when dissolved in concentrated hydrobromic acid and cobalt iodide dissolved in concentrated hydriodic acid.

---

* 'Roy. Soc. Proc.,' A, vol 118, p. 286 (1928).

Apparatus and Method of Observation.

The apparatus* previously described was again used. Since the principal absorption band of cobalt bromide, as compared with that of cobalt chloride, is situated farther towards the red end of the visible spectrum, where the dispersion of the apparatus is smaller, the wave-length interval between the different sets of observations was increased from 2 to 2·5 $m\mu$ in the region of 625 to 725 $m\mu$. At every wave-length value for which absorption measurements were obtained on the principal band, a minimum of 20 observations were made, and in the extreme red, where the sensitivity of the eye is poor, the number of observations was even larger. The average deviation from the mean absorption value E (where $E = \log_{10} I_0/I$, I_0 being the intensity of the radiant energy passing through the comparison cell filled with the solvent, and I the intensity of the radiant energy passing through the cell containing the solvent and the material under observation) was approximately the same as in the earlier work on cobalt chloride, *i.e.*, 0·025.

In the work with cobalt iodide in concentrated hydriodic acid, it was possible to make visual measurements on only a limited portion of the principal absorption band, and since the region of the spectrum under investigation is near the long wave-length limit of visibility, high accuracy was not to be expected. The component band at 697·5 $m\mu$ was, however, very well defined. In order to investigate the system completely it was necessary to employ a photographic method, using a spectrograph of special design (Adam Hilger, Ltd.), showing a dispersion of 5 cm. between 600 and 1000 $m\mu$. Special Kodak infra-red sensitive plates, freshly hypersensitised with ammonia, were used. The light source was a cored carbon arc, and the spectrum up to 900 $m\mu$ was recorded without difficulty. The photometer system was the ordinary Hilger rotating sector apparatus.

The plates were read from a photographic record obtained with a Moll registering microphotometer. The density curves for the comparison and the solution spectra were thus recorded and the points of intersection represented the wave-length values at which the absorptive power of the solute corresponded with the photometer setting (see Plates 1, 2). The data thus obtained are independent of the personal factor and extend beyond the red limit of visibility. For those wave-lengths accessible to both visual and photographic investigation, excellent agreement was obtained both in respect of extinction and wave-length determinations.

---

* A new model of the Hilger-Nutting spectrophotometer; Adam Hilger, Ltd., London.

Solutions.

Hydrogen bromide was prepared by the interaction of red phosphorus water and bromine* and a saturated aqueous solution of the gas was redistilled several times in the presence of a small amount of red phosphorus. The hydrobromic acid actually used (sp. gr. 1·57) was not fully saturated but was considerably stronger than the constant boiling mixture. The cobalt bromide solutions were prepared as follows: 0·2000 g. of a Kahlbaum preparation of nickel-free and alkali-free cobalt carbonate was dissolved in 100 c.c. of concentrated hydrobromic acid and 25 c.c. of this solution were diluted to 100 c.c. with hydrobromic acid. These solutions contained the equivalent of 5·50 g. of $CoBr_2 . 6H_2O$ per litre in the case of the concentrated solution and 1·375 g. of $CoBr_2 . 6H_2O$ in the case of the more dilute solution. The concentrated cobalt chloride solution was prepared in a similar manner, *i.e.*, 0·2000 g. of pure cobalt carbonate was dissolved in 100 c.c. of concentrated hydrochloric acid. The resulting solution contained the equivalent of 4·000 g. of $CoCl_2 . 6H_2O$ per litre of solution.

Hydriodic acid was prepared as follows: the constant boiling mixture was obtained by distilling an aqueous solution of hydriodic acid prepared by the interaction of hydrogen sulphide and iodine.† The colourless constant boiling mixture was obtained by distillation under reduced pressure in the presence of a little red phosphorus. Hydrogen iodide, prepared by the interaction of iodine and red phosphorus in the presence of hydriodic acid, was then passed into the constant boiling mixture, in the dark and in a cooled container, until the solution had become saturated with hydrogen iodide. This concentrated hydriodic acid was a pale straw colour (sp. gr. 2·0). The solution of cobalt iodide in hydriodic acid was prepared by adding 0·2000 g. of cobalt carbonate to 50 c.c. of the fuming acid; 5 c.c. of this solution was then made up to 20 c.c. with hydriodic acid. This latter solution contained the equivalent of 1·77 g. $CoI_2 . 6H_2O$ per litre of solution.

Discussion of Data.

A more detailed study of the absorption spectrum of cobalt chloride in concentrated hydrochloric acid in the blue and green portions of the visible spectrum has disclosed the presence of a number of maxima and inflexions. It seems probable that the absorption curve here, as in the principal band, owes its shape to the summation of overlapping component bands. It follows quite naturally that an attempt should be made to extend the analysis previously applied to the selective absorption between 600 and 720 $m\mu$ to the whole of the absorption spectrum under discussion. In order to observe fine structure in the blue and green regions of the spectrum, it is necessary to use concentrated solutions, and as a result of colloidal absorption some of the bands are slightly flattened out. This fact, together with the nature of the absorption curve on the steep side of the principal band, makes it very difficult to apply direct analytical methods to the entire curve.

---

* Mellor, 'Comprehensive Treatise on Inorganic and Theoretical Chemistry,' vol. 2, p. 168 (Longmans).

† Mellor, *loc. cit.*, p. 170.

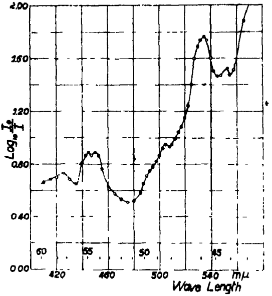

FIG. 1.—Absorption of Cobalt Chloride in Concentrated Hydrochloric Acid. 4·0 g. $CoCl_2 . 6H_2O$ per litre; cell thickness, 10 cm.

It was found, however, that of all the various systems tried, the only satisfactory basis of analysis was the original one applied to the principal band,* *i.e.*, the resolution of the curve into superimposed bands with frequencies of maximal absorption at integral multiples of 12·28 f.† The nicety with which this analysis applies, as is shown in Table I, leaves little doubt but that these bands are a continuation of the same system. Other bands may, of course, be present in addition to those indicated in Table I, but, as mentioned before, the effects of concentration and adjacent absorption bands have considerably reduced the sharpness of many of the weaker bands or possibly totally obscured some of them.

* *Loc. cit.*

† f. = fresnels = vibrations ÷ seconds × 10^{12}.

Table I.—The Analysis of the Absorption Spectrum of Cobalt Chloride in Concentrated Hydrochloric Acid, as based on a Frequency Difference of 12·28 f. between the Component Bands.

Multiple or band number.	Frequency.			Multiple or band number.	Frequency.		
	Calculated.	Observed.	Difference		Calculated	Observed.	Difference.
a 35	430	432	+2	48	589	593	+4
b 36	442	442	0	49	602	—	—
c 37	454	450	−4	50	614	610	−4
d 38	467	465	−2	51	626	—	—
e 39	479	478	−1	52	638	—	—
f 40	491	491	0	53	651	—	—
g 41	503	505	+2	54	662	664	+2
42	515	(probably present)		55	675	677	+2
43	527	(minimum at 524,		56	688	—	—
		probably absent)		57	700	704	+4
44	540	543	+3	58	712	—	—
45	552	—	—	59	724	—	—
46	565	561	−4	60	735	—	—
47	577	—	—				

On examining the absorption spectrum of cobalt bromide in concentrated hydrobromic acid (figs. 2 and 3) a marked similarity with cobalt chloride is at once apparent (*loc. cit.*). There is a definite shift of the entire absorption

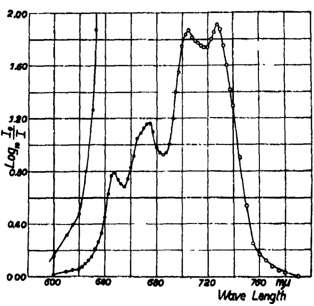

Fig. 2.—Absorption of Cobalt Bromide in Concentrated Hydrobromic Acid. 1·375 g. $CoBr_2 . 6H_2O$ per litre; cell thickness, 0·5 cm.

spectrum in the direction of smaller frequencies of vibration. This shift of an absorption band in the direction of smaller frequencies, concomitant with an increase in molecular weight without a marked change in the chemical or physical properties of the molecule, is to be expected from the fundamental physical concepts involved and has been observed in numerous cases in the study of the absorption spectra of similarly constituted compounds of different molecular weights.

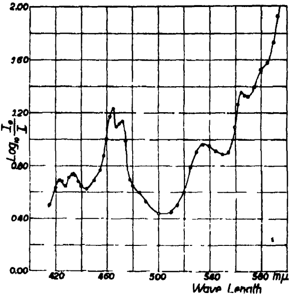

FIG. 3.—Absorption of Cobalt Bromide in Concentrated Hydrobromic Acid. 5·5 g. $CoBr_2 . 6H_2O$ per litre; cell thickness, 10 cm.

Although quite similar in shape to the cobalt chloride absorption band, the principal band of cobalt bromide (between 625 and 750 mμ) appears to be composed of four rather than six component bands. Had not the cobalt chloride system been analysed first, it is quite certain that the first attempt at analysis would be on what we shall term a "four basis" rather than a "six basis." Obviously both systems of analysis must be tried to determine whether there are in fact four components or whether the relative intensities of six components are such as to give a summation curve corresponding apparently with a four-band system.

The analysis on either basis is given both numerically and graphically in Table II and figs. 4 and 5. A four analysis fits the principal band as well as a six analysis, but as can be seen in Table II, the bands in the blue portion of the spectrum fit very poorly on the four basis. Not only does the analysis

Table II.—The Analysis of the Absorption Spectrum of Cobalt Bromide in Concentrated Hydrobromic Acid, as based on a Frequency Difference of 11·7 and of 17·75 between the Component Bands.

Multiple number.	Frequency difference of 17·75 (four basis).			Multiple number	Frequency difference of 11·7 (six basis).			Comparison‡ between chloride and bromide systems.	
	Calculations.	Observed.	Difference.		Calculated.	Observed.	Difference.	Bromide.	Chloride.
23	408	410	+2	35	409	408†	−1	+sss	+sss
24	426	428	+2	36	421	418†	−3	+ss	+ss
25	444	445	+1	37	433	430†	−3	+sss	+sss
26	462	463	+1	38	444	442†	−2	+ss	+ss
27	479	480	+1	39	456	455†	−1	+ss	+ss
28	496	501	+5	40	468	465†	−3	+ss	+ss
29	514	516	+2	41	479	476†	−3	+s	+s
30	532	535	+2	42	491	492†	+1	+	+
31	550	561	+11	43	503	501	−2	+	—?
32	568		−7	44	514	516	+2	+	+
33	586	—	-	45	526	—*	—	—	—
34	603	610	+7	46	538	535	−3	+s	+ss
35	621		−11	47	549	—*	—	—	—
		631	+10	48	561	561	0	+ss	+s
36	639		−8	49	573	—*	—	—	—
		649	+10	50	584	—*	—	—	—
37	656		−7	51	596	—*	—	—	-
		664	+8	52	608	610	+2	+	?
38	674		−10	53	619	—*	—	—	—
39	692	690	−2	54	631	631	0	+ss	+s
40	710	714	+4	55	643	649	+6	+ss	+s
				56	654		−5	?	—
				57	666	664	−2	+	+
				58	678	—*	—	—	-
				59	690	690	0	+s	
				60	701	—*	—	—	
				61	713	714	+1	+s	

* It will be noticed that from multiples 35 to 42 the sequence of component bands is uninterrupted, whereas from multiples 43 to 61 about half the components are missing. The failure to detect these bands may lessen the cogency of the conclusion that all the bands fall into one series, but the absence of the same multiples in both the chloride and bromide series tends to counterbalance this weakness in the argument.

† Based on analysis in fig. 4.

‡ Relative intensity as compared to adjacent bands is indicated by s, ss or sss. + indicates apparent presence as indicated by a maximum or inflexion in the absorption curve. — indicates apparent absence or no indication of a maximum or inflexion

into six bands fit better than into four, but the integral relations for the corresponding bands in the chloride and bromide systems are analogous. For example, the first band in each system is multiple 35, multiple number 40 corresponds to the band at the high-frequency edge of the principal band, and in the blue end of the spectrum bands 54 and 55 are most prominent in both systems. In the bromide analysis the constant difference, on the six basis,

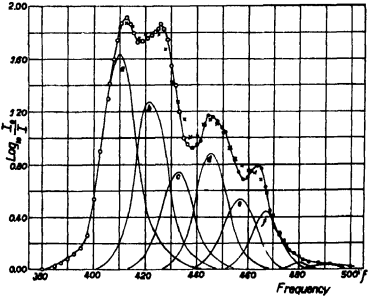

FIG. 4.—Analysis of the Principal Absorption Band of Cobalt Bromide in Concentrated Hydrobromic Acid into Six Component Bands. ○ = observed points; × = calculated points.

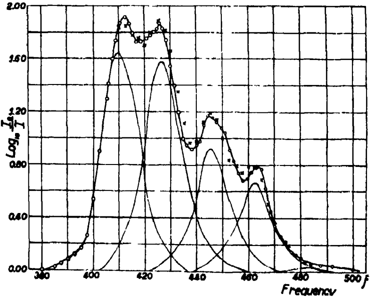

FIG. 5.—Analysis of the Principal Absorption Band of Cobalt Bromide in Concentrated Hydrobromic Acid into Four Component Bands. ○ = observed points; × = calculated points.

is 11·70 as compared with 12·28 for the chloride analysis. On the four basis the difference is 17·75, an increase in the constant frequency difference, whereas the contrary is to be expected. The smaller frequency difference in the bromide system means that the components will be closer together and more difficult to resolve. This fact, together with the smaller spectral dispersion and the location of the band in the far red portion of the visible spectrum may to some extent explain the failure to effect a direct experimental resolution of the principal bromide band into its six components.

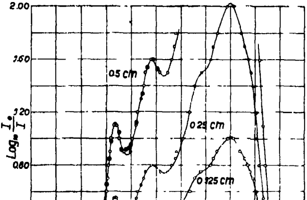

Fig. 6.—Absorption of Cobalt Iodide in Concentrated Hydriodic Acid. 1·77 g. $CoI_2 . 6H_2O$ per litre; cell thickness, 0 125 and 0 5 cm. (centre curve obtained from the other two). ● = visual; ○ = photographic.

Table III.—The Analysis of the Absorption Spectrum of Cobalt Iodide in Concentrated Hydriodic Acid, as based on a Frequency Difference of 10·79 f. between Component Bands.

Multiple or band No.	Wave-length.	Frequency.
a 35	795 mμ	377·6 = 35 × 10·79 f.
b 36	771	388 4 = 36 × 10·79
c 37	752	399·4 = 37 × 10·79
d 38	732	410·0 = 38 × 10·79
e 39	713	420·8 = 39 × 10·79
f 40	696	431·5 = 40 × 10 79

The absorption curve of cobalt iodide in concentrated hydriodic acid is similar to that of cobalt bromide in concentrated hydrobromic acid; it lies still farther in the direction of lower frequencies and extends appreciably into the infra red. From inspection of the curve, direct evidence of only four components is available. The curve has been analysed as before into four and six components (figs. 7 and 8), and each method satisfactorily reproduces the experimental results The choice between the six and four alternatives in the case of cobalt bromide in hydrobromic acid was made as a result of the detection of numerous additional bands in the blue region of the spectrum. For cobalt iodide in hydriodic acid such additional evidence could not well be obtained because fuming hydriodic acid inevitably contains a little free iodine which absorbs in the blue. Considerable absorption is shown by cobalt iodide in this portion of the spectrum, but the high general absorption prevents the observation of fine structure. Accordingly, any preference for either the six or four alternative in the case of cobalt iodide in hydriodic acid must rest entirely upon argument from analogy, the absorption of cobalt halides in concentrated halogen acids being considered as a whole.

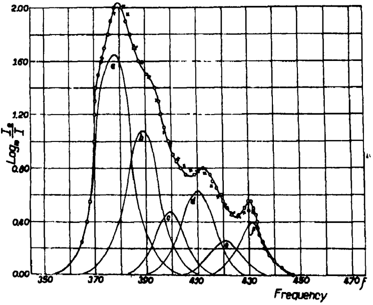

Fig. 7.—Analysis of the Absorption Curve of Cobalt Iodide in Concentrated Hydriodic Acid into Six Component Bands. ○ = observed points; × calculated points.

Observations made at various concentrations and thicknesses on all the halogen solutions confirmed the validity of Beer's law over a considerable range. In any of the three concentrated halogen acids the selective absorption corresponded with that of the cobalt salt of the same acid, even if the cobalt had been introduced originally as another halide. Cobalt fluoride in concentrated hydrofluoric acid exhibited only the pink colour given by cobalt halides in aqueous solution.

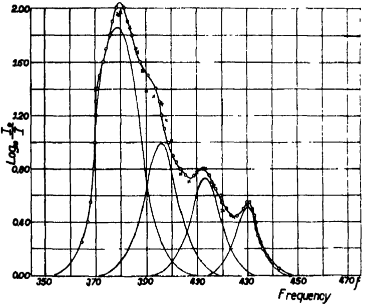

FIG. 8.—Analysis of the Absorption Curve of Cobalt Iodide in Concentrated Hydriodic Acid into Four Component Bands. ○ = observed points; × — calculated points

General Discussion.

Cobalt halides dissolved in the corresponding halogen acids exhibit selective absorption markedly different from that usually associated with cobalt salts in water. In the latter case the absorption is ascribed to the cobalt ion and is considered to be largely independent of the anion. On the other hand, the absorption of the systems investigated in this work is clearly influenced by the nature of the anion. As far as the frequency is concerned, the replacement of a lighter by a heavier halogen atom results in a shift of the absorption bands in the direction of lower frequencies, whilst as regards intensity, an increase in molecular weight increases the intensity of the low-frequency components as compared with the high-frequency components of the principal band.

For the solutions of cobalt chloride in concentrated hydrochloric acid, the resolution of the principal absorption band into its components can only be made on the assumption of *six* constituents, and although the four alternative would appear plausible for the principal band of the bromide, consideration of the selective absorption outside the principal band leads definitely to the rejection of the four basis in favour of the six basis for both the bromide and chloride systems. We know of no evidence for regarding the solutions of cobalt iodide in hydriodic acid as in any significant sense different from solutions of cobalt bromide in hydrobromic acid, and therefore an analysis proved to be valid for both the chloride and bromide solutions might reasonably be extended to include the iodide solutions. In addition, it is found that such an analysis reproduces the data with considerable accuracy, and reveals in the three systems the same integral relationships and a uniform trend in the fundamental frequency. By this method of analysis the principal band is composed in all cases of component bands, the frequencies of which are from 35 to 40 times the constant frequency difference between these components, this constant frequency difference being 12·28 for the chloride system, 11·70 for the bromide and 10·79 f. for the iodide.

The relative intensities of the components corresponding with even integral multiples of the fundamental frequency are less influenced by exchange of the halogen than are those of the components corresponding with the odd multiples. In the even series, the intensities of the components increase to approximately the same extent with increasing molecular weight, whereas in the odd series the first component (*a*) increases much more rapidly and bands (*c*) and (*e*) less rapidly than the other components.

Summary.

1. The absorption spectrum of cobalt chloride in hydrochloric acid has been determined between wave-length values of 400 and 600 $m\mu$.

2. It has been shown that the fine structure observed in this region is a continuation of a vibrational system which has previously been shown to apply to the absorption spectrum of cobalt chloride in hydrochloric acid, between 600 and 720 $m\mu$.

3. The absorption spectrum of cobalt bromide in hydrobromic acid has been determined throughout the visible portion of the spectrum. The curve has been analysed into a series of component bands, the centres of which are multiples of the frequency difference (11·70 f.) between the bands.

4. The absorption spectrum of cobalt iodide in hydriodic acid, between 500 and 900 $m\mu$, has been determined by a combination of visual and photographic methods, and has been analysed into a series of component bands, the centres of which are multiples of the frequency difference (10·79 f.) between the bands.

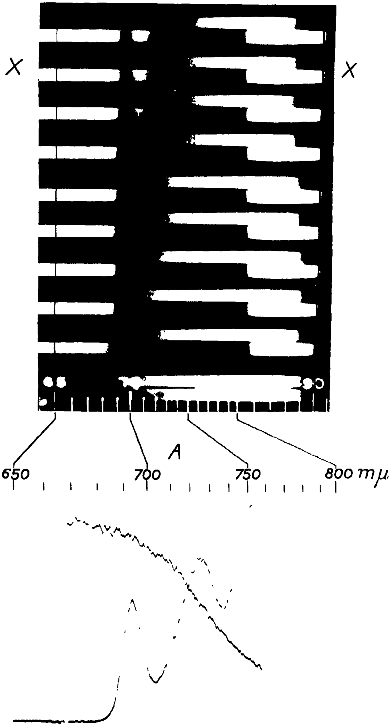

(*Facing p.* 32.)

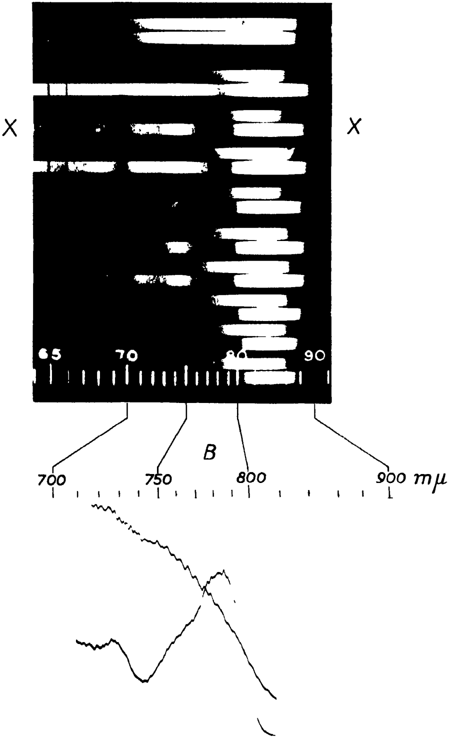
X
X
65
70
80
90
B
700
750
800
900 mμ

5 The same system of analysis applies to the cobalt chloride bromide and iodide data An increase in the molecular weight of the cobalt halide complex causes a decrease in the frequency difference The similarity of the curves indicates a similar constitution for the three cobalt halide complexes investigated

Our thanks are due to Prof E C C Baly F R S for his interest and advice in this work One of us (W R B) is indebted to the John Simon Guggenheim Memorial Foundation for a Fellowship

EXPLANATION OF PLATES

PLATE 1

Absorption Spectrum Plate and Microphotometer Record showing the first two Apparent Maxima in the Absorption Spectrum of Cobalt Iodide in Concentrated Hydriodic Acid 1 77 g CoI_2 $6H_2O$ per litre cell thickness 0 5 cm (microphotometer record that of the photographs marked ×)

PLATE 2

Absorption Spectrum Plate and Microphotometer Record showing the Inflexion and Last Maximum in the Absorption Spectrum of Cobalt Iodide in Concentrated Hydriodic Acid 1 77 g CoI_2 $6H_2O$ per litre cell thickness 0 125 cm (microphotometer record that of the photographs marked ×)

The Characteristics of a Karman Vortex Street in a Channel of Finite Breadth.

By H. Glauert, M.A.

(Communicated by G. I Taylor, F.R.S.—Received April 4, 1928 —Revised May 18, 1928.)

1. *Introduction.*

It is well known that the classical potential flow of a perfect fluid past a bluff body is not a satisfactory representation of the actual flow, and that, in particular, it fails to give any indication of the resistance or drag which is experienced by the body. If the body is of a long cylindrical shape with axis normal to the direction of motion, the flow will be the same in all planes normal to the axis, and may be conceived as proceeding in two dimensions only. In this case it is found experimentally that thin sheets of vorticity spring from the two sides of the body and enclose a dead-water region behind it, but owing to their essential instability these vortex sheets rapidly disintegrate and give rise to a succession of independent vortices which pass down stream in the form of a double vortex row. The characteristics of such a vortex street in its ultimate form far behind the body have been examined by Karman,* who derives an expression for the drag of the body in terms of the strength of the individual vortices and of the breadth of the vortex street. More recently the results of a comprehensive series of experiments on the flow past a flat plate have been published by Fage and Johansen,† and these results have been compared with Karman's theory. In view, however, of the fact that the experimental results are of necessity obtained from experiments in a channel of finite breadth, the present investigation has been undertaken to determine the constraint of the channel walls on the characteristics of the vortex street.

2. *Karman's Theory of the Vortex Street.*

Karman considers the behaviour in a perfect fluid of a double row of point vortices in the configuration shown in fig. 1, deducing the relationships which are necessary for the stability of the system, and the corresponding drag force on the body to which the vortex street is due It appears that the only stable configuration is that in which each vortex of one row is opposite the point mid-way between two successive vortices of the other row. Moreover, if h is

---

* 'Göttingen Nachr.,' p. 509 (1911), and p. 547 (1912).

† 'Roy. Soc. Proc.,' A, vol. 116, p. 170 (1927).

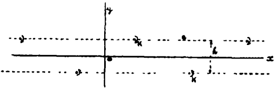

Fig. 1.

the breadth of the vortex street and a the distance between successive vortices of each row, the ratio of these two lengths is governed by the equation

$$\sinh \pi h/a = 1, \tag{1}$$

or numerically

$$h/a = 0\ 2806. \tag{2}$$

Choosing the origin of co-ordinates and the axes as in fig 1, the potential function of the flow due to the vortex street, expressed in terms of the complex co-ordinate $z = x + iy$, is

$$w_1 = \frac{iK}{2\pi} \log \left\{ \sin \frac{\pi}{a} (z_0 - z) \Big/ \sin \frac{\pi}{a} (z_0 + z) \right\}, \tag{3}$$

where

$$z_0 = \tfrac{1}{4}a + \tfrac{1}{2}hi \tag{4}$$

and the corresponding velocity distribution is

$$u - iv = \frac{dw_1}{dz} = -\frac{iK}{a} \cosh \frac{\pi}{a} h \Big/ \left(i \sinh \frac{\pi}{a} h + \cos \frac{2\pi z}{a} \right). \tag{5}$$

Finally, due to the mutual interaction of the vortices, the whole vortex system of fig. 1 moves to the left with the velocity

$$u_0 = \frac{K}{2a} \tanh \frac{\pi h}{a}, \tag{6}$$

and for the stable system this equation becomes

$$K = 2\sqrt{2}au_0. \tag{7}$$

The drag of the body which gives rise to the vortex street is calculated by Karman in two parts in the following manner: The first part, D_1, is derived by bringing the vortices to rest, so that the body is advancing with the velocity $(V - u_0)$ while the general mass of the fluid has the velocity u_0 in the opposite direction. Assuming the flow to be stationary with the potential function w, the force on the body is obtained by evaluating the integral

$$X - iY = \tfrac{1}{2}i\rho \int_c \left(\frac{dw}{dz}\right)^2 dz,$$

round a large contour enclosing the body. This calculation leads to the value

$$D_1 = \rho K^2/2\pi a - \rho u_0 Kh/a. \tag{8}$$

The second part of the drag is due to the fact that in time $a/(V - u_0)$ the body advances such a distance that a new pair of vortices is formed, and by calculating the consequent increase of momentum this second part of the drag is obtained as

$$D_2 = \rho (V - u_0) Kh/a. \tag{9}$$

The total drag is therefore

$$D = \rho (V - 2u_0) Kh/a + \rho K^2/2\pi a, \tag{10}$$

and by virtue of equation (7) the drag coefficient of the body, assumed to be of breadth b, is

$$k_D = \frac{D}{b\rho V^2} = \left(2 \cdot 828 - 1 \cdot 12 \frac{u_0}{V}\right)\frac{u_0 h}{Vb}. \tag{11}$$

The drag coefficient therefore depends mainly on the value of u_0h/Vb, and only to a small extent on the value of u_0/V independently.

Karman's theory, as expressed in the preceding equations, determines the configuration of the vortex street and the drag of the body in terms of the strength and spacing of the vortices, but the theory is incomplete, since it provides no criterion for determining the values of the ratios h/b and u_0/V. An attempt to complete the theory in the case of a flat plate has been made by Heisenberg.* The arguments used are by no means conclusive, but the final numerical values appear to be in good agreement with the experimental results. Heisenberg's analysis leads to the values

$$u_0/V = 0 \cdot 2295, \quad u_0h/Vb = 0 \cdot 3535, \tag{12}$$

and hence to the drag coefficient

$$k_D = 0 \cdot 909.$$

The actual conditions for a flat plate cannot differ greatly from those deduced by Heisenberg, and his values will therefore be used subsequently to obtain numerical estimates of the constraint due to the walls of a channel of finite breadth.

3. *Vortex Street in a Channel.*

Consider now a vortex street of breadth h in a channel of breadth H. The boundary conditions on the walls of the channel are satisfied by the introduction of the infinite series of images of the vortex street as illustrated in fig. 2, and the constraint experienced by the vortex street can be estimated as the velocity field of this series of images. In developing the analysis it is convenient to write

---

* 'Phys. Z.,' vol. 23, p. 363 (1922).

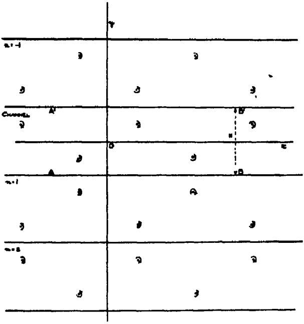

FIG. 2.

$$\sigma = 2\pi \mathrm{H}/a, \tag{13}$$

and to note that in any practical application the breadth h of the vortex street will not exceed one-sixth of the breadth H of the channel.* Thus e^{σ} is at least 40,000, and it is legitimate to develop the analysis on the assumption that e^{σ} is very large.

The velocity field due to the vortex street itself is

$$\frac{dw_1}{dz} = -\frac{i\mathrm{K}}{a}\cosh\frac{\pi}{a}h\Big/\left(i\sinh\frac{\pi}{a}h + \cos\frac{2\pi z}{a}\right),$$

and to obtain the effect of the n^{th} image of fig 2 we may use this same formula with the following modifications –

$$n \text{ odd},\quad \Delta z = \tfrac{1}{2}a + n\mathrm{H}i,$$

$$n \text{ even},\quad \Delta z = \qquad n\mathrm{H}i\,;$$

---

* The flow function for a vortex street of any breadth and the corresponding velocity of the vortices have been given by G. Jaffé: 'Ann. d. Phys.,' vol. 61, p. 173 (1920).

with n odd, therefore, we obtain for a single image of the vortex street

$$\frac{dw}{dz} = -\frac{i\mathrm{K}}{a}\cosh\frac{\pi}{a}h \Big/ \left\{i\sinh\frac{\pi}{a}h - \cos\left(\frac{2\pi z}{a} + n\sigma i\right)\right\},$$

and as e^{σ} is large, this expression becomes approximately

$$\frac{dw}{dz} = \frac{2i\mathrm{K}}{a}e^{-n\sigma}\cosh\frac{\pi}{a}h\left(\cos\frac{2\pi z}{a} + i\sin\frac{2\pi z}{a}\right).$$

Then, combining positive and negative values of n and retaining only the term involving the first power of $e^{-\sigma}$, we obtain as the effect of the system of images

$$\frac{dw_2}{dz} = \frac{4i\mathrm{K}}{a}e^{-\sigma}\cosh\frac{\pi}{a}h\cos\frac{2\pi z}{a}, \tag{14}$$

which is, in fact, simply the effect of the first pair of images

At the vortex $z = z_0$ of the vortex street, the interference of the image gives

$$\begin{aligned} u - iv &= \frac{4i\mathrm{K}}{a}e^{-\sigma}\cosh\frac{\pi}{a}h\cos\left(\frac{\pi}{2} + i\frac{\pi h}{a}\right) \\ &= \frac{4\mathrm{K}}{a}e^{-\sigma}\cosh\frac{\pi}{a}h\sinh\frac{\pi}{a}h, \end{aligned}$$

and hence the velocity u_0 of the vortices is reduced by the factor

$$\left\{1 - 8e^{-\sigma}\cosh^2\frac{\pi h}{a}\right\}. \tag{15}$$

This reduction is at most 0·04 per cent., and is quite negligible.

It appears, therefore, that the constraint of the channel walls does not exert any noticeable effect on the vortex street, and hence it is legitimate to assume that the stability criterion will be the same as in an unlimited fluid, and that Karman's equations (1) and (7) remain valid for the vortex street in a channel of finite breadth.

The potential function of the flow in the channel can be expressed as

$$\left.\begin{aligned} & w = w_1 + w_2 \\ \text{where} \quad & \\ & w_1 = \frac{i\mathrm{K}}{2\pi}\log\left\{\sin\frac{\pi}{a}(z_0 - z)\Big/\sin\frac{\pi}{a}(z_0 + z)\right\} \\ \text{and} \quad & \\ & w_2 = \frac{2i\mathrm{K}}{\pi}e^{-\sigma}\cosh\frac{\pi h}{a}\sin\frac{2\pi z}{a} \end{aligned}\right\}. \tag{16}$$

On the wall A′B′ of the channel the stream function is now obtained as

$$\psi_1 = -\frac{Kh}{2a} - \frac{K}{\pi} e^{-\frac{1}{2}\sigma} \cosh\frac{\pi h}{a} \sin\frac{2\pi x}{a}, \quad \psi_2 = \frac{K}{\pi} e^{-\frac{1}{2}\sigma} \cosh\frac{\pi h}{a} \sin\frac{2\pi x}{a},$$

so that

$$\psi = -Kh/2a.$$

Thus ψ is constant along the wall A′B′ as required, and there is a backward flow from right to left in the channel of amount Kh/a in unit time across any section such as BB′.

Hitherto we have considered only the conditions in the ultimate wake far behind the body, but it is now necessary to consider the flow as a whole. This flow may be represented diagrammatically as in fig. 3, and it is evident at once

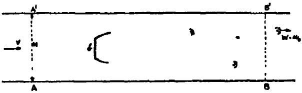

FIG. 3.

that the condition of continuity requires that the flow across AA′ shall be equal to the flow across BB′. At AA′ there is the undisturbed velocity V, and hence the flow VH. At BB′ in the distant wake there is a backward flow Kh/a due to the vortex street, and hence the general stream, on which this vortex system is superimposed, must have a velocity W greater than V. The vortices therefore pass down the channel with the velocity $(W - u_0)$, and the velocity W is determined by the equation

$$W = V + Kh/aH. \tag{17}$$

It is perhaps rather paradoxical that the constraint of the channel walls should cause no interference on the stream V far in front of the body, and no interference on the vortex street far behind it, and should yet be capable of producing the necessary increase of velocity to maintain the continuity of the flow.

The final stage of the calculation is to obtain a formula for the drag of the body. Following Karman's method, this drag force will be calculated in two parts, and will be based on a consideration of the flow relative to the vortices of the wake. The fluid is then streaming past the vortices with the velocity u_0, the body is advancing in the opposite direction with the velocity $(W - u_0)$ and the fluid in front of the body is coming to meet it with the velocity

$(u_0 - \mathrm{W} + \mathrm{V})$. The first part of the drag is obtained by evaluating the integral

$$\mathrm{X} - i\mathrm{Y} = \tfrac{1}{2}i\rho \int_c \left(\frac{dw}{dz}\right)^2 dz$$

round the contour ABB'A' of fig. 3. On AB and A'B', since dw/dz is real, the integral gives no contribution to X. On AA' we have

$$w = (u_0 - \mathrm{W} + \mathrm{V})\, z$$

and so this part of the integral gives

$$\mathrm{X} = \tfrac{1}{2}\rho\, (u_0 - \mathrm{W} + \mathrm{V})^2\, \mathrm{H},$$

or, by virtue of equation (17),

$$\mathrm{X} = \tfrac{1}{2}\rho u_0^2 \mathrm{H} - \rho u_0 \mathrm{K} h/a + \rho \mathrm{K}^2 h^2/2a^2 \mathrm{H}.$$

On BB', neglecting terms proportional to $e^{-1\sigma}$, we have as in an unlimited fluid

$$w = u_0 z + w_1,$$

where

$$w_1 = \frac{i\mathrm{K}}{2\pi} \log \left\{ \sin \frac{\pi}{a} (z_0 - z) \Big/ \sin \frac{\pi}{a} (z_0 + z) \right\},$$

and so

$$\left(\frac{dw}{dz}\right)^2 = u_0^2 + 2u_0 \frac{dw_1}{dz} + \left(\frac{dw_1}{dz}\right)^2.$$

But

$$\frac{\mathrm{K}^2}{2\pi a} \frac{d}{dz}\left(\frac{\sin 2\pi z/a}{i \sinh \pi h/a + \cos 2\pi z/a} \right) = -\left(\frac{dw_1}{dz}\right)^2 - 2u_0 \frac{dw_1}{dz},$$

and so

$$\left(\frac{dw}{dz}\right)^2 = u_0^2 - \frac{\mathrm{K}^2}{2\pi a} \frac{d}{dz}\left(\frac{\sin 2\pi z/a}{i \sinh \pi h/a + \cos 2\pi z/a} \right).$$

Hence for BB'

$$\mathrm{X} - i\mathrm{Y} = \tfrac{1}{2}i\rho \left[u_0^2 z - \frac{\mathrm{K}^2}{2\pi a} \frac{\sin 2\pi z/a}{i \sinh \pi h/a + \cos 2\pi z/a} \right]_{\mathrm{B}}^{\mathrm{B}'},$$

and for the second term the limits of integration may be regarded as infinite. Then

$$\mathrm{X} - i\mathrm{Y} = \tfrac{1}{2}i\rho \left\{ i u_0^2 \mathrm{H} - i\mathrm{K}^2/\pi a \right\}$$

or

$$\mathrm{X} = -\tfrac{1}{2}\rho u_0^2 \mathrm{H} + \rho \mathrm{K}^2/2\pi a,$$

and so the total for the first part of the drag is

$$\mathrm{D}_1 = \rho \mathrm{K}^2/2\pi a - \rho u_0 \mathrm{K} h/a + \rho \mathrm{K}^2 h^2/2a^2 \mathrm{H}. \qquad (18)$$

For the second part of the drag we have simply

$$\begin{aligned} \mathrm{D}^2 &= \rho\,(\mathrm{W} - u_0)\,\mathrm{K}h/a \\ &= \rho\,(\mathrm{V} - u_0)\,\mathrm{K}h/a + \rho\mathrm{K}^2h^2/a^2\mathrm{H}, \end{aligned} \tag{19}$$

and finally the total drag is

$$\mathrm{D} = \rho\,(\mathrm{V} - 2u_0)\,\mathrm{K}h/a + \rho\mathrm{K}^2/2\pi a + \tfrac{1}{2}\rho\mathrm{K}^2h^2/a^2\mathrm{H}. \tag{20}$$

which gives the drag coefficient

$$k_\mathrm{D} = \frac{\mathrm{D}}{b\rho\mathrm{V}^2} = \left(2{\cdot}828 - 1{\cdot}12\frac{u_0}{\mathrm{V}}\right)\frac{u_0h}{\mathrm{V}b} + 12\left(\frac{u_0h}{\mathrm{V}b}\right)^2\frac{b}{\mathrm{H}}. \tag{21}$$

This result is comparable with Karman's equation (11), and suffers from the same limitations that it is necessary to determine experimentally the values of u_0/V and h/b Moreover, there is no justification for assuming that these two ratios have the same values in a channel of finite breadth and in an unlimited fluid. The equation, therefore, cannot be used to determine the increase of drag of a body in a channel of finite breadth until some criteria have been established for determining the values of the two fundamental ratios. In the following section an attempt is made to develop the necessary extension of the analysis, but this further development is only of a tentative nature, and is based on rather uncertain hypotheses.

4 *The Generation of Vorticity*

To proceed further with the analysis, it is necessary to consider the conditions close to the body itself. From each side of the body there arises a sheet of discontinuity of velocity, but owing to their essential instability these sheets of discontinuity soon break up to form the separate vortices of the vortex street. Now let q_1 and q_2 be the velocities on opposite sides of the sheet of discontinuity, let p_1 and p_2 be the corresponding pressures, and let R be the rate of generation of vorticity at one side of the body. Then

$$\begin{aligned} \rho\mathrm{R} &= (p_1 + \tfrac{1}{2}\rho q_1^2) - (p_2 + \tfrac{1}{2}\rho q_2^2), \\ &= \tfrac{1}{2}\rho\,(q_1^2 - q_2^2) + (p_1 - p_2), \end{aligned}$$

and this result may also be expressed in the form

$$\rho\mathrm{R} = \tfrac{1}{2}\rho\,(\mathrm{V}^2 - q_2^2) + (p_0 - p_2).$$

where p_0 is the pressure of the undisturbed stream

The velocity q_2 in the dead-water region immediately behind the body may be assumed to be zero, and for a thin vortex sheet the pressure difference $(p_1 - p_2)$ may also be neglected. On this basis the rate of generation of vorticity becomes

$$R/V^2 = q_1^2/2V^2 = \tfrac{1}{2} + (p_0 - p_2)/\rho V^2. \tag{22}$$

Now the rate S at which vorticity passes down the wake in one row of the vortex street is less than the rate R at which the vorticity is generated at the side of the body, for some part of the positive and negative vorticity which is generated at the two sides of the body is annulled by partial mingling of the two streams of vorticity in the turbulent region behind the body. This view is expressed by Prandtl in an appendix to Heisenberg's paper,* and is confirmed by the experiments of Fage and Johansen.†

We shall write therefore

$$S = \lambda R, \tag{23}$$

where λ is less than unity and the value of S according to the previous analysis is

$$S = K(V - u_0)/a,$$

or

$$\frac{S}{V^2} = \frac{K}{aV}\left(1 - \frac{u_0}{V}\right). \tag{24}$$

The analysis for the flow in a channel of finite breadth will now be developed on the basis of the following assumptions: —

(1) The increase of the suction in the dead-water region behind the body, due to the constraint of the channel walls, is equal to the drop in pressure outside the vortex street far behind the body. This assumption is based on the conception that the vortex system behind the body is capable of maintaining a certain pressure difference between the fluid immediately behind the body and the fluid outside the vortex street far behind the body, and that this characteristic of the vortex system is not modified by the constraint of the channel walls.

(2) The values of K, $\sqrt{R}$, and $\sqrt{S}$, which are proportional to V in an unlimited fluid, will be assumed to be proportional to a certain effective velocity in the channel, and this effective velocity will be assumed to be the arithmetic mean of the velocities far in front of and far behind the body. This assumption implies that the factor λ has the same value in the channel and in an unlimited fluid.

---

* *Loc. cit.*

† *Loc. cit.*

Denoting values in the channel by accented letters, the first assumption leads to the equation

$$(\mathrm{R}' - \mathrm{R})/\mathrm{V}^2 = (p_2 - p_2')/\rho\mathrm{V}^2 = (\mathrm{W}^2 - \mathrm{V}^2)/2\mathrm{V}^2 = \mathrm{K}h/a\mathrm{VH},$$

while the second assumption gives

$$\mathrm{R}'/\mathrm{R} = \{(\mathrm{W} + \mathrm{V})/2\mathrm{V}\}^2 = 1 + \mathrm{K}h/a\mathrm{VH},$$

and hence it appears that

$$\mathrm{R} = \mathrm{V}^2. \tag{25}$$

Thus the assumptions as to the flow in a channel imply a definite value for the rate of generation of vorticity in an unlimited fluid, and hence the assumptions will be valid only for bodies which give rise to this rate of generation of vorticity. The validity of this conclusion will be examined more closely at a later stage of the analysis, but it may be stated here that this value of R appears to be correct for a body of bluff form. For a body of elongated shape the assumptions appear to break down, the weak point of the argument probably being the value assumed for the mean effective velocity. The subsequent analysis should be regarded therefore as applying to bodies of bluff form only.

The second assumption has led to the equation

$$(\mathrm{K}'/\mathrm{K})^2 = \mathrm{S}'/\mathrm{S} = \mathrm{R}'/\mathrm{R} = 1 + \mathrm{K}h/a\mathrm{VH},$$

and from the previous analysis we have

$$\frac{\mathrm{S}'}{\mathrm{S}} = \frac{a\mathrm{K}'\,(\mathrm{W} - u_0')}{a'\mathrm{K}\,(\mathrm{V} - u_0)} = \frac{u_0'\,(\mathrm{W} - u_0')}{u_0\,(\mathrm{V} - u_0)},$$

from which it follows that

$$\frac{u_0'}{u_0} = 1 - \frac{u_0}{\mathrm{V} - 2u_0}\,\frac{\mathrm{K}}{a\mathrm{V}}\,\frac{h}{\mathrm{H}}.$$

From these results we deduce the following equations for determining the characteristics of the vortex street in a channel of finite breadth.—

$$\left.\begin{aligned} \frac{u_0'}{u_0} &= 1 - \frac{2\sqrt{2}\,u_0/\mathrm{V}}{1 - 2u_0/\mathrm{V}}\left(\frac{u_0h}{\mathrm{V}b}\right)\frac{b}{\mathrm{H}} \\ \frac{\mathrm{K}'}{\mathrm{K}} &= 1 + \sqrt{2}\left(\frac{u_0h}{\mathrm{V}b}\right)\frac{b}{\mathrm{H}} \\ \frac{h'}{h} = \frac{a'}{a} &= 1 + \frac{\sqrt{2}}{1 - 2u_0/\mathrm{V}}\left(\frac{u_0h}{\mathrm{V}b}\right)\frac{b}{\mathrm{H}} \end{aligned}\right\}, \tag{26}$$

and it also appears that the value of the factor λ is

$$\lambda = 2\sqrt{2}\,\frac{u_0}{V}\left(1 - \frac{u_0}{V}\right). \tag{27}$$

Finally, the drag coefficient of the body, as given by equation (21), becomes

$$k_D' = (2 \cdot 828 - 1 \cdot 12\, u'_0/V)\,(u'_0 h'/Vb) + 12\,(u'_0 h'/Vb)^2\, b/H,$$

and by means of equation (26) we derive

$$k'_D - k_D = \left\{16 - 1 \cdot 58\,\frac{u_0}{V}\,\frac{1 - 4u_0/V}{1 - 2u_0/V}\right\}\left(\frac{u_0 h}{Vb}\right)^2 \frac{b}{H}. \tag{28}$$

The second term of this expression is quite negligible in practice, and we may therefore accept finally the value

$$k_D' = k_D + 16\left(\frac{u_0 h}{Vb}\right)^2 \frac{b}{H}. \tag{29}$$

5. *Comparison with Experimental Results*

In the case of a flat plate, Fage has obtained the following values of the drag coefficient as affected by the constraint of the channel walls :

H/b	-	42	21	14	$10\frac{1}{2}$
k_D	=	0·964	1·025	1·065	1·072

but the value of k_D at the lowest value of H/b appears to be so unreliable that it will be neglected in the subsequent discussion.

A detailed examination of the flow was made in the case $H = 14b$, and the following values were deduced .—

$$a'/b = 5 \cdot 25, \quad b\,(W - u_0')/a'V = 0 \cdot 146, \quad R'/V^2 = 1 \cdot 07.^*$$

To obtain corresponding calculated values we shall start with Heisenberg's values

$$u_0/V = 0 \cdot 2295, \quad u_0 h/Vb = 0 \cdot 3535, \quad h/b = 1 \cdot 54,$$

and then by means of equations (11) and (29) we calculate the following values for the drag coefficients :- ·

H/b	=	∞	42	21	14
k_D	=	0·909	0·957	1·004	1·052

Also by means of equations (26) we derive the following values in the special case $H = 14b$:—

$$u_0'/v = 0 \cdot 222, \quad h'/b = 1 \cdot 64, \quad W/V = 1 \cdot 071$$

and hence

$$a'/b = 5 \cdot 84, \quad b\,(W - u_0')/a'V = 0 \cdot 145, \quad R'/V^2 = 1 \cdot 071.$$

---

* Fage and Johansen, 'Phil. Mag.,' vol. 5, p. 417, table 5 (1928).

The agreement with the experimental values is quite good, except as regards the spacing of the vortices (a'/b), and in this case it may be noted that Karman and Rubach* found the value 5·50, which is higher than that given by Fage and Johansen.

In view of this numerical discussion it would appear that the assumptions of the previous section are valid for a flat plate. In the case of bodies of other shape, some results are given by Fage and Johansen,† but they are inadequate to serve as the basis of a detailed analysis. The following values for the rate of generation of vorticity have been extracted from Table V of their paper.—

Body.	H/b.	R'/V^2.
Flat plate	14	1·07
Circular cylinder...	25	1 01
Wedge	30	0·97
Ogival model	30	0·64
Long ogival model..	30	0·71

The values of R' for the flat plate and circular cylinder are consistent, approximately, with the conclusion that $R = V^2$, but it is evident at once that the assumptions of the previous section have broken down in the case of the longer models. The cause of this failure is almost certainly the assumption as to the mean effective velocity. For an ogival model of sufficient length, the velocity along the surface, apart from the effect of viscosity, must tend to the value $V(1 + b/H)$, and hence the rate of generation of vorticity will be approximately

$$R' = \tfrac{1}{2}V^2(1 + 2b/H).$$

For the ogival models this would imply $R' = 0 \cdot 53\ V^2$, and the values actually obtained in the experiments are intermediate between those which would be expected for a short model ($1 \cdot 02\ V^2$) and for a very long model ($0 \cdot 53\ V^2$). In the case of these long models, however, it is doubtful whether it would be possible to develop a satisfactory theory without taking account of the viscous boundary layer along the surface.

6. *Summary and Conclusions.*

By examining the conditions of flow in a channel of finite breadth a formula (21) has been developed for the drag due to the vortex street formed by a bluff body, but to apply this formula it is necessary, as in the case of Karman's formula itself, to determine experimentally the values of two fundamental ratios.

---

* 'Phys. Z.,' vol. 13, p. 49 (1912).

† 'Phil. Mag.,' vol. 5, p. 417 (1928).

An attempt to overcome this difficulty is made by means of certain assumptions as to the flow in a channel, which enable the constraint of the channel walls to be calculated from the flow in an unlimited fluid The final equations so obtained lead to conclusions in close agreement with the experimental results for a flat plate, but it appears that the assumptions are valid for bodies of bluff form only, and break down for bodies of elongated shape

---

Photoelectric Effect of Soft X-Rays

By G. B. BANDOPADHYAYA, M.Sc., State Scholar of the Government of India, King's College, London.

(Communicated by O W. Richardson, F R S.—Received May 7, 1928.)

For the investigation of soft X-rays, Richardson and Bazzoni* employed the method of ejection of photoelectrons from a metal plate under the action of the rays Subsequent investigations in this region were carried out by Richardson and Chalklin, Kurth, Mohler and Foote, Horton, Davies and Andrewes, Thomas, Compton and Thomas,† and also by others by the same method, with the view of determining voltages at which excitations of characteristic soft X-rays occur. More recently Richardson and Robertson‡ have employed this method for studying the relative soft X-ray emissivities of a large number of elements

Other methods have also been employed, among which the spectroscopic method of analysis may be mentioned.§ In this method, a pressure lower than 10^{-3} mm. can in the present state of things be hardly secured. It has been found* that the radiation from the residual gas at a pressure of 1 . 10^{-5} mm. is approximately equal to that of soft X-rays from a carbon target Further, the gas radiation increases linearly with pressure. So it can be easily understood what an important rôle the residual gas may be playing in the present spectroscopic methods.

---

* 'Phil. Mag.,' vol. 42, p. 1015 (1921)

† Richardson and Chalklin, 'Roy. Soc. Proc.,' A, vol. 110, p. 247 (1926); Kurth, 'Phys. Rev.,' vol. 18, p. 461 (1921); Mohler and Foote, 'Sci. Papers Bur. Standards,' No. 425 (1921), Horton, Andrewes and Davies, 'Phil. Mag.,' vol. 46, p. 721 (1923), and vol 110, p. 64 (1926); Thomas, 'Phys. Rev.,' vol. 25, p. 322 (1925); Compton and Thomas, 'Phys. Rev.,' vol. 28, p. 601 (1926).

‡ 'Roy. Soc. Proc.,' A, vol. 115, p. 280 (1927).

§ Millikan and Bowen, 'Phys. Rev.,' vol. 23, p. 1 (1924); Sieghbahn and Thoræus, 'Journ. Opt. Soc. America,' vol. 13, p. 235 (1926); Dauvillier, 'J. de Physique,' vol. 8, p. 1 (1927); T. H. Osgood, 'Phys. Rev.,' vol. 30, p. 567 (1927), etc.

At present, the photoelectric method of soft X-ray analysis seems to be most suitable. Though much work has been done in connection with determinations of characteristic excitation voltages, very little is known about the yield of photoelectrons, due to the same beam of soft X-rays, from different elements under similar conditions An investigation of this character may be of great importance to the soft X-ray worker and may throw some light on the mechanism of the liberation of photoelectrons by soft X-rays. Quite recently Miss Davies† has employed four different elements, iron, cobalt, nickel and copper, as photoelectric plates with the view of testing whether the nature of the photoelectric plate has any connection with the relative soft X-ray emissivity of different elements The present investigation is a continuation of Miss Davies' work with the improvement of a device for outgassing the photoelectric detectors. The quash apparatus was made by the Thermal Syndicate, Ltd , Wallsend-on-Tyne.

The tube is shown in two sections in figs. 1A and 1B, while fig 2 shows the more important parts and the circuit arrangements

All the joints and seals were made with tightly fitting brass-caps and a small quantity of hard sealing-wax. To get rid of occasional cracks in wax joints shellac varnish was employed, but this was avoided as far as possible.

A tungsten filament F (fig. 2) was glowed to a temperature of about 1800° C., and the electrons liberated were drawn to a copper plate by the application of positive potentials ranging from 200 volts to 500 volts. A part of the soft X-rays so generated passed between two copper plates c_1 and c_2, tapering from 4 mm. to 6 mm. in distance between them. A high potential difference of about 200 volts was maintained between them, which preliminary experiments showed to be more than sufficient to filter off ions and electrons from the beam. The filtered radiation fell on a photoelectric plate P, the electrons thus liberated were dragged to a hollow copper box B, on which a positive potential of about 50 volts was maintained. The positive charging up of the photoelectric plate P was recorded by a quadrant electrometer having a sensitivity of about 230 mm. per volt.

---

* Richardson and Chalklin, *loc. cit.*

† 'Roy. Soc. Proc.,' A, vol. 119, p. 543 (1928).

The photoelectric plate was mounted on a nickel framework with four vertical nickel pins 1 mm. in diameter. The elements employed were 2·5 cm. by 1·8 cm. and 1 mm. thick, with grooves 1 mm. wide along their lengths. Thus four different elements could be fitted into the framework P (fig. 1A). The framework had attached to it two small iron pieces p_1 and p_2, so that the plates could be rotated with an auxiliary electro-magnet and any one of the four plates might

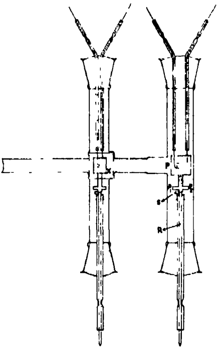

FIG. 1A.

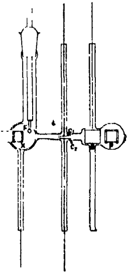

FIG. 1B.

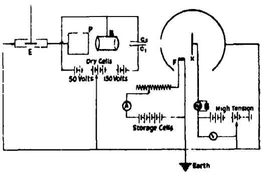

FIG. 2.

be brought in front of the beam of soft X-rays emanating from the copper plate. The whole body of the frame rested over a brass rod R as indicated by dotted lines in the diagram. There was a filament inside P which could be glowed to a very high temperature, and by applying a positive potential to P through the support R, the elements could be heated to a red heat and thus degassed. The X-ray copper plate was also mounted similarly and degassed in the same manner.

The apparatus was pumped by a mercury vapour pump (bottle type) backed by a first stage Volmer pump and a Hyvac pump. Further reduction in pressure was secured by putting liquid air over a charcoal tube. Auxiliary liquid air traps were also employed to trap mercury vapours.

Having obtained a preliminary pressure of about 10^{-6} mm, the tube was thoroughly heated and metal parts degassed in the manner mentioned before. The method of heating the elements by an internal electronic current was found very satisfactory because the external surfaces were not at all contaminated. The operation of degassing was continued a large number of times till the evolution of gas practically ceased.

All the readings of photoelectric currents recorded in this paper were taken at a pressure decidedly below 10^{-6} mm., probably at a pressure of the order of 10^{-7} mm. Twelve elements, carbon, aluminium, iron, cobalt, nickel, copper, molybdenum, silver, tantalum, tungsten, platinum and gold, were employed. These elements were commercially pure and all, with the exception of molybdenum and tungsten, which were obtained from the Tungsten Manufacturing Co. (London), were very kindly supplied to us by Johnson Mathey & Co.

The readings were taken in four settings of the apparatus, in each setting no alteration other than a change of the photoelectric plates was made Thus the geometry of the tube was kept constant throughout. Besides this, the copper plate used for the production of X-rays was sparingly used so as to avoid contamination as far as possible.

The electrical connections are indicated in fig. 2. The thermionic current was recorded with a micro-ammeter (Onwood Patent) shunted with a small resistance box. The micro-ammeter used was carefully calibrated with the help of suitable standard resistances and the calibrated values were used instead of the direct ones. Photoelectric currents were measured with an electrometer by the ordinary timing method. The voltages employed for the production of X-rays were supplied by small storage cells and were measured with a Weston voltmeter.

In Table I, values i_p/i_t* or photoelectric/thermionic currents observed with different elements by the action of X-rays from a copper plate at voltages ranging from 200 to 500 are inserted. These investigations were carried out in four settings labelled A, B, C and D. The dates are put down so as to show the reliability of the values on different days and also after a fresh setting. A small amount of correction must be applied to the voltages recorded by the voltmeter for (1) the work necessary to drag an electron out of the filament, and (2) the potential drop across the filament due to the heating current. To evaluate the magnitude of the correction to be applied due to source (1), one must know the temperature of the filament.† This was determined from the filament current, the potential difference between the two ends of the filament and the surface area of the filament. The temperature thus determined is approximately 2000° absolute. The value of the work function calculated from this as outlined by Richardson and Chalklin (*loc. cit.*) is equal to $+ 4 \cdot 9$ volts approximately.

The potential drop across the filament was approximately $+ 10$ volts throughout the whole investigation. The filament being a long one, about 12 cm., practically the whole of it was equally bright. Thus the average potential retarding the escape of electrons may roughly be taken to be 5 volts.

Hence the net correction factor is equal to $- 0 \cdot 1$ volt, which may be omitted as being within the source of error of reading the voltmeter.

As has been mentioned before, a very small fraction of the X-rays generated was incident on the photoelectric plates. If we assume (1) that soft X-rays are generated equally in all directions, and (2) that the number of electrons striking the anticathode per unit area is constant throughout the whole surface of the anticathode, then we can make an estimate of the fraction of the rays incident on the photoelectric plate. This has been worked out graphically and the fraction incident is $6 \cdot 50 . 10^{-4}$. Hence to get the values of the photoelectric currents that would have been recorded had the entire beam been utilised, the observed values have to be divided by $6 \cdot 5 . 10^{-4}$. It may be mentioned here that both the assumptions are improbable. In course of our earlier experiments with a design of tube similar to the one employed by Richardson and Chalklin, we found that the intensity of the beam normal to the anticathode

---

* It was found that for small thermionic currents of the order of 10^{-6} amp. such as were used in this investigation, i_p/i_t is a constant when the voltage is kept constant and i_t is varied. This was also found by Richardson and Chalklin and Richardson and Robertson (*loc. cit.*).

† Worthing and Forsythe, 'Phys. Rev.,' vol. 18, p. 144 (1921).

Table I (A).—Values of $\frac{\text{Photoelectric}}{\text{Thermionic}}$ Current for a Copper Anticathode.

(Photoelectric plates thoroughly degassed.)

Setting No.	Photoelectric Elements.	Dates	Values of $i_p/i_t \times 10^6$.			
			500 volts.	400 volts.	300 volts.	200 volts.
		1927.				
A.	Carbon ..	September 20	3·16	2·56	2·11	—
		September 21	3·07	2·45	2·09	—
		September 22	3·14	2·67	2·14	—
			(3·12)	(2·46)	(2·11)	
D.	Aluminium	December 15	30·5	22·8	—	10·0
		December 16	30·1	22·7	15·5	10·1
		December 17	29·3	22·0	14·9	9·35
			(30·0)	(22·5)	(15·2)	(9·82)
D.	Iron .	December 15	8·21	6·21	4·41	2·65
		December 16	8·38	6·23	4·25	2·82
			(8·30)	(6·22)	(4·33)	(2·73)
B.	Cobalt	October 21	3·32	2·71	2·05	—
		October 26	3·55	2·91	2·02	—
		October 27	3·47	—	2·15	—
			(3·45)	(2·81)	(2·07)	
A.	Nickel	September 20	8·35	6·44	4·65	3·04
		September 21	7·79	5·96	4·23	2·68
		September 22	7·69	5·83	4·31	(2·64)
			(7·94)	(6·08)	(4·40)	(2·79)
B.	Copper	October 21	5·74	4·24	3·30	2·06
		October 26	5·91	4·43	3·20	2·09
		October 27 ...	5·96	4·38	3·09	2·00
			(5·87)	(4·35)	(3·20)	(2·05)
C.	Copper	November 11	5·71	4·46	3·13	1·95
		November 12	5·98	4·28	3·11	1·98
		November 19	5·55	4·12	2·97	1·89
			(5·75)	(4·29)	(3·07)	(1·94)
D.	Silver	December 16	9·83	7·33	5·14	3·31
		December 17 .. .	9·50	7·10	4·80	3·01
			(9·67)	(7·22)	(4·97)	(3·16)
C.	Tantalum	November 11	5·01	3·69	2·65	1·72
		November 12 .. .	5·86	4·24	2·94	1·84
		November 19	5·32	3·86	2·69	1·72
			(5·37)	(3·93)	(2·76)	(1·76)

Table I (A)—(continued).

Setting No.	Photoelectric elements.	Dates.	Values of $i_p/i_t \times 10^3$.			
			500 volts.	400 volts.	300 volts.	200 volts.
		1927.				
C.	Molybdenum	November 11	4·22	3·15	2·15	1·40
		November 12	4·30	3·20	2·26	1·41
		November 19	4·03	3·32	1·99	1·33
			(4·18)	(3·22)	(2·13)	(1·38)
B.	Tungsten	October 21	4·64	3·53	2·72	1·77
		October 26	4·67	3·41	2·52	1·75
		October 27	4·76	3·52	2·43	—
			(4·69)	(3·49)	(2·56)	(1·76)
A.	Platinum	September 20	5·47	4·18	3·12*	1·95
		September 21	5·41	4·14	3·04	1·94
		September 22	5·35	4·13	2·92	1·91
			(5·41)	(4·15)	(3·03)	(1·93)
B.	Platinum	October 21	5·13	3·88	2·90	1·94
		October 26	5·30	4·00	2·99	1·98
		October 27	5·32	3·86	—	—
			(5·25)	(3·91)	(2·95)	(1·96)
A.	Gold	September 21	5·83	4·50	3·19	2·03
		September 22	5·84	4·45	3·13	2·09
			(5·84)	(4·48)	(3·16)	(2·06)
D.	Gold	September 15	5·93	4·36	3·07	—
		September 16	5·83	4·50	3·02	—
		September 17	5·73	4·22	—	—
			(5·89)	(4·13)	(3·05)	

was approximately twice of that of grazing angle. As in that tube there was no device for recording angles, no systematic readings were taken. In the present investigation a normal beam was employed, and computations of total intensities deduced from this will lead to slightly larger values. Our main object has been to test relative values.

Values of i_p/i_t inserted in Table I (A) are for thoroughly degassed photoelectric plates and those in Table I (B) for entirely undegassed elements. It will be seen that the latter values are higher, in general, except for aluminium. Also it will be seen that degassing affects relative values. As very little impor-

Table I (B).—Values of $\frac{\text{Photoelectric}}{\text{Thermionic}}$ Current for a Copper Anticathode.

(Photoelectric plates not degassed.)

No. of Setting.	Elements.	Dates.	Values of $i_p/i_t \times 10^9$			
			500 volts.	400 volts.	300 volts.	200 volts.
		1927.				
D	Aluminium	November 22	16·29	12·70	9·50	5·80
		November 23	16·72	12·87	9·33	5·92
			(16·51)	(12·79)	(9·42)	(5·86)
D.	Iron	November 22	13·01	9·87	7·38	4·41
		November 23	13·61	10·35	7·47	4·56
			(13·31)	(10·09)	(7·43)	(4·49)
A.	Nickel.	September 9	16·14	12·75	9·29	—
A.	Carbon	September 9	7·09	5·59	4·12	—
D.	Silver	November 22	11·31	8·40	6·21	3·81
		November 23	10·90	8·29	6·24	3·74
			(11·11)	(8·35)	(6·23)	(3·78)
A.	Gold	September 9	13·40	10·40	7·71	—
	Gold	November 22	14·70	11·47	8·33	5·07
		November 23	15·15	11·34	8·24	5·10
			(14·93)	(11·41)	(8·29)	(5·09)
A.	Platinum	September 9	14·49	11·26	8·60	—

tance can be attached to values of photoelectric currents from a gas-laden surface, I have determined this for 7 only out of the 12 elements that have been employed. In the last setting D, a plate of aluminium was present and this did not permit a strong heating operation. The procedure of degassing employed in this case was to bombard the plates with a smaller electronic current for a much longer period lasting over several hours for two or three days.

To show the experimental results more clearly, the values of i_p/i_t for different elements (the photoelectric efficiency) are plotted against atomic numbers of the various photoelectric plates, for X-rays from a copper anticathode at

500 volts and 400 volts in figs 3 and 4 respectively. The emission from aluminium, being very high, is omitted in the graphs. A glance at the figure

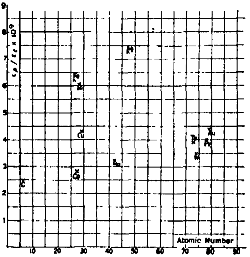

Fig. 3.

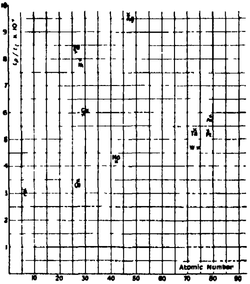

Fig. 4.

will show that there is no simple relationship between photoelectric efficiency and atomic number. It will be seen that the relative sensitivities are not far from what is observed under ultra-violet light. Thus aluminium, which is by far the most sensitive of all the twelve elements, is also so under ultra-violet light. Platinum and gold differ very little in sensitiveness while silver is decidedly more sensitive. Similar results have also been found by Suhrmann* under ultra-violet light. Again, carbon is only slightly sensitive to ordinary ultra-violet light† and to soft X-rays. Thus the results obtained in the present investigation do suggest there is a great deal of similarity in sensitiveness under soft X-rays and under ultra-violet light.

Richardson and Chalklin‡ have from their experiments inferred that the energy in a beam of soft X-rays is proportional to the square of the voltage. Miss E. Laird§ has confirmed this point from the duration of thermoluminescence caused by soft X-rays. This is analogous to ordinary X-rays and suggests strongly that the energy in a beam of soft X-rays is also approximately linearly distributed between the different frequencies according to

$$I_\nu \, d\nu = K(\nu_0 - \nu)\, d\nu, \tag{1}$$

where K is a constant, I_ν the intensity for frequency ν, and ν_0 the high frequency limit imposed by the voltage V on the tube and governed by Einstein's Law

$$V_e = h\nu_0. \tag{2}$$

We do not at present know the value of the constant K for soft X-rays, but we can take it as a definite constant for a particular anticathode. The simple formula (1) holds for ordinary X-rays, but systematic departures from it occur in the lower frequencies|| due to large absorption in the target itself. In the case of soft X-rays the factor of absorption in the target is expected to play a very great part even with a low atomic radiator like carbon, so much so that the energy emitted towards the low frequency side may be negligible. However, we will, as a first approximation neglect this effect for the sake of simplicity.

Let us consider the problem of ejection of photoelectrons. When a radiation of certain frequency ν is incident on a plate, it can knock out an electron from any orbit, having energy less than $h\nu$. Consequently, if we go on increasing ν by increasing the tube voltage we expect to get a number of discontinuities in the photoelectric current corresponding to the energies of the electrons in the photoelectric element itself. A large number of experimenters have tried

---

* 'Z. f. Physik,' vol. 33, p. 63 (1925).

† Roy, 'Roy. Soc. Proc.,' vol. 112, p. 599 (1926).

‡ *Loc. cit.*

§ 'Phys. Rev.,' vol. 29, p. 41 (1927).

|| Compare, for instance, Kulenkampff, 'Ann. d. Physik,' vol. 69, p. 548 (1922).

to investigate the characteristic excitation voltages of different anticathodes by the photoelectric method. It is likely that some of the breaks obtained by them may be due, not to the anticathode, but to the photoelectric plate. We may, however, find the breaks due to the latter factor in a simple way. Suppose, for instance, we determine the breaks due to two different anticathodes with the same photoelectric plate. There will be a number of common breaks due to the energies of the different electronic orbits of the photoelectric plate.

Kurth* has investigated soft X-rays from 12 to 1,000 volts for carbon, oxygen, aluminium, silicon, titanium, iron and copper, using a platinum photoelectric plate. There is no break common which may be attributed to platinum. Horton, Davies and Andrewes* have analysed five elements, aluminium, iron, nickel, copper and zinc, using a platinum plate. They have not got any break common. In a subsequent attempt, they increased their accuracy, and tested a few more elements, but no common break is present. Richardson and Chalklin have studied four different elements, carbon, iron, nickel and tungsten, at voltages ranging from 30 to 500 using a copper plate. None of the breaks are common to the four elements within the source of experimental error. Richardson and Chalklin have recently increased their accuracy very much, but their results, which are to be published soon, do not support our expectations.

Thomas, and Compton and Thomas* have investigated iron, cobalt, nickel, copper, carbon and tungsten between 1,000 volts to 10 volts. The breaks obtained by them are extremely numerous, but if we confine our attention to the critical potentials of iron, cobalt and nickel, then we find a regular sequence in all the breaks for the three elements in order of increasing atomic number. There is no common break such as we are looking for, although the degree of accuracy is of the order of one-thirtieth per cent.

From all these results, it seems likely that the characteristics of the photoelectric plate are not at all marked for tube voltages ranging from 1,000 to 10 volts. It is therefore probable that by far the greater number of photoelectrons come from the outermost valency orbit or from one or two orbits close to it.

The sensitiveness of different elements for the same beam of soft X-rays is to a great extent similar to ultra-violet light. Further, the photoelectric current per unit thermionic current is approximately proportional to voltage for voltages ranging from 50 to 500.* This suggests strongly some simple law governing the ejection of photoelectrons under soft X-rays. We will provisionally assume this law similar to the law of ejection of photoelectrons under ultra-violet light.

---

* *Loc. cit.*

Prof. O. W. Richardson† has shown that the number of photoelectrons ejected by ultra-violet light per unit intensity can be expressed as

$$N = C\,(\nu - \nu_t)/\nu^3, \tag{3}$$

where N is the number of photoelectrons liberated, ν the frequency of the incident light, ν_t the threshold frequency, and C a constant. Becker‡ has proposed an alternative formula, but it suffers from a serious drawback in as much as it does not explain the maximum effect at a frequency equal to $\frac{3}{2}\,\nu_t$. Dr. S. C. Roy (*loc cit.*) has investigated this point more closely and his results confirm equation (3). Combining equations (1) and (3) we get for the total number of photoelectrons generated

$$N = CK \int_{\nu_t}^{\nu_0} (\nu_0 - \nu)\,(\nu - \nu_t)\nu^{-3}\,d\nu.$$

Assuming $\nu_0 \equiv 300$ volts, $\nu_t \equiv 5$ volts; $\nu_0 \gg \nu_t$, and consequently the integral (4) reduces to

$$N = \tfrac{1}{2}\,CK\ \nu_0/\nu_t \text{ approximately.}$$

Since

$$h\nu_0 = Ve,$$

we have

$$N = \tfrac{1}{2}\,CK\,.\,Ve/h\nu_t.$$

Thus the number of photoelectrons liberated should be proportional to the voltage, a fact which is found to be approximately true.

When ordinary X-rays are thrown on a plate, the electrons come from a great depth and consequently there is a good deal of probability of compound photoelectric effect as has been found by Dr. Simons.§ In the case of soft X-rays, I found in the course of my investigations on absorption in gold and in aluminium that the intensity of soft X-rays at 350 volts falls to 0·6 per cent. by transmission through $1{\cdot}36\,.\,10^{-5}$ cm. of gold and to 0·1 per cent. by transmission through $7{\cdot}9\,.\,10^{-5}$ cm. of aluminium. So by far the greater number of electrons come from the first few layers, and consequently the probability of an electron already ejected undergoing a fresh *inelastic encounter* and thereby ejecting another photoelectron must be very small in comparison with primary electrons. Recently Mr. E. Rudberg* has studied the velocity distribution of photoelectrons ejected under soft X-rays, and has found that about 70 per cent. of the electrons liberated have energies less than 10 volts when the tube voltage is 700. This may imply either that softer radiations in the beam of soft X-rays are more effective in producing photoelectrons, or that the liberated electrons get their velocities diminished as a consequence of *elastic encounters* with atoms in course of their passage, or both. The data available at present are insufficient to ascertain the photoelectric effect of these radiations without ambiguity.

---

* Richardson and Chalklin, *loc. cit.*

† 'Phys. Rev.,' vol. 34, p. 119 (1912); 'Phil. Mag.,' vol. 23, p. 615 (1912), vol. 24, p. 570 (1912), etc.

‡ 'Ann. d. Physik,' vol. 78, p. 83 (1925).

§ 'Proc. Phys. Soc.,' vol. 37, p. 58 (1925).

In conclusion, I wish to express my deep sense of gratitude to Prof. O. W. Richardson for instructing me so kindly throughout the course of work. I wish also to thank my friends Dr. S. C. Roy and Mr. S. N. Ghosh for helping me in drawing the design of the tube, and the Government of Bihar and Orissa for the award of a scholarship.

---

* 'Nature,' vol. 119, p. 704 (1927).

The Electrolytic Behaviour of Thin Films. Part I.—*Hydrogen.*

By F. P. Bowden and E. K. Rideal.

(Communicated by T. M. Lowry, F.R.S.—Received May 9, 1928.)

Introduction.

Few investigations have been made on the electrolytic behaviour of very thin metallic films. Whilst the work of Oberbeck* and of Pring† reveals the fact that a deposited layer of metal but a few atoms thick will produce an electrode possessing all the electromotive properties of the massive metal, yet information is lacking on the alteration of the electromotive force as these layers are built up. It might be anticipated that the behaviour of the electrode during the deposition of the first few layers would lead to interesting results, giving some insight into the mechanism of electrode processes and the range of action of forces of adhesion. In view of this it was considered a matter of some interest to investigate how far it might be possible to obtain data on the electrode potential and the rate of solution of the deposited atoms during the building up of the first atomic layer.

The problem of metal ion deposition from aqueous solutions is complicated by the presence of other ions, such as the hydrogen ion, which can deposit simultaneously with the metal and affect the potential. For this reason the deposition of the hydrogen ion was first studied. It is well known that, in general, in order to bring about the continuous deposition of hydrogen ions at a metallic cathode, the potential must be maintained at a value considerably more negative than that of a reversible hydrogen electrode in the same electrolyte. The view most generally accepted is that this overpotential is due to an accumulation of electromotively active material on the electrode, and it has been suggested by various workers that it may consist of metallic hydrides, hydrogen atoms or negative hydrogen ions.‡ With the exception of a paper by Knobel,§ little work has been done in determining the actual quantity of hydrogen accumulated on the cathode during the establishment of overpotential. Knobel, making the assumptions that the material was atomic hydrogen, that the relation between the solution pressure of the hydrogen P and the surface concentration of atoms C_H is given by the relation $P = kC_H^n$, and that the potential is related to the pressure by the Nernst expression, calculated this quantity from the rate of growth of overpotential and found that for most metals it was considerably less than an atomic layer.

---

* ' Wied. Ann.,' vol. 31, p. 337 (1887).

† ' Z. Elektrochem.,' vol. 19, p. 255 (1913).

‡ ' Heyrovsky, ' Trans. Faraday Soc.,' vol. 19, p. 785 (1924).

§ ' J. Amer. Chem. Soc.,' vol. 46, p. 2613 (1924).

It is generally assumed that the relation between the potential and the concentration of active hydrogen is given by the Nernst expression

$$-\mathrm{E} = \frac{\mathrm{RT}}{\mathrm{F}} \log \frac{f\mathrm{C}_{\mathrm{H}}}{f\mathrm{C}_{\mathrm{H}^+}},$$

where C_{H} is the concentration of active hydrogen on the cathode surface and $f\mathrm{C}_{\mathrm{H}^+}$ is the activity of hydrogen ions in the solution. This assumption is open to criticism, for there appears little doubt that the electromotive behaviour of a substance in the form of a thin film at an interface differs in many respects from its behaviour in the bulk phase. The work of Guyot[*] and of Frumkin[†] on the change of potential at an air-liquid interface on the addition of a unimolecular film to the surface has shown that, over a considerable range, the alteration in potential is to a first approximation directly proportional to the surface concentration of the film forming material. Again, Langmuir[‡] has shown that for the emission of electrons from a tungsten surface coated with a single layer of cæsium atoms, the logarithm of the saturation current is directly proportional to the surface concentration of cæsium atoms. In this investigation it is found that the relation between the electrode potential and the surface concentration of active material is a linear one, viz.,

$$-\mathrm{E} = \beta\Gamma + \text{const.},$$

where E is the electrode potential and Γ is the true surface concentration of active hydrogen on the cathode surface. Moreover, the constant β is the same for all metals; thus the overpotential depends only on the surface concentration of the added hydrogen and is independent of the nature of the underlying metal. This quantity is very small indeed, the deposition of sufficient hydrogen to form only 1/3000th of an atomic layer raising the potential of the cathode 100 millivolts. Also it is shown that the rate of decay, $-d\Gamma/dt$, of the active material is not proportional to Γ^2 as usually assumed, nor to Γ as supposed by Heyrovsky,[§] but is an exponential function of the potential, viz.,

$$-\frac{d\Gamma}{dt} = k_1 e^{-k_1\mathrm{E}},$$

---

[*] 'Ann. d. Physique,' vol. 11, p. 506 (1924).

[†] 'Z. Phys. Chem.,' vol. 109, p. 34 (1924).

[‡] 'Science,' vol. 57, p. 57 (1923).

[§] 'Trans. Faraday Soc.,' vol. 18, p. 785 (1924); 'Rec. Trav. Chim.,' vol. 46, p. 582 (1927).

and thus also of the surface concentration

$$-\frac{d\Gamma}{dt} = k_1 e^{-k_2\Gamma}.$$

This relation holds for all the metals investigated It is shown that the behaviour of the electrode potential and the magnitude of the quantities involved is compatible with the assumption that the potential of the electrode is due to the presence of electric doublets on its surface, the electric moment of these doublets being equal to that given by a proton and a negative hydrogen ion separated from each other by a distance equal to the diameter of a hydrogen atom.

Apparatus.

The experimental method involved the measurement of the rapidly changing electrode potential during the initial deposition of active material on a cathode and during its subsequent decay. The usual commutator method was rejected as unsuitable since it measures the average of a large number of cycles and not the initial growth and decay; a cathode-ray oscillograph was unsatisfactory for the same reason. An oscillograph of the Duddell type could not be employed since no appreciable current must be drawn from the test electrode. The instrument finally adopted and which gave satisfactory results was an Einthoven string galvanometer supplied by the Cambridge Instrument Co. The sensitivity could be varied by altering the tension on the fibre, and as generally used was greater than 100 mm. per micro-ampere. The period could be decreased to 1/300th of a second. Electrode potentials were usually measured to the nearest millivolt. The general arrangement of the apparatus is shown in fig. 1.

Light from a 500-c.p. pointolite lamp A was focussed by a large condensing lens B on to the galvanometer, where it was further condensed by C on to the fibre D. The shadow of the fibre was magnified by the microscope E and fell on the camera H; with the camera at a distance of 1 metre the magnification effected was 600. The cylindrical lens F increased the intensity of illumination by condensing the light into a narrow band without affecting the horizontal magnification of the fibre. Another cylindrical lens I on the camera focussed this on to the sensitive paper. This lens had gradation marks scratched on it so that lines 1 mm. apart were reproduced on the photographic paper. The camera, as constructed, consisted of a light tight box and within this another compartment containing a 50-yard roll, J, of rapid bromide paper 6 cm. wide. The paper was fed through a spring slit K which maintained a constant tension on it, over the roller L on to the driving roller M. This roller was directly coupled to a clockwork (not shown) the speed of which could be varied by screwing fans of different size on to the fly wheel so that paper speeds varying from 0·5 to 60 cm per second could be obtained. The timing was given by an electrically driven tuning fork N of period 1/64 second vibrating in front of the lens I and throwing a shadow on the paper. At low paper speeds a rotating disc driven by a Wilberforce synchronous motor was employed instead. The galvanometer and the camera were mounted on concrete columns to diminish mechanical vibration. The circuit for exciting the magnetic field of the galvanometer is not shown, but the current was supplied from a constant e.m.f. of 220 volts.

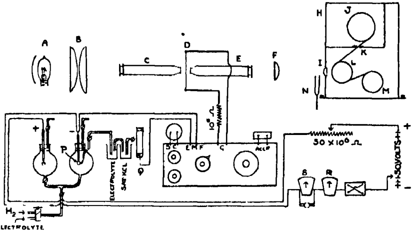

FIG. 1.

The potential of the test electrode P was measured against a saturated calomel electrode Q, a resistance of $10^6\ \Omega$ being included in the circuit so that the current drawn from the electrode was always very small. The galvanometer was calibrated by a potentiometer. The polarising current for the cell was supplied by a 50-volt battery of small accumulators with a variable resistance of several million ohms in the circuit. The larger currents were measured by a milli-ammeter R and the smaller by a uni-pivot micro-ammeter S (1 div. = 5×10^{-8} amps.). The apparatus was insulated by blocks of paraffin wax which rested on an equi-potential metal shield.

Preliminary Experiments.

It is necessary to consider the factors which determine the potential of a metal plate in a solution containing none or very few of its ions. For example, if a silver plate be immersed in N/5 . H_2SO_4, the potential being defined by the expression

$$-E = \frac{RT}{F}\log\frac{P_{Ag}}{fC_{Ag^+}}$$

should be infinitely negative at the moment of immersion, since $fC_{Ag^+} = 0$. There will, however, be rapid attainment of equilibrium between the electrode and all the ions in the solution, so that hydrogen ions will be deposited and the potential should remain constant at a value which is governed by the solution pressure of hydrogen on the electrode and the activity of the hydrogen ions in solution. Smits* has shown that if a silver or a copper electrode be immersed in pure water in the absence of oxygen or hydrogen, the potential attains the same value as would a hydrogen electrode in the same solution, indicating that the hydrogen pressure on the plate comes into equilibrium with the external pressure, viz., one atmosphere. In N/5 sulphuric acid, the hydrogen electrode potential on the saturated calomel scale is ca. $-0 \cdot 3$ V.; if at this potential the silver is in equilibrium with its ions in the solution, the concentration of the latter required by the above relation is 10^{-15} N. If for any reason the number of silver ions present in solution is greater than this, the potential will be more positive and will be determined by the value of this silver-ion concentration.

Experimentally it was found that for a silver plate immersed in N/5 . H_2SO_4 which had not been freed from oxygen, the potential was $+ 0 \cdot 25$ V. on the saturated calomel scale† and gradually became more positive on standing. If this potential were due to equilibrium between the silver plate and silver ions in the electrolyte, the necessary concentration of the latter would be 10^{-5} N. It was considered probable that silver ions were present in the electrolyte in the vicinity of the cathode in sufficient quantity to cause this potential, their solution being brought about by the oxygen dissolved in the electrolyte. To test this point N/5 . H_2SO_4 was freed from oxygen by prolonged boiling of the solution under reduced pressure, and cooling in a hydrogen atmosphere. The silver electrode (area 4 cm.^{2}) was cleaned in dilute nitric acid, washed, made cathodic in dilute sulphuric acid to reduce any oxide, removed, rapidly washed in distilled water, placed in a hydrogen atmosphere and oxygen-free electrolyte then admitted. The potential was now constant at a considerably more negative value, viz., + 0·03. This would correspond to a silver-ion concentration of less than 10^{-9} N at the electrode. It is probable that silver ions could still be present in this amount due to a trace of oxide on the electrode or to residual dissolved oxygen. If this were so, passage of a small current should deposit this silver and cause the potential to rise, *i.e.*, become more negative. A current density of 25 × 10^{-5} amps. cm ^{2} was passed and the potential rose in 0·35 second to − 0·76 V. This corresponds approximately to 9 × 10^{-5} coulombs per cm ^{2}, or enough to deposit ca. 9 × 10^{-10} gm. ions of silver. On opening the circuit the potential did not fall rapidly to that of the hydrogen electrode, as might be expected at first sight, but fell very slowly, taking 25 minutes to fall from − 0·76 to 0.

---

* 'Rec. Trav. Chim.,' vol. 44, p. 638 (1925).

† Unless otherwise stated, all potentials are given on the saturated calomel scale (hydrogen electrode $= -0 \cdot 25$ V. on sat. cal.), and the cell is at room temperature ca. 15° C. Negative potentials are spoken of as "high," positive as "low."

This behaviour is very different from that observed in solutions from which oxygen has not been rigorously excluded. In fig. 2, curve I shows the growth

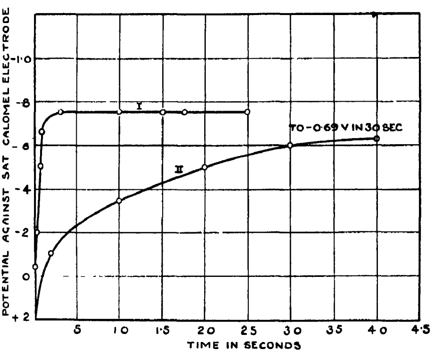

Fig. 2.

of potential at the silver cathode in oxygen free N/5 sulphuric acid on passing a current density of 25 × 10^{-5} amps. cm.^{2}. Curve II shows the growth when the electrolyte has not been freed from oxygen, all other experimental conditions being identical. In fig. 3 is shown the decay of potential on open circuit, curve I for oxygen-free electrolyte, curve II for ordinary electrolyte.

The marked effect which even a small amount of oxygen has on the apparent rate of growth and decay of hydrogen overpotential should be emphasised, since a very considerable number of experiments have been carried out in solutions which are open to the air or which contain dissolved oxygen. The fall of potential is in this case determined by the rate of supply of oxygen to the cathode and is not a measure of the natural decay of hydrogen overpotential. In ordinary solutions, photographs similar to those of Newbery* have been obtained showing a very rapid fall in the back electromotive force, the initial drop being too rapid to be recorded on the film. If, however, the solution be freed from oxygen, the decay rate is very much slower and can be followed from the moment of opening the circuit.† The bearing of this on the work of Oberbeck‡ should also be considered. For example, Oberbeck in one of his experiments placed a piece of silver in copper sulphate solution, made it cathodic, and determined the number of coulombs which passed before the

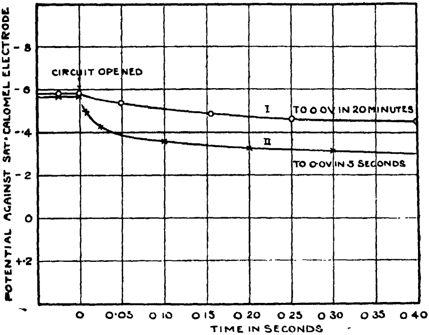

FIG. 3.

---

[*] 'Roy. Soc. Proc.,' A, vol. 111, p. 182 (1926).

[†] An air solution saturated with hydrogen behaves in an identical manner to an ordinary air solution, showing that the observed effects are due to the absence of dissolved oxygen and not to the presence of hydrogen.

[‡] 'Ann. der Physik,' vol. 31, p. 337 (1887).

silver cathode rose to the potential of copper. This was taken as a measure of the number of copper atoms deposited. It is apparent that this conclusion is unjustified: the initial potential of the silver plate in the copper sulphate solutions is that corresponding to equilibrium between the silver plate and the silver ions present in the solution, and before the potential can rise to that characteristic of copper these silver ions have to be deposited. If precautions were taken to prevent the occurrence of these silver ions in solution, the characteristic potential of the silver would initially be more negative than that of copper, and copper ions would deposit on the plate, causing the potential to fall without passage of any external current.

Measurement of Quantity of Material deposited on Cathode Surface during Establishment of Hydrogen Overpotential.

Two experimental methods were employed.

Method (a).—If the test electrode be made cathodic and a constant current I amps./cm.^{2} passed for a time T, the amount of material m gm. ions which accumulates on the cathode surface during the time T is given by

$$\frac{m}{F} = IT - \int_0^T i\,dt - \int_0^T \frac{E}{R}\,dt,$$

where i denotes the current which is equivalent to the loss of material at each instant due to natural decay. This rate of loss is a function of the potential. E is the electrode potential and R the resistance of the galvanometer circuit. Experimentally i can readily be determined for each value of E by measurement of the current density necessary to maintain the potential at that value. The last term represents the current drawn off through the galvanometer circuit and is in general negligible. It is not included in the second term, since during the determination of i there is no deflection of the galvanometer.

By plotting the observed rate of growth of potential and correcting for the natural loss during time of growth, the amount of material actually on the cathode can be determined.

A modification of this may be used. Since i falls off very rapidly with E (see later), by making I large, the last two terms become negligible if the potential change is measured for low values of E, so that over this range the current passed is a direct measure of the amount of material on the cathode.

Method (b).—In general, if the test cathode be polarised and the circuit then opened, the potential, in the absence of traces of oxygen, falls quite slowly. If now a current be passed in the reverse direction, the deposited material is removed from the cathode surface by electrolysis and the potential falls rapidly, the current passed being a direct measure of the amount of material removed.

These two methods, (*a*) that of depositing material on the cathode and measuring the growth of potential and (*b*) of forcing the material off the cathode and measuring the fall of potential, have been carried out on a number of metals. It was found that both methods gave the same result if the solution was free from dissolved oxygen. If, however, any oxygen were present, there was a large discrepancy between the two measurements, method (*a*) giving a value for the amount of material on the cathode which may be several hundred times greater than that given by method (*b*).

During the fall of potential on open circuit, arrests are frequently observed in the decay curve. These have been attributed to the formation of metallic hydrides,* but the work of one of us† has shown that they are in reality due to very small quantities of negative metal impurities which deposit on the cathode during electrolysis. Even in carefully purified solutions, if the cathode be subjected to prolonged electrolysis, this deposition can occur and affect the potential. Arrests in the decay curve due to this cause were occasionally observed in this work. The behaviour of the cathode under these conditions was erratic and methods (*a*) and (*b*) gave different values. In general, the excellent reproducibility of the results under widely varying experimental conditions and the agreement between methods (*a*) and (*b*) indicate that both oxygen and negative metal impurities are absent and that the growth of the potential of the electrode and its back electromotive force on open circuit is actually caused by the deposition of hydrogen.

Experimental.

The cell (see fig. 1) consisted of two glass bulbs each of 200 c.c. capacity connected at the base by a U-tube which could be closed by a tap. In the top orifice of each bulb was fitted a stopper, one carrying a platinum anode and inlet for hydrogen and the other the test cathode, a glass tube leading from the immediate vicinity of the cathode to the calomel electrode, and an outlet for hydrogen.

The cell could be evacuated and filled with hydrogen and the oxygen-free electrolyte blown in under hydrogen pressure through another inlet in the base of the cell, without coming into contact with air. Hydrogen from a cylinder was purified by passing through caustic potash and a long train of heated palladinised copper to remove oxygen. The water was purified by redistillation in a silica still and the sulphuric acid by redistillation in pyrex glass. The glassware was cleaned with chromic acid and distilled water before use.

---

* Newbery, 'Roy. Soc. Proc.,' A, vol. 111, p. 182 (1926).

† Bowden, 'Trans. Faraday Soc.,' vol. 23, p. 571 (1927).

Mercury.

The mercury electrode was contained in a glass cup and the procedure was either to run the purified mercury (withdrawn from the interior of a mass of mercury so as to be free from oxide) into the cell in an atmosphere of hydrogen and then admit the electrolyte, or to allow the liquid metal to flow in under the electrolyte.

In either case the initial potential of the electrode depended on the freedom or otherwise from traces of oxygen. It was generally about 0·0 volt but has been obtained as negative as − 0·15. Under similar conditions in ordinary solutions not freed from oxygen it is + 0·3 volt. The passage of a very small current is sufficient to deposit this mercury and establish a high hydrogen overpotential, *e.g.*, with a current density of 5×10^{-7} amps. cm.^{2} the potential is maintained at − 0·8 volt and on open circuit it falls only very slowly from this value.

Method (*a*).—In fig. 4 is shown the observed rise of potential on now passing

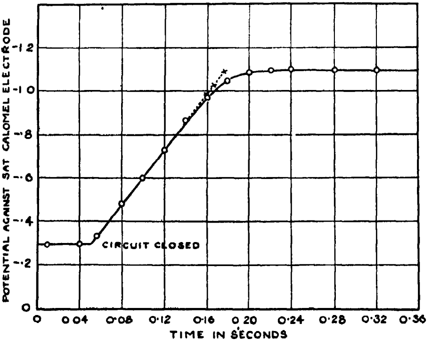

FIG. 4.

a current density of 4×10^{-5} amps. cm.^{2} The dotted line shows this corrected for loss during the period of growth. The current density/potential curves used for this correction will be considered later.

Method (*b*).—Fig. 5 shows the behaviour of the potential on opening the polarising circuit and passing the current in the reverse direction, making the

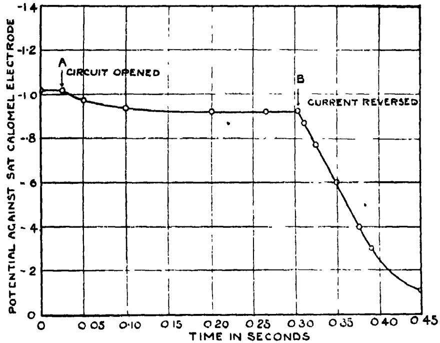

FIG. 5.

test electrode anodic: the current in this case is $4 \cdot 5 \times 10^{-5}$ amps. cm.^{2}. At the point A the circuit is opened and the slow fall in potential is due to the natural decay of the material from the surface, at B the circuit is closed in the reverse direction so that the material is removed electrolytically from the surface.

Both methods show clearly that if $\Delta\Gamma$ be the amount of material added to the surface and ΔE the increase in potential, then

$$-\Delta E/\Delta\Gamma = K,$$

where K is constant, or

$$-E = K\Gamma + \text{const.},$$

where Γ is the amount of active material on the cathode surface at the potential E. Thus the relation between the increase of potential and the amount of hydrogen added is a linear one and not logarithmic as might be expected if the deposited hydrogen behaved as an amalgam electrode of finite bulk concentration. Moreover, the amount of material deposited per square centimetre for every 100 millivolt rise in potential is very small indeed. Method (*a*) gives $6 \cdot 7 \times 10^{-7}$ coulombs/cm.^{2}/100 m.v. Method (*b*) gives $5 \cdot 9 \times 10^{-5}$ coulombs/cm.^{2}/100 m.v., or approximately 6×10^{-12} gm. ions. Taking the diameter of the hydrogen atom as 1×10^{-8} cm.^{2}, the number of coulombs required to deposit a monatomic layer is ca. $1 \cdot 7 \times 10^{-3}$ coulombs/cm.^{2}. If, then, the deposited material is atomic hydrogen, the potential is raised 100 m.v. for every 1/3000th of an atomic layer added. If the hydrogen is regarded as being adsorbed by the metal atoms, then (taking the diameter of a metal atom as 3×10^{-8} cm.) approximately 1/300th of the metal atoms in the surface is covered for a potential rise of 100 m.v. This linear relation is found to hold accurately over a potential range of — 0·2 volt to — 1·0 volt, and there is no evidence of deviation at more negative potentials. In the following table are given the results of a number of determinations of this quantity using both methods (*a*) and (*b*) under widely varying conditions of cathode area, current density, time of electrolysis and strength of solution. Considering the magnitude of the quantities involved the agreement is good, and within the limits of experimental error is independent of the above factors.

Area of cathode in square centimetres.	Solution.	Current in amps. × 10^6.	Method.	$\Delta\Gamma$ in coulombs/cm ^{2} × 10^7 to change potential 100 millivolts.
0·5	N/5 . H_2SO_4	8	(*a*)	6·7
0·5	,,	8	(*b*)	5·0
0·5	,,	8	(*b*)	6·0—Mean 5·9
0·33	N/500 . H_2SO_4	8	(*a*)	7·9
	,,	1	(*a*).	5·0
	,,	3	(*b*)	6·2—Mean 6·3
3·14	N/500 . H_2SO_4	24	(*b*) Few minutes electrolysis	5·3
	,,	24	(*b*)	5·4
	,,	54	(*b*) 3 hours electrolysis	5·2
	,,	24	(*b*) 45 hours electrolysis	5·3
	,,	126	(*b*)	6·1—Mean 5·8
3·14	N/5 . H_2SO_4	24·8	(*b*)	5·1
3·14	,,	24·8	(*b*)	5·2
14·4	,,	18	(*a*)	7·1
	,,	580	(*a*)	6·7
	,,	640	(*b*)	5·9
	,,	300	(*b*)	6·9—Mean 6·2
				Mean value 6·0 × 10^{-7}

Silver.

The cathode consisted of a sheet of pure silver, area 4·3 cm.², and the electrolyte was N/5 sulphuric acid. The behaviour was in all respects similar to that of mercury, the same linear relation being found between ΔΓ and ΔE. The magnitude of the quantities was, however, different and depended on the nature of the silver surface. This is shown in the following table; the values in the last column are the mean of several determinations using different current densities, and the maximum deviation from this mean is given.

Nature of surface.	Potential at CD of 1 × 10⁻⁵ amps. cm.².	Method.	$\Delta\Gamma$ in coulombs/cm.² × 10⁷ to change potential 100 milli-volts.
(i) Freshly etched with dilute HNO_3. Fine crystalline structure.	Volts. 0 465.	2 by (*a*) 4 by (*b*)	310 ± 40
(ii) Same as (i) but 20 hours old.	0 525	1 by (*a*) 2 by (*b*)	225 ± 13
(iii) Polished with "flour" sand-paper. Shows very scratched surface under the microscope.	0·60	2 by (*a*) 2 by (*b*)	100 ± 10

It will be seen that the amount of hydrogen added per apparent square centimetre of an etched silver surface to raise its potential 100 m.v. is about 50 times as great as that found for mercury. We must conclude that either the free energy of hydrogen deposited or adsorbed on silver is very much less than that of hydrogen on mercury, or else the accessible area of the silver cathode is very much greater than the apparent area.

Amalgamated Silver.

To investigate this point the surface of the sand-papered silver cathode was amalgamated with a very small amount of mercury, the surface being rubbed with another piece of silver for 30 minutes, giving a bright surface resembling mercury. The results were as follows:—

Nature of surface.	Potential for apparent CD of 1×10^{-3} amps. cm.^{2}	$\Delta\Gamma$ in coulombs/cm.^{2} $\times 10^7$ to change potential 100 millivolts.
Amalgam 1 hour old. Surface bright resembling mercury	$-0\cdot73$	$7\cdot3 \pm 0\cdot8$
Amalgam 20 hours old. Surface uniform grey and solid.	$-1\cdot06$	$7\cdot9 \pm 0\cdot7$
Amalgam 150 hours old. Surface solid. Dull grey and under microscope shows depressions and scratches of original sand papering.	$-0\cdot9$	$10\cdot5 \pm 0\cdot8$

The electrolyte was N/5 . H_2SO_4 as before, and the values given are the mean of several determinations using both methods (*a*) and (*b*) and with varying current densities. Since the amalgam is solid, the number of silver atoms in the surface must be high, yet it is seen that $\Delta\Gamma$ is practically the same as that found for pure mercury (6×10^{-7}), and only increases slightly as the surface becomes obviously rougher.

This indicates that the quantity of hydrogen which must be deposited on a metal plate to raise its potential 100 milli-volts is not a specific property of the metal atom, but depends only on the physical structure of the surface. The large differences found in the value of $\Delta\Gamma$ for etched, for polished and for amalgamated silver is due to the fact that the accessible area of the etched or polished surface (*i e.*, the total area of the metal which is accessible to hydrogen atoms and on which they can deposit or be adsorbed) is very much greater than its apparent area.

If A cm.^{2} is the accessible area of a metal cathode per apparent square centimetre, we may write equation (1), p. 73,

$$-\mathrm{E} = \mathrm{K}\Gamma/\mathrm{A} + \text{const.}$$

or

$$-\mathrm{E} = \beta\Gamma + \text{const.}, \tag{2}$$

where $\beta = \mathrm{K}/\mathrm{A}$ and is a constant, having the same value for all metals.

It appears that the magnitude of the hydrogen overpotential depends only on the true surface concentration of the added hydrogen and is independent of the underlying metal. The rate of removal of this added hydrogen (as measured by the current necessary to keep the surface concentration constant) does, however, vary greatly with the nature of the underlying metal. The behaviour of platinum lends strong support to these conclusions.

Platinum.

The following table shows the behaviour of platinum and platinised surfaces. The electrolyte was $N/5 . H_2SO_4$, and the values given are the mean of several determinations.

The platinum was deposited on the mercury electrolytically by adding known amounts of a platinum salt to the electrolyte.

It is seen that the accessible area of platinum foil is about twice, while that of platinum black is about 2000 times, its apparent area. If, however, the platinum be deposited not on to solid platinum but on to the liquid mercury, the atoms cannot form a sponge having a large area but lie in a plane surface having practically the same accessible area as the liquid mercury and giving the same value for $\Delta\Gamma$. The rate at which such a surface can catalyse the evolution of hydrogen is, however, many thousand times greater than a pure mercury surface.

Nature of surface.	Potential for an apparent C.D. of 10^{-8} amps. cm ^{2}.	$\Delta\Gamma$ in coulombs/cm ^{2} $\times 10^{7}$ to change potential 100 millivolts.
Bright platinum foil	$-0 \cdot 60$	13 (±1)
Platinised platinum "platinum black" as used for H_2 electrode.	$-0 \cdot 31$	11 000 (±2000)
Platinised mercury—		
(i) Pure mercury .	$-1 \cdot 19$	6 (±1)
(ii) Mercury surface covered with about 1/100 of an atomic layer of platinum.	$-1 \cdot 09$	5·1 (±0·5)
(iii) Mercury surface covered with several atomic layers of platinum.	$-0 \cdot 74$	5·0 (±0·5)

Relation between Surface Concentration of Hydrogen and its Rate of Decay.

In fig. 6 the logarithm of the apparent current density in amps. per cm.$^2 \times 10^{-7}$ is plotted against the observed electrode potential for the metals investigated. The electrolyte is N/5 sulphuric acid, so that the potential of the reversible hydrogen electrode is $-0 \cdot 3$ volt on this scale.

It is seen that over a wide range of current density the points lie accurately on a straight line. In fig. 7 the logarithm of the true current density, *i.e.*, the current per unit of accessible area, is plotted against the potential. The curves are marked with the same numbers as in fig. 6.

If E be the electrode potential and i the true current density, then

$$- E = b \log i + \text{const.}, \qquad (1)$$

where b is a constant.

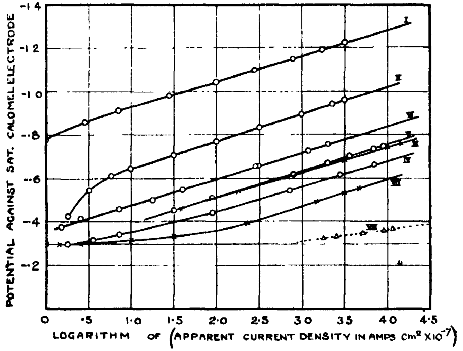

FIG. 6.

Curve I.—**Mercury.**
Curve II.—**Platinised mercury, 1/100 covered.**
Curve III.—**Platinised mercury, thin film of Pt.**
Curve IV.—**Etched silver, new.**
Curve V.—**Etched silver, old.**
Curve VI.—**Polished silver.**
Curve VII.—**Bright platinum.**
Curve VIII.—**Spongy platinum.**

(In Curve VIII the current density is expressed in amps. $\times 10^{-8}$ in order to bring it on the figure. It should be displaced two divisions to the right.)

Also it has been shown on p. 72 that

$$-E = \beta\Gamma + \text{const.}, \tag{2}$$

where β is a constant and where Γ is the true surface concentration of active hydrogen at the potential E.

Combining (1) and (2)

$$b \log i = \beta\Gamma + \text{const.} \tag{3}$$

But i is a direct measure of the velocity of the reaction by which the active hydrogen disappears from the plate or $-d\Gamma/dt = i$. Therefore equation (3) becomes

$$\log(-d\Gamma/dt) = \beta\Gamma/b + \text{const.}$$

or

$$-d\Gamma/dt = ke^{\beta\Gamma/b},$$

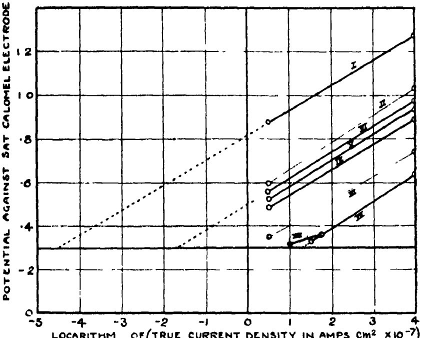

FIG. 7.

so that the rate of removal of the active hydrogen is an exponential function of its surface concentration.

The logarithmic relation between the current i and the potential holds accurately for all metals over a wide range of current density. In the case of high overvoltage metals such as mercury, deviation from this only occurs at very low current densities (less than 5×10^{-7} amps. cm^{-2}), and it is probable that this break is due to a trace of dissolved oxygen still present in the electrolyte, its rate of diffusion up to the cathode at this point becoming comparable with the current density, so causing the potential to fall below its equilibrium value. The supply of oxygen necessary for this is less than 5×10^{-12} gm. ions per second, and if any oxygen be admitted, the break occurs at much higher current densities. With low overvoltage metals such as platinum, hydrogen can be evolved at an appreciable rate without any overpotential, and it is only when this is exceeded that overpotential occurs.

In fig. 7 the graphs for mercury, polished silver and smooth platinum are extrapolated until they intersect a line drawn through the reversible hydrogen potential. The points of intersection are a measure of the maximum rate at which hydrogen can deposit reversibly on the respective metals. On mercury it is approximately 3×10^{-12} coulombs/sec., on polished silver 2×10^{-9} and on smooth platinum 2×10^{-6}. If for each metal the current be reduced below this value, no further decrease will occur in the cathode potential. If this maximum reversible current be denoted by i_0, then the overpotential η is given by

$$\eta = b (\log i - \log i_0),$$

where b is a constant.

This may be written

$$\eta = a + \mathrm{B} \log i,$$

where $a = - b \log i_0$.

This last relation between overpotential and the current density was first noted by Tafel* and has been confirmed by other workers.† These investigators found it to hold accurately for mercury but only approximately for other metals. In fig. 7 the value of b is practically the same for mercury, for silver, and for smooth platinum, viz., 0·120. The value obtained by Tafel for mercury was 0·110.

Since i represents the rate at which hydrogen is removed from the cathode surface per unit of accessible area, it is a measure of the specific catalytic activity of the surface for this reaction. It is seen that the curves in fig. 7 for the pure metals fall into three groups characteristic of mercury, silver and platinum, indicating the specfic activity of a particular atom; for example, platinum is not very different whether it exists in the form of platinum black or bright platinum, the apparent increase in activity being due mainly to the increase in the accessible area. For the respective metals, however, it differs very greatly, the rate at which platinum catalyses the deposition of hydrogen being 10^6 times greater than mercury per unit of accessible area of the surface, the surface concentration of hydrogen being the same in each case.

It is apparent that this experimental procedure gives an interesting method of investigating the areas of metallic surfaces and correlating it with their catalytic activity, and this will be considered in more detail later.

Mechanism of the Electrode Potential.

If the potential across the interface be due to a number of electric doublets, each possessing a finite electric moment, then the interfacial potential is given by

$$- \mathrm{E} = 4\pi n \mu, \tag{1}$$

---

* 'Z. Phys. Chem.,' vol. 50, p. 641 (1905).

† Lewis and Jackson, 'Z. Phys. Chem.,' vol. 56, p. 193 (1906); Harker and Adams, 'J. Phys. Chem.,' vol. 29, p. 205 (1925).

where E is the absolute potential difference, n is the number of doublets per square centimetre, and μ is the electric moment contributed by each doublet. If the number of doublets on the surface is increased, then the increase in potential is given by

$$- \Delta E = 4\pi \Delta n \mu. \tag{2}$$

Experimentally this linear relation is found, the cathode potential becoming 100 millivolts more negative for every $6 \times 10^{7} \times 6{\cdot}06 \times 10^{23} \div 96540 = 3{\cdot}7 \times 10^{12}$ hydrogen ions deposited per square centimetre of accessible surface and independent of the nature of the cathode. Substituting these values in (2) we obtain

$$\tfrac{1}{3} \times 0{\cdot}1 \times 10^{-2} = 4\pi\, 3{\cdot}7 \times 10^{12}\, \mu, \text{ whence } \mu = 7{\cdot}2 \times 10^{-18} \text{ E.S.U.}$$

If the electric moment be produced by a doublet consisting of an electron separated from a proton by a distance δ, we obtain

$$\mu = \epsilon\delta, \text{ whence } \delta = 7{\cdot}2 \times 10^{-18} /(4{\cdot}77 \times 10^{-10}) = 1{\cdot}5 \times 10^{-8} \text{ cm.}$$

This value is in agreement with that given for the diameter of the hydrogen atom, namely, 1×10^{-8} cm.

It is also significant that the rate of discharge of hydrogen is an exponential function of the potential

$$- d\Gamma/dt = k_1 e^{-k_2 E},$$

a relationship which is similar to that governing the emission of electrons across the double layer at a metallic surface.

It is found experimentally that if the deposited hydrogen be removed by electrolysis to a value below that corresponding to the reversible hydrogen electrode, the potential continues to fall with exactly the same gradient until well below the reversible potential, and only deviates from this when the number of metallic ions which go into solution becomes appreciable. For example, on polarising a silver electrode and then making it anodic, the linear relation between the amount of material removed and the fall of potential held over a range of $- 0{\cdot}9$ to $+ 0{\cdot}20$; beyond this it fell more slowly and exponentially to the silver value.

We are led to infer that the mechanism of the reversible hydrogen electrode is similar to the case of overpotential just considered, the number of doublets on the surface being here dependent only on the pressure of the gas. Whilst the absolute value of the hydrogen electrode potential is not known, the dropping electrode gives a value of $- 0{\cdot}28$ volt, which is equivalent to 1×10^{13} doublets per square centimetre, thus covering approximately 1 per cent. of the metal atoms in the surface. On deposition of hydrogen ions, doublets are formed which in turn must be discharged to form molecular hydrogen. The rate at which the discharge of these doublets can occur at the concentration corresponding to the reversible hydrogen potential varies from metal to metal. On mercury it is 2×10^7, on silver 1×10^{10} and on platinum 1×10^{13} doublets per second. Unless this rate of discharge be exceeded there is no overpotential. If this rate is exceeded, the surface concentration of the doublets increases and the electrode potential becomes more negative, the overpotential being directly determined by the number of doublets added to the surface. Since the equilibrium concentration of doublets is now exceeded, changes in the gas pressure will not affect appreciably the electrode potential.[*]

A possible mechanism by which these doublets are brought into existence may be suggested. The linkage between the metal and the deposited hydrogen atom is of such a nature that the hydrogen atom (possessing an electron affinity[†]) behaves as a negative ion which attracts to it a hydrogen ion from the solution, thus forming a doublet of a positive and negative hydrogen ion orientated on the surface. Discharge of this doublet involves the loss of an electron from the metal surface, and the rate at which it occurs is a function of the potential, viz., $-d\Gamma/dt = k_1 e^{-k_2 E}$, which is the same relation as that governing the emission of electrons from metals. When the doublet is discharged. the two hydrogen atoms unite to form a neutral hydrogen molecule.[‡]

Heyrovsky[§] on very different grounds has proposed a mechanism for hydrogen overpotential which is somewhat similar to the above in that it involves the formation of negative hydrogen ions on the electrode surface. It, however, involves the assumptions that the potential is proportional to the logarithm of the surface concentration of negative hydrogen ions and that the rate of removal of these ions is directly proportional to their surface concentration. The above experimental work does not support these assumptions.

---

[*] Knobel, 'J. Amer. Chem. Soc.,' vol. 46, p. 2751 (1924); Bircher and Harkins, *ibid.*, vol. 45, p. 2890 (1923).

[†] Joos and Huttig, 'Z. f. Physik,' vol. 39, p. 473 (1926).

[‡] Alternatively the potential change which occurs may be regarded as due simply to a flux of electricity across the boundary. Taking the dielectric capacity across the interface as unity, the thickness of the double layer is 1·5 Å.U., which is approximately the diameter of a hydrogen atom.

[§] 'Rec. Trav. Chim.,' vol. 44, p. 499 (1925), and vol. 46, p. 582 (1927).

Summary.

A quantitative investigation is made on the changes of electrode potential at the surfaces of metallic cathodes during the electrolytic deposition and removal of very small quantities of hydrogen. It is found that the electrode potential is a linear function of the surface concentration of the hydrogen; moreover, the potential of the polarised cathode depends only on the true surface concentration of the added hydrogen and is independent of the nature of the underlying metal. Apparent differences observed are due to differences in the real areas of the cathodes, and this gives a method of measuring the accessible area of metallic surfaces. The amount of hydrogen deposited is small, sufficient to form 1/3000th of an atomic layer, causing a change of 100 millivolts in the electrode potential. The rate of decay of the electromotively active hydrogen from the cathode surface is an exponential function of the potential. The general behaviour and the magnitude of the quantities involved can be explained on the assumption that the electrode potential is due to the presence of electric doublets on its surface, the electric moment of these doublets being that given by a proton and an electron separated from each other by a distance equal to the diameter of a hydrogen atom

Out best thanks are due to the Commissioners of the 1851 Exhibition for a Scholarship granted to one of us (F. P. B.) which made it possible to carry out this work, to Prof. T. M. Lowry, F.R.S., who communicated this paper, and to the Imperial Chemical Industries and the Cambridge Instrument Co. for assistance in obtaining the necessary apparatus

On the Electrolytic Behaviour of Thin Films. Part II.—*The Areas of Catalytically Active Surfaces.*

By F. P. Bowden and E. K. Rideal.

(Communicated by T. M. Lowry, F.R.S.—Received May 9, 1928.)

In a previous communication it was shown that by measurement of the quantity of hydrogen electrolytically deposited on a cathode surface in order to cause a given change in the electrode potential, it was possible to evaluate the accessible area of the surface, this area being defined as the total area accessible to hydrogen atoms and on which they can deposit or be absorbed. This procedure thus provides a third method, in addition to that of the examination of the thickness of oxide films by conductivity or interference methods or of the adsorption of suitable substances, for the determination of the areas of catalytic surfaces. Also, by measurement of the currents required to maintain the plates at a definite potential, the catalytic activities of the metals for the discharge of the hydrogen ions can be compared. In this paper the behaviour of electrolytically deposited and amagamated surfaces is considered in more detail, and the effect of different methods of treatment such as activation, annealing, rolling and electroplating on the area and catalytic activity is studied for a number of metals. The experimental procedure was in all details similar to that described in the previous communication.

Silver.

The behaviour of a silver cathode under changing surface conditions is shown in fig. 1, in which the logarithm of the apparent current density is plotted against the electrode potential. The electrolyte was oxygen-free N/5 sulphuric acid and the experimental conditions identical with those previously described.

For each surface the points lie accurately on a straight line and, with the exception of the graph for freshly amalgamated silver, the lines have the same slope. The reason for this change in gradient with a particular amalgam is not clear, but a similar effect is observed with a platinum/mercury surface. It is possibly occasioned by an alteration of the surface composition due to a change of the surface tension on increasing the interfacial potential. Thus the relative proportions of silver and mercury in the surface will change throughout the experiment so that the slope of the line will be different from that of a solid or nearly solid amalgam, where the concentration of the surface cannot alter during the period of the experiment.

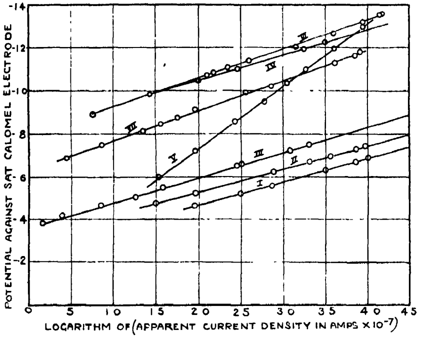

FIG. 1.

Curve I.—Silver, etched, new.
Curve II.—Silver, etched, 9 hours old.
Curve III.—Silver, polished.
Curve IV.—Pure mercury.
Curve V.—Silver amalgam 1 hour old.
Curve VI.—Silver amalgam 20 hours old.
Curve VII.—Silver amalgam 150 hours old.

By measurement of the quantity of hydrogen per apparent square centimetre deposited on the cathode surface in order to cause a given change in the electrode potential, the areas of these surfaces are determined. These are given in the following table (p. 82), the accessible area of a mercury surface being taken as equal to its apparent area.

Since, as has been shown, the electrode potential of a polarised cathode is determined solely by true surface concentration of hydrogen and is independent of the nature of the cathode, at any arbitrary potential the surface concentrations of hydrogen on all electrodes will be identical, and the rate of hydrogen evolution divided by the true area of the cathode will be a measure of the specific catalytic activities of the surfaces for hydrogen discharge. With the exception of curve V the slopes of the lines in fig. 1 are identical, so that the

Nature of surface.	$\Delta\Gamma$ coulomb/cm.^{2} $\times 10^7$ to change potential 100 milli-volts.	Accessible area per apparent square centimetre.	Hydrogen evolution per apparent square centimetre at 0·6 volt coul./sec. $\times 10^7$.	Hydrogen evolution per true square centimetre at 0·6 volt coul./sec. $\times 10^7$.
I.—Ag freshly etched with dilute HNO_3. Fine crystalline structure	310	51	1700	35
II.—Same as I but 20 hours old	225	37	440	12
III.—Polished with "flour" sand-paper	100	16	110	7
IV.—Pure mercury	6·0	1·0	0·01	0·01
V.—Ag amalgam 1 hour old. Surface bright resembling Hg	7·3	1·2	350	30
VI.—Amalgam 20 hours old. Surface grey and solid	7·9	1·3	0·02	0·016
VII.—Amalgam 150 hours old. Surface solid and rough	10·5	1·7	0·7	0·4

ratio of the catalytic activities will be the same whatever the potential chosen. Values for these at 0·6 volt are given in the last column of the table, and it will be noted that the catalytic activity of silver atoms is several thousand times that of mercury. In the case of pure silver a small variation (fivefold) in the specific activity with the treatment of the surface is observed, indicating that the configuration of the metal atoms as well as their nature and true area affects the total catalytic activity.

Platinum.

Fig. 2 illustrates the behaviour of platinum and platinised surfaces under similar experimental conditions.

Curve I was obtained with a piece of bright platinum foil. Curve II for platinum black was employed for a hydrogen electrode (the rate of hydrogen deposition was very rapid on this substance, necessitating the employment of a different scale, the current density in this case being given in amps. $\times 10^{-6}$). Curve III was obtained for pure mercury, the area of the cathode being 14·4 cm.^{2}. Curve IV shows this same cathode on which sufficient platinum has been deposited to cover about 1 per cent. of the surface. This was effected by adding a definite small amount of platinum salt to the electrolyte and electrolysing until the platinum was plated out. The appearance of the mercury surface was unchanged. Sufficient platinum was then added to form a thin bright film over the mercury, curve V. The surface now had a "stiff" appearance and was covered with large bubbles of hydrogen which adhered to it tenaciously. On open circuit the potential fell to — 0·3 volt, at which it remained constant so that the surface was functioning as a hydrogen electrode. On continued electrolysis at low current density the surface gradually changed, the platinum apparently dissolving very slowly in the mercury. Curve VI shows the surface after 3 days; the activity has decreased and the slope has changed. Curve VII after 5 days: there is a further decrease in the activity and the slope is becoming more normal. Curve VIII after 18 days: the slope is now nearly normal and the activity has decreased considerably.

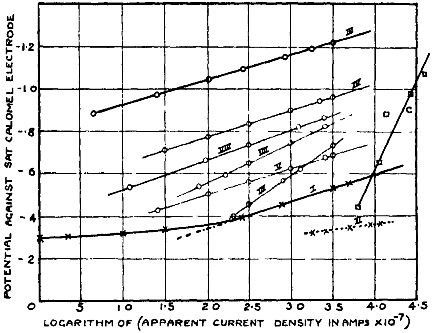

FIG. 2.

Curve I.—Bright platinum.

Curve II.—Platinum black.

Curve III.—Pure mercury.

Curve IV.—Mercury with 1 per cent. platinum.

Curve V.—Mercury with film of platinum.

Curve VI.—Mercury with film of platinum after 3 days.

Curve VII.—Mercury with film of platinum after 5 days.

Curve VIII.—Mercury with film of platinum after 18 days.

The accessible area of each of the surfaces is given in the following table :—

Nature of surface.	$\Delta\Gamma$ coul. $\times 10^7$ to raise potential 100 millivolts.	Accessible area per apparent square centimetre.	Hydrogen evolution per apparent square centimetre at 0·6 volt coul./sec. $\times 10^7$.	Hydrogen evolution per true square centimetre at 0·6 volt coul./sec. $\times 10^7$.
I.—Smooth platinum	13	2·1	11000	5500
II.—Platinum black	11000	1830	—	—
III.—Pure mercury	6	1·0	0·01	0·01
IV.—Hg surface with about 1 per cent. Pt	5·1	0·9	3·9	4·4
V.—Hg surface covered with thin layer of Pt	5·0	0·9	560	620
VI.—Platinised Hg after 3 days	5·0	0·9	1000	1100
VIII.—Platinised Hg after 5 days	7·0	1·1	160	140
VIII.—Platinised Hg after 18 days	4·8	0·8	31	40

The accessible area of bright platinum is about twice while that of platinised platinum is about 2000 times its apparent area. If, however, the platinum is deposited on a mercury surface, the area is sensibly the same as that of mercury; actually it is found to be very slightly less, and this may be a real effect due to the platinum atoms "freezing" the mercury and so preventing ripples which are normally present on the surface or else to the hydrogen bubbles adhering to the surface and decreasing the effective area. It is seen from the last column that the catalytic activity of platinum is very much greater than that of mercury (almost a million-fold) and the presence of relatively few platinum atoms on a mercury surface greatly increases the activity. At a potential of $-0\cdot35$ volt the rate of evolution of hydrogen on platinum black is $5\cdot6 \times 10^{-3}$ coul./sec. per apparent square centimetre, while on bright platinum it is 1×10^{-5} coul./sec. The rate of evolution per square centimetre of accessible surface is, however, 3×10^{-6} coul./sec. on platinum black and 5×10^{-6} coul./sec. on bright platinum, so that the specific catalytic activity of both forms of the metal is very nearly the same, the apparent increase in the activity of platinum black being due mainly to the increase in accessible area.

Carbon.

The electrode consisted of a piece of dense carbon rod 0·5 cm. diameter, as employed for carbon arcs, and was polished with flour sand-paper before use. The electrolyte was N/5 sulphuric acid and the experimental procedure as before. The relation between the potential and the logarithm of the apparent current density is given by curve C, fig. 2, and it is seen that in this case the points lie approximately on a straight line and that the slope is considerably greater than that observed for the metals, $b = 0{\cdot}84$. The accessible area of the surface was determined in the usual way, but the measurements are only approximate, since in the case of carbon the relation between the amount of hydrogen deposited and the potential is not linear over a wide range of potential.

	$\Delta\Gamma$ coul /cm. $\times 10^7$ to change potential 100 milli-volts.	Accessible area per square centimetre.	Hydrogen evolution per apparent square centimetre at 0 6 volt coul./sec. $\times 10^7$	Hydrogen evolution per true square centimetre at 0·6 volt coul./sec. $\times 10^7$.
Carbon rod after 2 hours	1970	328	-	—
Carbon rod after 20 hours	2200	366	10000	27

This method would measure the area of the carbon, which is wetted by the electrolyte, and it is found to be three to four hundred times the apparent area. The increase which occurs on prolonged electrolysis is probably due to electrolyte creeping farther into the capillaries in the carbon.

In the case of carbon a direct comparison has been made between the area as measured by the electrolytic method and that given by the adsorbtion of methylene blue. Pieces of the carbon rod were immersed in an aqueous solution of methylene blue and the amount adsorbed measured colorimetrically.* On the assumption that the methylene blue forms a unimolecular layer, the areas were as follows: –

Accessible area after 24 hours' immersion, 100 cm.^{2} per apparent cm.^{2}.
Accessible area after 48 hours' immersion, 140 cm.^{2} per apparent cm.^{2}.
Accessible area after 72 hours' immersion, 160 cm.^{2} per apparent cm.^{2}.
Accessible area after 96 hours' immersion, 165 cm.^{2} per apparent cm.^{2}.

The accessible area shows a steady increase with time, again indicating that the liquid is slowly penetrating the carbon. After 24 hours the area is 100 times the apparent area, which is about one-quarter of that found by the electrolytic method. Since the methylene-blue molecule is considerably larger than the hydrogen ion and diffuses more slowly, such a result might be expected.

---

* These surfaces were kindly measured by Dr. W. M. Wright.

Nickel.

A piece of hard nickel sheet 5·5 cms. in area was employed as the cathode and was subjected successively to different methods of treatment, polishing, activating, annealing, electroplating, etc., and the behaviour of each surface studied. The results are summarised in fig. 3 and in the following table. The experimental conditions were identical with those previously described and the values in the second column of the table are the mean of several determinations using different current densities. For any one surface the experimental variation was not more than 10 per cent.

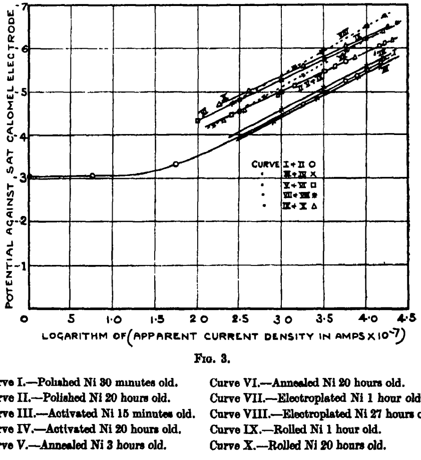

Fig. 3.

Curve I.—Polished Ni 30 minutes old.
Curve II.—Polished Ni 20 hours old.
Curve III.—Activated Ni 15 minutes old.
Curve IV.—Activated Ni 20 hours old.
Curve V.—Annealed Ni 3 hours old.
Curve VI.—Annealed Ni 20 hours old.
Curve VII.—Electroplated Ni 1 hour old.
Curve VIII.—Electroplated Ni 27 hours old.
Curve IX.—Rolled Ni 1 hour old.
Curve X.—Rolled Ni 20 hours old.

Nature of surface.	$\Delta\Gamma$ coul./cm.^{2} $\times 10^7$ to change potential 100 millivolts	Accessible area per apparent square centimetre	Hydrogen evolution per apparent square centimetre at 0·55 volt coul./sec. $\times 10^7$	Hydrogen evolution per true square centimetre at 0·55 volt coul./sec. $\times 10^7$.
I.—Polished Ni, new	75	13·3	10500	760
II.—Polished Ni, old	58	9·7	3390	350
III.—Activated Ni, new	276	46	11200	240
IV.—Activated Ni, old	176	29	8510	290
V.—Annealed Ni, new	65	10·8	3550	330
VI.—Annealed Ni, old	46	7·7	1780	230
VII.—Electroplated Ni, new	72	12	2340	180
VIII.—Electroplated Ni, old	57	9·5	1350	140
IX.—Rolled Ni, new	35	5·8	3550	610
X.—Rolled Ni, old	21	3·5	1410	400

It is seen from fig. 3 that when the logarithm of the apparent current density is plotted against the potential, the points lie accurately on a straight line, and that, with the exception of the electroplated nickel, the slope is the same for all the surfaces ($b = 0{\cdot}095$). For electroplated nickel $b = 0{\cdot}110$.

Initially the cathode was polished with flour sand-paper, the surface was bright and under a low-power microscope showed many scratches. The accessible area of this surface was 13 times its apparent area (compared with the value of 16 obtained for silver), and on electrolysis for 20 hours decreased to 9·7. This decrease of approximately 30 per cent. in the accessible area with ageing of the cathode is quite general for all surfaces. The cathode was then activated by alternate oxidation and reduction in an electric furnace. An oxide film $1{\cdot}2 \times 10^{-5}$ cms. thick (as measured by interference colours) was formed on the surface three times at a temperature of 560° C., being alternately reduced by hydrogen; the nickel was finally activated by reduction at 350° C.* The appearance under the microscope was unchanged except that the metal was slightly duller. The accessible area of this surface was now 46 times its apparent area, so that this treatment caused an increase in the surface in the ratio 9·6 : 46 or 1 : 4·8. With ageing of the cathode the accessible area decreased to 29. The cathode was then annealed by heating for 1 hour at 590° C. in an atmosphere of hydrogen. This caused the accessible area to decrease to 10·8, and after 20 hours' electrolysis to 7·7. After repolishing the cathode, it was electroplated in a buffered nickel sulphate bath with a current density of 0·002 amp. cm.^{2} for 1½ hours so that a thin bright coating of metal was formed, through which the marks of the sand-papering were still visible. The accessible area was approximately the same as that of a polished cathode. The effect of cold rolling on the nickel was to reduce the accessible area to 5·8, which on ageing further decreased to 3·5. It is evident that the accessible area of a metal surface can be altered very greatly by different methods of treatment from 3·5 times its apparent area for rolled nickel to 46 times for activated nickel. Accompanying this change there is little alteration in the appearance of the surface; if, however, a metal sponge is formed, as in the case of platinum black, the area can be increased some thousand times.

---

* This electrode was kindly activated by Dr. F. H. Constable.

The last column in the above table gives the rate of hydrogen evolution per square centimetre of accessible surface and is a measure of the specific catalytic activity of the surface for this reaction. In the case where the metal is not mechanically treated there is little change in the specific activity of the different surfaces; the increase in the total rate of catalysis which occurs on activation is due mainly to an increase in the accessible area. Moreover, the specific activity does not change appreciably on ageing of the cathode. If, however, the surface be mechanically treated by sand-papering or rolling, the specific activity is much greater and on ageing falls considerably. This indicates that the effect of alternate oxidation and reduction, the usual process of activation of metallic catalysts, is chiefly to increase the accessible area of the surface by altering the grain size. Violent mechanical treatment, however, although it increases the surface to a much less extent, increases the proportion of surface atoms which are out of the crystal lattice and which are catalytically the most active. Under the forces operating during the discharge of the hydrogen these atoms, which have been torn out of the crystal lattice, slowly return to it and the specific activity of the surface decreases. The activity of an electro-deposited surface is low.

Of the more recent work on the measurement of the true areas of metallic surfaces might be mentioned that of Constable,* in which a film of oxide is formed on the metal and its thickness measured by interference colours. The values found for the areas by this method are considerably less than those found by the electrolytic method described above. Such a result might be expected, since, in the interference method, a layer of oxide many thousand atoms thick is formed on the metal, and this would not be capable of detecting fine irregularities of the order of atomic size in the metal surface, while in the electrolytic method the area measured is that which is accessible to hydrogen ions.*

---

* 'Nature,' vol. 119, p. 349 (1927), and vol. 120, p. 769 (1927).

Summary.

The evaluation of the accessible area of cathode surfaces, by measurement of the amount of deposited hydrogen required to raise the potential by a definite increment, and a comparison of the catalytic properties of these surfaces by observation of the rate of hydrogen evolution, has been extended to silver platinum, carbon and nickel. The effect of amalgamation as well as of treatment of the surfaces by alternate oxidation and reduction, annealing, etching with acid, electroplating, sand-papering and rolling have been examined.

It is shown that the accessible area of a metal sponge such as platinum black may easily attain a value of 2000 times its apparent area. The accessible area of a sand-papered metal is about 10 times its apparent area, and in the case of nickel activation by alternate oxidation and reduction causes an increase of nearly fivefold. Rolling reduces the accessible area. The specific catalytic activity of the various metals for the electro-deposition of hydrogen differs very widely, but for any one metal the specific activity of the surfaces only suffer small variations by chemical or thermal treatment. Violent mechanical treatment, however, such as sand-papering or rolling, causes a marked increase in the activity, and this gradually diminishes with ageing of the cathode.

---

* The reference by Constable ('Roy. Soc. Proc.,' A, vol. 119, p. 197 (1928)) to this method rests on a misconception, since it does not involve the assumption that the cathode is covered with a complete unimolecular film of hydrogen, but simply that the quantity of electricity passed in order to cause a given change in the interfacial potential is proportional to the accessible area of the surface.—(*Added, July* 11, 1928.)

The Detonation-Wave in Gaseous Mixtures and the Pre-Detonation Period.

By William Payman, D.Sc., Ph.D.

(Communicated by H. B. Dixon, F.R.S.—Received May 11, 1928.)

[Plates 3–7.]

When an inflammable gas mixture, contained in a long horizontal glass tube closed at one end and open at the other, is ignited at the open end, a flame begins to move at a uniform rate towards the closed end. This initial spread of flame, which has been termed the "uniform movement," persists for some distance along the tube, but soon gives place to an accelerating movement, sometimes, but not always, vibratory, the mean speed of the flame increasing rapidly until finally, with certain mixtures, the detonation-wave is set up, the speed of the flame being extremely high but again becoming constant during this last phase. The speed of the uniform movement of flame and that of the detonation-wave both being constant, these phases of the propagation of flame lend themselves particularly well for measurement and observation, and have in consequence received much attention. The most striking difference between the two modes of propagation is in the order of speed attained. Thus, with a methane-oxygen mixture containing 50 per cent. of methane, the speed of the uniform movement of flame in a horizontal glass tube, 2·5 cm. in diameter, is only 2 metres per second, whereas the speed of the detonation-wave when set up in the same mixture is 2530 metres per second. There is good reason to believe that the difference between the two modes of propagation is not merely one of degree, and that they are, both physically and chemically, distinct.

During the intermediate phases the influence of either or both types of propagation may be observed. We may regard as "normal" that propagation (including the uniform movement) which takes place by conduction of heat, assisted by those factors which may increase conduction by increasing the efficiency of contact between hot and cold gases, namely, convection and turbulence.* In the detonation type of propagation the transfer of heat may still take place partly by conduction, but a new factor also enters, namely, the heating of unburnt gases by shock or pressure waves generated by the burning gases during their rapid inflammation. According to these definitions, during the true uniform movement of flame the transfer of heat should be effected by conduction alone between burning and unburnt gases. In the true detonation-wave itself, unburnt gases should be heated adiabatically to or above their temperature of instantaneous ignition by the pressure-wave produced by the burning gases, without conduction coming into play in the same sense. Though it is probable that neither of these conditions is attained, or is theoretically attainable, they may be taken as defining the ideal modes of propagation during what we may term the true uniform movement of flame and the true detonation-wave. The conditions under which the one type of propagation gives place to another so dissimilar are naturally of great theoretical interest.

---

* It has been suggested to me by Prof. C. H. Lees that this type of propagation is more properly described as propagation of flame by *transfer* of heat than by conduction.

A purely arbitrary and approximate, but nevertheless useful, distinction is to regard all flames the speed of propagation of which is appreciably less than that of sound in the gas mixture at ordinary temperatures (330 metres per second in air) as belonging to the normal type, whilst those in which the speed of propagation is of the same order or above this belong to the detonation type of inflammation.

The experimental investigation of the detonation-wave and the pre-detonation period has been limited mainly to the examination of the movements of the flame, photographic methods having been found particularly useful for this purpose.* The study of the detonation type of propagation of flame, and more particularly of the conditions under which detonation is set up and maintained, must, however, be incomplete without some knowledge of the mode of production and propagation of the shock- and pressure-waves, whose action mainly determines the type of propagation, and of their effects. Such waves have been studied mathematically, but have received comparatively little experimental treatment.

The present investigation has been carried out for the Explosives in Mines Research Committee of the Safety in Mines Research Board, with the primary object of ascertaining the effect on the external atmosphere of the detonation of a mining explosive in a shot-hole, since the compression-wave or "shock-wave" (*l'onde de choc*) thereby produced is one of the possible sources of ignition of firedamp in coal mines. The results of the work, in so far as they bear on the problems of the safety of explosives used in coal mines, are described in a series of publications of the Safety in Mines Research Board, of which two parts have already appeared.* The experiments have also given information with regard to the production of such waves and of their behaviour and effect during the pre-detonation and detonation periods with explosive gas mixtures, and it is this bearing of the work which will be discussed in this paper. An adaptation of an old optical device, the " Schlierenmethode " of Topler, has enabled photographic records to be obtained of the shape and appearance of the shock-wave, and of its speed of propagation, and these have been used to supplement and extend the information obtained by other workers using direct methods of photography only. The work already published deals with the propagation of the shock-wave through the atmosphere. It has shown that intense compression-waves may be sent through the air by detonating or rapidly burning explosives or gas mixtures, and that these may travel at speeds much greater than that of sound at the initial temperature of the air.

---

* Mallard and Le Chatelier, 'Ann. des Mines,' vol. 4, p. 274 (1883); Dixon, 'Phil. Trans.,' A, vol. 200, p. 315 (1903).

The momentary heating effect of these waves, resulting from the rapid compression of the gas mixture through which they pass, and the movement imparted to the gas mixture on their passage through it may have an appreciable effect on the propagation of flame through the mixture. During the propagation of what has been termed the detonation-wave (*l'onde explosive*) in gaseous mixtures, for example, it has been suggested that the heating effect of the shock-wave produced by rapidly burning gases is sufficient to raise the temperature of adjacent unburnt gases to their instantaneous ignition-point in the extremely short interval of time during which the shock-wave acts on these gases. The detonation-wave in a gas mixture is thus considered to be a shock-wave, produced by the rapid combustion of the gas mixture, and sufficiently intense to cause ignition of the gas mixture through which it passes, whilst being continuously maintained by the combustion thereby started, the latter fact explaining the constant rate at which the wave is propagated. This suggestion, due to Mallard and Le Chatelier,† is now generally accepted to explain the mode of production and propagation of the detonation-wave. The present paper is devoted to an examination of the waves produced before detonation, and to a study of the behaviour of these waves and of the flame during the pre-detonation period, in particular to examine the mode of inception of detonation in a gaseous mixture.

---

* "The Pressure Wave sent out by an Explosive," Part I, by W. Payman and H. Robinson. Part II, by W. Payman and W. C. F. Shepherd. 'Safety in Mines Research Board Papers,' No. 18 (1926), No. 29 (1927).

† 'C. R.,' vol. 95, p. 1354 (1882).

The initiation of detonation in gaseous mixtures presents a problem of great interest and complexity. Our main knowledge of the subject is based upon the classical researches of Mallard and Le Chatelier and of Dixon (*loc. cit.*), though their work has been supplemented recently by Laffitte* and by Egerton and Gates.† The photographic method with a rapidly moving plate or rotating film first adopted to study the movements of flame in gaseous explosions by Mallard and Le Chatelier was used by all, the gas mixtures being enclosed in a cylindrical tube of suitable material.

Mallard and Le Chatelier employed mixtures of carbon disulphide with oxygen or nitric oxide in their researches, these mixtures having been found to yield highly actinic flames. Their apparatus, in which the photographic paper could not be moved faster than 1 metre per second, failed to analyse the more rapid movements of the flame, but their conclusions are of interest. They are summarised by Prof. Dixon (*loc. cit.*) as follows:—

"When the gases were ignited by a flame at the open end of a long tube, the flame was propagated along the tube for some distance with a uniform slow velocity which Mallard and Le Chatelier regarded as the true rate of propagation by conduction. In the case of mixtures of carbon disulphide with nitric oxide, this period of uniform movement was succeeded by oscillations of the flame, which sometimes became of larger and larger amplitude and then died down, and sometimes gave rise to the detonation-wave. When carbon disulphide was mixed with oxygen the preliminary period of uniform movement was shorter and was immediately succeeded by the detonation-wave. These two mixtures appeared to be typical of other gaseous mixtures, carbon disulphide with oxygen resembling oxygen mixtures generally, carbon disulphide with nitric oxide resembling air mixtures generally.

"In the explosions starting at the open end of the tube the development of the detonation-wave was not progressive, but always instantaneous. On the other hand, when the mixture of carbon disulphide and nitric oxide was fired near the closed end of the tube the movement of the flame was uniformly accelerated, until the detonation-wave was set up."

The initiation of the detonation-wave and the initial phases of the explosion have been examined very thoroughly by Prof. Dixon, using many different inflammable gases. Perhaps his most interesting observation was that the detonation-wave starts suddenly, throwing back a strongly luminous wave (the retonation-wave) through the still burning gases, and leaving a dark space where it started The intensity of the retonation-wave led him to consider that the period before the detonation is distinguished "not only by a slower propagation of the flame, *i.e.*, of ignition, but also by a slower process of combustion. In the initial period the molecules of the gas might meet many times before chemical reaction occurred; in the detonation-wave the molecules might be so intensely agitated that most collisions between chemically opposite molecules would result in chemical change. At the point of detonation the rise of pressure must be exceedingly rapid owing to the increase of chemical action, and this pressure would produce not only the forward wave of detonation, but also a sudden backward wave of compression into the gases still slowly burning behind it."

---

* 'Ann. de Physique,' vol. 4, p. 587 (1925).

† 'Roy. Soc. Proc.,' A, vol. 114, pp. 137, 152 (1927).

A peculiarity was exhibited by many photographs at the point where detonation commenced, detonation apparently being set up some distance in front of the advancing flame. Le Chatelier suggested that this was due to the fact that the wave of detonation started in front of the flame and originated in an invisible wave which was proceeding in front of the flame. Dixon brought forward evidence which indicated that the discontinuity observed at the point where detonation was set up was due to halation on the photographs, the brighter record of the detonation-wave being enlarged.

During the initial phases of the explosion, however, before detonation was set up, Prof. Dixon showed that the movements of the flame were greatly affected by compression-waves, and obtained evidence that such waves advanced in front of the flame at the beginning of the explosion. His description of the origin of these waves is as follows: "When an explosive mixture is fired by a spark, the suddenly ignited gases must expand and transmit a compression-wave in both directions. This travels with the velocity of sound in the unburnt gas. The propagation of the flame from the firing point is in most gaseous mixtures less rapid than the velocity of sound in the unburnt gas, but the rate of propagation of the flame augments, much more rapidly in some mixtures than in others. If the tube is a long one the flame will overtake the sound-wave after a more or less prolonged chase, according to the nature of the mixture."

The work of Laffitte and of Egerton and Gates was devoted mainly to the examination of the effect of change of conditions, physical and chemical, on the duration of the pre-detonation period; or, alternatively, on the distance travelled by the flame before detonation was set up.

The present research provides visible evidence of the movements of the hitherto invisible compression-waves, the character of which has been previously postulated from their effects on the flame. A brief account of the experimental methods used will be necessary in order to explain the records obtained and reproduced here. For a detailed description, reference may be made to the 'Safety in Mines Research Board Papers' previously mentioned.

Rays of light from a suitable source are brought to a focus by means of a concave mirror on the objective of a camera, and the latter is focussed on the mirror so that on examining the ground-glass camera-screen one sees an image of the mirror illuminated by the source of light. If a straight-edged opaque screen is brought down gradually in front of the camera objective, the image of the mirror becomes darker and darker, as more of the light is cut off, until at the "critical position" the light is just cut off entirely The screen or diaphragm is set slightly in advance of this critical position and the optical setting is such that, when set, the diaphragm covers about half the camera objective.

Each point on the mirror will have a corresponding position on the image on the ground-glass screen. Hence, if the path of a ray be deflected at any particular point, the diaphragm will be in the critical position for all points but that one. If the deflection is in the right direction the ray of light will pass beyond the edge of the diaphragm and into the lens, so that the given point will be made visible (or brighter than its surroundings) in its true position in the image on the screen. It will be evident that the passage of a pressure-wave across the mirror will result, if the diaphragm is correctly placed, in the passage of a band of light across the camera image, and the shape of the moving band will be the shape of the advancing wave.

The camera is focussed on the mirror if the deflection takes place at the mirror. If it takes place some distance from the mirror, as in the present experiments, the camera is focussed on the plane in which the deflection occurs, though it must always point directly at the mirror.

A record of the movement of the wave as it travels along a tube is obtained by photographing the front of the shock-wave, moving horizontally, on to a film moving rapidly downwards, using a powerful mirror-arc lamp as the source of illumination.

The diaphragm in front of the objective is set so that a certain amount of light enters the camera when the gaseous medium between the mirror and camera is undisturbed. Deflections of light in opposite directions then have an effect on the camera image, in one direction increasing the amount of illumination at the point on the camera image corresponding to the point of deflection, in the other direction decreasing the amount of illumination. Thus if the passage of a band of increased density (*e.g.*, a shock-wave) across the field of view results in a record as a bright white line, the passage of a band of decreased density in the same direction will result in a record as a dark black line. Similarly, if a shock-wave travelling across the field of view in one direction is recorded as a bright white line, a shock-wave travelling in the opposite direction will be recorded as a dark black line.* This reversal may also be effected by covering different halves of the camera objective.

The optical nature of the experimental method renders it impossible to take photographs of the wave moving along a cylindrical glass tube. A tube with two optically flat and parallel glass windows along opposite sides would have served, but the expense of such an arrangement, which would be frequently shattered, rendered its adoption impossible. Instead of glass the thinnest obtainable sheets of transparent "cellophane" were used for the windows. Experiments showed that such windows remained intact until an appreciable time after the detonation-wave had passed. The explosion tube used in the majority of the experiments was an iron tube 1 metre long and 2·5 cm. in internal diameter. Along opposite edges were cut two parallel slots 30 cm. long, the maximum length which could be photographed with the optical arrangements used, and 4 mm. wide. These slots were closed with a sheet of cellophane wrapped tightly round the tube and gummed so as to be gas-tight. The tube was filled with the gas mixture by displacement, the volume of gas mixture used being about 10 times the capacity of the tube.

In order to obtain greater detail in the photographs a lens of long focal length, 43 cm., was used, a Teleros of aperture f/5·5. In addition to giving a larger magnification this was found to reduce the effects of halation. It must be remembered in comparing the records reproduced in this paper with those of earlier workers that the present ones cover a shorter run of the flame. The length of tube photographed was 30 cm. and the speed of film approximately 70 metres per second throughout. Ordinary orthochromatic film was found to give sharper and more detailed records than specially sensitive bromide paper such as Lumière.

Photographic Records of the Detonation-Wave.—The difference between the photographs obtained by the method of Le Chatelier and those obtained by the present method is illustrated by figs. 1 and 2, which show the record, obtained by each method, of a detonation-wave in a $CH_4 + 2O_2$ mixture traversing the last 30 cm. of a horizontal iron tube 1 metre long and 2·5 cm. in internal diameter, and closed at both ends. In both, photographs may be seen the record of the detonation-wave advancing from left to right and being

---

* It is assumed that the wave is always convex fronted.

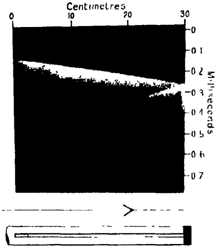

FIG. 1.—Detonation Wave in CH$_4$ + 2O$_2$
Direct Photograph.

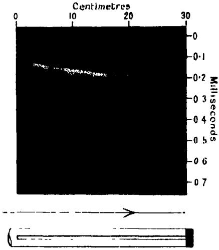

FIG. 2.—Detonation Wave in CH$_4$ + 2O$_2$.
Schlieren Photograph.

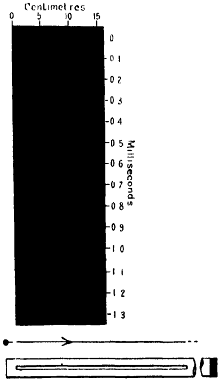

FIG. 3.—Uniform Movement in CH$_4$ + 2O$_2$.
Schlieren Photograph.

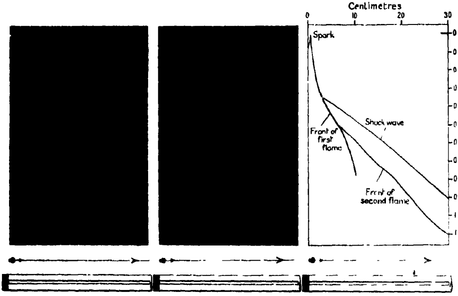

Fig. 4. Fig. 5 Fig. 6

Ignition near to one closed end of gas mixture $CH_4 + 2O_2$. Schlieren Photographs

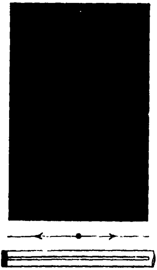

Fig. 7.—Ignition, 15 cm. from one closed end, of gas mixture $CH_4 + 2O_2$. Schlieren Photograph.

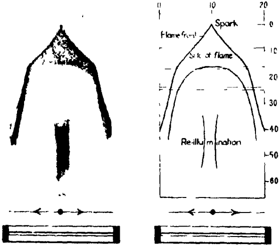

Fig. 8 Fig. 9.

Central Ignition in closed cylinder, 20 cm. long and 5 cm. in diameter, of gas mixture 4·2 per cent. C_2H_2 + 95·8 per cent Air.

Fig. 10.—Schlieren Photograph

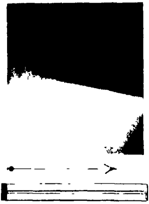

Fig. 11.—Direct Photograph

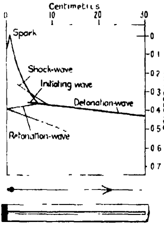

Fig. 12.

The Setting Up of Detonation in the Gas Mixture $C_2H_4 + 3O_2$.

Fig. 13.

The Effect of Restrictions

Fig. 14.

Fig. 15.

Schlieren Photographs of Ignitions of the Gas Mixture $CH_4 + 2O_2$.

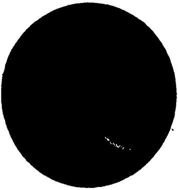

FIG. 16.

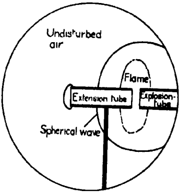

FIG. 17.

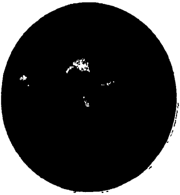

FIG. 18.
Instantaneous Photographs.

FIG. 19.—Direct Photograph.

FIG. 20.—Schlieren Photograph.

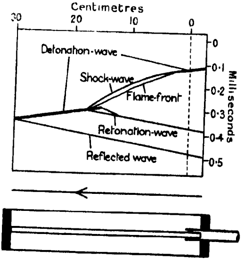

FIG. 21.
Moving Film Photographs.

reflected from the closed end of the tube, but the Schlieren photograph shows very clearly in addition the movements of the burnt gases behind the wave. The diaphragm in front of the camera objective for the Schlieren photograph is placed on the side which allows light refracted by a compression-wave moving from left to right to enter the camera, so that the detonation-wave shows up as a bright line compounded of the light so refracted and the light emitted by the burning gases themselves. The reflected wave is also a wave of compression, but as it moves from right to left, light from the arc, which is refracted, is sent off the camera lens on to the diaphragm, so that the front of the reflected wave tends to show as a darker line. Whether it does so or not depends upon the relative amounts of light refracted by the wave and emitted by the gases in the wave, this being illustrated as the gases lose their self-luminosity in the reflected wave as the latter proceeds farther away from the closed end of the tube.

It was found experimentally that the cellophane window remains intact for a period of about one five-thousandth of a second after the detonation-wave has passed.

Comparison between the Detonation-Wave and the Uniform Movement.—Stress was laid in the opening paragraphs of this paper on the great differences between the two modes of propagation of flame at constant speed in gaseous mixtures, during the uniform movement and during detonation.* These differences, which are mainly in the density or pressure in the flame front, in its luminosity, and in its speed, are illustrated by the two Schlieren photographs, figs. 2 and 3, showing records of flame movement in the same mixture, CH_4+2O_2. Fig. 2, to which reference has already been made, is a record of the detonation-wave; fig. 3 of the uniform movement, set up on igniting the mixture at an open end of the tube, the far end being closed. Only a portion of the record obtained is reproduced in fig. 3, which records the movement of the flame near the open end.

The Schlieren method itself brings out the difference in density. The flame during the uniform movement can be regarded as almost non-actinic in its effect on a photographic film moving at the high speed of the experiment. Being hot and free to expand, the gases in this flame have a density less than that of the unburnt gases, and, as the flame moves from left to right, refract light out of the camera lens on to the diaphragm, showing up as a black line. The difference between the speed of the detonation-wave (2320 metres per second) and that of the uniform movement (55 metres per second) in this mixture of methane and oxygen is brought out in a striking manner by these two photographs.

---

* See also Payman and Walls, 'J. Chem. Soc.,' vol. 123, p. 420 (1923).

The effect of three factors on the initial movement of the flame in gaseous mixtures fired in a tube closed at both ends has been examined—firstly, the position of the point of ignition (an electric spark); secondly, the presence of restrictions; and, thirdly, the intensity or type of the source of ignition.

The Effect of the Position of the Spark on the Initial Movement of the Flame in a Closed Tube.—To trace the effect of the position of the igniting spark a mixture of methane and oxygen, again of the composition $CH_4 + 2O_2$, was first used. The iron tube was 1 metre long and was closed at each end with rubber stoppers. One stopper held the electrodes, pieces of stout brass wire of the required length bent over and pointed at the ends. The exposure was timed by the dropping shutter of the camera, a knife-edge on which broke a wire in the primary circuit of an X-ray coil whose secondary was connected to the sparking electrodes. A small Leyden jar was connected in parallel with the electrodes, this being found to give a more uniform and reliable discharge, and also a more actinic spark.

For the first photograph, fig. 4, the spark was passed at a point 5 mm. from one end of the tube, and in this, as well as in most of the succeeding photographs, only the first 30 cm. of the tube was photographed. The end of the tube corresponds with the left-hand edge of the photograph. (In order to assist the description which follows of this photograph the details are reproduced diagrammatically in fig. 6.) The flame front advancing from left to right is again defined as a black line, whilst that portion of the flame which travels the short distance towards the near end of the tube, and therefore from right to left in the photograph, shows as a white line.* The compression-waves sent out by the burning gases are seen as a series of almost straight lines inclined across the film. Fig. 5 shows the reversal effect obtained by changing round the diaphragm on the front of the camera lens.

Leaving the consideration of the compression-waves till later, it will be observed that the flame appears immediately the spark has passed, and accelerates as it moves along the tube. After a short time the acceleration diminishes, and though a second flame appears to push through in advance and to progress at roughly constant speed, the initial flame front is seen to be retarded.

---

* The series of parallel vertical lines seen in all the Schlieren photographs are instrumental and have no significance. The position of the point of ignition is shown below each diagram by a black dot, and the direction of movement of the flame by an arrow. The film is moving upwards throughout.

A flame arrest has frequently been noted by investigators examining the movements of flame in gaseous mixtures contained in closed vessels, and two different explanations have been offered to account for it. The first is that the arrest is due to the compression-wave from ignition, moving at the speed of sound in the unburnt gases, and being reflected back from the far end of the tube.* This cannot be the explanation of the arrest recorded in fig. 4, since such a wave would only have travelled about half way towards the end of the tube when the flame was arrested. Further, as we shall see later, the flame moves outwards and is arrested almost symmetrically when the point of ignition is asymmetric.

The second explanation involves assumptions of gas surging or gaseous movements *en masse*, it being held in general that the arrest marks a point at which pressure behind the flame becomes equal to the pressure in front.

Two experimental observations may be referred to in this connection. Firstly, the gas surging or gaseous movement theory fails, just as did the wave-motion theory, to explain the simultaneous arrest of the flame, when the gas mixture is ignited asymmetrically in the explosion-tube. Secondly, when the mixture is fired at or close to one end, the point of arrest is the same whether the far end of the tube is opened or closed in a tube 1 metre long.

A more probable explanation is now offered. When an inflammable gas mixture is ignited at a point within a closed vessel, flame spreads simultaneously in all directions. During the first stage of propagation, before the flame touches the walls of the containing vessel, little heat will be lost by the flame, save to unburnt gases, except for that by radiation. When the flame touches the walls of the tube a second phase commences, heat being lost to the walls by conduction as the flame travels along in contact with them, and the flame speed being reduced. In the same way we may suppose that when a methane-oxygen mixture is ignited under the conditions of the present experiments, that is, in a closed tube 2·5 cm. in diameter and 1 metre long but some distance from one end, the flame starts outwards, first being spherical then becoming egg-shaped,† so that the most forward portion of the flame in each direction has travelled some distance along the tube before its equatorial belt touches the walls. The distance between the two ends of the flame may be quite large compared to the diameter of the tube before the portion touching the walls first is extinguished by them at that point. This extinction at the sides of the egg-shaped flame will result in propagation being now carried on solely by the two ends, that is, by two separate flames moving in opposite directions. Retardation probably commences as soon as the flame touches the walls or comes close enough to lose an appreciable amount of heat to them. The definite arrest of the flame would correspond to the moment of separation of the flame into two portions, so that the arrest would necessarily be simultaneous on each side of the point of ignition. This simultaneous arrest is shown in the next photograph, fig. 7, for which the point of ignition was moved to a point 15 cm. from the end of the tube. A similar simultaneous arrest of the flame front takes place not only under the conditions of the present experiments, but also under conditions such that the flame moves at appreciably different speeds towards the two ends of the tube.*

---

* Such an explanation was offered by Dixon for the retardation of the flame observed when a gas mixture was fired in short *narrow* tubes, and waves were seen crossing the burning gases from the points where the flames were checked (*loc. cit.*, figs. 54, 55, 64, 74, 75).

† Ellis and Wheeler, 'J. Chem. Soc.,' vol. 131, p. 313 (1927).

A separate series of experiments is being carried out in order to test the validity of this explanation under varying experimental conditions, but a photograph taken during another distinct investigation, and reproduced in fig. 8, shows an instance in which the break-up and arrest are simultaneous, in accordance with this suggestion. In this experiment a mixture of acetylene and air containing 4·2 per cent. of inflammable gas was ignited at the centre of a closed cylinder, the internal dimensions of which were length 20 cm. and diameter 5 cm., and which had a glass window along its whole length. The photograph was taken on bromide registration paper, so that the flame shows up black on a white background.†

The flame may be regarded, before it breaks, as a shell enclosing a non-luminous space. The outer edges of the flame, that is, the portions of the flame advancing towards the ends of the tube, are in line with the axis of the camera, which therefore records a considerable depth of flame, and shows up as a dark black line whose width gives some indication of the thickness of the flame front. The portions near the side of the tube are at right angles to the camera axis, and the depth of flame recorded is much less, so that the sides of the flame do not appear so black.

At any one instant the position of the flame behind the slit is indicated by a narrow horizontal section of the photograph. Three such sections are shown in the diagram fig. 9. At the instant shown in the uppermost section the flame is a complete spherical or egg-shaped shell. From the moment of ignition until the instant corresponding to the middle section the flame front has been accelerating, and the shell has been unbroken. Now, however, the flame is breaking and the break is rapidly increasing in size. At approximately the same instant the flame front begins to slow down. At the instant shown in the third section two distinct flames are observed, travelling in opposite directions.*

---

* Ellis, 'J. Chem. Soc.,' vol. 123, p. 1440 (1923).

† The tube was supported with its axis in a vertical position, but this has been shown horizontal in fig. 8 in order to compare directly with the other photographs.

In our discussion of fig. 4 only the primary flame has been considered. A second flame appears to push through the first in the region where it begins to slow down. This flame has no longer the clear-cut continuous outline of the initial flame, but resembles more the vibrating flame noted particularly with methane-air mixtures by Mason and Wheeler.† Since this second flame is undoubtedly helped along by compression-waves, which have their origin behind the flame front, the records of these waves may now be considered.

One of the most important observations from figs. 4 and 7 is that the shock-wave from the spark itself has little influence, probably none, on the propagation of the flame. This is evident from the photographs, and is still more so from the original negatives on which the faint spark-wave can be definitely seen. An idea of its position may be given. It starts out from the spark at an angle of approximately 45° to the edge of the film in both directions, its speed being slightly greater than that of sound in the mixture used. It appears to move almost immediately out of significant range of the burning gases.

The compression-waves which have such a marked effect on the flame, an effect from which their existence has previously been inferred, are shown to be much more marked than the spark-wave and to travel at a much greater speed, from which it can be safely concluded that their intensity is much greater. Their origin, however, is by no means clear. It is evident that they start in the still burning gases behind the flame front. Such marked compression-waves as the photographs disclose must arise from a sudden discontinuity in the conditions obtaining behind the flame front. Such a discontinuity can only arise from renewed chemical activity. There must, therefore, be renewed chemical activity behind the flame front.

Some observations by Prof. Dixon bear on this deduction. He has stated that "the collision of two flames in which detonation had not yet been determined gives rise to reflected waves more rapid and more luminous than the incident waves. Now these reflected waves cannot owe their increased velocity to the mechanical impact, which could only result in the reflected waves being copies of the incident waves. It is evident that chemical action must occur to assist these reflected waves, and therefore the combustion is obviously not complete when these waves return." Further, the retonation-wave sent back by a mixture on detonation was found to be "faster and more luminous when no other bright waves had been thrown back by the advancing flame before the point of detonation was reached."

---

* The further reillumination in the centre of the record will be considered later in this paper.

† 'J. Chem. Soc.,' vol. 117, p. 36 (1920).

More positive evidence that there can be and is renewed chemical activity some distance behind the flame front has been recently obtained by Ellis and Wheeler (*loc. cit.*). They have shown that in comparatively slowly burning mixtures this renewed chemical activity after the flame has passed through a mixture is indicated by a recrudescence of luminosity. This effect is also shown in fig. 8. In some of the later experiments of the present research, in which mixtures of hydrogen and oxygen were ignited by a fuse-head or a powder-fuse, the almost non-actinic flame suddenly became luminous a short distance behind the flame front, just before a strong compression-wave was sent out into the unburnt gases.

It can thus be regarded as established that the strong compression waves are caused by renewed chemical activity behind the flame front, that is, in gases in which the process of combustion has begun some time previously. What exactly this renewed activity is, activity renewed so rapidly as to send out strongly marked compression or shock-waves, remains to be discovered.

In some of the photographs obtained, for example fig. 5, the first shock-wave sent out by the flame can be observed as a single wave emerging from the flame front. In many others, for example fig. 14, the wave does not become visible until some distance in advance of the flame front. Close examination of the negatives leads to the conclusion that the apparently blank space is occupied by a faint triangle, composed of a mass of feeble compression waves, the later ones successively faster than the earlier, and so finally coalescing to form one strong wave which is visible on the print. This is indicated in a later photograph, fig. 24, whilst the joining of only two waves, a faster wave with a slower one in front of it, is shown in fig. 22.

The single wave in fig. 4 travels at a mean speed of approximately 500 metres per second. The minor waves from which this wave is produced do not appear to affect the initial flame as they pass through it, but later waves which follow the single wave, and travel at approximately the same speed, evidently assist the second flame. The undulations in the front of this flame appear to be due to a given wave or set of waves reaching the flame front, carrying it forward for a short distance and then leaving it behind, when another wave arrives and continues the process.

The Initial Movement of Flame with a Hydrogen-Oxygen and with an Ethylene-Oxygen Mixture in a Closed Tube.—When a mixture of hydrogen and oxygen, $2H_2 + O_2$ was ignited at (5 mm. from) the closed end of the experimental tube, a record was obtained similar in all respects to the one in which a methane-oxygen mixture was used, except that the flame throughout was faster. The distance of the point of arrest from the end of the tube is approximately the same as with the methane-oxygen mixture, despite the difference in speed of the flame, indicating that its position is determined merely by the shape and size of the containing vessel. The photograph obtained is reproduced later in the series (fig. 27) for comparison with another set of experiments.

Fig. 10, for which a mixture of ethylene and oxygen, $C_2H_4 + 3O_2$, was used, shows an additional feature, namely, the setting up of the detonation-wave. The initial flame starts out in much the same manner as in the methane-oxygen and hydrogen-oxygen mixtures, but detonation is set up suddenly whilst the flame is still accelerating. The cause of the detonation-wave being set up lies behind the advancing flame front, the increased chemical activity in the gases through which the flame-front has passed being sufficiently pronounced to produce a wave whose speed and intensity are of the order of those of the detonation-wave, which is set up immediately after the initiation-wave has passed through the flame front. The suddenly enhanced combustion in the initiating-wave at this moment, by reason of its passage through unburnt gas, results in a wave of retonation (which is a shock-wave) being sent back along the tube. The formation of the two waves, of detonation and retonation, at this point can be regarded as taking place on similar lines to the formation of the two flames moving in opposite directions from the point of ignition in a narrow tube; for where the shock-wave breaks through the flame-front, a new centre of disturbance is produced resulting in the formation of a spherical wave which impinges on the walls of the tube, two portions continuing to expand in opposite directions along the tube, giving the two separate waves of detonation and retonation.

In the same way the initiating-wave, the forerunner of the detonation-wave, and which has its origin at a position within the burning gases, sends out a wave travelling in both directions along the tube, as is shown more clearly when the point of ignition is moved some distance from the end of the tube.

The observation with this mixture that the setting up of the detonation-wave, as well as that of the preliminary shock-waves, is due to renewed chemical activity in gases through which the flame had passed some time before, led to a series of experiments to find under what circumstances the detonation-wave might be set up in advance of the flame, presumably by the strong compression-wave which the photographs show. Though this appeared quite possible, it was not observed in any mixture tried unless an obstruction was placed in the path of the flame, whether Schlieren or direct photographs were taken. When Schlieren photographs were taken the setting up of detonation was usually similar to that shown in fig. 10, and both detonation and retonation-waves always started quite definitely from a point behind the advancing compression-wave. The direct photograph reproduced in fig. 11 and obtained with the same mixture and point of ignition as that shown in fig. 10 also shows that the detonation-wave is set up within the burning gases. The apparent setting up of detonation in advance of the flame frequently recorded would appear to be an illusion due mainly, as suggested by Prof. Dixon, to the effects of halation, and partly due to the faintness of the flame record at this point. The use of a lens of long focal length with the resulting magnification is the probable explanation of the effect not being apparent in the present experiments, even when direct photographs were taken. This was confirmed by a repetition of the experiment recorded in figs. 10 and 11 using a wide aperture lens of much shorter focal length. The result was a photograph which indicated that detonation was set up in advance of the flame, though the effect was obviously one of halation

The photographs shown in figs. 10 and 11 show another feature of great interest. The flame starts out from the spark in much the same way as in a methane-oxygen mixture, but the Schlieren photograph shows the first compression-wave actually passing through the gases behind the flame-front. The wave starts in the gases and is not a wave reflected from the end of the tube, as is clearly shown by photographs to which reference has already been made for which the spark was moved farther from the end of the tube. The direct photograph offers more definite confirmation of the suggestion that the compression-wave is set up by renewed chemical activity behind the flame front, this renewed chemical activity being now evidenced by renewed luminosity. There is an important difference between the renewed luminosity observed in this experiment and that observed with comparatively slowly moving flames in air mixtures (compare fig. 8), for here the luminous effect is a growing one and spreads outwards, whilst with the slower flames the luminosity contracts. The two photographs, figs. 10 and 11, do not correspond perfectly, it having been found difficult to obtain exactly the same spread of flame in repeat experiments when ethylene was the inflammable gas.

The Effect of Restrictions.—The propagation of flame before detonation is set up is affected to a marked degree by the presence of restrictions in the experimental tube along which it has to pass. With comparatively slowly moving flames, such as those of methane and air, the usual effect of a constriction is to increase considerably the rate of propagation of flame.* With more rapidly moving flames in mixtures of inflammable gases with oxygen, the presence of a restriction in advance of the flame often results in a flame starting from the obstruction before the original flame reaches it, an effect which has been assumed, correctly as we shall see, to be due to adiabatic ignition by a pressure-wave which had preceded the flame.†

The record of an experiment with a mixture of methane and oxygen, $CH_4 + 2O_2$, is reproduced in fig. 13. The mixture was ignited close to one end of the experimental tube, in which had been placed an annulus of steel, 2 mm. thick, which reduced the diameter of the tube from 2·5 to 1·2 cm. at a point 10 cm. from the firing end. Its position is recorded on the photograph by a vertical black line. The vertical white line on the opposite side of the picture is instrumental and has no significance. It will be seen that the initial flame starts out as usual, but is retarded somewhat earlier and is then driven backwards. The first strong compression-wave (see, for example, fig. 4) cannot be detected in this photograph, but near the point where this wave, as deduced from previous experiments, would pass through the restriction, a second flame commences and travels comparatively slowly along the tube in the same direction as, but slightly in advance of, the initial flame. There is indication that later waves from behind the initial flame set up enhanced combustion behind the secondary flame that started beyond the restriction. This enhanced combustion soon causes a strong compression-wave which initiates the detonation-wave.

For fig. 14 the restriction was placed 20 cm. from the firing end. This photograph confirms the fact that the initiation of the flame at the restriction is due to the first strong compression-wave sent out from the initial flame. A flame can be seen moving outwards from either side of the restriction, at the point where it is hit by the compression-wave. For fig. 15, two restrictions were placed in the tube, and detonation has been set up at the second restriction. The increased combustion that occurs when waves strike obstructions is clearly illustrated by the increase in luminosity at the restrictions in these photographs.

---

* Chapman and Wheeler, 'J. Chem. Soc.,' p. 2139 (1926).

† Campbell and Woodhead, 'J. Chem. Soc.,' p. 32 (1926).

The Effect of Varying Cross-Section on the Speed of the Detonation-Wave.—Another important phenomenon of the propagation of the detonation-wave, which has received some attention during recent years, has been studied more particularly by Campbell.* He showed that whilst on passing from a wider to a narrower tube no alteration in the speed of the flame is observed, on passing from a narrower into a wider tube the flame slows down. These experiments have been repeated and confirmed by Laffitte (' C. R.,' 1924), who found also that the flame, after slowing down in the wider tube, eventually re-establishes its original speed. An explanation has been advanced (Payman and Robinson, *loc. cit.*) to the effect that the detonation-wave travelling along the narrow tube progresses approximately as a plane wave. On reaching the end of the narrow tube, the wave will begin to expand as a spherical wave and will slow down, as the spherical wave has been observed to do in other experiments not included in the present series. This decrease in speed is due to the fact that as the wave emerges into the wider tube the amount of gas to be, or being, compressed at any one instant is increasing more rapidly than the amount of the gases which are burning and producing the maintaining pressure-waves. The expansion will cease soon after the wave touches the walls of the wider tube. The wave-front, however, will now have gained on the maintaining, burning, gases, so that some distance separates them, and detonation will have been suppressed, a fact which is indicated by the diminution in speed. A definite length of run will therefore be necessary, even after the re-establishment of a plane shock-wave, before the detonation-wave itself is re-established. It has been found, in agreement with this explanation, that the time taken for the true detonation-wave to reappear is shorter the less the diameter of the wider tube, because the expansion of the spherical wave would be suppressed sooner in a narrower tube than in a wider.

This explanation is illustrated by two "spark Schlieren photographs," which are reproduced in figs. 16 and 18. By replacing the continuous source of illumination, the arc-lamp, by an electric spark of great actinic value but extremely short duration, a "snapshot" of the wave spreading spherically through the atmosphere when allowed to expand freely is obtained. For the first photograph, fig. 16, which should be compared with the explanatory diagram, fig. 17, a mixture of hydrogen and oxygen, $2H_2 + O_2$, was ignited in an iron tube, one end of which can be seen, as a black rectangle, on the right-hand side of the picture. This end was opened just before the mixture was fired. In line with the experimental tube, and a little distance from it, a short piece of tubing of the same diameter and open at both ends was placed. The mixture was fired some distance along the experimental tube so that detonation had been set up when the flame reached the open end. It will be seen that the atmospheric shock-wave, produced when the detonation-wave reached the open end, could spread outwards as a spherical wave, but a portion of it would be cut off by the extension tube, along which it would travel as an approximately plane wave. In this photograph it will be seen that the portion cut off is just emerging from the far end of the extension tube, and the difference in speed between the plane and spherical waves is evident, the spherical wave having lagged behind considerably. That the phenomenon is a natural result of wave-motion, and is not peculiar to the detonation-wave, is rendered clear by fig. 18, for which a wave produced by bursting a celluloid diaphragm by means of compressed air has been used, the extension tube in this instance being narrower than the experimental tube and continuous with it.

---

* ' J. Chem. Soc.,' vol. 121, p. 2483 (1922).

Fig. 19 shows a photographic record of an experiment, which is essentially a repetition of one carried out by Campbell, using the same method of photography. The only difference in the experimental arrangement was that no special fused joint was made between the two tubes, but the narrow tube was allowed to project 3 cm. through a rubber stopper and into the wider tube. In this way a continuous record could be obtained of the flame as it passed through the last 3 cm. of the narrower tube into the wider tube. The narrower tube was 12·5 mm., the wider 50 mm. in internal diameter, and the gas mixture used was of the composition $CH_4 + 2O_2$. The end of the narrow tube is at the right-hand side of the photograph and its edge is marked by a vertical black line. The detonation-wave can be seen travelling to the end of the narrower tube. The flame then temporarily falls off in speed, but the detonation-wave is again set up later.

Fig. 20 shows an exact repetition of this experiment, except that a Schlieren photograph was taken instead of a direct one, and fig. 21 gives an explanatory diagram. The separation of the shock-wave from the flame is shown to take place, the photograph serving as an illustration of the now generally accepted explanation of the mode of the propagation of the detonation-wave; that is to say, that the detonation-wave is a shock-wave, produced by the rapid combustion of a gas mixture, and sufficiently intense to cause ignition of the gas through which it passes, whilst being continuously maintained by the combustion thereby started.

The Ignition of a Gas Mixture by a Fuse or Detonator.—To complete the present series of experiments, a comparison has been made between ignition by other means with that of an electric spark, so-called "initiators" used for firing solid explosives being employed, and the gas mixture being electrolytic gas, $2H_2 + O_2$.

There are two types of initiators in general use, the powder fuse for gunpowder and the detonator for high explosives. The powder-fuse consists of a small cardboard cylinder plugged at one end with sulphur and containing a quantity of gunpowder. The detonator consists of a small metal cylinder containing a mixture of fulminate of mercury and chlorate of potash. When fired electrically, they each contain in addition a "fuse-head," which consists of a highly inflammable mixture of copper acetylide and collodion, in which firing wires are embedded. When fired alone, the fuse-head gives a small burst of flame and but little noise. The powder-fuse gives a larger volume of flame and a distinct report. The detonator gives a large volume of flame and the loud report distinctive of detonation. Schlieren photographs, obtained when (*a*) a 5-grain powder fuse, and (*b*) a No. 6 copper cased fulminate detonator are pushed through the stopper at one end of the experimental tube filled with air only, and fired, are shown in figs 22 and 23, respectively, whilst the dark portion in the upper left-hand corner of fig. 26 shows the type of record obtained in the same manner with a fuse-head only. With the fuse-head a faint shock-wave travelling approximately at the speed of sound can be seen on the negatives. With the powder-fuse (fig. 22), two pairs of shock-waves are sent out which first join to give one pair and finally produce a single wave. The gaseous products, which cut out light from the film and produce the dark portion in the photograph, are seen to be of much greater volume than with the fuse-head alone, and to advance much farther along the tube. The detonator (fig. 23) gives a wave moving rapidly and followed closely by the gaseous products of its detonation.

The different effects due to these mild, medium and strong sources of ignition of the hydrogen-oxygen mixture are shown in figs. 24, 25 and 26. After the first few centimetres travel the flame initiated by a fuse-head (fig. 26) proceeds in the same manner and at approximately the same speed as when the same mixture is fired by a spark (*cf.* fig. 27). Ignition may therefore not take place until some time after the fuse-head begins to fire. There appears to be

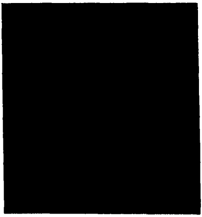

FIG 22.—Powder-fuse into Air

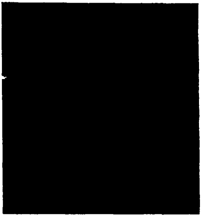

FIG 23.—Detonator into Air.

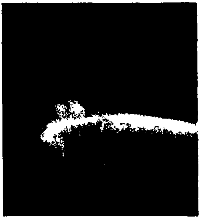

FIG. 24.—Ignition by Powder-fuse.

FIG 25.—Ignition by Detonator

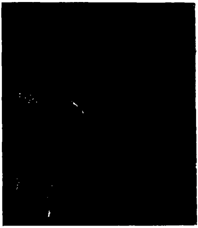

FIG. 26.—Ignition by Fuse-head.

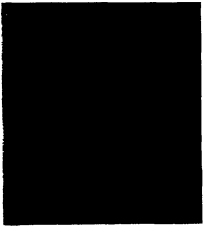

FIG. 27.—Ignition by Spark.

a similar lag, though by no means so considerable, when the mixture is fired by a powder fuse (fig. 24), and the more powerful nature of this mode of ignition is shown by the earlier initiation of detonation. When fired by a detonator (fig. 25), detonation is set up apparently instantaneously.

In conclusion, the author expresses his thanks to the Explosives in Mines Research Committee for permission to publish the results in this paper.

Summary.

An experimental method has been developed for photographing the invisible shock or compression-waves sent out through a gas mixture on the detonation of a solid or gaseous explosive in contact with the mixture, and has been applied to the study of the pre-detonation period and the inception of detonation in gaseous mixtures.

The effect of the position of the point of ignition on the initial movement of the flame in a closed tube has been examined, and an explanation advanced for the observed retardation of the flame, which suggests that it occurs simultaneously with the break-up of the flame front into two separate portions moving in opposite directions.

Visible evidence has been obtained of the movements of the hitherto invisible compression-waves, the character of which has been previously postulated from their effects on the flame. These are not due to the spark, as has been previously supposed, the spark-wave being comparatively feeble. The former waves travel at speeds much greater than that of sound in the gaseous medium through which they are passing, and appear to have their origin in the gases through which flame has passed and in which combustion has commenced some time previously. They appear to be due to renewed chemical activity of some kind behind the flame front. In the same way, under the experimental conditions, and with the mixtures used, the detonation-wave always appears to have its origin behind the flame front.

Other things examined by means of the experimental method were the influence of the compression-waves on the movements of the flame, when restrictions are present before detonation is set up, and their mode of propagation during the suppression of detonation when the flame passes from a narrow into a wider tube. Finally, a comparison was made between the inception of detonation in a gas mixture by different initiators.

The Zeeman Effect in the Band Spectrum of Helium.

By W. E. Curtis, D.Sc., Professor of Physics, Armstrong College, Newcastle-upon-Tyne, and W. Jevons, D.Sc., Lecturer in Physics, Military College of Science, Woolwich.

(Communicated by Prof. H. C. Plummer, F R S —Received May 15, 1928.)

1. *Introductory.*

Although a considerable amount of experimental work has been done on the Zeeman effect in band spectra, it is only recently that results of real value have been secured. The reasons for this may be summarised as follows :—

(*a*) The experimental difficulties are formidable, since -

(i) The intensities of band lines are much less than those of most atomic lines which have been investigated, and very long exposures are therefore necessary.

(ii) The small spacing of the lines prevents the use of a dispersing system of high resolving power, but economical in light, *e.g.*, a low-power prism spectrograph crossed by an echelon ; a large grating is practically essential.

(iii) The effects themselves are usually much smaller than for atomic lines, except for a few lines near the band-origin : unfortunately, these are in general of relatively low intensity, and are very liable to be confused with other lines of the band.

(*b*) Theoretical guidance has been lacking in most of the researches in question, and therefore such results as have been obtained are of little immediate value, since the interpretation of the lines themselves was not known. It is true that in recent years most of the lines studied have been allocated to branches by other workers, but it is a somewhat laborious and difficult task to correlate the two sets of data. We have been occupied for some time with such a systematic comparison, but the results are rather fragmentary, and not capable of presentation in a concise form. They clearly point to the desirability of new observations planned with regard to recent theoretical developments. Effort could then be concentrated in the directions most likely to yield definite results.

The band spectrum characteristics which are specially favourable for this type of investigation are as follows :—

(1) High absolute intensity, capable of being produced and maintained for long periods under the special conditions obtaining, *i.e.*, in a narrow gap traversed by an intense magnetic field, and development in a source permitting the use of a Back box in conjunction with the electromagnet, so that the pole-gap may be reduced to a smaller width than would be possible with a discharge tube.

(2) Lines comparatively few in number, spaced as widely as possible, and having their intensity maxima not too far from the band-origin. These characteristics are all associated with emitting molecules of small moment of inertia.

(3) As few branches as possible, consisting of single lines.

The helium band spectrum, upon the analysis of which one of us has been engaged, satisfies conditions (2) and (3) exceptionally well. It is less satisfactory as regards condition (1), since it has not yet been found possible to excite it with such great intrinsic brilliance as in many other cases. With increasing current density the band spectrum increases in intensity up to a maximum, and then declines. Further, it is not well developed in a tube of very small cross-section, such as is suitable for placing in the small air gap of an electromagnet. In an ordinary Plücker tube, for example, it can be obtained quite brightly in the bulbs, but is scarcely visible in the capillary. As it seemed possible, however, that both these difficulties might be considerably reduced by employing special forms of discharge tube and electromagnet, it was thought that observations for the Zeeman effect should be worth undertaking. It was clear from the outset that the instrumental facilities available, both spectroscopic and magnetic, would not suffice for a satisfactory quantitative study of the phenomena—that is to say, for resolution and measurement of the Zeeman patterns, but the scarcity of interpretable data on the subject seemed to justify an attempt to obtain even qualitative results.

2. *Experimental Arrangements.*

Two spectrographs were employed, (i) an Eagle spectrograph with a Rowland grating of 235 cm. radius of curvature, giving a dispersion of about 2·35 A./mm. in the third order, and (ii) a 1-cm. Fabry-Perot étalon in conjunction with a glass prism spectrograph (Hilger "constant deviation" type). The ranges of wave-lengths investigated with the grating were 4758–4365 Å.U. and 4161–3626 Å.U., whilst the range covered by the étalon spectrograph was 5000–4300 Å.U. approximately.

The discharge tubes used were of H pattern, with copper strip electrodes sealed into the upper ends of the vertical limbs, which were of circular section and about 1·5 cm. diameter. The horizontal limb consisted of a 16-cm. length of tubing of approximately elliptical cross-section,* the major axis of the ellipse being vertical and about 12 mm. internally, and the minor axis about 4 mm. internally. The considerations which led to the selection of this form of tube were as follows:—

As already mentioned, the band spectrum is developed only where the cross-section of the tube is fairly large– say half a square centimetre or more: hence, to investigate the spectrum in a magnetic field, with a tube of circular section, the pole-gap would have to be unduly widened, and the field intensity thereby seriously reduced. The elliptical tubing enabled a relatively large cross-section to be inserted in a reasonably narrow gap, the direction of the field being, of course, along the minor axis. The gap was about 8 mm., *i.e.*, very little more than would have been used if a capillary tube were admissible: thin sheets of mica were interposed between the tube and the pole faces.

Again, to secure sufficient luminosity for photography in the third order of the grating, it was necessary to observe the horizontal portion of the discharge end-on. The whole length of this limb of the tube had, therefore, to be enclosed in as uniform a field as possible. Fortunately, with the electro-magnet available this condition was nearly fulfilled: the magnet has large pole-pieces which taper to rectangular faces 14 cm. in length and 5 cm. in height. The tube was supported with the horizontal limb between these faces, and the vertical limbs just outside them, as indicated in fig. 1. It may be noted that in the line of the end-on observations a small portion of the discharge (at the junction of the vertical and horizontal limbs) was in a very much weaker field than the main (horizontal) portion. It is unlikely that this lack of homogeneity can have seriously impaired the resolution of Zeeman components of the He_2 band-lines, since those of the atomic He lines were clearly resolved in every grating spectrogram.

The earliest observations were made without a polarising prism (*i.e.*, perpendicular and parallel polarisations were superposed), and were confined to the bands of greatest photographic intensity: the whole apparatus was mounted as near as possible to the slit of the grating spectrograph, and exposures of about one hour sufficed; for such periods a current of 9 amperes could be maintained with safety in the magnet windings, giving a field of about

---

* As this elliptical tubing may be found useful for end-on observation of the discharge in other spectroscopic investigations, it may be mentioned that Messrs. James Powell and Sons (Whitefriars), Limited, Wealdstone, Middlesex, supply it in various sizes, both in lead- and in soda-glass.

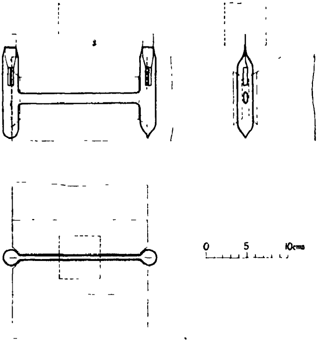

Fig. 1.—The disposition of the discharge tube in the pole-gap of the electromagnet, shown in side-elevation, end-elevation and plan. The right-angled prism used for the étalon exposures is shown in broken lines.

20,000 gauss in the 8-mm. gap. For the less intense bands the exposures necessary were about two hours, and the field current was reduced to 8 amperes, giving about 18,000 gauss. A field-on exposure and a no-field exposure were made on the same plate with the same instrumental settings.

In the later series of observations, in perpendicular and parallel polarisations separately, a lens was used to project on the slit the images of a central section of the horizontal limb of the discharge, and a double-image prism was interposed between the tube and the lens. In this series the exposures were much longer; in some cases about seven hours for one polarisation, even with the fast plates used (Ilford "Monarch"); for such periods a magnet-current of only 6 amperes could be maintained and the field was correspondingly smaller, about 15,000 gauss. For a given spectral region the exposures in the two polarisations were made on the same plate, but on two successive days, in order that the magnet might cool down overnight; a no-field exposure was also made on the same plate. Many trials were necessary before the three photographs on one plate were obtained with approximately equal densities.

For the exposures with the Fabry-Perot étalon, which were, as far as possible, made simultaneously with the grating exposures, the middle of the horizontal limb of the discharge was observed "broadside-on" by means of a right-angled prism supported over the tube and pole-gap, as shown in fig. 1. Thus the field was quite uniform over the portion of the discharge used in these observations. A second double-image prism and lens produced the polarised images on the slit of the étalon spectrograph, exactly as with the grating. The exposures necessary were of the same order as in the case of the grating.

3. *Notation: Tabulation of the Results of the Observations.*

Neither the grating nor the étalon spectrograms showed clear resolution of any line* of the He_2 bands into Zeeman components, although the splitting of the atomic He lines was very well shown in the grating plates. The effect of the field on the band-lines was shown as a broadening with a diminution of intensity, the broadening in the most marked cases being less than the width between the outer (⊥) components in the "normal" atomic Zeeman triplet. In the tables rough estimates of the degrees of broadening of the lines are indicated by letters: the estimates were made by direct comparison, without attempting actually to measure the widths, of the line without field and with field (both polarisations superposed).

(*a*) Not appreciably affected.
(*b*) Only very slightly affected.
(*c*) Slightly to moderately affected.
(*d*) Markedly affected.
(*e*) So greatly affected that the line was suppressed entirely or almost entirely. The significance of (*e*) is, of course, much greater for a strong line than for a weaker line: the apparent suppression of a very weak line does not necessarily imply a really big effect of the field.

In the case of lines for which two letters are given, the magnitude of the effect was more than usually difficult to decide: the first letter given was judged to describe the effect, though the second one given also seemed possible. Following the letter in the Z.E. column is, in some cases, the symbol ⊥ or ||, to denote the polarisation in which the width of the line appeared to be the greater; if resolution of the Zeeman components had been effected, the polarisation denoted by the symbol given would, presumably, be that in which the outermost components were stronger. The = sign indicates that the line was photographically recorded in both polarisations separately, but no difference could be detected in the ⊥ and ‖ widths. A blank space in this column indicates that although the line in question was present in the field-on spectrograms taken without the double-image prism, it could not be detected in those taken with that prism interposed.

---

* With one exception noted later (p. 123).

Table I gives the observations for lines which have been previously allocated to bands by Curtis,* Curtis and Long,† and Weizel and Füchtbauer.‡ Except in the case of one branch, to which particular reference will be made later (p. 124), only the first three lines of each branch are included in the table, as no effect was detectable with certainty in the grating plates for the fourth and succeeding lines of each of these branches. The electronic transitions are those given by Mulliken,§ but the rotational quantum numbers (j) are all less by one-half than those he used.¶ As he has pointed out,** this reduction is necessary in order to bring the values into accordance with the "true" j-values indicated by the new mechanics In further explanation of the tabulated j-values, it may be mentioned that Mecke†† recognised in the He_2 bands an extreme case of the phenomenon of alternating intensities of band-lines of symmetrical molecules—extreme in the sense that alternate lines in each branch are so weak that they have never been observed. Mulliken has developed a scheme of rotational energy levels in which (i) each level consists of two sub-levels A and B in ^1D and in ^1P states, and consists of only the B sub-level in ^1S states; and (ii) in accordance with Mecke's hypothesis of missing alternate lines, sets of alternate sub-levels are suppressed. The unsuppressed sub-levels are‡‡ .—

---

* 'Roy. Soc. Proc.,' A, vol. *101*, p. 38 (1922).

† 'Roy. Soc. Proc.,' A, vol. 108, p. 513 (1925).

‡ 'Z. f. Physik,' vol. 44, p. 431 (1927).

§ 'Proc. Nat. Acad. Sci,' vol. 12, p. 158 (1926).

¶ 'Phys. Rev.,' vol 28, p. 1202 (1926).

** p. 1204 of previous reference; also 'Phys. Rev.,' vol. 28, p. 506 (1906); and vol. 29, p. 649 (1927).

†† 'Phys. Z.,' vol. 26, p. 227 (1925).

‡‡ It is to be noted that the designations A and B for the rotational sub-levels are assigned in accordance with Mulliken's original scheme ('Phys. Rev.,' vol. 28, p. 1202 (1926)). He has recently ('Phys. Rev.,' vol. 30, p. 785 (1927)) proposed that this should be modified in order to bring it into harmony with theoretical conclusions of Hund. It was thought preferable, however, to adhere to the original notation in this communication, since the theoretical position is still hardly stable enough to justify such a change if confusion is liable to be introduced thereby.

In ^1S states, B sub-levels .... $j = 1, 3, 5, 7, \ldots$

In ^1P states $\begin{cases} \text{A sub-levels} \;.\; j = 1, 3, 5, 7, \ldots \\ \text{B sub-levels} \;..\; j = 2, 4, 6, 8, \ldots \end{cases}$

In ^1D states $\begin{cases} \text{A sub-levels} \;..\; j = 2, 4, 6, 8, \ldots \\ \text{B sub-levels} \;.\; j = 3, 5, 7, \ldots \end{cases}$

In view of these complications it seems desirable to designate a line fully by means of the rotational sub-levels of both (initial and final) states, as is done in Table I. For descriptive purposes, however, it is convenient to adhere to the usual method of designation by the branch letter and a numeral; for the numeral we shall here use the j-value of the final rotational sub-level.[*] The numeration used originally by Curtis has therefore to be modified in accordance with the following scheme, which gives the original and the present numerations for the first, second, third ..... lines of each branch of the bands included in Table I :--

Branch.	P	P′	Q	R	R′
Original	2, 3, 4, ...	1, 2, 3, ...	1, 2, 3, ...	2, 3, 4, ...	1, 2, 3, ...
Present	3, 5, 7, ...	2, 4, 6, ...	1, 3, 5, ..	2, 4, 6, ...	1, 3, 5, ...

The original symbols P′ and R′ are retained for convenience.

Finally, it must be noted that Mulliken has shown that the electronic states involved in the " main " Rydberg series of bands ($\tau P \rightarrow 2S$, $\tau = 3, 4, 5, \ldots 10$) and the related bands λ 6400 ($3S \rightarrow 2P$), λ 5730 ($3D \rightarrow 2P$) and λ 4546 ($4S \rightarrow 2P$) correspond to the triplet[†] terms of the He atom (formerly regarded as doublet terms—those of the so-called " ortho-helium doublets "), and that the electronic states of the " second " Rydberg series of bands ($\tau P \rightarrow 2S$, $\tau = 3, 4, 5, 6$) correspond to the singlet terms of the He atom (those of the so-called " par-helium singlets "). Mulliken suggests that two types of molecule are formed : one (which emits the " main " family of bands) composed of two ortho-He atoms each in the metastable $2\,^3S$ state, and another (which emits the " second " series of bands) composed of two par-He atoms each in the metastable $2\,^1S$ state ; it is convenient to designate these molecules as o-He_2 and p-He_2 respectively.

---

[*] In conformity with the National Research Council Bulletin on " Molecular Spectra in Gases," and with Kemble, Mulliken and Crawford, ' Phys. Rev.,' vol. 30, p. 438 (1927), to both of which reference is made in a later section.

[†] Burger, ' Z. f. Physik,' vol. 38, p. 437 (1926) ; Houston, ' Phys. Rev.,' vol. 29, p. 747 (1927).

The electronic states of both molecules appear to be of the singlet type, ^1S, ^1P, ^1D. Sommer,* in a study of effective quantum numbers, regards the electronic states for the ortho-He_2 bands as triplet, ^3S, ^3P, ^3D. A consideration of the missing lines of these bands seems, however, to support Mulliken's earlier view that these states, like those of par-He_2, are of singlet type. If they are actually triplet the separations are so small that, with the fields used, the Zeeman patterns may be expected to approximate closely to those which would be given by singlet electronic states, assuming that there is a molecular Paschen-Back effect of the same nature as the atomic.

The wave-lengths already recorded by Curtis and by Curtis and Long have been adopted in Table I. All the other wave-lengths tabulated have been determined from plates taken in the course of this investigation prior to the appearance of Weizel and Füchtbauer's paper. In every case our wave-length is close enough to theirs to show beyond doubt that both pertain to one and the same line. Lines given in the above-named investigations, but not satisfactorily recorded in our field-on plates, are excluded from Table I.

A few lines noted by Weizel and Füchtbauer as blended with neighbouring lines of the same band, or as hidden by stronger lines of another band, are resolved in our plates, which are of higher dispersion—*e.g.*, the first two Q-branch lines of the 1 → 1 band (λ 4668) of the *o*-He_2 system 3P → 2S, which are given as imperfectly resolved by Weizel and Füchtbauer, are quite separate in our plates (see Table I), again, in the P branch of the same band the first two lines are not given by Weizel and Füchtbauer (who remark that the second line is hidden by a stronger line), but are present in our plates. More noteworthy, however, is the fact that in the *o*-He_2 system 4P → 2S (Table I) our plates show the fifth line of the Q branch as an anomalous doublet in both the 1 → 1 band (λ 3689) and the 0 → 1 band (λ 3926), *i.e.*, a perturbation exactly like that found by Curtis and Long in the case of the corresponding line of the 0 → 0 band (λ 3676): the three measured doublet separations are: 0 → 0 band, 6·5 cm.$^{-1}$; 1 → 1 band, 6·6 cm.$^{-1}$; 0 → 1 band, 6·8 cm.$^{-1}$. Weizel and Füchtbauer give only one component of the anomalous doublet in the 1 → 1 and in the 0 → 1 band.

---

* 'Proc. Nat. Acad. Sci.,' vol. 13, p. 213 (1927); 'Nature,' vol. 120, p. 841 (1927).

Table I.—Effects on Band Lines of P → S and S → P Systems (Grating Observations).

Branch	Line (Initial and Final Sub-levels j′ → j″)	o-H₂ System 3P → 2S								o-H₂ System 4P → 2S											
		0 → 0 Band				1 → 1 Band				0 → 0 Band				1 → 1 Band				0 → 1 Band			
		λ_{air}	$\nu_{vac.}$	Z E	Notes	λ_{air}	$\nu_{vac.}$	Z E	Notes	λ_{air}	$\nu_{vac.}$	Z.E	Notes	λ_{air}	$\nu_{vac.}$	Z.E.	Notes	λ_{air}	$\nu_{vac.}$	Z E	Notes
P	$2_B \to 3_B$	4658·78	21458·8	bc =(?∥)	i					3683·02	27143·9	bc ?=		3695·65	27051·2	?	vii viii	3933·68	25414·3	?	vii
	$4_B \to 5_B$	64·83	421·5	ab =						88·29	105·1	ba =		3700·79	013·6	·		39·05	379·7	b	
	$6_B \to 7_B$	75·67	381·3	a =		4692·49	21304·7	a		94·31	061·0	b =	v					44·98	341·9	b	v
Q	$1_A \to 1_B$	4648·48	21506·4	d ∥	ii	4668·05	21416·3	d	iii	3676·49	27192·0	d ∥		3689·29	27097·8	ab		3926·56	25460·3	d	
	$3_A \to 3_B$	49·35	502·3	b ?∥		68·44	414·5	a		77·11	187·5	b =(?∥)		89·88	093·5	b		26·93	458·0	c ?∥	
	$5_A \to 5_B$	51·00	494·8	ab ?∥					iv	78·22	179·3	b =					iv	27·54	454·0	b =	
	$7_A \to 7_B$	53·32	484·0	a =		70·67	404·8	a		79·84	167·4	b =		92·54	073·9	bc		28·46	448·5	b =	
	$9_A \to 9_B$	56·35	470·1	a =		73·63	390·7	c		81·29 82·17	156·7 150·2	ad² ?∥ d ∥	ii	94·16 95·06	062·1 055·5	de e	vi ix	28·77 29·81	446·1 439·3	?c de	vi x
R′	$2_B \to 1_B$	4642·38	21534·7	b =(?∥)						3672·77	27219·7	b					viii	3922·34	25487·8	?b	viii xi
	$4_B \to 3_B$	37·34	558·1	a =						69·86	241·3	b =		3682·82	27145·4	?a		18·66	511·7	ab	
	$6_B \to 5_B$	33·18	577·4	a =						67·74	257·0	b =	v	80·94	159·4	c	v	15·57	531·9	c	v

Branch	Line (Initial and Final Sub-levels j′ → j″)	o-H₂ System 4S → 2P			
		0 → 0 Band			
		λ_{air}	ν_{vac}	Z E.	Notes
P′	$1_B \to 2_B$	4551·82	21963·2	ba	vii
	$3_B \to 4_B$	58·20	932·4	a	
	$5_B \to 6_B$	64·82	900·6	a	
Q	$1_B \to 1_A$	4545·80	21992·2	c ∥	
	$3_B \to 3_A$	46·21	990·2	b ?∥	
	$5_B \to 5_A$	46·93	986·7	ab	
R	$3_B \to 2_B$	4537·14	22034·1	?	vii
	$5_B \to 4_B$	31·71	060·6	a	
	$7_B \to 6_B$	26·66	085·1	a	

Branch	Line (Initial and Final Sub-levels j′ → j″)	p-H₂ System 4¹P → 2¹S				p-H₂ System 5¹P → 2¹S			
		0 → 0 Band				0 → 0 Band			
		λ_{air}	ν_{vac}	Z E	Notes	λ_{air}	ν_{vac}	Z E	Notes
P	$2_B \to 3_B$	4010·12	24929·9	ba ?=					vii
	$4_B \to 5_B$	16·47	890·5	ba =		3646·39	27416·0	b	
	$6_B \to 7_B$	23·58	846·5	a =		52·54	370·4	b	
Q′	$1_A \to 1_B$	4002·30	24978·5	d ∥		3634·36	27507·2	?	vii xii
	$3_A \to 3_B$	03·17	973·2	ba =		35·15	501·4	c	
	$5_A \to 5_B$	04·73	963·4	ab =		36·50	491·2	b	
R″	$2_B \to 1_B$	3997·85	25006·4	ad ⊥					vii
	$4_B \to 3_B$	94·36	028·1	a =					
	$6_B \to 5_B$	91·78	044·4	ab =					

NOTES TO TABLE I.

See p. 114 for notation used to describe Z.E. observations.

(i) The doubt as to the grating observations of this line in the two polarisations separately is resolved by the étalon observations, which give it unmistakably as broader in ⊥, in agreement with the theoretical expectation.

(iii) The best spectrogram in ‖ polarisation shows this line just resolved into a symmetrical doublet, separation about *one-third-*" normal."

(iii) These lines were unresolved by Weizel and Füchtbauer.

(iv) Hidden by the stronger line Q (15) of the 0 → 0 band of the same system.

(v) Perturbation (displacement) does not show any specially large Zeeman effect.

(vi) Perturbation (anomalous doublet). both components show large Zeeman effects.

(vii) The lines of this branch are so faint in the field-on plates that no certain conclusions can be drawn as to their Zeeman effects.

(viii) These two lines are not given by Weizel and Füchtbauer, but are shown in our plates both without and with field. Their Zeeman effects, however, are uncertain, the first line being too faint, and the second too near P (9) of the 0 → 0 band of the same system.

(ix) This component of Q (9) is not given by Weizel and Füchtbauer It appears to be a very close doublet, the fainter component being suppressed by the field

(x) This component of Q (9) is not given by Weizel and Füchtbauer.

(xi) Weizel and Füchtbauer give the wave-*numbers* of these two lines, together with the wave-*lengths* of two neighbouring lines ($\lambda\lambda$ 3922·58 and 3918·92, both of which are present in our plates).

(xii) The possibility that the He line λ 3634·37 may be feebly developed in addition to the superposed Q (1) renders the Z.E. observation uncertain.

4. *Bands of* P → S *and* S → P *Systems.*

In order to discuss the significance of the observations for the He_2 bands shown in Table I, we must first quote briefly the theoretical predictions of Kemble* for the Zeeman patterns of band-lines, especially those of bands due to electronic transitions between ^1P and ^1S states, since each of the He_2 bands in Table I may be considered to correspond to such a transition.†

All theories yet developed predict for the Zeeman patterns of the lines of each branch of a band (i) a symmetry about the position of the line without the field; (ii) a width which is greatest for the faint lines (of lowest j-values) near the band-origin and diminishes rapidly as j increases, so that lines remote from the origin are not appreciably affected by the field, and (iii) a complexity which increases with j (*i.e.*, increases as the width decreases), each energy level of the molecule becoming split by the magnetic field into (exactly or approximately) $2j$ equidistant magnetic sub-levels.

Further, electronic energy levels of the ^1S type are unaffected by the field, and the same is very nearly true of levels of the ^2S, and, indeed, of any S type. Thus bands corresponding to any S → S electronic transition should show no Zeeman effect of the first order of magnitude: this prediction has been verified experimentally by Watson and Perkins‡ in the case of the $^1S \rightarrow {}^1S$ bands of AgH.

---

* 'N. R. C. Bulletin' on "Molecular Spectra in Gases," pp. 337–343, and 352, 'Phys. Rev.,' vol. 27, p. 799, abs. 19 (1926), and vol. 30, p. 438 (1927).

† See note on p. 117.

‡ 'Phys. Rev.,' vol. 30, p. 592 (1927).

Bands corresponding to a transition P→S or S→P should show Zeeman patterns due entirely to the splitting of the rotational energy levels of the P electronic state. For the ^1P state Kemble predicts that a rotational energy level should split into $(2j+1)$ magnetic sub-levels, with an over-all range of $2\Delta\nu_n/(j+1)$, where $\Delta\nu_n = eH/4\pi mc^2 = 4{\cdot}70 \, . \, 10^{-5}\,\mathrm{H}\ \mathrm{cm.}^{-1}$, the half-width of the "normal" Zeeman triplet in atomic spectra, and j is the "true" total rotational quantum number (corresponding to the total angular momentum) as given by the new quantum mechanics.*

In the case of the Ångstrom ($^1S \rightarrow {}^1P$) bands of CO, the "true" values of j'' are identical with the values of the ordinal number (M) for the lines in each of three branches, M being unity for the first observed line in each branch. Hence the Zeeman pattern for the Mth line in a branch should consist of $(2M+1)$ equidistant components in a range of $2\Delta\nu_n/(M+1)$, the predicted intensities being given by expressions also obtained by Kemble. Kemble, Mulliken and Crawford† have summarised these theoretical results for the transition $^1S \rightarrow {}^1P$ by means of diagrams showing the number, spacing and relative intensities of the components in the ⊥ and ‖ polarisations in the predicted patterns for the first four lines of each branch. They have obtained striking experimental confirmation of these predictions in the case of the Ångstrom bands of CO. Their diagrams apply not only to the corresponding twelve lines (having $j'' = 1, 2, 3, 4$) of any $^1S \rightarrow {}^1P$ bands, but also to the lines having $j' = 1, 2, 3, 4$ in each branch of any $^1P \rightarrow {}^1S$ bands, *e.g.*, those of CO (the "4th positive" bands), AlH, Na_2, SiO and CS. For $^1P \rightarrow {}^1S$ bands the pattern for the line R (j) due to the (electronic and Δj) transition $(^1P, j+1) \rightarrow (^1S, j)$ is identical with that for the CO Ångstrom band-line P $(j+1)$, due to the reverse transition $(^1S, j) \rightarrow (^1P, j+1)$; and, similarly, the predicted pattern for the line P (j) is identical with that for the CO Ångstrom line R $(j-1)$: that is to say, the patterns for the R and the P branches are interchanged, while the Q-branch patterns are identical for the two ($^1S \rightarrow {}^1P$ and $^1P \rightarrow {}^1S$) band-systems. Experimental verification has been obtained by Watson and Perkins (*loc. cit.*) in the case of the $^1P \rightarrow {}^1S$ band $(0 \rightarrow 0)$ of AlH.

In applying the predictions for CO to the He_2 bands shown in Table I, account must be taken of the suppression of alternate rotational energy sub-levels A and B. The results may conveniently be summarised as in Table II.

---

* As already mentioned on p. 115, j, according to the new quantum mechanics, is less by $\frac{1}{2}$ than the value given by the older "conventional" quantum theory.

† *Loc. cit.* (see fig. 1, p. 444).

Table II.—Predicted Zeeman Effects for $^1S \rightarrow {}^1P$ and $^1P \rightarrow {}^1S$ Band-lines of He_2.

Type of Band (Electronic transition, and example in He_2).	He_2 band-line.			CO Ångstrom band-line having same or reverse transition, and, therefore, the same Zeeman pattern.	Number of Zeeman components	Width of Zeeman pattern in terms of width of "normal" triplet
	Rotational transition.	Original notation.	Present notation.			
$^1S \rightarrow {}^1P$ o-He_2 : 4546, 4030	$1_B \rightarrow 2_B$ $3_B \rightarrow 4_B$	P′ (1) P′ (2)	P′ (2) P′ (4)	P (2) P (4)	5 9	$\frac{1}{3}$ $\frac{1}{5}$
	$1_B \rightarrow 1_A$ $3_B \rightarrow 3_A$	Q (1) Q (2)	Q (1) Q (3)	Q (1) Q (3)	3 7	$\frac{1}{2}$ $\frac{1}{4}$
	$3_B \rightarrow 2_B$ $5_B \rightarrow 4_B$	R (2) R (3)	R (2) R (4)	R (2) R (4)	5 9	$\frac{1}{2}$ $\frac{1}{3}$
$^1P \rightarrow {}^1S$ o-He_2 : 4648, 4668, 3676, 3689, 3926 p-He_2 : 4002, 3635	$2_B \rightarrow 3_B$ $4_B \rightarrow 5_B$	P (2) P (3)	P (3) P (5)	R (2) R (4)	5 9	$\frac{1}{3}$ $\frac{1}{5}$
	$1_A \rightarrow 1_B$ $3_A \rightarrow 3_B$	Q (1) Q (2)	Q (1) Q (3)	Q (1) Q (3)	3 7	$\frac{1}{2}$ $\frac{1}{4}$
	$2_B \rightarrow 1_B$ $4_B \rightarrow 3_B$	R′ (1) R′ (2)	R′ (1) R′ (3)	P (2) P (4)	5 9	$\frac{1}{3}$ $\frac{1}{5}$

See remarks on electronic states of o-He_2 on p. 117.

From this table it is seen that the Zeeman patterns for the first two lines of the three branches of either type of He_2 band in Table I are given by Kemble, Mulliken and Crawford's diagrams for P (2), P (4); Q (1), Q (3); R (2), R (4). These diagrams form the basis of fig. 2, which has been made to include the He_2 bands of the P → S type as well as those of the S → P type by the addition of the notation and transitions given in Table II for each type; those for P → S bands are given above, and those for S → P below, against each pattern.

The lengths of the vertical lines represent the predicted intensities, the parts above and below the horizontal lines corresponding to the parallel and the perpendicular polarisations respectively. For both polarisations superposed the intensities of the components are indicated by the heights of the dots above the horizontal lines.

With the aid of the diagrams we can enumerate a few salient features which should be observed with a spectrograph of resolving power just not sufficient to reveal the full details of the patterns of these lines :—

(i) In each band the first Q-branch line should be the most favourable for resolution into Zeeman components ; failing resolution there should be a very marked broadening (half-" normal ") in the || polarisation, and also in the superposed polarisations, and a less marked broadening in the ⊥ polarisation.

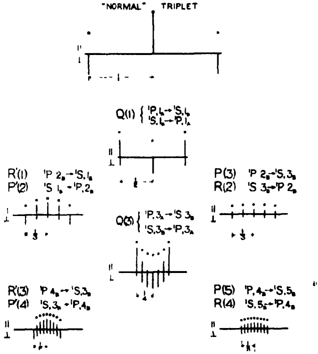
"NORMAL" TRIPLET
$Q(1)$ $\{ {}^1P,1_b \to {}^1S,1_b$; ${}^1S,1_b \to {}^1P,1_a$
$R'(1)$ ${}^1P\,2_a \to {}^1S,1_a$
$P'(2)$ ${}^1S\,1_a \to {}^1P,2_a$
$P(3)$ ${}^1P\,2_b \to {}^1S,3_a$
$R(2)$ ${}^1S\,3_b \to {}^1P\,2_a$
$Q(3)$ $\{ {}^1P,3_a \to {}^1S\,3_a$; ${}^1S,3_b \to {}^1P,3_a$
$R'(3)$ ${}^1P\,4_a \to {}^1S,3_a$
$P'(4)$ ${}^1S,3_a \to {}^1P,4_a$
$P(5)$ ${}^1P,4_b \to {}^1S,5_a$
$R(4)$ ${}^1S,5_b \to {}^1P,4_a$
||
⊥

Fig. 2.—Predicted Zeeman patterns for the first two lines of each branch of ${}^1P \to {}^1S$ and ${}^1S \to {}^1P$ bands of He_2. The unit employed in expressing the half-width is $\Delta\nu_n$, the "normal" atomic displacement.

(ii) Next to Q (1) in case of resolution of Zeeman pattern should come the first lines of the P and R′ branches in a P → S band, and those of the P′ and R branches in a S → P band. Just inadequate resolving power should show the first R′ or P′ line markedly broadened in the ⊥ polarisation and in the superposed polarisations, but less markedly broadened in the || polarisation. That is to say, the changes of broadening with polarisation should be opposite to those for Q (1). For the first P or R line the difference of breadth in the || and ⊥ polarisations should be in the same sense as for R′ or P′, but less marked, perhaps inappreciable.

(iii) The second Q line should be still less easy of resolution. With just insufficient resolving power there should be a broadening more marked in the || polarisation and in the superposed polarisations than in the ⊥ polarisation, as in the case of Q (1).

(iv) The second lines of the P (or P′) and R′ (or R) branches should be less broadened than the second Q line: the effects should be of the same kind as for the first lines of the same branches, but still less marked.

(v) Succeeding members of each branch should behave in the manner described in (iii) and (iv), but to a progressively diminishing extent, the effect becoming quite inappreciable before high *j*-values are reached. The absence of alternate lines in each branch means, of course, that the effects should appear to diminish more rapidly than in a band of similar type in which every line is developed, as in the cases of CO and AlH.

We will now return to the observational results shown in Table I. In a preliminary report* (prior to the appearance of the theoretical investigation referred to above) we described the main features of the earlier of our observations on the prominent band near λ 4648, the 0 → 0 band of the *o*-He_2 system 3P → 2S. Though made with inadequate resolving power and field strength, the observations are, it may be stated at once, in qualitative agreement with the above theoretical predictions for a $^1P \rightarrow {}^1S$ band. Thus in this band the Q (1) line shows the greatest broadening, which was estimated to be of the order two-thirds-" normal," and was found to be appreciably greater in the ∥ than in the ⊥ polarisation (*cf.* (i) above). In one of the grating plates obtained subsequently, Q (1) is just resolved in the polarisation into a symmetrical doublet, with a separation which has been found on measurement to be of the order one-third-" normal " ; whilst the measurement is not sufficiently precise to exclude positively the possibility of a half-" normal " separation, the two-thirds-" normal " previously reported (*loc. cit.*) is certainly an over-estimate. Further, the first lines of the R′ and P branches (R′ (1) and P (3) in the present notation) are less broadened than Q (1). The broadenings of these two lines in the ∥ and ⊥ polarisations were very difficult to compare in the earlier plates ; it first appeared that while the broadening of R′ (1) was probably greater in the ⊥ than in the ∥ polarisation, the opposite was the case in P (3), which was reported (*loc. cit.*) to show an effect similar to, but smaller than, that for Q (1). This last observation is not sustained by examination of subsequent plates in which this band was more heavily recorded in the two polarisations separately ; in the grating plates no difference of the broadenings of P (3) in the ∥ and the ⊥ polarisation is detected with any certainty (*cf.* (ii) above), but in the étalon plates the broadenings of both R and P lines are clearly shown to be greater in the ⊥ polarisation, while those of the Q lines are greater in the ∥ polarisation. In the étalon plates these effects are seen to diminish rapidly in each branch, with increase of rotational quantum number, but they are definitely traceable up to the fifth or sixth line (*cf.* (v) above).

---

* Curtis and Jevons, 'Nature,' vol. 116, p. 746 (1925).

Broadly speaking, the effects just described for the λ 4648 band are also observed in the other bands shown in Table I.

Particular mention must be made of the Q branches of all three bands, 0 → 0, 1 → 1 and 0 → 1, of the o-He_2 system 4P → 2S. In each case the broadening, which is greater in the || than in the ⊥ polarisation, as in the preceding band 3P → 2S just described, is greatest for the first Q line, and rapidly diminishes with increasing j-values, becoming almost inappreciable in the grating plates at the fourth line. At the fifth line Q (9), which, as was pointed out on p. 117, is an anomalous doublet with a separation of about 6·6 cm.$^{-1}$, the Zeeman broadening, instead of remaining almost inappreciable, becomes very large for both components of the anomalous doublet in each of the three bands of the system. In the 0 → 0 band the long-wave component λ 3682·17 of the perturbed Q (9) is broadened as much as, or perhaps slightly more than, Q (1): the short-wave component λ 3681·29 shows a still larger effect, being so diffuse in the field as to be almost invisible. The 1 → 1 and the 0 → 1 bands are so faint that no certain conclusions can be drawn from the observations, but it appears that in the 1 → 1 band the long-wave component λ 3695·06 is itself a close doublet whose fainter component is suppressed by the field. These three bands also show perturbations in the third lines of their R′ and P branches ($\Delta j = 6 \rightarrow 5$, and $6 \rightarrow 7$ respectively), but these lines do not appear to show any specially large Zeeman effect. If such exists, it is certainly much less in magnitude than for the perturbed Q (9), so that we may perhaps associate abnormal magnitude of Zeeman effect with the latter type of perturbation, namely, a splitting of the initial rotational energy sub-level, as distinct from the more commonly occurring displacement type. It would thus seem quite probable that the splitting in question has a magnetic origin.

5. *A New Band of o-He_2 and Unallocated Lines.*

In the regions covered by our plates there are a great many (over 300) lines recorded which have not yet been allocated to bands, although they must, with very few exceptions, be due to the helium molecule, since no trace of any impurity but hydrogen (atomic) has been found in the spectrum. It is not proposed to give here a complete list of these lines, but only to mention those which show particularly large effects.

There is a conspicuously regular group of lines in the neighbourhood of the He line λ 4472, noted by McLennan, Smith and Lea,* who regarded it as composed of a P and a P′ branch. In the course of an analysis of the He_2 spectrum which is now being made by one of us (W. E. C.) in conjunction with Mr. A. Harvey, it has appeared that the branches in question are in reality of R and Q type respectively.† They have a common set of initial levels and the final levels are the B and A rotational sub-levels of the 2P electronic state of *o*-He_2. The initial state is apparently single, and has an effective electronic quantum number 3·93, but its term designation is at present uncertain, and will be referred to here as Z. It shows certain unusual characteristics which will be described in another paper. The preceding term 3Z has also been identified in combination with 2P of *o*-He_2, giving two branches similar to the above in the region λλ 5950–6080, for which no magnetic data are available.

Particulars of the 4Z → 2P branches are given in Table III.

Table III.—Effects on Band-Lines of *o*-He_2 System 4Z → 2P.

Branch.	Line (initial and final sub-levels $j' \to j''$).	Int.	λ_{air}.	ν_{vac}.	Z.E.	Notes.
Q	$3_B \to 3_A$	1	4467·22	22,379·04	?	i
	$5_B \to 5_A$	1	78·03	325·02 *	*e* ⊥	i
	$7_B \to 7_A$	6	89·88	266·10	*d* ⊥	ii
	$9_B \to 9_A$	1–	4502·23	205·03	*ed*	
	$11_B \to 11_A$	0	15·16	141·40	?	
R	$3_B \to 2_B$	6	4458·43	22,423·16	*de* ⊥	
	$5_B \to 4_B$	8	63·32	398·60	*d* ⊥	
	$7_B \to 6_B$	8 ?	69·10	360·59	*d* ?	iii
	$9_B \to 8_B$	9	75·56	337·31	*d* ⊥	
	$11_B \to 10_B$	6	82·51	302·67	*d* ⊥	
	$13_B \to 12_B$	6	89·88	266·10	*d* ⊥	ii
	$15_B \to 14_B$	3	97·54	228·16	*d* ⊥	
	$17_B \to 16_B$	1	4504·54	193·64	*cd* ⊥	iv
	$19_B \to 18_B$	0	14·81	143·13	*cd* ?	

NOTES TO TABLE III.

See p. 114 for notation used to describe Z.E. observations.

i. Ghost superposed *on present plates.* Intensity estimated *from* plates *taken* with 10 feet grating of Imperial College, South Kensington.

ii. Blend of Q (7) and R (12).

iii. Recognition of effect difficult owing to proximity of ghost.

iv. Probably perturbed.

---

* 'Roy. Soc. Proc.,' A, vol. 113, p. 183 (1926).

† The R branch is the same as McLennan, Smith and Lea's P, but the Q branch differs considerably from their P′.

It will be seen that the broadenings are very marked throughout both branches, in striking contrast to the bands due to S → P combinations. In view of the known behaviour of the 2P state, we must conclude that the 4Z state is responsible for the relatively large effects observed. An attempt was made to estimate the amount of the broadening in the case of the stronger (R) branch, with the following results :—

R (2)	R (4)	R (6)	R (8)	R (10)
0·41	0·71	?	0·94	$0{\cdot}51 \times 2\Delta\nu_n$

These measurements are necessarily quite rough, since they are liable to be influenced by the intensity of the line ; but it seems clear that the effect is not only larger than that characteristic of S → P bands, but is related to the *j*-values in quite a different manner. Whereas previously the effect diminished rapidly as *j* increased, here it increases to a maximum and then shows a tendency to diminish. The broadening of the R lines is very much greater in the ⊥ polarisation than in the ∥, and the same appears to be true of the Q lines, although the polarisations are observable separately for only two of the latter.

It is worthy of note that the étalon observations on the R lines of this band in the absence of a magnetic field strongly suggest that they are sensibly broader than those of the S → P bands. This would indicate that a fine structure may have something to do with the unusual type of Zeeman effect.

In Table IV a list is given of unallocated lines which show well-marked broadenings in the field. This includes all lines of appreciable strength for

Table IV.—Effects on Lines Unallocated to Bands.

Int.	λ_{air}.	ν_{vac}.	Z.E.	Int.	λ_{air}.	ν_{vac}.	Z.E.
4	4679·78	21,362·6	*d*	2	4146·50	24,110·0	*e*
0	4516·92	22,132 8	*cb*	2	38·15	158·6	*e*
1	09·56	168 9	*d*	2	4044 21	719 7	*e*
1	02·35	204 4	*d*	6	18·99	874 9	*d*
1	4495 55	238·0	*d*	8	07·67	945·1	*d* — (?⊥)
1	89·31	268 9	*e*	6	3976 75	25,139·1	*d* ⊥
1—	83·75	296 5	*cd*	6	73·94	156 9	*e*
6	42 88	501 6	*dc* ⊥	4	63 90	220·6	*dc* =
5	42 40	504 1	*cd* ?⊥	4	3801·79	26,296 0	*de*
4	22·73	604·1	*d* ?=	5	3796·83	330·3	*d*
7	14 02	649 8	*d* ?=	5	91·93	364·3	*d*
7	02·60	707·5	*d* ∥	3	87·56	394·8	*d*
7	4396·93	736·8	*cd* ⊥	2	70·96	510·9	*ed*
8	95·14	746·2	*cb* ?∥	3	65·61	548·6	*ed*
4	92·67	758·4	*d* ∥				

which effects of magnitude *d* and *e* on our scale have been definitely established. There are many others showing unmistakable effects, but it does not appear that any useful purpose would be served by listing them at present. It is hoped, however, that the observations will be of material assistance in detecting regularities in the more complex regions which still remain to be analysed. The utility of the present results in this connection may be illustrated by reference to the lines bracketed together in Table IV. The similarity of the Zeeman effects affords a valuable confirmation of the proposed arrangement in two branches.

6. *Summary.*

The Zeeman effects in two regions of the helium band spectrum have been investigated in fields up to 20,000 gauss with an 8-foot concave grating (third order) and a Fabry-Perot 1-cm. étalon. Resolution of the magnetic components has only been effected in one case, but a great many instances of broadening, sometimes quite considerable in amount, have been observed, and some information as to the polarisation of the components has been obtained by means of a double image prism.

In the case of those bands which are due to transitions between S and P electronic states, the results are completely in accordance with theoretical predictions. The effects rapidly decrease in amount (*i.e.*, width of pattern) with increase of rotation, and the polarisation of the outer components is opposite in character for Q and PR type branches. In the case of another band, details of which have not been previously published, a totally different behaviour has been observed. The effects are relatively large throughout both Q and R branches (the P branch being too weak to observe), and they show similar polarisations. The final state of this band is known to be the 2P electronic state of the ortho-He_2 molecule, but the relation of the initial electronic state to the known term sequences of He_2 is not clear. It is designated as 4Z, it shows certain other peculiarities besides the exceptional magnetic behaviour.

A list is given of lines which show large magnetic effects, but are as yet unallocated to bands.

The authors have pleasure in thanking the Government Grant Committee of the Royal Society and the Research Fund Committee of Armstrong College for the Hilger micrometers used in these observations, and Prof. E. N. da C. Andrade for the use of the grating spectrograph and the electromagnet.

Studies in the Infra-Red Region of the Spectrum. Part I.—*Description of Prism Spectrometer and Apparatus.*

By Sir Robert Robertson, F.R.S., and J. J. Fox, D.Sc., Government Laboratory.

(Received June 21, 1928.)

INTRODUCTION.

For a projected investigation on the rate of decomposition of an explosive gas, arsenic hydride, it became necessary to know its absorption in the region of the infra-red From preliminary trials with a small infra-red spectrometer, a series of absorption bands possessing certain regularities was observed in this region, whereupon a larger prism instrument was obtained capable of giving values up to 17 μ.

Interest in the absorption spectrum of arsenic hydride led to the exploration of the same region for phosphine and for ammonia. In the following papers will be described the apparatus and methods adopted and the results found for these three gases, together with a comparison of inter-relationships and their bearing on molecular structure.

Many difficulties of technique had to be overcome, partly on account of the laboratory being situated near traffic and electric stations, and partly on account of incompleteness, it is thought, in the prescriptions and precautions described in the literature for work in this region. Thus attention had to be paid to the necessity for keeping the source of energy constant, for calibrating the mechanism for reading wave-lengths, for shielding the thermopile from variations in air pressure, for keeping a close watch on the temperature of the prism, especially when made of rocksalt, on account of the high temperature coefficient of its index of refraction, for accurate alignment of the observation tubes containing the gas, and for obtaining a galvanometer of great sensitiveness and freedom from external perturbations.

All these precautions must be adopted for accurate work, and it is necessary to maintain a constant watch on the whole apparatus lest " bands " of small intensity emerge which are in reality the effect of instrumental errors. Small irregularities in the bands themselves must be investigated very carefully for the same reason.

ARRANGEMENT OF APPARATUS.

The room in which the work was carried on was in the basement of the Government Laboratory and furnished with stone benches on brick piers; gas, water and electric power at 100 and 200 volts were available. It was the custom to work at a temperature as near to 18° C. as possible, as all readings were ultimately corrected for deviations of the index of refraction of the respective prisms from this temperature. In warmer weather, however, the temperature of the room was adjusted so as to keep the relative humidity as low as practicable, lest moisture should unduly affect bare rocksalt plates and lenses.

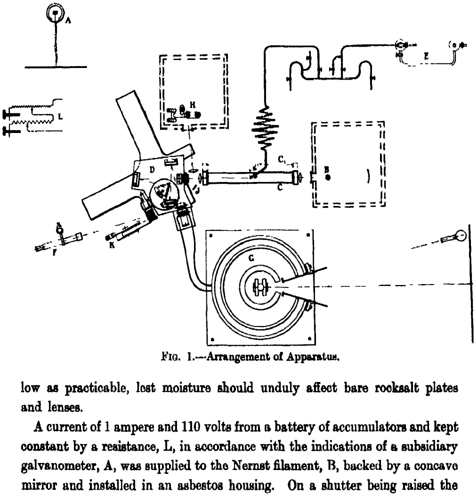

FIG. 1.—Arrangement of Apparatus.

A current of 1 ampere and 110 volts from a battery of accumulators and kept constant by a resistance, L, in accordance with the indications of a subsidiary galvanometer, A, was supplied to the Nernst filament, B, backed by a concave mirror and installed in an asbestos housing. On a shutter being raised the radiation passed through a rocksalt lens of 21 cm. focus and 5 cm. aperture and thence through an observation tube, C or C_1, the one empty, the other containing gas, mounted on a rocking arrangement for throwing them alternately into the optical path. A Toepler pump and taps were so arranged that gas could be drawn from the container E, passed to or withdrawn from an observation tube, and a " Hyvac " pump in series assisted in the evacuation of the system (see fig. 1).

After leaving the observation tube the beam was focussed on the collimator slit of the housed Hilger No. 2 infra-red spectrometer D, furnished with either a rocksalt prism (for which its wave-length drum was engraved), a quartz or a fluorite prism, and having a Wadsworth mirror for securing minimum deviation. To propel the wave-length drum smoothly the velvet-covered periphery of a low-geared wheel, K, engaged with the milled head of the drum, while the scale on the drum was read by the telescope F.

On emerging from the second slit of the spectrometer the radiation was received by a Hilger 20 element bismuth-silver thermopile, enclosed in an airtight casing, while the current generated here was carried by glass-encased leads to a galvanometer, G, of the Paschen type.

For calibration of the instrument as set up, the beam from a mercury lamp, H, was reflected into the spectrometer by means of the mirror, J, that could be swivelled into position when it was required for this purpose.

One operator regulated the current to the Nernst by observing the spot of light from the galvanometer A, opened or closed the shutter of the Nernst housing by means of a cord, brought the required observation tube into the optical path by means of lines, and observing the marking on the wave-length drum through the telescope F, caused it to progress a step in wave-length.

A second observer took the readings of the throw of the galvanometer G, recording the energy passing through the observation tubes of which the difference represents absorption.

SOURCE OF RADIATION.

Nernst Filaments.

Several sources of infra-red radiation were examined, and as a result it was decided to use Nernst filaments, since these gave the most uniform supply having regard to the intensity at different regions of the spectrum.

The Nernst filaments were 1·8 mm. diameter, 25 mm. long, and they last at least 250 hours. Attempts made to use laboratory-made rods and tubes of the same composition as that of the filament were not successful with the direct current used, owing to the formation of small arcs at the terminals where the fine platinum wires are inserted. On the whole, the Nernst filament is a satisfactory source of radiation for absorption work, as it attains a fairly high temperature (about 1600° K.) and has a good proportion of its emitted energy in the infra-red. Other sources of the radiation failed to give as much energy in the infra-red. Such were nichrome wire wound in a helix and almost surrounded by a mantle of fireclay. This was useful, however, in settling whether a hitherto unrecorded absorption band in fluorite was due to the prism of that substance or to a minimum in the energy curve of the Nernst filament. The carbon arc was much too unsteady for use. The Nernst filament mounted in a suitable holder was enclosed in an asbestos house which also contained the concave reflector and was supplied with a shutter to let out the radiation.

Control of Current.

Constancy of supply of current from the electric mains, both when taken directly and when balanced against a high-tension floating battery or passed through a bank of tungsten filament lamps, having been found unattainable, a battery of 25 six-volt, 60 ampere-hour storage cells was taken to supply current for the Nernst filament at 110 volts and 1 ampere. This battery was not discharged below one-half of its capacity. As there were some fluctuations, a small portion of the current was shunted through a D'Arsonval galvanometer with scale at 1 m. and balanced against a high-capacity cadmium cell, kindly supplied by Sir Richard Threlfall, to whom we are also indebted for the suggestion to raise all wires from the bench by supporting them on glass insulators. Except with a new filament, or one nearing the end of its life, the galvanometer spot remained fairly steady with a range of 2 cm on the scale and required only an occasional adjustment of the resistance to bring it back to zero. That this deviation is negligible is shown by the fact that 25 cm. on this subsidiary galvanometer scale represents 1 per cent. variation in the total energy as measured by the main galvanometer. The accompanying diagram shows the electrical arrangements.

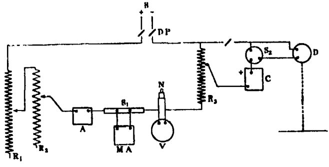

FIG. 2.—R_1, R_2, R_3, Variable rheostats with lead screw adjustments. B, mains leading from storage battery. A, Ammeter. M.A., Microammeter. V, Voltmeter. C, Large-capacity cadmium cell. D.P., Double-pole switch. N, Nernst filament D, D'Arsonval galvanometer. S_1, Shunt. S_2, Universal shunt.

Mounting for Filament and Lenses.

To prevent any shift in position due to vibration, it was found advantageous to insert the vertical supports for framework containing lenses and for the filament in heavy cones of lead with plane bases, as in Fig. 3. The frames and stems of the mirrors and lenses should be of massive construction.

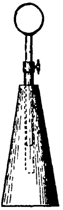

FIG. 3.—Mounting for Filament and Lens.

Housing of Filament.

As draughts were found to affect the constancy of the energy sent out from the incandescent filament, the filament and mirrors were enclosed in a frame-work covered with two layers of asbestos board with slag wool between them. This framework has a sloping roof from the apex of which the heated air passed through a chamber containing composition piping carrying a supply of cold water. In this way heat from the filament could be prevented from warming the air of the room, but this arrangement was not always used. Constancy of air flow past the filament, as well as a good supply of cold air, was secured by having a fairly large aperture at the bottom of the housing.

Effect of drying the System.

Energy curves in the region of $6 \cdot 25\ \mu$ showed a series of bands which coincided with those observed by Eva v. Bahr,* Hettner,† and Sleator and Phelps‡ for water vapour. To eliminate as much water as possible from the path of the beam, the apparatus was experimentally dried by solid drying agents and a stream of dried nitrogen in the spectrometer casing, and by passing dried CO_2 free air into the Nernst housing and into the space between these.

As the bands persisted they could not be attributed to water vapour in the path of the beam, nor do they arise from variations in the emitted energy of the Nernst filament, since they are reproduced when the radiation from an incandescent nichrome wire is used. The remaining possibilities are that they are due to some occlusion of water in the rocksalt windows or adsorption on them, or to a specific spectrum of fluorite. The latter is not likely since two inflexions of the energy curve (at 6·2 and 6·7 μ) with the rocksalt prism agree with similar ones with fluorite

---

* 'Deut. Phys. Ges.,' vol. 15, p. 737 (1913).

† 'Ann. der Physik,' vol. 55, p. 476 (1918).

‡ 'Astrophys J., vol. 62, p. 28 (1925).

Water in or on rocksalt windows seems, therefore, the most likely cause of the bands.

As the absorption of a gas is calculated from the difference between the energy passing through two similar tubes, one empty and one full of gas, these bands should not affect the percentage absorption at any point, when the empty tubes have been so adjusted as to pass the same energy.

This point was investigated further by interposing at 3·46 μ a column of dry HCl gas in the path of the radiation during a set of observations in front of a tube of an absorbing gas (ammonia) as well as the blank tube. In this region HCl has one of its most pronounced bands, but the absorption band of ammonia was in no way altered by the presence of the absorbing column of HCl gas in the separate tube. A similar observation was made by Sleator in his investigation of water vapour.*

Having regard to these experiments and considerations, the effect of water was discounted, especially when it was found that when the water bands occurred in a portion of the spectrum of a gas where there was no absorption, compensation occurred as between the two tubes, and a smooth record was obtained.

Optical System within the Housing.

After many arrangements of mirrors had been tried for obtaining the greatest energy from the filament, the simplest one, and that which gave the least loss of energy, was to place the filament in the main optical path directly facing the spectrometer slit and with a reflecting mirror (silvered and of 11 cm. focus and 5·5 cm. aperture) behind it. By this means some of the reflected radiation was returned along the path of the direct radiation, and an advantage of about 30 per cent. was secured. No disturbing effects were observed with this arrangement, as was shown by the shape of the energy curve at different regions of the spectrum when the reflecting mirror was omitted. The beam, on leaving the house, was passed through the rocksalt lens and brought to a focus on the slit of the spectrometer, after it had traversed the shorter observation tubes when these were placed in front of the spectrometer. When longer observation tubes were used, the best procedure was to focus the beam within the tube, but very near to the end. The beam therefore diverged from this point, but as this was close to the end of the tube the diverging beam occupied only about one-half of the aperture of the rocksalt end. It was picked up just outside the tube by a rocksalt lens, focussed on to the slit and adjusted to give maximum galvanometer deflection.

---

* 'Astrophys. J.,' vol. 62, p. 47 (1925).

Shutter.

A shutter of aluminium plate working in guides passed or cut off the radiation leaving the house, and was worked by means of a cord and pulley.

OBSERVATION TUBES AND ROCKER.

In fig 1 the observation tubes are shown between the source of radiation and the spectrometer, this being the position in which most of the work was done. As the full radiation contains light of short wave-length, it may affect chemically the gas under observation, and a slight decomposition was, in fact, noticed with AsH_3; an alternative scheme can, however, be adopted whereby the radiation is first dispersed by the prism, then passed by the second slit of the spectrometer through the gas, and focussed on to the thermopile situated in a special chamber (see *infra*, p 144). Advantages possessed by the former method are greater compactness, so that less energy is lost by reason of distance, with better insulation of the thermopile from variations in temperature of the room. The results given by the two methods are, however, identical both as to position of the bands and as to their intensity, as was brought out by a special experiment on three bands of NH_3, in which a quartz prism was used.

Single versus Double Tube.

In a system in which gas has to be retained in an absorption tube with transparent ends, it is necessary to compare the absorption of the gas in the tube at any given wave-length with that of a similar tube containing no gas, at the same wave-length.

The merits of two methods of working may be considered.

(1) The absorption of the gas may be measured in a single fixed tube by filling it with gas and exploring a small region of the spectrum. After removal of the gas by evacuation or by displacement with dry purified air, the same region of the spectrum is traversed. In this way the energy passing through the gas at any wave-length may be compared with that passing through a tube when no gas is present. This is the method used by Coblentz,* Burmeister† Brinsmade and Kemble,‡ Schaefer and Thomas,§ Becker,‖ Schierkolk.¶

---

* 'Investigations of Infra-Red Spectra.' Carnegie Inst. of Washington, 1905.

† 'Deut. Phys. Ges.,' vol. 15, p. 589 (1913).

‡ 'Proc. Nat. Acad. Sci.,' vol. 3, p. 420 (1917).

§ 'Z. Physik,' vol. 12, p. 330 (1923).

‖ 'Z. Physik,' vol. 34, p. 255 (1925).

¶ 'Z. Physik,' vol. 29, p. 277 (1924).

(2) The other method, and the one used for the most part in these investigations, is to bring alternately into the optical path two tubes, the one containing the gas and the other gas-free. These two tubes were made identical in size, had polished parallel ends, were fitted with plane parallel rocksalt end-plates parallel to one another, and were brought alternately into position by the rocking arrangement described below. In spite of certain difficulties at first found in using two tubes, of which a short account will be given, it is thought that their use has certain advantages over the employment of a single tube. Thus, readings in both the gas tube and the empty tube are made on one setting of the spectrometer, and so no error can arise in reproducing the exact spectrometer setting for both conditions. This is specially important where the energy from the Nernst filament is altering rapidly with the wave-length. As an example, at 4·220 μ the energy corresponded to a galvanometer throw of 19 cm., while at 4·233 μ the throw is 14·3 cm., a difference of nearly 25 per cent. It is clear that in such a case it is difficult to reset the wave-length drum or spectrometer circle with the accuracy necessary to avoid an error as small as 1 per cent. Moreover, method (1) involves an interval of time for emptying the tube; during this interval there is a possibility of sufficient change in temperature of the prism, particularly with rocksalt, to produce an alteration in refractive index, and so of wave-length setting. Changes in the sensitiveness of the galvanometer may also occur during this interval, thus failing to reproduce the correct quantity of energy appropriate to each reading. But the greatest advantage is in speed of working, time being saved that in method (1) is taken up in clearing the tube of gas. Apart from the time lost in the frequent evacuation of the tube, the total number of readings is reduced in the proportion of four to six. This method is also used by E. v. Bahr,* who compares with path in air, Imes,† who compensates by end-plates alone, and by Okubo.‡

Description of Observation Tubes.

Two lengths of tube were generally used according as strong or faint bands were being explored.

The shorter tubes were made of pyrex glass, 50 mm. in diameter and 100 mm. long, and had side-tubes with taps for admitting gas. Cut to the same length and with the ends made parallel, the tubes were fitted gas-tight with plane parallel rocksalt windows, 6·5 mm. thick, and the assembled system brought to parallelism by back-reflection.

---

* 'Deut. Phys. Ges.,' vol. 15, p. 731 (1913).

† 'Astrophys. J.,' vol. 50, p. 251 (1919).

‡ 'Sci. Rep. Tôhoku Univ.,' vol. 12, p. 39 (1913) ('Sci. Abs.,' p. 3453 (1923)).

The longer tubes were made of soda-glass and were 50 mm. in diameter and 450 mm. in length; otherwise they were similar to the shorter tubes. Some experiments were made with tubes of the same length, but of 25 mm. diameter.

Attachment of End-Plates.

Reliance was placed on the parallelism of the ends of the tubes and of the optically worked rocksalt plates to get the plates ultimately parallel as experimentally determined by back reflection. The plates had only the thinnest film of vaseline between them and the ends of the glass tubes, and were kept in position by the screw cap shown in Fig. 4. The tubes when fitted are tested to stand a vacuum overnight.

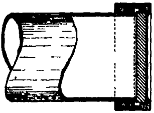

Fig. 4.—Attachment of End-Plate.

Mounting for Tubes.

Each pair of tubes was mounted in a rocker so devised that by means of cords worked from a distance by the operator who changed the wave-length

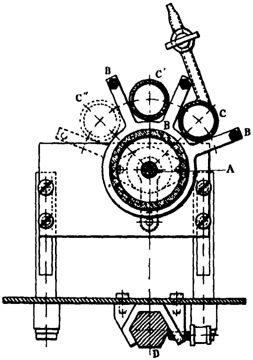

Fig. 5.—Rocking Support for Tubes. A, Axle of rocker. B, Saddles for holding tubes. C, C', C", Position of tubes. D, Attachment to optical bench.

reading, either tube could be brought into the optical path and each exactly into the same position. In fig. 5 will be seen the rocker supporting the tubes.

Correcting the Tubes.

At the start of these experiments when long and narrower tubes, 25 mm. in diameter, were used, it was observed that the same beam did not always produce the same deflection of the galvanometer when sent through the two empty tubes in turn. The tubes were then adjusted by means of packing so that equal deflections were obtained for the radiation passing through each tube for some particular wave-length, but it became apparent that this equality did not hold for other wave-lengths. So-called "end corrections" were then determined over small ranges of the spectrum and with varying widths of slit, but as time went on it became clearer that these corrections between the two tubes, which are the percentage differences in deflection given by the empty tube as compared with the other, both being empty, were to be attributed to a particular region of the spectrum irrespective of the energy passed through, which is governed by the slit-width.

Curves giving percentage corrections at different wave-lengths for the difference in energy from the two tubes were therefore constructed and applied to the experimental data from which the absorption curves were drawn. These corrections were determined for the regions in which all three prisms, quartz, fluorite and rocksalt, were used.

Reflection from the walls of the tubes or selective absorption by them being suspected as the reason for want of equality of energy as shown by galvanometer throw, the short tubes were installed and the beam so arranged that it was brought to a focus beyond the farther window and on the collimator slit of the spectrometer, thus avoiding reflections from the sides.

When the tubes, of which the ends had been tested for parallelism by back reflection, had been placed approximately parallel to one another in the rocker, a quartz prism being in the spectrometer, they were adjusted by packing so as to give equality of galvanometer throw over a fair range of the spectrum (1 to $3 \cdot 5\,\mu$), but a deviation was still found about $2 \cdot 95\,\mu$, where one of the tubes permitted about 5 per cent. more energy to pass than the other, both tubes being empty. By experiment this deviation was proved not to be due to reflection from the glass walls as the interposition of diaphragms showed; nor to differences in the rocksalt windows, as the same effect was obtained on reversing the tubes; nor to an interference effect due to the reflecting mirror behind the filament, as it was reproduced when the filament alone was used;

nor to the contents of the tube being absorbent, as it was obtained equally when they were filled with dry CO_2-free air or highly evacuated. It was also obtained when the tubes were both filled with ammonia gas at atmospheric pressure.

At this stage the results were considered, especially as the region where this deviation was observed coincided with an absorption band of quartz given by Coblentz as having a maximum at 2·9 μ, and found by us from many energy curves at 2·95 μ. As reflections from the glass walls of the tubes had been eliminated, suspicion fell on the relative alignment of the tubes in the rocker being still faulty.

The experiment was then made of tilting one of the tubes slightly until equality of throw was secured in the region where deviation had previously been observed (in the neighbourhood of 2·95 μ). As a result, equality of throw was obtained for the two tubes throughout the rest of the spectrum (1 to 3·4 μ with a quartz prism).

Similarly with a fluorite prism in the spectrometer, it was necessary to make the final adjustment of the tubes so that equality of throw was obtained about the region of 4·26 μ, where there is an absorption band in fluorite.

When a rocksalt prism is used there is much less difficulty in securing uniformity, as rocksalt has no sharp absorption bands up to 17 μ.

The explanation of this want in uniformity in energy registered for the two tubes apparently for particular wave-lengths only when they are not exactly parallel to one another or with their ends not parallel to the plane of the slit is as follows :—

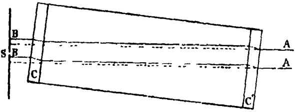

Fig. 6

The two tubes, one destined to contain the gas, must be set exactly when empty so that the faces of C, C′, themselves made of plane plates, are parallel to the plane of the slit opening S, to ensure that the energy falling on the slit is the same from both tubes. If one tube is displaced a little from this position, as in fig. 6, then the beam of light A, A, which is arranged to impinge symmetrically on the slit, is displaced as at B, B. It can be ascertained readily that the energy from the Nernst filament is not uniform over the whole slit-width. Any displacement of the image, therefore, means that the energy reaching the slit is liable to vary if the end-plates of the two tubes are not in exactly the same positions relative to the slit. It may be shown that when the tubes are only slightly out of alignment, the shape of the absorption curve does not alter to any serious extent provided that the energy from the source, as measured by the galvanometer deflection, is not altering rapidly from wave-length to wave-length. In the case illustrated in fig 7, where three points *a*, *b*, *c* are close together on the energy curve of the source of radiation, a value *d* may be taken to represent the small difference in galvanometer deflection due to imperfect alignment of one of the tubes. Then the fraction of the total energy gained or lost by this defect in alignment is given by d/aa', d/bb', and d/cc', which are nearly constant values. The effect of this on an absorption band in the region *a*, *b*, *c* is to produce a slight apparent alteration in the intensity of the band. If, however, the energy is varying rapidly, as in fig. 8, or if the radiation suffers selective absorption in any part of the optical train (*e.g.*, a quartz prism at 2·95 μ, where there is comparatively large absorption) the circumstances are different. In this case, suppose the tubes are again out of adjustment so as to give the difference of deflection *d'* as in the previous case. At neighbouring points *a*, *b*, *c* of rapidly falling energy, the error due to faulty alignment now becomes d'/aa', d'/bb', d'/cc', and these fractions are no longer nearly equal. At points *e*, *f*, *g*, the effect is equally marked but in an opposite direction. A little consideration will show that the total effect from *a* to *g* is to produce a spurious band, resulting from the faulty alignment. Great care, therefore, is necessary in checking the setting of the two tubes in every part of the spectrum where the optical train itself exhibits selective absorption, or where the energy of the source of radiation is altering rapidly. In fact, the accuracy of the setting of the tubes may be checked by comparing the energy curves of the source of radiation at those parts of the spectrum where this state of affairs is known to exist.

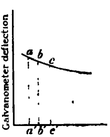

Fig 7.

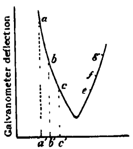

Fig 8.

It will also be clear that the method of using one tube alone in the case where the energy is varying rapidly is liable to produce serious errors, since it is necessary to ensure that the spectrometer is brought back exactly to its original position on a rapidly rising or falling curve of energy. This is especially difficult, particularly when a rocksalt or fluorite prism with a high temperature coefficient of index of refraction forms the dispersing system and when an interval of time elapses between the two observations on the gas-filled and empty tube, as is generally the case.

TRANSFERENCE OF GAS.

The pure gases were prepared as described in Part II and stored over mercury in containers which were connected to the observation tube through a gas pumping arrangement consisting of Hyvac and Toepler pumps as in fig. 9. All joints were of glass to diminish the risk of air entering the system at any point. The arrangement enabled the observation tubes and connections to be evacuated and the gas transferred either to the observation tube at any desired pressure or to be removed from the observation tube and transferred back to the container.

Rubber joints, even for tubes in close contact inside the rubber, were abandoned after a time as these introduced a possible source of contamination of the gas, and rubber is unreliable for preventing leakage.

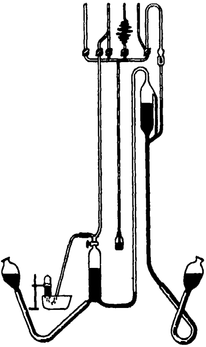

Fig. 9.—Apparatus for Transference of Gas.

When dealing with gases like PH_3, which are liable to flash in the presence of oxygen, or with AsH_3 or PH_3, which in the presence of oxygen are easily decomposed by light, it was necessary to have these arrangements. As the observation tube containing gas had to be moved out of its position after every reading to make way for the empty control tube, the glass connecting tube had to take the form of a spiral as shown in fig. 1.

MERCURY LAMP FOR CALIBRATION.

In order to obtain a rapid check on the setting of the spectrometer, a mercury lamp of the open type, running on a current of 2·5 amps, and having an intense arc about 4 cm. long, was permanently installed (see fig. 1) in such a manner that the radiation from the lamp could be reflected normally on to the slit without disturbing the setting of the rest of the apparatus. This was done by opening a shutter on the side of the housing for the mercury lamp and passing the radiation from the lamp through a quartz lens of 2·8 cm. aperture and 6·9 cm. focus on to a small plane mirror attached to the optical bench by means of a swivel joint and capable of being swung into position for reflecting the mercury light into the spectrometer.

SPECTROMETER.

The instrument used was one of Hilger's No 2 type, with a wave-length drum calibrated for a 60° rocksalt prism. It was furnished with Hilger's symmetrical slits capable of being opened by the rotation of a divided ring, two mirrors of 45 mm. aperture with a focus of 22·9 cm, and with a Wadsworth mirror 5·2 cm. by 4·4 cm. on the prism table. The mirrors were adjusted and the prism set according to the instructions issued with the instrument, with the aid of a jig also supplied to secure minimum deviation. Around the instrument a wooden housing was erected for the purpose of keeping off draughts and enabling as dry an atmosphere as possible to be maintained within it by means of a drying agent, and the instrument was anchored to the stone bench by cement applied to the three feet. A thermometer passed through the roof of the housing and had its bulb near the prism.

Little attention seems to have been paid by many workers in this region to the temperature of the prisms, and especially when that is made of rocksalt. As the temperature coefficient of the index of refraction of rocksalt varies rapidly with changes in temperature, considerable errors may be introduced by omitting to take this into consideration. Attention was directed by us to this feature in a letter to 'Nature,'* and the same effect is considered in

---

* 'Nature,' vol. 119, p. 818 (1927).

Part II, p. 150, when dealing with the correction of Paschen's values of refractive index for temperature.

The prisms used had the following dimensions :—

	Angle.	Height.	Length of face.	For region.
	° ′ ″	cm	cm.	
Quartz (Cornu)	60 2 38 (N.P.L.)	4·1	6·5	To 3·5 μ
Fluorite	59 59 47 (N.P.L.)	3·75	3·0	3·5 to 8 μ
Rocksalt	60 0 9 (N.P.L.)	4·3	5·5	8 to 17 μ

Movement of Wave-Length Drum.

The wave-length drum was divided to read in μ for the rocksalt prism. To avoid heating the instrument by proximity of the hand, this wave-length drum was driven by a wheel with velvet on its periphery, this in turn being driven by slow gearing. In addition, a telescope was levelled on the pointer of the drum so that the divisions could be more accurately read and interpolations made between the markings. It was found, however, that the wave-length drum was subject to a more or less periodical error, and so had to be calibrated by the method described in the following paper.

Protection for the Rocksalt Prism.

The prism as supplied was coated with a thin film of celluloid to prevent tarnishing of the prism from moisture. This had to be abandoned on account of the absorption bands, due to nitrocellulose in the celluloid. Trowbridge[*] investigated the absorption of nitrocellulose in celluloid films in the infra-red region and found bands at 3 μ, 5·89 μ, about 7·7 μ, and about 9·4 μ. In addition to these, we have found strong absorption bands at 11·9 and 13·35 μ. It was not until the celluloid was removed from the prism and from all rocksalt lenses and faces in the optical system that fine structure of many of the bands, especially beyond 8 μ, was obtained. A serious disadvantage in having a celluloid coating is the cutting down of the available energy passing through the system; this involves widening the slits unduly, so that the radiation departs much more than is desirable from the monochromatic condition. The effect of this is that fine bands are missed, because the slit-width is too great to give the necessary purity of spectrum for resolution of the finer structure. By having a drying agent within the housing of the spectrometer, trouble with the prism due to the hygroscopic character of rocksalt was avoided.

---

[*] 'Phys. Rev.,' vol. 27, p. 282 (1908).

Effect of Temperature on Prisms.

On account of the change in refractive index with temperature, which is especially important in the case of rocksalt (see Part II, p. 150), it was necessary to know the temperature of the prism, and this was taken every quarter of an hour by means of the thermometer during the progress of an experiment. Since the temperature throughout an experiment altered very slowly (*e.g.*, not over 1° in eight hours), it was assumed that the prism itself had sufficient time to acquire the temperature actually recorded by the thermometer alongside it.

THERMOPILE.

The thermopile made by Hilger was a 20-junction bismuth-silver thermopile, and in the instrument as supplied was housed in a brass pocket just beyond the second slit.

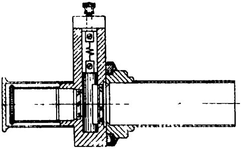

FIG 10.—Airtight Thermopile Holder.

Airtight Housing of Thermopile

It was found necessary to modify the instrument by designing an air-tight holder for the thermopile, as in fig. 10. Before this was done, it was observed that fluctuations occurred when the galvanometer was connected to the thermopile on windy days, or when doors were closed in the neighbourhood. The matter was investigated by Sir Richard Threlfall, who concluded that the effect was due to a pulse of pressure affecting the air in contact with the thermopile, which thereby registered adiabatic heating or cooling. That this was so was confirmed by placing the thermopile and leads to the galvanometer in a sealed bell-jar connected to a mercury manometer. By slowly raising the reservoir of the manometer, the galvanometer could be kept steady, but by raising it even by one millimetre, with a jerk, a large excursion of the spot took place. After the thermopile had been enclosed in an airtight holder, the galvanometer indication remained steady, even on closing the door of the room sharply. The airtight holder was furnished with a tap to enable it to be evacuated, but probably on account of the mass of the elements of the thermopile, only an insignificant advantage was obtained on evacuating.

Protection from Temperature Drift.

Round the holder containing the thermopile was placed a wooden cell with a lid, and between this and the thermopile holder, coarse worsted was inserted as an insulator. This was found materially to reduce drift of the galvanometer caused by local variations in temperature. The drift actually observed was, in general, so small and regular that no error was introduced from this source.

Arrangement of Airtight Thermopile outside Spectrometer.

For certain work, as, for example, when the radiation from the source is passed first through the spectrometer, which now acts as a monochromatic illuminator, and thence through the observation tubes, a protected thermopile is required outside the instrument and beyond the observation tubes. In such cases, the arrangement shown in fig. 11 was used.

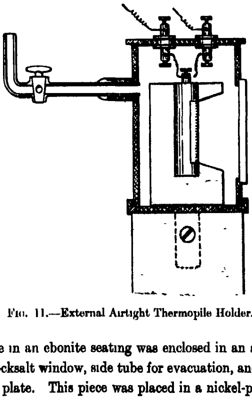

Fig. 11.—External Airtight Thermopile Holder.

The thermopile in an ebonite seating was enclosed in an airtight brass box, furnished with rocksalt window, side tube for evacuation, and copper terminals let into an ivory plate. This piece was placed in a nickel-plated box brightly plated outside and blackened within, this nickel box being in turn enclosed in a similar but larger one, with an ebonite distance piece fixed to a rigid metal stand. The air space between the nickel boxes was packed with worsted.

Galvanometer Leads.

An important point in this matter is the desirability of keeping all leads from the thermopile to the galvanometer fixed in position, as disturbances seem to be possible from the swaying of the leads. This was secured by passing the leads through long glass tubes which were securely fastened to the walls and benches to prevent any movement.

GALVANOMETER.

On account of the proximity of electric power stations and railways, the galvanometer was affected by electromagnetic impulses, whilst mechanical vibrations from the traffic in the Strand caused perturbations so that for a long time any critical work had to be done on holidays and after midnight. Of these troubles, the former was the more readily overcome, and that by suitable shielding; the latter has been met by suspending the instrument.

Paschen Galvanometer.

As at first erected the Paschen galvanometer of the suspended moving of magnet type and made by the Cambridge Instrument Company had as a shielding two conical bells of soft iron, the outer weighing 70 kg. and the inner 25 kg., coaxially situated over the instrument, which had a brass casing with vertical brass tube for carrying the attachment of the suspension. Through a horizontal slot 12 cm. in length and 0·7 cm. wide the galvanometer mirror was illuminated. Two magnets on arms projecting through the extremities of the slot were used to control the sensitiveness, which in this original instrument was approximately $1 \cdot 7 \times 10^{-10}$ amps. (for scale $1\frac{1}{2}$ m. away) with a period of 13 seconds.

As a mercury surface plainly showed that the bench on which the instrument then rested was in a state of quiver, to keep down the irregularities of the spot of light due to these mechanical vibrations, various devices such as rubber sheet, sorbo rubber, motor cycle tyre, tennis balls, fibre boards, felt and brown paper and combinations of these were tried. The best results were obtained with three or four glass plates intercalated with a few sheets of brown paper.

While this reduced the smaller excursions of the spot of light, they still persisted, but in addition occasional larger perturbations seriously interfered with work. As there were indications that these larger excursions were due to electromagnetic impulses, the advice of the N.P.L. was sought, and the Director kindly asked Dr. Dye, F.R.S., to consider the further magnetic shielding of the instrument. Dr. Dye thereupon devised a nest of Stalloy rings placed horizontally over each other, practically enclosing the brass casing of the instrument, and this was later supplemented by a tape of another permeable alloy (mu-metal) wound round the outer surface of the inner soft iron bell and prevented from moving by an adhesive. The magnets which penetrated between the inner bell and the Stalloy rings could still be used for controlling the field of the magnets on the suspension, efficient shielding from external magnetic influences being at the same time secured.

Disturbances of small period, however, still persisted, and it was thought that these might be due to mechanical vibrations affecting the suspension if it were not attached so as to hang vertically. Prof. A. V. Hill was good enough to recommend a lighter suspension made by Mr. A. C. Downing, and this, while it produced no marked improvement as regards mechanical disturbances, gave a sensitiveness of $1 \cdot 0 \times 10^{-10}$ amps. for 1 mm. of scale at $1 \cdot 5$ m. for a period of 7 seconds.

Downing Galvanometer.

A Downing galvanometer of the Paschen type was then installed and has been used for most of the work. The apparent advantage of having a cylindrical mu-metal shield close to the intrument failed on account of difficulty in working up the sensitiveness by the control magnets even when these were increased in strength The former shielding by the soft iron bells, the inner being wound with mu-metal tape, and by the nest of Stalloy rings was then put back with a heavy block of lead on the rings to prevent their relative movement. To obviate overdamping effects the four coils of the galvanometer were connected in series parallel, thus reducing the coil resistance from 18 to $4 \cdot 5$ ohms and making it more nearly equal to that of the thermopile ($6 \cdot 9$ ohms). The sensitiveness of this instrument could be worked up to give a deflection of 1 mm. per 7×10^{-11} amps at a period of 9 seconds and with the scale at $1\frac{1}{4}$ m. To obtain greater stability and, consequently, greater accuracy of observation, the instrument was generally used at a sensitiveness of 10×10^{-11} amps. and a period of $7 \cdot 5$ seconds.

The same field control magnets actuated from the slit were used with this galvanometer, but in addition a long very feeble bar magnet that could be moved round a vertical axis was attached to the top of the outer bell for the purpose of bringing the spot of light on to a suitable position of the scale, without affecting the general sensitiveness of the instrument.

This instrument was satisfactory for critical work at night, but could still not be used by day when mechanical tremors from traffic penetrated to the building, or during high winds.

Suspension of the Galvanometer.

We were fortunate at this stage in enlisting the interest of Mr. R. W. Paul, who designed a method of suspending the instrument and its shielding from a steel rail running across the corner of the room. This consisted of a slate platform 45 cm. square attached to a gunmetal spider by four 135 cm. brass rods The centre of the spider held an inverted cup which fitted over another cup resting upon the rail. It was originally intended that the weight should rest on a hard rubber ball placed between the two cups, but while the tremor had disappeared excursions of the spot of light were still observed, nor were these removed by a harder rubber ball nor by a steel ball. An improvement was obtained by placing between the rims of the cups a pad of filter papers, at *a*, and on following this up by using in this position seven sheets of filter papers mechanical disturbances practically disappeared.

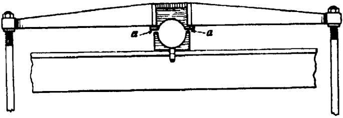

FIG. 12.—Suspension of Galvanometer

It is important in erecting the galvanometer on the suspended platform to adjust levels on the addition of each consecutive part. The instrument has been used for the last year during the day with total disturbances rarely exceeding 1 mm., and it is due to this that expeditious work can now be put through without having to wait for times when the streets are free from traffic.

Method of Reading.

When using the Paschen galvanometer (period 13 secs.), the position of rest of the spot of light was taken as the reading, the time taken for an observation being 16 seconds. The Downing galvanometer (period 7·5 secs.) gave an appreciable swing back after deflection and the end point of this swing back was taken as the reading. Comparison showed this method of reading to be more reproducible and also the time taken for an observation to be considerably less (8 secs. as compared with 16 secs.).

Determination of Sensitiveness.

The absolute sensitiveness of the galvanometer was checked periodically by measurement of the deflection (using the back swing as in ordinary readings) caused by 0·002 volt tapped from a potentiometer and passing through 100,000 ohms in series with the galvanometer.

It is with pleasure that we acknowledge the kindness of many friends who have assisted us in the course of this work: Sir Richard Threlfall, G.B.E., M.A., F.R.S., Mr. F. Twyman, F.R.S., Dr. D. W. Dye, F.R.S., Mr. R. W. Paul —already mentioned in the text; Yarrow Prof. O. W. Richardson, F.R.S.; Dr. F. Freeth, F.R.S., for the loan of a small infra-red spectrometer with which preliminary work was done; Mr. S. A. Pollock for the loan of apparatus; and Messrs. Castner-Kellner for synthetic ammonium chloride. But we desire also to record our satisfaction with the great assistance we have received from Mr. E. S. Hiscocks, M.Sc., in conducting the experiments, and our indebtedness to Mr. F. S. Bepge for his devotion and skill in instrumental work.

Studies in the Infra-Red Region of the Spectrum. Part II.—*Calibration of Prism Spectrometer; General Procedure; and Preparation of Pure Ammonia, Phosphine and Arsine.*

By Sir Robert Robertson, F.R.S., J. J. Fox, D.Sc., and E. S. Hiscocks, M.Sc.

Calibration of Prism Spectrometer.

(1) *Instrument.*

The instrument used was a No. 2 Hilger infra-red spectrometer fitted with a "wave-length drum." It soon became evident that the wave-length drum required calibration on account of the chance of periodic errors in the screw thread. If the screw remains constant, it would be better to have the drum marked in angles which could be referred to the refractive indices of the material of the respective prisms used. As any one prism varies in the refractive index with temperature, reading of wave-length on a wave-length drum can be accurate only for one temperature.

(2) *Calibration of Wave-Length Drum in Terms of Angle of Rotation of Prism Table.*

A plane mirror was mounted vertically at the centre of rotation of the prism table and an illuminated scale set up parallel to it exactly 5 metres away. The image of the scale in the mirror was observed by means of a fixed telescope with cross wires in the eyepiece. Zero was taken as 0·5893 on the drum, which was set successively on about 80 of its graduation marks and the scale image coinciding with the cross wires noted for each setting. The displacement of the image in millimetres in each case was thus observed, and as the distance from the scale to the mirror was accurately known, the tangent of the angle of rotation and thence the angle itself was obtained within 2 seconds of arc. Three observers agreed closely in their observations, from which a curve was drawn connecting drum calibration marks with angle of rotation (first graph).

(3) *Calibration of Wave-Length Drum for use with Rocksalt Prism.*

The refractive indices of rocksalt determined by Paschen[*] were used. Since these determinations had been made at varying temperatures (14·6° to 18·8° C.)

---

[*] 'Ann. der Physik,' IV, vol. 26, pp. 120, 1029 (1908).

it became necessary to adopt a standard temperature, 18° C. being chosen. The values of the refractive index were recalculated to this temperature (Table I) by means of the temperature coefficient of the refractive index of rocksalt as measured by Liebreich.* Outside the range (0·6 to 8·8 μ) investigated by Liebreich, extrapolations of his values were used. The corrected refractive indices were then plotted against wave-length on a large scale graph, readable to 0·00001 of refractive index and 0·002 μ (second graph). In this table all refractive indices are given with respect to air and those stated to the sixth decimal place are the corrected Paschen values, the rest of the values being obtained from the graph.

Table I.—Refractive Index of Rocksalt corrected to 18° C.

λ (in μ).	*n*.	λ (in μ).	*n*.	λ in (μ).	*n*.
0·58932	1·544313	5·600	1·51709	11·200	1·48632
0·78576	1·536145	5·8932	1·515908	11·500	1·48404
0·88398	1·534040	6·200	1·51474	11·7864	1·481783
0·9822	1·532464	6·4825	1·513541	12·000	1·48004
1·1786	1·530386	6·700	1·51262	12·300	1·47750
1·500	1·52848	7·0718	1·511006	12·600	1·47492
1·7680	1·527458	7·400	1·50951	12·9650	1·471690
2·000	1·52677	7·6611	1·508288	13·250	1·46907
2·3573	1·525870	7·9558	1·506734	13·500	1·46672
2·600	1·52532	8·200	1·50547	13·800	1·46386
2·9466	1·524537	8·500	1·50388	14·1436	1·460529
3·250	1·52386	8·8398	1·501984	14·450	1·45741
3·5359	1·523190	9·100	1·50043	14·7330	1·454384
3·850	1·52241	9·400	1·49860	15·000	1·45130
4·12524	1·521655	9·700	1·49671	15·3223	1·447491
4·400	1·52064	10·0184	1·494681	15·600	1·44437
4·700	1·51991	10·300	1·49275	15·9116	1·441023
5·0092	1·518902	10·600	1·49067	16·200	1·43793
5·300	1·51807	10·900	1·48853		

From the above graph were read the refractive indices corresponding to the drum markings for which the angle of rotation is known from (2). With these corrected values for refractive index at 18°, the theoretical angles of rotation from 0·5893 were calculated. The differences between the calculated and observed angles of rotation, after conversion into terms of wave-length, were plotted against drum graduation marks to give the correction in μ to be applied at any point on the drum when the instrument is set for minimum deviation for 0·5893 μ (third graph).

It should be noted that Paschen's refractive indices for rocksalt given in Landolt and Börnstein's Tables, 1912, as for 18° C. are actually the values for the various temperatures given in the paper quoted.

---

* 'Verh. Phys. Ges.,' vol. 13, p. 1 (1911).

(4) *Calibration of Wave-Length Drum for use with Quartz Prism.*

The determinations of refractive index made by Rubens,* Carvallo† and Paschen‡ were considered. Many of Rubens' results are stated only to the fourth decimal place, and those of Carvallo in several cases do not fall upon a smooth curve when plotted against wave-length. Paschen's determinations were therefore accepted, particularly as these were determined at 18°.

Paschen's values of refractive index were plotted against wave-length for the range 0·5 to 3·1 μ on a graph readable to 0·00001 of refractive index and 0·001 μ (fourth graph). Owing to the poor dispersion of fluorite between 3·0 and 3·5 μ it was decided to use quartz in this region also. The dispersion curve of quartz was therefore extended to 3·5 μ by means of Rubens' determinations of refractive index (*loc. cit.*) Refractive indices corresponding to 50 different wave-lengths were read from this curve and the corresponding rotation angles calculated starting from 0·5893 μ as zero and with the angle of the prism as determined at the National Physical Laboratory. The angles calculated in this way were plotted against wave-length on a graph readable to 2″ and to 0·0005 μ (fifth graph), and from this graph the rotation angles corresponding to wave-length intervals of 0·05 μ from 0·5 to 3·5 μ were read off. These angles were then applied to the curve connecting drum readings with angle of rotation By this means a series of drum graduation marks corresponding with the wave-lengths was arrived at. These corresponding values were plotted against each other on a large scale, and from the graph the wave-length corresponding to any drum graduation mark could be determined (sixth graph).

(5) *Calibration of Drum for use with Fluorite Prism.*

Paschen's determinations of the refractive index of fluorite§ were accepted and corrected to 18° C. by means of Liebreich's determinations (*loc. cit.*) of the temperature coefficient of refractive index. In Table II is given a list of these corrected refractive indices with respect to air. The values corresponding to wave-lengths stated to three places of decimals are interpolated.

The values were plotted against wave-length on a graph readable to 0·00001 of refractive index and 0·001 μ over the range 0·5 to 9·1 μ (seventh graph). Values of refractive index corresponding to about 65 wave-lengths were read

---

* 'Ann. der Physik,' vol. 51, p. 381 (1895); *ibid.*, vol. 54, p. 476 (1896).

† 'C. R.,' vol. 126, p. 728 (1898).

‡ 'Ann. der Physik,' vol. 35, p. 1005 (1911).

§ 'Ann. der Physik,' vol. 4, p. 290 (1901); *ibid.*, vol. 41, p. 670 (1913).

Table II.—Refractive Indices of Fluorite corrected to 18° C.

λ (in μ).	n.	λ (in μ).	n.	λ (in μ).	n.
0·48615	1·437072	2·3573	1·42201	6·300	1·38110
0·58758	1·433907	2·5537	1·42088	6·4825	1·37828
0·65630	1·432519	2·6519	1·42025	6·700	1·37457
0·72818	1·431427	2·9466	1·41829	6·900	1·37111
0·76653	1·430928	3·2413	1·41616	7·0718	1·36804
0·8840	1·42982	3·400	1·41493	7·300	1·36376
1·0140	1·42885	3·5359	1·41382	7·500	1·35991
1·08304	1·428449	3·8306	1·41120	7·6612	1·35680
1·1786	1·42791	3·950	1·41011	7·900	1·35197
1·3756	1·42689	4·1252	1·40852	8·100	1·34773
1·4733	1·42645	4·4199	1·40559	8·2505	1·34444
1·5715	1·42601	4·550	1·40420	8·500	1·33879
1·7680	1·42508	4·7146	1·40236	8·700	1·33415
1·8688	1·424567	5·0092	1·39903	8·8398	1·33079
1·9153	1·42436	5·3036	1·39526	9·100	1·32437
1·9644	1·42411	5·600	1·39126	9·300	1·31932
2·0626	1·42361	5·8932	1·38715	9·4291	1·31612
2·1608	1·42310	6·100	1·38412		

from this curve and the corresponding angles of rotation calculated, again starting from the angle corresponding to 0·5893 μ as zero. Drum markings corresponding to the calculated angles of rotation were read from the drum angle curve and plotted against wave-length, thus giving the drum calibration marks in terms of wave-length (eighth graph).

Since the helical motion of the "wave-length drum" permits of very fine setting of the prism table, the scheme described furnishes a means of setting the prism at any desired wave-length with considerable accuracy.

(6) *Setting of the Spectrometer.*

In using this or other types of infra-red spectrometer with Wadsworth constant deviation setting, it is necessary to fix a zero position, usually the mean of the sodium lines at 0·5893 μ. From this zero, positions in the infra-red are arrived at by calculation from the known refractive index of the prism used, or by the use of known points in the infra-red spectrum, which must be determined by bolometric methods or by means of a thermopile. There are few places in the infra-red region which are so accurately ascertained that they can be relied on for setting a prism. The commonly accepted practice of using the emission line about 4·4 μ for CO_2, or the quartz reflection lines at 8·3 and 8·41 μ is approximate only, for the lines are not sharp. The exact position of the centres of the emission lines of CO_2 is not shown sufficiently to serve for any accurate work; and, further, it is difficult to decide on a centre of the CO_2 emission line since the centre shifts as the instrument warms up. Better positions may be found from the absorption position of a quartz or fluorite prism itself at 2·95 and 4·26 μ respectively. A good bench mark, however, is that given by the emission line at 1·014 μ of the mercury arc in quartz. This line is sharp and has sufficient intensity for use with a delicate galvanometer and thermopile.

A slight error in setting at 0·5893 μ is intensified in the infra-red. Accordingly, the procedure adopted was to set at 0·5893 μ (or 0·5461 μ) visually, as accurately as possible, and adjust so that this line fell on the centre of the thermopile slit when the drum was set at the correct mark. The prism table was then turned to the position which it should occupy to permit line 1·014 μ to fall on the centre of the thermopile as calculated from the refractive index. Readings of the energy, as measured by the galvanometer, are taken on each side of this position, the prism table being moved into known consecutive positions by means of the wave-length drum. A curve is drawn connecting galvanometer throw and drum readings, and the position of the maximum of the curve is ascertained. Should this not coincide with the calculated position of 1·014 μ on the drum for the prism in hand, the Wadsworth mirror is moved slightly and the readings are repeated. This procedure is gone through again until the correct position for the Hg line 1·014 μ on the drum graduation, as calculated above from the curve drum graduation/wave-length for the particular prism used, is arrived at. It has been found that when the prism is set for minimum deviation on this line and for 0·5893 μ or 0·5461 μ, other places in the infra-red fall into line. During a set of actual measurements of absorption by a gas, the constancy of the spectrometer setting is checked by ascertaining that the line 1·014 μ is still at the same spectrometer setting. For this purpose the mercury lamp permanently installed (see Part I, p 130) is used.

The graphs used for calibration in this part have not been reproduced, but the data of general interest are given in Tables I (rocksalt) and II (fluorite).

(7) *Calibration of Galvanometer.*

It was noticed that occasional variations occurred in the sensitiveness of the galvanometer. The sensitiveness was therefore determined periodically by measurement of the deflection caused by a known current. A potentiometer system was installed so that it could be introduced by means of a double switch into the thermopile-galvanometer circuit when desired. A current of 0·002 volt from this potentiometer was sent through a standard 100,000-ohm resistance in series with the galvanometer, and the deflection measured, the back swing being used as in ordinary readings. The sensitiveness of the galvanometer was maintained so that this deflection was 180 mm. ± 10 mm. with a scale $1\frac{1}{2}$ m. away, and this corresponds with a deflection of 1 mm. for approximately 1×10^{-10} amps.

GENERAL PROCEDURE.

Preliminary Arrangements.

In the foregoing section are indicated the preliminary arrangements necessary for setting the instrument and its parts.

Thus the Nernst filament will have been tested as to its condition and together with its reflecting mirror set in a position relative to the spectrometer to give the greatest possible throw of the galvanometer, the rocksalt lenses before and after the observation tubes having also been adjusted.

The observation tubes will have been chosen as to their length, long tubes for exploring faint bands, and shorter tubes for well-marked bands, an advantage of the shorter tubes being a diminished length of path with consequently smaller loss of available energy. The tubes themselves will have been assembled so that the end-plates are parallel to themselves as shown by back reflection, and set in the rocker so as to be parallel to one another (see Part I, p. 136), and checked throughout the spectrum for equality of galvanometer throw when both are empty.

In order to obtain as good resolution as possible and yet have throws of the galvanometer of such a magnitude that any differences between the empty and the gas tube can be accepted as real differences due to the absorption by the gas when calculated as a percentage of the energy passing through the empty tube, the slits of the spectrometer will be set so that in the region explored only throws of from 200 to 100 mm. on the scale at 1·5 m. are accepted. Usually the collimator and thermopile slits were opened to the same extent, but to take in a more extended region of the spectrum it was the practice to widen the former, but not beyond twice the width of the back slit.

In the spectrometer the prism will have been set up vertically and in minimum deviation, and the instrument oriented so that the beam enters normally, filling the collimating mirror with light. The prism will have been chosen with reference to its dispersion in the region of the spectrum to be explored, quartz up to 3·5 μ when it ceases to be transparent, thence to 8 μ a fluorite prism, followed by a rocksalt prism up to 17 μ.

Calibrations of the instrument will have been made, such as checking the positions indicated by the drum with real angular rotation of the prism table, and calibrations for the immediate experiment by setting visually on the line at 0·5461 μ, by observations on the mercury line at 1·014 μ, and by checking at the known positions of inflection of the energy curve in the case of quartz and fluorite.

The galvanometer will have been tested as described in this part, p. 153, to ensure that it is working at its full sensitiveness, and that there is no disturbing influence, and the spot of light will have been adjusted by the feeble controlling magnet, if necessary, so as to fall on a convenient part of the scale.

These arrangements being satisfactory, the following is the method of conducting an experiment:—

Course of an Experiment.

The room having been maintained at a fairly constant temperature and above that of the outer air to reduce the relative humidity and so save the rocksalt lenses and plates, the Nernst filament is kept at a steady state of incandescence for half an hour before starting, and the temperature, as shown by the thermometer alongside the prism in the spectrometer housing, is read every quarter of an hour from now onwards.

A start is made by setting the wave-length drum at the desired position and reading the galvanometer with the shutter down—Blank$_1$. By means of the cord the shutter on the Nernst housing is raised and radiation passed through the empty tube, giving reading — A. Another reading is then taken with the shutter down, as a precaution against drift—Blank$_2$, and then by moving the rocker so as to bring the gas tube into alignment and again opening the shutter a further reading of the galvanometer is taken — B. The cycle is repeated by lowering the shutter, taking a reading Blank$_1$, and then proceeding to the next higher wave-length.

Tabulated, the readings appear as on p. 156.

To calculate percentage of absorption the readings of the empty tube (A) and of the gas tube (B) are respectively diminished by the means of Blanks$_{1.2}$ and Blanks$_{2.1}$, the difference is taken and expressed as a percentage of the total energy passing through A. If there is no absorption this is zero, but if the gas is absorbing this appears as a band when plotted as ordinate against wave-length or wave-number as abscissa, thus showing percentage of absorption.

	W.L. reading	Blank$_1$ centimetres on scale.	A centimetres on scale.	Blank$_2$ centimetres on scale.	B centimetres on scale.	A.	B.	A−B.	Absorption.	
Gas—PH$_3$ Pressure—760 mm. Prism—Fluorite .. Tubes—450 mm. × 50 mm. Temperature—17·7° C.	μ.								per cent.	Slits $\begin{cases} 0\cdot1 \text{ mm.} \\ 0\cdot05 \text{ mm.} \end{cases}$ Nernst filament— Amps, 1·05. Volts, 98.
	2·52	12·6	0·6	12 5	0·4	12 0	12·0	0 0	0·0	
	2 54	12·2	0·3	12 0	0·1	11·8	11·8	0 0	0 0	
		11·8								
Gas—NH$_3$. Pressure—190 mm. Prism—Rocksalt Tubes—100 mm. × 50 mm. Temperature—17·1° C.	9·44	17·6	4·5	17·5	10·1	13·1	7·4	5·7	43·5	Slits $\begin{cases} 0\cdot2 \text{ mm.} \\ 0\cdot1 \text{ mm.} \end{cases}$ Amps., 1·05. Volts, 107.
	9·46	17·5	4 6	17·3	11·0	12·8	6·3	6·5	50·8	
	9·48	17·3	4·5	17·2	11·6	12·8	5·6	7·2	56·2	
	9·50	17·2	4·6	17·2	11·8	12·6	5·4	7·2	57·1	
	9·52	17·2	4·7	17 0	11·5	12·4	5 5	6 9	55·7	
	9·54	17·1	4·8	16 9	11·0	12·2	5·9	6·3	51·6	
	9·56	17·0	4·7	16·9	9·9	12·3	7·0	5·3	43·1	
		16·9								

A correction for slit-width has been worked out by Paschen* for the case where the slit-width is of the dimensions of the bolometer strip. This was not applied here, as the slit-widths used were narrow compared with the thermopile slit, and the resulting correction calculated according to Paschen's method was too small to be of importance. Since the absorption is 98 per cent. or so in certain regions, there is clearly no room for such corrections to be applied.

Determination of the position of the maximum of the band is simple when the band has been well resolved and the maximum represents a peak of the rotation spectrum; it is not, however, so accurate in the case of an unresolved or partially resolved oscillation band. When this is symmetrical, the mean position of the band is taken; when unsymmetrical and partially resolved, the maximum is chosen having regard to any indications of structure that may be present.

As a false idea of the symmetry of a band is given by plotting wave-lengths, the diagrams are shown in wave-numbers in one centimetre, the reciprocals of the wave-lengths in μ ($1\ \mu = 0 \cdot 001$ mm.) The wave-numbers would be multiplied by 3×10^{10} to obtain frequencies per second.

PREPARATION OF AMMONIA.

Materials.

Ammonium chloride—obtained through Dr. Slade—was the specially pure salt manufactured by the Castner Kellner Co. from synthetic HCl and synthetic NH_3. This salt was crystallised before use and gave no action with Fehling's solution, cadmium chloride solution nor silicotungstic acid; it also gave a perfectly white residue on evaporation with concentrated HNO_3, and from these tests was judged to be free from pyridine, hydrazine and other organic impurities.

Phosphorus pentoxide—obtained from Sir R. Threlfall—gave no turbidity on boiling with mercuric chloride solution and was thus free from traces of lower oxides.

Calcium oxide was freshly ignited just before use.

Mercury was carefully cleaned and dried before use.

Apparatus and Procedure.

The arrangement of apparatus is shown in fig. 1. Ammonia generated in the litre flask A by gently warming a mixture of damp solid ammonium chloride and 50 per cent. KOH solution was allowed to escape at the two-way tap X until samples were completely absorbed by water. The apparatus to the right of X was evacuated by means of a pump attached to G, after which gas was allowed to enter the apparatus as far as E, passing in the first place through the moisture trap B immersed in a freezing mixture, then through the tube C (3 × 100 cm.) filled with freshly ignited lime, and the U-tube D containing KOH sticks and lime. At the two-way tap E further samples were taken, whereupon the gas was allowed to enter the first section of the fractionating system consisting of three condensing bulbs J, K and M, each connected by barometric heads with the non-return traps H, L and N respectively, M being connected through the P_2O_5 tube O to the gas reservoir P. The bulb J having been immersed in a mixture of solid CO_2 and chloroform, ammonia gas was passed until about 6 ml. of liquid had condensed. The tap E was then closed and the freezing mixture transferred from J to K, when the liquid in J evaporated, gas escaping at H, until 4 or 5 ml. liquid remained The tap W was then opened and K cooled until about 3 ml. of liquid had condensed in K, when W was closed, the fraction remaining in J again being allowed to escape. This process was repeated between K and M, the middle fraction from M being collected over mercury in the reservoir P.

---

* 'Ann. der Physik,' vol. 60, p. 663 (1897).

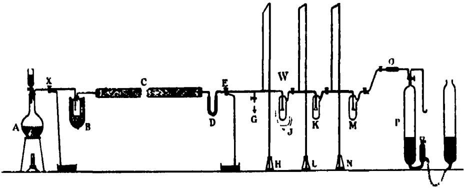

Fig. 1 —Apparatus for the Preparation of Pure Ammonia.

These precautions were taken and the materials chosen so as to ensure that the NH_3 had none of the ordinary impurities and was quite free from moisture. For a few seconds after the gas came into contact with the P_2O_5 some slight signs of interaction were observed. Before it was used the NH_3 was left in contact with the P_2O_5 for 48 hours, but no contraction was observed during this time.

PREPARATION OF PHOSPHINE.

Materials.

Phosphonium iodide, pure, obtained in sealed tubes.
Caustic soda solution, 50 per cent.

Apparatus and Procedure

The arrangement of apparatus is shown in fig. 2. The apparatus to the right of the tap E, constructed entirely of glass, was evacuated by means of a Toepler pump attached at P, tubes M and O containing P_2O_5 and U-tube N, KOH sticks. Nitrogen introduced through A was passed by means of the mercury and $CuSO_4$ trap C through the $CuSO_4$ bubbler D, whence it went to the flue through the tube W until B was deemed to be free from oxygen. Phosphonium iodide crystals were quickly introduced into B and the tube sealed with wax. Nitrogen was again passed for several minutes. A solution of 50 per cent. KOH was run into B from the funnel F, and after phosphine had been evolved for a short time, E was opened and G immersed in a Dewar flask of liquid air. When evolution of gas in B ceased, E was closed and all uncondensed gases pumped off at P. The solidified PH_3 in G was then allowed to evaporate, the gas escaping through the mercury and copper sulphate trap H to D, until samples taken from P showed complete absorption in $CuSO_4$ solution. A little more gas was sent to waste and the middle fraction from G

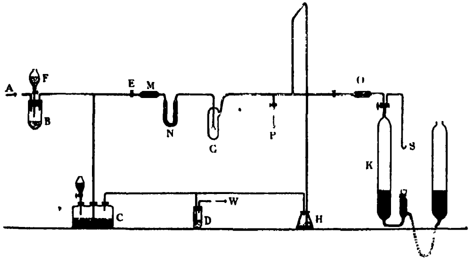

FIG. 2.—Apparatus for the Preparation of Pure Phosphine

collected over mercury in the reservoir K, control samples also being taken at S and tested for complete absorption in $CuSO_4$ solution.

PREPARATION OF ARSINE.

Materials.

Alloy of (approximately) 53 per cent. *Zinc* and (approximately) 47 per cent. *Arsenic* prepared as described by Cohen.*

Apparatus and Procedure.

The same apparatus and procedure were used as in the preparation of phosphine, except that hydrogen was used as the washing gas; the KOH in N was replaced by $CaCl_2$ and solid CO_2 and chloroform used in place of liquid air for liquefaction. B was replaced by a 200 ml. flask containing zinc-arsenic alloy and the arsine was generated by warming this with 30 per cent. H_2SO_4 run in from F.

The results obtained in the exploration of the absorption spectra of the gases NH_3, PH_3 and AsH_3 are recorded in Part III, and a discussion of them will be found in Part IV.

---

* 'Z. phys. Chem.,' vol. 25, p. 483 (1898).

Studies in the Infra-Red Region of the Spectrum. Part III.—*Infra-Red Absorption Spectra of Ammonia, Phosphine and Arsine.*

By Sir Robert Robertson, F R.S., and J. J. Fox, D.Sc.

Introduction.

In this part will be given a general description of the absorption bands found in these three gases, together with curves showing their occurrence in the region up to 17 μ, and evaluations of the maxima of the absorption bands. In Part IV the relationships of the bands to each other in one gas, and to corresponding bands in the other gases, where these occur, will be discussed.

A description of the apparatus is given in Part I, and of its calibration and of the general procedure in Part II, which also gives the methods of obtaining the gases pure. It is only necessary, therefore, to say here that in order to get the best definition of which this prism instrument is capable, the galvanometer was maintained at its highest sensitiveness, the spectrometer slits were closed down so that no more than 200 mm or less than 100 mm. were read on the galvanometer scale, the longer tubes were selected for the examination of faint bands and the shorter tubes for strong bands, and the exploration was conducted at pressures varying from 1 to 1/16 or 1/32 atmosphere.

With this prism instrument the quality of resolution was as follows · Bands were unresolved below 2·2 μ (quartz prism), bands were partially resolved from 2·2 μ (quartz), from 4 μ (fluorite) and from 5 μ (rocksalt); and bands were resolved to show fine structure from 3 μ (quartz), from 6 μ (fluorite) and from 8 μ (rocksalt).

Unresolved bands show one peak of which the centre near the top is taken as the position of the oscillation band, partially resolved bands show usually three peaks of which the central one is taken for calculating the oscillation frequency, the side peaks being also evaluated; while for resolved bands the positions of the maxima of rotation imposed on the oscillation band are recorded.

Although in practice the readings in the first place were recorded on a wave-length basis, they have all been converted into wave-numbers per centimetre for purposes of calculation and comparison, and the figures have also been constructed to show percentage absorption/wave-number, since the use of wave-length as abscissa gives an erroneous picture of a band system. In the curves, wave-lengths are indicated, but only at a few positions, and to avoid interrupting the curves a row of dots is shown at every tenth experimental point on the graph The hatched markings within parallel lines represent the extent of the region in W.N. passed by the back slit.

Of the three gases, NH_3 has been explored from 2·3 to 14 μ by Coblentz,* who used a rocksalt prism throughout and called attention to certain regularities in the bands, and from the visible to 14 μ by means of prisms of quartz, fluorite and rocksalt by Schierkolk,† with whose values we are in general, and in some cases in close, agreement (see Table I), but our arrangements have permitted of a better resolution of the spectrum of this gas, especially after 2·5 μ. One of the bands of NH_3, at 3 μ, has been examined by Spence,‡ whose values agree with ours, allowing for the better resolution he obtained with a grating. In the case of another band of NH_3, at 10·55 μ, Colby and Barker,§ also with a grating, in a note give two values coinciding with ours for maxima of absorption. Badger in a note to 'Nature'‖ reports on bands of NH_3 in the farther infra-red and calculates a moment of inertia for the molecule.

We have found no record in the literature of the absorption spectra of phosphine nor of arsine in the near infra-red.

GENERAL COMPARISON OF THE ABSORPTION SPECTRA OF NH_3, PH_3 AND AsH_3 (OSCILLATION BANDS).

In fig. 1 are graphs of the absorption bands found in the three gases in the region from 1 to 17 μ, set out to show a general comparison. From the experimental data the contour of the bands has been in all cases traced for 1 atmosphere pressure, and also at a quarter atmosphere for other bands. Long tubes are used except for bands II, I and 10·55 μ of NH_3, II, I and α of PH_3 and AsH_3.

As it was not possible to include in this figure the fine structure of all the bands, where this has been obtained, more detailed curves (figs. 2 to 7, corresponding to Tables II to VIIA) showing partial and more complete resolution are given later. To facilitate identification of corresponding bands where these occur in the three gases, the sequences of the bands have been indicated by the same numerals and letters as are given in Table I.

---

* 'Investigations of Infra-red Spectra,' Carnegie Institution of Washington, p. 53 (1905).

† 'Z. f. Physik,' vol. 29, p. 277 (1924).

‡ 'Opt. Soc. Am.,' vol. 10, p. 127 (1925).

§ 'Phys. Rev.,' vol. 29, p. 923 (1927).

‖ 'Nature,' vol. 121, p. 492 (1928).

Table I.—Oscillation Bands of NH_3, PH_3 and AsH_3.

Band.	NH_3.									PH_3.								AsH_3.							
	Wave-length.	Wave-number.	Schierkolk's values for NH_3.	Prism	Tubes.	Resolution	Absorption percentage at atmospheres.			Wave-length.	Wave-number.	Prism.	Tubes.	Resolution	Absorption percentage at atmospheres			Wave-length.	Wave-number.	Prism	Tubes.	Resolution	Absorption percentage at atmospheres.		
							1	$\frac{1}{4}$.	$\frac{1}{8}$						1.	$\frac{1}{4}$.	$\frac{1}{8}$						1.	$\frac{1}{4}$	$\frac{1}{8}$.
VII	μ.		μ.							μ								μ 0 6 (ca)	16667	Q	LW	N	12		
VI																		1·634	6120 0	Q	LW	N	7		
F	1·023	9775 2	(1 016)	Q	LN	N	8																		
V	1·212	8250·8	(1·20)	Q	LN	N	11			1 783	5608 5	Q	LW	N	13			1 951	5125 6	Q	LW	N	8		
E	1 307	7651·1	(1 298)	Q	LN	N	11																		
IV	1 513	6609·4	(1 493)	Q	LW	N	67			2 193	4560 0	Q	LW	PR	43	17		2 364 2 403 2 441	4230 1 4161 5 4096 6	Q	LW	PR	80	44	30
δ																		2 550	3921·6						
D	1 663	6013·2	(1·643)	Q	LW	N	20																		
E′										2 696	3709 2	Q	LW	N	9										

Table I (continued).

Band.	NH_3.									PH_3.								AsH_3.							
	Wave-length.	Wave-number.	Schierkolk's values for NH_3	Prism.	Tubes.	Resolution	Absorption percentage at atmospheres			Wave-length.	Wave-number.	Prism.	Tubes.	Resolution.	Absorption percentage at atmospheres.			Wave-length	Wave-number.	Prism	Tubes.	Resolution	Absorption percentage at atmospheres		
							1.	¼.	⅛.						1	¼.	⅛.						1	¼.	⅛.
	μ.		μ.																						
																		3·178	3146·6	Q	LW	PR	64	27	
III	1·967	5083·9	(1·935)	Q	LW	P	83		24	2·929	3413·7	Q	LW	P	67	27		3·235	3091·2	F	LW	N	57		
																		3·316	3015·7	F	SW	N	21		
																		3·378	2960·3	Q	LW	PR	17	7	
γ										3·107	3218·5	Q	LW	N	9			3·461	2889·3				12	6	
																		3·506	2852·3				8	4	
	2·220	4504·0																							
C	2·264	4416·9	(2·239)	Q	LW	PR	97	57	30																
	2·315	4319·6																							
										3·353	2982·4														
D′										3·407	2935·1	Q	LW	PR	14										
										3·462	2888·5														

E''																			3·683	2715·2	F	LW	N	5	
II	2·916	3429·8		Q	LW	PR		65	43	4·169	2398·7							4 562	2192·0						
	2·996	3335·6	(2·974) (Spence 3·0022) (Coblentz 2·98)		SW	PR	70	35		4 297	2327·2	F	SW	PR	95	75	61	4 713	2121·9	F	SW	PR	95	89	81
	3·096	3227·9		F	SW	N	57			4 437	2253·9							4 860	2057·5						
β										4 722	2117·7	F	SW					5 207	1920·5	F	SW	PR	29	12	
										4 924	2031·0							5 393	1854·2				28	10	
										5·057	1977·2							5·514	1813·4				27	8	
4·05 μ	ca. 4·05	2469	(3 896)																						
I	6·132	1630·9	(6 136) (Coblentz 6·1)	F	SW	R	92	75	50	8·889	1125·0	RS	SW	R	80	55	37	9·946	1005·4	RS	SW	R	79	71	55
				RS	SW	PR	87	67																	
α										10·068	993·2	RS						11·037	906·0	RS					
10·55 μ	10·322	968·8	(10·315) (Coblentz 10·4) (Barker 10·3)	RS	SW	R	80	72	65																
	10·710	933·7	(10·669) (Coblentz 10·75) (Barker 10·7)	RS	SW	R	80	75	70																
A'										14·778	676·7	RS	LW	N	22	15									
a	15 906	628·6		RS	LN	N	52	30																	

For ease in referring to them the oscillation bands have been given numbers in accordance with the sequence into which they are considered to fall. Broadly, it may be said that while NH_3 exhibits a more complicated spectrum, all three gases have in common a main sequence of harmonic bands, these being given numerals I, II, ...; NH_3 has a second sequence, not represented in PH_3 nor in AsH_3, and indicated by capital letters C, D, ..., a faint sequence of which the farthest band measured is a member, indicated by small letters, *a*, *b*, ..., together with a band at 4·05 μ and a well-defined and resolved band at 10·55 μ; PH_3 and AsH_3, in addition to the main series, have each a sequence indicated by A′, B′, ..., and A″, B″, ..., and a sequence not represented in NH_3, to which numerals α, β, ... are given.

In Table I are also included the values found for NH_3 by Coblentz and Schierkolk, and for the bands of NH_3 examined by Spence and by Colby and Barker; the materials of the prism (Q = quartz, F = fluorite, RS = rocksalt); the dimensions of the observation tubes (SW = 10 cm. long × 5 cm. wide, LW = 45 cm. long × 5 cm. wide, LN = 45 cm. long × 2·5 cm. wide); the nature of the resolution (N = not resolved, PR = partially resolved, R = resolved); and the percentage of absorption found at 1, $\frac{1}{4}$ and $\frac{1}{8}$ atmosphere. Later tables give some results at lower pressures. The underlined values in Table I relate to more or less resolved central branches of the bands.

Main Sequence (NH_3, PH_3 and AsH_3,—I, II, ..).

These bands (I to VI) form a nearly harmonic sequence whose relationships will be discussed in Part IV. As a rule their intensity decreases towards the visible. The sequence in NH_3 springs from a simple fundamental band at 6·132 μ (1630·9 W.N.), but in PH_3 and AsH_3 from fundamentals at 8·889 μ (1125 W.N.) and 9·946 μ (1005·4 W.N.) respectively, which themselves form bands fused with the fundamentals of another sequence (α, β, ...).

All the bands of this main sequence are of the same type (Type 2, see Part IV, fig. 9), characterised by an intense zero (Q) branch with less intense side branches (P and R). Fine structure has been found superimposed on this general contour in band I and band II (partially) of NH_3, in band I of PH_3 and band I of AsH_3. In addition this general contour is observable in bands III of NH_3, III and IV of PH_3 and III and IV of AsH_3, the remaining bands of this sequence in the respective gases being distinct but unresolved (see Part IV.)

Second Sequence (NH_3– C, D, ... ; PH_3—A′, B′, ... ; AsH_3—A″, B″, ...).

In NH_3 this sequence starts with the strong band, C, apparently tripartite, and its members C, D and E, as well as the band at 4·05 μ, occur at approximately intermediate positions between bands of the main sequence.

In PH_3 occurs a less well-defined sequence A′, D′, E′, and in AsH_3 a similar sequence A″, C″, E″, both sequences being incomplete.

The members of this second sequence in the respective gases are not related to one another in the same simple fashion as are the members of the main sequence in each gas.

Third Sequence (PH_3, AsH_3,—α, β, ...).

This sequence, taking origin in Q branches at 10·068 μ and 11·037 μ on the short W.N. side of the composite bands of PH_3 and AsH_3, whose centres are at 9·146 and 10·412 μ respectively, has also members which are tripartite. It is not represented in NH_3.

Sequence X—or Rotation—(NH_3—*a*, *b*, ...).

Of this sequence the first band *d* appears at 628·6 W.N. (15·91 μ) It is simply related to the band *a* of NH_3 found by Rubens and Wartenberg* at about 159 W.N. (63 μ) and the succeeding members of the sequence can be traced superimposed on the fine structure of band 10·55 μ (see Part IV).

Band 10·55 μ (NH_3).

This band, of which the central dip is at 948·1 W.N., has been resolved and has the peculiar feature of having two Q branches close to one another (Type 3, see Part IV, fig. 9). Its general contour so far is unique in the spectrum of these gases, and apparently it has no members associated with it in simple harmonic fashion, as far as 17 μ.

In the cases where any of the above bands has been resolved into fine structure, the details are given in the following section.

ROTATION-OSCILLATION BANDS.—*Tables* II *to* VII, *figs.* 2 *to* 7.

Of those bands or regions which have been resolved the numerical data giving the wave-numbers of the rotation maxima, their wave-number differences, and wave-lengths will be found in Tables II to VII, with the corresponding curves in figs. 2 to 7. From the direction of greater to smaller wave-number the rotation maxima are numbered ... 3, 2, 1 to the zero of a band (Q), and beyond the zero 1′, 2′, 3′, ...

---

* 'Rev. Phy. Ges. Verh.,' vol. 13, p. 796 (1911).

The following is a list of the figures and tables :—

Figures.	Tables.
Fig. 1—Oscillation bands of NH_3, PH_3 and AsH_3.	Table I—Oscillation bands of NH_3, PH_3 and AsH_3.
Fig 2 -Ammonia—Band I.	Table II—Structure of band I of NH_3.
	Table IIA—Intermediate region between bands I and 10·55 μ of NH_3.
Fig. 3 -Ammonia—Band II	Table III—Structure of band II of NH_3.
Fig. 4—Ammonia—Band at 10·55 μ.	Table IV—Structure of band at 10·55 μ of NH_3.
Fig. 5—Phosphine -Band I and band α.	Table V—Structure of band I of PH_3.
	Table VA—Structure of band α of PH_3.
Fig 6—Phosphine--Band II.	Table VI—Structure of band II of PH_3
Fig. 7—Arsine—Band I and band α.	Table VII—Structure of band I of AsH_3.
	Table VIIA—Structure of band α of AsH_3
Fig 8—Arsine—Band II.	
	Table VIII—Effect of pressure on maxima of absorption bands.
	Table VIIIA—Effect of pressure on the area under the absorption bands.

The data obtained for oscillation and rotation-oscillation bands will be discussed in Part IV, in which the numbering of tables is consecutive with those in this part.

Robertson and Fox.

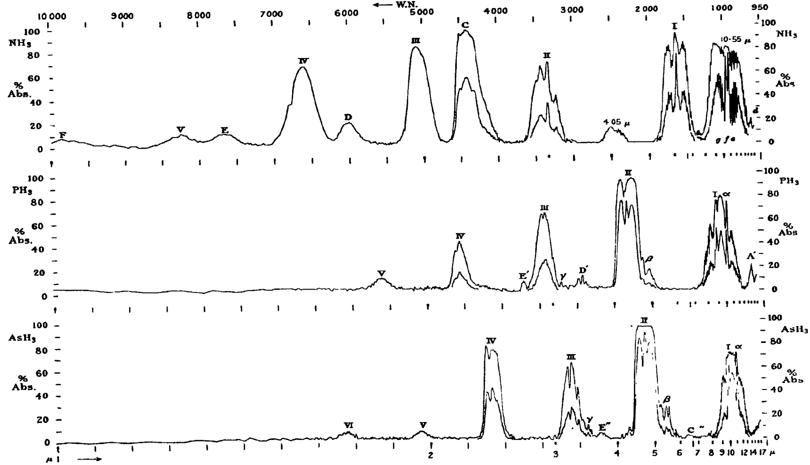

FIG. 1.—Oscillation Bands of NH_3, PH_3 and AsH_3.

(Facing p. 168.)

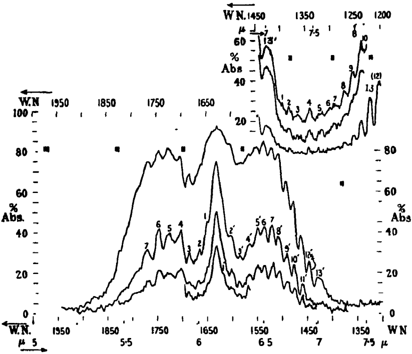

FIG. 2.—Ammonia. Band I and Intermediate Region, Bands I to 10·55 μ

The curves from top to bottom are for 1 atm , ½ atm , ¼ atm and $\frac{1}{16}$ atm pressure: using short wide tubes.

Inset curves. top, 20 per cent. high, long wide tubes; middle, 10 per cent. high, long wide tubes; bottom, short wide tubes—all at 1 atm. pressure.

(See Tables II, IIA.)

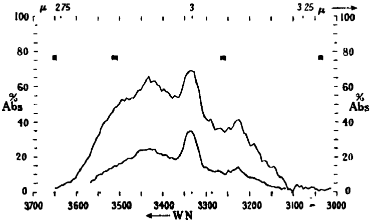

FIG. 3.—Ammonia. Band II.

Curves at 1 atm. (top) and ½ atm. pressure (bottom): short wide tubes.

(See Table III.)

ROTATION BANDS.

Table II.—Structure of Band I of NH_3.

(Fluorite prism ; short tubes)—see fig. 2.

Band.	1 atmosphere.		½ atmosphere.		¼ atmosphere.		1/16 atmosphere.		Mean W.N.	Δ W.N.	Mean W.L.	Band.
	W.N.	W.L.	W.N.	W.L.	W.N.	W.L.	W.N.	W.L.				
7	1766·9	μ. 5·660	1769·9	μ. 5·650	1766·9	μ. 5·660		μ.	1767·9 ±1·5	22·5	μ. 5·66	7
6	1746·1	5·727	1746·1	5·727	1744·9	5·731			1745·4 ±0·6	19·8	5·73	6
5	1725·6	5·795	1725·6	5·795	1725·6	5·795			1725·6 ±0	22·4	5·79	5
4	1703·6	5·870	1702·4	5·874	1703·6	5·870			1703·2 ±0·6	17·6	5·87	4
3	1684·9	5·935	1684·9	5·935	1686·3	5·930	1686·3	5·930	1685·6 ±0·7	20·4	5·93	3
2			1663·9	6·010	1666·4	6·001	1665·2	6·005	1665·2 ±1·2	16·3	6·00	2
1			1640·3	6·063	1649·3	6·063	1648·2	6·067	1648·9 ±0·5	18·0	6·06	1
0 (Q)	1627·6	6·144	1630·0	6·135	1631·3	6·130	1631·3	6·130	1630·9 (3)	13·0	6·13	0
1′					1617·9	6·181	1617·9	6·181	1617·9 ±0	15·9	6·18	1′
2′	1601·5	6·244	1602·5	6·240	1601·5	6·244	1601·5	6·244	1602·0 ±0·5	16·3	6·24	2′
3′			1585·0	6·309	1586·0	6·305	1586·0	6·305	1585·7 ±0·5	19·1	6·31	3′
4′	1564·2	6·393	1564·2	6·393	1566·7	6·383	1568·9	6·374	1566·6 ±2·2 (3)	18·1	6·38	4′
5′	1548·5	6·458	1548·5	6·458	1548·5	6·458			1548·5 ±0	12·8	6·46	5′

6′	1534·9	6·515	1534 9	6 515	1537 2	6 505			1535·7 ±1 1	15 6	6·51	6′
7′	1520·9	6 575	1519·7	6 580	1519·7	6 580			1520·1 ±0 6	14 4	6·58	7′
8′	1505·1	6·644	1506·0	6 640	1506 0	6 640			1505 7 ±0 4	15 3	6 64	8′
9′	1490·1	6·711	1490 1	6 711	1491 0	6·707			1490 4 ±0 4	14 4	6 71	9′
10′	1476 0	6·775	1476 0	6·775	1476 0	6 775			1476 0 ±0	16 1	6 77	10′
11′	1460·4	6 847	1459 6	6 851	1459 6	6 851			1459 9 ±0·4	13 8	6 85	11′
12′	1446 1	6 915	1446 1	6 915	1446 1	6 915			1446·1 ±0	19 6	6 91	12′
13′	1426 5	7 010							1426 5		7 01	13′

Schierkolk (' Z. f. Physik,' vol. 29, p. 285 (1924)) has resolved this band partially and gets the following maxima :—

5·677, 5·742, 5·816, 5·863, 6·136 (Q)
6·325, 6·392, 6·461, 6·503, 6·573, 6·618, 6·703.

Table IIA.—Intermediate Region between Bands I and 10·55 μ of NH_3—see fig. 2 (inset).

Band.	1 atmosphere.		1 atmosphere.		½ atmosphere.		Mean W.N.	Δ W.N.	Mean W.L.	Band.
	W.N.	W.L.	W.N.	W.L.	W.N.	W.L.				
		μ.		μ.		μ.			μ.	
13′ (see also Table II)	1427 3	7·006	1427 3	7 006			1427 3	31 0	7 01	13′
1			1396 3	7 162			1396 3	13 6	7 16	1
2	1382·7	7·232	1381 8	7·237	1383 5	7 228	1382 7	16 8	7 23	2
3			1365 9	7 321			1365 9	24·6	7 32	3
4	1341·3	7 455	1341 3	7 455	1341 3	7 455	1341 3	21·3	7·46	4
5	1320 0	7·576	1320 0	7 576			1320 0	15 5	7·58	5
6			1304·5	7 666			1304·5	13 7	7·67	6
7	1290 8	7·747	1290·8	7·747			1290 8	21 0	7·75	7
8	1269·8	7 875	1269·8	7 875	1269 8	7 875	1269 8	15·5	7·88	8
9			1253 9	7 975	1254·7	7 970	1254·3	17 7	7 97	9
10	1236 6	8 086	1236·6	8 086	1236 6	8 086	1236 6		8 09	10
13 (see Table IV)							(1218 2)		(8·209)	13

Table III.—Structure of Band II of NH_3.

(Quartz prism ; short tubes) see fig. 3.

Band.	G L.			Results of Spence (with grating).			Band.
	W.N.	W.L.	Δ W.N	W N.	W.L.	Δ W N.	
		μ.			μ.		
5	3435·2	2·911		3430·4	2·9151		5
			16·4			19·4	
4	3418·8	2·925		3411·0	2·9317		4
			19·8			19·0	
3	3399·0	2·942		3392·0	2·9481		3
			25·2			19·1	
2	3373·8	2·964		3372·9	2·9648		2
						18·9	
1				3354·0	2·9815		1
						23·1	
0	3335·6	2·998		3330·9	3·0022		0
			26·5			15·9	
1′	3309·1	3·022		3315·0	3·0166		1′
			18·5			20·5	
2′	3200·6	3·039		3294·5	3·0354		2′
			19·4			20·9	
3′	3271·2	3·057		3273·6	3·0547		3′
			27·6			20·2	
4′	3243·6	3·083		3253·4	3·0737		4′
			15·7			19·7	
5′	3227·9	3·098		3233·7	3·0924		5′
			15·6			19·3	
6′	3212·3	3·113		3214·4	3·110		6′
			22·5			21·3	
7′	3189·8	3·135		3193·1	3·1318		7′
			23·2			21·3	
8′	3166·6	3·158		3171·8	3·1528		8′
			20·0			19·1	
9′	3146·6	3·178		3152·7	3·1719		9′
			17·7			17·8	
10′	3128·9	3·196		3134·9	3·1899		10′

Table IV—Structure of Band 10·55 μ of NH_3.

(Rocksalt ; short tubes)—see fig. 4.

Band.	1 atmosphere.		½ atmosphere.		¼ atmosphere.		$\frac{1}{16}$ atmosphere.		Mean W.N.	Δ W.N.	Mean W.L.	Band.
	W.N.	W L.	W.N.	W.L.	W.N.	W.L.	W N.	W.L.				
13		μ.	1218 2	μ. 8·209		μ.		μ.			μ.	13
12	1202·2	8 318	1201·8	8 321	1198·6	8 343			1200 9 ±1 8		8·327	12
11	1183·4	8 450	1183 0	8 453	1180·1	8 474			1182 2 ±1 5	18·7	8·459	11
10	1161·7	8·608	1162 7	8·601	1162 5	8·602			1162·3 ±0 4	19·9	8 604	10
9	1140 6	8·767	1142 7	8 751	1141 3	8 762			1141 5 ±1 0	20 8	8·760	9
8			1123·5	8 901	1122 1	8 912			1122·8 ±0 7	18 7	8 906	8
7			1109·3	9·015	1110 1	9·008			1109 7 ±0 4	13·1	9 011	7
6			1094·9	9 133	1093 5	9·145			1094 2 ±0 7	15·5	9·139	6
5			1076 5	9 289	1077 4	9·282			1077 0 ±0 5	17·2	9 285	5
4			1056·7	9·463	1057 4	9 457			1057 0 ±0 3	20 0	9 460	4
3			1037 9	9 635	1038 5	9 629			1038 2 ±0·3	18·8	9 632	3
2	1015·4	9·848	1016 3	9 840	1015·5	9 847			1015 7 ±0 4	22 5	9 845	2
1	997·7	10 023	997·3	10 027	996 8	10 032			997 2 ±0 3	18 5	10 028	1
Q			968·4	10·326	968 4	10·326	969 6	10 314	968 8 ±0 6	28·4	10 322	Q
Q−1					956 9	10 450	957 7	10·442	957·3 ±0 4	11·5	10·446	Q_{-1}
										9 2		

Zero			949 2	10·535	947 8	10 551	948 5	10·543	948·1 ±0·3	14·4	10 547	Zero
Q′			933 2	10 716	933 5	10 712	934·3	10·703	933·7 ±0 5	20·3	10 710	Q′
1′			914 3	10 937	913·0	10 953	912 9	10·954	913 4 ±0 7	20 4	10·948	1′
2′	893 5	11 192	893 1	11·197	892·6	11 203			893 0 ±0 4	20·2	11·198	2′
3′	873 3	11 451	872 8	11 458	872 2	11 465			872 8 ±0 5	19 4	11 457	3′
4′	853 5	11 716	853 8	11·712	853 3	11 719			853 4 ±0 2	19 5	11 718	4′
5′	834 4	11 985	834 0	11 991	833 4	11 999			833 9 ±0 5	19 0	11 992	5′
6′	815 5	12 263	814 5	12 278	814 6	12 270			814 9 ±0 6	16 5	12 271	6′
7′			797 8	12 535	799 1	12 514			798 4 ±0 6	8 7	12 525	7′
8′			789 7	12 663	789 8	12 662			789 7 ±0 0	8 8	12 663	8′
9′	780 4	12 814	781 8	12·791	780 6	12 810			780 9 ±0 7	12 5	12 806	9′
10′			768 7	13 009	768 1	13 019			768 4 ±0 3	20 5	13 014	10′
11′	748·9	13 353	747 3	13 381	747 4	13 380			747 9 ±0 8	9 7	13 371	11′
12′	739 4	13 524	739 0	13 531	738 1	13 548			738 2 ±0 1	9 8	13 546	12′
13′	728·0	13·737	728 1	13 735	729 2	13 713			728 4 ±0 6	17·4	13 729	13′
14′	712 1	14 043	712 2	14 041	711 7	14 051			711 0 ±0 2	18 7	14 065	14′
15′	692 0	14 451	692 6	14 439					692 3 ±0 3		14 445	15′

Schierkolk (*loc. cit*) in a partial resolution of this band gives the following values for some of the rotation maxima of this band: 7·855, 8·002, 8·10. 8 223, 8·339, 9·237, 9·463, 9·575, 9·838, 9·987. 10 315 (Q). 10 669 (Q′), 11·153. 11·443, 11·686, 11·965, 12·215, 12·49, 12·63, 12·77, 12·99, 13·34. 13·52, 13·72, 14·02.

Colby and Barker (*loc. cit.*) give the value 10·3 μ for Q and 10·7 μ for Q′

Coblentz (*loc. cit.*) also has resolved a portion of this band and gets the following values 10·4 (Q). 10·75 (Q′), 11·18, 11·43, 11·69. 11·98 12·3, 12·78 and 13·7.

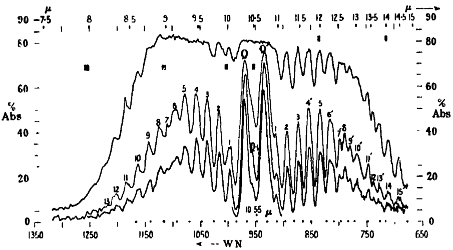

FIG. 4.—Ammonia. Band at 10·55 μ.

The curves from top to bottom at 1 atm, $\frac{1}{2}$ atm., $\frac{1}{8}$ atm. and $\frac{1}{16}$ atm. pressure. short wide tubes. (See Table IV)

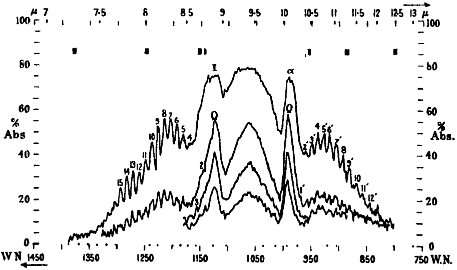

FIG. 5.—Phosphine. Bands I and α.

The curves from top to bottom are for 1 atm., $\frac{1}{2}$ atm., $\frac{1}{8}$ atm. and $\frac{1}{16}$ atm. pressure: short wide tubes. (See Table V)

Table V.—Structure of Band I of PH_3.

(Fluorite prism ; short tubes)—see fig. 5.

Band.	1 atmosphere.		$\frac{1}{2}$ atmosphere.		$\frac{1}{4}$ atmosphere.		$\frac{1}{16}$ atmosphere.		Mean	Δ W.N.	Mean W.L.	Band.
	W.N.	W.L.	W.N.	W.L.	W.N.	W.L.	W.N.	W.L.	W.N.			
		μ.		μ.		μ.		μ.			μ.	
15	1294·0	7·728	1294·0	7·728					1294·0 ±0		7·73	15
										12·0		
14	1282·0	7·800	1282·0	7·800					1282·0 ±0		7·80	14
										10·7		
13	1270·6	7·870	1272·1	7·861					1271·3 ±0·6		7·87	13
										11·4		
12	1259·9	7·937	1259·9	7·937					1259·9 ±0		7·94	12
										11·8		
11	1248·4	8·010	1247·8	8·014					1248·1 ±0·3		8·01	11
										11·1		
10	1236·7	8·086	1237·3	8·082					1237·0 ±0·3		8·08	10
										11·6		
9	1225·8	8·158	1225·1	8·162					1225·4 ±0·3		8·16	9
										10·6		
8	1214·8	8·232	1214·8	8·232					1214·8 ±0		8·23	8
										11·4		
7	1203·7	8·308	1203·1	8·312					1203·4 ±0·3		8·31	7
										11·7		
6	1192·0	8·389	1191·5	8·393					1191·7 ±0·2		8·39	6
										11·9		
5	1179·1	8·481	1180·5	8·471					1179·8 ±0·7		8·47	5
										11·0		
4	1168·5	8·558	1169·2	8·553					1168·8 ±0·3		8·56	4
										13·8		
3			1155·0	8·658					1155·0		8·66	3
										11·6		
2	1143·5	8·745	1142·8	8·750	1144·1	8·740			1143·4 ±0·6		8·74	2
Q			1126·7	8·875	1126·7	8·875	1128·0	8·865	1127·1 ±0·6		8·87	Q
									1125·0 (R.S.)		8·89	

Table VA.—Structure of Band α of PH_3.

(Rocksalt prism; short tubes)—see fig. 5.

Band.	1 atmosphere.		½ atmosphere.		Mean W.N.	Δ W.N.	Mean W.L.	Band.
	W.N.	W.L.	W.N.	W.L.				
		μ.		μ.			μ.	
1′			972·1	10·287	972·1		10·287	1′
2′	961·0	10·406	961·0	10·406	961·0	11·5	10·406	2′
3′	950·0	10·526	949·1	10·536	949·5	10·0	10·532	3′
4′	939·1	10·648	940·0	10·638	939·5	10·9	10·644	4′
5′	928·6	10·769	928·6	10·769	928·6	11·1	10·769	5′
6′	917·5	10·899	917·5	10·899	917·5	11·2	10·899	6′
7′	905·9	11·039	906·7	11·029	906·3	13·8	11·034	7′
8′	892·1	11·210	892·9	11·200	892·5	11·1	11·204	8′
9′	881·8	11·341	881·0	11·351	881·4	11·6	11·345	9′
10′	869·4	11·502	870·2	11·492	869·8	14·1	11·497	10′
11′	855·7	11·686			855·7	10·8	11·686	11′
12′	844·9	11·836	844·9	11·836	844·9		11·836	12′

Table VI.—Structure of Band II of PH_3.

(Fluorite; short wide tubes)—see fig. 6.

P branch.			R branch.		
W.N.	Δ W.N.	W.L.	W.N.	Δ W.N.	W.L.
		μ			μ
2414·3	11·0	4·142	2280·5	8·8	4·385
2403·3	11·0	4·161	2271·7	9·3	4·402
2392·3		4·180	2262·4	10·6	4·420
			2251·8	11·2	4·441
			2240·6	10·0	4·463
			2230·6		4·483

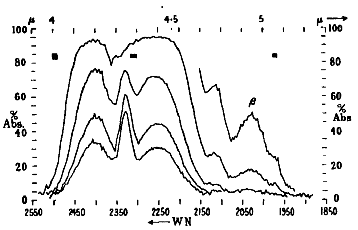

FIG. 6.—Phosphine. Bands II and β.

The curves from top to bottom are for 1 atm., ½ atm , ¼ atm. and $\frac{1}{16}$ atm. pressure : short wide tubes. (See Table VI)

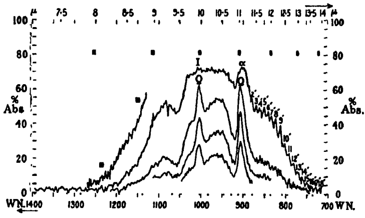

FIG. 7.—Arsine. Bands I and α.

The curves from top to bottom are for 1 atm , ½ atm , ¼ atm. and $\frac{1}{16}$ atm. pressure : short wide tubes. The broken curve for 1 atm. pressure : long wide tubes. (See Tables VII and VIIA.)

Table VII.—Structure of Band I of AsH_3.

(Fluorite and rocksalt prisms)—see fig. 7.

Fluorite prism.		Rocksalt prism.		Δ W.N.
W.N.	W.L.	W.N.	W.L.	
	μ.		μ.	
1253·1	7·980			
1245·6	8·028			7·5
1236·7	8·086			8·9
1226·5	8·153			10·2
1219·5	8·200			7·0
1212·7	8·246	1210·6	8·260	7·9
1201·8	8·321			9·8
1192·7	8·384			9·1
1186·8	8·426	1185·3	8·437	6·7
1179·1	8·481			6·9
1170·4	8·544	1170·1	8·546	8·9
1160·9	8·614			9·3
1151·8	8·682			9·1
		1116·4	8·957	
		1105·6	9·045	10·8
		1097·6	9·111	8·0
		1089·2	9·181	8·4
		1081·2	9·249	8·0

Table VIIA.—Structure of Band α of AsH_3.

(Rocksalt prism ; short tubes)—see fig. 7.

Band.	1 atmosphere.		½ atmosphere.		¼ atmosphere.		Mean W.N.	Δ W.N.	Mean W.L.	Band.
	W.N.	W.L.	W.N.	W.L.	W.N.	W.L.				
1′		μ.		μ.		μ.			μ.	1′
2′	880·6	11·356	879·9	11·365	882·2	11·335	880 9	11·3	11·352	2′
3′	869 8	11·497	870 6	11 486	868·4	11·516	869·6	8·2	11·500	3′
4′	861·4	11·609	862·2	11·598	860·7	11·618	861·4	10·1	11 609	4′
5′	850·9	11·752	851 7	11·741			851·3	9·2	11·747	5′
6′	841·7	11·881	842·5	11·870			842·1	10·1	11·875	6′
7′	832·6	12·010	831·3	12 029	832·0	12·019	832·0	8·8	12·019	7′
8′	822·4	12 159	823·9	12·138			823·2	11·0	12·148	8′
9′	811·8	12·318	812·5	12·307			812 2	10·3	12·312	9′
10′	802·1	12·467	802·8	12·456	800·9	12·486	801·9	10 2	12·470	10′
11′	791·5	12 635	792·8	12·614	790·3	12·653	791 7	10·3	12·631	11′
12′	781·1	12·802	781·8	12 791	781·2	12·801	781 4	11·8	12·798	12′
13′	769·3	12·999			769·9	12·989	769·6	11·4	12·994	13′
14′	758·2	13 190					758·2	8·1	13·189	14′
15′	750·1	13·331					750·1	8·9	13·331	15′
16′	741·2	13·492					741·2	10·5	13·492	16′
17′	730·7	13·685					730·7	9·1	13·685	17′
18′	721·6	13·858					721·6		13·858	18′

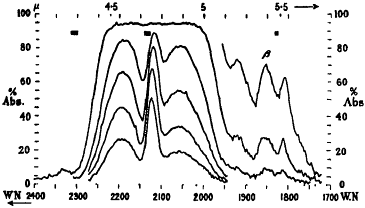

Fig. 8.—Arsine. Bands II and β.

The curves from top to bottom are for 1 atm, $\frac{1}{2}$ atm, $\frac{1}{4}$ atm., $\frac{1}{16}$ atm and $\frac{1}{32}$ atm. pressure: short wide tubes. The broken curve is for 1 atm pressure: long wide tubes.

Table VIII.—Effect of Pressure on Maxima of Absorption Bands at the Central Frequency.

NH_3—Band I.

Band.	Pressure atmospheres.	Absorption per cent.	Calculated absorption assuming Beer's Law.	Difference from observed absorption, per cent
7	1·0	75	79	+ 4
	0·25	32	(32)	(0)
	0·125	16	18	+ 2
6	1·0	80·5	89	+ 8·5
	0·25	42	(42)	(0)
	0·125	21	24	+ 3
5	1·0	82	87	+ 5
	0·25	40	(40)	(0)
	0·125	20	22·5	+ 2·5
4	1 0	78	88	+10
	0·25	41·5	(41·5)	(0)
	0·125	22·5	23·5	+ 1
3	1·0	69	75	6
	0·25	30	(30)	(0)
	0·125	16	16	0
	0·062	11	8	− 3
2	1·0	78	78	0
	0·25	32	(32)	(0)
	0·125	16	17	+ 1
	0·062	9·5	9·0	− 0·5
1	1·0	—	—	—
	0·25	45	(45)	(0)
	0·125	23	26	+ 3
	0·062	15	14	− 1

Table VIII (continued).

NH_3—Band I (continued).

Band.	Pressure atmospheres.	Absorption per cent.	Calculated absorption assuming Beer's Law.	Difference from observed absorption, per cent.
Q	1·0	92 5	99	+ 6·5
	0·25	75	(75)	(0)
	0·125	50	50	0
	0·062	33	30	− 3
1′	1·0	—	—	—
	0·25	—	—	—
	0·125	27	(27)	(0)
	0·062	19	15	− 4
2′	1·0	84	85	+ 1
	0·25	38	(38)	(0)
	0·125	22	21	− 1
	0·062	13	11	− 2
3′	1·0	74	73	− 1
	0·25	28 5	(28 5)	(0)
	0·125	16	15	− 1
	0·062	9·5	8	− 1 5
4′	1·0	79	81	+ 2
	0·25	34	(34)	(0)
	0·125	19·5	19	− 0·5
	0·062	14	10	− 4
5′	1 0	82	89	+ 7
	0·25	42·5	(42·5)	(0)
	0·125	24	25	+ 1
6′	1·0	85	89	+ 4
	0·25	42·5	(42·5)	(0)
	0·125	23·5	25	+ 1·5
7′	1·0	81·5	90	+ 8·5
	0·25	43·5	(43·5)	(0)
	0 125	25	25	0
8′	1·0	78	85	+ 7
	0·25	38	(38)	(0)
	0·125	21	21	0
9′	1·0	65	74	+ 9
	0·25	29	(29)	(0)
	0·125	15·5	16	+ 0·5
10′	1 0	55	67	+12
	0·25	24	(24)	(0)
	0·125	12·5	13	+ 0·5
11′	1·0	41	47	+ 6
	0·25	14·5	(24)	(0)
	0·125	9	8	− 1
12′	1·0	25·5	27	+ 1·5
	0·25	7·5	(7·5)	(0)
	0·125	4·5	4	− 0·5

Table VIII (continued).

NH_3—Band at 10·55 μ.

Band.	Pressure atmospheres.	Absorption per cent.	Calculated absorption assuming Beer's Law.	Difference from observed absorption, per cent.
12	1·0	37	41	+ 4
	0·25	12	(12)	(0)
	0·125	7	6	− 1
11	1·0	55	53	− 2
	0·25	17	(17)	(0)
	0·125	10	9	− 1
10	1·0	67	70	+ 3
	0·25	26	(26)	(0)
	0·125	15	14	− 1
9	1·0	77	83·5	+ 6·5
	0·25	36	(36)	(0)
	0·125	19	20	+ 1
8	1·0	83	88	+ 5
	0·25	42	(42)	(0)
	0·125	25	24	− 1
	0·062	13	12	− 1
7	1·0	82	90	+ 8
	0·25	44	(44)	(0)
	0·125	24	25	+ 1
	0·062	13	14	+ 1
6	1·0	82	94	+12
	0·25	50	(50)	(0)
	0·125	29	29	0
	0·062	16	16	0
5	1·0	80	96	+ 16
	0·25	56	(56)	(0)
	0·125	33	34	+ 1
4	1·0	80	97	+ 17
	0·25	57	(57)	(0)
	0·125	37	34	− 3
3	1·0	80	96	+17
	0·25	55	(55)	(0)
	0·125	37	33	− 4
2	1·0	80	93	+13
	0·25	49	(49)	(0)
	0·125	31	29	− 2
1	1·0	77	80	+ 3
	0·25	33	(33)	(0)
	0·125	23	18	− 5
Q	1·0	81	99	+18
	0·25	72	(72)	(0)
	0·125	65	47	−18
	0·062	55	28	−27

Table VIII (continued).

NH$_3$—Band at 10·55 μ (continued).

Band.	Pressure atmospheres.	Absorption per cent.	Calculated absorption assuming Beer's Law.	Difference from observed absorption, per cent
Q′	1·0	80·0	99	+19
	0·25	75·0	(75)	(0)
	0·125	70·5	50	-20·5
	0·062	58	30	−28
1′	1·0	77	86	+ 9
	0·25	39	(39)	(0)
	0·125	21·5	22	+ 0·5
	0·062	12·5	12	− 0·5
2′	1·0	75	87	+12
	0·25	40	(40)	(0)
	0·125	25	22	− 3
3′	1·0	77	91	+14
	0·25	45	(45)	(0)
	0·125	27	26	− 1
4′	1·0	77	94	+17
	0·25	50	(50)	(0)
	0·125	33	30	− 3
5′	1·0	76	94	+18
	0·25	50	(50)	(0)
	0·125	31	30	− 1
6′	1·0	75	91	+16
	0·25	45	(45)	(0)
	0·125	27·5	26	− 1·5
7′	1·0	70	83	+13
	0·25	36	(36)	(0)
	0·125	21	20	− 1
8′	1·0	70	87	+17
	0·25	40	(40)	(0)
	0·125	25	23	− 2
9′	1·0	69	90	+21
	0·25	44	(44)	(0)
	0·125	19	25	+ 6
10′	1·0	64	75	+11
	0·25	30	(30)	(0)
	0·125	19	16	− 3
		PH$_3$—Band α.		
Q	1·0	75	97	+22
	0·25	58·5	(58·5)	(0)
	0·125	41·5	36	− 5·5
	0·062	29	20	− 9

Table VIII (continued).

PH_3—Band α (continued).

Band.	Pressure atmospheres.	Absorption per cent.	Calculated absorption assuming Beer's Law.	Difference from observed absorption, per cent.
3′	1·0	42	61	+19
	0·25	21	(21)	(0)
	0·125	13	11	− 2
	0·062	11·5	6	− 5·5
4′	1·0	45·5	62	+16·5
	0·25	21·5	(21·5)	(0)
	0·125	16	11	− 5
5′	1·0	50·5	67	+16·5
	0·25	24·5	(24·5)	(0)
	0·125	18·5	13	− 5·5
6′	1·0	50	67	+17
	0·25	24	(24)	(0)
	0·125	17·5	13	− 4·5
7′	1·0	50	65	+15
	0·25	23	(23)	(0)
	0·125	16	12	− 4
8′	1·0	45	63	+18
	0·25	22·5	(22·5)	(0)
	0·125	17	12	− 5
9′	1·0	40	59	+19
	0·25	20	(20)	(0)
	0·125	15	11	− 4

PH_3—Band II.

Band.	Pressure atmospheres.	Absorption per cent.	Calculated absorption assuming Beer's Law.	Difference from observed absorption, per cent.
R	1·0	94	99	+ 5
	0·25	76·5	(76·5)	(0)
	0·125	50	51	+ 1
	0·062	35	30	− 5
Q	1·0	—	—	—
	0·25	75	(75)	(0)
	0·125	61	50	−11
	0·062	51·5	30	−21·5
P	1·0	95	99	+ 4
	0·25	72	(0)	(0)
	0·125	45	47	+ 2
	0·062	30	27	− 3

Table VIII (continued).

AsH$_3$—Band II.

Band.	Pressure atmospheres.	Absorption per cent.	Calculated absorption assuming Beer's Law.	Difference from observed absorption, per cent
R	1·0	95	100	+ 5
	0·25	85	(85)	(0)
	0·125	66	61	− 5
	0·062	45	38	− 7
	0·031	26·5	22	− 4·5
Q	1·0	95	100	+ 5
	0·25	89	(89)	(0)
	0·125	81	67	−14
	0·062	68	42	−26
	0·031	51	24	−27
P	1·0	95	100	+ 5
	0·25	81·5	(81·5)	(0)
	0·125	55·5	57	+ 1·5
	0·062	34	34	0
	0·031	19·5	19	− 0·5

Table VIIIa.—Effect of Pressure on the Area under the Absorption Bands.

NH$_3$—Band I.

Band.	Pressure atmospheres.	Absorption per cent.	Calculated absorption assuming Beer's Law.	Difference from observed absorption, per cent
R branch	1·0	49	64	+15
	0·25	23	(23)	(0)
	0·125	12	12	0
Q branch	1·0	91	97	+ 6
	0·25	59	(59)	(0)
	0·125	31	36	+ 5
P branch	1·0	56	67	+11
	0·25	24	(24)	(0)
	0·125	13	13	0

Table VIIIA (continued).

NH_3—10·55 μ.

Band.	Pressure atmospheres.	Absorption per cent.	Calculated absorption assuming Beer's Law.	Difference from observed absorption, per cent.
R branch	1·0	58	70	+12
	0·25	26	(26)	(0)
	0·125	15	14	− 1
Q branch	1·0	76	96	+20
	0·25	54	(54)	(0)
	0·125	31	32	+ 1
	0·062	22	18	− 4
Q′ branch	1·0	76	96	+20
	0·25	55	(55)	(0)
	0·125	39	32·5	− 6·5
	0·062	28	18	−10
P branch	1·0	58	71	+13
	0·25	27	(27)	(0)
	0·125	15	14	− 1

PH_3—Band α.

Q branch	1·0	60·5	86	+25·5
	0·25	38	(38)	(0)
	0·125	25	21	− 4
	0·062	19	11	− 8
P branch	1·0	30·5	51	+20·5
	0·25	16	(16)	(0)
	0·125	12	9	− 3

PH_3—Band II.

R branch	1·0	70	92	+22
	0·25	54	(54)	(0)
	0·125	35	27	− 8
	0·062	20	14	− 6
Q branch	0·25	63·5	(63·5)	(0)
	0·125	48	40	− 8
	0·062	40	22	−18
P branch	0·25	51	(51)	(0)
	0·125	28	30	+ 2
	0·062	20	17	− 3

Table VIIIA (continued).

AsH_3—Band II.

Band.	Pressure atmospheres.	Absorption per cent.	Calculated absorption assuming Beer's Law.	Difference from observed absorption, per cent
R branch	0·25	52	(52)	(0)
	0·125	33	31	− 2
	0·062	14	17	+ 3
Q branch	0·25	79	(79)	(0)
	0·125	70	54·5	−15·5
	0·062	35	32	− 3
P branch	0·25	41·5	(41 5)	(0)
	0·125	60	64	+ 4
	0·062	13	20	+ 7

Studies in the Infra-Red Region of the Spectrum. Part IV.—*Discussion of Absorption Bands of Ammonia, Phosphine and Arsine.*

By Sir Robert Robertson, F.R S., and J. J. Fox, D Sc.

(*Note.*—The numbering of figures and tables in this part runs consecutively with those in Part III.)

OSCILLATION BANDS.

Types of Bands in the Near Infra-Red.

Of absorption bands in the infra-red which are partially or more completely resolved, the following four types (fig. 9) have been observed in the work of others and ourselves.

Type 1 occurs in dipoles such as HCl, HBr and HF[*] and is absent in NH_3, PH_3 and AsH_3. Type 2 is characteristic of the Main Sequence of bands common to NH_3, PH_3 and AsH_3, and appears in the infra-red spectrum of CH_4[†]; type 3, so far found only in the band of NH_3 at 10·55 μ, contains two Q branches; while type 4 exhibits the fusion of two distinct bands, of which the zero branches in PH_3 and AsH_3 are the first members of a distinct series of harmonics.

---

[*] Imes, 'Astrophys. J.,' vol. 50, p. 251 (1919).

[†] Colby, 'Astrophys. J.,' vol. 62, p. 73 (1925).

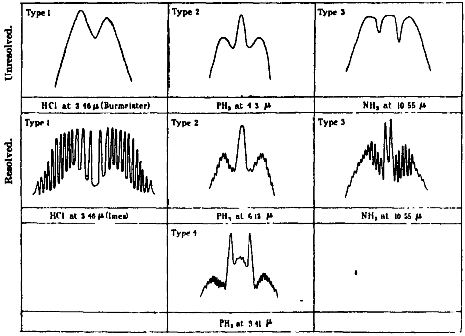

Fig. 9.

RATIOS OF CORRESPONDING OSCILLATION BANDS COMMON TO NH_3, PH_3 AND AsH_3.

Table IX.—Ratios of Position of Bands.

Main Sequence—NH_3, PH_3, AsH_3.

Band :	I.	II.	III.	IV.	V.	
NH_3—W.N.	1630·9	3335·6	5083·9	6609·4	8250·8	
PH_3—W.N.	1125·0	2327·2	3413·7	4560·0	5608·5	
AsH_3—W.N.	1005 4	2121·9	3091·2	4161·5	5125·6	
Ratio $\frac{PH_3}{NH_3}$	0·689	0·697	0·672	0·680	0·680	Mean 0·685
Ratio $\frac{AsH_3}{PH_3}$	0·893	0·911	0·905	0·912	0·914	Mean 0·907

Third Sequence—PH_3, AsH_3.

Band :	α.	β.	γ.
PH_3—W.N. . . .	993·2	2031·0	3218·5
AsH_3—W.N. .	906·0	1854·2	2889·3
Ratio $\frac{AsH_3}{PH_3}$ . .	0·912	0·913	0·900

It will be seen that there are nearly constant ratios between the vibration numbers of the members of the Main Sequence common to the three gases, and that the Second Sequence found in PH_3 and AsH_3 has a ratio similar to that in the main series for these two gases. There are thus certain degrees of freedom common to these gases.

From the change in frequency of vibration of similar bands with change in mass, it should be possible to calculate the distance of the heavy atom to the plane of the hydrogens, by assuming some law of force, and a tetrahedral structure.

INTER-RELATIONSHIPS OF BANDS OF EACH GAS (HARMONICS).

Table X.—Harmonic Relationships of Oscillation Bands.

Main Sequence—NH_3, PH_3, AsH_3.

	I. ($n=1$)	II. ($n=2$)	III. ($n=3$)	IV. ($n=4$)	V. ($n=5$)	VI. ($n=6$)
NH_3 W.N.	1630·9	3335·6	5083·9	6609·4	8250·8	
W.N. Δ		1704·7	1748·3	1525·5	1641·4	
Simple ratios of I	(1630·9)	3261·8	4892·7	6523·6	8154·5	
Difference from observed	(0)	73·8	191 2	85·8	96·3	
$\frac{W.N.}{n}$	1630·9	1667·8	1694·6	1652 4	1650·1	
PH_3 W.N.	1125·0	2327·2	3413·7	4560·0	5608·5	
W.N. Δ		1202 2	1086·5	1146·3	1048·5	
Simple ratios of I	(1125 0)	2250 0	3375 0	4500·0	5625 0	
Difference from observed .	(0)	77 2	38·7	60 0	16 5	
$\frac{W.N.}{n}$.	1125·0	1163·6	1137·9	1140·0	1121·7	
AsH_3 W.N.	1005 4	2121·9	3091·2	4161·5	5125 6	6120·0
W.N. Δ		1116·5	969·3	1070·3	964·1	994·4
Simple ratios of I	(1005·4)	2010·8	3016·2	4021·6	5027·0	6032·4
Difference from observed	(0)	111·1	75·0	139·9	98·6	87·6
$\frac{W.N.}{n}$	1005·4	1060·9	1030·4	1040·4	1025·1	1020 0

Table X. (continued).

Second Sequence—NH$_3$, PH$_3$, AsH$_3$.

Band :	A		B		C		D		E
NH$_3$									
W.N.	—		—		4416·9		6013·2		7651·1
W.N. Δ						1596·3		1637·9	
$\frac{\text{W.N.}}{n}$.	—		—		1472·3		1503·3		1530·2

Band :	A′		B′		C′		D′		E′
PH$_3$									
W.N.	676·7		—		—		2935·1		3709·2
W.N. Δ				(3×752·8)				774·1	
$\frac{\text{W.N.}}{n}$.	676·7						734		742

Band :	A″		B″		C″		D″		E″
AsH$_3$									
W.N. .	(ca. 500)		—		ca. 1550 weak		—		2715
W.N. Δ				(2×525)				(2×582)	
$\frac{\text{W.N.}}{n}$.	(500)		—		517				543

Third Sequence—PH$_3$ and AsH$_3$.

Band :	α.		β.		γ.		δ.
PH$_3$							
W.N.	993·2		2031·0		3218·5		
W.N. Δ		1037·8		1187·5			
$\frac{\text{W.N.}}{n}$	993·2		1015·5		1072·8		
AsH$_3$							
W.N.	906·0		1854·2		2889·3		3921·6
W.N. Δ		948·2		1035·1		1032·3	
$\frac{\text{W.N.}}{n}$	906		927·1		963·1		980·4

Table X (continued).

Sequence X—NH_3, or rotation.

Band:	*a.*	*d.*	*e.*	*f.*	*g.*
W.N.	(150) (R. & W.)	628·6	783·4	948·1	1108·5
W.N. Δ	(159)	(3×156·5)	154·8	164·7	160·4

Main Sequence: NH_3, PH_3, AsH_3—I, II, ...

The members of this sequence may be considered as to the extent to which they follow a harmonic ratio. For dipoles such as HCl Kratzer* considered that as a result of the compounding of rotation with oscillation the frequency values of the harmonics were less than whole multiples of the fundamental by a small quantity x, as in the equation $\nu = n\nu_0 (1 - nx)$

While the bands of the Main Sequence will be seen in Table X, where the W.N. of the band is divided by n, to be approximately multiples of the fundamental, in none of the three gases NH_3, PH_3, or AsH_3 does Kratzer's relation hold. Nor do the values obtained agree with such an equation, even if it were justifiable, in which x is positive, but with some exceptions they exhibit a small departure from simple ratios.

In all cases the value for the fundamental ($n = 1$) is low when compared with the values for the other bands divided by their ordinal number. The greater complexity of the movements in these molecules apparently has the effect of influencing the strictly harmonic relationships of the bands in a much less simple manner than attributed by Kratzer to dipoles, and it may be found possible to connect the deviations from true harmonic ratios with the intensity of neighbouring bands. This is a feature which is absent in hydrogen halides which have a simple sequence of harmonics, whereas other bands or sequences of bands occur in the gases under review, mingled with the members of the main harmonic series.

Second Sequences: NH_3—C, D, ...; PH_3—A′, B′, ...; AsH_3—A″, B″, ...

NH_3.—Starting with an intense band at 4416·9 (2·264 μ) a sequence follows with increase in W.N. not very different from that of the Main Sequence of NH_3. From its intensity this band might be taken as the first of a series, but the W.N. Δ between the members of this sequence would point to an origin being about 1470 W.N. ($6\cdot8\ \mu$), where no definite effect can be observed. Nor is there any definite band about 2940 W.N., where the second member of the series might be expected to fall.

---

* 'Z. f. Physik,' vol. 3, p. 289 (1920).

It would, therefore, seem that this band or sequence has no simple origin.

Hettner* from the values given by Schierkolk (*loc. cit.*) has attributed this band and its associates to combinations of bands I and $10\cdot55\ \mu$, but the results do not agree well with this assumption when either Schierkolk's or our values are taken. With the values for W.N. found by us, the comparison is as follows :—

$\nu_1 = 948\cdot1$ W.N. (Centre of band at $10\cdot55\ \mu$.)
$\nu_2 = 1630\cdot9$ W.N. (Centre of band I.)
$\nu_1 + \nu_2 = 2579$ W.N. Nearest band is 2469. Difference $= 110$ W.N.
$\nu_1 + 2\nu_2 = 4209\cdot9$ W.N. Band C is $4416\cdot9$ „ $= 207\cdot0$ „
$\nu_1 + 3\nu_2 = 5840\cdot8$ W.N. Band D is $6013\cdot2$ „ $= 172\cdot4$ „
$\nu_1 + 4\nu_2 = 7471\cdot7$ W.N. Band E is $7651\cdot1$ „ $= 179\cdot4$ „
$\nu_1 + 5\nu_2 = 9102\cdot6$ W.N. Band F is $9772\cdot5$ „ $= 669\cdot9$ „

Equally, the members of this sequence might be considered as intermediate bands between the members of the Main Sequence thus :—

Between centres of bands—

I and II mid-position $= 2483\cdot2$ W.N , nearest band is 2469 W.N. Difference $= -14$ W.N.

II and III mid-position $= 4209\cdot7$ W.N., nearest band C is $4416\cdot9$ W.N. Difference $= 207\cdot2$ W.N.

III and IV mid-position $= 5846\cdot6$ W.N., nearest band (D) is $6013\cdot2$ W.N. Difference $= 166\cdot6$ W N.

IV and V mid-position $= 7430\cdot1$ W.N., nearest band (E) is $7651\cdot1$ W.N. Difference $= 221\cdot0$ W.N.

If the limits of the absorption bands could be more accurately ascertained, there are indications that another band occurs midway between the ends of bands I and $10\cdot55\ \mu$ at No. 4 (see inset of fig. 2).

The agreement is much the same whether the members of this sequence be taken as being combination bands of bands I and $10\cdot55\ \mu$ or of two neighbouring bands.

Whichever view be favoured, no explanation is afforded of the great intensity of band C, for which nor for its concomitants is there an analogue in PH_3 or

---

* 'Z. f. Physik,' vol. 31, p. 273 (1925).

AsH_3. In fact, neither the procedure of combining the frequencies nor taking them as intermediates is quite satisfactory as a method of accounting for the bands.

PH_3.—The sequence A′ ... starts with a band at 676·7 W.N. (Table X), and in the same gas are found bands at 2935·1, D′, and 3709·2, E′. Rock-salt begins to absorb so strongly about 600 W.N. that it is impossible to say, without using a sylvin prism, if the band found at 676·7 W.N. is a simple band or the beginning of an analogue of the band 10·55 μ of NH_3. The spacing between D′ and E′ is in only moderate agreement with the third of the distance between A′ and D′, but, as stated, the position of A′ is not quite established. It will be observed that B′ is missing; C′ would fall within band II; band D′ is tripartite.

AsH_3.—The sequence A″ ... starts with a band at about 500 W.N., but, for the same reason as given above, it is not more than indicated. A second member, B″, would lie within band I, and a faint band, C″, is found. The next member, D″, would lie within band II and again there is a faint band E″. These bands C″ and E″ have the feature of being approximately equidistant from the bands of the Main Sequence on either side of them.

The ratios of the W N $\frac{A''}{A'}$ and $\frac{E''}{E'}$ are 0·74

Third Sequence: PH_3, AsH_3,—α, β, ...

The members of this sequence take their origin in the zero branches lying towards the smaller W N. of the composite bands whose central positions are about 9·4 and 10·4 μ respectively. Again they fail to obey Kratzer's principle for dipoles, the second member being greater instead of less than twice the W.N. of the fundamental. In the direction of the visible they have an ascending value for $\frac{\text{W.N.}}{n}$, and when partially resolved are characterised by being tripartite like the members of the Main Sequence, and by having a ratio as between the respective gases not unlike that of the members of that sequence (Table IX).

These bands are found in similar positions on the smaller W.N. side of the bands of the Main Sequence.

This sequence is peculiar to PH_3 and AsH_3 and has no traceable analogue in NH_3: thus it represents a degree of freedom possessed by the heavier molecules.

ROTATION-OSCILLATION BANDS.

Partially Resolved Bands.

The following wave-number differences have been observed between the P and Q and R branches of the partially resolved bands.

Table XI.—Wave-Number Differences from Zero to Position of Maximum Absorption in Side Branches.

Main Sequence, I, II, … .

Gas.	Band.	R to Q W N	Q to P W.N.	Mean W.N.
NH_3	I	95·7	95·2	98·2
	II	94·2	107·7	
PH_3	I	76·3	73·0	73·5
	II	71·5	73·3	
AsH_3	I	72·6	45·0	63·8
	II	70·1	64·1	
	III	55·4	75·5	

Third Sequence.

Gas.	Band.	R to Q W N	Q to P W.N.	Mean W.N.
PH_3	α	68·8	64·6	68·5
	β	86·7	53·8	
AsH_3	α	54·4	39·0	55·1
	β	66·3	40·8	

Main Sequence.

Here these bands are all tripartite, the intensities of the side members affording a measure of the probability of the occurrence of a rotation at right angles to the plane of oscillation, since it was shown by Rayleigh* that under these circumstances, in addition to a frequency of oscillation ν_0, there would be found two others, $\overline{\nu_0 + \nu_r}$ and $\overline{\nu_0 - \nu_r}$. In Table XI are given the mean values for the differences of the maxima of the side branches from the centres of the bands. These maxima, P and R branches, are less easy to evaluate than the central Q branches, which are much more definite.

---

* 'Phil. Mag.,' vol. 24, p. 410 (1892).

The values are used later to compare the moments of inertia of the molecules of the gases on the basis of the kinetic theory for the most probable rotational frequency with those determined from the fine structure.

Third Sequence.

Here the bands are sometimes so merged with neighbouring bands that they are still more difficult to evaluate. They take their origin in the Q branches of the composite bands of PH_3 and AsH_3, which lie towards the smaller W.N. at 10·068 and 11·037 μ respectively, and are not found in NH_3.

Sequence X, NH_3—*a*, *b*, ... (See Table X.)

This sequence is considered later as pertaining to rotation, as it appears to have its origin in band of NH_3 found by Rubens and Wartenberg[*] by means of reststrahlen in the farther infra-red about 63 μ (159 W.N.). It recalls a sequence of bands of water vapour described by Hettner[†] and ascribed by him to an effect of rotation carried from a band in the far infra-red towards the visible.

A band, *d*, of fair intensity (fig. 1) is found at 628·6 W.N. which corresponds to the third harmonic. The next, *e* (fig. 1), corresponds to a disturbance in the regular sequence of rotation bands at 783·4 W.N., followed, *f*, by the centre of the oscillation band at 10·55 μ and another disturbance, *g*, in the rotation bands at 1108·5 W.N. The averages of these differences in W.N. is 158·2.

This rotation, slow as compared with the frequency of the oscillation bands, is much faster than the frequency of rotation as deduced from the fine structure on bands I, II and band 10·55 μ (see below). In the sequel it is thought to be due to the rotation of the hydrogen atoms round an axis dropped from the nitrogen nucleus on the plane of the hydrogen atoms.

RESOLVED BANDS. (Tables II to VIIA, figs. 2 to 7.)

In these tables are collected the data obtained for the fine structure of the bands which have been resolved, and figs. 2 to 7 illustrate their contour and the rotation maxima, at pressures of 1, $\frac{1}{2}$ in some cases, $\frac{1}{4}$, $\frac{1}{8}$, $\frac{1}{16}$ and occasionally $\frac{1}{32}$ atmospheres of the respective gases.

The structure of these bands may be shortly discussed.

---

[*] 'Verh. d. D. phys. Ges.,' vol. 13, p. 796 (1911).

[†] 'Ann. der Physik,' vol. 55, p. 476 (1918).

NH_3, Band I. (Table II, fig. 2.)

In this band the mean of the differences in W.N. between the rotation maxima is 17·1 W.N. These differences, however, are greater on the side of larger W.N., which is contrary to what was found by Imes (*loc. cit.*) in the hydrogen halides, but similar to the experience of Levin and Meyer* for ethane. The following diagram gives the intensity of the bands and the W.N. differences for a pressure of ½ atmosphere.

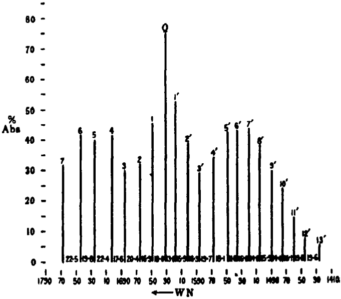

FIG. 10.—Rotation-Oscillation Maxima in Band I, NH_3—½ atmosphere.

A more regular series of differences is obtained according to the method of Imes by dividing the differences between corresponding rotation maxima on each side of the zero branch by twice their ordinal number in these two ways :—

Ordinal number.	—	½ $\frac{W.N}{m}$	—	½ $\frac{W.N.}{m}$	
		W.N.			
$m = 1$	1–1′	15·5	[1–2′	23·4]	
$m = 2$	2–2′	15·8	2–3′	19·9	19·3
$m = 3$	3–3′	16·6	3–4′	19·8	
$m = 4$	4–4′	17·1	4–5′	19·4	
$m = 5$	5–5′	17·7	5–6′	19·0	
$m = 6$	6–6′	17·5	6–7′	18·8	
$m = 7$	7–7′	17·7	7–8′	18·8	
				Mean 19·8	

---

* 'J. Opt. Soc, Am.,' vol. 16, p. 137 (1928).

It is to be noted that 1′ is very weak, but apparently distinct, especially with reduced pressure, and seems to represent a jump of less than 1 quantum, as is assumed to occur in Kratzer's treatment of the region at 3·46 μ of HCl, where, however, no indication of an inflexion was observed. The second procedure has the advantage of eliminating the region requiring a fractional quantum number and gives differences thereafter of W.N., 19·3 W.N. on the average.

NH_3, *Intermediate Region between Bands* I *and* 10·55 μ. (Table IIA, fig. 2 inset.)

This region possesses features some of which have already been mentioned (see p. 194). In the undisturbed portion of the region the mean W.N. Δ is 17·9.

NH_3, *Band* II. (Table III, fig. 3.)

It was important to determine the fine structure of this band, in the first place, to see if the W N. Δ is the same for different members of the same sequence, Cooley* having found in CH_4 a variation from band to band, and also to ascertain if on the smaller W.N. side of the band any imposed bands occurred similar to those (β, γ) found in this position in PH_3 and AsH_3. Allowing for the less favourable conditions of the use of a prism in this region, the differences in W.N. of the rotation maxima on the average agree with those obtained by Spence, who has also explored this band, but with a grating, the values being 20·3 and 19·7 W.N. respectively. It would appear, therefore, that these two bands I and II of this sequence of NH_3 have fine structure of rotation bands of the same frequency, and that there is no sign of such bands as are enclitic on the side of band II of PH_3 and AsH_3.

NH_3, *Band at* 10·55 μ. (Table IV, fig. 4.)

This band is of a type not hitherto properly explored, having side branches, but with a double zero branch. The fine structure shows in places a regular spacing of rotation maxima with interruptions at intervals. In fig. 11 the intensities of the rotation maxima at ½ atmosphere pressure are shown, together with their W.N. differences.

---

* 'Astrophys. J.,' vol. 62, p. 73 (1925).

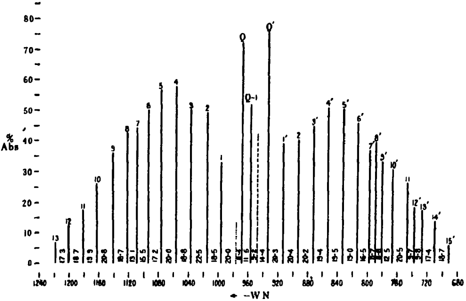

FIG. 11.—Rotation-Oscillation Maxima in Band 10·55 μ—⅛ atmosphere.

On inspection of the spacings of the rotation bands some regularities appear:—

Bands 12 to 8, average	Δ 19·5 W.N.	mean = 19·6 W.N.
,, 6 to 1, average	Δ 19·4 ,,	
,, Q to central dip	Δ 20·7 ,,	
,, Q′ to 7′, average	Δ 19·3 ,,	
,, 10′ to 11′	Δ 20·5 ,,	
,, 13′ to 15′, average	Δ 18·1 ,,	
Bands 8 to 6, average	Δ 14·4 W.N.	mean = 13·8 W.N.
,, central dip to Q′	Δ 14·4 ,,	
,, 9′ to 10′	Δ 12·5 ,,	
Bands 7′ to 9′, average	Δ 8·8 W.N.	mean = 9·3 W.N.
,, 11′ to 13′, average	Δ 9·8 ,,	
Band 1 to Q	Δ 28·4 W.N.	

Thus, if the W.N. Δ of the majority of the maxima be taken as 1, spacings occur at half, two-thirds and one and a half times this spacing.

It may be that the space between the zero branches is not equally divided. A band small, but increasingly evident as the pressure is reduced, occurs midway between the centre and the branch Q, reminiscent of the half-quantum band presumed by Kratzer to exist in this region of the 3·46 μ band of HCl, but experimentally missing. The interval from the central dip to the branch Q′ shows no break of this kind and is two-thirds of the regular spacing distance It is not clear whether the departure from the regularity found in this portion of the band is to be expected on such grounds as Kratzer advances for HCl, or whether, as is supported by the following considerations, it is due to a disturbance caused by an imposed vibration belonging to another system of bands.

If the mean positions be taken of those regions on either side of the branches Q and Q′, which depart from the regular spacing of 19·3 W.N., they are found to lie as follows:—

Mean between 8 and 6 = 1108·5 W.N.: distance from central dip = 160·4 W.N.

Mean between 7′ and 10′ = 783·4 W.N.: distance from central dip = 164·7 W.N.

It thus appears that the disturbances (*e* and *g* in fig. 1) and the central region (*f*) are equally spaced and at a W.N. interval which is the same as that from (*e*) to the next band on the long W.L. side (*d*) at 628·6 W.N. As the band *d* is four times this W.N. difference, and as the frequency of the band of NH_3 found by Rubens and Wartenberg (*loc. cit.*) has the same value (159 W.N.), it has been assumed that this imposed sequence has its fundamental at this W.N. This is so tabulated above as "Sequence X, NH_3."

It will also be observed that between the zero branch Q and rotation band 1 there is a W.N. difference of 28·4, pointing, it may be, to a missing line indicated by a dotted line in fig. 11, thus dividing the interval into approximately one and a half times the principal spacing (19·6).

On the Q side of the band the first maximum observed (No. 1) is taken as $\frac{3}{2}$, the second $\frac{5}{2}$ and so on, up to No. 6; on the Q′ side the first maximum is taken as 1′, the second 2′, and so on, up to 6′. The values for these are $\frac{2}{3}$ of 28·4, 18·5, 22·5, 18·8, 20·0, 17·2 and 20·3, 20·4, 20·2, 19·4, 19·5, 19·0, of which the mean is 19·6 W.N. This is used later in calculation of moment of inertia of the molecule.

PH_3, *Band* I. (Table V, fig. 5.)

This band, which forms the member on the larger W.N. side of the composite band, whose centre is about 1060 W.N., has been resolved by fluorite on the larger W.N. side of its Q branch (1125 W.N.). The region intermediate between this Q branch and the Q branch at 993·2, which pertains to the series number α ..., has not been well resolved.

In Table V are given the values for the rotation-oscillation maxima of the R branch of band I, the mean of their W.N. differences being 11·5 W.N.

PH_3, *Band* α. (Table VA, fig. 5.)

This band, the other member of the above-mentioned composite band, has been resolved by rocksalt on its smaller W.N. side. The values for the rotation-oscillation bands of its P branch are given in Table VA, the mean of their W.N. differences being 11·6 W.N., a value similar to those on the side of band I of PH_3.

PH_3, *Band* II. (Table VI.)

An attempt was made to obtain values for the fine structure on the P and R branches. The mean of the values for W.N. Δ given in Table VI are 11 and 10 W.N. respectively, roughly corroborative of the values in band I, but the quality of resolution was poor.

AsH_3, *Band* I. (Table VII, fig. 7.)

This band is situated on the larger W.N. side of a composite band in a fashion like band I of PH_3. The structure of its R branch is not very well resolved, but has maxima coinciding when determined with a rocksalt as well as with a fluorite prism, showing a mean W.N. Δ for the rotation-oscillation bands of 8·5 W.N.

AsH_3, *Band* α. (Table VIIA, fig. 7.)

This band, again as in PH_3, the member of the composite band towards the smaller W.N. side, when resolved by rocksalt, gives a mean W.N. Δ for the oscillation bands of its P branch of 10·0 W.N.

EFFECT OF PRESSURE ON INTENSITY AND AREA OF BANDS.

In these papers (Tables VIII and VIIIA) we have given data for the percentage absorption of some unresolved bands taken at the position of the central frequencies, and also similar data in some cases for the bands of the fine structure. Since the pressure of the gas did not appear to lead to displacement of the central frequencies of the sharp bands, it became of interest to ascertain whether the alteration of absorption at these central frequencies, with alteration of pressure of the gas, followed any law such as Beer's law. In some cases at full atmospheric pressure the bands are fused and in these cases the central frequency is taken as that derived from the sharper resolved band at lower pressures, for example, in band NH_3 at 10·55 μ. This inquiry is of some interest in view of the statement made by Hettner* that when the absorption becomes continuous owing to fusion of the bands the absorption law holds.

Since the intensity of the transmitted radiation falls off with increase of pressure, we applied the expression $I = I_0 e^{-kp}$, where I is the intensity of the transmitted and I_0 of the original radiation, p the pressure, and k an absorption constant for the band under consideration. It will be observed from Table VIII that for the lower pressures, particularly for the bands of the fine structure of NH_3 band I and band 10·55 μ, this exponential expression fits the observations with remarkable accuracy and the results are generally within the experimental error. There is, however, a strong deviation at full atmospheric pressure, no doubt connected with the fusion of the bands. While the Q branch of NH_3 band I likewise fits the equation, the Q and Q′ branches of NH_3 band 10·55 μ are altogether outside it. Again, it is found that the bands II of PH_3 and AsH_3, in which the Q branches diverge widely, have P and R branches falling fairly well within the rule.

While it cannot be stated that there is any generalisation which can be made on the intensities of the central frequencies, it can be said that in the resolved bands the rule is followed at the lower pressures for the bands of the fine structure.

We have evaluated the area under the contour of the same bands (Table VIIIA), thus obtaining the total absorption over the branches of the band, including its fine structure. The results of this treatment follow closely the results obtained from considering the central frequencies alone.

There is thus no doubt that when the band is well resolved the intensity of absorption follows some form of exponential decrement. Since this is the case it would appear that, except when a large concentration of gas is present, the radiation penetrates the column of gas and is absorbed by a comparatively small fraction of the total number of molecules present.

CONSIDERATION OF STRUCTURE OF BANDS.

Central Frequency of Bands.

Where complicated bands occur as in NH_3 band I, an exact position can be assigned to the central frequency of the band. A set of values can be drawn up for this centre determined by the method of least squares from the means of the W.N. of two maxima of the same ordinal number in the P and R branches. For band I, NH_3 for example, these may be represented by the expression ν (in W.N.) $= 1631 \cdot 8 + 0 \cdot 23\, m^2$, in which $m = 0, 1, 2, 3, \ldots$, the observed value being 1630·9 W.N.

---

* 'Phys. Z.,' vol. 27, p. 788 (1926).

Fine Structure of Bands of NH_3 *and Moments of Inertia.*

Band I of NH_3 shows a certain asymmetry for the spacing of the rotation maxima of absorption of the bands, arising from the spacing being somewhat different in the P and R branches. Band II has not been resolved so well as to permit of any decision on this point. The observed W.N. differences in band I yield an average of 19·6 in the R branch (Table II and fig. 2) and 15·7 in the P branch, but if the procedure adopted on p. 198 is used, the W.N. difference is 19·8. With band 10·55 μ the branch on the side of higher frequency of Q (Table IV and fig. 4) has a spacing of 20·2 W.N. and that on the other side of Q′ a spacing of 19·0. If, however, the disturbed regions of this band are left out of consideration, the W.N. difference as far as bands 6 and 6′ respectively is 19·6, or nearly the same as for band I, provided the spacing Q to 1 is considered as a $\frac{3}{2}$ spacing.

For band II, the first harmonic of band I, the average spacing is 20·3 W.N., which may be compared with Spence's value of 19·7. In this band, too, the method of p. 198 comparing 2 with 2′ and so on leads to a mean value of 20·8, which may be considered as some confirmation of the value 20·3, the mean of all the observations on this band.

It will be seen from the foregoing that the average spacings, from which the moment of inertia may be calculated, are 19·8 for band I, 20·3 for band II and 19·6 for band 10·55 μ. These values indicate that the rotation-oscillation bands here considered are all affected by the same frequency of rotation of the molecule. It would be of interest to have the fine structure of other bands of NH_3 resolved, especially band C, of which the peculiar features are great intensity and absence of earlier members of its sequence. It is hoped to investigate this point with apparatus of greater dispersion.

The moments of inertia may be calculated from the expression $J = \frac{nh}{4\pi^2 \Delta \nu}$ on the supposition that the angular velocity of rotation is constant, where $\Delta \nu$ is the spacing between the maxima of the fine structure. The following results are obtained :—

Band.	$\Delta\nu$.	$J \times 10^{40}$.
I	19·9	2·78
II	20·3	2·72
	19·7 (Spence)	2·81
10·55 μ	19·6	2·82
Region between I and 10·55 μ	20·0	2·77

In this table the value for the last row is determined by considering the differences 3–5, 2–6, 1–7 of fig. 2 inset (Table IIA). With band I the value of $\Delta\nu$ falls from 19·9 to 18·8, see p. 198, the moments of inertia corresponding to these being $2 \cdot 78 \times 10^{-40}$ and $2 \cdot 98 \times 10^{-40}$ gr cm.^{2} If we take this increase into consideration together with the quantum condition $J\omega = mh/2\pi$, it is clear that as the velocity of rotation increases, the radius of gyration increases with rise of ordinal number, since the mass of the molecule remains constant. For the mean of the above moments of inertia, $2 \cdot 78 \times 10^{-40}$, the radius of gyration is $0 \cdot 82 \times 10^{-8}$ cm. In a letter to 'Nature'* Badger writes that from an examination of the region 55 to 130 μ he gets rotation bands of NH_3, from which he deduces a moment of inertia of $2 \cdot 77 \times 10^{-40}$ gm. cm.^{2}, a value almost identical with ours.

If the band observed by Rubens and Wartenberg at 63 μ be considered a rotation band, the corresponding moment of inertia is $0 \cdot 35 \times 10^{-40}$. It is not easy to decide, without further inquiry with apparatus of greater resolving power, whether other spacings are present in the fine structure of the NH_3 bands.

Fine Structure of Bands of PH_3 *and Moments of Inertia.*

For PH_3 the spacing differences determined from the fine structure of bands I and α (Tables V and VA, fig. 5) are 11·5 and 11·6 W.N. respectively, equivalent to a moment of inertia of $4 \cdot 78 \times 10^{-40}$, from which the radius of gyration comes out at $1 \cdot 025 \times 10^{-8}$ cm The W N. difference for band II of PH_3 (Table VI, fig. 6) is either 10 or 11, but is not so accurately determined as is the case for the other bands.

Fine Structure of Bands of AsH_3 *and Moments of Inertia.*

For bands I and α of AsH_3 (Tables VII and VIIA, fig. 7) W.N. differences of 8·5 and 10·0 respectively are obtained, corresponding to moments of inertia $6 \cdot 51 \times 10^{-40}$ and $5 \cdot 53 \times 10^{-40}$. This difference may or may not be real. With the first value the radius of gyration is $1 \cdot 165 \times 10^{-8}$ cm, with the second $1 \cdot 07 \times 10^{-8}$ cm.

---

* 'Nature,' vol. 121, p. 942 (1928).

Calculation of Radii.

The radii of gyration of the three gases may be compared with the radii of their mean collision area found by Rankine* from the measurement of viscosity of the gases.

The following comparison brings out the difference between the length of the radii according to these :—

	Radii of gyration, cm. × 10^{-8}.	Half diameter of mean collision area (Rankine), cm. × 10^{-8}.	Ratio.
NH_3	0·82	1·43	1·74
PH_3	1·03	1·70	1·65
AsH_3	1·17 or 1·07	1·77	1·51 or 1·65

As might be expected, the radius of the mean collision area is greater than that found by us for the radius of gyration. They have, however, a fairly constant ratio the one to the other.

Comparison of Moments of Inertia derived from Energy Relation.

It is of some interest for comparison to calculate the moments of inertia of the three gases from the classical energy relation for three degrees of freedom $\frac{1}{2}J(2\pi\nu)^2 = \frac{3}{2}kT$, where k is Boltzmann's constant. This may be carried out from the values of W.N. differences (Table X) of the Q branches from the maxima of absorption of the P and R branches, which may be considered as most probable frequencies at room temperature. Taking W.N. 98·2, 73·5 and 63·8 for NH_3, PH_3 and AsH_3 respectively, the moments of inertia are $3{\cdot}49 \times 10^{-40}$, $6{\cdot}24 \times 10^{-40}$ and $8{\cdot}28 \times 10^{-40}$. These values may thus be compared with the moments of inertia deduced above from the fine structure of the bands :—

	$J_1 \times 10^{40}$ from band structure.	$J_2 \times 10^{40}$ from energy relations.	Ratio J_2/J_1.
NH_3	2·78	3·49	1·26
PH_3	4·78	6·24	1·30
AsH_3	5·53 or 6·51	8·28	1·27 or 1·49

---

* 'Trans. Faraday Soc.,' vol. 17, p. 719 (1922).

It will be observed that there is a fairly constant ratio between the moment of inertia as calculated by the two methods, indicating that the factor used with kT should be less than $\frac{3}{2}$.

MOLECULAR MODEL OF MOLECULES NH_3, PH_3, AsH_3.

It is interesting to consider how the different modes of oscillation of molecules such as NH_3 may arise, and for this purpose some molecular model has to be taken. A tetrahedral molecule of four atoms may have $(3n - 6)$ or 6 degrees $(n = 4)$ of freedom and some of these degrees of freedom may be associated with valency bonds of the various atomic linkages, and so with the structure of the molecule. The sequence and complexity of the bands, however, appear to be greater in number than can be accounted for by consideration of valency bonds alone. Since the H atoms are not joined together by any valency linkage, oscillations arising from the three H atoms, or from two relatively to one another constitute degrees of freedom which are only remotely connected with the valencies of the atoms of the molecule.

From purely chemical considerations it is not easy to decide whether the N and the three H atoms are in one plane. The existence of optically active forms of substituted ammonium compounds is not decisive on this point, since it may be argued that as soon as one of the H atoms is replaced by a group the simple configuration of the NH_3 molecule is thereby disturbed.

Hund* from a consideration of the polarisation and laws of force between the ions arrived at the conclusion that as soon as the polarisation reached the value where an equilibrium position was established, whereby the four ions formed a tetrahedron with three equal side faces, then this tetrahedron was stable. The existence of oscillation bands of various frequencies in the infra-red spectrum of NH_3 shows that the ions are separating and one of the modes of vibration may be considered to be the oscillation of N against the plane of the H atoms. In such a case Hund's condition will clearly be fulfilled, and a tetrahedral structure will be required for the model. In favour of this view is the large temperature effect on the dielectric constant of gaseous NH_3, recorded by Watson,† together with its large electric moment. We may therefore accept the view that the NH_3 molecule is a tetrahedron, although it is not necessary to place the N atom at any great distance from the plane of the H atoms. In such a case modes of vibration can be: (1) N against the plane of 3 H atoms, that is, along a line directed towards the centre of gravity of the molecule, (2) N against one H atom; (3) H in a direction at right angles to the line joining it to the centre of gravity of the system; and (4) N in a manner similar to (3). It is not necessary in the first mode of vibration to suppose that all three H atoms are in phase.

---

* 'Z. f. Physik,' vol. 31, p. 99 (1925).

† 'Roy. Soc. Proc.,' A, vol. 117, p. 43 (1927).

In addition to these oscillations, this model may rotate about the centre of gravity, as well as about an axis through the line joining the N atom to the centre of gravity. We have so far been able to discover only two definite W.N. differences in NH_3 (about 20 and 160 W.N.). Of these the former, giving the larger moment of inertia, is most likely to be associated with that rotation which is about an axis through the centre of gravity and parallel to the plane of the H atoms. The other, since it has a smaller moment of inertia, may arise from a rotation of the hydrogen atoms round an axis passing through the N and the centre of gravity of the system. Other W.N differences might have been taken, as is done by Hund (*loc. cit.*) from some of the rotation bands on band 10·55 μ, but as these lie in the region apparently disturbed by the imposition of the system originating at 63 μ (see above, p. 200), we have not included them.

If the atoms of the molecule are all in one plane, (1) becomes more difficult to conceive, although possible, but the other oscillations are possible. In this coplanar model the rotation might well occur solely round an axis through the N at right angles to the plane, rotation of the molecule round a median line or one parallel to two H atoms being less easy to conceive. Another coplanar model would be one in which one H atom is at a greater distance from the N than the other two. There is no evidence for considering this likely, since no certain experimental data are known to indicate that one H is different from the others in NH_3.

Attempts have been made to identify certain bands with specific bonds in NH_3. Thus the work of Salant* on the infra-red spectra of liquid amino- and imino-compounds indicates that the band at 2·998 μ persists so long as there is one N–H group. Ellis,† also working with liquids, showed that the N–H oscillation is required to account for bands about 1·03 μ and 1·5 μ, corresponding, however, to our bands F and IV, F not being in that harmonic sequence which has 6·13 μ as fundamental. On the other hand, Salant‡ stated that the band at 6 μ became very weak with secondary and tertiary amines, concluding from this that the band at 6·1 μ is not the fundamental of which band 3 μ is a harmonic. This evidence is not at all conclusive for the reason above given for substitution in ammonia. From the similarity in ratio of the related bands of the Main Sequence in the three gases examined by us and from their inter-relationships, there appears to be definite evidence that the bands of the sequences described (pp. 190–197) are "harmonics" arising for similar degrees of freedom in the molecules displaced a little compared with the simple harmonic ratios.

---

* 'Proc. Nat. Acad. Sci.,' vol. 12, p. 74 (1926).

† 'J. Am. Chem. Soc.,' vol. 50, p. 685 (1928).

‡ 'Nature,' vol. 119, p. 926 (1927).

In favour of the view that there are at least three distinct oscillation sequences in NH_3, of which the band at 6·13 μ is the fundamental of one sequence, we have the fact that it is possible to separate the complicated infra-red oscillation bands of NH_3 into one set of harmonics, commencing with 6·13 μ, another, of which the strong band C is the third member, and the band at 10·55 μ. This same selection is taken by Hund as corresponding to the three frequencies required by his calculations, and is used by him as confirmation of his model.

If the band at 3 μ is admitted to represent the oscillation corresponding with the N–H oscillation in substituted ammonias, which in this case happens to be coincident with a valency bond, it would seem to follow that band I at 6·13 μ is the fundamental corresponding to the N–H degree of freedom in NH_3. It may further be considered that the N–H oscillation is likely to be faster than the N-H_3 oscillation, which would be an argument for regarding the band at 10·55 μ as arising from this slower oscillation, thus leaving band C at 2·264 μ to be accounted for. This may be derived from a degree of freedom due to an oscillation of H at right angles to the line joining it to the centre of gravity of the NH_3 model. The fundamental of this band should occur about 6·8 μ, but this band is missing.

An alternative speculation, in which band I at 6·13 μ is again assigned to the degree of freedom corresponding to the band N–H, would be to consider that band 10·55 μ arises from the oscillation of N parallel to the plane of the 3H (4), this being likely to be slower than N against one H. The emergence of C as a third and strong member of a sequence, without an obvious fundamental, might arise from some violent feature such as an oscillation of the nitrogen penetrating the plane of the H atoms.

The considerations leading to a tetrahedral structure for NH_3 apply likewise to PH_3 and AsH_3. A harmonic sequence of five oscillation bands equally well defined with those in NH_3 is found in PH_3, and, in addition, two other sequences are discernible. A tetrahedral structure is thus indicated for this molecule also, and this is supported by Watson (*loc. cit.*), who finds that PH_3

has an electric moment, smaller indeed than that of NH_3, but still of considerable magnitude, and with a definite temperature coefficient. At least one mode of oscillation in PH_3 (represented by the "Main Sequence") is similar to one in NH_3. From rotation data only one moment of inertia has been found, and generally the vibrations of PH_3 appear to be less complicated than those of NH_3.

Equally in AsH_3 occurs a sequence of six oscillation bands in the Main Sequence, with apparently two other sequences. In arrangement of its oscillation bands AsH_3 is much more like PH_3 than NH_3, and possesses a series (α, β, ...) similar in form and disposition to one in PH_3. From rotation data its moment of inertia is much nearer to PH_3 than to NH_3. The similarity of the oscillation bands would point again to a tetrahedral structure were it not that Watson (*loc. cit.*) finds such a small electric moment and temperature coefficient of dielectric constant. However, if we may regard the electric moment of the molecule in the tetrahedral model as the product of the distance of the heavy atom from the three H atoms and the charges of the ions, then it is not safe to suppose that any alteration of the polarisation is measured merely by the magnitude of this product. As soon as the heavy atomic nucleus moves a small distance from the H atoms, the effect of the electron shroud comes into play, and this acts in the opposite direction to the original electric moment. Therefore, the electric moment as measured by the product of distance and charges is reduced by an amount depending on the electron shroud. This is greater in the order N, P, As, so that, from this consideration alone, a smaller electric moment would be expected, and the model for PH_3 could still be regarded as tetrahedral like NH_3.

From the graphs and tables it is clear that the oscillation frequencies become slower in the order, from NH_3, to PH_3, to AsH_3, and the wave-number differences in the rotation bands show that the molecules rotate more and more slowly in the same order.

The Kinetics of the Decomposition of Calcium Carbonate Hexahydrate.

By B. TOPLEY, M.A., and J. HUME, B.Sc.

(Communicated by Sir Harold Hartley, F.R.S.—Received May 19, 1928.)

Up to the present, so far as we are aware, the kinetics of reactions directly involving two solid phases have not been examined quantitatively in connection with a theory of the mechanism. Qualitative suggestions have been made (*cp.* G. N. Lewis,* Macdonald and Hinshelwood†) to account for the autocatalysis observed in particular cases of such reactions

Langmuir‡ drew attention to the importance of the *interface* between the two solid phases for dynamic equilibrium in systems of the type · $\text{Solid}_1 \rightleftarrows \text{Solid}_2 + \text{Gas}$, and Langmuir's suggestion was applied by Crowther and Coutts§ to explain the results obtained in a study of the dehydration of certain salt hydrates.

The object of the experiments described here was to investigate the mechanism of an "interface" reaction, with special reference to the influence of temperature. From this point of view we have studied dilatometrically the rate of decomposition of calcium carbonate hexahydrate

$$CaCO_3 . 6H_2O = CaCO_3 + 6H_2O$$

in contact with pure water—a reaction which has already been studied qualitatively,‖ where details of the dilatometric method of following the reaction have been given.

The following is a summary of the conclusions previously reached which are relevant to this paper :-–

(1) Calcium carbonate hexahydrate is unstable in contact with water at all temperatures above 0°. The decomposition product is calcite, and there is no sign of the formation of lower hydrates as intermediate stages in the decomposition.

(2) The rate of the change is greatly affected by the inclusion in the hydrate of small quantities of foreign substances apparently in solid solution; the

---

* 'Z. Phys. Chem.,' vol. 52, p. 310 (1905).

† 'J. Chem. Soc.,' vol. 127, p. 2767 (1925).

‡ 'J. Amer. Chem. Soc.,' vol. 38, p. 2263 (1916).

§ 'Roy. Soc. Proc.,' A, vol. 106, p 215 (1924).

‖ Hume and Topley, 'Proc. Leeds Phil. Soc.,' vol. 1, p. 169 (1927).

stabilising influence of different substances is very specific, and for the same included substance the retardation of decompostition increases with the amount included.

(3) The velocity increases as the reaction proceeds, passing through a maximum at about 50 per cent. decomposition.

(4) The autocatalysis is not eliminated by grinding the crystals to a fine state of subdivision.

(5) It was suggested that the autocatalysis could be explained on the assumption that the reaction proceeds at the interface hydrate-calcite, the rate being proportional to the area of this interface.

(6) The reaction rate is extremely sensitive to temperature.

(7) The decomposition reaction is endothermic.

The most interesting point is the interpretation of the very large effect of temperature on the reaction rate; but before any theoretical significance can be attached to the temperature coefficient it is necessary to show that the velocities actually measured at different temperatures refer to comparable states of the system. It is desirable, therefore, to discuss in some detail what we believe to be the mechanism of the change.

The basic idea of an "interface" reaction is that the only molecules (ions or ionic groups) which react are those in a layer immediately adjacent to molecules (ions or ionic groups) in the space lattice of the resultant solid phase. This assumption is fundamental for the explanation of the apparent autocatalysis observed as the reaction proceeds; thus, the state of affairs when the reaction takes place in a mass of reactant consisting of a large number of very small crystals or crystal fragments is as follows: The rate of change observed dilatometrically is an average result at any moment for all the particles present; as an experimental fact the curve obtained by plotting "fraction decomposed" against time is sigmoid in form (see fig. 1, curve 1). There are, *a priori*, several possibilities, but closer consideration rules out all except one of these:—

(1) The reaction takes place within the space lattice of the reactant solid in a manner analogous to a homogeneous gas reaction, *i.e.*, the change proceeds at points distributed at random throughout the space lattice of the solid. This would lead to a curve in which the maximum velocity is at the beginning of the reaction.

(2) There is the possibility that the reaction might begin at points distributed at random throughout the solid, and then be propagated outwards from these "nuclei." This would give rise to an acceleration as the reaction proceeds.

Both (1) and (2) are inherently improbable, however, in the present case, since there is a considerable expansion when the hydrate decomposes to calcite and liquid water, and it is difficult to see how this can occur in the interior of the solid.

(3) It may be supposed that the actual commencement of the change is restricted to the surface of the particles, which are mutually independent. The propagation of the change then takes place from the surface inwards. Three cases present themselves :—

(*a*) The surface rapidly becomes almost completely covered with points where " nuclei " of calcite have formed ; the resulting interface would approximate to a spherical shell, and would move inwards at a constant linear rate (k cms. per second). The reaction velocity after t seconds is then given by

$$\frac{d\alpha}{dt} = \frac{3k}{a} - \frac{6k^2t}{a^2} + \frac{3k^3t^2}{a^3},$$

where $d\alpha/dt$ is the fractional change per second, and a cms. is the radius of a particle, assumed spherical. (A decomposition curve of this type has been observed in the reaction $Ag_2CO_3 \longrightarrow Ag_2O + CO_2$ and is being further investigated.)

(*b*) If the frequency with which " nuclei " form on the surface of any one particle is small, relative to the rate at which the change spreads through the particle once the nucleus has formed, then the average curve for many particles will conform to the monomolecular law. (Finely ground monoclinic sulphur shows this behaviour when changing to the rhombic form.)

(*c*) An intermediate case between (*a*) and (*b*) is important: when the frequency of nucleus formation on the surface of a particle and the rate of propagation of the change from the point where a nucleus has formed are relatively such that the majority of the particles have at least one nucleus before more than a very small fraction of the total reaction has taken place, then the total area of the interface for all the particles will increase as the reaction proceeds, and pass through a maximum. The observed reaction rate is proportional to the area of this interface.

It would seem that the sigmoid form of the decomposition curve of calcium carbonate hexahydrate corresponds to the last of these possible cases (3*c*). It may be mentioned here that C. N. Hinshelwood and E. J. Bowen* explained the acceleration which they observed in the irreversible decomposition of potassium permanganate, ammonium dichromate, and tetranitraniline as due to a progressive break up of the crystals with consequent increase of effective surface; the reaction was regarded as taking place in a zone near the surface; hence the increase in velocity as the change proceeds isothermally. Also the variation of effective surface rendered the temperature coefficient useless for determining the heat of activation. These considerations, however, do not apply to the accelerated decomposition of calcium carbonate hexahydrate. In the first place, the acceleration is not removed by finely grinding the crystals; also microscopic observation of the decomposing hydrate lends some support to the mechanism suggested (3c). But more significant evidence was obtained in experiments in which the temperature was varied during the decomposition. The following figures show the effect of raising the temperature for a short time, and then lowering it to its original value; the velocity returns to its original value, provided that the two tangents measured at the lower temperature and the intermediate tangent at the higher temperature are all obtained on an approximately linear part of the curve.

---

* 'Phil. Mag.,' vol. 40, p. 569 (1920).

Experiment 1.		Experiment 2.	
Temperature.	Tangent	Temperature.	Tangent.
°	Per cent. per minute.	°	Per cent. per minute.
0	0·027	0	0·036
15·4	1·99	15·4	1·37
0	0·026	0	0·30

The increase in velocity must therefore be due entirely to a true temperature coefficient of reaction rate, and not to a spurious effect such as an increase of effective surface due to break-up of the crystals at the higher temperature; if such a break-up occurred, it could not be reversed by lowering the temperature.

Microscopic examination of the solid product of decomposition shows that it consists of minute calcite rhombohedra, frequently aggregated into a pseudomorph of the original hexahydrate crystal. The conception of the change as the advance of a continuous interface between the two solid phases offers no explanation of the formation of well-defined rhombohedral crystals of calcite. Possibly the calcite side of the interface consists in the first place of a continuous layer of Ca^{++} and CO_3^{--} ions arranged relatively to one another approximately as they are in the calcite lattice; as this thin layer grows in thickness, a process akin to recrystallisation may be imagined to take place, in which the minute crystals with definite faces are formed. We assume that this process whatever its nature, does not influence the rate of the primary reaction.

On the basis of the mechanism described above (3c), it becomes possible to make an estimate of the absolute rate of propagation of the reaction through the solid: the observed acceleration up to about 50 per cent. decomposition must mean that the number of nuclei from which the change spreads in any one particle is quite limited—of the order of one to five. As a first approximation, the experimental curve can be roughly reproduced by calculation on the assumption that change begins at one nucleus only in each particle simultaneously. Taking the particles as approximately spherical, the fraction decomposed (α) after time t seconds is given by the expression

$$\alpha = \tfrac{1}{2}\left(\frac{kt}{a}\right)^3 - \tfrac{3}{16}\left(\frac{kt}{a}\right)^4,$$

where a is the particle radius and k the linear rate of propagation of the change in centimetres per second.

Fig. 1, curve 1, is an experimental curve obtained with ground particles of radius 0·009 cm. Fig. 1, curve 2, is the corresponding curve given by the above expression, when $a = 0{\cdot}009$ and k has the value $3{\cdot}4 \times 10^{-7}$ cm. per sec. obtained by substituting the value of t taken from the experimental curve when $\alpha = 59{\cdot}3$ per cent. It will be seen that the experimental curve

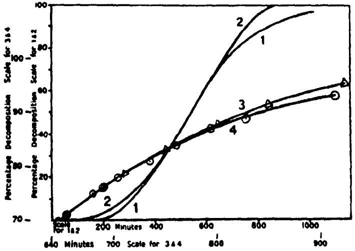

○ Experimental Points.
△ Calculated Points.
● Points from which k_1 is calculated.

FIG. 1.

falls below the calculated curve in the early stages of the reaction. This may reasonably be attributed to the simplifying assumption that each particle starts at zero time with a single nucleus; actually, it is clear that the number of nuclei per particle must be less than one at the beginning of the reaction, and increase until at about 70 per cent. to 80 per cent. decomposition the surface has become completely covered. Therefore, in the last stages of the reaction the interface will approximate to a spherical shell, and the form of the expression should be given approximately by the expression

$$\alpha_1 = 3\left(\frac{k_1t_1}{a_1}\right) - 3\left(\frac{k_1t_1}{a_1}\right)^2 + \left(\frac{k_1t_1}{a_1}\right)^3.$$

Fig. 1, curve 3, is calculated by this expression, where t_1 and a_1 are respectively the time in seconds and the fraction of the original amount of hexahydrate which has undergone change; the formula is applied to calculate the form of the curve from 71·25 per cent. decomposition of the original amount of hexahydrate onwards. α_1 in the formula refers to the fraction of the spherical "core" of volume (100 — 71·25) per cent. of the volume of the original particle, and a_1 is the radius appropriate to this spherical core. The value of $k_1 = 1 \cdot 7 \times 10^{-7}$ cm. per sec. is obtained from two points on the experimental curve. Fig. 1, curve 4, is a repetition of the upper part of curve 1 on a larger scale, for comparision with curve 3.

Here the experimental curve still falls off more rapidly than the calculated curve; this is probably to be attributed to the fact that the particles could not be obtained quite uniform in size, but varied over the range of radius 0·0078 to 0·011 cm.—the increasing discrepancy being caused by the earlier extinction of the smaller particles.

The values of k calculated from the first part of the experimental curves and of k_1 calculated from the later part of the curves should be the same. The experimental curve (fig. 1, curve 1 and curve 4) is typical of many that have been obtained; in practice, k is always between two and three times as great as k_1. The cause of this is that k is calculated over the range 0 per cent. to 59·3 per cent. decomposition, on the assumption that the change in that region is spreading from one nucleus only per particle, whereas actually the average number is greater than this. Nevertheless, the mean of k and k_1 should give the true rate of linear propagation of the reaction correct to within, say, a factor of five; the method of calculation is, of course, very rough, but under the circumstances an attempt to calculate k by a more precise method would hardly be justified. This, however, is not a serious drawback, since for the purpose of correlating the *absolute* rate of the reaction with the temperature coefficient, this degree of accuracy for k is sufficient.

EXPERIMENTAL.

The experiments were done with crystals grown from lime-sucrose solutions, and from a solution containing $CaCl_2 + NaOH + NH_4Cl + 0\cdot5$ per cent. $CuCl_2$. The method of precipitation is given in the earlier paper.

The selection of particles of the same size was done by allowing the ground-up crystals to fall down a wide tube of known length, filled with, and immersed in, ice-cold water; samples were collected at the bottom which had fallen during definite time intervals; the size of the particles was calculated by Stokes' law.

Experiments which support the View that the Reaction proceeds by spreading outwards from a Limited Number of Nuclei.

The form of the decomposition curve and the closeness with which different parts of it can be reproduced by calculated curves have already been mentioned. The formula applicable to spreading from one nucleus per particle gives for the velocity of the reaction at any moment

$$\frac{d\alpha}{dt} = \tfrac{3}{16} \cdot \frac{k^3t^2}{a^4}(8a - 3kt) - \tfrac{3}{16} \cdot \frac{k^4t^3}{a^4}$$

and for the fraction decomposed when $d\alpha/dt$ has its maximum value

$$\alpha = 16/27 = 59\cdot3 \text{ per cent.}$$

In practice, using crystals of uniform size, the maximum velocity is found between 50 per cent. and 60 per cent. decomposition.

A consequence of the view that the change spreads from a limited number of nuclei is that the rate $d\alpha/dt$ should increase as the radius of particle diminishes; the maximum rate (*i.e.*, when the fraction decomposed is $\alpha = 16/27$) is equal to $8k/9a$. A sufficient subdivision would produce particles so small that the formation of a nucleus would be followed almost immediately by complete decomposition of the particle; the acceleration would thus be eliminated; but since this does not happen with any ordinary amount of grinding in an agate mortar, it is possible to test experimentally the conclusion that the maximum rate varies inversely as the particle radius. The following results were obtained at 12·03° with similarly "sized" particles of $CaCO_3 . 6H_2O$ prepared from solutions containing sucrose :—

Experiment No.	Radius of particle in centimetres (= a).	$\frac{da}{dt}$ when $\alpha = 16/27$.	$a \times \frac{da}{dt}$.
1	0·0115	21 35	0·246
	0 00529	43·75	0·232
2	0 0115	17·40	0·200
	0 00529	38 70	0·205
3	0·115	19 10	0·220
	0 00529	43 70	0·231

The constancy of the figures in the last column is satisfactory.

The Influence of Temperature.

The effect of temperature on the rate of reaction has been measured by a method which eliminates uncertainty caused by the changing area of the interface. The reaction was followed for part of its course with the dilatometer in a thermostat at one temperature; the dilatometer was then transferred to another thermostat at a different temperature, and the remainder of the reaction followed at the new temperature. The temperature coefficient is obtained from the ratio of the two tangents to the decomposition curve immediately before and after the change.

The use in this way of four thermostats set at temperatures spaced approximately equally between 0° and 14° gave strictly comparable values for the reaction rate at four different temperatures. Four dilatometers containing particles of the same size were immersed in the thermostat at the highest temperature. One dilatometer was left in the same thermostat until decomposition was complete; each of the other three dilatometers was transferred to one of the lower temperature thermostats when decomposition had proceeded to between 40 per cent. and 50 per cent. The value of k in absolute units was calculated *for the highest temperature* by each of the two formulæ already discussed, applied respectively to the early and late parts of the curve. The mean of the two values of k was taken as representing the true linear rate of propagation of the change at the temperature in question; then the values for k at the other temperatures were obtained by multiplying the first value of k by the appropriate ratio of tangents.

It was found that the experiments must be restricted to the temperature range 0° to about 15°, because of the strongly endothermic nature of the reaction ; above about 15° the reaction proceeds so rapidly that the isothermal condition cannot be maintained. This limitation is not very serious, since the change in velocity is about forty-fold in that range. The thermostats were controlled to within 0·02°.

The following table gives the results of experiments done in this way, and the data are plotted in fig. 2 as $\log_{10} (k \times 10^9)$ against $10^4/T$ (abs.). Values of the empirical Arrhenius constant calculated from *dln* . *d*/*d*T = A/RT^2 are included in the table.

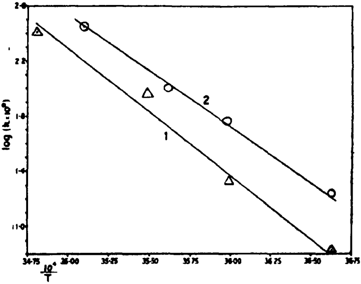

Fig. 2.

Crystals prepared from solutions containing	T (abs.).	k (cms. sec.$^{-1}$).	A.
Cu $(NH_3)_4^{++}$	287·17 281·78 277·83 273 00	$2·53 \times 10^{-7}$ $9\ 00 \times 10^{-8}$ $2\ 15 \times 10^{-8}$ $6\ 75 \times 10^{-9}$	41,350
Sucrose ..	285 00 280·80 278 00 273 00	$2·79 \times 10^{-7}$ $9·91 \times 10^{-8}$ $5\ 69 \times 10^{-8}$ $1\ 72 \times 10^{-8}$	36,780

Other values obtained for A .—

Cu $(NH_3)_4^{++}$	37,380
Sucrose	40,210

Discussion.

The Kinetics of the Reaction.—It is recognised that the explanation of the behaviour of calcium carbonate hexahydrate put forward above has not been established beyond question ; nevertheless, it is of interest to use it as a basis for an attempt to relate together the absolute reaction rate and its temperature coefficient.

When an ion (or molecular group of atoms) in the interface between two solid phases ceases to be part of the first and becomes part of the second solid, the ion must undergo a change of position ; one may reasonably assume that such a change of position takes place in virtue of the thermal vibration, and take for the frequency ν the figure 5×10^{12} per second, as representing the order of magnitude involved.

Of the vibrations undergone by any one ion in the interface, only a certain fraction β result in chemical change.

A rough value of β can be calculated if we write

$$k = \beta \,.\, \nu \,.\, \lambda,$$

where λ is the mean distance between successive ionic layers in the hydrate and k is the linear rate of propagation of the reaction, in cm. sec.$^{-1}$.

From the density of $CaCO_3 \,.\, 6H_2O$ ($= 1{\cdot}82$) $\lambda = 5 \times 10^{-8}$ cm. approximately.

For $CaCO_3 \,.\, 6H_2O$ crystals (prepared from a solution containing $Cu\,(NH_3)_4{}^{++}$) k was found to be $6{\cdot}75 = 10^{-9}$ at 273° abs.

Hence

$$\beta = 2{\cdot}7 \times 10^{-14}.$$

The fraction β must also be related to the temperature coefficient ; if we assume that the only condition which a vibration of an ion in the interface layer of the hydrate must fulfil, in order that it shall contribute to the chemical reaction, is that there shall be associated with that vibration an energy greater than some minimum value E, then β can, in principle, be calculated from the distribution of energy among vibrations in the interface lattice.

It seems, however, that no simple assumption about the distribution of energy and the number of degrees of freedom involved can lead to a value of β which is of the same order as the value calculated above from k.

Thus, if every reacting ion has previously been activated in one degree of freedom (*e.g.*, vibration across the interface), then β should be of the order $e^{-A/RT}$ (where $A = 41350$ and $T = 273°$), that is, of the order $6{\cdot}7 \times 10^{-34}$.

If it is supposed that two or three adjacent ions must be activated simultaneously, then howsoever the energy is divided up among them in order to account for the observed temperature coefficient, β is still far too small.

Possibly the association in some way of six molecules of water with the ions provides a large number of degrees of freedom among which the energy is distributed; this would be a case roughly analogous to that of unimolecular gas reactions involving complex molecules. But the expression given by Hinshelwood* and Fowler and Rideal† for the fraction of molecules having a total energy (in n energy terms) exceeding E cannot be applied in the present case (*i e.*, $A = 41350$ and $T = 273°$) when n exceeds about 22; and with only 22 energy terms it leads to a value of $\beta = 1 \cdot 7 \times 10^{-25}$, still far too small.

Nevertheless, if the mechanism suggested above does correspond at all closely to the truth, it seems reasonable to look for an explanation of the very high temperature coefficient in the possibility of a large number of degrees of freedom being concerned in the activation process.

One point which requires mention is the question whether the temperature of the layers of reactant near the interface is affected to an appreciable extent by the reaction in the interface; if this were so, the difficulty in connection with the temperature coefficient would be increased, because, if the temperature coefficient is in error from this cause, the experimental value must represent a lower limit, since the reaction is endothermic

Summary.

The velocity of the reaction $CaCO_3 . 6H_2O = CaCO_3 + 6H_2O$ has been studied dilatometrically.

The absolute rate of propagation of the chemical change in the solid has been deduced from the experimental results, and the temperature coefficient of the rate has been measured over the range 0° to 15°.

A kinetic mechanism is suggested which involves the vibration frequency of ions in the interface between the two solid phases, and the distribution of energy among the vibrating ions.

---

* 'Roy. Soc. Proc.,' A, vol. 113, p. 230 (1926).

† 'Roy. Soc. Proc.,' A, vol. 113, p. 570 (1927).

The Band Spectrum of Water Vapour.—III.

By David Jack, M.A., B.Sc., Assistant and Carnegie Teaching Fellow, The University, St. Andrews.

(Communicated by O. W. Richardson, F.R.S.—Received June 6, 1928.)

1. *Introduction.*

In previous papers,[*][†] details have been given of bands in the spectrum of water vapour, including the arrangement of the bands 2608 and 3428 into P, Q, and R branches. Measurements have also been given of a series of singlet lines[*] lying close to the head of the band 2811 and similar in structure to the singlet series observed by Watson[‡] near the head of the band 3064. The advances which have recently been made in the theory of band spectra throw a considerable amount of light on their structure, and in the present communication it is proposed to apply the new methods to the analysis of the water-vapour bands.

The conception which has been emphasised by several writers in the last few years is the close analogy which exists between molecular and atomic spectra. The electronic state of a molecule is characterised by the same features as are found in atoms, and in particular is associated with an electronic quantum number corresponding to Sommerfeld's inner quantum number for an atom. The outer electrons in a molecule are responsible for energy changes which are comparable in their nature and amount with those associated with the outer electrons of "corresponding" atoms. Mulliken, in a series of papers[§] in the 'Physical Review,' has discussed at length this analogy between atomic and molecular spectra, and in the sixth paper of the series has proposed a suitable notation which will be employed here.

The various electronic states are classified as S, P, D, ..., on analogy with the S, P, D, ... states in line spectra. These states are subject to multiplicity which is classified into two types. The first type is analogous to the multiplicity observed in line spectra, and the various sub-levels are distinguished by numerical subscripts, 1, 2, ..., added to the term symbol, F. The second type has no parallel in line spectra and in this case literal subscripts, A, B, are employed. This type, frequently referred to as σ-type multiplicity, is attributed to the effect of rotation on the component, σ, of the electronic angular momentum parallel to the axis of figure.

---

[*] 'Roy. Soc. Proc.,' A, vol. 115, p. 373 (1927).

[†] 'Roy. Soc. Proc.,' A, vol. 118, p. 647 (1928).

[‡] 'Astrophys. J.,' vol. 3, p. 145 (1924).

[§] 'Phys. Rev.,' vol. 28, pp. 481 and 1202 (1926); vol. 29, pp. 391 and 637 (1927); vol. 30, pp. 138 and 785 (1927).

The angular momentum of the rotating nuclei is denoted m (in units $h/2\pi$), and the component of the electronic orbital angular momentum parallel to the axis of figure, σ_k. The resultant of m and σ_k is denoted j_k, while the resultant of j_k and s, the angular momentum of electron spin, is denoted j. Consider the case in which both the initial and the final levels are doublet electronic levels (1, 2), and suppose also that both are further subject to doubling of the rotational type (A, B). Then corresponding to each value of j, in both initial and final states, there are four sub-levels. If transitions between any initial and any final level be permitted, subject to the selection principle for j by which $\Delta j = \pm 1, 0$, then there are 48 possible transitions. Transitions for which $\Delta j = -1, 0$, and $+1$ are denoted respectively **P**, **Q**, **R**, where $\Delta j = j' - j''$. The actual sub-levels involved are indicated by subscripts, for example, a transition from a 1A initial to a 2B final level when $\Delta j = -1$, is denoted $\mathbf{P}_{1A2B}(j)$, j being the final value, j''.

Further selection rules are, however, put forward which limit the number of transitions, and these will now be considered. In Hund's case b which is of special interest here, s is parallel or antiparallel to j_k so that $j = j_k \pm s$, and if j_1 and j_2 correspond to the substates 1 and 2, then $j_1 = j_k + s$, and $j_2 = j_k - s$. This in fact defines the meaning of the subscripts, 1 and 2. If now s is given the usual value, $\frac{1}{2}$, it is evident that in a 1 to 2 transition where j_1 and j_2 have the same value, $\Delta j_k = -1$. Such a transition would normally be denoted **Q**, but now in view of the transition $\Delta j_k = -1$ of j_k, it is called a P-form **Q** and is written $^{\mathbf{P}}\mathbf{Q}$. Similarly, for a 2 to 1 transition where j_2 and j_1 have the same value, $\Delta j_k = +1$, and the result is an R-form **Q**, $^{\mathbf{R}}\mathbf{Q}$.

The second selection rule which is usually imposed is that $\Delta j_k = \pm 1, 0$. This makes impossible both **P** transitions from a 1 state to a 2 state and **R** transitions from a 2 state to a 1 state. The former change makes $\Delta j_k = -2$, giving a "double P-form," the latter makes $\Delta j_k = +2$ giving a "double R-form" transition. This cuts out 8 transitions, reducing the total number to 40.

At present no definite rules are laid down as to how the subscripts, A and B, are to correspond to the physical properties of the substates concerned, but if the normal (intense) **P** and **R** branches be taken to correspond to transitions, A to B or B to A, then the following additional selection rule may be stated.

In A to B or B to A transitions $\Delta j_k = \pm 1$, and in A to A or B to B transitions $\Delta j_k = 0$. This reduces the total number of transitions from 40 to 20.

In the special case where one or other of the states is a rotationally single S state, half the above transitions automatically drop out and the total number of transitions permitted by the selection rules is 10.

2. *Simplification of Notation.*

The notation defined above is somewhat cumbersome but it can generally be simplified considerably without loss of definiteness. The Δj_k index can always be omitted when it is the same as the letter denoting the j transition, *e.g.*, $^{P}\mathbf{P}$ may be written simply $\mathbf{P}$. In special cases, such as that of the water-vapour bands considered here, further simplification may be introduced.

The water-vapour bands arise from transitions between ^{2}S (doublet S) initial and ^{2}P final states[*] Following Mulliken,[†] the rotationally single initial states will be denoted A. Since, therefore, the B subscript does not appear in the initial states, combinations like $\mathbf{P}_{1B1A}$, $\mathbf{Q}_{2B2B}$, do not occur, and the symbols, $\mathbf{P}_{1A1B}$, $\mathbf{R}_{1A1B}$, $\mathbf{Q}_{1A1A}$ may, without ambiguity, be contracted to $\mathbf{P}_1$, $\mathbf{R}_1$, $\mathbf{Q}_1$. For convenience a table showing the 10 transitions permitted by the above selection rules is given below.

Table I.

Main branches.				Satellites.
Here.	Mulliken.	Here.	Mulliken.	
$\mathbf{P}_1$	$^{P}\mathbf{P}_{1A1B}$	$\mathbf{Q}_1$	$^{Q}\mathbf{Q}_{1A1A}$	$^{P}\mathbf{Q}_{1A2B}$
$\mathbf{P}_2$	$^{P}\mathbf{P}_{2A2B}$	$\mathbf{Q}_2$	$^{Q}\mathbf{Q}_{2A2A}$	$^{R}\mathbf{Q}_{2A1B}$
$\mathbf{R}_1$	$^{R}\mathbf{R}_{1A1B}$			$^{Q}\mathbf{P}_{2A1A}$
$\mathbf{R}_2$	$^{R}\mathbf{R}_{2A2B}$			$^{Q}\mathbf{R}_{1A2A}$

The table includes both the complete symbols according to Mulliken and the contractions used here. The satellites will be given in full. The classification into main branches and satellites is the result of intensity considerations.

---

[*] 'Phys. Rev.,' vol. 30, p. 395 (1927).

[†] 'Phys. Rev.,' vol. 30, p. 792 (1927).

3. *Old and New Notation.*

According to the new meaning attached to subscripts 1 and 2, transitions between two levels with subscripts 1 give rise to the higher frequency components of the doublets, and transitions between levels with subscript 2 to the lower frequency components. As a result, the subscripts 1 and 2 formerly applied to the water-vapour bands have to be interchanged, *e g*, a line formerly denoted $\mathbf{P}_2$ now becomes $\mathbf{P}_1$. The next point which arises is that of the connection between the old empirical "*m*" of Heurlinger, and *j*. This question, as that of the interchange of the numerical subscripts, has already been referred to* in connection with Kemble's work on the water-vapour bands. It appears, then, that the two components of a doublet have different values of *j*, these values differing by unity They have, however, the same value of j_k so that if, for the higher-frequency component of a doublet, $j_1 = 2$, then for the lower-frequency component $j_2 = 1$. Accordingly Heurlinger's $\mathbf{P}_1(m)$, $m = 2$, becomes $\mathbf{P}_2(j)$, $j = 1$, and Heurlinger's $\mathbf{P}_2(m)$, $m = 2$, becomes $\mathbf{P}_1(j)$, $j = 2$. A complete list of old and new symbols will be given later.

4. OH *Bands. Main Branches.*

From consideration of intensities, the most probable transitions are those corresponding to the symbols classed under main branches in Table I. For the **P** and **R** branches the transitions are between 1A and 1B, or 2A and 2B states, while for the **Q** branches the transitions are 1A to 1A, and 2A to 2A. The σ-type doubling (A, B), and crossing over are capable of accounting for the failure of the combination principle,

$$\mathbf{R}(j-1) - \mathbf{Q}(j) = \mathbf{Q}(j-1) - \mathbf{P}(j), \tag{1}$$

when applied to the main branches. Kemble† has given an explanation of the variation of the doublet separation in the water-vapour bands with *j*, but his theory does not take account of the σ-type doubling.

The main branches are defined, in terms of Mulliken's notation, by the relations,

$$\left.\begin{aligned} \mathbf{P}_1(j) &= \mathbf{F}'_{1A}(j-1) - \mathbf{F}''_{1B}(j) \\ \mathbf{Q}_1(j) &= \mathbf{F}'_{1A}(j) \quad\;\; - \mathbf{F}''_{1A}(j) \\ \mathbf{R}_1(j) &= \mathbf{F}'_{1A}(j+1) - \mathbf{F}''_{1B}(j) \end{aligned}\right\}, \tag{2}$$

and similarly for $\mathbf{P}_2$, $\mathbf{Q}_2$, $\mathbf{R}_2$. Here the quantity ν_0 is supposed for convenience to be included in $\mathbf{F}'$. Making use of the above expressions the $\mathbf{F}_1$ terms were evaluated for the band 3064, apart from an additive constant. Similarly an independent set of values was obtained for the $\mathbf{F}_2$ terms.

---

* 'Roy. Soc. Proc.,' A, vol. 118, p. 652 (1928).

† 'Phys. Rev.,' vol. 30, p. 395 (1927).

5. *Satellites.* **P** *and* **R.**

Heurlinger[*] observed that some of the lines of the bands 3064 and 3122 are accompanied by faint lines lying very close to the main lines. These faint lines he called satellites and gave data on 18 satellites of the band 3064. Fortrat[†] gives much more extensive lists of satellites in a paper in which he discusses the Zeeman effect in these bands More recently Watson[‡] measured two series of Q satellites not mentioned by Heurlinger or Fortrat.

Consider first the satellites of the **P** and **R** branches. The most probable P- and R-form satellites, according to Table I, are ${}^{\mathrm{P}}\mathrm{Q}_{1\mathrm{A}2\mathrm{B}}$ and ${}^{\mathrm{R}}\mathrm{Q}_{2\mathrm{A}1\mathrm{B}}$. These are defined by

$$\left.\begin{aligned} {}^{\mathrm{P}}\mathrm{Q}_{1\mathrm{A}2\mathrm{B}}(j) &= \mathrm{F}'_{1\mathrm{A}}(j) - \mathrm{F}''_{2\mathrm{B}}(j) \\ \text{and} \qquad {}^{\mathrm{R}}\mathrm{Q}_{2\mathrm{A}1\mathrm{B}}(j) &= \mathrm{F}'_{2\mathrm{A}}(j) - \mathrm{F}''_{1\mathrm{B}}(j) \end{aligned}\right\}, \tag{3}$$

Now,

$$\left.\begin{aligned} {}^{\mathrm{P}}\mathrm{Q}_{1\mathrm{A}2\mathrm{B}}(j) - \mathrm{P}_2(j) &= \mathrm{F}'_{1\mathrm{B}}(j) - \mathrm{F}'_{2\mathrm{B}}(j-1) \\ \text{and} \qquad \mathrm{R}_1(j-1) - {}^{\mathrm{R}}\mathrm{Q}_{2\mathrm{A}1\mathrm{B}}(j-1) &= \mathrm{F}'_{1\mathrm{B}}(j) - \mathrm{F}'_{2\mathrm{B}}(j-1) \end{aligned}\right\}. \tag{4}$$

In Table II are given the differences on the left-hand side of equation (4). The results should be the same both for the P and for the R differences. Since the data on the satellites are subject to considerable irregularities, the values from both Heurlinger's and Fortrat's tables are given. The results in columns 2 and 3 are in good general agreement with those in columns 4 and 5, as they ought to be if the above interpretation is correct

Table II.

j.	${}^{\mathrm{P}}\mathrm{Q}_{1\mathrm{A}2\mathrm{B}}(j) - \mathrm{P}_2(j)$.		$\mathrm{R}_1(j-1) - {}^{\mathrm{R}}\mathrm{Q}_{2\mathrm{A}1\mathrm{B}}(j-1)$	
	Heurlinger.	Fortrat.	Heurlinger.	Fortrat.
3	—	0·74	—	—
4	0·77	0·76	0·73	0·73
5	0 92	0 96	1·02	0·99
6	—	—	1·06	1·23
7	1·41	1·38	1·47	1·45
8	1 45	1·30	—	0·93*
9	—	1·80	1·84	1·60
10	—	2 10	2·19	0·79*
11	—	2·64	—	0·91*
12	—	2·50	—	—

* These values appear to be irregular, probably due to inaccuracy in the measurement of the faint lines.

---

[*] " Untersuchungen über die Struktur der Bandenspektra," Lund (1918).

[†] 'J. de Physique,' vol. 5, p. 20 (1924).

[‡] 'Nature,' vol. 117, p. 157 (1926).

6. *Term Values.*

Table II gives the values of $F'_{1B}(j) - F'_{2B}(j-1)$, and these may be used to obtain the connection between the F_1 and F_2 levels. The differences of the values of $F'_{1B}(j)$ and $F'_{2B}(j-1)$ already determined (with different arbitrary zeros) were compared with the values in Table II, and the correction which must be applied to the F_1 values to correlate them with the F_2 values, ascertained.

Fig. 1 is a diagram showing a few of the energy levels in the band 3064. The F_1 levels have all been drawn to a uniform scale. The spacing of the A and B levels has been magnified five times, and the spacing of the 1 and 2 initial levels 10 times. Transitions between the various levels are indicated in the usual way by arrows. The transition marked S will be referred to in § 8.

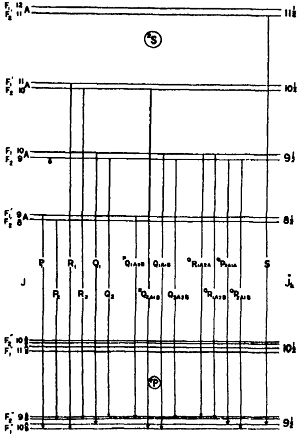

FIG. 1.

7. Q *Satellites.*

The Q satellites measured by Watson may next be considered. Watson states that these satellites obey the combination relation (1) if Q is taken to refer to Watson's satellite lines. It follows directly from this relation, the numerical test of which is contained in Table III, that

$$Q^{*}_{1}(j) = F'_{1A}(j) - F''_{1B}(j).$$

These satellites are therefore to be represented, in the present notation, by $Q_{1A1B}(j)$ and $Q_{2A2B}(j)$.

Now

$$\left.\begin{aligned} Q_{1A1B}(j) - Q_{1}(j) &= F''_{1A}(j) - F''_{1B}(j) \\ \text{and} \qquad Q_{2A2B}(j) - Q_{2}(j) &= F''_{2A}(j) - F''_{2B}(j) \end{aligned}\right\}. \tag{5}$$

Columns 2 and 4 of Table IV show the values of the differences on the left-hand side of (5), while columns 3 and 5 give the corresponding values of the differences on the right-hand side, obtained from the calculated values of F. The figures in column 2 should agree with those in column 3, and similarly for columns 4 and 5. When allowance is made for the obvious irregularity of the experimental data on Q_{1A1B} and Q_{2A2B}, it is seen that the results are consistent with this interpretation of the satellites.

Table III.

j.	$R_1(j-1) - Q^{*}_1(j)$	$Q^{*}_1(j-1) - P_1(j)$.	$R_2(j-1) - Q^{*}_2(j)$.	$Q^{*}_2(j-1) - P_2(j)$.
8	—	—	289·01	—
9	292 27	—	325·30	326·36
10	330·48	331·62	361·15	361 38
11	363·17	363·00	396·50	395·82
12	399·21	399·57	431·28	429·52
13	433·41	431·77	465·42	463·00
14	466 58	465 27	496·79	495·60
15	498 63	498·06	529·26	529·81
16	532 47	531 15	561·93	561 93
17	—	561 19	591·63	592·26
18	595 20	—	626·51	624 25
19	624·18	622·91	650·78	649·53
20	653·74	653·61	683 35	684·06
21	683 64	681·98	709·66	708·55
22	709·27	709·67	737·73	737·91
23	739·70	739·41	—	763·52

Q* represents Watson's Q satellites.

---

* The star is added to indicate that the lines in question are Q satellites and not main branch lines.

Table IV.

j.	$Q_{1A1B}(j) - Q_1(j)$.	$F''_{1A}(j) - F''_{1B}(j)$.	$Q_{2A2B}(j) - Q_2(j)$.	$F''_{2A}(j) - F''_{2B}(j)$.
8	—	—	1·83	1·17
9	5·20	2·65	2·00	1·60
10	2·80	4·21	2·07	2·24
11	5·70	4·46	2·17	2·68
12	4·89	5·77	2·59	3·84
13	5·89	6·65	2·82	3·99
14	6·66	7·21	5·35	5·37
15	8·54	8·56	6·30	5·93
16	8·01	9·31	6·34	6·91
17	—	9·76	8·71	7·51
18	10·23	11·37	5·29	8·75
19	12·62	12·75	11·98	9·77
20	13·28	14·28	9·35	10·85
21	14·39	16·05	12·51	12·12
22	17·86	16·80	12·51	12·72
23	15·85	18·20	—	—
24	10·92	—	—	—
25	18·06	—	—	—

In these Q satellites the transitions violate the σ-selection rule in that they arise from transitions from A to B states while at the same time $\Delta j_k = 0$. That some of the OH satellites probably violate the σ-selection rule was suggested by Mulliken.*

There still remain several series of Q satellites to be accounted for. There appear to be at least five different series of Q satellites in Fortrat's lists, which do not include those just discussed. There only remain two unused symbols in Table I, and to those may be added the two, ${}^{Q}P_{2A1B}$ and ${}^{Q}R_{1A2B}$, which violate the σ-selection rule. These four are probably capable of accounting for four of the above satellites, but the precise interpretation of the satellites is a little uncertain on account of errors of measurement, which, judging from the figures in Fortrat's tables, are likely to be considerable. To account for the fifth series it would seem necessary to assume further multiplicity of the energy levels. It is just possible that very narrow rotational doubling may actually be present in the initial levels. If this were so Watson's satellites might be represented by B to B transitions. The evidence for the existence of rotational doubling in the initial levels is very slender and will not, therefore, be further stressed here.

8. *The Singlet Series.*

The question now arises as to the possibility of explaining the singlet series by transitions between the levels represented in fig. 1. The singlet series measured by Watson will here be referred to as singlet series I, and that measured by the author as singlet series II. Owing to the proximity of singlet series I to the band 3064 it is natural to expect some close relation between the two, and similarly for singlet series II and the band 2811.

---

* 'Phys. Rev.,' vol. 30, p. 793 (1927).

The main branches of the water-vapour bands do not follow exactly a parabolic law. In the higher-frequency component branches (new subscript 1) the second differences of the wave-numbers always show a marked numerical increase with increasing j, while in the lower-frequency component branches (new subscript 2) there is a corresponding numerical decrease. In this respect the singlet series show a strong similarity to the higher-frequency branches. It seems natural, therefore, to expect combination relations between the singlet series and $\mathbf{P}_1$, $\mathbf{Q}_1$, $\mathbf{R}_1$, rather than $\mathbf{P}_2$, $\mathbf{Q}_2$, $\mathbf{R}_2$.

Let the lines of the singlet series be represented by $\mathbf{S}(j)$, the lowest value of j being taken as 2 on analogy with $\mathbf{P}_1$, $\mathbf{Q}_1$, $\mathbf{R}_1$. If the series, $\mathbf{S}$, be then represented on the same Fortrat diagram as the $\mathbf{P}_1$, $\mathbf{Q}_1$, $\mathbf{R}_1$ branches, fig. 2, it appears, so far as the accuracy of the diagram goes, that

$$\mathbf{S}(j) - \mathbf{R}_1(j+1) = \mathbf{Q}_1(j) - \mathbf{P}_1(j+1). \tag{6}$$

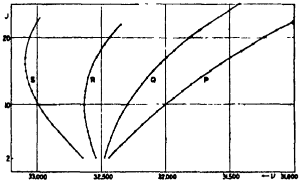

FIG. 2.

This relation is subjected to a numerical test in Table V. The first part of the table relates to combinations between the band 3064 and singlet series I. If the relation held accurately $\mathbf{S}(j)$ should correspond to the transition, $\mathbf{F}'_{1A}(j+2)$ to $\mathbf{F}''_{1A}(j)$. This follows immediately on replacing $\mathbf{P}$, $\mathbf{Q}$, $\mathbf{R}$ in (6) by the appropriate terms. It is observed, however, that the values in column 2 are less than those in column 3, which fact would indicate that the initial $\mathbf{S}(j)$ level is $\mathbf{F}'_{2A}(j+1)$ and not $\mathbf{F}'_{1A}(j+2)$. Column 4 gives the difference, column 3–column 2, which, if the initial $\mathbf{S}(j)$ sub-level is really $\mathbf{F}'_{2A}(j+1)$, should be equal to $\mathbf{F}'_{1A}(j+2) - \mathbf{F}'_{2A}(j+1)$. The values of

Table V.

(1) j.	(2) $S(j) - R_1(j+1)$.	(3) $Q_1(j) - P_1(j+1)$.	(4) Column 3 − Column 2.	(5) $F'_{1A}(j+2) - F'_{2A}(j+1)$.
Band 3064 and Singlet Series I.				
2	82·82	83·61	0·79	0·76
3	116·76	117·77	1·01	0·96
4	151·37	153·91	2·54	1·15
5	186·04	187·73	1·69	1·50
6	220·84	222·70	1·96	1·73
7	255·53	257·37	1·84	1·60
8	289·92	292·15	2·23	2·27
9	324·12	226·42	2·30	2·03
10	357·78	360·20	2·42	2·60
11	390·88	393·87	2·99	2·67
12	424·00	426·88	2·88	3·03
13	456·04	459·38	3·34	3·17
14	487·57	491·40	3·93	3·44
15	518·92	522·61	3·69	3·67
16	549·36	553·18	3·82	3·88
Band 2811 and Singlet Series II				
2	82·76	83·52	0·76	0·85
3	117·23	117·90	0·67	0·74
4	151·48	152·60	1·12	0·87
5	186·70	187·72	1·02	1·11
6	220·59	222·74	2·15	1·56
7	255·50	257·76	2·76	1·11
8	289·96	292·23	2·27	1·86
9	324·40	326·58	2·18	2·09
10	358·12	360·37	2·25	2·22
11	389·00*	394·01	5·01*	2·78
12	423·50*	427·22	3·72*	2·61
13	456·98*	549·20	2·22*	2·77
14	487·65	491·65	4·00	3·07
15	519·41	522·90	3·59	3·69
16	549·47	553·33	3·86	3·91
17	579·41	583·16	3·75	4·19
18	608·79	612·31	3·52	3·87

* Turning point of *S* series. Lines not completely resolved.

the latter difference, previously obtained, are given in column 5. The agreement between columns 4 and 5 is very good indeed, so that the interpretation of the singlet series,

$$S(j) = F'_{2A}(j+1) - F''_{1A}(j), \tag{7}$$

receives very strong support from the experimental data.

The second part of the table shows the corresponding results for the band 2811 and singlet series II. The figures in the last column are obtained by making use of the fact that the final levels in both bands, 3064 and 2811, are the same.

The actual combination relation should therefore be

$$\mathbf{S}(j) - {}^{\mathrm{B}}\mathbf{Q}_{2\mathrm{A}1\mathrm{B}}(j+1) = \mathbf{Q}_1(j) - \mathbf{P}_1(j+1), \tag{8}$$

instead of (6). The experimental data by which this relation may be tested directly are very unsatisfactory, since they involve the rather irregular values for the R satellites, of which only a few are available in any case The less direct method used in Table V is, therefore, much to be preferred as it is likely to be very much more reliable. It should be observed that, although the S series of the bands 3064 and 2811 are very weak compared with the main branches of these bands, yet they are capable of being measured with the same accuracy as the main branches since they lie in regions free from other lines. Exposures may be increased sufficiently to give really intense photographs of the singlet series without any difficulty.

9. *Selection Rules.*

The combination principle provides very strong evidence for the interpretation of the singlet series as stated in equation (7). The most striking feature of the singlet series is, then, that it violates the Δj_k selection rule, $\Delta j_k = \pm 1, 0$. The transition, $\mathbf{F}'_{2\mathrm{A}}$ to $\mathbf{F}''_{1\mathrm{A}}$, together with the transition, $\Delta j = +1$, leads to the conclusion that $\Delta j_k = +2$.

Remarkable as this result[*] may appear, it is, however, to be expected from the position of the **S** curve in the Fortrat diagram, fig. 2. The **P** branch and all its satellites lie close together and correspond to $\Delta j_k = -1$, irrespective of Δj. The **Q** branch and all its satellites correspond to $\Delta j_k = 0$, the **R** branch and its satellities to $\Delta j_k = +1$. Now, each group (main branch and its satellites) is defined by a particular value of Δj_k, irrespective of Δj, and occupies a definite narrow region in the diagram. The regions corresponding to each value of Δj_k are well separated, and consequently, from the position of **S** on the high-frequency side of **R**, it seems reasonable to attribute the **S** branch to a transition, $\Delta j_k = +2$. The **S** branch is therefore to be considered as a double R-form **R** branch, say $^{\mathrm{S}}\mathbf{R}$.

---

[*] *Cf.* 'Nature,' vol. 121, p. 793 (1928). Dieke, Takamine, and Suga, referring to helium, make the following statement: "The band $2p - 3y$ has three branches which have the appearance of a Q-branch, a P-branch and a branch in which the *effective* rotational quantum number decreases by two units."

This interpretation suggests the question as to the possible occurrence of a double P-form branch, where $\Delta j_k = -2$. Unfortunately, the experimental data available cannot be expected to provide any evidence on this point, since if such a branch does occur, its low intensity together with its position in a dense region of intense lines will make its observation a matter of considerable difficulty. In most band spectra there is considerable overlapping of the bands, but in this respect the water-vapour spectrum is particularly suitable for the study of double R-form branches.

From the foregoing discussion it seems that the only selection rule which holds ***rigidly*** is the rule, $\Delta j = \pm 1, 0$. That is to say, the resultant of all the angular momenta can change only by ± 1 or 0 in any one transition, whereas the component momenta *may* change by an amount greater than unity under certain conditions. At the same time it may be said that the *most probable* transition of any momentum component is ± 1 or 0, although this rule cannot be taken as final.

10. *Summary*

The water-vapour bands can be interpreted as arising from transitions between ^2S and ^2P levels. The ^2P levels are subject to σ-type doubling (A, B), while the ^2S levels are probably rotationally single The **P** and **R** main branches are due to transitions, 1A to 1B, and 2A to 2B, while the **Q** branches show " crossing over," 1A to 1A, and 2A to 2A. Other combinations give rise to satellites, in some of which the σ-selection rule does not hold.

The most striking feature exhibited by these bands is the presence of a singlet branch for which the combination principle definitely indicates a transition of two units in j_k. It is therefore concluded that, although the j selection rule, $\Delta j = \pm 1, 0$, probably holds rigidly, the other selection rules (j_k and σ) are only an expression of the *most probable* transitions and cannot be taken as final.

The connection between the old and new notation is given in Table IV (p. 234), which also serves to summarise the interpretation of the various branches.

Table VI.

Main branches.		**Satellites.**	
Old.	**New.**	**Old.**	**New.**
$P_1(2)$	$P_2(1)$	H, F $\sigma P_1(2)$	${}^{P}Q_{1A2B}(1)$
$P_2(2)$	$P_1(2)$	$\sigma R_2(2)$	${}^{R}Q_{2A1B}(2)$
$Q_1(2)$	$Q_2(1)$	W $\sigma Q_1(2)$	$Q_{2A2B}(1)$
$Q_2(2)$	$Q_1(2)$	$\sigma Q_2(2)$	$Q_{1A1B}(2)$
$R_1(2)$	$R_2(1)$	Fortrat's	* ${}^{Q}P_{2A1A}(2)$
$R_2(2)$	$R_1(2)$	$\sigma Q_1(2)$	${}^{Q}R_{1A2A}(1)$
		$\sigma Q_2(2)$	${}^{Q}P_{2A1B}(2)$
			${}^{Q}R_{1A2B}(1)$
		Singlet series	Double R-form $S_{2A1\backslash}(2)$

F., Fortrat. H., Heurlinger. W., Watson. * Probable interpretation.

The writer is deeply indebted to Prof. H. Stanley Allen for the keen interest he has taken in the work of this paper and for much helpful discussion.

The Electrical Condition of Hot Surfaces during the Adsorption of Gases. Part II.—*A Nickel Surface at Temperatures up to* 850° *C.*

By G. I. Finch and J. C. Stimson.

(Communicated by W. A. Bone, F R S.—Received June 15, 1928.)

Introduction.

It was shown in Part I* of the present series of researches that a gold or silver surface becomes charged when heated in vacuo or in contact with various gases, and that the charge on the surface depends, in the main, upon the temperature and the nature of the gas, and also to some extent upon the previous history of heating of the surface; but is independent, within wide limits, of the gas pressure. In view of the close bearing which these results undoubtedly have upon the nature and mechanism of heterogeneous catalysis, the investigation is being extended to an examination of the electrical conditions of a variety of other surfaces. In what follows an account is given of the experimental results obtained with a nickel surface at temperatures up to 850° C.

Experimental.

The apparatus previously described and illustrated in Part I† was employed in all experiments to be described below, a rolled-up nickel 20 S.W.G. sheet, 7 cm. by 12 cm., being suspended in the vertical quartz vessel by means of a narrow nickel tape cut from the sheet itself. The sheet had been previously washed with petroleum ether, no attempt having been made to remove the thin oxide film. The surface charge was measured by means of a Lindemann electrometer. The experimental procedure was essentially that followed and described in Part I.

Experimental Results.

In all the experiments to be described below in which the surface was heated in contact with gases the pressure could be varied within wide limits (between 1 mm. and 760 mm.) without in any way affecting the charge on the surface.

Series A. In Vacuo.

The nickel sheet was heated to 480° C. in a vacuum below 10^{-5} mm. during 7 days (168 hours), towards the end of which period the charge settled down to a constant value of — 1·45 volt. Thereupon the in vacuo charge-temperature curve was determined, the result being recorded in fig. 1, curve Vacuo

---

* 'Roy. Soc. Proc.,' A, vol. 116, p. 379 (1927).

† *Loc. cit.*, p. 380 and fig. 1.

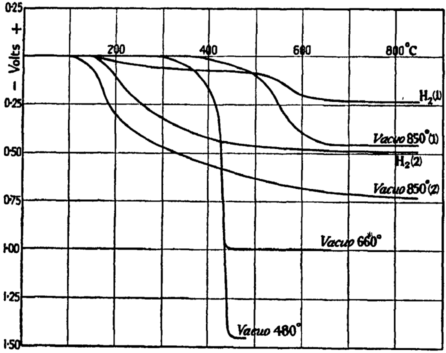

FIG. 1.

480°. In a similar manner, the in vacuo charge-temperature curves of the nickel sheet, after previous heating of sufficient duration to ensure constancy of the in vacuo charges having been attained, were determined for 660° (— 1·00 volt) and 850° (— 0·46 volt) respectively. The results are recorded in fig. 1, curves Vacuo 660° and 850° (1).

Series B.—Hydrogen.

The 850° in vacuo charge-temperature curve was twice redetermined, both with falling as well as with rising temperature. The resulting curves were identical, within the limits of experimental error, with that previously obtained and shown in fig. 1, curve Vacuo 850° (1). The surface was, therefore, certainly in a settled condition.

With the surface at 850° and giving the in vacuo charge of — 0·46 volt corresponding to that temperature, hydrogen was admitted into the apparatus. Within 5 minutes the charge had fallen to — 0·23 volt, at which value it remained constant throughout 7 days heating in hydrogen at 850°. The apparatus was then evacuated to below 10^{-5} mm, whereupon, within 30 minutes, the previous in vacuo charge of $-0 \cdot 46$ volt at 850° was restored. The corresponding charge-temperature curves are recorded in fig. 1, curves H_2 (1) and Vacuo 850° (1). On repeating these experiments, the hydrogen charge at 850° rose to $-0 \cdot 49$ volt (previously $-0 \cdot 23$ volt) which on evacuation gave way to a constant in vacuo charge of $-0 \cdot 73$ volt at 850° (previously $-0 \cdot 46$ volt) within 30 minutes. After checking the electrical circuit we were unable to account for the change in these charges other than by concluding that the activating powers of the nickel surface had undergone profound change as a result of a single treatment with hydrogen. In putting forward this view, however, we have not lost sight of the fact that the in vacuo charge remained unchanged after the first hydrogen treatment. It is possible that two such treatments were necessary before the surface was in such a "hydrogen-normalised" condition as indicated by the new in vacuo charge of $-0 \cdot 73$ volt. Four successive determinations of both the hydrogen and the in vacuo charge-temperature curves up to 850° were carried out. The results which agreed within the limits of experimental error, thus showing that the surface had completely settled down to a hydrogen-normalised condition, are recorded in fig. 1, curves H_2 (2) and Vacuo 850° (2).

Series C.—Oxygen.

The oxygen charge at 850° was found to be $-0 \cdot 33$ volt. The corresponding charge-temperature curve is shown in fig. 2, curve O_2. During this experiment the nickel sheet absorbed a considerable quantity of oxygen, and became

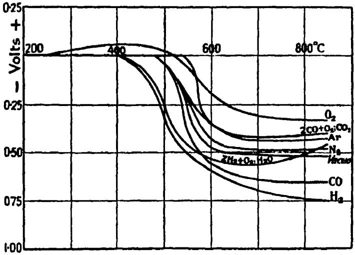

Fig. 2.

coated with oxide. In 18 hours, for example, at 850° the oxygen pressure fell from 100 to less than $0 \cdot 1$ mm. On evacuation a constant in vacuo charge of $- 0 \cdot 52$ volt at 850° was attained within 45 minutes. The corresponding charge-temperature curve is recorded in fig. 2, curve Vacuo. Three repeat experiments confirmed these results. It should be pointed out that during the determination of this in vacuo charge the surface was covered with a dense and thick film of oxide which was stable at 850°, since it gave off no oxygen, as was shown by the fact that within 30 hours after closing the stopcock, T_1 (see Part I, p. 381, fig. 1), between the apparatus and the pumping system, the pressure rose from below 10^{-5} mm. to only about 10^{-3} mm., a pressure rise of the same order as that obtained under otherwise similar conditions but with the nickel sheet reduced, and probably due, in the main, to slight gas evolution from the grease freshly exposed as a result of closing the stopcock, T_1.

Hydrogen was next admitted to the apparatus, the surface being heated to 850°. Within 5 minutes a constant hydrogen charge of $- 0 \cdot 75$ volt was attained Before proceeding to carry out the determination of the charge-temperature curve for this gas, however, fresh quantities of hydrogen were admitted to the apparatus until the oxide film on the surface had been completely reduced. The hydrogen charge-temperature curve of the reduced surface is shown in fig 2, curve H_2. It will be noted that the hydrogen charge at 850° is the same for both the oxidised and the reduced surface.

A determination of the in vacuo charge-temperature curve for the reduced surface gave a result identical with that obtained with the heavily oxidised surface and recorded in fig. 2, curve Vacuo.

In further experiments, to be described below, the surface was heated with several different gases. In all cases the subsequently determined in vacuo charge-temperature curves agreed with that recorded in fig. 2, curve Vacuo. Similarly the hydrogen and oxygen charge-temperature curves recorded in fig. 2, curves H_2 and O_2, could always be repeated, irrespective of the nature of the gas with which the surface had previously been in contact. It will be convenient to refer to the nickel surface as "fully normalised" when giving these charge-temperature curves. It will be noted that at least one thorough oxidation and reduction of the surface at 850° was necessary in order to normalise it completely. The oxygen charge could always be removed within 45 minutes evacuation.

Series D.—Carbonic Oxide.

At 850° a constant carbonic oxide charge of $- 0 \cdot 65$ volt was fully established within 5 minutes. The corresponding charge-temperature curve is recorded in fig. 2, curve CO. On evacuating during several hours at 850°, the carbonic oxide charge remained unchanged, and although evacuation below 10^{-5} mm. at this temperature was prolonged over a continuous period of 5 days, this charge remained perfectly steady. During this period the surface was frequently earthed, as indeed was the case in all charge determinations made in the course of our experiments, sometimes during a period of many hours. On re-insulation of the surface the carbonic oxide charge was invariably rapidly restored to its full value.

On admission of oxygen to the evacuated apparatus, however, the carbonic oxide film on the surface was rapidly burnt off, the full oxygen charge of − 0·33 volt at 850° being established within 5 minutes.

Series E.—Electrolytic Gas, Steam, Carbonic Oxide "Knall" Gas and Carbon Dioxide.

On bringing either one of the above gases or gaseous mixtures into contact with the surface at 850°, the in vacuo charge of − 0·52 volt gave way to the respective gas charge within 5 minutes. At 850° these charges were as follows:—

Electrolytic gas, − 0·46 volt; steam, − 0·46 volt; carbonic oxide "Knall" gas, − 0·40 volt; carbon dioxide, − 0·40 volt.

The corresponding charge-temperature curves are shown in fig. 2, curves $2H_2 + O_2$ and H_2O, $2CO + O_2$ and CO_2. The curves for the two former and the two latter gases are identical at all temperatures.

On evacuation the above charges were completely removed and the in vacuo charge fully restored within 45 minutes.

Series F.—Nitrogen and Argon.

At 850°, the nitrogen and argon charges were − 0·48 and − 0·43 volt respectively, and were established within 5 minutes of admission of the gas in question. The corresponding charge-temperature curves are shown in fig. 2, curves N_2 and Ar. On evacuation the in vacuo charge was restored within 45 minutes.

Series G.—Mixtures of Nitrogen or Argon with Oxygen or Hydrogen.

On referring to Part I, p. 393, fig. 11, and to fig. 2 (this paper) it will be seen that the argon and nitrogen charge-temperature curves for silver and nickel lie close to each other, the argon charge being, however, slightly less negative throughout than that due to nitrogen. On gold, on the other hand (see Part

I, p. 392, fig. 9), we found that the argon charge was throughout more negative than that of nitrogen. It was thought that this might possibly be due to an impurity, probably hydrogen, in the argon then employed. The amount of such adventitious impurity could not, however, have exceeded 0·2 per cent. If this explanation were correct, the activity of hydrogen in charging up a surface must greatly exceed that of argon. In order to test this point and further to compare the activity of nitrogen with oxygen or hydrogen a series of experiments were carried out in which argon or nitrogen was diluted with a small amount of oxygen or hydrogen and brought into contact with the nickel surface at 850°. The results are recorded in the following table:—

Table I.—Charges on a Nickel Surface at 850°.

Gas.	Charge (volts).	Gas.	Charge (volts).	Gas.	Charge (volts).
In vacuo	−0·52	Argon	−0·43	Nitrogen	−0·48
Oxygen	−0·33	Argon + 2·0 per cent. oxygen	−0·33	Nitrogen + 2·0 per cent. oxygen	−0·33
Hydrogen	−0·75	Argon + 2·0 per cent. hydrogen	−0·75	Nitrogen + 2·0 per cent hydrogen	−0·75

These results show that both hydrogen and oxygen are far more active than either argon or nitrogen, and there seems to be little room for doubt that the argon charge-temperature curve for gold recorded in Part I, p. 392, fig. 9, was displaced towards the hydrogen curve by the presence of a trace of the latter gas in the argon employed in those experiments. We are carrying out further experiments in order to test this conclusion further.

Discussion of the Results.

In Part I of the present series of researches a hypothesis was formulated in order to account for the electrical charging up of a hot gold or silver surface in contact with various gases. This hypothesis was put forward on that occasion with the main object of indicating the lines upon which the investigation could be continued to the best advantage. The experimental results which we have obtained with the nickel surface not only support this hypothesis, but also enable it to be extended in certain important directions.

In the light of the facts hitherto forthcoming, the most probable explanation of the charging up of a hot nickel surface in contact with a gas or gaseous mixture is essentially in accordance with that previously advanced in Part I in connection with the charging of gold or silver surfaces. According to that hypothesis, molecules of gas in contact with the hot nickel surface are adsorbed on to the surface of the metal, whereupon a certain proportion of such adsorbed molecules become charged or "activated." Such activation may take place in either one or both of two ways, both of which proceed to equilibrium.—

(i) Some molecules become positively charged and remain in this state on the surface, the corresponding negative charges quitting the surface, which thus becomes positively charged.

(ii) Other adsorbed molecules become negatively charged and remain in this condition on the surface, which thus acquires a negative charge

Depending on the temperature, the surface charge with oxygen may be either positive or negative, the former over the lower, the latter throughout the higher temperature ranges; thus tending to show that, in the case of oxygen, the adsorbed molecules are activated in both ways, the observed charge at any temperature being the algebraic sum of the individual charges due to each type of activation In the case of nickel, (i) predominates below 520°, and (ii) above this temperature. With the remaining gases examined the charges were invariably negative, from which the conclusion may be drawn that activation took place mainly or exclusively in the manner indicated in (ii).

In Part I, in order to account for the negative charging of a gold or silver surface in vacuo, it was suggested that such charging might be due to activation of the vapour of the metal itself. In the case of both gold and silver conclusive evidence of volatilisation was obtained. With nickel, however, such was not the case. It is true that we did find on conclusion of our experiments a film of nickel deposited on the cooler portions of the quartz vessel, though it might well be that such deposit was due, not to the evaporation of the metal as such, but to the formation and subsequent decomposition of nickel carbonyl. Hughes and Bevan,* however, have found that when a nickel wire is heated to dull redness in a vacuum or in hydrogen, volatilisation occurs. But in view of the profound effect which not only the maximum temperature to which the nickel (and also gold or silver) surface was raised, but also successive reductions and oxidations had upon the whole course of the in vacuo charge-temperature curve, it may well be that the surface undergoes structural change of a permanent nature as a result of such treatments, and that such change involves rearrangement of the surface atoms. The changes in the in vacuo and hydrogen charge-temperature curves obtained in our earlier experiments with the nickel sheet (Series B and C), as a result of successive reductions and oxidations, and by which the surface was brought into what has been called above the "fully normalised" condition, may also be due to rearrangement of surface atoms into another more stable configuration.

---

* 'Roy. Soc. Proc.,' A, vol. 117, p. 101 (1927).

The new facts revealed relating to the ease or otherwise with which the charge due to a gas can be removed from a nickel surface by evacuation are of special significance, since they now enable a sharp distinction to be drawn between different kinds of adsorption of gases on metallic surfaces. Benton* has attempted to distinguish between two types of adsorption, *i.e.*, between the adsorption of gases by inert materials such as charcoal and, on the other hand, by metals; adsorption in the former case being roughly proportional to the ease with which the gas can be liquefied, whereas in the latter case the adsorption is highly specific. The distinction between the two types of adsorption thus illustrated is, however, by no means sharp.

At 850°, with the sole exception of carbonic oxide, the charges due to all gases were in our experiments readily removed from nickel within 45 minutes (hydrogen within 30 minutes) evacuation. In the case of carbonic oxide, however, the charge remained completely unaffected even by prolonged evacuation, and could only be removed by burning off with oxygen. From these facts and from those previously established and set forth in Part I, we conclude that a gas can be held adsorbed on a hot metal surface in at least five different ways, as follows :—

(i) The gas is held physically in an electrically neutral condition in the form of a condensed layer which even at 850° is, as has been shown by Langmuir,† at least of monomolecular thickness.

(ii) The gas is held loosely in an electrically charged condition, whereby the surface itself acquires a charge, which can be removed with complete restoration of the in vacuo charge proper to the surface within 30 to 60 minutes by evacuation alone at 850°. As examples may be cited H_2, N_2, CO, CO_2, H_2O and Ar, in the case of gold; N_2 and Ar, in the case of silver (no experiments were carried out with this metal in contact with CO, CO_2 or H_2O); and all these gases together with oxygen, but excepting carbonic oxide, in the case of nickel.

(iii) The gas is held more firmly than in (ii) in a condition approximating to unstable, loose chemical combination; for example, O_2 on gold, and O_2 or H_2 on silver. In these cases the respective gas charges can only be removed with difficulty, and the necessary time of evacuation increases with the time during which the surface was previously in contact with the gas.

---

* 'J. Am. Chem. Soc.,' vol. 45, p. 887 (1923).

† 'Trans. Faraday Soc.,' vol. 17, p. 607 (1922).

(iv) The gas is held in a still firmer manner than as outlined in (iii); the surface, however, continues to exhibit the charge characteristic of the gas in question even after prolonged evacuation. The one example of this type of combination so far revealed in the course of this investigation is that of carbonic oxide on nickel.

(v) The gas is bound chemically to the surface and the resulting stable chemical compound undergoes no dissociation at temperatures up to 850°. In this case the in vacuo charge on the oxidised surface is the same as the in vacuo charge characteristic of the reduced oxygen-free surface. The one example which we have so far been able to study is that of oxygen on nickel, where direct evidence was obtained, not only of compound formation (absorption of a large volume of oxygen by the hot surface, coupled with the change in appearance at the surface from a bright metallic lustre to a matt greenish-black), but also of the stability of the resulting nickel oxide at 850° Thus oxygen, when once it is firmly chemically combined with nickel, does not give rise to the charge otherwise characteristic of that gas.

From these facts we conclude that (*a*) only one of the two constituent atoms of an activated carbonic oxide molecule, probably the carbon atom, is directly attached to the surface, (*b*) this atom is held thereto with great tenacity; (*c*) that atom, probably oxygen, which is not in direct contact with the surface is mainly responsible for the carbonic oxide charge; (*d*) the formation of stable nickel oxide proceeds by stages through adsorption, followed by activation as in (ii) but not as in (iii), both oxygen atoms being finally attached directly to the surface.

The different types of adsorption outlined above, together with their respective salient characteristics, are tabulated below in Table II, in the fourth column of which examples of each type of adsorption are diagrammatically represented in the manner which, in our opinion, best takes into account the facts hitherto established.

Table II.

Type of adsorption.	Charge at 850°.	Time of evacuation required to remove charge at 850°.	Diagrammatic representations of typical examples.	Nature of adsorption.
(i)	None	—	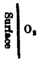	Electrically neutral physical attraction resulting in condensation of a layer of at least monomolecular thickness.
(ii)	Negative	30 to 60 minutes, independent of previous time of contact of gas with surface	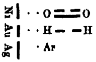	Electrical attraction, one bond between the atoms being weakened and one atom loosely held to the surface.
(iii)	Negative	Several hours, increasing with previous time of contact of gas with surface	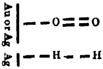	Electrical attraction, the bond or bonds between atoms being loosened, one atom being held more firmly to the surface than in (ii).
(iv)	Negative	Cannot be removed by evacuation	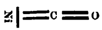	Electrical attraction, free valencies of the carbon atom linked with the surface.
(v)	None	—	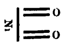	Atoms held separately and securely on surface, forming a definite and stable chemical compound.

Thus at least five stages can now be distinguished between the mere physical adsorption of a gas by a surface and definite stable chemical combination. Moreover, it would seem that in all cases of these in all probability (i) and (ii) always occur successively, and that thereafter may follow either (iii), (iv) or (v), according to the characters of the surface and the gas; and it is also probable that in any given case and circumstance a particular gas may be present in more than one stage of association with the surface.

The results obtained with mixtures of combining gases in their equivalent proportions and their resulting reaction products are in agreement with those recorded in Part I, and support the view therein put forward that charges due to the reaction products, which are similar to those due to the reacting mixtures, represent the average charging effect of the products of their dissociation.

No evidence has as yet been forthcoming as to the occlusion, *i.e.*, absorption, of gases by any of the surfaces hitherto examined. Steacie and Johnson*

---

* 'Roy. Soc. Proc.,' A, vol. 112, p. 542 (1926).

Chemical Equilibrium in the Vapour of a Mixture of Paraffins and Unsaturated Hydrocarbons.

By H. A. Wilson, F.R.S., Rice Institute, Houston, Texas.

(Received June 9, 1928.)

In a previous paper* on "Chemical Equilibrium in a Mixture of Paraffins" the composition of the mixture in equilibrium at any temperature and pressure was calculated on the assumption that only paraffins C_nH_{2n+2} were present. The condition for equilibrium among the members of any homologous series in the vapour was shown to be $p_n = p_1 f^{n-1}$, where p_n denotes the partial pressure of the nth member of the series and f is a quantity less than unity which is approximately independent of n.

In the present paper unsaturated hydrocarbons containing one or more double bonds as well as paraffins will be supposed present in the mixture. The homologous series to be considered are therefore the paraffins C_nH_{2n+2}, the olefines C_nH_{2n} with one double bond, the diolefines C_nH_{2n-2} with two double bonds, and other series C_nH_{2n-4}, C_nH_{2n-6}, C_nH_{2n-8}, . . ., containing 3, 4, 5, . . . double bonds.

Let p_n denote the partial pressure of the paraffin C_nH_{2n+2} so that $p_n = p_1 f^{n-1}$, and let p denote the sum of the partial pressures of all the paraffins so that $p = p_1 + p_2 + p_3 + \ldots = p_1/(1-f)$. In the same way let p_n' denote the partial pressure of the olefine C_nH_{2n} so that $p_n' = p_2' f'^{n-2}$, and let p' denote $p_2' + p_3' + p_4' + \ldots$ so that $p' = p_2'/(1-f')$. Also let p_n'' denote the partial pressure of C_nH_{2n-2}, p_n''' that of C_nH_{2n-4}, and so on. We have then $p'' = p_3''/(1-f'')$, $p''' = p_4'''/(1-f''')$ and similar equations for the other homologous series.

We may suppose the olefines formed by the hypothetical reaction $C_nH_{2n+2} = C_mH_{2m+2} + C_{n-m}H_{2(n-m)}$. The equilibrium constant K′ of this reaction is equal to $p'_{n-m}p_m/p_n$ or to $p_2' f^{n-m} f'^{n-m-2}$. We have

$$\log K' = H'/RT + \log T + C'$$

approximately where H′ is the heat of the reaction, R the gas constant, T the absolute temperature and C′ a constant. This is Planck's approximate equation for K′ obtained by supposing that the sum of the molecular heats is unchanged by the reaction.

---

* 'Roy. Soc. Proc.,' A, vol. 116, p. 501 (1927).

According to Thomsen's determinations of the heats of formation of hydrocarbons the heat of the reaction H′ is independent of n and m and equal to − 14,800 calories per mol. The constant C′ unfortunately is not known accurately but it can be roughly estimated. It is equal to $C_m + C'_{n-m} - C_n$ where C_n is the chemical constant for C_nH_{2n+2}, C_m that for C_mH_{2m+2}, and C'_{n-m} that for $C_{n-m}H_{2(n-m)}$. If we suppose the chemical constant for a hydrocarbon containing n carbon atoms equal to $a + bn$ where a and b are constants, then we have $C' = a$. The chemical constant for methane when the pressure is measured in atmospheres is equal to 5·7 and that for molecules containing about 3 carbon atoms is about 9, so that b is about $(9 - 5{\cdot}7)/2$, and therefore a is about 4. It cannot be much less than 4, and if it is taken to be much greater than 4 the results of the present theory do not agree with the facts, so we shall take it to be equal to 4. If this value of C′ is in error the general character of the influence of temperature and pressure on the proportion of unsaturated hydrocarbons in the vapour will not be affected but the numerical values deduced from the theory will require modification.

The equation for K′ with $R = 2$ and $C' = 4$ is

$$\log K' = -\,7400/T + \log T + 4.$$

According to this $K' = p_2' f^{m-n} f'^{n-m-2}$ is independent of n and m so that we must have $f = f'$ and $K' = p_2' f^{-2}$ or $p_2' = K'f^2$. The equilibrium total partial pressure p' of all the olefines is therefore given by

$$p' = p_2'/(1-f) = K'f^2/(1-f).$$

We may suppose the diolefines produced by the hypothetical reaction

$$C_nH_{2n+2} = C_mH_{2m+2} + C_lH_{2l+2} + C_{n-m-l}H_{2(n-m-l)-2}.$$

The equilibrium constant of this reaction is given by the equation

$$\log K'' = H''/2T + 2\log T + C''.$$

The heat of this reaction according to Thomsen's experiments is − 2 × 14800 calories and the constant C″ should be approximately double C′. Hence we have

$$\log K'' = -\,14800/T + 2\log T + 8,$$

so that

$$\log K'' = 2\log K' \qquad \text{and} \qquad K'' = K'^2.$$

Since K″ is independent of n, m and l we must have $f = f''$ so that

$$K'' = p_1 p_3'' f^{-4}.$$

Hence the total partial pressure of the diolefines is given by

$$p'' = p_3''/(1-f) = \mathrm{K}''f^4/p_1(1-f).$$

In the same way for the hydrocarbons C_nH_{2n-4} we obtain $\mathrm{K}''' = p_1^2\, p_4'''\, f^{-6}$, $\mathrm{K}''' = \mathrm{K}'^3$ and $p''' = p_4'''/(1-f) = \mathrm{K}'''f^6/p_1^2(1-f)$. Similar results follow for the series C_nH_{2n-6}, C_nH_{2n-8}, etc.

Now let P denote the total pressure so that $\mathrm{P} = p + p' + p'' + \ldots$. Substituting the values found we get

$$\mathrm{P} = p + \mathrm{K}'f^2/(1-f) + \mathrm{K}'^2f^4/p(1-f)^2 + \mathrm{K}'^3f^6/p^2(1-f)^3 + \ldots,$$

which gives

$$1/(\mathrm{P}-p) + 1/p = (1-f)/\mathrm{K}'f^2,$$

provided $\mathrm{K}'f^2/p(1-f)$ is less than unity.

Putting $y = (\mathrm{P}-p)/\mathrm{P}$ we get $y(1-y) = \mathrm{K}'f^2/\mathrm{P}(1-f)$, so that

$$y = \tfrac{1}{2} - \sqrt{\tfrac{1}{4} - \mathrm{K}'f^2/\mathrm{P}(1-f)}.$$

By means of this equation y or the fraction of the total pressure P due to unsaturated hydrocarbons in a state of equilibrium with liquid and vapour both present may be calculated. K′ is given by the equation

$$\log \mathrm{K}' = -\,7400/\mathrm{T} + \log \mathrm{T} + 4$$

and the values of the fraction f at any temperature and pressure may be obtained from the charts given in the previous paper (*loc. cit.*). The charts give the values of $x = 4 - 2f$.

The following table gives the calculated equilibrium percentages of the total pressure due to unsaturated hydrocarbons when liquid and vapour are both present at several temperatures and pressures.

Temperature.	15 atmospheres.	30 atmospheres.	60 atmospheres.
°F.	Per cent.	Per cent.	Per cent.
750	17	6	2
775	23	8	3
800	38	11	4
825	—	15	6
850	—	22	8
875	—	36	10

It appears that doubling the pressure should diminish the unsaturated compounds in the vapour to about one-third while raising the temperature 50° F. should about double them.

The maximum possible molecular percentage of unsaturated bodies in the vapour is 50 when $K'f^2/P(1-f)$ is equal to $\frac{1}{4}$. If $K'f^2/P(1-f)$ with the values of f taken from the chart is greater than $\frac{1}{4}$ then the equation for y cannot be satisfied so that no equilibrium with both liquid and vapour present is possible. In this case therefore decomposition will go on until only vapour remains. This is the case at 15 atmospheres and 825, 850 and 875° F.

It is well known that the amount of unsaturated compounds is diminished by increasing the pressure, but so far as the writer is aware no numerical data are available for comparison with the calculated values. It is also well known that when oil is heated at low pressures rapid decomposition goes on until only vapour and coke remain, and that this does not occur at higher pressures.

If the constant C' in the equation for $\log K'$ is taken to be greater than 4 then the calculated percentages of unsaturated compounds is increased, and the calculated temperatures at which equilibrium, with the liquid and vapour present, becomes impossible are lowered.

When oil is kept at temperatures near 800° F solid coke is deposited from it. The rate of coke formation increases rapidly as the temperature is raised. Coke may be regarded as a mixture of very highly unsaturated hydrocarbons. It always contains some hydrogen.

When three phases vapour, liquid and solid coke are present then, according to the phase rule, a system having two independent constituents has only one degree of freedom so that the equilibrium pressure is determined by the temperature. It follows that when oil is kept at constant temperature and pressure and coke is deposited exact equilibrium will not in general be reached while all the three phases remain. If the rate of coke formation is small, which is usually the case in practice, the liquid and vapour will soon reach very approximate equilibrium with compositions determined approximately by the temperature and pressure in accordance with the theory given above and in the preceding paper. As the amount of coke increases the amount of liquid present will decrease and eventually only coke and vapour will remain, and then complete equilibrium will be possible at the given temperature and pressure.

Since the equilibrium amount of unsaturated bodies is decreased either by raising the pressure or lowering the temperature, and since coke may be regarded as a highly unsaturated body, we should expect the rate of coke formation to be diminished either by raising the pressure or lowering the temperature.

If oil is kept at a constant temperature in a closed vessel of constant volume, then if the temperature is high enough for coke to form we should expect decomposition to go on with increasing pressure until the pressure reaches the equilibrium value which may not happen until only coke and vapour remain. During this process, provided the rate of coke formation is not too great, the compositions of the liquid and vapour should be approximately determined by the temperature and pressure in accordance with the theory given above.

Observations of the Height of the Ozone in the Upper Atmosphere.

By F. W. P. Götz, Dr phil. nat. (Lichtklimatisches Observatorium, Arosa), and G. M. B. Dobson, D.Sc., F.R.S.

(Received June 13, 1928.)

It has been shown that there is a close connection between the amount of ozone in the upper atmosphere and the pressure conditions in the upper part of the troposphere and the lower part of the stratosphere.* MM. Cabannes and Dufay,† and also MM. Lambert, Déjardin and Chalonge‡ have measured the height of this ozone and found that it is about 40 to 50 kms. above the earth's surface It is remarkable that the ozone situated at so great a height should be so closely connected with variations of pressure much lower down, and as the observations of the height of ozone which have been published up to the present have been confined to a relatively small number of days, it seemed desirable to make further measurements.

As the amount of ozone in the atmosphere varies both with the season of the year§ and also with the pressure distribution in the lower layers, it is important to see whether the height of the ozone shows variations of any similar nature.

Some 50 fairly satisfactory measurements of the height have now been made at Arosa, and though the conclusions must still be regarded as provisional, yet their importance with regard to theories of the cause of the variations of the amount of ozone makes it desirable to publish them without waiting a further year or so which must elapse before more certain conclusions can be drawn.

* 'Roy. Soc. Proc.,' A, vol. 114, p. 521 (1927).

† 'J. de Physique,' vol. 8, p. 125 (1927).

‡ 'C. R.,' vol. 183, p. 800 (1926).

§ Götz, 'Beiträge z. Physik d. fr. Atmosphäre,' vol. 13, p. 15 (1926).

The principle of the method of obtaining the height of the ozone is the same as that used by the former observers, and is as follows: Measurements are made by spectrographic means of the amount of ozone through which the sunlight has passed before reaching the earth's surface. Dividing this thickness by the secant of the sun's zenith distance (sec Z), we obtain the equivalent vertical thickness of the ozone layer. So long as the sun is high, its zenith distance as seen from the ozone layer will be the same whatever the height of that layer, but when the sun is low the point where the sun's ray strikes the ozone layer will be at a great distance from the observer and the curvature of the earth will cause the sun's zenith distance at the ozone layer to be less than that at the observer, and the difference will increase as the sun approaches the horizon. Thus the thickness of the ozone layer deduced from the zenith distance as measured by the observer will be too small when the sun is low. In a similar way, if a value of the zenith distance is used which corresponds to a height greater than that of the ozone layer, the calculated amount of ozone will be too great when the sun is low. Hence, if the ozone really remains constant during the observations, we can find a height such that the corresponding values of the zenith distance will lead to a constant ozone value, and this height will, in fact, be the true average height of the ozone.

In practice five curves are drawn showing the changes in the amount of ozone through each day, calculated on the assumptions that the ozone is at heights of 0, 30, 40, 50 and 60 kms. respectively. The curve which indicates the most constant ozone value through the day is taken as being based on the correct assumption for the height of the ozone. Two typical sets of curves are given in fig. 1 and fig 2, showing both a satisfactory determination of the height and also a day when real changes in the amount of ozone made the results indefinite.

It is important to realise that in all these measurements it is presupposed that there is no regular diurnal change in the amount of ozone, and if there is such a change, the heights found will be wrong. The fact that the heights obtained when the sun is rising agree with those found when it is setting is some evidence that there is no great error from this cause. On the other hand, the recent paper of M. Chalonge,* giving an account of preliminary measurements of the ozone at night, indicates that the amount of ozone may be greater by night than by day. To get further information on this point, the mean ozone value at Arosa when the sun is about 12° above the horizon in the morning was compared with the corresponding value in the evening. It appears

---

* 'C. R.,' February, 1928.

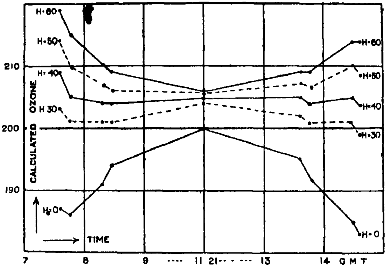

FIG 1.—Date, December 30, 1927.

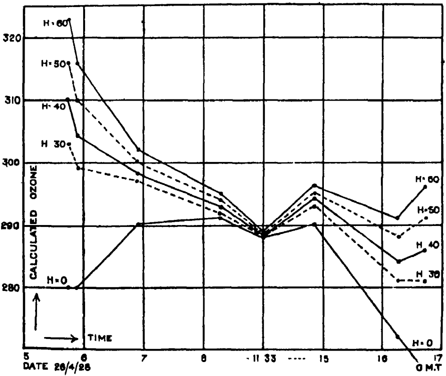

FIG. 2.—Date, April 26, 1928.

that there is a very small difference of 0·001 cm. between the average values in the two cases, the evening value being the smaller. This difference is too small to be relied upon, but as it appears in each of three groups into which the days were divided it may be real, and the change is in the same sense as that indicated by M. Chalonge.

The light-gathering power of the spectrograph employed was not large and the wave-lengths used for deducing the amount of ozone were well within the ozone absorption band, so that there was not enough light to take photographs when the sun was less than about 12° above the horizon. This seriously limited the possible accuracy of the measurements, and the best observations may have an error of at least 5 kms., but the mean of a number of observations should be reliable, though the apparent changes from day to day are obviously due to errors.

Again, a small change in the constant of the spectrograph* giving the ratio of the intensity of the two wave-lengths used, which would be obtained if the instrument could be taken right outside the atmosphere, makes a considerable difference to the height deduced. This constant is very difficult to determine accurately, and there may be a small error of 5 kms. or so which will be constant throughout all the observations, making the heights too great or too small. Thus it is possible that the difference in the average height given here and that found by the French observers may be due to this cause.

In deducing the height of the ozone there are two different lines on which we may proceed. Either we may take a few observations near sunrise or sunset, when the magnitude of the correction to sec Z due to the effect of the curvature of the earth and the height of the ozone is changing rapidly, and find a height for the ozone layer which should make the ozone values so obtained as uniform as possible; or, on the other hand, we may take all the values obtained through the day and find a height for the ozone layer which shall make the average of the values obtained in the middle of the day agree as well as possible with those near sunrise or sunset. In the first case we shall be but slightly troubled by errors due to slow progressive changes in the amount of ozone, but small erratic changes in the amount of ozone from minute to minute and errors of observation will produce a large effect. We have found that on many days the average ozone value remains very constant throughout the whole day, but there are often small irregular changes from minute to minute of the order of 0·005 cm. of ozone. Thus it seemed that the second method might probably be the best on the whole. This was confirmed by estimating the height on a number of days by both methods, when it was found that while the average height for the group of days was the same which ever method was used, the variability from day to day was twice as great with the first method as with the second. Consequently, we have adopted the second method of estimating the heights.

---

* For full details of the method of measuring the amount of ozone, see 'Roy. Soc. Proc.,' A, vol. 110, p. 660 (1926).

The error due to personal differences in estimating the heights from the curves is very small, as shown by the fact that two people independently arrived at closely similar results. By far the greatest error is, of course, that due to real changes in the amount of ozone during the observations.

When exposures of several minutes have to be made at times when the value of sec Z is changing rapidly, the mean value of sec Z cannot strictly be used, since the light is weaker during the half of the exposure when the sun is lower. The effect of this has been calculated and, where necessary, it has been allowed for, but as the difference of sec Z at the beginning and end of an exposure is not generally greater than 0·3, this is seldom necessary. The effect of refraction has also been calculated, but it is negligible for this work.

The measurements give the mean height of the ozone and afford no evidence of the height of its upper and lower limits.

Results of Observations.

The following table gives the results of all observations which were not spoilt by large changes in the amount of ozone during the time that the observations were being made. The last column is added to give an idea of the reliability of each value, the poorer values generally being due to changes in the actual amount of ozone, except in midwinter when the range of sec Z which is available is very small.

Fig. 3 shows the estimated heights of the ozone layer plotted against the time of year. There seems to be evidence of an increase in the height of the ozone between autumn and spring, which would correspond to the increase in the average amount of ozone during this time. Whether this indicates a real seasonal variation in the height of the ozone cannot be settled until at least a full year's observations have been made.

In order to see whether there were any variations in the height of the ozone corresponding to the variations associated with cyclones and anti-cyclones, the estimated heights have been plotted against the amount of ozone in fig. 4, but to avoid effects of a possible annual variation, the amount of ozone is shown as the difference from its monthly mean value. Here again further observations are needed, but there is a strong indication that the height is greater when the amount of ozone is greater. (If the height be plotted against surface pressure no connection is apparent, but it must be remembered that the

Table I

Date	Estimated height.	Ozone value	Surface pressure	Character of height estimate	Date	Estimated height	Ozone value.	Surface pressure	Character of height estimate
1927.	kms.	cms. × 10⁻³.	mm. Hg.		1928	kms	cms × 10⁻³.	mm Hg	
Aug 29 p m	32	235	616·7	Poor	Jan 1 a m p.m.	32	279	610·8	Poor
Sept. 13 p.m	40	268	612·2	Good	,, 2 a m p.m.	34	264	609·8	Poor
,, 14 p.m.	37	262	611·3	Fair	,, 3 a.m. p.m	32	239	606·1	Poor.
,, 15 a.m.	30	256	610·3	Good.	,, 10 p.m	22	244	610·2	Poor.
,, 21 p.m.	47	236	613·9	Fair	,, 11 a m p m.	23	249	608·9	Poor
Oct. 2 p.m.	34	225	—	Poor.	,, 12 p m.	52	283	610·0	Poor.
,, 7 a.m.	31	258	613·2	Poor.	,, 26 a.m p.m	32	251	614·4	Poor.
,, 8 p m.	41	238	612·7	Fair	Feb 5 p.m	41	268	613·7	Poor.
,, 9 a.m. p.m.	30	235	616·0	Good.	,, 8 a.m. p.m.	24	261	620·4	Fair.
,, 10 a m. p.m.	42	218	615·8	Good	,, 16 a m p m	32	234	613·7	Good
,, 13 p.m.	41	217	610·5	Poor.	,, 21 a m. p m.	40	263	615·3	Poor.
,, 14 p.m	35	217	607·5	Good.	,, 22 a.m. p m	35	258	614·9	Poor.
,, 19 a m.	22	223	607·1	Poor.	,, 24 a.m. p.m	29	256	612·2	Poor.
,, 20 p m.	27	227	610·3	Poor.	,, 25 p m.	27	263	615·8	Fair.
,, 25 a m. p.m.	22	224	614·9	Fair.	Mar. 18 a.m p m	52	280	611·3	Fair.
,, 28 a m p.m.	30	214	615·5	Fair	,, 20 p.m	44	293	605·0	Poor.

Oct. 30 a.m. p.m.	42	203	614·9	Good.	April 9 a.m.	32	276	609·5	Fair.
„ 31 a.m. p.m.	32	200	612·6	Poor	„ 20 p.m.	47	315	603·9	Fair.
Nov. 3 p.m	42	186	619·4	Good	„ 25 a.m.	32	307	611·9	Fair.
„ 4 a.m p.m.	31	190	616·2	Fair	„ 29 p.m	32	304	603·7	Poor
„ 6 a.m.	12	215	602·5	Poor	May 2 a.m	52	275	605·0	Poor.
„ 15 a.m. p.m.	32	267	608·7	Fair	„ 7 a m	49	304	600·8	Fair.
Dec. 2 a.m p.m.	27	246	610·5	Good.	„ 11 a m.	62	342	605·7	Poor.
„ 8 a.m. p.m	42	263	603·6	Fair.					
„ 11 a.m. p m.	32	232	605·0	Poor.					
„ 14 a m p m.	21	219	600·7	Poor.					
„ 19 p.m.	52	266	603·0	Poor.					
„ 25 a m. p.m.	42	259	597·5	Poor.					
„ 30 a.m. p.m.	30	269	604·6	Poor					
„ 31 p.m.	32	270	608·3	Poor.					

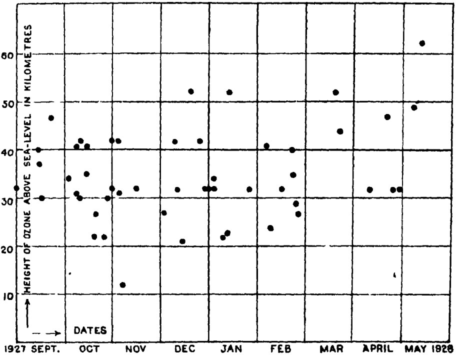

Fig. 3.—Estimated Ozone Height.

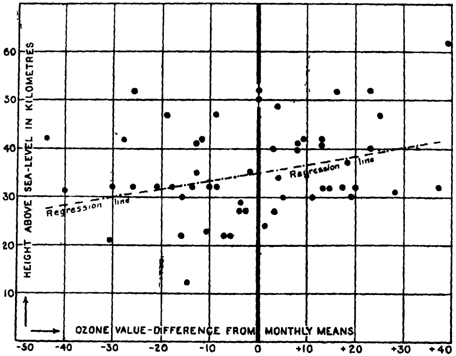

Fig. 4.—Estimated Ozone Height and Ozone Value (Difference for Monthly Means.)

correlation between the ozone value and absolute *surface* pressure is but small, as may be seen by plotting the values in Table I.)

The importance of the conclusion indicated by fig. 4 is that the increase in the amount of ozone associated with cyclones must occur in the upper part of the ozone layer rather than in the lower part This rules out all such hypotheses as, that the ozone is dragged downwards by descending currents in cyclonic regions, thus increasing the thickness of the layer. It is, of course, possible that in regions where the amount of ozone is highest, the height of the layer may also be greatest, and that changes both in the amount and average height are due to bodily movement of large masses of air.

In this work we are very much indebted to Mr. R. W M. Gibbs, who has measured nearly all the spectra from which the height of the ozone is estimated, which measurement is most laborious. The instruments used were those employed in the previous work, and their cost was met by a grant from the Royal Society, for which we again record our thanks Finally, we are indebted to the Department of Scientific and Industrial Research for a grant for assistance in the necessarily heavy work of measuring spectra and computing the ozone values.

Summary.

Measurements have been made of the height of the ozone layer in the upper atmosphere over Arosa (Switzerland). It appears that the height is greatest when the amount of ozone is large, and least when the amount is small. There is also evidence of an increase of height from autumn to spring. Further measurements are necessary to confirm these conclusions. The average height seems to be between 30 and 40 kms. above sea-level.

The Forces on a Body placed in a Curved or Converging Stream of Fluid.

By G. I. TAYLOR, F.R.S.

(Received June 14, 1928.)

Introduction.

The force which a body experiences when placed in a converging stream of fluid has a certain practical interest in aeronautics because the flow in the centre of a parallel-walled wind tunnel is of this type. The convergence is due to the retardation of a layer of air close to the walls. This retarded layer increases in thickness as the air passes down the channel, thus causing a corresponding increase in the velocity in the central part of the channel. This increase in velocity is associated with a decrease in pressure in accordance with Bernoulli's equation, the pressure in a Pitot tube being very nearly constant down the channel at all points outside the retarded layer.

In measuring the resistance of models of airships it has been customary to correct the observed readings by subtracting what is called the "horizontal buoyancy," *i. e.*, the force which would act on the body if the air were a stationary fluid in which the existing pressure gradient down the channel was maintained by some external force like gravity. Expressed mathematically, if dp/dx is the pressure gradient, *i.e.*, the gradient of static pressure in the channel, and V the volume of the body, the "horizontal buoyancy" is $-V\dfrac{dp}{dx}$. This correction to the measured resistance of an airship model is believed to be approximately correct from the point of view of wind tunnel practice, and the primary object of the present work was to find out how far it is justified from the point of view of hydrodynamical theory.

Previous Work.

An extremely simple treatment has already been given by Max M. Munk,* but this is limited to a very special class of body, namely, the body which can be represented as regards its external flow by a simple source and an equal sink placed at a finite distance apart. When the distance apart is large so that the flow due to the source at the position of the sink is small compared with the general flow of the fluid, the body consists of two rounded ends connected by a middle body which is parallel to the stream lines of the converging or diverging stream, *i.e.*, the body is a long truncated cone, rounded off at the ends. For such a body the force acting in a converging stream of a perfect fluid is actually equal to the "horizontal buoyancy," $-\mathrm{V}\frac{dp}{dx}$.

---

* 'Some New Aerodynamical Relations,' Report No. 114, National Advisory Committee for Aeronautics. Washington, 1921.

In the other limiting case, when the source and sink are infinitely close together, Munk pointed out that the force is $-\frac{3}{2}\mathrm{V}\frac{dp}{dx}$, the body being in this case approximately a sphere; and he deduced that for bodies of intermediate length the factor by which the "horizontal buoyancy" must be multiplied in order to find the force acting on such a body when placed in a converging stream is intermediate between 1·0 and 1·5. Munk indicates that the force acting on bodies derived from any known distributions of sources and sinks could also be treated in the same way

The forces acting on a small sphere in a stream circulating in a multiply-connected space has been studied by Lord Kelvin.* The limitation imposed by the supposition that the space is multiply-connected does not affect the result, however, because the force acting on the sphere must depend only on the direction, curvature and convergence of the stream in the neighbourhood of the sphere. Though he does not express it in this way, Kelvin's result may be reduced to the simple statement that the resultant force on the sphere is in the direction of the pressure gradient in the fluid, irrespective of the direction of flow, and it is equal to the pressure gradient multiplied by 1·5 times the volume of the sphere. This result may be regarded as a generalisation of Munk's result for a sphere in a straight converging flow, to the case when the flow is also curved.

Scope of the Present Work and Results.

In the present work these results are extended to bodies of any shape placed in a curved and converging or diverging stream, or even in a stream which converges in one place and diverges in a plane at right angles to it. In the case of a straight converging stream the actual value of the factor by which the "horizontal buoyancy" must be multiplied is calculated and shown to be equal to $1+\alpha$, where $\alpha\rho\mathrm{V}$ is the virtual addition to the mass of the body which must be added to its own mass to account for its resistance to accelerated motion in the direction of the stream lines and ρV is the mass of fluid displayed by the body. This is true whether the convergence is symmetrical in all planes through the direction of the flow or not. It will be recognised at once that Munk's and Kelvin's expressions for a sphere are particular cases of this general result.

---

* "On the Motion of Rigid Solids in a Liquid circulating irrotationally through perforations in them or a Fixed Solid," 'Phil. Mag.' (1873).

This result is extended to find the direction and magnitude of the force which acts on a small body of any shape placed in a curved or converging stream. It is found that Kelvin's result for a sphere (that the resultant force acts in the direction of the pressure gradient) is true for bodies of any shape provided that the body is placed so that one of its possible "directions of permanent translation" is parallel to the direction of the stream so that no couples act on it. When the body is placed in any other position, however, Kelvin's result for a sphere is no longer applicable. It is curious that Kelvin first published his result as a general one applicable to bodies of any shape, but on revising his paper later he recognised that his analysis applied only to the case of a sphere.

In general, a body placed in a straight uniform stream of fluid experiences couples about axes at right angles to the stream. The additional couples due to a small amount of convergence or curvature of the stream were calculated. These, however, appear of little interest because in a real fluid the observed couples usually differ very widely from those calculated. On the other hand, even in a real fluid there is a very large class of bodies which experience no couple about an axis parallel to the direction of the stream. Accordingly, the couples about the direction of the flow in a curved and converging stream were calculated and the results tested experimentally. The analysis shows that certain types of asymmetry in the stream react on certain types of asymmetry in the body and cause it to rotate about the stream direction into some definite orientation. Thus, if a body with the type of asymmetry possessed by a rod bent into a circular arc is suspended at its centre of gravity in a curved stream so that it can rotate about the direction of the stream which is parallel to the chord of the arc, it will take up a position so that the plane of the arc coincides with the plane containing the curved stream lines; but the direction of curvature of the arc is opposite to that of the stream lines. This was verified experimentally.

A body with the type of asymmetry possessed by a tetrahedron about the line joining the centres of opposite edges reacts with a stream in which the centre stream line is straight but the convergence is asymmetrical, being greatest in one plane through the direction of the stream and least in the plane at right angles to it. Such a stream was created by sucking air by means of a vacuum cleaner through a vertical channel two walls of which were parallel glass plates, the remaining two walls being made of bent metal sheet so that the stream first converged and then afterwards diverged. Bodies with the required type of symmetry were hung in this stream by fine silk threads, and it was found that in every case they set themselves in the positions indicated by theory. They rotated through 90° on being lowered through the point of maximum constriction from the converging to the diverging part of the channel. This also was predicted by theory.

Components of Force on a Body in a Curved and Converging Stream.

The kinetic energy of a system consisting of a fluid circulating in a cyclic space and containing a small sphere moving with velocity components $\dot{x}$, $\dot{y}$, $\dot{z}$ has been given by Lord Kelvin in the form

$$2\mathrm{T} = (\mathrm{M} + \tfrac{1}{2}\rho\mathrm{V})(\dot{x}^2 + \dot{y}^2 + \dot{z}^2) + 2\mathrm{K}, \tag{1}$$

where K is the energy of the cyclic motion when the sphere is held at rest, M is the mass of the sphere and V its volume. If x, y, z are the co-ordinates of the centre of the sphere, K may be regarded as a function of x, y, z.

The simplest method for finding K is to use an artifice due, I think, to Dr. Horace Lamb. If M is made equal to the mass of the fluid displaced and if the sphere is made to move with the fluid in its neighbourhood, then the energy T is the same as what it would be if the sphere were absent, the space being occupied by fluid. This assumption implies that the sphere is so small that the changes in the velocity of the undisturbed stream in a distance equal to the diameter of the sphere is small compared with the velocity of the stream Using this assumption, then

$$2\mathrm{K} = \text{constant} - \tfrac{3}{2}\rho\mathrm{V}(u^2 + v^2 + w^2), \tag{2}$$

where u, v, w are the components of velocity in the stream before the introduction of the sphere, at the point afterwards occupied by its centre.

To find the motion Kelvin used some general dynamical equations, proving that certain coefficients vanish in the case of a sphere. It is not necessary, however, to use these equations to find the force which acts on the body when held at rest in the circulating fluid. If the body be displaced slowly through a short distance whose components are δx, δy, δz, the change in K must be

$$-(\mathrm{X}\delta x + \mathrm{Y}\delta y + \mathrm{Z}\delta z),$$

where X, Y, Z are the components of force acting on the body.

Hence

$$X = -\frac{\partial K}{\partial x} = \frac{3}{4}\rho V\frac{\partial}{\partial x}(u^2+v^2+w^2)$$

If p is the pressure in the undisturbed motion i e before the introduction of the sphere $p+\frac{1}{2}\rho(u^2+v^2+w^2)$ is constant since the motion is a steady one so that

$$X = -\frac{3}{2}V\frac{\partial p}{\partial x}$$

and similarly

$$Y = -\frac{3}{2}V\frac{\partial p}{\partial y} \qquad Z = -\frac{3}{2}V\frac{\partial p}{\partial z} \tag{3}$$

In this example the fluid is circulating in a cyclic region but the force on the sphere must depend only on the convergence and curvature of the undisturbed stream lines in its vicinity so that the formula (3) is general for any type of undisturbed flow provided that the changes in velocity in a length equal to the diameter of the sphere are small compared with the velocity of the stream

To apply this method to bodies of any shape one may write T_0 for the energy in the fluid surrounding a body when it moves without rotation in a fluid at rest at infinity If u v w are the components of its velocity*

$$2T_0/\rho = Au^2+Bv^2+Cw^2+2A'vw+2B'wu+2C'uv \tag{4}$$

where A B C A' B' C' are six constants which depend only on the shape of the body They are determined relative to some axes fixed in the body Equation (2) then takes the form

$$2K/\rho = \text{constant} - V(u^2+v^2+w^2) - 2T_0/\rho \tag{5}$$

As in the case of the sphere

$$X = -\frac{\partial K}{\partial x} \qquad Y = -\frac{\partial K}{\partial y} \qquad Z = -\frac{\partial K}{\partial z}$$

so that

$$\left.\begin{aligned} X &= \frac{1}{2}\rho V\frac{\partial}{\partial x}(u^2+v^2+w^2)+\frac{\partial T_0}{\partial u}\frac{\partial u}{\partial x}+\frac{\partial T_0}{\partial v}\frac{\partial v}{\partial x}+\frac{\partial T_0}{\partial w}\frac{\partial w}{\partial x}\\ Y &= \frac{1}{2}\rho V\frac{\partial}{\partial y}(u^2+v^2+w^2)+\frac{\partial T_0}{\partial u}\frac{\partial u}{\partial y}+\frac{\partial T_0}{\partial v}\frac{\partial v}{\partial y}+\frac{\partial T_0}{\partial w}\frac{\partial w}{\partial y}\\ Z &= \frac{1}{2}\rho V\frac{\partial}{\partial z}(u^2+v^2+w^2)+\frac{\partial T_0}{\partial u}\frac{\partial u}{\partial z}+\frac{\partial T_0}{\partial v}\frac{\partial v}{\partial z}+\frac{\partial T_0}{\partial w}\frac{\partial w}{\partial z} \end{aligned}\right\} \tag{6}$$

---

* See Lamb's 'Hydrodynamics' 4th edn p 155

These expressions may be simplified by taking the axis of x parallel to the stream at the point considered. In that case $v = w = 0$, and

$$\frac{\partial T_0}{\partial u} = Au, \quad \frac{\partial T_0}{\partial v} = C'u, \quad \frac{\partial T_0}{\partial w} = B'u.$$

Also some of the partial differentials $u\frac{\partial u}{\partial x}$, $u\frac{\partial v}{\partial x}$, etc., are proportional to the components of the pressure gradient, thus with this choice of axes

$$\rho u \frac{\partial u}{\partial x} = -\frac{\partial p}{\partial x}, \quad \rho u \frac{\partial u}{\partial y} = \rho u \frac{\partial v}{\partial x} = -\frac{\partial p}{\partial y}, \quad \rho u \frac{\partial u}{\partial z} = \rho u \frac{\partial w}{\partial x} = -\frac{\partial p}{\partial z},$$

so that

$$\left.\begin{aligned} X &= -(V + A)\frac{\partial p}{\partial x} - C'\frac{\partial p}{\partial y} - B'\frac{\partial p}{\partial z} \\ Y &= -(V + A)\frac{\partial p}{\partial y} + \rho C'u\frac{\partial v}{\partial y} + \rho B'u\frac{\partial w}{\partial y} \\ Z &= -(V + A)\frac{\partial p}{\partial z} + \rho C'u\frac{\partial v}{\partial z} + \rho B'u\frac{\partial w}{\partial z} \end{aligned}\right\}. \qquad (7)$$

From these equations it will be seen that in the particular case when $B' = C' = 0$, *i.e.*, when the body has one of its axes of permanent translation parallel to the direction of flow so that it would experience no couples in a uniform stream, the resultant force is in the direction of the pressure gradient and equal to $(V + A) \times$ (maximum pressure gradient).

An ellipsoid, for instance, placed with one of its principal axes in the direction of the stream would experience a force acting in the direction of the pressure gradient in the undisturbed stream. The magnitude of this force would differ according to which axis was parallel to the stream; thus, if the long axis were parallel to the stream the force would be smaller than if a shorter axis were in that direction. In general, however, when the direction of the stream is not parallel to one of the axes of permanent translation, the force acting on the body is not in the direction of the pressure gradient.

The particular case of a converging flow with a straight central stream line is of special interest because, as has already been pointed out, it is the condition which may be expected in the middle of a parallel-sided wind tunnel. In this case $\frac{\partial p}{\partial y} = \frac{\partial p}{\partial z} = 0$, so that $X = -(V + A)\frac{\partial p}{\partial x}$ and no restriction is placed on the shape of the body. This is the generalised form of the expression obtained by Munk for a sphere and a certain class of elongated bodies of revolution. The "virtual mass" of a body in accelerated motion through a fluid is $A\rho$. This is sometimes expressed in the form $\alpha V\rho$, where $\alpha = A/V$ so that $X = -(1+\alpha)\,V\,\frac{\partial p}{\partial x}$. $(1+\alpha)$ is the factor by which the "horizontal buoyancy" should be multiplied in order to find the effect of convergence on the resistance of an airship model hung in a horizontal wind tunnel.

In order to estimate the value of $(1+\alpha)$ in the case of a body whose shape approximates to that of an airship, it seems useful to give the value of $(1+\alpha)$ for a prolate spheroid of eccentricity e moving parallel to its long axis.

In that case*

$$(1+\alpha)^{-1} = \frac{1}{e^2} - \frac{1-e^2}{2e^3}\log\frac{1+e}{1-e}. \tag{8}$$

It is customary in aerodynamical work to use the expression "fineness ratio" to indicate the ratio of the length to maximum diameter of an airship shape. The fineness ratio, β, for a spheroid is $(1-e^2)^{-\frac{1}{2}}$. From these formulæ the following Table I was calculated :—

Table I.

β.	$1+\alpha$.	β.	$1+\alpha$.
1·00	1·50	3·64	1·093
1·34	1·35	5·08	1·057
1·81	1·24	7·12	1·035
2·5	1·16		

It will be seen that for this series of shapes the factor by which the "horizontal buoyancy" must be multiplied decreases from 1·5 for the sphere ($\beta = 1{\cdot}00$) to 1·057 for a body five times as long as its maximum diameter.

In a recent paper† I have given a simple method by which the "virtual mass" of any airship shape derived from a system of sources and sinks may be found. Suppose that a system of sources and sinks m_1U, m_2U, ... m_rU, ..., placed at points (x_1, y_1, z_1), (x_2, y_2, z_2) ..., in a stream of fluid flowing with uniform velocity $-U$ parallel to the axis of x has been found to represent the flow round a body of volume V. The "virtual mass" of this body in accelerated motion was shown to be[*]

---

* This expression was first calculated by integrating the pressure over a spheroid due to the flow from a source placed on the axis. It was only after finishing the calculation that it was found that (8) gives also the expression for the "virtual mass."

† "The Energy of a Body moving in an Infinite Fluid, with an Application to Airships," 'Roy. Soc. Proc.,' *supra*, p. 13.

$$\rho \mathrm{A} = \rho \Sigma m_r x_r - \rho \mathrm{V}. \tag{9}$$

When placed in a converging stream this body experiences a force

$$\mathrm{X} = -\rho(\mathrm{A}+\mathrm{V})\frac{\partial p}{\partial x}.$$

Hence from (9)

$$\mathrm{X} = -(\Sigma m_r x_r)\frac{\partial p}{\partial x}. \tag{9A}$$

This is equivalent to Munk's formula. It can only be applied when the requisite distribution of sources and sinks is known.

Verification of Equation (7) *in a Simple Case.*

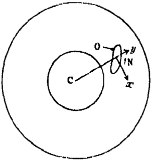

FIG. 1.

It is of interest to notice why the terms in C′ and B′ must come into the expressions for the forces. Consider, for example, the case of a body, O, placed between two concentric circular cylinders (see fig. 1) with liquid circulating between them. Let u be the velocity of the fluid at the radius r where the body is situated.

Now consider a displacement in which the body rotates through an angle $\delta\theta$ about the axis C of the cylinders. Since there is no change in the circulation round the inner cylinder, such a displacement does not alter the energy of the system. If there is a couple N acting on the body owing to its being placed so that the direction of the stream is not one of its axes of permanent translation, then there must also be a force X in the direction of motion so that the work done during the displacement is zero. Hence

$$\mathrm{X}r\,\delta\theta - \mathrm{N}\,\delta\theta = 0 \qquad \text{or} \qquad \mathrm{X} = \mathrm{N}/r. \tag{10}$$

Now the couple on a body moving parallel to the axis of x, which may be taken in the direction of flow as shown in fig. 1, is[†]

$$\mathrm{N}/\rho = v\frac{\partial \mathrm{T}_0}{\partial u} - u\frac{\partial \mathrm{T}_0}{\partial v} = -\mathrm{C}'u^2. \tag{11}$$

---

[*] *Loc. cit.*, equation (21). There given as $\rho \mathrm{A} = \rho\int_{x_1}^{x_2} mx\,dx - \rho \mathrm{V}$, which is the form of (9) above, suitable for a continuous distribution of sources along a line.

[†] Lamb, 'Hydrodynamics,' 4th edn., p. 159.

Hence from (10) and (11)

$$X = -\rho C' u^2/r.$$

But

$$\frac{\partial p}{\partial r} = \rho u^2/r.$$

Hence

$$X = -C' \frac{\partial p}{\partial r} = -C' \frac{\partial p}{\partial y}. \tag{12}$$

Comparing (12) with (7) it will be seen that for the particular case when

$$\frac{\partial p}{\partial x} = \frac{\partial p}{\partial z} = 0,$$

the first of formulæ (7) is verified by this very simple argument.

As regards the practical application of equations (7) it will be seen that convergence in a stream of fluid produces an effect on lift as well as on drag. Thus, for a wind tunnel for which $\frac{\partial p}{\partial y} = \frac{\partial p}{\partial z} = 0$, the convergence produces an effect on lift, Y, equal to $+\rho C' u \frac{\partial v}{\partial y}$. In the case where the convergence is the same in all axial planes, as in a wind tunnel of square or circular section, $\frac{\partial v}{\partial y} = -\frac{1}{2}\frac{\partial u}{\partial x}$, so that the effect on lift is

$$+\tfrac{1}{2}C' \frac{\partial p}{\partial x}. \tag{13}$$

It appears, therefore, that the effect of convergence on lift may be of the same order of magnitude as that on drag.

Determination of Forces and Couples by Integration of Pressures over the Surface of the Body.

The formulæ (7) were not originally obtained by the simple process described in the first part of this paper. They were first derived by laborious integration of pressures over the surface of the body, a process made possible by Green's theorem, which enabled the integrations to be transformed into integrations over a spherical surface.

For finding the couples acting on the body, equation (5) giving K in terms of *u*, *v*, *w* is of no value. It is true that couples about axes perpendicular to the direction of the stream could be derived from (5), but these would only be the couples which would act on the body in a uniform stream. This can be illustrated by reversing the argument in the example given in the preceding section. To determine the changes in these couples owing to convergence, or the couple acting about the direction of the stream, it would be necessary to determine K to a higher order of approximation than can be done by Dr. Lamb's artifice. It is clear, for instance, that rotation of the body about the direction of the stream makes no change in (5), for T_0 is unaltered by such a rotation, so that as far as (5) goes one might conclude that the couple is zero.

To find the couples, therefore, I found it necessary to revert to my original method and to expand both the disturbed and the undisturbed stream in a series of spherical harmonics.

Representation of the Undisturbed Stream.

The velocity potential of a uniform stream of fluid is represented by a spherical harmonic function of the first degree. In general three terms are necessary to determine the three components of velocity, but we shall simplify the formulæ by taking the direction of the stream at the origin as the line $\theta = 0$ when we use spherical polar co-ordinates, or the axis of x when we use Cartesian co-ordinates.

Convergence or curvature in the stream lines near the origin may be represented, to the degree of approximation required, by spherical harmonics of the second degree. The general expression for the velocity potential of a curved and converging stream may, therefore, be written in the form

$$\phi_0 = r\mathrm{S}_1 + r^2\mathrm{S}_2, \tag{14}$$

where S_1 and S_2 are surface harmonics of the first and second degrees. When the velocity at the origin is parallel to $\theta = 0$ and equal to U,

$$\mathrm{S}_1 = -\mathrm{U}\cos\theta, \tag{15}$$

the most general form of S_2 is

$$\mathrm{S}_2 = \mathrm{G}\left(\tfrac{3}{2}\cos^2\theta - \tfrac{1}{2}\right) + (\mathrm{H}\cos\omega + \mathrm{J}\sin\omega)\cos\theta\sin\theta + (\mathrm{E}\cos 2\omega + \mathrm{F}\sin 2\omega)\sin^2\theta, \tag{16}$$

when ω is the angular co-ordinate of an axial plane so that

$$\left.\begin{aligned} x &= r\cos\theta \\ y &= r\sin\theta\cos\omega \\ z &= r\sin\theta\sin\omega \end{aligned}\right\}. \tag{17}$$

If G is positive the flow is diverging; if G is negative it is converging. If $\mathrm{H} = \mathrm{J} = 0$ the stream line through the origin is straight. If $\mathrm{H} = \mathrm{J} = \mathrm{E} = \mathrm{F} = 0$ the flow is symmetrical about the axis of x. If

$H = J = F = 0$ the stream is symmetrical about the planes $y = 0$, $z = 0$, and if, in addition, $G = 2E$ the motion is two-dimensional, the stream lines being parallel to the plane $y = 0$.

If $G = E = F = 0$ the stream lines are curved but do not converge in any axial plane and the direction of maximum pressure gradient is at right angles to the stream lines. If, in addition, $J = 0$ the stream lines lie in the plane $z = 0$, and if H is then positive the centre of curvature of the central stream line is in the direction $\theta = \frac{1}{2}\pi$, $\omega = \pi$, *i.e*, it lies on the negative side of the axis of y.

If $H = 0$ and J is positive the central stream line lies in the plane $y = 0$ and its centre of curvature lies in the negative side of the axis of z.

Representation of the Disturbed Flow.

The disturbed flow may be represented by the velocity potential

$$\phi = \phi_0 + \phi_1 = r^2 S_2 + r S_1 + r^{-2} s_1 + r^{-3} s_2 + \ldots + r^{-m-1} s_m + \ldots, \quad (18)$$

where s_m is a surface spherical harmonic of degree m.

Forces found by Integration of Pressures.

Since the motion is steady $p/\rho + \frac{1}{2}(u^2 + v^2 + w^2)$* is constant. If the components of the resultant force on the body are X, Y, Z,

$$\frac{X}{\rho} = \tfrac{1}{2}\iint_\iota l\,(u^2 + v^2 + w^2)\,ds, \qquad \frac{Y}{\rho} = \tfrac{1}{2}\iint_\iota m\,(u^2 + v^2 + w^2)\,ds,$$

$$\frac{Z}{\rho} = \tfrac{1}{2}\iint_\iota n\,(u^2 + v^2 + w^2)\,ds,$$

the suffix ι shows that the integration extends over the surface of the body and l, m, n are the direction cosines of the outward drawn normal to the surface of the body.

These expressions may be transformed by Green's theorem in the forms

$$\left.\begin{aligned} \frac{X}{\rho} &= \tfrac{1}{2}\iint_0 (u^2 + v^2 + w^2)\,l\,ds - \iint_0 (lu + mv + nw)\,u\,ds \\ \frac{Y}{\rho} &= \tfrac{1}{2}\iint_0 (u^2 + v^2 + w^2)\,m\,ds - \iint_0 (lu + mv + nw)\,v\,ds \\ \frac{Z}{\rho} &= \tfrac{1}{2}\iint_0 (u^2 + v^2 + w^2)\,n\,ds - \iint_0 (lu + mv + nw)\,w\,ds \end{aligned}\right\}, \quad (19)$$

---

* Note that u, v, w are used here and in succeeding pages as the components of velocity at any point in the fluid. In the first part of the paper up to equation (13) they represent the components of velocity in the fluid before the introduction of the solid.

the integrations extending over any surface O which completely surrounds the body. Taking O as a sphere of radius r it is found that

$$\frac{\mathrm{X}}{\rho} = \tfrac{1}{2}\iint_{\mathrm{O}} \cos\theta \left\{\left(\frac{1}{r}\frac{\partial\phi}{\partial\theta}\right)^2 + \left(\frac{\partial\phi}{\partial r}\right)^2 + \frac{1}{r^2\sin^2\theta}\left(\frac{\partial\phi}{\partial\omega}\right)^2\right\} ds$$
$$- \iint_{\mathrm{O}} \left\{\left(\frac{\partial\phi}{\partial r}\cos\theta - \frac{\partial\phi}{r\partial\theta}\sin\theta\right)\frac{\partial\phi}{\partial r}\right\} ds, \qquad (20)$$

with similar expressions for Y/ρ and Z/ρ.

Now the value of X/ρ is independent of r, and ds is $r^2 \sin\theta\, d\omega\, d\theta$, so that it is only necessary to pick out terms in the integrands of (20) which contain r^{-2} as a factor All other terms must vanish when integrated over the sphere of radius r. It is hardly worth while to complete the whole operation because we should ultimately only find the expressions given in equations (7), but it seems worth while to verify, say, the first term in the expression for X/ρ.

Substituting from (14) and (18) in (20) and picking out only terms in r^{-2} in the integrands, it is found that

$$\frac{\mathrm{X}}{\rho} = \iint_{\mathrm{O}} \left\{4\mathrm{S}_2 s_1 \cos\theta - 2\sin\theta\left(\mathrm{S}_2\frac{\partial s_1}{\partial\theta} - s_1\frac{\partial \mathrm{S}_2}{\partial\theta}\right) + \frac{\partial \mathrm{S}_2}{\partial\theta}\frac{\partial s_1}{\partial\theta}\cos\theta\right.$$
$$\left. + \cos\theta \operatorname{cosec}^2\theta \frac{\partial \mathrm{S}_2}{\partial\omega}\frac{\partial s_1}{\partial\omega}\right\} r^{-2} ds. \qquad (21)$$

Taking the case when $\mathrm{H} = \mathrm{J} = 0$ so that the centre line of the undisturbed flow is straight, and substituting for s_1, its most general value

$$a_1 \cos\theta + a_2 \sin\theta\cos\omega + a_3 \sin\theta \sin\omega,$$

and for S_2 from (16), it is found that the only terms in (21) which do not vanish are those containing $a_1\mathrm{G}$ thus:

$$\iint_{\mathrm{O}} 4\mathrm{S}_2\, s_1 \cos\theta\, r^{-2}\, ds = \tfrac{32}{15}\pi a_1 \mathrm{G},$$

$$\iint_{\mathrm{O}} 2\sin\theta\left(\mathrm{S}_2\frac{\partial s_1}{\partial\theta} - s_1\frac{\partial \mathrm{S}_2}{\partial\theta}\right) r^{-2}\, ds = \tfrac{64}{15}\pi a_1 \mathrm{G},$$

$$\iint_{\mathrm{O}} \frac{\partial \mathrm{S}_2}{\partial\theta}\frac{\partial s_1}{\partial\theta}\cos\theta\, r^{-2}\, ds = \tfrac{24}{15}\pi a_1 \mathrm{G},$$

$$\iint_{\mathrm{O}} \cos\theta \operatorname{cosec}^2\theta \frac{\partial \mathrm{S}_2}{\partial\omega}\frac{\partial s_1}{\partial\omega} r^{-2}\, ds = 0,$$

so that from (21)

$$\mathrm{X} = \frac{32 + 64 + 24}{15}\pi a_1 \mathrm{S}\rho = 8\pi a_1 \mathrm{G}\rho. \qquad (22)$$

Remembering that $H = J = 0$ in (16), it can be shown that

$$\frac{\partial p}{\partial y} = \frac{\partial p}{\partial z} = 0,$$

so that the value of X from (7) is

$$X = -(V + A)\frac{\partial p}{\partial x}. \tag{23}$$

In comparing the two expressions for X given in (22) and (23) we must first calculate the value of $\partial p/\partial x$ at the origin in the undisturbed flow. The velocity along the central stream line before the introduction of the body is

$$u = -\left[\frac{\partial \phi_0}{\partial r}\right]_{\theta=0} = [-S_1 - 2rS_2]_{\theta=0},$$

so that the rate of change in pressure along the axis of x is

$$\frac{\partial p}{\partial x} = -\frac{\partial}{\partial x}(\tfrac{1}{2}\rho u^2) = -\rho\left[u\frac{\partial u}{\partial x}\right]_{\theta=0} = -\rho U[-2S_2]_{\theta=0} = 2\rho GU. \tag{24}$$

It remains to find the relationship between a_1 and A. a_1 is the coefficient of $\cos\theta/r^2$ or x/r^3 in the expansion of the velocity potential of the disturbed motion in spherical harmonics. We can regard the disturbed motion as consisting of two parts, one due to the term rS_1 in the undisturbed motion and the other to the term r^2S_2. Let the coefficients of x/r^3 in these two parts be a_1' and a_1'' respectively, so that

$$a_1 = a_1' + a_1''. \tag{25}$$

So far we have made no assumptions as to the relative magnitudes of the terms r_1S_1 and r^2S_2 in ϕ_0. If now we make the assumption made in obtaining (7) that the changes in velocity of the undisturbed stream in a distance comparable with the linear dimensions of the body are small, then a_1'' is small compared with a_1'. Now a_1' is the coefficient of x/r^3 in the expansion of the disturbed motion due to a uniform stream of velocity U flowing past the body. This is identical with the coefficient of x/r^3 in the expansion of the velocity potential in spherical harmonics of the flow produced by moving the body with velocity $-$ U in an infinite fluid at rest.

The connection between this coefficient and the expression for the energy of a body moving without rotation in an infinite fluid has been discussed by the author in a previous paper.* As a particular case of the formulæ in that paper the coefficient of x/r^3 in the expansion of the velocity potential due to a velocity $-$ U parallel to the axis of x is

$$-U(A + V)/4\pi, \tag{26}$$

---

* *Loc. cit.*, p. 13.

where A and V have the same meaning as in (7). If we neglect a_1'' compared with a_1', we can therefore write

$$4\pi a_1 = -(\mathrm{A}+\mathrm{V})\,\mathrm{U}. \tag{27}$$

Taking the value of a_1 from (27) and of G from (24) and substituting them in (22), it will be found that

$$\mathrm{X} = 8\pi a_1 \mathrm{G}\rho = (4\pi a_1)(2\mathrm{G}\rho) = -2(\mathrm{A}+\mathrm{V})\,\mathrm{U}\mathrm{G}\rho = -(\mathrm{A}+\mathrm{V})\frac{\partial p}{\partial x},$$

which is identical with the expression (23) derived from the first part of the paper.

In the same way the rest of formulæ (7) can be found by direct integration of the pressures over the surface of the body.

Couples found by Integration of Pressures over the Surface of the Body.

If Lρ, Mρ, Nρ are the component couples,

$$\mathrm{L} = \frac{1}{\rho}\iint_s p\,(mz - ny)\,ds = \tfrac{1}{2}\iint_s (ny - mz)\,(u^2+v^2+w^2)\,ds. \tag{28}$$

First the integral will be transformed into an integral over an outer surface 0 completely surrounding the body, thus:

$$\tfrac{1}{2}\iint_s ny\,(u^2+v^2+w^2)\,ds = \tfrac{1}{2}\iint_0 ny\,(u^2+v^2+w^2)\,ds$$
$$-\tfrac{1}{2}\iiint y\,\frac{\partial}{\partial z}(u^2+v^2+w^2)\,dx\,dy\,dz, \tag{29}$$

the volume integral extending between the body and the outer surface 0. Remembering that $\frac{\partial u}{\partial x}+\frac{\partial v}{\partial y}+\frac{\partial w}{\partial z}=0$ and at the surface of the body $lu+mv+nw=0$,

$$-\tfrac{1}{2}\iiint y\,\frac{\partial}{\partial z}(u^2+v^2+w^2)\,dx\,dy\,dz$$
$$= -\iiint y\left(u\frac{\partial w}{\partial x}+v\frac{\partial w}{\partial y}+w\frac{\partial w}{\partial z}\right)dx\,dy\,dz$$
$$= -\iint_0 yw\,(lu+mv+nw)\,ds$$
$$+\iiint w\,\frac{\partial}{\partial x}(yu)+\frac{\partial}{\partial y}(yv)+\frac{\partial}{\partial z}(yw)\,dx\,dy\,dz$$
$$= -\iint_0 yw\,(lu+mv+nw)\,ds + \iiint wv\,dx\,dy\,dz.$$

The integral $-\frac{1}{2}\iint_s mz\,(u^2+v^2+w^2)\,ds$ can be treated in the same way, and by adding the two results it is found that

$$\mathrm{L} = \tfrac{1}{2}\iint_0 (ny-mz)(u^2+v^2+w^2)\,ds - \iiint_0 (yw-zv)\,(lu+mv+nw)\,ds. \tag{30}$$

If now the outer surface be taken on a sphere of radius r, $ny - mz = 0$ so that

$$\left.\begin{aligned} \mathrm{L} &= \iint_0 (yw-zv)\frac{\partial\phi}{\partial r}\,ds. \\ \text{Similarly,}\qquad \mathrm{M} &= \iint_0 (zu-xw)\frac{\partial\phi}{\partial r}\,ds. \\ \mathrm{N} &= \iint_0 (xv-yu)\frac{\partial\phi}{\partial r}\,ds. \end{aligned}\right\}. \tag{31}$$

Expressing u, v, w in terms of the velocity potential

$$\left.\begin{aligned} yw - zv &= -\frac{\partial\phi}{\partial\omega} \\ zu - xw &= \frac{\partial\phi}{\partial\theta}\sin\omega + \frac{\partial\phi}{\partial\omega}\cot\theta\cos\omega \\ xv - yu &= -\frac{\partial\phi}{\partial\theta}\cos\omega + \frac{\partial\phi}{\partial\omega}\cot\theta\sin\omega \end{aligned}\right\}, \tag{32}$$

and substituting these expressions in (31)

$$\left.\begin{aligned} \mathrm{L} &= -\iint_0 \frac{\partial\phi}{\partial\omega}\frac{\partial\phi}{\partial r}\,ds \\ \mathrm{M} &= \iint_0 \left(\frac{\partial\phi}{\partial\theta}\sin\omega + \frac{\partial\phi}{\partial\omega}\cot\theta\cos\omega\right)\frac{\partial\phi}{\partial r}\,ds \\ \mathrm{N} &= \iint_0 \left(\frac{\partial\phi}{\partial\theta}\cos\omega + \frac{\partial\phi}{\partial\omega}\cot\theta\sin\omega\right)\frac{\partial\phi}{\partial r}\,ds \end{aligned}\right\}. \tag{33}$$

The remainder of this paper will be devoted to the discussion of L.

Since L has a definite value independent of the radius of the sphere over which the integration is taken, it is only necessary to pick out terms in $\frac{\partial\phi}{\partial\omega}\frac{\partial\phi}{\partial r}$

which contain the factor r^{-2}. Differentiating the expression (18) for ϕ with respect to r and ω, multiplying and picking out terms in r^{-2},

$$-\iint_0 \frac{\partial\phi}{\partial\omega}\frac{\partial\phi}{\partial r}\,ds = \iint_0 \left(2s_1\frac{\partial S_1}{\partial\omega} - S_1\frac{\partial s_1}{\partial\omega}\right) r^{-2}\,ds$$
$$+ \iint_0 \left(3s_2\frac{\partial S_2}{\partial\omega} - 2S_2\frac{\partial s_2}{\partial\omega}\right) r^{-2}\,ds, \qquad (34)$$

and since S_1 does not contain ω when the axis of x is parallel to the stream direction at the origin, the first of these integrals vanishes so that

$$L = \iint_0 \left(3s_2\frac{\partial S_2}{\partial\omega} - 2S_2\frac{\partial s_2}{\partial\omega}\right) r^{-2}\,ds. \qquad (35)$$

Now S_2 is

$$G\left(\tfrac{3}{2}\cos^2\theta - \tfrac{1}{2}\right) + (H\cos\omega + J\sin\omega)\cos\theta\sin\theta$$
$$+ (E\cos 2\omega + F\sin 2\omega)\sin^2\theta \qquad (36)$$

and s_2 may be expressed in its most general form

$$s_2 = g\left(\tfrac{3}{2}\cos^2\theta - \tfrac{1}{2}\right) + (h\cos\omega + j\sin\omega)\cos\theta\sin\theta$$
$$+ (e\cos 2\omega + f\sin 2\omega)\sin^2\theta. \qquad (37)$$

It will be seen that only four kinds of terms can occur in (35), namely, those containing Hj, hJ, Ef, eF; all others vanish when integrated over the surface of the sphere.

To find the coefficient of Hj take $J = E = F = 0$, then

$$L = Hj\int_0^{\pi}\int_0^{2\pi}(-3\sin^2\theta\cos^2\theta\sin^2\omega - 2\sin^2\theta\cos^2\theta\cos^2\omega)\sin\theta\,d\omega\,d\theta$$
$$= -\tfrac{4}{3}\pi Hj. \qquad (38)$$

Similarly the term in Jh is $+\tfrac{4}{3}\pi Jh$.

To find the coefficient of Ef put $H = J = F = 0$

Then

$$L = Ef\int(-6\sin^4\theta\sin^2 2\omega - 4\sin^4\theta\cos^2 2\omega)\,r^{-2}\,ds = -\tfrac{32}{5}\pi Ef.$$

Hence this complete expression for L is

$$L = \tfrac{4}{3}\pi(Jh - Hj) + \tfrac{32}{5}\pi(Fe - Ef). \qquad (39)$$

. Each of these terms represents the reaction between some type of asymmetry in the body and a corresponding type of asymmetry in the flow. If the changes in velocity of the undisturbed stream in a distance comparable with the linear dimensions of the body are small compared with the velocity of the undisturbed stream, we can use the same argument to find h, j, e and f that we previously used to find the coefficient a_1 which occurs in finding the force component X in (22). Thus h, j, e and f are the coefficients of four of the terms in the harmonic of the second degree in the expansion of the velocity potential due to the motion of the body with velocity $-$ U parallel to the axis of x in an infinite fluid.

The first two harmonics in the velocity potential due to a movement of the body with velocity $+$ U are therefore

$$\begin{aligned}\phi' = r^{-2}(-a_1 \cos\theta - a_2 \sin\theta \cos\omega - a_3 \sin\theta \sin\omega) \\ - r^{-3}\{g(\tfrac{3}{2}\cos^2\theta - \tfrac{1}{2}) + (h\cos\omega + j\sin\omega)\sin\theta\cos\theta \\ + (e\cos 2\omega + f\sin 2\omega)\sin^2\theta\}. \quad (40)\end{aligned}$$

Though it is not possible to express the coefficients in the harmonics of the second degree in terms of the coefficients occurring in the energy equation, as it is in the case of the harmonics of the first degree; yet it is possible to see what kind of asymmetry in the body will give rise to positive values of the coefficients h, j, e and f.

Consider, for instance, what kind of body might be expected to give rise to a flow for which $j = e = f = 0$ but h is not zero. The simplest such body is a sphere with its centre not at the origin.

The velocity potential due to a sphere of radius a with its centre at small distance η along the axis of y and moving with velocity U parallel to the axis of x is

$$\phi' = \tfrac{1}{2}\mathrm{U}\frac{a^3x}{\{x^2 + (y-\eta)^2\}^{3/2}} = \tfrac{1}{2}\mathrm{U}a^3\left\{\frac{x}{r^3} + \frac{3\eta xy}{r^5}\right\}.$$

The harmonic of the second degree is therefore

$$\tfrac{3}{2}\mathrm{U}a^3\eta r^{-3}\cos\theta\sin\theta\cos\omega,$$

so that comparing this with (40) it will be seen that

$$g = j = e = f = 0 \quad \text{and} \quad -h = \tfrac{3}{2}\eta\mathrm{U}a^3.$$

Hence from (39)

$$\mathrm{L} = \tfrac{4}{3}\pi h\mathrm{J} = -2\pi\eta\mathrm{U}a^3\mathrm{J}. \quad (41)$$

Since with positive values of J and η, L is negative, the couple tends to turn the sphere about the axis of x as though its centre were attracted towards the centre of curvature of the central stream line, which for positive values of J is in the negative part of the axis of z.

This result can be verified because in the case of a sphere the resultant force necessarily acts through its centre, and from (7) is

$$\mathrm{Z} = -2\pi a^3\frac{\partial p}{\partial z}.$$

It can be shown that $\frac{\partial p}{\partial z} = \text{JU}$, so that

$$\text{Z} = -2\pi a^3\text{JU} \quad \text{and} \quad \text{L} = \text{Z}\eta = -2\pi a^3\text{JU}\eta,$$

which agrees with (41).

Experimental Verification of Expression for Couples on Bodies in Curved Streams.

In the case of a sphere capable of rotation about an axis which does not pass through its centre there is a resultant force when it is placed in a curved stream. This lateral force makes it difficult to use such a body for experimental demonstration, accordingly a body was devised which when suspended under gravity might be expected to give rise to a pronounced value for the coefficient h of (40) without necessarily giving rise to lateral force. Such a body is shown in fig. 2. It was an elongated body of revolution the centre line of which was afterwards bent into an arc of a circle so that it looked like a small bologna sausage.

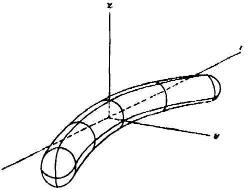

FIG. 2.

If such a body be set in the position shown in fig. 2 so that the curvature of the centre line lies in the plane $z = 0$ and the centre of curvature lies in the positive part of the axis of y, then the effect of the curvature of the centre line would be to increase the velocity of the flow at points in the negative side of the axis of y and to decrease it at points on the positive side. This is exactly opposite to the effect of moving the centre of a sphere from the origin to a distance η out along the positive side of the axis of y. It will be seen, therefore, that if the body shown in fig. 2 is moved parallel to the axis of x in the positive direction, the coefficient of the harmonic $r^{-3} \cos\theta \sin\theta \cos\omega$

in the corresponding expansion of ϕ' will be negative while that of $r^{-3}\cos\theta\sin\theta\sin\omega$ will be zero.

Hence from (40) h is positive and $j = 0$.

Taking the case of the undisturbed flow for which $\mathrm{H} = \mathrm{E} = \mathrm{F} = 0$ and J is positive, *i.e.*, curved flow in which the stream lines are parallel to the plane $y = 0$ and the centre of curvature in the negative part of the axis of z, it will be seen from (39) that L is positive so that a couple acts on the body tending to turn it towards the position where the centre of curvature of the middle line of the body is in the positive side of the axis of z. It appears, therefore, that a body of this shape should set itself so that the curvature of its centre line is in the same plane as the curvature of the stream lines but in the opposite direction. It has two positions of equilibrium, one stable and the other unstable.

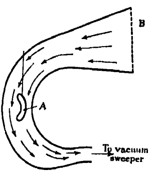

Fig. 3. — Experiment on a Curved Body in a Curved Stream of Air.

A body of this form was hung by a fine silk thread in the curved stream created by a vacuum sweeper sucking air through a curved channel formed by two bent pieces of sheet metal between two parallel glass plates. The apparatus is shown in fig. 3, which needs little explanation. In that figure A is the body and B is some fine gauze fitted into the mouth of the apparatus to prevent disturbances in the outside air from affecting the flow. The apparatus was mounted so that the air in the neighbourhood of the middle of the body was descending vertically.

Result.—Directly the vacuum sweeper was started the body swung into the position shown in fig. 3. This is what was predicted mathematically.

Experimental Verification of Formulæ for Converging and Diverging Flow.

Next suppose the central stream line of the undisturbed flow is straight so that $\mathrm{H} = \mathrm{J} = 0$, and let us consider the expression $\mathrm{L} = \frac{32}{3}\pi\,(\mathrm{F}e - \mathrm{E}f)$.

The quantities E and F represent differences in the amount of convergence or divergence of stream lines in different axial planes through the central stream line. We have already pointed out, for instance, that if $\mathrm{H} = \mathrm{J} = \mathrm{F} = 0$ and $\mathrm{G} = 2\mathrm{E}$ the stream lines are all parallel to the plane $y = 0$. A convenient method for obtaining a stream having a pronounced value of E is therefore to make a channel two of whose walls are parallel (in the actual apparatus glass plates) and the remaining two are made from sheet metal bent into the form shown in fig. 4. If the axes are chosen so that the plane $y = 0$ is parallel to the glass sheets, and if the axis of x is the central line of the apparatus, the

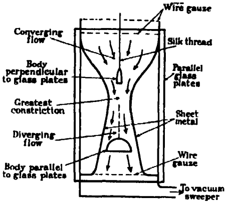

FIG. 4.—Experiment on a Flattened Body in Converging and Diverging Flow.

positive direction being downwards, then $E = \frac{1}{2}G$ is negative in the converging upper part of the apparatus and positive in the lower diverging part.

Referring to the expression (39) for L, it will be seen that E occurs associated with f. For an experimental verification, therefore, we must find what shape a body must be made in order that it may give rise to a pronounced value for f.

Referring to (40), $-f$ is the coefficient of $r^{-3} \sin^2 \theta \sin 2\omega$ in ϕ'. We shall first find what kind of small alteration must be made to a sphere in order that the velocity potential of the flow round it may contain a term of the type $r^{-3} \sin^2 \theta \sin 2\omega$. Let $r = a + b\chi(\theta, \omega)$ be the equation to the body, b being small compared with a, and χ a function of θ and ω. This will produce a velocity potential

$$\phi' = \tfrac{1}{2}Ua^3r^{-2} \cos \theta - fr^{-3} \sin 2\omega \sin^2 \theta,$$

provided $lU = -\dfrac{\partial \phi'}{\partial r}$, where l is the direction cosine of the normal to the surface of the body.

Since b is small compared with a

$$l = \cos \theta + \frac{b}{a} \sin \theta \frac{\partial}{\partial \theta} \chi(\theta, \omega),$$

so that

$$b \frac{\partial}{\partial \theta} \chi(\theta, \omega) = -3fU^{-1}a^{-3} \sin 2\omega \sin \theta,$$

or

$$b\chi(\theta, \omega) = 3fU^{-1}a^{-3} \sin 2\omega \cos \theta = b' \sin 2\omega \cos \theta. \qquad (42)$$

In order to form a picture of the shape of the body whose equation is

$$r = a + b' \sin 2\omega \cos \theta, \tag{43}$$

one can imagine a series of sections by planes perpendicular to the axis of x. These are shown in figs. 5A and 5B. Fig. 5A gives the sections of the half of the body for which x is positive and fig. 5B for the negative half. It will be seen that the essential feature is that the body is circular in the central section and that it has a flattened nose and tail, but the direction of flattening at the nose is at right angles to the direction at the tail and each is at 45° to the axes of y and z. The asymmetry is, in fact, that possessed by a tetrahedron about the line joining the mid-points of opposite edges. If a body of this shape is

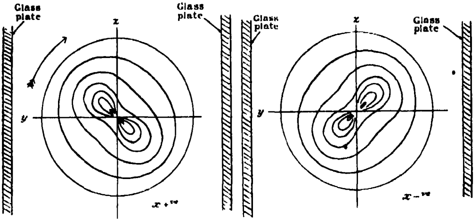

Fig. 5A. Fig. 5B.

Sections of the Body $r = a + b' \cos\theta \sin 2\omega$ by Plane Perpendicular to the Axis, *i.e.*, $\theta = 0$.

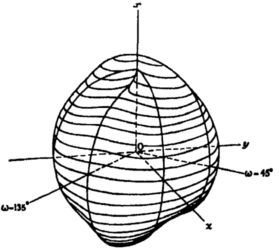

Fig. 5C.—Perspective Sketch of $r = a + b' \cos\theta \sin 2\omega$.

placed in a converging stream of fluid it gives rise to a value of f equal to $\frac{1}{3}b'Ua^3$, so that

$$L = -\tfrac{32}{3}\pi Eb'Ua^3. \tag{44}$$

In the converging part of the apparatus shown in fig. 4 E is negative, so that L is positive. The reaction between the fluid and the body is therefore such that the body tends to turn in the direction of increasing ω, namely, that shown by the arrow in fig. 5A.

Since the wind is blowing downwards in the apparatus shown in fig. 4, figs. 5A and 5B show the contours of the body when seen from *below*. The positions of the glass plates in the apparatus of fig. 4 are also shown in figs. 5A and 5B: it will be seen from the direction of the arrow in fig. 5A that in the converging channel the body tends to set itself so that the flattened lower end is parallel to the glass plates while the flattened upper end is perpendicular to them. This is a position of stable equilibrium. Another stable position can evidently be found by rotating the body through 180° round the wind direction, and these are two intermediate unstable positions of equilibrium at right angles to them.

A perspective sketch of the body $r = a + b' \cos\theta \sin 2\omega$ is shown in fig. 5C.

If the body is lowered through the point of maximum constriction of flow into the diverging part of the channel in the apparatus shown in fig. 4, E changes sign. The stable positions of equilibrium become unstable and unstable positions become stable. The body should therefore rotate through a right angle as it passes from the converging to the diverging part of the channel.

These predictions were completely verified. The body used was not, in fact, the body whose equation is $r = a + b' \sin 2\omega \cos\theta$, because the flow round bodies which are nearly spherical is known to be quite unlike the flow contemplated in hydrodynamical theory. In order that the actual flow may resemble at all closely the theoretical irrotational flow, the body must be smooth and elongated. Accordingly a body was made in which the essential feature of the symmetry about the wind direction, or axis of x, of the body represented by (43) was preserved, but the length was six times the maximum diameter. This body was made by flattening the two ends of a circular cylinder into two knife edges at right angles to one another, as shown in fig. 6. It was then rounded off carefully so that there were no sharp edges to spoil the flow except the knife edges at the nose and tail. It was suspended by a silk thread at S and hung in the wind tunnel shown

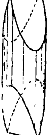

FIG. 6.

in fig. 4, so that it would be raised or lowered through the central part of the channel.

When a draught was created by applying a vacuum sweeper to the lower end of the channel, the body set itself so that the upper knife edge was perpendicular to the glass plates when it was in the upper converging part; but it turned through a right angle when lowered through the point of maximum constriction into the diverging part of the channel.

It appears, therefore, that the predictions of mathematical theory as to the effect of two types of asymmetry in the flow on corresponding types of asymmetry in the body are completely verified by experiment.

It is well known that the flow of fluid past a body differs considerably from that contemplated by irrotational theory even in the case of elongated bodies, but the flow at the forward end is far more like the theoretical flow than that behind the mid-ship section. In order to separate the effects of asymmetry of the flow and the body at the forward end from those at the after end, the body shown in the perspective sketch (fig. 7) was made. One end was cut to a knife edge like the body previously described, while the other end was turned to a point in a symmetrical ogival shape like the nose of an airship. There were no sharp edges except at the nose and tail of the body.

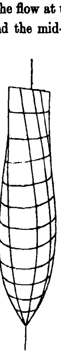

FIG. 7. — Body with circular cross-sections in lower half, finishing in a point, and elliptical cross-sections in upper half with knife-edge on top.

When hung in the converging channel with its point downwards and knife edge upwards, this body set itself with its knife edge perpendicular to the glass plates. When hung in the converging channel with the point on top, the knife edge at the bottom set itself parallel to the glass plates. It appears, therefore, that the agreement between theory and experiment extends to the tail end of the body when the body is of the "easy" shape shown in fig. 7

A body cut into the shape of half a magnifying lens and hung from the middle point of its curved edge set itself perpendicular to the glass plates in the converging part and parallel to them in the diverging part. The two positions of this body are shown in fig. 4.

A body shaped like a whole magnifying lens or disc sets itself in the same position as that assumed by the half disc. If the flow were accurately the irrotational flow contemplated by theory, the stream should exert no directive effect on a body with this kind of symmetry. Failure of the stream lines to close in at the after end of the body in manner indicated by irrotational theory would, however, weaken the negative directive effect of the rear portion compared with the positive effect of the front portion. It seems clear that this is the reason for the observed orientation of a lenticular-shaped body hung from a point in its curved edge. An oblate spheroid with one of its maximum diameters along the wind direction behaves in the same way. The experiments here described are very easy to carry out with a domestic vacuum cleaner, but in making a body like that shown in fig. 7 great care has to be exercised to keep it symmetrical and to hang it symmetrically. In my experiments I controlled it with a magnet, inserting a small magnet in the body perpendicular to the axis When the flow was established I removed the control.

In conclusion I should like to express my thanks to Mr. W. S. Farren for preparing the three perspective sketches of figs. 2, 5c and 7, and to Sir Ernest Rutherford for facilities for making the experiments.

On the Decomposition of Ammonia by High-Speed Electrons.

By Prof. J. C. McLennan, F.R.S., and Gilbert Greenwood, M.Sc., University of Toronto

(Received June 28, 1928.)

Introduction.

During recent years a knowledge of the ammonia equilibrium has attained a great technical importance. The fact that ammonia decomposes under the action of an electric spark or on passing through a red-hot tube was known as long ago as in the time of Priestly. It was, at this time, regarded as a complete decomposition. The first indication of a certain quantity of the ammonia remaining undecomposed, and thus of the balanced nature of the action, was obtained by Deville[*] in 1805. Measurements on the variation of the equilibrium with temperature, at atmospheric pressure, were made by Haber and Oordt.[†] They found that at 1020° C. the equilibrium mixture contained only 0·012 per cent. by volume of ammonia, whilst at 27° C. the concentration of ammonia was 98·51 per cent. However, at this low temperature the speed of attaining the equilibrium was very slow. Many investigations have been carried out by various methods and different results obtained. The photochemical decomposition was investigated by Kuhn,* who reported that the decomposition was complete. The equilibrium under the action of α-rays has been studied by Lind and Bardwell,† and these authors concluded that equilibrium would be established when 83·3 per cent. of the ammonia was decomposed. Decomposition by means of the silent electric discharge was studied by Le Blanc and Davies,‡ who found that the equilibrium was not governed by the ordinary laws of mass action.

---

[*] 'C. R.,' vol. 60, p. 317 (1865).

[†] 'Z. f. anorg Chem.,' vol. 44, p. 341 (1905).

Experiments with low-voltage electrons have been carried out by Anderson,§ and by Caress and Rideal.|| In these experiments, however, the gases were in contact with the glowing filament, which produced the electrons, and thus thermal effects, as instanced by the work of Schwab,¶ Hinshelwood and Burk,** might be present. It seemed, therefore, of interest to investigate the decomposition of ammonia by means of electron bombardment under such conditions that the thermal effects were eliminated, and a possibility of attaining this was offered by the use of the new Coolidge cathode-ray tube.

Description of Apparatus.

A diagrammatic sketch of the apparatus is given in fig. 1. The cathode-ray tube, which was constructed in this laboratory, was similar to that described by Coolidge.†† It consisted essentially of a large glass bulb B, with three side arms. One of these served for the introduction, and the holding in position, of the hot filament C. A second arm carried the conical-shaped copper tube D, along which the cathode rays passed, to emerge finally through a thin window of " resistal " metal mounted in the metal end-piece, and supported by a grid. The third side-arm led to a mercury-vapour diffusion pump, and a rotary oil pump, which served to evacuate the tube. The accelerating potential was applied between the filament and the copper tube. It was produced by means

---

* 'C. R.,' vol. 177, p. 956 (1923); 'J. de Chem. Phys.,' vol. 23, p. 521 (1926).

† 'J. Am. Chem. Soc.,' vol. 50, p. 745 (1928).

‡ 'Z. f. Elektrochem.,' vol. 14, p. 361 (1908).

§ 'Z. f. Physik,' vol. 10, p. 54 (1922).

|| 'Roy. Soc. Proc.,' A, vol. 115, p. 684 (1927).

¶ 'Z. f. phys. Chem.,' vol. 128, p. 161 (1927).

** 'J. Chem. Soc.,' vol. 127, p. 1105 (1925).

†† 'J. Franklin Inst.,' vol. 202, p. 693 (1926).

of a transformer, used in conjunction with a mechanical rectifier. The centre of the transformer was earthed, and, as a result of this, the filament was at a

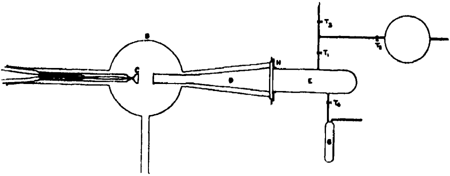

FIG. 1.

high negative potential whilst the copper-tube window and end-piece were at a high positive potential. Both ends had therefore to be insulated. The filament was heated by a battery of about 12 volts, which was supported on an insulating table. Junction between the glass of the tube and the end-piece was made by means of a wax seal, and in order to keep this seal hard it was cooled by a stream of cold water, which was circulated round it by a pump. This cooling device also had to form an insulated system.

The ammonia gas to be submitted to the action of the cathode rays was contained in the vessel E. This vessel fitted into an annular groove at H in the metal end-piece, and a vacuum-tight seal was made by means of wax. Leading into the reaction vessel was a tube from a reservoir, in which ammonia gas could be stored. This supply could be closed off by means of the tap T_1. Evacuation of the reaction vessel could also be effected through this tap by means of a T-piece, and a tube leading to a pump. A second tube led from the reaction vessel to a McLeod gauge. In order to prevent any mercury being shot over from this gauge into the reaction vessel, a trap G was inserted between the two. The gauge could also be closed off from the reaction vessel by means of a tap T_4. A calibration of the potential applied to the tube was made by means of a graduated spark-gap supplied by the Victor X-Ray Corporation of Chicago.

Preparation of the Gases and their Analysis.

Ammonia.—The gas was liberated from a strong aqueous solution by gentle heating. It was passed through a drying train consisting of tubes of quicklime and tubes of phosphorus pentoxide. The dried gas was then solidified in a fractionating vessel by means of liquid air. Any adventitious permanent gases were removed by the evacuation of both the fractionating vessel and the storage reservoir Fractionation was carried out, and the middle fraction only of the ammonia was collected in the reservoir.

Nitrogen.—This gas was prepared by the action of bromine on an aqueous solution of ammonia. The moist gas was passed through a liquid air-trap and through tubes containing caustic potash to remove traces of bromine, through calcium chloride to remove traces of ammonia, and finally through tubes of phosphorus pentoxide. The dried gas was collected in a suitable storage vessel. A quantity of the gas could be passed from this vessel into the ammonia reservoir, and in this way a mixture of the two gases made. The approximate composition of the mixture was controlled by readings on a pressure gauge connected to the ammonia reservoir.

Hydrogen.—The hydrogen was prepared by the electrolysis of a baryta solution in a suitable eudiometer. The oxygen was allowed to escape whilst the hydrogen was led through a liquid-air trap, and a series of phosphorus pentoxide drying tubes into the same storage vessel as was used for the nitrogen. Mixtures of hydrogen and ammonia could be made when desired.

Analysis of the Mixtures —A side-tube from the ammonia reservoir led to a simple analysis apparatus, in which the volume of the dry gas mixture could be read. The sample was then driven over into an absorption vessel containing strong sulphuric acid. When the ammonia was absorbed, the residual gas (nitrogen or hydrogen) was drawn back into the measuring vessel, and again measured under the same pressure as before.

Experimental Procedure.

The reaction vessel was filled with the experimental gas in the following manner: By means of the pump, the vessel and the connecting tubes as far as the tap T_2 of the gas reservoir were evacuated to a pressure of about 1/50 mm. The pump was then shut off by means of the tap T_3 and the experimental gas allowed to enter the vessel to a pressure of about 3 cm. The system was again evacuated to the low pressure, and gas admitted a second time. Small quantities of gas were then removed by the pump, and the pressure read each time on the gauge until the desired gas pressure in the vessel was reached. In this way the pressure could be adjusted to within 1/25 mm. of any desired value. The tap T_1 was then closed and a pressure reading made: after 15 minutes a second pressure reading was made as a test for the absence of leaks. If there had been no change in pressure during the 15 minutes, the actual experiment could be started. If, however, there was a leak the taps had to be cleaned, or the wax joint at H improved, and the filling of the tube repeated.

The cathode rays were now switched on and bombardment of the gas carried out for a definite period of time, usually 2½ minutes. The rays were then turned off and the pressure of the gas measured. The rays were then turned on again, and after a further period of time another pressure measurement made. That this mode of measurement—stopping the bombardment during the reading of the pressure—is justified is shown by the fact that the same pressure readings are obtained immediately after stopping the bombardment and after waiting another 15 minutes, without turning on the rays. This fact is also of importance in showing that the increase of pressure was not due to a rise of temperature Further proof of this is to be found in an experiment carried out with argon (see later) Throughout the whole course of this argon experiment, there was no increase in pressure, thus proving conclusively that the increase was not due to a rise of temperature. Since the ratio of the reaction vessel to the total volume of the system—*i e.*, the ratio of the quantity of gas irradiated to the total volume of gas—was known, a small correction could be applied to allow for the gas in the gauge being shielded from the action of the rays.

Preliminary Results.

An experiment carried out in the manner described above, with ammonia at a pressure of about 1 mm., showed a doubling of the pressure—*i e.*, complete decomposition—in about three minutes. An examination of the time-pressure curve, from the point of view of chemical kinetics, showed that the action was monomolecular, except for the final stages. Similar results have been obtained by Pohl* in investigations of the decomposition of ammonia by means of the silent electric discharge. Since the metal end-piece was at a high potential, and the gas in the reaction chamber at a low pressure, one might suspect that the decomposition was due to a silent electric discharge, especially since a distinct glow was to be seen in the reaction chamber. An attempt to eliminate this discharge was made by shielding the ammonia gas from any electric fields by coating the chamber with tinfoil, which was brought into intimate contact with the charged metal end-piece. To prevent any discharge taking place in the McLeod gauge itself, a large metal vessel, provided with doors, was built up round the gauge. The doors could be opened after an experiment in order to read the pressure. Under these conditions the decomposition of the ammonia was quite different from the monomolecular reaction caused by the silent discharge. A test experiment with argon was made at this stage. After irradiation for one hour with the cathode rays there was no increase of pressure, thus showing that no gas was being liberated from the walls of the vessel or the gauge, nor—as previously mentioned—was elevation of temperature playing any part. At this stage of the work another interfering factor was noticed. It was found that sometimes the pressure-time curves were straight lines, and at other times curves decreasing in slope and gradually approaching a constant pressure value. It was soon found that the straight lines were only obtained when a new glass reaction chamber was used, or when the chamber had been exposed to the atmosphere for some considerable time. Beginning with a new chamber, the straight line type of decomposition was obtained for the first two or three experiments, the next experiment would be of an intermediate character, and after this the second type of curve would be obtained. This final type of curve could be repeated as many times as desired. Now a straight-line time-pressure curve for decomposition indicates that the rate of the reaction is independent of the concentration of the reacting gas. The usual cause of such behaviour is to be sought in a surface reaction, and this would seem highly probable, on account of the change in the nature of the reaction, after the surface had been out of contact with the air for some time. A varying sensitivity of silica surfaces has been noted by Hinshelwood and Burk in the thermal decomposition of ammonia. A possible explanation of the observed phenomenon is that glass, in its original state, possesses the property of catalytically decomposing ammonia under the influence of cathode rays, and that this property is destroyed by prolonged exposure to ammonia, hydrogen or nitrogen. The experiments about to be described were all carried out with the glass vessel in the final non-active state.

---

* 'Ann. d. Physik,' vol. 21, p. 879 (1906).

The Decomposition of Pure Ammonia.

The first series of experiments to be carried out under the conditions described above was designed to test the effect of varying the voltage applied to the tube. In these experiments the pressure of the ammonia gas—*i.e.*, its concentration—was kept constant: the current passing through the cathode-ray tube was also constant. The pressure of the ammonia was 1 mm., and the tube current 0·2 m. amp. The general type of pressure-time curve is shown in fig. 2: the pressure, which rose rapidly at first, gradually tended to a fixed value, beyond which it did not increase. Since the pressure change which accompanied decomposition was known from the equation

$$2NH_3 = N_2 + 3H_2,$$

it was very simple to calculate, from the increase of pressure, the quantity of

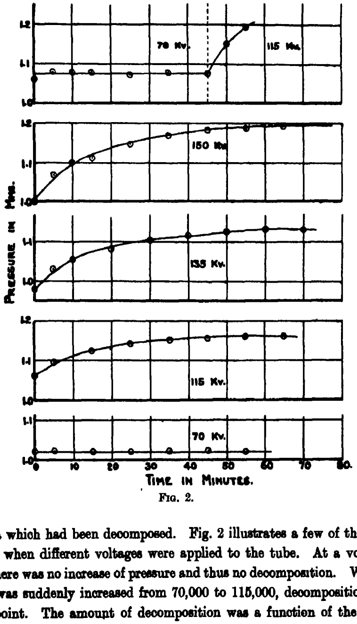

FIG. 2.

ammonia which had been decomposed. Fig. 2 illustrates a few of the curves obtained when different voltages were applied to the tube. At a voltage of 70,000 there was no increase of pressure and thus no decomposition. When the voltage was suddenly increased from 70,000 to 115,000, decomposition set in at this point. The amount of decomposition was a function of the applied voltage. Table I gives details of the results thus obtained.

Table I.

Voltage	50	70	100	115	135	150	165 thousand volts
Pressure of NH_3	1·06	1·02	1·01	1·06	0·98	0·99	1·02 mm.
% decomposition	0	0	5·5	9·6	15·3	19	24·5

These measurements give the somewhat surprising result that the percentage decomposition of the ammonia is a linear function of the voltage applied to the cathode-ray tube. This is well illustrated by the graph of fig. 3. An extrapolation of the straight line to the axis of zero decomposition gives a critical value of voltage of 82,000 volts. One might expect that this critical voltage was the voltage required to bring the electrons through the window of the tube. Confirmation of this view was obtained by making " blue print " pictures of the electron beam in the manner described by Coolidge. When the voltage applied to the tube was 80,000, no impression was obtained on the sensitive paper, whilst an applied voltage of 85,000 gave a distinct picture of the electron beam.

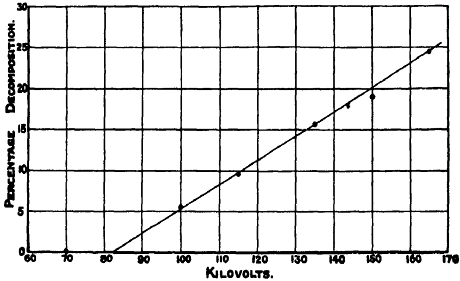

Fig. 3.

The second series of experiments was a test of the variation of the decomposition with the pressure of the ammonia, the value of the applied voltage and the filament current being constant. Their values were 115,000 volts and 0·2 m.amp. respectively. Time-pressure curves of the type described were obtained, and details of the results are given in Table II.

Table II.

Pressure	0·68	0·85	1·06	1·29	1·60	2·24	2·58	3·26	4·07 mm.
% decomposition	29·4	15·2	9·6	8·1	6·1	4·0	3·1	2·4	0

These results are illustrated graphically in fig. 4. It will be seen that the amount of decomposition was very sensitive to pressure changes. At low pressures—0·68 mm.—it was comparatively large, and was changing rapidly. It was impossible, with the McLeod gauge used, to obtain results at pressures much lower. At higher pressures, but still only a few millimetres of mercury, it was impossible to obtain evidence of any decomposition.

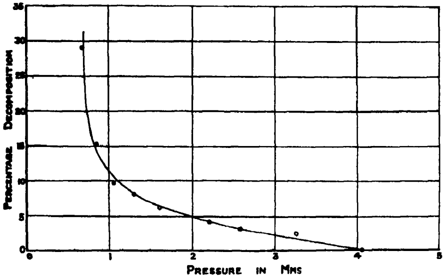

FIG. 4.

Let us consider the decomposition process as presented by the time-pressure curves of fig. 2 in greater detail. When the action begins—*i.e.*, for $t = 0$—the speed of the change of pressure is a measure of the speed of the action

$$NH_3 \rightarrow N + 3H$$

assuming that any formation of molecular hydrogen or nitrogen proceeds at a much greater rate. At later stages of the action other processes are set up, *e.g.*, the reverse action

$$N + 3H \rightarrow NH_3$$

and also possibly a retarding action of the nitrogen, the hydrogen, or of both, upon the decomposition of the ammonia. Thus at any point after a time, x, the speed at which the action is proceeding is the resultant of the speeds of these various actions. Now the measure of the speed of the action at the time x is given by the tangent to the time-pressure curve at this point. Thus the tangent to the curve at the time 0, or at the point where the primary action is free from these secondary effects, will be a measure of the speed of the primary decomposition. The change of pressure, over short time intervals during the first stages of the decomposition, was determined from the curves, and these rates of change plotted against the quantity of decomposed ammonia. The rate of change for zero decomposition was then determined by extrapolation. In this way the following figures were obtained :—

Table III.—Variation of Speed of Decomposition with Pressure of Ammonia.

Pressure of NH_3	0·68	0·85	1·06	1·29	1·60	2·24	2·58	3·26 mm.
dp/dt mm. per min.	0·070	0·075	0·062	0·065	0·060	0·065	0·065	0·065

Mean dp/dt = 0·066.

Table IV.—Variation of Speed of Decomposition with Applied Voltage.

Applied voltage	100	115	135	150	165 thousand volts.
dp/dt mm. per min.	0·042	0·062	0·072	0·090	0·105

It is thus to be seen from these tables that, with an electron beam of constant speed and intensity, the rate of the primary decomposition is independent of the pressure of the ammonia—that is to say, that each electron, having a definite velocity dependent on the constant applied voltage, is responsible for the decomposition of a definite quantity of ammonia molecules. In other words, the ratio

$$R = \frac{\text{number of ammonia molecules decomposed}}{\text{number of electrons causing decomposition}}$$

is independent of the pressure of the ammonia.

From the second set of values (those for the experiments carried out at constant pressure with electrons of different speeds) it is to be seen that this ratio increases with the speed of the electrons.

These facts are, qualitatively at least, in agreement with the data on the composition of the equilibrium mixture. Consider first the experiments at constant voltage. The speed of the decomposition of the ammonia is independent of its pressure. Now equilibrium will be attained when the speed of the reverse action becomes equal to this speed of decomposition. The speed of this reverse action will be proportional to the number of collisions between the H and N atoms, *i.e.*, proportional to the amount of these atoms, or to the pressure of the ammonia. Hence, as the pressure increases the speed of re-combination will increase, and thus the quantity of ammonia in the equilibrium mixture will increase. In the case of the experiments at constant pressure and increasing electron speed, the rate of the decomposition increases with the speed of the electron, whilst we may assume that the rate of reunion is a process affected only slightly, or not at all, by the electrons, and that it will thus remain constant. Thus the amount of ammonia in the equilibrium mixture will decrease with increasing electron speed.

The Effect of the Decomposition Products on the Course of the Decomposition.

As described above, the effect of the presence of hydrogen and nitrogen in the proportion of three volumes to one is to cause a stopping of the reaction and the establishing of an equilibrium. It will therefore be of interest to investigate the effect of adding either nitrogen or hydrogen to the gas mixture. Mixtures of hydrogen and ammonia and of nitrogen and ammonia were made and submitted to the action of cathode rays produced when 115,000 volts were applied to the tube. The tube current was again 0·2 m. amp. Experiments were carried out at various pressures, and the results compared with those previously obtained for pure ammonia under these same conditions. Table V gives the values obtained using a mixture of ammonia and nitrogen containing 14·1 per cent. of nitrogen.

Table V.

Total pressure	0·81	1·10	1·37	2·2 mm
Part pressure of NH_3	0·70	0·95	1·18	1·99 mm.
% decomposition	33·0	20·0	13·1	7·4

Table VI gives similar results obtained using a mixture of ammonia and hydrogen containing 9·1 per cent. of hydrogen.

Table VI.

Total pressure	0·65	0·77	0·99	1·25	1·64 mm
Part pressure of NH_3	0·59	0·70	0·90	1·13	1·49 mm
% decomposition	15·0	12·9	8·4	5·5	0·9

These values are illustrated by fig. 5, where the percentage decompositions are plotted against the reciprocals of the pressure of the ammonia. The presence of excess nitrogen has the property of increasing the quantity of ammonia decomposed when the equilibrium has been established, whilst the presence of excess hydrogen decreases the amount of decomposition. It is therefore at once evident that the ordinary laws of mass action do not apply to this equilibrium, since both an excess of hydrogen and an excess of nitrogen would result in there being a small quantity of ammonia decomposed when the equilibrium was established. This result may be compared with that of Le Blanc and Davis, who found that in the decomposition of ammonia by the silent electric discharge the mass laws could not be applied, and that the presence of excess hydrogen decreased the speed of decomposition, whilst the presence of excess nitrogen increased it. Further light can be thrown on the specific effects of the excess of hydrogen or of nitrogen by determining their effects on the primary decomposition process by the method already used in the case of pure ammonia. Table VII gives the results so obtained.

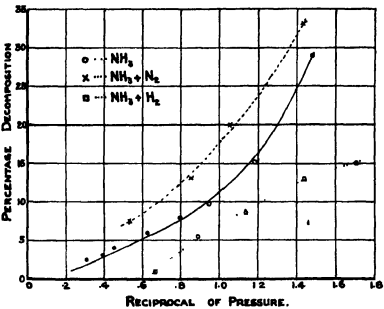

FIG. 5

Table VII.

Excess of nitrogen (14·1 per cent.).		**Excess of hydrogen (9·1 per cent.).**	
Part pressure of NH_3.	$\frac{dp}{dt}$	**Part pressure of NH_3.**	$\frac{dp}{dt}$
mm.		mm.	
0·70	0·065	0·65	0·029
0·95	0·060	0·70	0·020
1·18	0·067	0·90	0·024
1·99	0·070	1·25	0·018
Mean = 0·065.		**Mean = 0·023.**	

It is again to be seen that the speed of the decomposition is independent of the absolute value of the gas pressure, and that the presence of extra nitrogen has no effect on the speed. Just as in the previous experiment, the addition of extra ammonia—*i.e.*, increasing the pressure from 0·68 to 3·26 mm.—had no effect on the speed of decomposition, so is the extra nitrogen quite inert. In the case, however, of additional hydrogen, the result is different; the diluent is no longer inert, the speed of decomposition is decreased. The amount by which the speed is decreased is constant for mixtures containing the same proportion of hydrogen.

I desire to acknowledge my indebtedness to the National Research Council of Canada and to the Carnegie Corporation for aid in helping me to meet the cost of this investigation.—J.C.M.

An Investigation of the Absorption Spectra of Water and Ice, with Reference to the Spectra of the Major Planets.

By Prof. J. C. McLennan, F.R.S., R. Ruedy, D.Sc., and A. C. Burton, M.A.

(Received June 28, 1928.)

[Plates 8–10.]

The spectra of the light of the sun reflected from the major planets—Jupiter, Saturn, Uranus and Neptune—were photographed by Slipher* in 1909. These spectra showed a general similarity in that there were a number of absorption bands superimposed on the ordinary solar spectrum. The intensity and width of these absorptions varied from planet to planet, increasing in general from Jupiter to Neptune in the order quoted. Of the chemical identity of the bands little is known. Some—C and F, fig. 4, for example—can be attributed to absorption by atomic hydrogen in the atmospheres of the planets; others might be due to water-vapour, though other water-vapour bands do not appear. The outstanding unidentified bands† which are common to the spectra of the four planets are (see fig. 4, Plate 10):—

(*a*) At $\lambda = 5430$ Å.—A rather weak band in the spectra of Jupiter and Saturn, but very strong in those of Uranus and Neptune

(*b*) At $\lambda = 6190$ Å.—This is the mid-point of a conspicuous and dense band appearing in the spectra of all the four planets, broadening from a width of some 50 Å in that of Jupiter to some 200 Å in that of Neptune. Although quite strong in the spectrum of Jupiter, it showed no tendency to become resolved in the high dispersion plates taken of the spectrum of this planet.

(*c*) A strong double band at $\lambda = 7200$ to 7260 Å recorded in the spectra of Saturn and Jupiter, and probably just as strong in those of Uranus and Neptune, but not recorded because of the insensitiveness of the plates in this region.

About these three bands Slipher says: " There is no hint as to the identity of the band at λ 5430 or of that at λ 6190. The band at λ 7200 is practically coincident with the strongest band of water-vapour, but, as none of the other water-vapour bands are visible in the spectra, the quantity of water on these planets is at most only comparable with that in the telluric air."

---

* 'Lowell Observatory Bulletin,' No. 42 (1909).

† There is a strong unidentified band at $\lambda = 5762$ Å in the spectrum of Neptune. It appears in the spectrum of Uranus as well, but Slipher states it is to be seen on only a part of his plates for Jupiter and Saturn.

The Absorption of Water.

As a starting point in the investigation, the absorption of water was examined.

Abney,[*] in 1883, investigated the absorption of water in cells up to 2 feet in thickness, using a thermocouple, for the purpose of comparison with the solar thermograms obtained by Langley. His curves show absorption maxima at $\lambda = 7200$ Å and a slight maximum at $\lambda = 6200$ Å, even with $\frac{1}{8}$-inch of water only. The latter band has been observed and noted visually by Russell and Lapraik,[†] using 14 feet of water. The most complete investigation was made by Aschkinass[‡] in 1895, using a bolometer. He obtained curves of absorption using different thicknesses of water from a few centimetres up to 100 cms. The curve for 100 cms. of water shows a maximum at $\lambda = 6100$ Å, and, in addition, smaller maxima at $\lambda = 5550$ and 5150 Å, though the absorption here is very slight. Hufner and Albrecht,[§] working with 125 cms. of water, used a visual comparison method, but obtained a steady increase of transmission coefficient rather than maxima of absorption. There have been numerous measurements on the water-vapour and water bands in the infra-red at $0 \cdot 81\,\mu$ and longer wave-lengths, and most of these bands have been resolved into their components by Sleator and Phelps,[||] Hettner,[||] Collins[||] and Witt [||] The ultra-violet bands have been examined by Jack [¶]

It was evident that there was a possibility of identifying the band at 6190 Å in the planets with an absorption band of water As the latter apparently had not been recorded photographically it was thought desirable to take photographs of a continuous spectrum through considerable lengths of water, and to compare the results with the planetary spectra.

The source used was a "Pointolite" lamp, which gives a spectrum that is completely continuous in the visible region. The spectrograph was a constant deviation instrument made by The Adam Hilger Co. Ilford panchromatic plates were used in the first instance.

---

[*] 'Roy. Soc. Proc.,' A, vol. 35, p. 330 (1883).

[†] 'J. Chem. Soc.,' vol. 21, p. 168 (1881).

[‡] 'Ann. Phys. Chem.,' vol. 55, p 401 (1895).

[§] 'Ann. Phys. Chem ,' vol. 42, p 1 (1891).

[||] Sleator, 'Astrophys. J.,' vol. 48, p. 125 (1918); Sleator and Phelps, 'Astrophys. J.,' vol. 62, p. 48 (1925); Hettner, 'Ann. d. Physik,' vol. 55, p. 476 (1918); Collins, 'Phys Rev.,' vol. 20, p. 486 (1922); Witt, 'Z. f. Physik,' vol. 28, p. 249 (1924).

[¶] 'Roy. Soc. Proc.,' A, vol. 115, p. 373 (1927).

A photograph taken through 100 cm. of distilled water showed no distinct absorption band in the region studied. A glass tube 4 metres long was then used. The photographs obtained are shown in Plate 8, fig. 1. (*a*) is the Neon spectrum, which is used for comparison throughout the photographs; (*b*) is the spectrum of the light through 4 metres of water, and (*c*) was obtained with the tube empty and the same time of exposure; (*d*) and (*e*) are from exposures with the tube full and empty respectively, the relative times of exposure being adjusted to give the same density in the green, in order to see if any absorption band were visible there.

A glass tube giving a column of water 21·5 metres long was then constructed and used. The results are shown in Plate 8, fig. 2. A comparison with the tube empty is, of course, not possible here, as the same exposure would produce complete blackening of the plate. Various exposures were tried to see if any absorption in the green could be observed, but comparisons with the spectra through the empty tube show that the absorption band found by Aschkinass, if present, is too faint to be apparent photographically even with this length of water. (*b*) is one of such photographs (the comparison being Mercury). Green sensitive plates gave a similar negative result.

The photographs with 4 metres of water show a diffuse absorption band with its sharper edge at about $\lambda = 5990$ Å, extending to about 6350 Å. The centre of this band is coincident with that of the band in the planetary spectra; its breadth is a little greater than that in the spectrum of Neptune, but considerably broader than in the spectra of the other planets. With the longer column, the short wave-length edge is shown much more distinct and sharp at about $\lambda = 5995$ Å, the other edge not being distinctly visible. There is the edge of a second band at about 6550 Å, which seems to coincide with an absorption strong in the spectra of Neptune and Uranus, but weak in those of Saturn and Jupiter.

Slipher used Seed plates that had been sensitised by dyeing in a dicyanine solution. Eastman 40 plates, which closely correspond, were therefore sensitised in a bath containing dicyanine and ammonia, the usual formula and method of operation being used (see Scientific Papers of Bureau of Standards, No. 422, 1921). The bathing rendered the plates sensitive up to about 7600 Å.

Plate 10, fig. 4, shows the spectra obtained by Slipher, and beneath is a photograph taken through 4 metres of water on a sensitised plate. The similarity of the two bands visible on the plate to those in the spectrum of Neptune is obvious. The second band (whose edge was visible on the panchromatic plates) is seen to extend from about 6560 to 6700 Å. Then there is a bright place on the spectrum, with its centre at about 6800 Å, and the edge of a heavy band beginning at about 7000 Å.

In the spectra of both Uranus and Neptune, and to a less degree in those of the others, there is a broad band at 6670 Å, which is practically coincident with a bright place in the water spectrum. In addition, there is in the spectrum of Neptune a strong broad band starting at 7020 Å ; it is present faintly in the spectra of Jupiter and Saturn, and probably in that of Uranus, though here the spectrum is too faint for certainty. This may be identified with the edge of a third band obtained with water at 7000 Å. The lower plate shows the sensitivity of the dicyanine bathed plates. As can be seen, there is quite a pronounced maximum sensitivity at about 7000 Å.

The uncertainty of the results obtained with the use of dicyanine is well known, and it is thought that the small apparent shifts of intensity may be attributed to the action of the dye, as well as to the differences in the intensity distributions of the source used in the laboratory and of sunlight It is believed that the broad heavy absorptions in the red, at any rate in Uranus and Neptune, are identical with those of water.

The band at 5430 Å in the green remains unidentified. It is seen that although Aschkinass obtained maxima of absorption in this region using 1 metre of water by a radiometric method, photography with as much as 21·5 metres of water was unable to show such maxima. The absorptions of very great thicknesses of water have been observed by the lowering of instruments into the sea and lakes, by Aitken,* Bertel,* Aufsess,* Vogel,* Pietenpol,* and others. The methods used were, in general, rough observation only, the aim being in many cases other than purely physical. None of the later observers record selective absorption in the green, but Vogel, 1895, observed that in the light of the " Blue Grotto " there was a strong absorption between the Frauenhofer lines E and *b* (5270 and 5170 Å). On the other hand, Bertel records that the green light was present in depths up to 300 metres. The evidence points to the conclusion that though water may have a selective absorption in this region, the band at 5430 Å in the planets is not due to water.

---

* Aitken, 'Roy. Soc. Proc.,' Edin., vol. 11, p. 472 (1882); Bertel, 'Bull. de l'Inst. Oceanog.,' Monaco, No. 219 (1911); Aufsess, 'Inaug. Diss.,' München (1903), Vogel, 'Pogg. Ann.,' vol. 6, p. 325 (1875), and vol. 54, p. 175 (1895); Pietenpol, 'Trans. Wisconsin Acad. Sci.,' vol. 19 (1918).

The Absorption of Ice.

Until 1914 it was thought that the extremely vigorous circulation of the atmospheric clouds of the major planets must indicate very high temperatures, but the delicate radiometric measurements of Coblentz have shown on the contrary that the surface temperature is probably as low as − 140° C. Russell* suggests that there is a warmer temperature at the surface of the planets, and that their atmospheres contain layer upon layer of clouds of condensed gases, such as carbon dioxide, at levels where the temperature is appropriate.

It was thought of interest, therefore, to obtain photographs of the absorption of ice in the visible region, to see if they showed marked differences from those of water, and which of the two more nearly resembled the planetary spectra

Saunders,† in 1899, was the first to study the absorption of ice from the visible to $3 \cdot 2\ \mu$ Bode,‡ in 1909, found that it absorbed 93 per cent. of the energy at $1\ \mu$ with a thickness of only 0·01 cm. Plyler,§ in 1924, using a bolometer, investigated the infra-red absorption from $0 \cdot 7\ \mu$. He found that the bands of water-vapour and of water were present, but were shifted towards the longer wave-lengths. He looked upon it as confirming Sutherland's|| suggestion that water is a mixture of $(H_2O)_2$ and $(H_2O)_3$, and that ice is $(H_2O)_3$.

It was found impossible to obtain great lengths of natural ice that were sufficiently clear, or to freeze a column of clear ice, so a number of blocks of artificial ice, each a little over a metre in length, were used. When the faces of these had been rendered clear and plane by the application of a hot steel plate, and they were placed end to end, they were found to transmit a remarkable amount of light. Photographs of the spectrum of the source were taken through 4 metres, 8 metres and 14 metres of ice. No estimate of the actual absorption coefficients can be made from the photographs, as the loss of light by scattering and reflections at the faces of the blocks was large. Plate 9, fig. 3, shows the result.

There is a very marked difference from the absorption by water, as will be seen on comparison of fig. 3 (*d*) with fig. 2 (*a*) The absorption by ice has no distinct edge, but gradually increases. There is evidently a considerable shift of the absorption bands towards the longer wave-lengths, there being

---

* 'Scientific American,' p. 312 (1927).

† 'Johns Hopkins Univ. Circ.,' No. 140 (1899).

‡ 'Ann. d. Physik,' vol. 30, p. 326 (1909).

§ 'J. Opt. Soc. of America,' vol. 9, p. 545 (1924).

|| 'Phil. Mag.,' vol. 50, p. 460 (1900).

in ice very little absorption in the region where, with water, the absorption is very strong.

Fig. 5 shows the curves given by a Moll microphotometer with the various

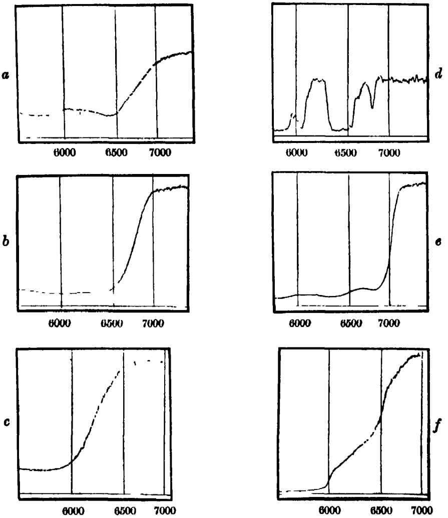

Fig. 5.

plates. (*a*) is that for 4 metres of water, (*b*) for 4 metres of ice. It will be seen that the band, at 6100 Å with water, is present in the spectrum obtained with ice (though not obvious in the prints), but shifted towards the longer wave-lengths by some 200 or 300 Å. (*c*) is for 14 metres of ice, while (*f*) is for the 21·5 metres of water. The shift of intensity is again recorded. (*d*) is taken from Slipher's spectrum of Uranus, and (*e*) is for 4 metres of water with the sensitised plate.

Sutherland* arrived at his conclusions that water is a mixture of $(H_2O)_2$ and $(H_2O)_3$, and ice is $(H_2O)_3$ from considerations of a large number of the physical peculiarities of water He looked upon the melting of ice as a phenomenon of dissociation rather than one of a pure change of state The fact that ice contracts on melting while its latent heat is positive is an indication of the validity of his theory He calculated that the dissociation heat of $(H_2O)_3$ to $(H_2O)_2$ was 180 calories per gramme

Perrin† has fully discussed, and Franck‡ has accurately verified the relation for dissociation processes

$$h\, d\nu = D$$

where D is the dissociation energy per molecule Using for D the value given by Sutherland, we get for the shift of wave length

$$d\lambda = 400\ \text{Å},$$

which is, at any rate, of the order observed Thus dissociation may explain the observed displacement of the bands

Summary

The absorption of water has been taken with columns 4 metres and 21 5 metres long Using plates sensitised by dicyanine, three absorption bands have been photographed in the red each of which can be identified with bands in the planetary spectra

The absorption of ice has been found using lengths up to 14 metres There is a marked difference from that of water the intensities being shifted towards the longer wave lengths

It is concluded that the absorptions in the red common to the four major planets can be attributed to water, not as vapour or as ice, but in the liquid state Water vapour at very low temperatures might explain the absorption, but this can hardly be tested in the laboratory (the vapour pressure being so very low) How this absorption by liquid water can arise is not suggested The absorption in the green at 5430 Å cannot be attributed to water and its identity is unknown Search is being made for it in the absorption of certain liquefied gases

We wish to thank Dr Harold Jeffreys for suggestions in connection with this investigation One of us (J C M) desires to acknowledge his indebtedness to the National Research Council of Canada and to the Carnegie Corporation for aid in meeting the cost of this investigation

---

* *Loc cit.*

† Perrin, 'Ann de Physique,' vol 9, p 1 (1919)

‡ Franck, 'Z f Physik,' vol 43, p 155 (1927)

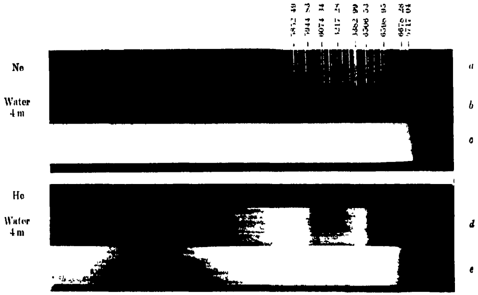

FIG. 1.

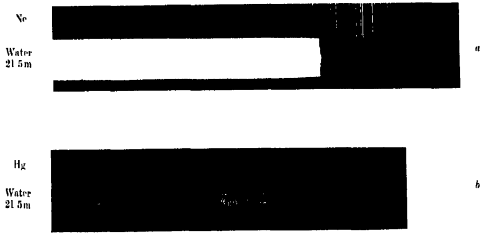

FIG. 2.

(*Facing p.* 302.)

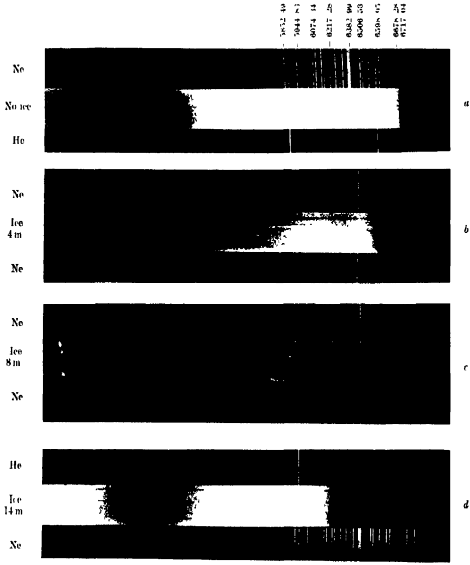

FIG 3.—Absorption of Ice.

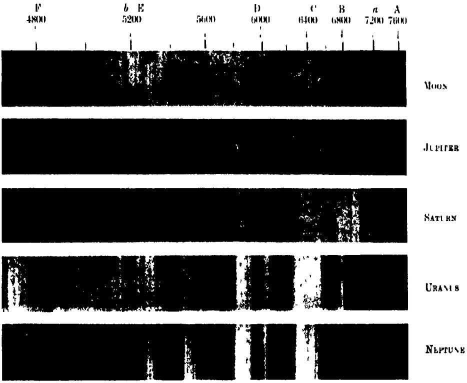

Fig 4a.—The Spectra of the Moon and the Major Planets

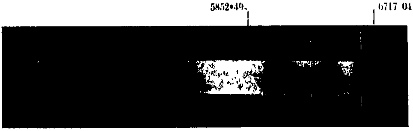

Fig 4b.—The Spectrum of Water.

Fig. 4c.—The Spectrum of Dicyanine.

On the Luminescence of Solid Nitrogen under Cathode Ray Bombardment *

By Prof. J. C. McLennan, F.R.S., H. J. C. Ireton, M.A., and E. W. Samson, M.A.

(Received June 28, 1928.)

[Plate 11.]

Introduction.

After the discovery by Vegard† of the luminescence which occurred in solid nitrogen under cathode ray bombardment at the temperature of liquid hydrogen, considerable interest was attached to it on account of his attempt to explain the well-known auroral green line as due to this luminescence under certain conditions in the upper atmosphere. His theory of the auroral line was not corroborated by the experiments of McLennan‡ and others, who showed that the line was due to oxygen. But the luminescence in solid nitrogen retained a very considerable interest as an outstanding example of the phenomenon of luminescence. From this point of view its spectrum and its properties were further studied in this laboratory where there were available all the necessary facilities for low temperature research. The investigation was commenced by McLennan, Ireton and Thomson,§ and the present research was a continuation of their work. Its object was to photograph the spectrum more completely, and to obtain further data in connection with the luminescence which might lead to an adequate explanation of the phenomena observed.

Apparatus for Producing the Luminescence.

The apparatus for producing the luminescence was with some few improvements in detail, the same as that described by McLennan, Ireton and Thomson.§ Use was made of a type of cathode ray tube designed by Dr. Coolidge,‖ of the General Electric Company. With such a tube it was possible to obtain

---

* One of the authors, Mr. E. W. Samson, is indebted to the National Research Council of Canada for the award to him of a Studentship that enabled him to participate in this research.

† 'Commun. Phys. Lab. Univ. Leiden,' No. 175; 'Ann. d. Physik,' vol. 79, p. 377 (1926).

‡ 'Roy. Soc. Proc.,' A, vol. 108, p. 501 (1925), and vol. 114, p. 766 (1927).

§ 'Roy. Soc. Proc.,' A, vol. 116, p. 1 (1927).

‖ 'J. Franklin Inst.,' vol. 202, p. 693.

high velocity cathode rays outside the generating tube. The essential details of the apparatus are shown in fig. 1.

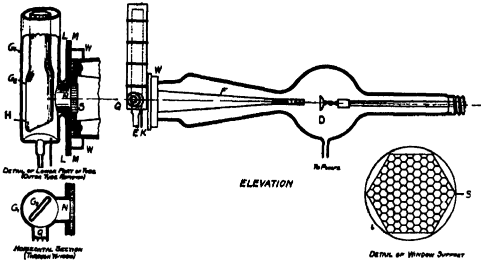
G₁
G₂
H
L M
W
N
S
W
L M
Q
W
F
E K
D
To Pumps
ELEVATION
S
Detail of Lower Part of Tube (Outer Tube Removed)
G₁
G₂
N
Q
Horizontal Section (Through Window)
Detail of Window Support

FIG. 1

In the cathode ray tube itself a high vacuum was maintained. The electrons were projected at a high voltage out of a hot tungsten filament at D. They travelled down the centre of the copper tube F, and passed right through a thin window of a nickel alloy foil at N,* into the outer chamber of the vacuum flask G_1. The tube was operated usually at a voltage near 150,000 volts, and with a current of about half a milliampere. These were supplied by a Victor Snook special transformer, with rotary rectifier, capable of giving voltages up to 200,000 and currents as high as 30 milliamperes.

Liquid hydrogen contained in the inner flask G_2 of a double-walled German silver flask, served to freeze nitrogen, which was passed between the two walls, on the outside of the inner wall. The electrons passed through the foil window N, impinged on the frozen nitrogen, and produced a bright yellow green luminescence. The bottom H of the inner flask was flattened and set at an angle of 45 degrees so that the luminescence could be observed or photographed through a quartz window Q, which was placed in the side of the outer wall of the flask. The outer chamber of the flask was kept evacuated during the operation of the apparatus. The nitrogen was produced by the action of ammonium chloride and sodium nitrite solutions when heated. The gas was passed through drying tubes of P_2O_5 and CaO and a liquid air trap before

---

* These foils were kindly given to me by Dr. Coolidge.—J.C.M.

I

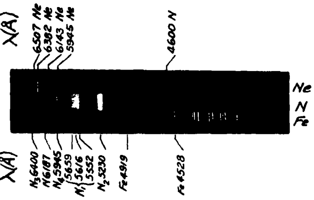

II

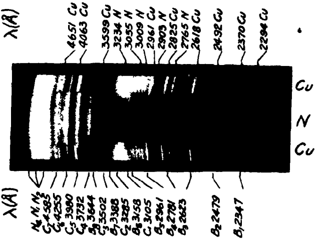

III

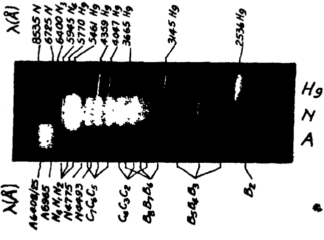

(*Facing p.* 1305.)

admission to the flask. Fresh nitrogen was admitted every half or three-quarters of an hour during an experiment.

The Luminescence Spectrum.

The spectrum of the luminescence from the solid nitrogen was photographed throughout the spectral region from 2000 A.U. to about 8600 A.U., by means of spectrographs of very high light power.

Spectrogram I (Plate 11) was taken with a small glass spectrograph having a direct vision prism. An exposure of 9½ hours was given using a panchromatic plate. The lower comparison is the iron arc spectrum, the upper is the neon discharge tube spectrum. The central spectrum is that of luminescent solid nitrogen. It shows the prominent visible bands denoted by Vegard with the symbols N_2, N_1, and N_4, namely, those at the mean wave-lengths 5230, 5609, and 5945 A.U. On the same plate there appears a very faint narrow band at 6187 A.U , and a broad band, also very faint, extending from 6360 to 6500 A.U., with its maximum intensity at 6400 A.U. This latter band is probably the one photographed by Vegard between 6320 and 6580, which he called N_3. In the blue there is a broad continuous band between 4300 and 4900 A.U. with its maximum at 4600 A U.

A strong band at 8535 A.U. was photographed on an infra red plate with the same spectrograph.

In order to get photographs over a large range of the spectrum, with moderate exposures, a small quartz spectrograph with a 60 degree prism was used. It gave spectrograms in fairly good focus over the whole range from 2000 to 8600 A.U., and had an F number about 2. Its low dispersion, as well as its small F number, rendered it a powerful instrument for the detection of bands. When it was in use the slit was made as wide as possible consistent with good definition, thereby further increasing the intensity of the bands on the plate. The measurements of the maxima of bands on photographs taken with such an instrument were, of course, subject to considerable error. Spectrograms II and III (Plate 11) were taken with this spectrograph.

Spectrogram II (Plate 11) shows two distinct series of bands, one series consisting of narrow bands extending down into the ultra-violet, the other consisting of broad bands degraded towards the red. The wave-lengths of the maxima in these series are given in Table II, with the wave-numbers and wave-number differences. The differences for each series decreases gradually towards the lower wave-numbers. The series of broad bands, denoted by C, was observed by Vegard* when the solid nitrogen was bombarded with canal rays, but the other series, denoted by B, was not. The comparison spectrum shown on each side of the nitrogen spectrum is that of the copper arc.

Table I.

A.U.		A.U.		A U		A.U.	
2347	B_1	3055		3732	C_4	5552	
2479	B_2	3105	C_1	3980	C_5	5616	N_1
2623	B_3	3158	B_6	4255	C_6	5659	
2765		3234		4493		5945	N_4
2781	B_4	3285	C_2	4585	C_7	6187	
2903		3388	B_7	4775		6400	N_3
2961	B_5	3502	C_3	5230	N_2	6725	
3009		3644	B_8			8535	

Table II.

B_1	2347	4259		C_1	3105	3220	
			226				177
B_2	2479	4033		C_2	3285	3043	
			222				188
B_3	2623	3811		C_3	3502	2855	
			216				176
B_4	2781	3595		C_4	3732	2679	
			219				167
B_5	2961	3376		C_5	3980	2512	
			210				162
B_6	3158	3166		C_6	4255	2350	
			215				170
B_7	3388	2951		C_7	4585	2180	
			208				
B_8	3644	2743					

Spectrogram III (Plate 11) was obtained with 11 hours' exposure on an infra red (neocyanin) plate, dyed with dicyanin to render it sensitive to the yellow and red regions to which it is ordinarily insensitive. The upper comparison is the spectrum of a mercury arc lamp, the lower is the spectrum produced in an argon discharge tube. In the red and infra red it shows the bands at 8535 and 6400 A.U., and a new band at 6725 A.U. The rest of the spectrum is the same as that on Spectrogram II.

All the bands which were observed are recorded in Table I.

Visual Observations.

The three strong bands N_1, N_2 and N_4 could be seen in a hand spectroscope. It was noted that the N_2 and N_4 bands had an appreciable period of decay, while the N_1 band appeared to vanish instantly the source of excitation was cut off. This observation was confirmed by viewing the glowing surface directly through colour filters which were capable of isolating each of the three bands. The colour was a strong yellow green during the excitation, which changed to blue green when the excitation stopped. The blue green then faded over a period of 2 or 3 minutes. If the solid nitrogen were allowed to warm up slightly after the luminescence had apparently ceased, however, the bands flashed out quite strongly again for a short time, and the N_1 band was present with the others. This always occurred when the liquid hydrogen evaporated. The appearance of the bands thus showed that they were all phosphorescent, since energy which could give rise to all of them was stored up during excitation. At liquid hydrogen temperature therefore the N_1 band was in the lower instantaneous state. At a little higher temperature it became thermoluminescent. As the temperature of the solid nitrogen rose gradually after the liquid hydrogen had gone, a point was reached where the luminescence effects disappeared totally, a short time before the nitrogen itself evaporated This was the upper temperature limit of the luminescence, and was therefore between the temperatures of liquefaction of hydrogen and melting of nitrogen, that is, between 21° K. and 62·5° K., and it was appreciably below the latter.

---

* *Loc. cit.*

The luminescence was viewed through a double image Wollaston prism to test for polarisation of the visible light. If there were any systematic polarisation a difference of intensity of the two images should have appeared at some point as the prism was rotated. No such effect was found. Colour filters were used to isolate each of the N_2 and N_4 bands. No effect was observed. Faint polarisation however, might have escaped observation by this method.

The Decay Curves.

Measurements were made on the rates of decay of the two strong bands N_2 and N_4 These measurements were made with a simple photometer for low brightnesses designed by Karrer and Poritsky,* at the Nela Research Laboratories, Cleveland, Ohio, and kindly lent to us by the latter. The instrument consisted of a Lummer-Brodhun cube through which the object and comparison light were viewed. The comparison light was from the interior surface of a paper fibre sphere which was diffusely illuminated by a small electric lamp. The intensity of the illumination could be altered by means of a variable aperture between the lamp and the surface. Scale readings of the size of the aperture could be taken, and the curve of relative depletion of the intensity with the scale readings was known. Colour filters were used which were capable of isolating each of the bands from all other bands which were strong enough to have an appreciable effect on the intensity. In making the measurements the photometer was directed towards the phosphorescent surface, and the colour filter was placed over the eyepiece. The photometer scale was set so that the variable aperture was wide open, and the strength of the comparison light was adjusted by means of a rheostat until there was a match of intensity with the phosphorescence a few seconds after the electron bombardment was stopped. The rheostat was then left at this position and readings were taken in the following manner. The photometer scale was set at a given reading, so that the illumination of the comparison field was determined. The solid nitrogen was bombarded for 10 seconds with the cathode rays at a definite voltage, then the bombardment was stopped and a stop watch started simultaneously. The watch was stopped when the intensity of the phosphorescence matched that of the comparison in the photometer field. The photometer reading and the time on the stop watch were recorded. Such readings were taken over the range of the scale of the photometer. Sets of such readings were taken for each of the band N_2 and N_4.

---

* 'J.O.S.A.,' and 'R.S.I..' vol. 8, p. 355 (1924).

The readings were plotted with the time as abscissa, and the relative intensity corresponding to the photometer reading, as ordinate, and a curve drawn.

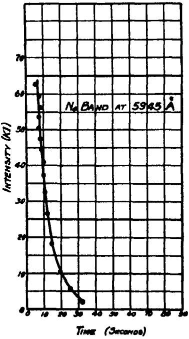

GRAPH I

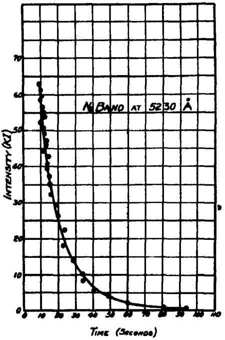

GRAPH II.

Such curves are shown in the graphs I and II, representing the decay of the N_4 and N_2 bands respectively. Representative points from these curves were then plotted with time as abscissa, and the reciprocal of the square root of the relative intensity as ordinate. Such curves, plotted from I and II are shown in graphs III and IV. The curves were seen to consist of two distinct sections, each being a straight line. Graph V, plotted in a similar manner from readings on the N_2 band at lower intensities, shows three straight lines of different slopes. Each straight line apparently represents a distinct process in the decay, following an equation of the form $I(a + bt)^2 = 1$, where I is the intensity, t the time, and a and b are constants which are different for each process. The upward breaks in the curves characterise what is known as the "vanishing type" of phosphorescence, as opposed to the "persistent type" in which the breaks are downward. Cathodoluminescence is usually of the "persistent type." The intensity scale in the graph V is different

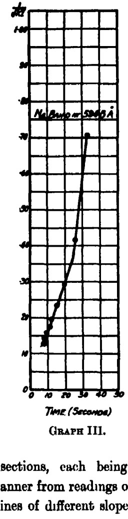

GRAPH III.

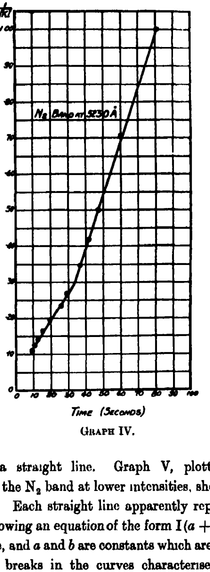

GRAPH IV.

from that in IV. On account of the lower intensity of the N_4 band it was uncertain whether there was a third section of the curve similar to that for the N_2 band. Apart from the characteristic form of the curves no definite relationships have been established.

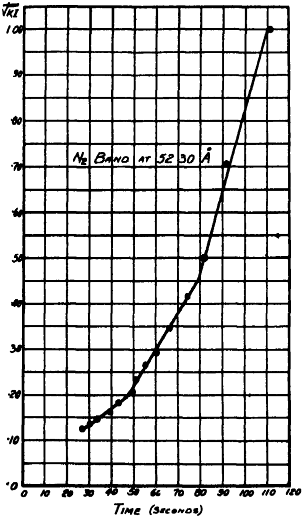

GRAPH V.

Possibility that the Luminescence is due to Hydrogen.

The presence of a small quantity of a metal in solid solution in a diluting medium often constitutes a phosphore, in which the phosphorescent spectrum is characteristic of the metal itself. This fact suggested the search for an impurity which might cause the luminescence in solid nitrogen. T. Tanaka[*]

---

[*] 'J.O.S.A.' and 'R.S.I.,' vol. 8, p. 316 (1924).

plotted a curve which showed, for a large number of metals, a relationship of the atomic weight to the average frequency difference of the two or more characteristic band series of the metal. The average frequency difference of the two band series which occur in solid nitrogen, when compared to this curve, was seen to be too high to correspond to any metal on the curve, but formed a reasonable production of the curve to the atomic weight of hydrogen. It did not correspond at all to the atomic weight of nitrogen. This, together with the fact that hydrogen was known to be present in our apparatus in small amounts during the experiments, indicated that hydrogen might have formed the active centre for the luminescence in solid nitrogen. Presence of adsorbed hydrogen in the solid nitrogen in such proportion as to constitute a phosphore would seem quite possible at such low temperature. The evidence is as yet, however, inconclusive.

Summary.

(1) The spectrum of the luminescence emitted when solid nitrogen was bombarded with high velocity electrons was photographed by means of spectrographs of high light power throughout the region from 2000 A.U. to 8600 A.U.

(2) In addition to the well-known bands N_1 at about 5609 A.U., N_2 at 5230 A.U., and N_4 at 5945 A.U., several bands were found in the red and infra red. One with its maximum at 6400 A.U., probably that designated by Vegard as N_3, was recorded with long exposures. A strong infra red band occurred at 8535 A.U., a red band at 6725 A.U., and a faint narrow band at 6187 A.U.

(3) In the region of shorter wave-lengths there were found two well-defined series of bands with nearly constant wave-number differences. There were also several other bands which did not fit into these series.

(4) It was shown that the bands N_1, N_2 and N_4, at 5609, 5230 and 5945 A.U. respectively were all phosphorescent bands, N_2 and N_4 being in the persistent state at liquid hydrogen temperature, while N_1 was in the lower instantaneous state, but appeared as thermoluminescence at a little higher temperature.

(5) There was no marked polarisation of the light of the visible bands.

(6) The rates of decay of the bands N_2 and N_4 were measured individually, and it was found that the phosphorescence of each belonged to the "vanishing type." There were two distinct stages in the decay of N_4, three in the decay of N_2. Each stage fitted an equation of the form $I(a + bt)^2 = 1$ where I represents the intensity, t the time, a and b constants.

(7) If the phosphorescent light was due to an active metallic centre in a diluting medium, then the large frequency differences in the two band series suggests hydrogen as the active centre.

Further Investigations of the Spectrum of Singly-Ionised Carbon (C II).

By A. FOWLER, D.Sc., F.R.S., Yarrow Research Professor of the Royal Society, and E. W. H. SELWYN, B.Sc., Imperial College, South Kensington.

(Received July 4, 1928.)

Introductory.

In a previous paper* it was shown that a considerable number of lines attributed to singly-ionised carbon (C^+ or C II) could be arranged in a regular system of doublet series, involving transitions of a single electron. Numerous lines which appeared to belong to C II remained unclassified, but further analysis of the spectrum has been greatly facilitated by subsequent theoretical developments. In accordance with Hund's theory, quartet as well as doublet terms are to be expected, and several of these additional terms have now been identified. The present communication gives an account of the newly classified lines, and includes improved measurements for some of the lines previously considered.

Observational Data.

The wave-lengths of most of the additional lines involved in the present discussion were determined in the course of the investigation of the doublet system. The sources included the spark between graphite poles in air, the spark in hydrogen, the arc *in vacuo*, and vacuum tubes of carbon dioxide. In the spark at atmospheric pressure, most of the lines are too diffuse for accurate measurement and wave-lengths were consequently determined chiefly from vacuum tubes. The vacuum tube spectra of oxygen under similar varied conditions served for the elimination of lines due to oxygen in the CO_2 spectra.

By comparing spectra produced under different conditions of pressure and strength of discharge, the lines representing successive stages of ionisation could be sorted out with considerable certainty. In many cases the assignment of lines to C II was confirmed by their behaviour in the spark in air, since lines representing the higher stages of ionisation do not appear on the less refrangible side of λ 2300 in this source. As previously observed by Lockyer, Baxandall and Butler, however, some of the lines of C III in this region are brought out when the carbon spark is passed in an atmosphere of hydrogen.†

---

* A. Fowler, 'Roy. Soc. Proc.,' A, vol. 105, p. 299 (1924).

† 'Roy. Soc. Proc.,' A, vol. 82, p. 541 (1909).

In the spark spectrum, it may be noted, lines of carbon are readily distinguished from lines of nitrogen and oxygen by using a rather long spark gap, so that the carbon lines are localised near the electrodes while the gas-lines extend right across the gap.

An additional source which has been employed is the "vacuum spark" or "hot spark." In the ordinary region of observation this has been found to be about equivalent to the carbon spark in hydrogen, which, as already remarked, includes the more prominent lines of C III as well as lines of C II. Lines of C IV, in this region of the spectrum, are readily obtained in vacuum tubes, as first observed by Merton.* In the region of short wave-lengths a strong condensed spark in hydrogen has been found to give all the lines which have been recorded in the vacuum spark, and to exhibit the chief lines of C IV with as great a relative intensity as has been recorded by Millikan in the "hot spark." In vacuum tube spectra it is not uncommon to find the C IV doublet at λ 1550 of intensity similar to that of the C I triplet on its longer wave-length side, and in some photographs it has been found of much greater intensity. It appears that where vacuum tube observations are convenient, they should be of greater experimental value on account of their wide range and comparative ease of operation.

The most convenient source for observations of C II in the region of short wave-lengths is the vacuum arc; in this case the C I and C II lines are strongly developed, whilst only the more fundamental lines of C III appear with any considerable intensity, and even the "D" lines of C IV at λ 1550 are relatively feeble. As a comparative source, the carbon spark in hydrogen, with varying amounts of self-induction, provided useful confirmation of the classification of lines according to the different stages of ionisation; spectra ranging from predominant C I and C II to predominant C III and C IV were obtained in this way over the region λ 2000 to λ 1200, which is the limit when a fluorite window is interposed between the sparking tube and the slit of the vacuum spectrograph. With the vacuum arc as source, the fluorite window being removed, photographs have been taken as far as λ 800, some of them in the second and higher orders of the grating. The 1-metre concave grating in use was ruled at the National Physical Laboratory and gives extremely good definition and resolution—the C I triplet at λ 1561 is readily resolved into its three components in the first order—but no lines have been obtained of wave-length shorter than λ 800 with this instrument.

Important contributions to the investigation of the spectrum of C II have been made by Bowen in his classification and remarkably accurate measurements of lines in the extreme ultra-violet.[*] These measurements have been adopted so far as they go, and have been used as standards for additional determinations. Some of the lines which occur in the visible spectrum of C II have also been classified by C. Mihul,[†] in agreement with the results which had already been obtained in the course of the present investigation.

---

* 'Roy. Soc. Proc.,' A, vol. 91, p. 498 (1915).

Most of the brighter lines in the region less refrangible than λ 2300 have been measured in the first order of a 10-foot grating and several of them in the third order. From λ 2300 to λ 3900 other lines were measured on photographs taken with Hilger's large quartz spectrograph (E.1) and from λ 3900 to λ 7300 with glass spectrographs of large dispersion. Some of the lines in the red which have been found to form multiplets, however, are very faint and the wave-lengths of such lines are probably subject to considerable errors. A specially adjusted quartz spectrograph by Bellingham and Stanley, obtained with the aid of the Government Grant Committee, has also been used for the region λ 1840 to λ 2300.

Predicted Terms.

Most of the terms of C II may be considered as arising from the addition of an electron, in various orbits, to a C III core. The configurations corresponding with the deepest terms of C III, and Bowen's term values are as follows :—

Configuration.				Terms.
1_1	2_1	2_2		
2	2		$1s^2\,2s^2$	$2s\,{}^1S_0$ 375463
2	1	1	$1s^2\,2s\,2p$	$2p\,{}^3P_1$ 331939 ; $2p\,{}^1P_1$ 273110

It should be remarked that while there are good grounds for the value assigned to $2p\,{}^3P_1$ the other values depend upon the identification of λ 2297 (ν 43524) with ${}^1S_0$—${}^3P_1$, and there is at present no confirmation of this assignment. The terms ${}^1S_0$ and ${}^1P_1$, however, are probably correct relatively to each other.

The series dealt with in the previous paper are derived by the addition of an electron to the core in its most stable state ($2s\,{}^1S$). The corresponding configurations and terms are shown under A in Table I, where the previous notation has been modernised as shown below.—

---

[*] 'Phys. Rev.,' vol. 29, p. 231 (1927).

[†] 'C.R.,' vol. 184, p. 1648 (1927).

Previous notation.	Present notation.
$2\ (1)\ \pi_1$	$2p\ {}^2P_2$
$2\ (1)\ \pi_2$	$2p\ {}^2P_1$
$3\ (2)\ \sigma$	$3s\ {}^2S_1$
$3\ (2)\ \delta_1$	$3d\ {}^2D_3$
$3\ (2)\ \delta_2$	$3d\ {}^2D_2$
$4\ (3)\ \phi_1$	$4f\ {}^2F_4$
$4\ (3)\ \phi_2$	$4f\ {}^2F_3$
x	$2p'\ {}^2S_1$

A second family of terms arises when the fifth electron is added to a C III core in the $2p\ {}^3P$ state. This includes quartet and doublet terms as shown under B in Table I. The terms of this group are conveniently distinguished by "priming" the electron symbols which are used as prefixes to the term symbols, as in previous papers.*

Other doublet terms, arising from the addition of an electron to a C III core in the $2p\ {}^1P$ state, are also possible. From $3s'$ downwards these would be similar in type to the doublet terms tabulated for the ${}^3P$ state of the core but none of these has been identified, and they are not included in the table.

Still another group of terms, as found by Bowen in the spectrum of the similarly constituted atoms of N III, corresponds to a displacement of both the 2_1 electrons to 2_2 orbits, as shown under C in Table I. The system of double primes which has become generally familiar does not appear to be completely applicable to this group, and the terms are accordingly distinguished by the prefix $2p^3$.

The combinations to be expected are indicated by the rules for electron transitions; namely, $\Delta k = \pm 1$ for one electron, and, if there are simultaneous transitions of two electrons, $\Delta k = 0$ or 2 for the second ($k = 1, 2, 3, \ldots$ for $s, p, d, \ldots$). They are most conveniently shown by the diagram at the corner of the table, but it should be noted that combinations are further restricted by the selection rule for inner quantum numbers, *i.e.*, $\Delta j = \pm 1$ or 0, with $0 \rightarrow 0$ forbidden. Combinations of terms connected by broken lines are possible, but are unlikely to be of any great intensity.

In Table I the electron configurations are exhibited first in the usual tabular

---

* 'Roy. Soc. Proc.,' A, vol. 117, p. 317 (1927), and vol. 118, p. 34 (1928).

Table I.—Predicted Terms of C II.

	K	L		M			N				O		Electrons outside rare gas shell.	Adopted prefix.	Terms.	*Combination Possibilities.*
	1_1	2_1	2_2	3_1	3_2	3_3	4_1	4_2	4_3	4_4	5_1	5_2				
A	2	2	1										$2s^2$ $2p$	$2p$	^2P	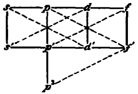
	2	2		1									$2s^2$ $3s$	$3s$	^2S	
	2	2			1								$2s^2$ $3p$	$3p$	^2P	
	2	2				1							$2s^2$ $3d$	$3d$	^2D	
	2	2					1						$2s^2$ $4s$	$4s$	^2S	
	2	2						1					$2s^2$ $4p$	$4p$	^2P	
	2	2							1				$2s^2$ $4d$	$4d$	^2D	
	2	2								1			$2s^2$ $4f$	$4f$	^2F	
	2	2									1		$2s^2$ $5s$	$5s$	^2S	
B	2	1	2										$2s$ $2p^2$	$2p'$	^4P	^2S ^2P ^2D
	2	1	1	1									$2s$ $2p$ $3s$	$3s'$	^4P	^2P
	2	1	1		1								$2s$ $2p$ $3p$	$3p'$	^4S ^4P ^4D	^2S ^2P ^2D
	2	1	1			1							$2s$ $2p$ $3d$	$3d'$	^4P ^4D ^4F	^2P ^2D ^2F
	2	1	1				1						$2s$ $2p$ $4s$	$4s'$	^4P	^2P
	2	1	1					1					$2s$ $2p$ $4p$	$4p'$	^4S ^4P ^4D	^2S ^2P ^2D
	2	1	1						1				$2s$ $2p$ $4d$	$4d'$	^4P ^4D ^4F	^2P ^2D ^2F
	2	1	1							1			$2s$ $2p$ $4f$	$4f'$	^4D ^4F ^4G	^2D ^2F ^2G
C	2		3										$2p^3$	$2p^3$	^4S	^2P ^2D

form, and again, omitting electrons belonging to the completed rare gas shell, in a form which is more convenient for writing; *e.g.*, $2s^2\,2p$ means that there are two electrons in the $2s$ or 2_1 level, and one in the $2p$ or 2_2. Terms which have actually been identified are printed in heavy type. In addition, the combination $2p'\,{}^4\mathrm{P}$—$2p^3\,{}^4\mathrm{S}$ has been identified by Bowen, but the terms themselves have not yet been evaluated.

Doublet Term Values.

In the revision of the regular doublet terms, no sufficient reason has been found to change the original values, except those which depended upon measurements of lines in the extreme ultra-violet, for which more accurate determinations have since become available through the work of Bowen. Thus the terms $2p'\,{}^2\mathrm{S}_1$ (previously "x") $= 100164\cdot9$ and $3s\,{}^2\mathrm{S}_1 = 80121\cdot12$ have been retained and utilised for amending the value of $2p\ {}^2\mathrm{P}$, giving $\mathbf{2p\,{}^2P_2} = 196595\cdot0$, $2p\,{}^2\mathrm{P}_1 = 196659\cdot0$. In deriving the $2p'\,{}^2\mathrm{P}$ terms from these the values have been slightly adjusted to accord with the $\Delta\nu$ more accurately determined from the combination $2p'\,{}^2\mathrm{P}$-$2p^3\,{}^2\mathrm{D}$. Higher doublet terms from the previous paper have been utilised for the identification of additional lines in the extreme ultra-violet; namely, $2p\,{}^2\mathrm{P}$--$5d$, $6d$, $7d\,{}^2\mathrm{D}$. The agreement between calculated and observed values is fairly satisfactory.

The $2p'$ doublet terms, and thence $2p^3\,{}^2\mathrm{D}$, it should be noted, have been determined from combinations with the main doublet terms, so that all the values assigned to doublet terms are in correct relation with each other. In other words, all these terms are referred to the limit ${}^1\mathrm{S}$ of the C III core.

The term $2p^3\,{}^2\mathrm{P}$ has not been identified; from the irregular doublet law, as applied to C II, N III and O IV, its value is estimated at about 25500, but corresponding combinations with $2p'$ doublet terms have not been certainly recognised.

Quartet Term Values.

There are three sequences of two terms each, from which the quartet terms can be calculated with reasonable accuracy by the use of the simple Rydberg formula. Thus, from the known differences of the respective pairs of terms, with $\mathrm{R} = 109737$, the following results are obtained:—

$$\begin{array}{ll}
\Delta\nu & \\
42586 & \left\{\begin{array}{l} 3s'\,{}^4\mathrm{P}_1 = 82850 \\ 4s'\,{}^4\mathrm{P}_1 = 40264 \end{array}\right. \\
31077 & \left\{\begin{array}{l} 3p'\,{}^4\mathrm{S}_2 = 64954 \\ 4p'\,{}^4\mathrm{S}_2 = 33877 \end{array}\right. \\
33064 & \left\{\begin{array}{l} 3p'\,{}^4\mathrm{D}_1 = 68123 \\ 4p'\,{}^4\mathrm{D}_1 = 35059 \end{array}\right.
\end{array}$$

$$3s'\,{}^4\mathrm{P}_1 - 3p'\,{}^4\mathrm{S}_2 = 17896$$
$$3s'\,{}^4\mathrm{P}_1 - 3p'\,{}^4\mathrm{D}_1 = 14727$$

If the calculated term values were entirely consistent, the differences shown on the right would have been equal to the observed lines $\nu = 17724$ and $\nu = 14730$ respectively. The deviations are not great, and the adoption of $3s\,{}^4\mathrm{P}_1 = 82850$ will clearly provide a basis for quartet term values which is probably not far from exact. It should be mentioned, however, that the terms $3d'\,{}^4\mathrm{P}_1$ and $4d'\,{}^4\mathrm{P}_1$, with $\Delta\nu = 21963$, when treated in the same way, yield term values nearly 1100 units smaller than those given by the other pairs of terms.

The terms which have now been identified and evaluated are collected in Table II, where wave-number separations of multiple terms are also indicated. As already remarked, the value of the deep term $2p'\,{}^4\mathrm{P}$ has not been found, for although Bowen has identified the combination $2p'\,{}^4\mathrm{P} \cdot 2p^3\,{}^4\mathrm{S}_2$ ($\nu = 98972$, etc.) neither of these terms has been recognised in other combinations. Hund's rule that of the terms arising from a given configuration, the one of highest multiplicity is usually the deepest, suggests that $2p^3\,{}^4\mathrm{S}_2$ is greater than $2p^3\,{}^2\mathrm{D}$ ($= 46196$), and consequently, since $2p'\,{}^4\mathrm{P}_3—2p^3\,{}^4\mathrm{S}_2 = 98973$, that $2p'\,{}^4\mathrm{P}$ is greater than 145170. It is somewhat disappointing that the intercombination $2p\,{}^2\mathrm{P}—2p'\,{}^4\mathrm{P}$, representing the two deepest terms of the spectrum, has not been found. The corresponding lines would be expected to have wave-numbers less than 51425, and thus to occur in a part of the spectrum which has been well explored.

Table II.—Terms of C II.

(A.)

$2p\,{}^2\mathrm{P}_1$	196659	64·0	$3s\,{}^2\mathrm{S}_1$	80121·12	$3d\,{}^2\mathrm{D}_2$	51109·01	1·45	$4f\,{}^2\mathrm{F}_{34}$	27679·95
${}^2\mathrm{P}_2$	196595				${}^2\mathrm{D}_3$	51107·56			
			$4s\,{}^2\mathrm{S}_1$	39424·57				$5f\,{}^2\mathrm{F}_{34}$	17702·54
$3p\,{}^2\mathrm{P}_1$	64934·32	11 13			$4d\,{}^2\mathrm{D}_2$	28535·08	0·41		
${}^2\mathrm{P}_2$	64923·19		$5s\,{}^2\mathrm{S}_1$	23310·82	${}^2\mathrm{D}_3$	28534 67		$6f\,{}^2\mathrm{F}_{34}$	12282·80
$4p\,{}^2\mathrm{P}_1$	34140·30	5·92			$5d\,{}^2\mathrm{D}_2$	18164·2			
${}^2\mathrm{P}_2$	34134·38								
					$6d\,{}^2\mathrm{D}_{23}$	[12558]			
					$7d\,{}^2\mathrm{D}_{23}$	[9193]			

Table II (continued).

(B.)

†$2p'$	$^4P >$ 145170		$^2S_1$ 100164 9		$^2P_1$ 86033·9	*41·2*	$^2D_3$ 121728·1	*1·2*
	$\Delta\nu$ *29 : 21*				$^2P_2$ 85992 7		$^2D_2$ 121726 9	
$3s'$	$^4P_1$ *82850·00	*23·76*					(^2P)	
	$^4P_2$ 82826·24	*44·97*						
	$^4P_3$ 82781·27							
$3p'$	$^4S_2$ 65126 01		$^4P_1$ 63389·68	*16·30*	$^4D_1$ 68120·20	*14 70*	^{2}(S P D)	
			$^4P_2$ 63373 38	*22·43*	$^4D_2$ 68105 50	*25·01*		
			$^4P_3$ 63350·95		$^4D_3$ 68080·49	*36 27*		
					$^4D_4$ 68044 22			
$3d'$	$^4P_3$ 50972·7	*−21·5*	$^4D_1$ 53258·5	*5 6*	$^4F_2$ 54063 9	*14 3*	^{2}(P D F)	
	$^4P_2$ 50951·2	*−14·2*	$^4D_2$ 53252 9	*8 7*	$^4F_3$ 54049 6	*19 6*		
	$^4P_1$ 50937·0		$^4D_3$ 53244·2	*10 3*	$^4F_4$ 54030·0	*27 6*		
			$^4D_4$ 53233·9		$^4F_5$ 54002 4			
$4s'$	$^4P_1$ 40264·44	*24·02*					(^2P)	
	$^4P_2$ 40240·42	*46·08*						
	$^4P_3$ 40194·34							
$4p'$	$^4S_2$ 34049·1		^4P [33100]		$^4D_1$ 35056·4	*14 3*	^{2}(S P D)	
					$^4D_2$ 35042·1	*22 0*		
					$^4D_3$ 35020·1	*33 4*		
					$^4D_4$ 34986·7			
$4d'$	$^4P_3$ 29006·23	*−20 50*	^{4}(D F)				^{2}(P D F)	
	$^4P_2$ 28985·73	*−11·90*						
	$^4P_1$ 28973 83							

(C.)

$2p^3$	$^4S_2 >$ 46200		^2P [25500]		$^2D_3$ 46196 2	*−5·1*
					$^2D_2$ 46191·1	

* Calculated by Rydberg formula as basis of quartet terms.

† The $2p'$ term values are referred to the ^1S limit, while the other terms of group B are referred to ^3P.

The above estimate of the value of $2p'$ ^4P, it should be noted, is referred to the ^1S state of the C III core, and, following a suggestion made by Prof. H. N. Russell, the term might be written in the form $2p'$ (^1S) ^4P. Its value referred to the ^3P state, or $2p'$ (^3P) ^4P, which would be expected to be in Rydberg sequence with $3p'$ ^4P, would be greater than this by the difference $^1S_0 - {}^3P_1$ of C III. Bowen has taken this to be 43524 (representing the supposed C III "resonance" line λ 2297) and assuming this to be correct, the value of $2p'$ ^4P referred to the ^3P limit would be $>$ (145170 + 43524), or $>$ 188694. In view of its great intensity, however, it is possible that λ 2297 may not be the resonance line of C III, and that a line of higher wave-number should have been selected. The order of magnitude is, nevertheless, generally confirmed by a comparison of the doublet p P and quartet p' P terms, from which it may be inferred that $2p'\,{}^4$P, referred to the ^{3}P limit of C III, is probably not much smaller 196595. A value of, say, 193000 would not be inconsistent with the values assigned to $3p'\,{}^4$P and $4p'\,{}^4$P.

Thus, in searching for combinations between the doublet terms of groups A and C with the quartet and doublet terms of group B, the latter (except the $2p'$ terms which are already evaluated with reference to the ^{1}S limit) must be reduced by an amount representing $^1S_0$—$^3P_1$ of the C III spectrum. Attempts to trace such combinations, however, assuming alternative possible identifications of the resonance line of C III, have so far been unsuccessful.

Doublet Combinations.

The doublet combinations which have been identified are collected in Table III. This includes all the lines considered in the previous paper, and additional lines which have been identified by Bowen and the authors. For lines in the extreme ultra-violet which have not yet been measured with great accuracy the calculated wave-numbers, enclosed in square brackets, are indicated for comparison with the values corresponding with the observed wave-lengths. Other calculated lines are also distinguished by brackets.

Quartet Combinations.

The quartet combinations which have been identified are collected in Table IV.

Unclassified Lines.

Among the unclassified lines are two complex doublets which may possibly involve doublet terms of group B, none of which beyond the first row ($2p'$) has yet been evaluated. These may be represented as follows :—

? $3s'$	$^2P_2$		$^2P_1$
? $3p'\,{}^2D_2$	16381·95 (1)	*19·48*	16401·43 (3)
	10·75		
$^2D_3$	16392·70 (5)		

? $4d'$	$^2P_2$		$^2P_1$
? $3p'\,{}^2D_2$	37854·2 (1)	*5·0*	37859·2 (2)
	7·3		
$^2D_3$	37846·9 (3)		

There is also an unclassified pair λλ 3167·95 (3), 3165·51 (4), Δν 24·33, which is notable for the sharpness of its lines.

Table III.—Doublet Combinations of C II.

	$2p\,{}^2P_2$ 196595·0	*64 6*	$2p\,{}^2P_1$ 196659 0	$3p\,{}^2P_2$ 64923·19	*11 13*	$3p\,{}^2P_1$ 64934 32	$4p\,{}^2P_2$ 34134·38	*5 92*	$4p\,{}^2P_1$ 34140 30	$4f\,{}^2F_{43}$ 27679 95	$5f\,{}^2F_{43}$ 17702 54	$6f\,{}^2F_{43}$ 12282 80
$2p'\,{}^4P$ > 145170	[<51425]											
$2p'\,{}^2D_2$ = 121726 9 $2p'\,{}^2D_3$ = 121728·1	 *74866 9 (10)		74932 1 (8)	 *56804 0 (2)		56790 8 (1)	 *87595 6 (2)			 [94048]	 [104026]	 [109445]
$2p'\,{}^2S_1$ = 100164 9	*96430 (6)	*63 7*	96493·8 (6)	35241 75 (10)	*11 06*	35230 69 (8)	[66030 5]					
$2p'\,{}^2P_1$ = 86033·9 $2p'\,{}^2P_2$ = 85992 7	*110561 7 (7) *41 5* 110603 2 (8)	*62 7* *62 8*	110624 4 (8) *41 6* 110666 0 (7)	 [21069 5]			 [51858 5]					
$3s\,{}^2S_1$ = 80121 12	*116474 0 (6)	*64 2*	116538 2 (5)	15197 93 (10)	*11 13*	15186 80 (8)	45986 74 (2)	*5·92*	45980 82 (1)			
$3d\,{}^2D_2$ = 51109 01 $3d\,{}^2D_3$ = 51107 56	[145486] [145487] *145486 1 (5)	 *63 1*	[145550 0] 145549 2 (5)	[13814 18] 13815 63 (8)		13825 31 (6)	[16974 63] 16973 32 (3)		16968 46 (2)	23428 99 (8) 23427 61 (10)	33405 71 (4)	38825 45 (1)
$4s\,{}^2S_1$ = 39424 57	[157170] †157183 (1)		[157234]	25498 65 (8)	*11 06*	25509 71 (6)	§					
$4d\,{}^2D_2$ = 28535 06 $4d\,{}^2D_3$ = 28534 67	[168060] *168062 (2)		[168124] 168127 (2)	[36388 11] 36388 52 (6)		36390 24 (5)	 §			 §		 [16252]
$5s\,{}^2S_1$ = 23310 82	[173284] †173190 (1)		[173348]	41612 37 (2)	*10 90*	41623 27 (1)	§					
$5d\,{}^2D_{32}$ = 18164 2	[178431] †178412		[178495]	46759 34 (1)	*10 50*	46769 84 (1)	[15970 2]			§	§	§
$6d\,{}^2D_{32}$ = [12558]	[184037] †184026 (2)		[184101]	[52365]			[21576]			[15122]	§	§
$7d\,{}^2D_{32}$ = [9193]	187402 †187546 (1)		[187466]	[55730]			[24941]			[18487]	§	§

* Measurements and classification by Bowen. † Observations by Lang all but 173190 observed also by Millikan and by Simeon. § Out of range

	$2p^3\,{}^2D_3$ 46196 2	*−5·1*	$2p^3\,{}^2D_2$ 46191·1
$2p'\,{}^4P$ > 145170	[>98974]		
$2p'\,{}^2D_3$ = 121728 1 *−1·2* $2p'\,{}^2D_2$ = 121726 9	[75531·9] [75530 7] 75531 0(7)		[75537·0] [75535 8]
$2p'\,{}^2P_1$ = 86033 9 *41 2* $2p'\,{}^2P_2$ = 85992 7	 39796·46(10)	 *5·07*	39842·77(8) *41 24* 39801·53(4)

Table IV —Quartet Combinations of C II.

	$3s\,{}^4P_3$ 82781 27	*44 97*	P_2 82826 24	*23 76*	P_1 82850 00	$4s\,{}^4P_3$ 40194 34	*46 08*	P_2 40240 42	*24 02*	P_1 40264 44	$3d\,{}^4P_3$ 50972 7	*−21 5*	${}^4P_2$ 50951 2	*−14 2*	P_1 50937 0
$3p'\,{}^4D_1$ = 68120 20			14706 06 (0)	*23 73*	14729 79 (2)			27879 62 (2)	*23 86*	27855 76 (1)			[17169 0]		17183 7 (0)
14 70			*14 61*		*14 82*			*14 38*		*(15 27)*					*15 5*
D_2 = 68105 50	14675 72 (0)	*44 95*	14720 67 (3)	*23 94*	14744 61 (2)	[27911 1]		27865 24 (2)	*(24 7)*	*27840 49 (2)	[17132 8]		17154 4 (1)	*13 8*	17168 2 (0)
25 01	*25 03*		*25 10*					*(24 75)*					*25 0*		
D_3 = 68080 49	14700 75 (3)	*45 02*	14745 77 (4)			27886 23 (1)	*(45 74)*	*27840 49 (2)			17107 5 (0)	*21 9*	17129 4 (1)		
36 27	*36 30*					*36 43*					*36 0*				
D_4 = 68044 22	14737 05 (6)					27849 80 (4)					17071 5 (2)				
$3p'\,{}^4S_2$ = 65126 01	17655 13 (4)	*45 10*	17700 23 (3)	*23 89*	17724 12 (2)	24931 26 (2)	*45 74*	24885 52 (1)	*23 89*	24861 63 (0)	14153 6 (1)	*21 1*	14174 7 (1)	*14 2*	14188 9 (0)
$3p'\,{}^4P_1$ = 63389 68			19436 65 (2)	*23 57*	19460 22 (0)										
16 30			*16 19*		*16 30*										
P_2 = 63373 38	19408 01 (3)	*44 83*	19452 84 (1)	*23 68*	19476 52 (3)										
22 43	*22 33*		*22 43*												
P_3 = 63350 95	19430 34 (0)	*44 93*	19475 27 (3)			[23157]					§				
$4p'\,{}^4S_2$ = 34049 1	[48732]					§					16923 4 (1)	*21 7*	16901 7 (0)	*13 3*	16888 4 (0)

	$3d\,{}^4D_4$ 53233 9	*10 3*	D_3 53244 2	*8 7*	D_2 53252 9	*5 6*	D_1 53258 5	$3d\,{}^4F_5$ 54002 4	*27 6*	F_4 54030 0	*19 6*	F_3 54049 6	*14 3*	F_2 54063 9
$3p'\,{}^4D_1$ = 68120 20					[14867 3]		14861 7 (0)							†14056 2 (1)
14 70							*(14 8)*							*14 0*
D_2 = 68105 50			†14861 7 (0)	*(9 1)*	14852 6 (0)	*(5)*	*14846 9 (0)					†14056 2 (1)	*(14 0)*	*14042 2 (2)
25 01			*25 10*		*24 4*							*(25 9)*		
D_3 = 68080 49	*14846 9 (0)	*(10 6)*	14836 3 (0)	*(8 1)*	14828 2 (0)					14050 7 (1)	*20 4*	14030 3 (0)		[14017]
36 27	*(36 6)*		*36 0*							*36 2*				
D_4 = 68044 22	14810 3 (2)	*10 0*	14800 3 (0)					*14042 2 (2)	*(27 7)*	14014 5 (0)				
$4p'\,{}^4D_1$ = 35056 4														†19007 5 (3)
14 3														
D_2 = 35042 1												†19007 5 (3)		[19022]
22 0												*(22 0)*		
D_3 = 35020 1										†19007 5 (3)	*(22 0)*	19029 5 (1)	*(14 9)*	*19044 4 (0)
23 4										*(36 9)*				
D_4 = 34986 7	18248 (0)							19015 7 (2)	*(28 7)*	*19044 4 (0)				

$2p\,{}^4P_3 - 2p^3\,{}^4S_2$ = 98972 5 (6)
28 6
P_2 S_2 = 99001 1 (6)
21 5
P_1 S_2 = 99022 6 (5)
$2p^3\,{}^4S_2 > 46196$

$3p\,{}^4S_2 - 4d'\,{}^4P_3$ = 36119 78(2)
−20 50
S_2 P_2 = 36140 28(1)
−11 90
S_2 P_1 = 36152 18(0)
$4d\,{}^4P_3$ = 29006 23

*† Used more than once
§ Out of range

Catalogue of Lines attributed to C II.

Table V is a catalogue of all the lines between λ 7236 and λ 2137 which have appeared to be attributable to C II. The wave-lengths, followed by numbers in brackets representing rough estimates of intensity, are given in the first column, the corresponding wave-numbers in the second, and the classification, where ascertained, in the third column.

Table V. List of C II Lines, λ 7236—λ 2137.

λ.	ν	
[7237]	[13814·18]	$3p\ {}^2P_2$ $3d\ {}^2D_3$
7236·19 (8*n*)	13815·63	P_2 D_2
7231·12 (6*n*)	13825·31	P_1 D_2
*7139·68 (00)	14002·39	
*7133·52 (0)	14014·47	$3p'\ {}^4D_4$—$3d'\ {}^4F_4$
*7125 49 (0)	14030 26	D_2 F_3
7119·4₅ (2)	14042·16	$\{D_4$ F_5 $\{D_2$ F_2
7115·13 (2-)	14050 69	D_3 F_4
7112·36 (1)	14056 16	$\{D_3$ F_3 $\{D_1$ F_2
7063 4 (1*n*)	14153 6	$3p'\ {}^4S_2$—$3d'\ {}^4P_3$
7052·9 (1*n*)	14174·7	S_2 P_2
7045·8 (0*n*)	14188·9	S_2 P_1
6812 19 (0)	14675·72	$3s'\ {}^4P_3$—$3p'\ {}^4D_2$
6800·50 (3)	14700·75	P_2 D_2
6798·04 (1)	14706 06	P_2 D_1
6791·30 (3)	14720·67	P_3 D_3
6787 09 (2)	14729 79	P_1 D_1
6783·75 (6)	14737 05	P_3 D_4
6780·27 (2)	14744 61	P_1 D_2
6779 74 (4)	14745·77	P_2 D_3
6754·75 (0)	14800·32	$3p'\ {}^4D_4$—$3d'\ {}^4D_3$
6750·22 (2)	14810·25	D_4 D_4
6742·05 (0)	14828·20	D_3 D_2
6738·36 (1)	14836·32	D_3 D_3
6733·56 (0)	14846·89	$\{D_3$ D_4 $\{D_2$ D_1
6730·79 (0)	14852 59	D_2 D_2
6726·84 (0)	14861·73	$\{D_2$ D_3 $\{D_1$ D_1
6721·67 (0)	14873·17	
6707·60 (0)	14904·35	
6582 85 (8)	15186·80	$3s\ {}^2S_1$—$3p\ {}^2P_1$
6578 03 (10)	15197·93	S_1 P_2
*6243·98 (0)	16011 02	
*6115·21 (0)	16348·15	
6102·59 (0)	16381 95	
6098 62 (3)	16392·70	
6095 37 (2)	16401·43	
5919 60 (0)	16888 4	$3d'\ {}^4P_1$—$4p'\ {}^4S_2$
5914·92 (0)	16901 7	P_2 S_2
5907 36 (1)	16923 4	P_3 S_2
5891 65 (3)	16968 18	$3d\ {}^2D_2$—$4p\ {}^2P_1$
5889·97 (5)	16973·32	D_3 P_2
[5889·5]	[16974 6]	D_2 P_2
5856·09 (2)	17071 5	$3p'\ {}^4D_4$—$3d'\ {}^4P_3$
5843 77 (0)	17107·5	D_3 P_3
5836 31 (1)	17129 4	D_3 P_2
5827·80 (1)	17154·4	D_2 P_2
5823·13 (0)	17168·2	D_2 P_1
5817 87 (0)	17183·7	D_1 P_1
5662·51 (4)	17655·13	$3s'\ {}^4P_3$—$3p'\ {}^4S_2$
5648·08 (3)	17700·23	P_2 S_2
5640 50 (2)	17724 12	P_1 S_2
5478·6 (0)	18248	$3d'\ {}^4D_4$—$4p'\ {}^4D_4$
5272·56 (1)	18961·4	
5259·62 (3)	19007·5	$3d'\ \{{}^4F_4,\ F_3,\ F_2\}$—$4p'\ \{{}^4D_3,\ D_2,\ D_1\}$
5257·36 (2)	19015·7	F_5 D_4
5253 55 (1)	19029·5	F_3 D_3
5249·43 (0)	19044·4	F_4 D_4

* Merrill (private communication).

Table V—continued.

λ.	ν	
5151·08 (3*d* ?)	19408 01	$3s'\,^4P_2-3p'\,^4P_3$
5145·16 (5)	19430·34	$P_3 \quad P_3$
5143·49 (2)	19436 65	$P_2 \quad P_1$
5139·21 (1)	19452 84	$P_2 \quad P_2$
5137·26 (0)	19460 22	$P_1 \quad P_1$
5133·29 (2)	19475 27	$P_3 \quad P_2$
5132 96 (3)	19476·52	$P_1 \quad P_2$
5121·60 (0)	19520 1	
5119 55 (1)	19527 6	
5114·07 (1)	19548 5	
4964·90 (1)	20135 8	
4618·85 (2*d* ?)	21044 3	
4411·52 (2)	22661·58	
4411 20 (2)	22663 22	
4410 06 (1)	22669 08	
4374·28 (2)	22854 50	
4372·49 (1)	22863 87	
4371 59 (0)	22868 57	
4267 27 (10)	23427 61	$3d\,^2D_3-4f\,^2F_{43}$
4267·02 (8)	23428 99	$D_2 \quad F_3$
4074·89 (1)	24533 70	
4074·53 (2)	24535 80	
4070·30 (3)	24561 30	} C II ?
4068·97 (3)	24569·33	
4021·13 (0)	24861 63	$3p'\,^4S_2-4s'\,^4P_1$
4017·27 (1)	24885·52	$S_2 \quad P_2$
4009·90 (2)	24931·26	$S_2 \quad P_3$
3980·35 (2)	25116 34	
3952·08 (1)	25296 00	
3920·677 (8)	25498 65	$2p\,^2P_2-2s\,^2S_1$
3918·977 (6)	25509·71	$P_1 \quad S_1$
3889·18 (1)	25705·10	
3885·99 (0)	25726·21	
3876·670 (1)	25788 05	
3876·409 (2)	25789 79	
3876·188 (4)	25791·26	
3876·051 (1)	25792 17	
3590·87 (2)	27840 49	$3p'\begin{cases}^4D_3\\ \;\,D_2\end{cases}\!-4s'\begin{cases}^4P_2\\ \;\,P_1\end{cases}$
3589 67 (4)	27840·80	$D_4 \quad P_3$
3588·92 (1)	27855 61	$D_1 \quad P_1$
3587 08 (2)	27865 24	$D_2 \quad P_2$
3585·83 (2)	27879·62	$D_1 \quad P_2$
3584·98 (1)	27886 23	$D_3 \quad P_3$
3361·75 (1)	29737·90	
3361·09 (2)	29743·74	
3167 95 (3)	31557·05	
3165·51 (4)	31581·38	
2992 63 (4)	33105·71	$3d\,^2D_{32}-5f\,^2F_{43}$
2967·91 (3)	33683·93	
2967 31 (2)	33690·75	
2885 47 (2*n*)	34646·26	
2837 602 (8)	35230 69	$2p'\,^2S_1-2p\,^2P_1$
2836·710 (10)	35241·75	$S_1 \quad P_2$
2801·36 (2*n*)	35686·45	
2767 75 (2)	36119 78	$3p'\,^4S_2-4d'\,^4P_3$
3766·18 (1)	36140 28	$S_2 \quad P_2$
2765·27 (0)	36152·18	$S_2 \quad P_1$
[2747 34]	[36388 1]	$2p\,^2P_2-2d\,^2D_3$
2747 31 (6)	36388 52	$P_2 \quad D_1$
2746·50 (4)	36399·24	$P_1 \quad D_2$
2725·90 (1)	36674 3	
2725 29 (1)	36682 5	
2724 87 (0)	36688·1	
2641 44 (3)	37846·88	
2640 93 (1)	37854·18	
2640 58 (2)	37859·20	
2595·07 (1*n*)	38523·1	
2592 00 (2*n*)	38568 7	
2574·86 (1*n*)	38825·5	$3d\,^2D_{32}-6f\,^2F_{43}$
2512 03 (8)	39796·46	$2p'\,^2P_2-2p^3\,^2D_3$
2511 71 (4)	30801·53	$P_2 \quad D_2$
2509·11 (7)	39842·77	$P_1 \quad D_2$
2402 40 (2)	41612·37	$3p\,^2P_2-5s\,^2S_1$
2401·77 (1)	41623·27	$P_1 \quad S_1$
2191 37 (2)	45619 3	
2177 66 (1)	45906·4	
2174·14 (1)	45980·82	$3s\,^2S_1-4p\,^2P_1$
2173·86 (2)	45986·74	$S_1 \quad P_2$
2163·60 (5)	46204·7	
2137·93 (2)	46759·34	$3p\,^2P_2-5d\,^2D_{32}$
2137·45 (1)	46769·84	$P_1 \quad D_2$

Table VI is a list of carbon lines which have been observed between λ 2137 and λ 1894; the distinction between C II and C III by experimental behaviour is somewhat difficult in this region, but suggested or known origins are indicated.

Table VI.—Lines of Carbon between λ 2137 and λ 1894.

λ_{air}	ν.	
2092 40 (4)	47776·8	C III ?
2016 92 (1*d* ?)	49564 5	,,
2010 18 (5)	49730·6	,,
2000 67 (4)	49743·3	,,
λ_{vac}		
1988 05 (1)	50300 5	C II ?
1979 79 (3)	50510 4	C III ?
1979 35 (4)	50521 6	,,
1931 03 (10)	51785 9	C I
1923 52 (4*d* ?)	51988 0	C III
1923·13 (5)	51998·6	
1894·49 (2)	52784·6	C III ?

Table VII includes lines of carbon below λ 1760 which have been classified as part of the C II spectrum. All of these occur in the vacuum arc, in

Table VII.—Classified Lines of C II λ 1760—λ 534.

λ_{vac}	ν		λ_{vac}	ν	
			*858 561 (1)	116474 0	$2p\ {}^2P_2 - 3s\ {}^2S_1$
*1760·85 (2)	56790 8	$2p'\ {}^2D_2 - 3p\ {}^2P_1$	858 088 (0)	116538 2	$P_1 \quad S_1$
1760·44 (3)	56804 0	$D_3 \quad P_2$			
			*687 351 (5)	145486 1	$2p\ {}^2P_2 - 3d\ {}^2D_3$
*1335·703 (10)	74866 9	$2p\ {}^2P_2 - 2p'\ {}^2D_3$	687·053 (5)	145549·2	$P_1 \quad D_2$
1334·541 (10)	74932·1	$P_1 \quad D_2$			
			†636·2 (2)	157183	$2p\ {}^2P_{21} - 4s\ {}^2S_1$
1323·96 (7)	75531·0	$2p'\ {}^2D_{32} - 2p^3\ {}^2D_{32}$			
			*595·02 (2)	168062	$2p\ {}^2P_2 - 4d\ {}^2D_3$
*1141·61 (2)	87595·6	$2p'\ {}^2D_{32} - 4p\ {}^2P_{21}$	594 79 (2)	168127	$P_1 \quad D_2$
*1037 021 (7)	96430 1	$2p\ {}^2P_2 - 2p'\ {}^2S_1$	†560 5 (2)	178412	$2p\ {}^2P_{21} - 5d\ {}^2D_{32}$
1036·336 (5)	96493 8	$P_1 \quad S_1$	†543 4 (1)	184026	$2p\ {}^2P_{21} - 6d\ {}^2D_{32}$
			†533·5 (1)	187441	$2p\ {}^2P_{21} - 7d\ {}^2D_{32}$
*1010·382 (3)	98972 5	$2p'\ {}^4P_3 - 2p^3\ {}^4S_2$			
1010·090 (3)	99001·1	$P_2 \quad S_2$			
1009·870 (5)	99022·6	$P_1 \quad S_2$			
*904·472 (2)	110561·7	$2p\ {}^2P_2 - 2p'\ {}^2P_1$			
904·133 (2)	110603 2	$P_2 \quad P_2$			
903·960 (2)	110624 4	$P_1 \quad P_1$			
903·620 (2)	110666 0	$P_1 \quad P_2$			

* λ and classification by Bowen ('Phys. Rev.,' vol. 29, p. 233 (1927)).
† Mean λ, Millikan, Simeon, and Lang.

company with lines of C I. Other observations of the vacuum arc have been made by Simeon[*] and of the vacuum spark by Millikan and Bowen[†] and by Lang[‡]. Wave lengths and classification of lines of C I have been given in a previous paper[§].

Summary

The paper gives the results of a further investigation of the spectrum of singly ionised carbon (C II) as observed over a wide range in various sources. Previous results for the regular doublet system have been revised and numerous lines have been classified in the quartet system which is predicted by Hund's theory. A catalogue of all the lines which appear to be attributable to C II in the region λ 7200 to λ 2137 is included and also a list of classified lines of shorter wave length.

One of the authors (E. W. H. S.) is indebted to the Department of Scientific and Industrial Research for a grant which has enabled him to take part in this investigation.

---

[*] Roy. Soc. Proc. A, vol. 102, p. 484 (1922) and vol. 104, p. 368 (1923).

[†] Phys. Rev. vol. 23, p. 8 (1924) and other papers.

[‡] Phil. Trans. A, vol. 224, p. 377 (1924).

[§] Roy. Soc. Proc., A, vol. 118, p. 34 (1928).

BAKERIAN LECTURE.—*The Aurora and its Spectrum.*

By Prof. J. C. McLENNAN, F.R.S., Professor of Physics and Director of the Physical Laboratory, University of Toronto.

(Lecture delivered June 28, 1928—MS received August 7, 1928.)

[PLATES 12-17.]

I.—THE POLAR AURORA.

The beauty of the Polar Aurora, when it is seen in its full glory, has always deeply impressed those who have seen it, and has excited many to search for the true nature and cause of its occurrence. It occurs in both hemispheres, that in the northern being designated as *Aurora Borealis*, and that in the south as *Aurora Australis*. The frequency of occurrence varies with latitude and is greatest in the two zonal regions that make angles of about 20° with the earth's magnetic axis. Auroral displays are generally accompanied by magnetic storms, and a view commonly held is that both phenomena are due to streams of electrons emitted by the sun. Such streams, Prof. Birkland has shown, must necessarily describe paths on coming under the influence of the earth's magnetic field that follow closely the course of the streamers in an auroral display.

The polar aurora appears with varying intensities and in various forms and colours. At times it is seen as a weak, diffuse, formless luminosity; at other times it appears as luminous draperies, bands or arcs, and often only as luminous beams or rays.

These forms are sometimes stationary and at other times they undergo movements more or less rapid. Pulsating types of luminosity have also been observed. The feebly luminous, diffuse types of aurora are usually greenish-yellow. In the case of curtain and arc forms with ray structure and of low elevation, the colour is also greenish-yellow. Blue, red, violet and other colours may occur however, especially in the more intense and moving varieties of auroræ. In the case of displays at enormous heights, auroræ of a red-violet colour have been seen, and curtains of a violet-grey colour have been observed that gradually became transformed into a feeble, diffuse mass of luminosity of a violet-mauve colour. Spectrograms taken of the light of such auroræ indicate exceptionally strong intensity in the radiation of the shorter wave-lengths.

Since 1907 Prof. Størmer* has devoted much time and effort in Norway at Oslo, Bygdø, Bossekop, and other stations, in the direction of determining the height and position of auroral displays. The method used involved the simultaneous photography of an aurora from two or more stations separated by distances varying from 4·5 to 258 km. With the instruments developed by him good photographs can be obtained with exposures of only a second. A pair of such photographs, kindly given me by Prof. Størmer, are shown in Plate 12, figs. 1 and 2. They were taken in March, 1926. Fig. 1 shows an auroral curtain photographed by Prof. Størmer at Bygdø, and fig. 2 the same aurora photographed simultaneously by Carsten Borchgrevink at Tømte, 48 km. to the N.N.W. of Bygdø. The stars γ, δ, ϵ, ζ and η of the Great Bear are shown very clearly in both pictures. The parallax referred to these stars, it will be seen, is considerable. Measurements made on the plates showed that the altitude of the lowest border of the auroral curtain was unusually high, for four points at the foot of the rays gave the altitudes 135, 132, 131 and 137 km. above the earth. The summits of the rays reached at least a height of 350 km.

From hundreds of photographs that he has taken, Prof. Størmer has calculated the heights of the upper and lower edges of many auroral displays. His results show that very few displays occur below 80 km., and that above this level the number increases rapidly with the most frequent occurrences, beginning at a height of 106 km. Above this height the number of auroræ falls off rapidly. Some, however, have been observed as high as 500 km. and 750 km. One notable aurora† was observed by Størmer on September 8, 1926, in the region between Iceland and the Shetlands, that extended to the enormous height of 1000 km. A point of interest that emerged from Prof. Størmer's work is that the auroral displays observed at Oslo extended generally much higher in the atmosphere than those observed at Bossekop near Finland.

The Auroral Spectrum.

Angstrom‡ appears to have been the first to have made observations on the spectrum of the aurora. This was in 1869. He had expressed the opinion that one should expect the spectrum to be the same as that of the electrical discharge in air, but this he did not find to be so, for he obtained only a "green line at λ 5567 and in addition three very faint lines in the blue region, all of which were of unknown origin." Since the work of Angström a number of

---

* 'Geophys. Pub. Norske Vid. Akad.,' vol. 4, No. 7.

† Størmer, Gerland's 'Beitr. z. Geophys.,' vol. 17, p. 254 (1927).

‡ 'Pogg. Ann.,' vol. 137, p. 161 (1869).

Fig. 1.—Auroral Curtain photographed at Bygdo at 18h 36m. The stars γ, δ, ε, ζ, η, Ursæ Majoris are seen.

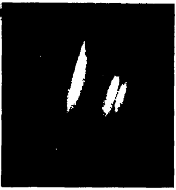

Fig. 2.—The same, photographed simultaneously by Carsten Borchgrevink at Tomte.

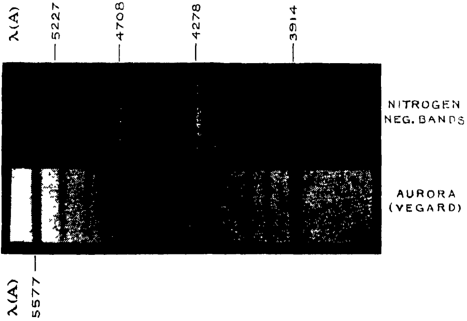

Fig. 3.

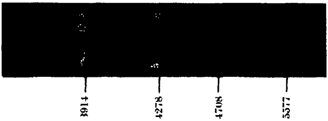

Fig. 4.—The Spectrum of an Aurora and of the Negative Bands of Nitrogen by Lord Rayleigh.

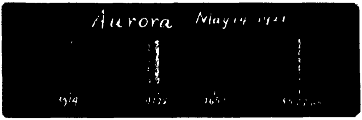

Fig. 5.—The Spectrum of an Aurora by Dr. Slipher.

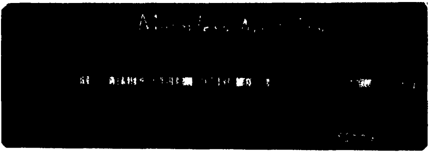

Fig. 6.—The Spectrum of the Light from the Moonless Night Sky by Dr. Slipher.

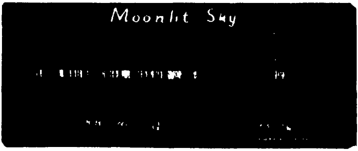

Fig. 7.—The Spectrum of the Light from the Moonlit Sky by Dr. Slipher.

investigators have studied the auroral spectrum, but with the exception of Gyllenskiold* in 1886, no one appears to have done anything of an extensive nature until the brilliant series of studies initiated by Prof. Vegard† in the winter of 1912–13 was undertaken. The results of Vegard's work up to 1926 have been collated and are summarised in Table I. In addition to the wave-lengths given in the table, a spectral line or band of weak intensity has been observed in the spectrum of the aurora, whose wave-length has been variously given by different observers as λ 5269, λ 5205, λ 5200, λ 5233, λ 5210, λ 5239, λ 5207, λ 5200, λ 5228, λ 5235, λ 5166, λ 5230. Special observations made by Vegard‡ in 1927 gave values between λ 5220 and λ 5269 for this band. In his later work dealing with the red region of the auroral spectrum, Vegard reports a spectral line at λ 5944 and one at λ 6320, both slightly masked by a diffuse band. He also observed a line or band at λ 6565.

Table I.

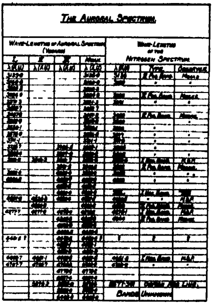

THE AURORAL SPECTRUM.

WAVE-LENGTHS OF AURORAL SPECTRUM (VEGARD)

WAVE-LENGTHS OF THE NITROGEN SPECTRUM

BANDS UNKNOWN

A characteristic photograph of the spectrum of the polar auroral light, taken by Prof. Vegard,§ is reproduced in the lower part of fig. 3 (Plate 12). Other typical ones taken by Lord Rayleigh and Dr. V. M. Slipher respectively are shown in figs. 4 and 5 (Plate 13).

---

* 'Observations faites au Cap Thordsen, Spitzberg, par l'Exp. Suéd.,' vol. 2, p. 158.

† 'Phil. Mag.,' vol. 46, pp. 193, 577 (1923); 'Ann. d. Physik,' vol. 79, p. 377 (1926).

‡ 'Naturw.,' vol. 15, p. 438 (1927).

§ 'Nature,' vol. 119, p. 349 (1927).

The Non-Polar Aurora.

The polar aurora occurs at irregular intervals and evidently therefore only when some special conditions prevail. On the other hand, it has been known since 1901 that the night sky can and does glow with a faint green light. Through the work of Wiechert, Campbell, Lord Rayleigh, Slipher, Babcock,* and others, we have learned that this soft green light is continually and continuously emitted in all latitudes by all parts of the night sky when the latter is moonless and cloudless, also when it is moonlit, and even when it is moderately overclouded. Its existence is not conditional upon the occurrence of magnetic storms or upon the display of polar auroræ. Photographs of the spectrum of the light of the night sky, taken by Dr. Slipher and given to me by him for reproduction, are shown in figs. 6 and 7 (Plate 13). From these and others we now know that the most characteristic and possibly only feature of the spectrum of the light from the night sky is a faint yellow-green spectral line that has been identified with the strong line near λ 5577 in the spectrum of the light of the polar aurora.

Since both spectra have this interesting line near λ 5577 in common, it has become customary for writers, following the practice of Lord Rayleigh,† to use the term non-polar aurora as a designation for this phenomenon of the emission of a faint greenish-yellow light by the night sky; but in doing so, it is not to be understood that the polar and non-polar aurora are thought to have of necessity the same origin or to be produced necessarily by the same agent.

The Band Spectrum of Nitrogen.

By far the greater portion of the spectrum of the polar aurora finds its interpretation in certain features of the band spectrum of nitrogen. This latter spectrum has been analysed in part by many investigators, including Birge, Hopfield, Dr. Sponer, and A. H. Poetker.‡ Through the work of the last mentioned especially, some outstanding difficulties have been cleared up, and it is now possible to formulate definitely the systems of vibrational energy levels that correspond to and originate in the lower electronic transitions within the molecules of this gas.

---

* Wiechart, 'Phys. Z.,' vol. 3, p. 365 (1901); Campbell, 'Lick Obs. Bull.,' vol. 5, p. 46 (1908) and 'Ast. Soc. Pol.,' vol 29, p. 218 (1917), Rayleigh, 'Roy. Soc. Proc.,' A, vol. 100, p. 367 (1922), vol. 101, p. 114 (1922), and vol 106, p. 117 (1924); Slipher, 'Astrop J.,' vol. 49, p. 266 (1919), and vol. 55, p. 73 (1922), and 'Nature,' vol. 109, p. 55 (1922); Babcock, 'Astrop. J.,' vol. 57, p. 209 (1923).

† 'Roy. Soc. Proc.,' A, vol. 119, p. 11 (1928).

‡ Birge and Hopfield, 'Nature,' vol. 116, p. 15 (1925); Hopfield, 'Phys. Rev.,' vol 27, p. 801 (1926); Sponer, 'Proc. Nat. Acad. Sci.,' vol. 13, p. 100 (1927), Poetker, 'Phys. Rev.,' vol. 30, p. 812 (1927).

The energy levels corresponding to these lower electronic transitions are shown in fig. 8, the excitation potentials inscribed being those of the 0 → 0 vibrational band for each electronic transition The band system corresponding to the lowest electron transition in the nitrogen molecule has for

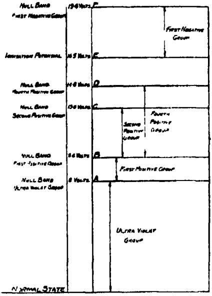

Fig. 8.

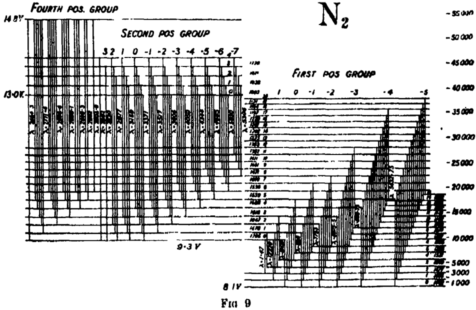

Fig 9

the excitation potential of its 0 → 0 band 8·1 volts, and consequently the bands are all in the extreme ultra-violet.

The vibrational band systems for others of the lower electron transitions, together with their usual designations, their vibration quantum numbers, their frequency differences and a suitably inscribed wave-number scale of reference, are shown in fig. 9. The wave-lengths of the heads of the First

Table II.

Nitrogen. First Positive Band Spectrum.

Wave-Lengths (λ = I. Å. Air).

Approximate Positions of Band Heads.

n' / n	0	1	2	3	4	5	6	7	8	9
0	10491 10420									
1	8911 57 8892 08 8862·53									
2	7753 05 7739 56	8722·28 8703·31 8675·46	9927 9860							
3	6875·5	7626 13 7613 0	8451 73 8523·15 8496 88	9657 9599						
4	6186·73	6788·61	7504·0 7491·0	8369 02 8351 45 8326·16	9409 9362					
5	3632 75	6127·37	6704·75	7386·5 7374·0	8204·62 8187·38 8163·65	9180 9133				
6	5178·?	5592·88	6069·06	6623·57	7273·0 7260·9	8047·26 8030·23 8007 63				
7		5153·7	5553·73	6013 58	6544·88	7164·6 7152·2	7896·28 7879·72 7858·07			
8			5126 5	5515·59	5959 05	6468 6				
9				5098·7	5478·47	5906·01	6394·6			
10						5442·33	5854 4	6322·82		
11						5033·6	5407·13	5804·14	6252 81	
12							5030·85	5372 82	5755 19	6185·13

References { A. H. Poetker, 'Phys. Review,' p. 812 (December, 1927).
Datta, 'Phil. Mag.,' vol. 48, p. 686 (1924).

positive bands are given in Table II, and those of the Second positive group in Table III.

Table III.—Nitrogen-Second Positive Band Heads.

n \ n'	0	1	2	3	4	5	6	7	8	9	10	11
0	3371	3577	3805	4059	4344	4668						
1	3159	3339	3536	3755	3998	4269	4574	4917				
2	2977	3136	3309	3500	3710	3942	4201	4490	4814			
3	2820	2962	3116	3285	3469	3671	3894	4131	4416	4723		
4		2814	2953	3104	3267	3446	3642	3857	4094	4356	4648	4975

The exeitation potential of the 0 → 0 band of the Fourth positive group is about 5·5 volts, and the wave-lengths of the band heads of this system, as far as they are known, fall between λ 3000 and λ 2650.

For singly ionised molecules of nitrogen the most easily excited vibrational band system is known as the First Negative Band group. The excitation potential of the 0 → 0 band of this sytem is approximately 3·1 volts and the wave-length of the head of this band is λ 3914. Those of the heads of the three bands next in importance are respectively λ 4278, λ 4708 and λ 5227. The wave-lengths of the band heads for the complete system are shown in Table IV.

Table IV - -Nitrogen-First Negative Band Heads.

n \ n'	0	1	2	3	4	5	6	7
0	3914	4278	4708	5227				
1	3581	3884	4237	4651	5150			
2		3563	3857	4199	4599	5075		
3		3208	3548		4167	4554	5018	
4			3206				4515	4961
5								4485

Identification of the Band Spectrum of the Polar Aurora.

From fig. 3, and also from figs. 4 and 5, it will be seen that one of the outstanding features of the spectrum of the polar aurora is a set of four well-marked bands with heads as shown at or near λλ 3914, 4278, 4708 and 5227. These bands it is now generally agreed are among the leading members of the first negative band spectrum of gaseous nitrogen. The comparison photographs shown make this quite evident. The auroral spectrum includes three additional though less intense bands of this system, and these and the four already mentioned are designated as such in Table I. A less important feature of the spectrum of the polar aurora is a set of some 16 bands of low intensity. These it is now possible to identify with members of the Second positive band system of nitrogen. They are indicated in Table I and recorded in full in Table III. Two other bands in Table I, λ 5925 and λ 6465, remain still unidentified, but it seems likely that one, if not both of them, belong to the First positive band system of nitrogen. This system of bands is given in Table II. Their intensities as recorded by Poetker (*loc. cit.*) are tabulated in fig. 10. The wave-length λ 6465 would seem to originate in the transition $n = 8$ to $n' = 5$, and the wave-length λ 5929 which may be the same as that given by Vegard in the account of his later investigations as occurring at λ 5945 may originate in the transition $n = 8$ to $n' = 4$. If the two wave-lengths be not identical, the one could be taken to correspond to the transition $n = 9$ to $n' = 5$ and the other to the transition $n = 8$ to $n' = 4$. The wave-length at λ 6320 which Vegard found particularly strong in the spectrograms of the light of auroræ that had a noticeably reddish hue, could belong to the First positive band system of nitrogen and be given by the transition $n = 10$ to $n' = 7$.

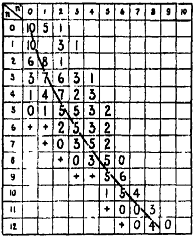

$n \backslash n'$	0	1	2	3	4	5	6	7	8	9	10
0	10	5	1								
1	10		3	1							
2	6	8	1								
3	3	7	6	3	1						
4	1	4	7	2	3						
5	0	1	5	5	3	2					
6	+	+	2	5	3	2					
7		+	0	3	5	2					
8			+	0	3	5	0				
9				+	+	5	6				
10						1	5	4			
11						+	0	0	3		
12							+	0	4	0	

FIG. 10.—N2. First Positive Group.

An observation that may have a bearing on the colour of auroræ was recently made in the course of an investigation by Dr. R. Ruedy, Mr. J. M. Anderson and myself. We were making a study of the distribution of intensity among the after-glow bands of active nitrogen when the rare gases, helium and argon, were in turn mixed with smaller and smaller quantities of nitrogen. With both gases we found that with small percentages of nitrogen in the mixture the afterglow became quite red in colour, and finally with the last traces of nitrogen the glow strongly resembled the well-known red light given out by neon in a tube of large diameter. The mixtures that exhibited this very red glow contained very probably much less than ½ per cent. of nitrogen. When the afterglow was of this character we found on photographing its spectrum, that the only bands that appeared were λ 6394, λ 6469 and λ 6545. A reference to fig. 10 and Table II will show what appears to be an obvious connection between them and infra-red wave-lengths that have been observed in auroral spectra.

The Auroral Green Line.

Table I contains a list of 11 wave-lengths other than those that can be identified with certain bands in the spectrum of nitrogen. Of these 10 are between λ 3000 and λ 5000. None of them appears to be assignable to the arc spectrum of atomic nitrogen. The only wave-lengths of this category that one might expect to obtain with an excitation approximately the same as that which produces the First negative band system, are either far down in the ultra-violet or too far up in the infra-red to be recorded. Three or four of them agree fairly well with wave-lengths in the first spark spectrum of atomic nitrogen but as a group it does not appear to be possible to identify them with any known important group of wave-lengths in this spark spectrum.

With the possible exception of one of them, λ 4378·9, none of the wave-lengths referred to between λ 3000 and λ 5000 appear to be assignable to the spectrum of atomic oxygen. In view of recent developments this wave-length has a special interest attached to it, and it may be that it will prove, on further investigation, to be identifiable with the close triad $\nu = {}^3S_1 - {}^3P_{012}$ (λ 4368) of the quintet-triplet spectral term system of atomic oxygen.

Probably the most important wave-length by far in the spectrum of the polar aurora is that near λ 5577. For long it defied identification. At various times suggestions were put forward as to its origin that on investigation failed to receive corroboration. In 1925, however, it was shown by the writer* in collaboration with his associate, Dr. Shrum, that this famous green line could be obtained from atomic oxygen when the latter was subjected to suitable electrical excitation.

This remarkable line in the spectrum of oxygen has been found to exhibit great variations in intensity when the conditions of its production have been varied. In a vacuum tube discharge in pure oxygen the line is generally absent, very faint or masked by a band spectrum originating in molecular oxygen according to the pressure of the gas. By the use of a vacuum tube some 30 to 40 cm. long and 2·5 cm. in diameter, containing one or other of the rare gases helium, neon, or argon, in a highly purified state at a pressure of about 3 cm. of mercury, this spectral line can be brought out with very great intensity when oxygen obtained from potassium permanganate, for example, and also highly purified, is added at a partial pressure of about 3 mm. of mercury. While helium added in excess to oxygen enhances the intensity of the line, neon with the same partial pressure does so too, and to a greater extent. With argon, however, the enhancement can be very great. In one test specially designed for the purpose. the enhancement obtained with argon was nearly 20 times that obtained with neon.

---

* 'Roy. Soc. Proc.,' A, vol. 108, p. 501 (1925).

By varying the mode of excitation it was found that the line can be obtained most readily with strong intensity when a current of 100 milliamps. or over is passed through a discharge tube of the type shown in fig. 11, and of the dimensions given above, from a 2000 volt direct current generator.

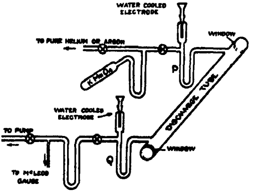

Fig. 11.

A spectrogram obtained with a mixture of oxygen and helium is shown in Plate 14, fig. 12, and one with a mixture of oxygen and argon in Plate 14, fig. 13. The partial pressure of the rare gas was about the same in both cases, but the times of exposure were different, and approximately in the ratio of the intensities of the wave-length λ 5330 in the two reproductions. As the plates show, the intensity of the line λ 5577, obtained with argon was much greater than that of the line λ 5330, while with helium its intensity was somewhat less than that of λ 5330.

In seeking for an explanation of this effect of the inert gases, one recalls that inert gases are known to have a small potential drop throughout the discharge. In xenon, for example, with a tube 15 mm. in diameter, and in argon with one 50 mm. in diameter, the voltage gradient is barely 1 volt* per centimetre, whereas in oxygen at the same pressure it is of the order of 10 volts. By adding only a small trace of oxygen to an inert gas—argon, for example—the potential gradient will be that of the inert gas, and the oxygen spectral lines produced will be limited to those of correspondingly low-excitation energy.

---

* McLennan, Ruedy and Howlett, 'Trans. Roy. Soc., Canada,' vol. 22, p. 79 (1928).

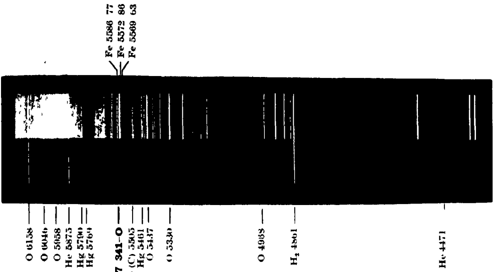
Fe 5586 77
Fe 5572 86
Fe 5569 63
O 6158
O 6046
O 5958
He 5875
Hg 5790
Hg 5769
5577 341–O
He (C) 5505
Hg 5461
O 5437
O 5330
O 4968
H_2 4861
He 4471

FIG. 12.

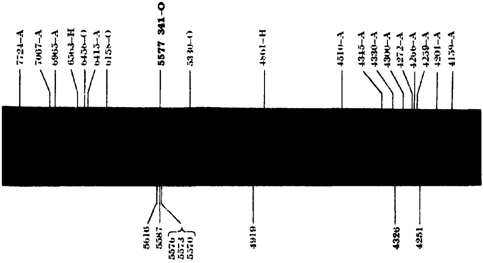
7724–A
7067–A
6965–A
6563–H
6456–O
6415–A
6158–O
5577 341–O
5330–O
4861–H
4510–A
4345–A
4330–A
4300–A
4272–A
4266–A
4259–A
4201–A
4159–A
5616
5587
5576
5573
5570
4919
4326
4251

FIG. 13.

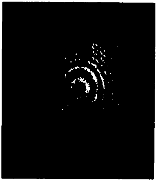

Fig. 14

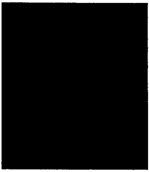

Fig. 15

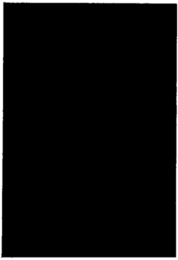

Fig. 18.—One Order.

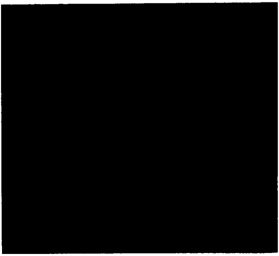

Fig. 19.—Two Orders.

Zeeman Effect Oxygen λ 5577·341 Echelon Normal separation

There is still another fact to be considered in connection with the case of inert gases. It is well known that atoms in the metastable states are able to transfer their energies to the atoms of a foreign gas. According to Franck, atoms in metastable states excite other atoms in such a way as to cause them to emit mainly lines that require approximately the same energy as that which is stored up in the metastable atoms themselves. Those energy transfers appear to have the preference that impart as little kinetic energy as possible to the atoms involved. A remarkable example is found in the character of the hydrogen band spectrum obtainable from hydrogen excited in the presence of argon. The bands in this case are limited to those originating in such molecules as are endowed with three quanta of rotational energy in their initial state. Effects of a similar kind can be obtained from mixtures of helium or argon with a very little nitrogen.

The identity of the oxygen green line with the green line of the aurora was finally and definitely established by measurements of precision made on both wave-lengths with a Fabry and Perot interferometer. A reproduction of the system of interference band obtained by Babcock (*loc. cit.*) with the light of the auroral green line, is shown in Plate 15, fig. 14, and that of the bands obtained by McLennan and McLeod[*] with the light of the oxygen green line, is in Plate 15, fig. 15. From the clear definition of the bands of the interference patterns it is evident that the light used was highly monochromatic, and in both cases corresponded to a sharply-defined very narrow spectral line. From Babcock's measurements the wave-length of the auroral green line was found to be λ 5577·35 ∓ 0·005 I.Å. with a line width of not more than 0·035 I.Å. The measurements on the oxygen green line showed its wave-length to be 5577·341 ∓ 0·004 I Å. with a spectral line width of 0·030 I.Å.

The Position of the Auroral Green Line in the Spectral Term Scheme of Atomic Oxygen.

A reference to standard works on the subject will show that the wave-length scheme of the ordinary triplet-quintet spectral term system of atomic oxygen has been fully worked out, and that there is no place available in it for λ 5577·341. It follows, therefore, that this wave-length must belong to one or other of the two singlet-triplet term schemes provided by the Heisenberg-Hund-Russell[†] theory for atomic oxygen, in addition to the triplet-quintet system. This complete spectral term scheme as it has been built up from the three fundamental spectral terms, ${}^4\bar{S}_2$, ${}^2D_{23}$ and ${}^2P_{12}$ of a nitrogen-like core, is given in Table V. A diagram showing the relative values of the deeper spectral terms of the scheme is given in fig. 16. The problem before us is to fit the wave-length of the auroral green line into this term scheme. Information that may help in solving this problem can be obtained by a consideration of some of the features of the polar and non-polar auroral spectra.

---

[*] 'Roy. Soc. Proc.,' A, vol. 115, p. 515 (1927).

[†] Heisenberg, 'Z. f. Physik,' vol. 32, p. 841 (1925); Hund, *ibid.*, vol. 33, p. 345 (1925).

Table V.

Nitrogen

n_k	1_1	2_1	2_2	3_1	3_2	3_3	Terms
	2	2	3	—	—	—	${}^4S_2$ ${}^2D_{23}$ ${}^2P_{12}$

Oxygen.

A

n_k	1_1	2_1	2_2	3_1	3_2	3_3	Terms
	2	2	3	—	—	-	${}^4\bar{S}_2$
	2	2	4	—	-	-	${}^3P_{012}$
	2	2	3	1	-	-	${}^5S_2$ ${}^3S_1$
	2	2	3	—	1	-	${}^5P_{123}$ ${}^3P_{012}$
	2	2	3	—	—	1	${}^5D_{1234}$ ${}^3D_{123}$

B

n_k	1_1	2_1	2_2	3_1	3_2	3_3	Terms
	2	2	3	–			${}^2D_{23}$
	2	2	4	—	-	-	${}^1D_2$
	2	2	3	1	—	—	${}^3\bar{D}_{123}$ ${}^1D_2$
	2	2	3	—	1	—	${}^3\bar{F}_{234}$ ${}^3D_{123}$ ${}^3P_{012}$ ${}^1F_3$ ${}^1D_2$ ${}^1P_1$

C

n_k	1_1	2_1	2_2	3_1	3_2	3_3	Terms.
	2	2	3	—	—	—	${}^2P_{12}$
	2	2	4	-	-	-	${}^1S_0$
	2	2	3	1	—	—	${}^3P_{012}$ ${}^1P_1$
	2	2	3	—	1	—	${}^3D_{123}$ ${}^3P_{012}$ ${}^3S_1$ ${}^1D_2$ ${}^1P_1$ ${}^1S_0$

The "first negative bands" of nitrogen that appear so prominently in the spectrum of the auroral streamers are due to singly ionised nitrogen molecules—that is, to molecules which have lost one electron. The excitation potential of these bands, as the diagram of fig. 8 shows, is about 20 volts.

The "positive bands" are due to non-ionised nitrogen molecules and can be excited with less stimulation than the first negative bands. An excitation potential of about 14 5 volts will serve to bring out the second positive bands and one of 11 5 volts to bring out the first positive group

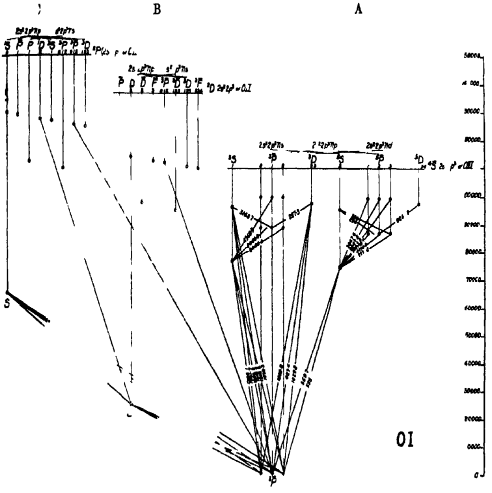

FIG 16

Since the nitrogen bands are absent from the spectrum of the light of the night sky it is clear that the excitation potential required for the production of the auroral green line must be less than 11 5 volts It is known that oxygen is readily dissociated into neutral atoms on absorbing radiation of wave length about λ 1750 and this fact when considered in conjunction with the results of investigations in other directions has made it practically certain that 7 1 volts is very approximately the dissociation potential of oxygen As the two resonance potentials for atomic oxygen are respectively 9 48 volts ($\nu = {}^3P_{012}$ $^3S_1 = 76788$ λ 1302) and 9 11 volts ($\nu = {}^3P_{012} - {}^5S_2 = 73760$

λ 1356) it follows that under a stimulus having an excitation potential of 11·5 volts or less, molecular oxygen cannot be made in one act to emit any radiation belonging to the triplet-quintet spectral system of atomic oxygen, since the residual excitation potential available after 7·1 volts is abstracted for dissociation will not be more than 4·4 volts at most.

If, however, we assume that in the production of the light of the auroral green line in the night sky the process involved is a two act one, of which one represents dissociation, then it can happen that neutral atoms of oxygen will be subjected to an excitation of 11·5 volts. In this case the resonance radiation λ 1302—λ 1356 will be emitted, and the radiation λ 8446 ($^3S_1$—$^3\bar{P}_{012}$) and λ 7775 ($^5S_2$—$^5\bar{P}_{123}$) as well. As the resonance radiation is in the extreme ultra-violet and cannot therefore penetrate the atmosphere, it cannot be recorded photographically in observations made at the earth's surface even if emitted. As to the radiations λ 8446 and λ 7775, all one can say is that such radiations have never been recorded up to the present on spectrograms of the light of the night sky. It would appear, then, from all the evidence accumulated so far, that the equivalent excitation potential of the agency responsible for the emission by the night sky of the auroral green light cannot at most be greater than 11·5 volts, and may be very much less.

With such an excitation potential as a maximum applied to molecules or even to atoms of oxygen, the only transitions available for the production of radiation giving rise to the auroral green line λ 5577·341 are limited to those between the low levels $^1S_0$, $^1D_2$ and $^3\bar{P}_{012}$ in pairs.

Confirmation of this view is found in the fact that the wave-lengths λ 4368 and λ 3947 do not appear in the spectra of the light of the night sky. This would show that under the conditions that give rise to the emission of radiation from the night sky corresponding to the auroral green line there is not sufficient energy available to raise the oxygen in the upper atmosphere to the atomic levels involved in the production of the wave-lengths λ 4368 and λ 3947.

It follows from this that there cannot be sufficient energy available to permit of electronic transitions to the low $^{3,1}P$ levels of the $^1S_0$ system from higher ones in it, or to the low $^{3,1}\bar{D}$ levels of the $^1D_2$ system from higher ones in it.

Moreover it is certain that an electron jump from any one of the low $^{3,1}P$ levels of the $^1S_0$ system to the $^1S_0$ level or from any one of the low $^{3,1}\bar{D}$ levels of the $^1D_2$ system to the $^1D_2$ level would give rise to radiation too far in the ultra-violet region to include λ 5577.

This follows from the fact that the resonance lines of the $^3\bar{\bar{P}}_{012}$ system which are of the same order are far down in the ultra-violet region. We are limited then to the consideration of transitions between the low levels $^1S_0$, $^1D_2$ and $^3\bar{P}_{012}$.

Two of these levels, $^1S_0$ and $^1D_2$ are known to be metastable ones, and transitions between them or between either of them and one of the stable levels $^3\bar{P}_{012}$ with the emission of radiation, have been held until recently to be "forbidden." Such transitions would involve the violation of either one or both of the inner quantum number and the electronic azimuthal quantum number selection rules. Collisions of the second line have been considered until recently as the only means of bringing about transitions between metastable atomic states and stable ones

Before proceeding to consider more fully the subject of the emission of radiation by atoms in metastable states, it may be well to consider why it is that the oxygen green line is possibly with one or two exceptions the only constituent of the oxygen spectrum that is obtained on spectrograms of the light of the polar aurora where an excitation potential as high as 19·6 volts is known to be operative The wave-length λ 4368 has been referred to earlier in this paper. Its quantum equivalent corresponds to an excitation potential of 2·83 volts. This added to 9·48, the resonance potential of oxygen, gives 12·31 volts, and this in turn added to 7·1, the dissociation potential of oxygen, gives 19·4 volts. This voltage is practically equal to the excitation potential of the first negative bands of molecular nitrogen—the bands that constitute one of the most outstanding features of the auroral spectrum. It is possible then that the wave-length observed by Vegard at λ 4378·9 in the auroral spectrum may be that of the unresolved oxygen arc triplet λ 4368. If this should be so, it would indicate that the agent responsible for producing the polar aurora—probably slow-moving electrons—could in one act dissociate a molecule of oxygen into two atoms with one of them left in an excited state suitable for the emission of radiation of the wave-lengths λ 4368. A reference to the diagram of fig. 16 will show that with a stimulus having an excitation potential of 19·4 volts operating on molecules of oxygen, we should have some excited atoms produced capable of emitting radiation with the wave-length λ 3947, as well as others capable of emitting the radiation λ 4368. It is interesting to note in this connection that Table I contains a wave-length λ 3942 that I have assigned, following Vegard, to the Second positive band system of nitrogen. It may be, however, that this wave-length should have been identified with the atomic oxygen arc triad, $^5S_2 - {}^5\bar{P}_{123}$, having wave-lengths approximately equal to λ 3947. The two groups of wave-lengths λ 4368 and λ 3947 are apparently the only ones in Table I that molecules of oxygen subjected to a 20-volt excitation can be made to emit in a single act process involving dissociation.

It would appear then that to account for all the features of the spectrum of the polar aurora that are known and understood, a 20-volt excitation of molecular nitrogen and of molecular oxygen would suffice, if applied occasionally and at irregular intervals. Such excitation could be provided by streams of electrons emitted by the sun from time to time, if they reached the atmospheric zone of the earth in which auroræ occur with an energy equivalent of 20 volts.

There is a very definite distribution of auroral displays in time as well as in space. The number of displays per year varies from year to year in such a way that every eleventh year there is a maximum of auroral activity. It is known that the number of spots on the sun also varies from year to year with a maximum every eleven years. A long series of observations on polar auroræ and sunspots has shown that this is not mere coincidence, and that the maxima occur at approximately the same time. There must therefore be some connection between the aurora and the kind of volcanic activity that produces the sunspots and prominences on the sun. It is fairly certain that the sun gives off streams of electrons at such times of activity and that some of these electron streams strike the earth's atmosphere and excite the molecules there to emit the light of the aurora. If such electrons were all stopped in the upper layers of the atmosphere, it would follow that the aurora might not appear below such a level as the 80–90 km. limit.

The ever-present green light from the night sky may possibly be due as well to electrons emitted by the sun or to electrons from some source other than the sun, but it is more likely in this case that the atoms of oxygen are excited to emit the auroral green light by ultra-violet radiation of short wave length which must be emitted by the sun, but which cannot penetrate the denser lower layers of the atmosphere. Consideration arising from a study of the reflection of radio waves by the Heaviside-Kennelly layer, and from investigations on the amount and distribution of ozone in the upper atmosphere, lend confirmation to this view.

Radiation from Atoms in Metastable States.

In an earlier part of this paper I have pointed out that the only possible energy levels associated with atomic oxygen that can be involved in the emission of the auroral green light are the two lowest $^1S_0$ and $^1D_2$ metastable levels and the lowest stable $^3P_{012}$ levels. Transitions involving any two of these levels accompanied by the emission of radiation would have been deemed "forbidden" prior to last autumn on account of the so-called "Selection rules." It was shown by Bowen,* however, that the eight strong nebular wave-lengths given in Table VI could originate in transitions, ordinarily classed as forbidden, from metastable states associated with the atomic systems Oxygen II, Oxygen III, and Nitrogen II. These transitions are shown in the diagrams of fig 17. Bowen's view has received general acceptance and the discovery that the strong lines in the spectra of nebulæ originate in this way furnishes conclusive evidence that metastable states are not absolutely stable, and that they, too, are states from which spontaneous transitions accompanied by the emission of radiation can occur. The probability of the occurrence of such a transition in unit time is, however, extremely small. Under terrestrial conditions collisions of the second kind with other atoms, or with the walls of a discharge tube, are so frequent that a spontaneous jump with the emission of radiation having the wave-length of a nebular spectral line seldom occurs. In highly rarefied nebulæ, however, collisions of the second kind occur but rarely, and the time interval between collisions can be very long compared with the life periods of atoms or atom ions in their metastable states. In nebulæ transitions of this kind have time to occur, and the existence of the characteristic spectral lines of nebulæ constitutes a proof that they do.

Table VI—Spectral Wave-lengths of Nebulæ.

Wave-lengths. λ (I A).	Transition.	Atom I on System.
7325·0	$^2D_{32} - {}^2P_{12}$	Oxygen II
6583·6	$^3\overline{P}_2 - {}^1D_2$	Nitrogen II
6548·1	$^3\overline{P}_1 - {}^1D_2$	Nitrogen II
5006·8	$^3\overline{P}_2 - {}^1D_2$	Oxygen III
4958·9	$^3\overline{P}_1 - {}^1D_2$	Oxygen III
4363·2	$^1D_2 - {}^1S_0$	Oxygen III
3726·2	$^4\overline{S}_2 - {}^2D_3$	Oxygen II
3728·9	$^4\overline{S}_2 - {}^2D^2$	Oxygen II

In the upper atmosphere in the region in which the polar and non-polar auroræ occur the conditions of pressure and density cannot be very different

---

* 'Nature,' vol. 120, p. 473 (1927).

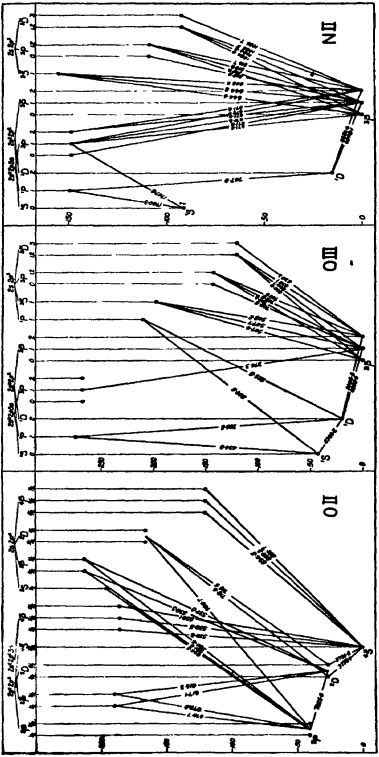

Fig. 17.

from those that obtain in nebulæ. In this fact we find strong justification for our view that the auroral green line must originate in a transition from one or other of the metastable states $^1S_0$ and $^1D_2$, in which atoms of oxygen are left as a result of the action of solar radiation direct or indirect on molecular oxygen found in the upper atmosphere.

Of the life periods of metastable atoms little is known. One can only say it is great compared with the life periods of atoms in normally excited states which are of the order of 10^{-8} secs. Recent investigations by Dorgelo* have shown that the life period of the metastable states of some of the rare gas atoms can reach as high values as 10^{-3} or 10^{-2} secs.

The Zeeman Effect.

With a view to reaching a decision as to what electronic transition in the atoms of oxygen gives rise to the auroral green line, a special effort was recently made by the writer with the assistance of his co-workers, Mr H. J. McLeod and Dr Richard Ruedy, to determine the Zeeman effect of the line. A complete account of the investigation will appear elsewhere, but a summary of the results achieved on account of the interest attached to them should be included in this communication. Our efforts were first of all directed to obtaining the oxygen green line with as strong intensity as possible, and it was found that best results could be obtained by using a direct current generator for producing the electrical discharge. The machine used for this purpose operated at 2000 volts and was capable of giving a current of 1 ampere.

By means of rheostats attached to the machine the current could be modified at will. In our actual experiments we found that the green line could be obtained quite strongly for a period of over an hour when a current of between 30 and 40 milliamperes was passed through the discharge tube, provided great care was taken to ensure the purity of the rare gas used and of the oxygen with which it was mixed. Care had always to be taken to remove as much gas as possible from the electrodes if the green line was to be kept at a strong intensity throughout runs of long duration.

The coil for producing the magnetic field was wound on a brass tube 3·2 cm. in diameter. It was 35 cm. long, and had an outside diameter of 8 cm. It was made with ten layers of No 16 B. & S gauge enamelled single silk-covered wire. Each layer was separated from the neighbouring one by ebonite strips, $\frac{1}{32}$ of an inch by $\frac{1}{8}$ of an inch, laid parallel to the axis of the coil, and about 1 cm. apart. The whole coil was enclosed in an outer brass tube with plates of brass joining the ends of the outer tube to those of the inner tube. The wire terminals of the coil were brought out through watertight insulating bushings inserted in the end plates. The covering brass tube was provided with an inlet tube at one end and an exit one at the other, so that when heavy currents were sent through the coil, water from the mains could be forced between the various windings to keep the wires from getting too hot.

---

* 'Z. f. Physik,' vol. 34, p. 766 (1925).

The total number of turns in the coil was 2390, and the number of turns per centimetre was 68·28. This gave a field of 85·74 gauss per ampere at the centre of the coil. By means of an exploring coil the field along the axis was carefully investigated and found to be uniform over a length of 25 cm. During our experiments the current in the magnetising coil was kept at 30 amperes, which gave a magnetic field slightly over 2500 gauss.

The discharge tube was made of pyrex glass 2·8 cm. in diameter. At both ends it was provided with clear plane glass windows. One end of the tube was re-entrant, the inner portion being 1 cm. in diameter and 3·5 cm. long. The electrode at this end was an aluminium cylinder located in the space between the outer and re-entrant portions of the tube. This form of tube was used so as to make certain that the portion of the discharge emitting the light under investigation was in that portion of the space within the coil where the magnetic field was uniform. Besides, with the tube having this form it could be readily slipped into or out of the coil at will. The other end of the tube was provided with two electrodes of magnesium and one of aluminium, all three being inserted in side tubes attached to the main one. The magnesium electrodes were used when purifying the gas in the tube, and the aluminium one when the discharge was passed through the gas for the purpose of having observations made on the Zeeman effect. Some observations were made with a mixture of argon and oxygen and others with a mixture of neon and oxygen.

The longitudinal Zeeman patterns were photographed and the special equipment used for the purpose consisted of a very fine Echelon spectrograph* backed by a constant deviation spectrograph with camera attached. All were made by the Adam Hilger Co. The Echelon spectrograph had 45 plates, 14·76 mm. in thickness, with a width of step of 1 mm. With this instrument differences in wave-length of 0·007 Å could be measured readily for wave-lengths close to λ 5577·341. With the special apparatus arranged in the manner indicated it was possible to get photographs of the Zeeman patterns of a number of wave-lengths in the one setting. In the experiments made by us, photographs were obtained of the magnetically resolved components of several of the rare gas wave-lengths along with those of the wave-length of the auroral green line of the oxygen spectrum. From the separations of the magnetically resolved components of the rare gas wave-lengths for which the Zeeman effect was already known the magnitude of the actual magnetic fields employed in the resolution could be found and used as a check on the calculated values.

---

* This instrument was a gift to the Physical Laboratory of the University of Toronto by Messrs. Samuel and Benjamin, of London and Toronto.

Under the conditions of our experiments the Neon wave-length λ 5852·487 was found particularly suitable for the magnetic field determinations. According to Beck it is magnetically resolvable into a triplet with a separation of the outer components 31/30ths of that of the outer components of a normal triplet

In our experiments the wave-length of the Oxygen auroral green line λ 5577·341 was found to be resolvable under longitudinal observation into a Zeeman triplet with a separation equal to that between the other components of a normal doublet. Beautifully clear resolution was obtained with exposures of 60 min, and it was found possible to maintain the condition of the experiment constant for a period of this duration. In some experiments Astronomical green sensitive plates were used, and in others Cramer's Iso-Chromatic plates (medium). Fig. 18 (Plate 15) shows the original line, and the resolution of the wave-length obtained when the light was concentrated in one order of the interference pattern. Fig. 19 (Plate 15) shows the resolution obtained when the light was concentrated in two orders.

It was not possible to observe or photograph the transversal effect, but the evidence seems clear that the resolution was that of a normal triplet.

The results obtained in this investigation confirm the conclusions drawn from visual observations by McLennan, McLeod and McQuarrie* in 1927.

Table VII.

Zeeman resolutions for transitions between metastable states and stable ones

$\nu = {}^1D_2 - {}^1S_0 = \frac{(0)\,1}{1}$

$\nu = {}^3P_0 - {}^1S_0 = \frac{0}{1}$

$\nu = {}^3P_1 - {}^1S_0 = \frac{(0)\,3}{2}$

$\nu = {}^3P_2 - {}^1S_0 = \frac{(0)\,3}{2}$

$\nu = {}^3P_0 - {}^1D_2 = \frac{(0)\,1}{1}$

$\nu = {}^3P_1 - {}^1D_2 = \frac{(0)(1)\,1\,2\,3}{2}$

$\nu = {}^3P_2 - {}^1D_2 = \frac{(1)\,1\,(2)\,2\,3\,4}{2}$

The Zeeman resolutions corresponding to the various transitions possible between atomic states represented by ${}^1S_0$, ${}^1D_2$ and ${}^3P_{012}$, and calculated according to the ordinary rules laid down for normal and anomalous Zeeman effects under weak fields, are given in Table VII. From this table it will be seen that the only transitions giving normal Zeeman triplets are $\nu = {}^1D_2 - {}^1S_0$ and $\nu = {}^3\overline{P}_0 - {}^1D_2$. It is necessary to decide then which of these two transitions gives rise to the auroral green line. From fig. 17 it will be seen that strong lines exist in nebular spectra corresponding to the transition $\nu = {}^3\bar{P}_{12} - {}^1D_2$, and that lines corresponding to the transition $\nu = {}^3\bar{P}_0 - {}^1D_2$ are either absent from nebular spectra or appear with intensities too weak for detection. Or it may be that the line represented by $\nu = {}^3\bar{P}_0 - {}^1D_2$, if it existed in nebular spectra, would not be separated sufficiently from the one given by $\nu = {}^3P_1 - {}^1D_2$ to be readily detected. If, then, we assume that the frequency of the auroral green line be given by $\nu = {}^3\bar{P}_0 - {}^1D_2$, we should expect, judging from what obtains in nebular spectra, that lines with frequencies $\nu = {}^3\bar{P}_1 - {}^1D_2$ and $\nu = {}^3\bar{P}_2 - {}^1D_2$ would accompany the auroral green line and appear with much greater intensities. As the wave number differences ${}^3\bar{P}_0 - {}^3\bar{P}_1$ and ${}^3P_1 - {}^3P_2$ for the lowest atomic levels of oxygen are known, and are 67 cm. and 159 cm. respectively, it is clear that such spectral lines should be easily detectable. From the fact that these lines do not appear either in the spectra of polar and non-polar aurora or in the spectrum of oxygen when the radiation of the wave-length λ 5577·341 is emitted by it, we must conclude that the green line cannot be represented by $\nu = {}^3\bar{P}_0 - {}^1D_2$, but must be given by $\nu = {}^1D_2 - {}^1S_0$.

---

* 'Roy. Soc. Proc.,' A, vol. 114, p. 1 (1927).

Our analysis of the polar and non-polar spectra has led us quite definitely to the conclusion that the atomic transition involved in the production of the auroral green line must be a low level one in the atom of oxygen. The only possible spectral levels that can be involved are the metastable ones ${}^1S_0$ and ${}^1D_2$, and the stable ones ${}^3\bar{P}_{012}$. With the magnetic resolution of the wave-length λ 5577·341 that we have succeeded in photographing so clearly, it would appear to be impossible to reach any other conclusion than that the auroral green line has its origin in atomic oxygen and is due to a transition between the low metastable energy states represented by ${}^1D_2$ and ${}^1S_0$. This conclusion is of some interest for it is not in accordance with a view recently published by L. A. Sommer.* In a short note by him that appeared recently he assigned the auroral green line λ 5577·341 to the low level transition ${}^3\bar{P}_1 - {}^1S_0$ in the atomic system of oxygen, and stated that he found the line resolved under longitudinal observation into a doublet with 3/2 times the separation of the outer components of a normal triplet.

If we may take the transitions taking place in the atom ion system of Oxygen III which give rise to nebular spectral lines as indicative of what might be expected to occur with the atomic system of Oxygen I under conditions of high rarefaction, it would follow from our conclusion that the auroral green line originates in the atoms of oxygen and has a frequency given by

---

* 'Naturw.,' vol. 13, p. 210 (1928)

$\nu = {}^1D_2 - {}^1S_0$, that both polar and non-polar auroral spectra should contain lines corresponding to $\nu = {}^3\bar{P}_{12} - {}^1D_2$ and possibly to $\nu = {}^3\bar{P}_0 - {}^1D_2$ as well. Moreover, such spectral lines should have wave-lengths longer than λ 5577·341. They would probably be, however, too far in the infra-red region to be recorded with λ 5577·341 in night sky work, unless plates specially stained were used. During the course of our investigations of the spectral lines obtainable with oxygen-argon mixture, it was found when plates stained with neocyanin were used, that a line always came out on them at or near λ 7600 whenever, and only whenever, the auroral green line came out strongly. A second strong sharp line was also recorded at λ 2977, when the oxygen auroral green line was strong. Neither was obtained on the plates with oxygen or with argon alone. Both lines always appeared to be single and were never accompanied by a second second line with a wave-number difference of 67 cm.$^{-1}$ or 158 cm^{-1} (${}^3P_{02} - {}^3\bar{P}_1$). No wave-lengths appeared at either λ 6363·8 or at or near λ 3200. This led us to conclude that the wave-length λ 2977 could not be given by one of the frequencies $\nu = {}^3\bar{P}_{012} - {}^1S_0$, and the wave-length λ 7600 not by any one of the frequencies $\nu = {}^3\bar{P}_{012} - {}^1D_2$. This point is, however, worthy of further investigation, and as photographic plates suitably stained enable one to record spectral lines as far up as λ 10000, it should be possible to photograph with the spectrographs that have been developed recently for night sky work the infra-red spectrum of both the polar and the non-polar auroral light and obtain a record of the wave-lengths $\nu = {}^3\bar{P}_{012} - {}^1D_2$ if they have a real existence in such light. The infra-red spectrum of the light of the electrical discharge in argon-oxygen mixtures should also be more fully explored to see if the conditions that give the auroral green line with strong intensity also favour the emission of radiation that can correspond to one or more of the frequencies $\nu = {}^3\bar{P}_{012} - {}^1D_2$.

Daily Variations in the Intensity of the Auroral Green Light from the Night Sky.

Lord Rayleigh* has recently given an account of the results of a very extensive survey organised by him and carried out with the co-operation of a number of workers, on the intensity of the light of the auroral green line from the night sky, as observed at a number of stations scattered over the world. The broad result of this investigation is that while the intensity of this light varied for the most part irregularly its values at all stations were included in the same general range of intensities that were found to apply to observations in England. Indications were obtained of an annual periodicity with a maximum intensity in October in the Northern hemisphere and in April in the Southern hemisphere. Lord Rayleigh's observations in England have also indicated a progressive increase in intensity from year to year for the last four years.

---

* 'Roy. Soc. Proc.,' A, vol. 119, p. 11 (1928).

As this increase has occurred during the rise from sunspot minimum to sunspot maximum, it is thought by him to indicate a periodicity in the 11-years' period of the solar cycle.

At the close of his paper Lord Rayleigh states that he has overcome most of the difficulties connected with the use of a photo-electric cell, and that in preliminary observations made with it during some months past he has been able to follow the changes in intensity of the night sky light from hour to hour on clear nights.

Some observations I have recently made with the help of my associates, Mr. H. J. C. Ireton and Mr. J. H. McLeod, are of interest in connection with this matter, for they appear to show quite definitely that from sunset onwards there is a gradual increase in the intensity of the auroral light received from the zenith of the clear night sky. Our observations showed that the intensity reached a maximum in about an hour and a half after midnight, and from that time onwards until sunrise, gradually lessened.

In this investigation two lines of procedure were followed. In the one case a continuous record of the intensity was obtained by means of a filter and slit moved at a uniform rate over a photographic plate, and in the other a sequence of records of intensity was obtained by photographing the auroral green line with one or other of a number of spectrographs of high light power. With the most efficient of the spectrographs used it was found possible to obtain satisfactory spectrograms of the green line radiation from the zenith of the night sky with exposures as short as 30 minutes.

Some of our observations were made at a point a few miles north of Toronto. A few were made at Esterhazy, Saskatchewan, but most of them were made through the courtesy and with the help of Dr. V. M. Slipher, at the Lowell Observatory, Flagstaff, Arizona, U.S.A.

Four spectrographs were used for this work, and their speeds varied by amounts that at first sight may seem surprising. The considerations which should guide one in the design of a spectrograph for work of this kind (observation of variations in the intensity of a single spectral line) may perhaps be recorded here with advantage.

Instrument No. 1.—In our first spectrograph, an instrument assembled at my request by the Adam Hilger Co., the collimator was provided with a simple lens of focal length about 12 cm. The prism was a direct vision one of high dispersion, which happened to be immediately available, with an aperture of about 10 × 13 mm. The camera lens was an F/1·9 Dallmeyer photographic lens with a focal length of 2 inches. With this instrument it was found possible to record the green line very faintly at Toronto with a total exposure of about 16 hours. The dispersion of this instrument was considerable for its small size, the spectrum range per millimetre being only 60 Å.

It was desirable for the purpose of these experiments to increase as greatly as possible the speed of the spectrograph. High dispersion, *per se*, is no cause of lack of intensity in the spectrography of sharp spectral lines, but it was with the prism used in this instrument associated with high absorption (as it usually is), with a large loss of light by reflection from the glass surfaces and, most serious of all, with a small aperture

Instrument No. 2.—In the second spectrograph the collimator lens was a photographic F/2·7 one, having a focal length of 3 inches. The prism was a dense flint one, and had a refracting angle of 60°. The refractive index was $\mu = 1\cdot621$. For a camera lens the 2-inch focus camera lens belonging to Instrument No. 1 was used In tests made with this instrument at Saskatchewan observable records of the green line were obtained with an exposure of 4 hours on a moonless night in December. A whole night's exposure of about 10 hours at Toronto gave a fairly good record.

Instrument No. 3.—In spectrograph No. 3 the collimator and camera lenses were identical, and were Taylor-Hobson F/2 anastigmats of focal length 2 inches. The prism was of dense flint glass, with refracting angle 60° and refractive index $\mu = 1\cdot64695$. With this instrument a good spectrogram of the auroral green light was obtained in 8 hours at Toronto, on a clear moonless night. In this case Eastman Green sensitive plates were used. With this instrument it was found that the green line could be recorded with an exposure of 2 hours and 40 minutes, at the Lowell Observatory at Flagstaff, Arizona, when Cramer Isochromatic plates were used. Exposures of 4 hours with this instrument at Flagstaff gave excellent spectrograms.

A few points that became clear to us through our experience in using these three instruments may be mentioned. First, there was much loss of light incurred by the use of compound uncemented lenses. The loss at each surface of an element of a lens for light falling perpendicularly upon it was found to be as much as 4 to 5 per cent. Secondly, in the spectrography of extended light sources such as the sky, the focal length of the collimator lens has no direct effect on the "speed" of the spectrograph. It is true that a lens of very short focal length may require, for its whole aperture to be effective, special attention to be paid to the jaws of the slit in order that they do not obstruct light passing through them at high obliquity, and for this reason the collimator lens had better be of long focus, say not less than ten times the effective aperture. It is desirable too that the slit should not be too narrow, or the individual grains of the photographic plate might not be fully illuminated; and although this can be remedied very simply by widening the slit, it is perhaps an argument against choosing a collimating lens of excessively long focus.

The factors of prime importance are A, the effective area of the *camera* lens as limited by the prism, and F, its focal length; and if we ignore loss of light by absorption and reflection, the relative speeds of spectrographs intended for the photography of well separated bright lines are given by the expression A/F.

Instrument No. 4.—By far the most speedy instrument we employed was one Dr. V. M. Slipher kindly allowed my collaborator, Mr. Ireton, to use. In its construction it fulfilled most of the requirements set forth above. The details of this spectrograph, hitherto unpublished, are given here with Dr. Slipher's permission, as follows. Its collimator lens was an ordinary visually corrected lens such as is found in the finder of a telescope. It consisted of two elements, one of flint and one of crown glass separated by a ring of paper. Its focal length was 16 inches and its diameter 2 inches. The prism was made by Brashear and was of Mantois glass. It had refracting angles of 64°, 56° and 60°. Its faces were approximately 4 inches by 2½ inches. The camera lens was a single one made by John E. Mellish, of St. Charles, Illinois, U.S.A. Its focal length was 2 inches and its diameter 2 inches. With this instrument very strong records of the green line were obtained at Flagstaff in 30 minutes.* It had a dispersion of about 250 to 300 Å per millimeter.

---

* In the data collected in the following table there is a sufficient explanation of the different speeds of the four instruments —

Camera.	Prism.	Collimator focus.	Camera focus = F.	Area of effective aperture = A.	Approximate dispersion Å.U. per mm.	Relative speed.		Exposures with which good records were obtained.
No. 1, Hilger	D V.	4½″	2″ *f*/1·9	0·12	60	0·06	1·0	16 hours.
No. 2, Toronto make	60°	3″	2″ *f*/1·9	0·78	500	0·39	6·5	10 hours.
No. 3, Toronto make	60°	3″	3″ *f*/2	1·76	300	0·59	9·8	8 hours.
No. 4, Dr. Slipher, one prism instrument	64° 56° 60°	16″	2″ *f*/1	3·14	250–300	1·57	26·0	30 minutes.

(1) In the column headed "Approximate dispersion" the numbers given have been calculated from the data that were available at the time of writing.

(2) The collimator focal length has no effect on the exposure (within wide limits).

(3) For sharp lines on dark ground the dispersion per millimeter has little effect on exposure, but high dispersion is associated with high absorption and reflection from the glass surface.

(4) It follows (ignoring loss of light by absorption and reflection) that the relative speeds are—effective area of aperture of camera lens/focal length of camera lens

Fig. 20

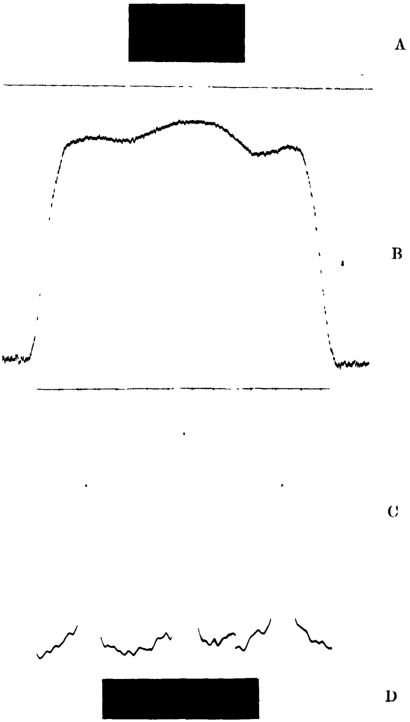

Fig. 21.

Exposures were made at Flagstaff with Instruments Nos. 3 and 4, on the moonless portions of nights between April 15 and April 24 last, and the detailed results of this work will appear in another place.

Illustrations of the records of the auroral green line obtained with Instrument No. 4 are shown in the reproduction D of fig. 21 (Plate 17). Each was obtained with an exposure of 2 hours 30 minutes. The one on the left was obtained between 8.40 p.m. and 11.10 p.m., the centre one between 11.10 p.m. and 1.40 a.m., and the one on the right between 1.40 a.m. and 4.10 a.m On this night the sun set at 7.01 p.m. and rose in the morning at 5.50 a.m., the moon rose at 5 34 a.m. The sky was described as fairly good during the night, but best during the first period of exposure.

Moll photometric tracings of the lines in D, fig. 21, are shown in C, fig. 21. The central photograph, it will be seen, shows the line strongest.

Filter Experiments.

The filter camera was made so that a plate in which there was a carefully made slit covered by a glass filter could be slowly moved over a photographic plate that was held close up to it. The motion was provided by an ordinary alarm clock. The pitch of the screw moving the plate with the slit in it was $\frac{1}{8}$ of an inch, and the width of the slit was $\frac{1}{8}$ of an inch. The clock rotated the screw once each hour, so that excepting for the first and last hours of exposure, each point illuminated on the photographic plate was exposed for 1 hour. The filter used was one of the " auroral filters " kindly provided by Lord Rayleigh with the photometer referred to in his recent communication (*loc. cit.*). The photograph reproduced in fig. 20 (Plate 16) shows the spectrum of the light from a pointolite lamp that was transmitted by this filter.

The transmission was practically limited to a range of 250 Å, between λ 5450 and λ 5700. The filter was therefore well suited for observations on the night sky light corresponding to the auroral green line. The exposures were made with the photographic plate in a horizontal position, so that it was directly exposed to the whole of the sky. One of the records obtained is shown slightly enlarged in A of fig. 21 (Plate 17). A Moll tracing of the distribution of intensity is shown in B, fig. 21. The exposure was begun at 8.30 p.m. and was ended at 5.34 a.m. on the same night as the spectral lines shown in D, fig. 21, were photographed.

In order to make the meaning of the tracing shown in B, fig. 21, clear, let us suppose the apparatus started at 8 p.m. with the slit and filter moving to the right. The portion of the photographic plate that was under the right-hand edge of the slit at 8 p.m. would then be exposed to the sky until the left-hand side of the slit passed over it. This portion of the plate would therefore have recorded on it the effect of light falling on it between 8 p.m. and 9 p.m. Each point on the plate to the left of that just referred to would either not have been exposed at all or would have been exposed for a time somewhere between zero and 1 hour. This explains the sharp increase in intensity up to a maximum value shown by B of fig. 21. Where the maximum begins, corresponds to the point from which the right-hand side of the slit started. The point at which the microphotometer first rises to full value gives the mean intensity of the light between 8 and 9 p.m. This point should be taken as 8.30 p.m., and this means that at that point on the microphotometer curve the intensity is for the hour whose centre time is 8.30 p.m. Similar reasoning shows that the point in that part of the curve corresponding to the morning where the curve starts to drop sharply, corresponds to the mean intensity of the light for the last hour of exposure. The time of this point should be recorded as one-half an hour before the time at which the instrument was shut off in the morning.

From the tracing shown in B, fig. 21, it is evident that while the intensity of the night skylight was continually changing, there is clear evidence of a gradual increase in intensity during the first half of the night, followed by a decrease in the second half. As to this feature, the tracings in B, fig. 21, and C, fig. 21, agree, which goes to show that in using the auroral filter there was justification for supposing that it practically transmitted only the light of the auroral green line.

Exposures were made with the filter camera during suitable portions of the nights between April 15 and April 23, and with most of the exposures indications were obtained of this gradual increase in the intensity of the green light from the sky during the first part of the night. In order to bring this point out more clearly the results obtained were combined in a composite tracing.

As the total time of exposure for each plate was known it was possible to mark on all the microphotometer curves a series of points corresponding to each half-hour of the night. For example, in the case of an exposure from 8 p.m. to 4 a.m., a total duration of 8 hours, the horizontal portion of the microphotometer tracing would correspond to 7 hours, *i.e.*, from 8.30 p.m. to 3.30 a.m., and this horizontal portion could be divided into 14 equal parts, giving 15 points on the curve, each pair of points being separated by a distance corresponding to half an hour.

If h_0 represents the deflection of the microphotometer galvanometer for the part of the plate where no image was recorded, and h is the deflection for any point in the image, see B, fig. 21, then the blackening of the plate is given by log h_0/h. The heights h and h_0 were measured for each half-hour point on the tracing for each night, and the blackening was calculated for each of these points. Then the mean blackening for a series of nights was calculated for each of the same points of time, and in this way a mean value was obtained for the blackening corresponding to each half-hour for a series of nights. Two curves were plotted showing the mean blackening as a function of the time during the night. These are shown in fig. 22. The upper is a curve for full exposures on five consecutive nights, *i.e.*, from 9.10 p.m. to 3.40 a.m. The lower is for the mean blackening from 11.40 p.m. to 3.40 a.m. for nine consecutive nights, the first five nights of which were the same as before.

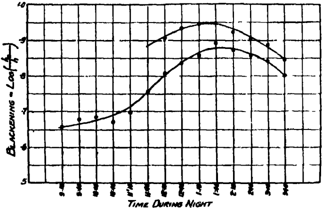

FIG. 22.

In order to get a mean curve that could be compared more directly with the original microphotometer traces obtained from the plates for each night, h_0 was taken as 90 mm. (this being the approximate value of h_0 for the series of curves), and h was then calculated from the mean blackening for each interval. The mean h was then plotted against the time and gave the curves shown in fig. 23 and fig. 24. Fig. 23 is for the five days April 15 to 19 inclusive, for the time 9.10 p.m. to 3.40 a.m., and fig. 24 is for the nine days April 16 to 23 inclusive, from 11.40 p.m. to 3.40 a.m. Both curves show a maximum intensity at about 1.40 a.m.

Information regarding weather conditions at the Lowell Observatory for the period of the investigation is given in Table VIII, and data relating to the exposures made are recorded in Table IX.

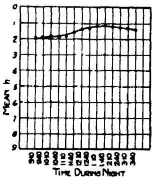

Fig. 23

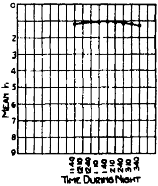

Fig. 24.

Table VIII.—Weather Conditions for Nights at Flagstaff.

Night of April 15. Clouds in the north-east all night, but fair in other regions Better after midnight.

Night of April 16. Sky uniformly hazy throughout the night Slightly less hazy in north and west

Night of April 17 Sky somewhat hazy like the 16th during first period, but clear after 11 o'clock and perfect after 1 o'clock

Night of April 18 Sky fairly good but best during first period

Night of April 19. Sky slightly overcast during first period, but quite clear after 11 o'clock.

Night of April 20 Sky clear, transparency good.

Night of April 21. Sky clear but not brilliant.

Night of April 22. Sky good.

Night of April 23 Sky good

Night of April 24. Sky good.

Table IX.—Data on Exposures.

Night.	Sun set	Exposure.	Moon rose	Sun rose
April 15	6.58 p m.	8.30 p m to 3 50 a m.	3 54 a.m	5 54 a m
,, 16	6 59 ,,	8.30 ,, ,, 4 21 ,,	4 28 ,,	5 53 ,,
,, 17	7 00 ,,	8 30 ,, ,, 4 21 ,,	4 61 ,,	5 51 ,,
,, 18	7.01 ,,	8 30 ,, ,, 4 21 ,,	5 34 ,,	5.50 ,,
,, 19	7.01 ,,	8.30 ,, ,, 4 21 ,,	6 08 ,,	5 48 ,,
			Moon set	
,, 20	7 02 ,,	8.30 ,, ,, 4 21 ,,	7.32 p m.	5 47 ,,
,, 21	7 03 ,,	8.50 ,, ,, 4.10 ,,	8.48 ,,	5.46 ,,
,, 22	7 04 ,,	10 05 ,, ,, 4 10 ,,	10.00 ,,	5 45 ,,
,, 23	7 05 ,,	11 15 ,, ,, 4.10 ,,	11.14 ,,	5 43 ,,
,, 24	7 06 ,,	12 10 a m ,, 4 10 ,,	12 09 a.m	5 42 ,,

While the records of intensity obtained in this investigation cannot be described as other than meagre, they were made with great care and under conditions most favourable for obtaining reliable and accurate information.

These experiments appear to be the first to give evidence of the existence of a diurnal variation in the intensity of the light from the night sky, with a maximum in the intensity of the light giving rise to the auroral green line occurring at or near one hour and a half after midnight. It is desirable that the experiments described here should be continued and extended to include observations at as many points on the earth as possible.

The results recorded here seem to indicate quite definitely that a diurnal radiation and solar radiation may, in some way, as yet obscure, be connected with the origin of the non-polar auroral light. It will be interesting to see if any connection can be established between the daily variations known to occur in the state of ionisation of the upper atmosphere and the variation indicated here in the intensity of the night sky light.

The observational material collected in studies on the height and thickness of the ozone layer in the upper atmosphere should be examined to see if any relation can be found between these factors and the intensity of the night sky radiation Some results obtained by Chalonge* appear to show that the ozone layer remains of constant thickness during any individual night, and that it is thicker at night than during the day. It may be noted here that in the course of some observations made at Toronto, with the help of Dr. Richard Ruedy and Mrs. Krotkov, during the past year, heights for the ozone layer were found of 49·4, 47, 53, 55 and 57 km

These values are of the same order as those found by Dobson and Harrison, Fabry and Buisson and Cabannes and Dufay† at other points on the earth's surface.

In concluding this paper I desire to express my deep appreciation of the loyal co-operation of various associates from time to time. These include Messrs. Shrum, McLeod, McQuarrie, Ireton, McLay, Ruedy, Ball, Thompson, Anderson, Grayson-Smith, Wilhelm, and Chappell I am grateful to Dr. Sliphcr for courtesies extended during the recent visit of my associate, Mr. H. J. C. Ireton, to the Lowell Observatory, and to the Superior of the Roman Catholic Seminary near Toronto for his hospitality at times during the past winter. I desire to express my thanks to Lord Rayleigh, too, for valuable advice in our development of spectrographs of high light power. To Mr. Frank Twyman, F R S., I am indebted for valuable advice and information freely given on numerous occasions. For aid granted to meet in part the cost of investigations dealt with above I am indebted to the National Research Council of Canada and to the Carnegie Corporation.

---

* 'C R,' vol. 186, p. 440 (1928).

† Dobson and Harrison, 'Roy. Soc. Proc,' A, vol. 110, p. 660 (1926), and vol. 114 p 521 (1927); Fabry, 'Proc Phys Soc,' vol. 39, p. 1 (1927); Cabannes and Dufay, 'J. de Physique,' vol. 7, p. 257 (1926), and vol. 8, pp. 125, 353 (1927), also 'C. R.,' vol. 182, p. 331 (1926).

A Series of Bessel Functions connected with the Lattice-Points of an n-Dimensional Ellipsoid.

By J. R. WILTON.

(Communicated by G. H. Hardy, F R S.—Received March 8, 1928.)

This paper is a continuation of the earlier part of the argument of a recent communication to the London Mathematical Society,* to which I shall refer as L.P. II, but the explanation is sufficiently full to enable it to be read without having the earlier paper at hand.

1. *Explanation of Notation.*

Let

$$P_1(m_i) = P_1 = \sum_{i=1}^{n} \sum_{j=1}^{n} a_{ij} m_i m_j \qquad (a_{ij} = a_{ji})$$

be a positive-definite quadratic form whose coefficients a_{ij} are rational. Let D be the discriminant of P_1, and let DQ_1, be the form adjoint to P_1, so that the discriminant of Q_1 is $1/D$, and P_1/D is adjoint to Q_1.

Let $p_1, p_2, \dots, p_n$ and $q_1, q_2, \dots, q_n$ be two sets of rational numbers such that

$$0 < p_i < 1, \qquad 0 < q_i < 1 \qquad (i = 1, 2, \dots, n);$$

let $P = P_1(m_i + p_i)$ and $Q = Q_1(m_i + q_i)$, and let H and K be, respectively, the least integers such that HP and KQ are positive integers for all integer values of the variables m_i.

Further, let,

$$r_P(x) = \sum_{P=x} e^{-2\pi i \Sigma mq} \qquad (x > 0),$$

where

$$\Sigma mq = m_1 q_1 + \quad + m_n q_n,$$

and the sum is to be taken over all positive and negative integer values of $m_1, \dots, m_n$ for which $P = x$, so that $r_P(x)$ is zero unless Hx is an integer. Let

$$R_P(x) = \sum_{h=1}^{Hx}{}' \, r_P\left(\frac{h}{H}\right) = \sum_{0 < P \leq x}{}' \, e^{-2\pi i \Sigma mq},$$

where the accent denotes, in each case, that if Hx is an integer, the terms for which $P = x$ are to be halved.

---

* Wilton, "A Series of Bessel Functions connected with the Theory of Lattice-Points," 'Proc. London Math. Soc.' (not yet published). I shall not have occasion to refer explicitly to an earlier paper (L.P. I), "The Lattice-Points of an n-Dimensional Ellipsoid," 'J. London Math. Soc.,' vol. 2, p. 227 (1927).

In the same way let

$$r_Q(x) = \sum_{Q=x} e^{2\pi i \Sigma mp}, \quad R_Q(x) = \sum_{k=1}^{Kx}{}' \, r_Q\left(\frac{k}{K}\right) = \sum_{0<Q\leqq x}{}' \, e^{2\pi i \Sigma mp}.$$

If indices indicate (fractional) integration, defined when $\kappa > 0$ by the equation,

$$R^{(\kappa)}(x) = \frac{1}{\Gamma(\kappa)} \int_0^x R(u)(x-u)^{\kappa-1}\, du,$$

we have

$$R_P^{(\kappa)}(x) = \sum_{0<P\leqq x}{}' \, (x-P)^\kappa e^{-2\pi i \Sigma mq} / \Gamma(\kappa+1),$$

with a corresponding equation for $R_Q^{(\kappa)}(x)$.

Finally the function $\psi_P^{(\kappa)}(x)$ is defined by the equation

$$\frac{\psi_P^{(\kappa)}(x)}{\sqrt{D}} = \eta_P \frac{x^\kappa}{\Gamma(\kappa+1)} - \eta_Q \frac{\pi^{\frac{1}{2}n} x^{\kappa+\frac{1}{2}n}}{\sqrt{D}\,\Gamma(\kappa+\frac{1}{2}n+1)} + R_P^{(\kappa)}(x),$$

where

$$\eta_P = 1 \quad \text{if} \quad p_1 = p_2 = \ldots = p_n = 0, \quad \text{otherwise} \quad \eta_P = 0,$$

and

$$\eta_Q = 1 \quad \text{if} \quad q_1 = q_2 = \ldots = q_n = 0, \quad \text{otherwise} \quad \eta_Q = 0;$$

and $\psi_Q^{(\kappa)}(x)$ is defined by the corresponding equation, in which, it must be remembered, $1/D$ takes the place of D.

2. *Statement of the Problem.*

Lemma 1.—*With the notation of* § 1, *if* $\kappa > -1$, $\lambda = 1$ *if* $\kappa > \frac{1}{2}(n-5)$, *and otherwise* $\lambda = [\frac{1}{2}n - \kappa - \frac{1}{2}]$, $x > 0$, $N > 0$, $n \geqslant 2$, *then*

$$(2.1) \quad \sqrt{D}\left\{\pi^\kappa \psi_Q^{(\kappa)}(x)\, e^{2\pi i \Sigma pq} - \sum_{h=1}^{HN}{}' \, r_P\left(\frac{h}{H}\right)\left(\frac{Hx}{h}\right)^{\frac{1}{4}n+\frac{1}{2}\kappa} J_{\frac{1}{2}n+\kappa}\left(2\pi \sqrt{\frac{hx}{H}}\right)\right\}$$

$$(\Sigma_1) \qquad = \pi^\lambda \int_N^\infty \left(\frac{x}{\sigma}\right)^{\frac{1}{4}n+\frac{1}{2}\kappa+\frac{1}{2}\lambda} J_{\frac{1}{2}n+\kappa+\lambda}\{2\pi\sqrt{(\sigma x)}\}\psi_P^{(\lambda-1)}(\sigma)\, d\sigma$$

$$(\Sigma_2) \qquad - \sum_{k=0}^{\lambda-1} \pi^k \left(\frac{x}{N}\right)^{\frac{1}{4}n+\frac{1}{2}\kappa+\frac{1}{2}k} J_{\frac{1}{2}n+\kappa+k}\{2\pi\sqrt{(Nx)}\}\, \psi_P^{(k)}(N)$$

$$(\Sigma_3) \quad + \eta_Q\left\{\sum_{k=1}^{[\frac{1}{2}n]} \frac{\pi^{\frac{1}{2}n-k}}{\Gamma(\frac{1}{2}n-k+1)} N^{\frac{1}{2}n-k}\left(\frac{x}{N}\right)^{\frac{1}{4}n+\frac{1}{2}\kappa-\frac{1}{2}k} J_{\frac{1}{2}n+\kappa-k}(2\pi\sqrt{(Nx)}) + \Theta_n(x)\right\}$$

$$= \Sigma_1 + \Sigma_2 + \Sigma_3,$$

say, where $\Theta_n(x) = 0$ *when n is even, and when n is odd,*

$$\Theta_n(x) = \sqrt{\frac{2}{\pi}}\,(2\pi x)^\kappa \int_{2\pi\sqrt{(Nx)}}^\infty \frac{J_{\kappa+\frac{1}{2}}(t)}{t^{\kappa+\frac{1}{2}}}\, dt,$$

and J *is the Bessel function of the first kind.*

The lemma results from the combination of Theorems B and B′ of L.P. II. It is not necessary for the truth of the lemma that the q_i should be rational; this restriction is introduced for the sake of the application. Further, λ may be any positive integer not less than the values stated; and, in fact, (2.1) will be employed with $\lambda = [\frac{1}{2}n + \frac{1}{2}]$, when the series for $\psi_P^{(\lambda-1)}(\sigma)$, corresponding to that for $\psi_Q^{(\kappa)}(x)$ on the left of (2.1), is convergent, though not absolutely convergent.*

The problem is to determine an "Abschätzung," in terms of x and N, for the expression on the left of (2.1). I believe that this has not been previously attempted in quite the same form except when $\kappa > \frac{1}{2}(n-1)$, so that the series is absolutely convergent,† and in the particular case when $n = 2$, $\kappa = 0$, $p_i = q_i = 0$. The theorem stated below is a generalisation of this case, which is due to Hardy.‡

THEOREM.—*If* $\kappa > -1$, $x \geqslant \text{A} > 0$, $\text{N} \geqslant \text{A}$, $n \geqslant 2$, *then*

$$(2.2) \quad \text{S}(\kappa, \text{N}, x) = \pi^{\kappa}\psi_Q^{(\kappa)}(x)e^{2\pi i\Sigma pq} - \sum_{h=1}^{\text{HN}}{}' r_P\left(\frac{h}{\text{H}}\right)\left(\frac{\text{H}x}{h}\right)^{\frac{1}{2}n+\frac{1}{2}\kappa} \text{J}_{\frac{1}{2}n+\kappa}\left\{2\pi\sqrt{\left(\frac{hx}{\text{H}}\right)}\right\}$$
$$= \text{O}\left(x^{\frac{1}{2}n+\frac{1}{2}\kappa-\frac{3}{4}}\text{N}^{\frac{1}{2}n-\frac{1}{2}\kappa-\frac{3}{4}+\epsilon}\right) + \text{O}\left(x^{\frac{1}{2}n+\frac{1}{2}\kappa-\frac{1}{2}+\epsilon}\text{N}^{-\frac{1}{2}\kappa-\frac{1}{2}}\right) + \phi(\kappa, \text{N}, x),$$

for every $\epsilon > 0$, *where*

(i) $$\phi(\kappa, \text{N}, x) = 0,$$

if

$$[\text{K}x] + 1 - \eta \geqslant \text{K}x \geqslant [\text{K}x] + \eta \qquad (\tfrac{1}{2} \geqslant \eta > 0),$$

or if Kx *is an integer and* $\kappa = 0$;

(ii) *for arbitrary values of* x,

$$\phi(\kappa, \text{N}, x) = \text{O}\left(x^{\frac{1}{2}n+\frac{1}{2}\kappa-1+\epsilon}\text{N}^{-\frac{1}{2}\kappa}\right), \qquad \text{if } \kappa \geqslant 0,$$

while (Kx *not being an integer*)

$$\phi(\kappa, \text{N}, x) = \text{O}\left(x^{\frac{1}{2}n-1+\epsilon}\right)\left\{(\text{K}x - [\text{K}x])^{-|\kappa|} + (1 + [\text{K}x] - \text{K}x)^{-|\kappa|}\right\},$$

if $0 > \kappa > -1$.

---

* L.P. II, Theorems C and C′.

† E. Landau, 'Berlin. Akad. Ber.,' vol. 31, p. 458 (1915), for the case when κ is an integer; the general case is due to Müntz, 'Berlin. Sitzungsb.,' vol. 24, p. 81 (1925).

‡ 'Roy. Soc. Proc.,' A, vol. 107, p. 623 (1925), Theorem 3. Hardy omits the term $\phi(\kappa, \text{N}, x)$, which is, in his case, $\text{O}(x^{\epsilon})$.

It is possible, at heavy cost,* to improve slightly upon the theorem; namely, if the second O-term on the right of (2.2) be multiplied by $\log x$, the theorem is true, when $n \geqslant 5$ and $\kappa > 0$, if we put $\epsilon = 0$ throughout.†

3. *Proof of the Theorem.*

Lemma 2.—*If* $n \geqslant 2$, $\psi_P(x) = O(x^{\frac12 n-\frac12})$, *and*

$$\psi_P^{(\kappa)}(x) = O(x^{\frac12 n-\frac12+\epsilon}) \qquad (0 < \kappa < \tfrac12 n - \tfrac12)$$

for every $\epsilon > 0$.

As stated in L.P. II,‡ this is a crude theorem, very far from representing all that is known. It shows that

$$\text{(3.1)} \qquad \Sigma_2 = O\left\{\underset{0 \leqq k \leqq \lambda-1}{\operatorname{Max}} x^{\frac14 n+\frac12\kappa-\frac14} N^{\frac14 n-\frac12\kappa-\frac34+\epsilon}\left(\frac{x}{N}\right)^{\frac12 k}\right\}.$$

Thus, if $A > 0$, and $N \geqslant Ax$,

$$\text{(3.11)} \qquad \Sigma_2 = O(x^{\frac14 n+\frac12\kappa-\frac14} N^{\frac14 n-\frac12\kappa-\frac34+\epsilon}),$$

and if $N < Ax$, remembering that $\lambda \leqslant \frac12 n + \frac12$,

$$\text{(3.12)} \qquad \Sigma_2 = O(zx^{\epsilon}), \text{ where } z = x^{\frac12 n+\frac12\kappa-\frac12} N^{-\frac12\kappa-\frac12}.$$

It is evident that

$$\text{(3.13)} \qquad \Sigma_3 = O(x^{\frac14 n+\frac12\kappa-\frac34} N^{\frac14 n-\frac12\kappa-\frac34}),$$

which is clearly included in (3.11).

The sole difficulty in the proof of the theorem lies in the determination of an upper bound to the integral Σ_1. The final result is contained in equations (3.5) to (3.53). I find it necessary to assume that $\lambda = [\frac12 n + \frac12]$, and therefore

$$\text{(3.2)} \quad \pi^{\lambda-1}\psi_P^{(\lambda-1)}(\sigma)\, e^{-2\pi i \Sigma pq} = \sum_{k=1}^{\infty} r_{Q'}\left(\frac{k}{K}\right)\left(\frac{K\sigma}{k}\right)^{\frac14 n+\frac12\lambda-\frac12} J_{\frac12 n+\lambda-1}\left\{2\pi\sqrt{\left(\frac{k\sigma}{K}\right)}\right\},$$

---

* The improvement requires (i) that $r_Q(x)$ shall be $O(x^{\frac12 n-1})$, and (ii) in order that in the first O term N^{ϵ} should be replaced by 1, the assumption that, in Lemma 7, $\epsilon = 0$ for integer values of $\kappa < \frac12 n - \frac12$. Of these (i) is certainly true when $n \geqslant 5$—that it is not true when $n = 4$ is shown by Walfisz, 'Math. Z.,' vol. 26, p. 66 (1927)—but, slight as is the improvement on the elementary (3.321), I am not aware that a proof has been given without employing $\psi_Q(x) = O(x^{\frac12 n-1})$, $n \geqslant 5$, a deep theorem due to Walfisz, *ibid.*, vol. 19, p. 300 (1924), and Landau, *ibid.*, vol. 21, p. 126 (1924). The assumption (ii) is classical when $\kappa = 0$ (see footnote † following Lemma 7); but when $\kappa > 0$ it requires

$$\psi_Q(x) = O\left(x^{\frac12 n-1+\frac{1}{n+1}-\epsilon}\right) \text{ for } some\ \epsilon > 0;$$

and when $0 > \kappa > -1$ I do not know whether it is true or not.

† In case $n = 4$ we may put $N^{\epsilon} = 1$ and replace x^{ϵ} by $\log^3 x$; for, when $n = 4$, $r_Q(x) = O(x \log^2 x)$ (Landau, *loc. cit.*), and this must be multiplied by $\log x$.—See (3.51).

‡ Lemmas 2 and 4.

where

$$Q' = Q_1(m_\iota - q_\iota) \qquad (\iota = 1, 2, \dots, n),$$

and

$$(3.21) \qquad r_{Q'}(x) = \sum_{Q'=x} e^{-2\pi i\Sigma mp} = r_Q(x),$$

as is seen by changing the sign of m_ι $(\iota = 1, 2, \dots, n)$.

By the asymptotic expansion of the Bessel function,

$$(3.3) \qquad J_{\frac{1}{2}n+\kappa+\lambda}\{2\pi\sqrt{(\sigma x)}\} = \pi^{-1}(\sigma x)^{-\frac{1}{4}}\phi(\sigma, x) + \chi(\sigma, x),$$

where

$$\phi(\sigma, x) = \cos s_1 - C(\sigma x)^{-\frac{1}{2}}\sin s_1,$$

$$(3.30) \qquad s_1 = 2\pi\sqrt{(\sigma x)} - \tfrac{1}{2}\pi(\tfrac{1}{2}n + \kappa + \lambda + \tfrac{1}{2}),$$

C is a constant, the precise value of which is of no consequence, and

$$\chi = \chi(\sigma, x) = O(\sigma x)^{-5/4};$$

so that, in Σ_1, if we choose $\varepsilon < \frac{1}{4}$ in Lemma 2,

$$(3.31) \qquad \pi^\lambda \int_N^\infty \left(\frac{x}{\sigma}\right)^{\frac{1}{2}n+\frac{1}{2}\kappa+\frac{1}{2}\lambda} \chi\psi_P^{(\lambda-1)}(\sigma)\,d\sigma = O(z),$$

where z is defined by (3.12).

LEMMA 3.—*If* $n \geqslant 2$, $\kappa > -1$, $\lambda = [\frac{1}{2}n + \frac{1}{2}]$, *and* $\psi_P^{(\lambda-1)}(\sigma)$ *is given by* (3.2), *change of order of integration and summation is permissible in* Σ_1; *and if* $\phi = \phi(\sigma, x)$ *is defined by* (3.3),

$$(3.32) \quad \Sigma_1 = O(z)$$
$$+ e^{2\pi i\Sigma pq} x^{\frac{1}{2}\kappa+\frac{1}{2}} \sum_{k=1}^{\infty} r_Q\left(\frac{k}{K}\right)\left(\frac{Kx}{k}\right)^{\frac{1}{2}n+\frac{1}{2}\lambda-\frac{1}{2}} \int_N^\infty \sigma^{-\frac{1}{2}\kappa-\frac{1}{2}}\,\phi J_{\frac{1}{2}n+\lambda-1}\left\{2\pi\sqrt{\left(\frac{k\sigma}{K}\right)}\right\}d\sigma,$$

provided that, when $0 > \kappa > -1$, Kx *is not an integer.*

The series (3.2) is uniformly convergent* over any finite interval (N, N′) of values of σ; hence, by Dini's test,† the change of order is permissible if the series of integrals in (3.32), when taken between the limits N and T, converges uniformly over the infinite interval $T \geqslant N$.

Omitting the argument of the Bessel function, and observing that

$$\sigma^{\frac{1}{2}n+\frac{1}{2}\lambda-\frac{1}{2}} J_{\frac{1}{2}n+\lambda-1} = \frac{1}{\pi}\sqrt{\left(\frac{K}{k}\right)}\frac{d}{d\sigma}\left(\sigma^{\frac{1}{2}n+\frac{1}{2}\lambda} J_{\frac{1}{2}n+\lambda}\right),$$

---

* L.P.II, Theorems C and C′.

† Bromwich, 'Theory of Infinite Series' (1926), p. 502, Theorem C.

we have, on integrating by parts,

$$\int_N^T \sigma^{-\frac{1}{4}\kappa-\frac{3}{4}}\,\phi J_{\frac{1}{2}n+\lambda-1}\,d\sigma = \frac{1}{\pi}\sqrt{\left(\frac{K}{k}\right)}\Big[\sigma^{-\frac{1}{4}\kappa-\frac{1}{4}}\,\phi J_{\frac{1}{2}n+\lambda}\Big]_N^T$$

$$-\frac{1}{\pi}\sqrt{\left(\frac{K}{k}\right)}\int_N^T \sigma^{-\frac{1}{4}\kappa-\frac{5}{4}}\left\{\sigma\frac{d\phi}{d\sigma}-\left(\tfrac{1}{4}n+\tfrac{1}{2}\lambda+\tfrac{1}{4}\kappa+\tfrac{1}{4}\right)\phi\right\} J_{\frac{1}{2}n+\lambda}\,d\sigma.$$

Since*

(3.321) $$r_Q(k/K) = O\left(k^{\frac{1}{2}n-1+\epsilon}\right) \qquad (\epsilon > 0),$$

the series of integrated parts is absolutely convergent, and is $O(N^{-\frac{1}{4}\kappa-\frac{1}{4}})$, uniformly with respect to T. And, in fact,

$$\sum_{k=1}^{\infty} r_Q\left(\frac{k}{K}\right)\left(\frac{K}{k}\right)^{\frac{1}{4}n+\frac{1}{2}\lambda-\frac{1}{4}}\int_N^T \sigma^{-\frac{1}{4}\kappa-\frac{3}{4}}\,\phi J_{\frac{1}{2}n+\lambda-1}\,d\sigma$$

$$=\sqrt{x}\sum_{k=1}^{\infty} r_Q\left(\frac{k}{K}\right)\left(\frac{K}{k}\right)^{\frac{1}{4}n+\frac{1}{2}\lambda}\int_N^T \sigma^{-\frac{1}{4}\kappa-\frac{3}{4}}\,J_{\frac{1}{2}n+\lambda}\sin s_1\,d\sigma + O(N^{-\frac{1}{4}\kappa-\frac{1}{4}})$$

$$=\frac{\sqrt{x}}{\pi}\sum_{k=1}^{\infty} r_Q\left(\frac{k}{K}\right)\left(\frac{K}{k}\right)^{\frac{1}{4}n+\frac{1}{2}\lambda+\frac{1}{4}}\int_N^T \sigma^{-\frac{1}{4}\kappa-1}\sin s_1\cos s_2\,d\sigma + O(N^{-\frac{1}{4}\kappa-\frac{1}{4}}),$$

uniformly with respect to T, where

(3.322) $$s_2 = 2\pi\sqrt{(k\sigma/K)} - \tfrac{1}{2}\pi\left(\tfrac{1}{2}n+\lambda+\tfrac{1}{2}\right).$$

The whole expression is $O(N^{-\frac{1}{4}\kappa})$ if $\kappa > 0$; and if

$$-1 < \kappa < 0,$$

it is, by the second theorem of the mean,

(3.33) $$O(N^{-\frac{1}{4}\kappa-\frac{1}{4}})\left|\sum_{k=1}^{\infty} k^{\frac{1}{4}n-\frac{1}{2}\lambda-\frac{5}{4}+\epsilon}\int_N^{T'}\sin\left\{2\pi\sqrt{\sigma}\left(\sqrt{x}-\sqrt{\frac{k}{K}}\right)-\tfrac{1}{2}\pi\kappa\right\}\frac{d\sigma}{\sqrt{\sigma}}\right|$$
$$+\,O(N^{-\frac{1}{4}\kappa-\frac{1}{4}}),$$

where $N < T' \leqslant T$. If $\kappa = 0$, (3.33) is $O(N^{-\frac{1}{4}})$ for every x, and if $-1 < \kappa < 0$, it is $O(N^{-\frac{1}{4}\kappa-\frac{1}{4}})$ provided that Kx is not an integer. This proves the lemma.

From the asymptotic expansion of the Bessel function†

(3.4) $$J_{\frac{1}{2}n+\lambda-1} = \pi^{-1}K^{\frac{1}{4}}(k\sigma)^{-\frac{1}{4}}\left\{S_1\cos\left(s_2+\tfrac{1}{2}\pi\right) - S_2\sin\left(s_2+\tfrac{1}{2}\pi\right)\right\}$$
$$+\,O\left(\sigma^{-m-\frac{1}{4}}k^{-m-\frac{1}{4}}\right),$$

where m is an integer $\geqslant 1$, and

$$S_1 = 1 + \frac{A_1}{k\sigma} + \dots + \frac{A_{m-1}}{(k\sigma)^{m-1}},$$

$$S_2 = \frac{1}{(k\sigma)^{\frac{1}{2}}}\left\{B_0 + \frac{B_1}{k\sigma} + \dots + \frac{B_{m-1}}{(k\sigma)^{m-1}}\right\},$$

---

* Landau, 'Göttinger Nachr.,' p. 687 (1922).

† G. N. Watson, 'Theory of Bessel Functions,' p. 199 (1922).

in which $A_1, \ldots, B_{m-1}$ are constants whose precise value is immaterial. They are, of course, independent of k.

In (3.32) we may replace $J_{\frac12 n+\lambda-1}$ by

$$-\pi^{-1}K^{\frac12}(k\sigma)^{-\frac12}(S_1 \sin s_2 + S_2 \cos s_2),$$

provided that we introduce a remainder term

$$O(x^{\frac12 n+\frac12\kappa+\frac12\lambda-\frac12}N^{-\frac12\kappa-m}) = O(x^{\frac12 n+\frac12\kappa}N^{-\frac12\kappa-m}). \tag{3.41}$$

LEMMA 4.—*If* $\delta > 0$, *and* $N \geqslant x^{\delta}$, *and if m is chosen so that*

$$2m \geqslant 1 + 1/\delta,$$

then, under the conditions of Lemma 3,

$$\pi\Sigma_1 = -e^{2\pi i\Sigma pq}x^{\frac12\kappa}\sum_{k=1}^{\infty} r_Q\left(\frac{k}{K}\right)\left(\frac{Kx}{k}\right)^{\frac12 n+\frac12\lambda-\frac12}$$
$$\times\int_N^{\infty}\sigma^{-\frac12\kappa-1}\{\cos s_1(S_1\sin s_2+S_2\cos s_2)-C(\sigma x)^{-\frac12}\sin s_1\sin s_2\}\,d\sigma+O(z). \tag{3.42}$$

The truth of the lemma follows from (3.41), since the integral on the right of (3.42) is clearly

$$\int_N^{\infty}\sigma^{-\frac12\kappa-1}\phi(S_1 \sin s_2 + S_2 \cos s_2)\,d\sigma + O(x^{-\frac12}k^{-\frac12}N^{-\frac12\kappa-1}).$$

Consider now any term of the integral (3.42) other than

$$\int \sigma^{-\frac12\kappa-1}\{\cos s_1 - C(\sigma x)^{-\frac12}\sin s_1\}\sin s_2\,d\sigma. \tag{3.43}$$

Such a term is a constant multiple of

$$k^{-\frac12 p}\int_N^{\infty}\sigma^{-\frac12\kappa-\frac12 p-1}\begin{matrix}\cos\\ \sin\end{matrix}(s_1 \pm s_2)\,d\sigma \qquad (p = 1, 2, \ldots, 2m-1). \tag{3.44}$$

In the corresponding term $\Sigma_1^{(p)}$ of (3.42) divide the interval of summation with regard to k into the three parts

$$(1, \tfrac12 Kx), \qquad (\tfrac12 Kx, 2Kx), \qquad (2Kx, \infty).$$

In the first part the integral (3.44) is, by the second theorem of the mean,

$$O(k^{-\frac12 p}N^{-\frac12\kappa-\frac12 p-\frac12}x^{-\frac12}) = O(k^{-\frac12}N^{-\frac12\kappa-1}x^{-\frac12});$$

in the second it is $O(k^{-\frac12}N^{-\frac12\kappa-\frac12})$; and in the third it is

$$O(k^{-\frac12 p-\frac12}N^{-\frac12\kappa-\frac12 p-\frac12}) = O(k^{-\frac12}N^{-\frac12\kappa-1}x^{-\frac12}).$$

Hence, for every value of p,

$$\Sigma_1^{(p)} = O\left(x^{\frac12 n+\frac12\kappa+\frac12\lambda-\frac34}N^{-\frac12\kappa-1}\right) + O\left(x^{\frac12 n+\frac12\kappa+\frac12\lambda-\frac34}N^{-\frac12\kappa-\frac12}\sum_{\frac12 Kx}^{2Kx} k^{\frac12 n-\frac12\lambda-\frac34+\epsilon}\right)$$
$$= O(zx^{\epsilon}).$$

We are left with the integral (3.43), which may be regarded as replacing the integral in (3.42).

LEMMA 5.—*Under the conditions of Lemma* 3

$$\Sigma_1^{(0)} = x^{\frac12\kappa-\frac12}\sum_{k=1}^{\infty} r_Q\left(\frac{k}{K}\right)\left(\frac{Kx}{k}\right)^{\frac12 n+\frac12\lambda-\frac14}\int_N^{\infty}\sigma^{-\frac12\kappa-1}\cos(s_1 \pm s_2)\,d\sigma = O(z).$$

Divide the interval of summation into the three parts

$$(1,\ Kx - Kx^{\theta}),\qquad (Kx - Kx^{\theta},\ Kx + Kx^{\theta}),\qquad (Kx + Kx^{\theta},\ \infty),$$

where $0 < \theta < 1$; and as in the case of (3.44), apply the second theorem of the mean to the integral in the first part and the third, and the first theorem of the mean in the second part. In the first partial interval

$$\sqrt{(Kx)} - \sqrt{k} \geqslant Ax^{\theta-\frac12}\qquad (A > 0),$$

and in the third

$$\sqrt{k} - \sqrt{(Kx)} \geqslant Bk^{\theta-\frac12}\qquad (B > 0).$$

Hence

$$\Sigma_1^{(0)} = O\left(N^{-\frac12\kappa-\frac12}x^{\frac12 n+\frac12\kappa+\frac12\lambda-\frac34}\right)\left\{\sum_{1}^{Kx} x^{\frac12-\theta}N^{-\frac12}k^{\frac12 n-\frac12\lambda-\frac34+\epsilon}\right.$$
$$\left. + x^{\theta}\,.\,x^{\frac12 n-\frac12\lambda-\frac34+\epsilon} + \sum_{Kx}^{\infty} N^{-\frac12}k^{\frac12 n-\frac12\lambda+\epsilon-\theta-\frac14}\right\} = O(z),$$

provided that

$$\tfrac34 + \epsilon < \theta < 1 - \epsilon\qquad (\epsilon < \tfrac18),$$

the lower bound being necessary for the convergence of the last series in case n is even.

Again, since

$$\int_N^{\infty}\sigma^{-\frac12\kappa-1}\sin(s_1 + s_2)\,d\sigma = O\left\{\frac{N^{-\frac12\kappa-\frac12}}{\sqrt{k}+\sqrt{(Kx)}}\right\},$$

the integral is $O(N^{-\frac12\kappa-\frac12}x^{-\frac12})$ when $k \leqslant Kx$, and $O(N^{-\frac12\kappa-\frac12}k^{-\frac12})$ when $k \geqslant Kx$. It now follows from Lemmas 4 and 5 that

$$(3.5)\quad \Sigma_1 = e^{2\pi i\lambda p}\frac{x^{\frac12\kappa}}{2\pi}\sum_{k=1}^{\infty} r_Q\left(\frac{k}{K}\right)\left(\frac{Kx}{k}\right)^{\frac12 n+\frac12\lambda-\frac14}\int_N^{\infty}\sigma^{-\frac12\kappa-1}\sin(s_1-s_2)\,d\sigma + O(zx^{\epsilon})$$

where

$$s_1 - s_2 = 2\pi\sqrt{\sigma}\,\{\sqrt{x} - \sqrt{(k/K)}\} - \tfrac12\pi\kappa.$$

(i) Let x be included in a closed interval which does not contain an integer value of $\mathrm{K}x$; there is then a number η such that

$$[\mathrm{K}x]+\eta \leqslant \mathrm{K}x \leqslant 1+[\mathrm{K}x]-\eta \qquad (0<\eta\leqslant \tfrac12).$$

In this case

$$\Sigma_1 = \mathrm{O}\,(x^{\frac12\kappa}\mathrm{N}^{-\frac12\kappa-\frac14})\left\{\sum_{k=1}^{[\mathrm{K}x]}\frac{|r_{\mathrm{Q}}|}{\sqrt{(\mathrm{K}x)}-\sqrt{k}}+\sum_{k=1+[\mathrm{K}x]}^{2\mathrm{K}x}\frac{|r_{\mathrm{Q}}|}{\sqrt{k}-\sqrt{(\mathrm{K}x)}}\right.$$

$$\left.+\,x^{\frac12 n+\frac12\lambda+\frac14}\sum_{k=2\mathrm{K}x}^{\infty}k^{\frac12 n-\frac12\lambda-5/4+\epsilon}\right\}+\mathrm{O}\,(zx$$

In the first sum

$$\frac{1}{\sqrt{(\mathrm{K}x)}-\sqrt{k}}=\frac{\sqrt{(\mathrm{K}x)}+\sqrt{k}}{\mathrm{K}x-k}<\frac{2}{\eta}\,\frac{\sqrt{(\mathrm{K}x)}}{[\mathrm{K}x]+1-k},$$

and in the second

$$\frac{1}{\sqrt{k}-\sqrt{(\mathrm{K}x)}}<\frac{2}{\eta}\,\frac{\sqrt{k}}{k-[\mathrm{K}x]}.$$

Therefore

$$\Sigma_1=\mathrm{O}\left(x^{\frac12 n+\frac12\kappa-\frac14+\epsilon}\,\mathrm{N}^{-\frac12\kappa-\frac14}\sum_{k=1}^{\mathrm{K}x}\frac{1}{k}\right)+\mathrm{O}\,(zx^{\epsilon})=\mathrm{O}\,(zx^{\epsilon}\log x), \tag{3.51}$$

in which $\log x$ is without significance unless $\epsilon=0$ *

(ii) If $\mathrm{K}x$ is an integer, the particular term $k=\mathrm{K}x$ vanishes if $\kappa=0$; it diverges if $\kappa<0$; and if $\kappa>0$ it is

$$-\,e^{2\pi i\Sigma pq}\,\frac{\sin\frac12\kappa\pi}{\kappa\pi}\left(\frac{x}{\mathrm{N}}\right)^{\frac12\kappa} r_{\mathrm{Q}}\,(x).$$

It is interesting to note that, when $\mathrm{N}>x$, this may be the dominating term of Σ_1.

(iii) If $\mathrm{K}x$ may approach arbitrarily near to an integer value, the two terms for which $k=[\mathrm{K}x]$ and $k=1+[\mathrm{K}x]$ must be considered separately. When $\kappa=0$ the two integrals in (3.5) corresponding to these two values of k are of the form

$$\int_a^{\infty}\frac{\sin t}{t}\,dt=\mathrm{O}\,(1);$$

and if $\kappa>0$ they are clearly $\mathrm{O}\,(\mathrm{N}^{-\frac12\kappa})$. Hence, if $\kappa\geqslant 0$,

$$\Sigma_1=\mathrm{O}\,(zx^{\epsilon})+\mathrm{O}\,(x^{\frac12 n+\frac12\kappa-1+\epsilon}\mathrm{N}^{-\frac12\kappa}). \tag{3.52}$$

And, finally, if $-1<\kappa<0$, the integral in Σ_1 corresponding to $k=[\mathrm{K}x]$ is

$$2\,(2\pi)^{\kappa}\{\sqrt{x}-\sqrt{([\mathrm{K}x]/\mathrm{K})}\}^{\kappa}\int_y^{\infty}t^{-\kappa-1}\sin\,(t-\tfrac12\kappa\pi)\,dt,$$

where

$$y=2\pi\sqrt{\mathrm{N}}\,\{\sqrt{x}-\sqrt{([\mathrm{K}x]/\mathrm{K})}\},$$

---

* That $\epsilon=0$ is true when $n\geqslant 5$; *v.* footnote * on p. 361.

and, since $0 < \kappa + 1 < 1$, the integral is $O(1)$, uniformly with respect to N and x. Hence in this case, if Kx is not an integer,

$$(3.53)\quad \Sigma_1 = O(x^{\frac{1}{2}n-1+\epsilon})\{(Kx-[Kx])^{-|\kappa|} + (1+[Kx]-Kx)^{-|\kappa|}\} + O(zx^{\epsilon}).$$

Lemma 6.—*If* $\delta > 0$, $A > 0$, *and* $x^{\delta} \leqslant N \leqslant Ax$, $x \geqslant B > 0$, $\kappa > -1$, $\epsilon > 0$, $n \geqslant 2$, *and if, when* $-1 < \kappa < 0$, x *belongs to a closed interval within which there is no integer value of* Kx, *then*

$$(3.6)\qquad S(\kappa, N, x) = \Sigma_1 + \Sigma_2 + \Sigma_3 = O(zx^{\epsilon}),$$

where z is defined by (3.12).

This follows, by collecting results, from (3.12), (3.13), (3.5), (3.51) and (3.52).

But, when $N \leqslant Ax$,

$$\sum_{h=1}^{HN}{}' r_P\left(\frac{h}{H}\right)\left(\frac{Hx}{h}\right)^{\frac{1}{2}n+\frac{1}{2}\kappa} J_{\frac{1}{2}n+\kappa}\left\{2\pi\sqrt{\left(\frac{hx}{H}\right)}\right\}$$
$$= O(\Sigma\,|r_P|\,h^{-\frac{1}{2}n-\frac{1}{2}\kappa-\frac{1}{4}}x^{\frac{1}{2}n+\frac{1}{2}\kappa-\frac{1}{4}})$$
$$(3.61)\qquad = O(x^{\frac{1}{2}n+\frac{1}{2}\kappa-\frac{1}{4}}N^{\frac{1}{2}n-\frac{1}{2}\kappa-\frac{1}{4}}\log N)\qquad (\kappa \leqslant \tfrac{1}{2}n-\tfrac{1}{2}),$$

by partial summation, since $\Sigma\,|r_P| = O(N^{\frac{1}{2}n-1})$. The log N is introduced so as to include the particular case $\kappa = \frac{1}{2}n - \frac{1}{2}$. If $\kappa > \frac{1}{2}n - \frac{1}{2}$ the series is absolutely convergent, and is $O(x^{\frac{1}{2}n+\frac{1}{2}\kappa-\frac{1}{4}})$.*

Lemma 7.—*If* $n \geqslant 2$, $x > A > 0$, $\frac{1}{2}n - \frac{1}{2} > \kappa > -1$, $\epsilon > 0$,

$$\psi_Q^{(\kappa)}(x) = O\left(x^{\frac{1}{2}n-1+\frac{\kappa+1}{n+1}+\epsilon}\right) + O(x^{\frac{1}{2}n-1+\epsilon})\{(Kx-[Kx])^{\kappa} + (1+[Kx]-Kx)^{\kappa}\}.$$

The proof consists in the observation that (3.6) and (3.61) are both $O\left(x^{\frac{1}{2}n-1+\frac{\kappa+1}{n+1}+\epsilon}\right)$ when N is chosen so that

$$Bx^{\frac{n-1}{n+1}} \leqslant N < Cx^{\frac{n-1}{n+1}}\qquad (B > 0).$$

The second term in the "Abschätzung" of $\psi_Q^{(\kappa)}(x)$ is, of course, significant only when $-1 < \kappa < 0$, and Kx is allowed to approach arbitrarily near to an integer value.

Lemma 7, when $\kappa = 0$, is classical; it is due to Landau, who proved it, when $q_1 = \ldots = q_n = 0$, so long ago as 1912.† In subsequent papers he extended the theorem and refined upon it to the extent of showing that $\epsilon = 0$.‡ All Landau's proofs are by complex analysis. A proof by real analysis (Pfeiffer's method) in the case when $p_1 = \ldots = p_n = 0$ (as well as $q_1 = \ldots = q_n = 0$) has been given by van der Corput.* When $\kappa > 0$ the lemma may be derived from the particular cases $\kappa = 0$ and $\kappa > \frac{1}{2}n - \frac{1}{2}$ by the use of a mean value theorem due to M. Riesz.† When $0 > \kappa > -1$ I believe it to be new.

---

* See footnote † on p. 360.

† 'Göttinger Nachr.,' p. 687 (1912).

‡ 'Berlin. Aka. Ber.,' p. 458 (1915); 'Wiener Sitzungsb.,' IIa, vol. 124, p. 445 (1925); 'Göttinger Nachr.,' p. 209 (1915).

To have assumed, instead of proving, Lemma 7 would not have shortened the proof of the theorem by half a page.

It is now possible to improve upon (3.1). For, returning to the definition of Σ_2 in Lemma 1, since $\lambda - 1 \leqslant \frac{1}{2}n - \frac{1}{2}$, it is clear from Lemma 7 that

$$(3.7) \qquad \Sigma_2 = O\left\{\operatorname*{Max}_{0 \leq k \leq \lambda - 1} x^{\frac{1}{4}n+\frac{1}{2}\kappa-\frac{1}{4}} N^{\frac{1}{4}n-\frac{1}{2}\kappa-\frac{1}{4}+\epsilon} \left(x\, N^{-\frac{n-1}{n+1}}\right)^{\frac{1}{2}k+\frac{1}{2}}\right\}.$$

Thus, if $A > 0$, and $N > Ax^{\frac{n+1}{n-1}}$.

$$(3.71) \qquad \Sigma_2 = O\left(x^{\frac{1}{4}n+\frac{1}{2}\kappa-\frac{1}{4}} N^{\frac{1}{4}n-\frac{1}{2}\kappa-\frac{1}{4}+\epsilon}\right);$$

and, if $N \leqslant Ax^{\frac{n+1}{n-1}}$,

$$(3.72) \qquad \Sigma_2 = O(zx^{\epsilon}).$$

The equations (3.71) and (3.72), together with (3.13) and (3.51) to (3.53), prove the theorem in case $N \geqslant x^{\delta}$, $\delta > 0$. To complete the proof it is sufficient to show that there is a $\delta > 0$ such that the left-hand side of (2.2) is $O(zx^{\epsilon})$ when $N \leqslant x^{\delta}$.

(i) If $\kappa > \frac{1}{2}n - \frac{1}{2}$, $\quad S(\kappa, N, x) = O\left(x^{\frac{1}{4}n+\frac{1}{2}\kappa-\frac{1}{4}}\right)$,

and there is obviously a $\delta > 0$, *e.g.*, $\delta = \frac{1}{2}(n-1)/(\kappa+1)$, such that

$$\tfrac{1}{2}n + \tfrac{1}{2}\kappa - \tfrac{1}{2} + \epsilon - \tfrac{1}{2}\delta(\kappa+1) > \tfrac{1}{4}n + \tfrac{1}{2}\kappa - \tfrac{1}{4}.$$

(ii) If $\kappa \leqslant \frac{1}{2}n - \frac{1}{2}$, it follows from Lemma 7 that

$$S(\kappa, N, x) = O\left(x^{\frac{1}{2}n-1+\epsilon+\frac{\kappa+1}{n+1}}\right) + O\left\{x^{\frac{1}{4}n+\frac{1}{2}\kappa-\frac{1}{4}+\delta\left(\frac{1}{4}n-\frac{1}{2}\kappa-\frac{1}{4}+\epsilon\right)}\right\},$$

and the condition is satisfied, for both terms, if $\delta < (n-1)/(n+1)$.

The following corollary to the theorem is a generalisation of a theorem stated by Hardy‡ in the particular case of the lattice-points of the circle ($\kappa = 0$).

---

* 'Nieuw Archief voor Wiskunde,' vol. 13, p. 125 (1919).

† 'Acta Univ. Hungaricæ,' vol. 1, p. 114 (1923). The theorem is stated as Lemma 3 of L.P. II, and is there employed for a similar purpose.

‡ Hardy, *loc. cit.*, equation (4.12). The term $O(x^{\kappa})$ should be added on the right on account of the discontinuities of $\overline{P}(x)$ for integer values of x.

Corollary.—If $n \geqslant 2$, $\kappa > -1$, $\epsilon > 0$, $A > 0$, $B > 0$, *and* $A \leqslant N < Bx^{\frac{n+1}{n-1}}$, *then*

$$\pi^{\kappa}\,\psi_Q^{(\kappa)}(x)\,e^{2\pi i \Sigma pq} = \sum_{h=1}^{HN}{}' r_P \left(\frac{h}{H}\right)\left(\frac{Hx}{h}\right)^{\frac14 n+\frac12\kappa} J_{\frac12 n+\kappa}\left\{2\pi\sqrt{\left(\frac{hx}{H}\right)}\right\}$$
$$+\, O\left(x^{\frac14 n+\frac12\kappa-\frac14+\epsilon} N^{-\frac12\kappa-\frac12}\right) + \phi(\kappa, N, x),$$

where $\phi(\kappa, N, x)$ *is defined in the statement of the theorem. In particular, if* $B > A > 0$ *and*

$$Ax \leqslant N \leqslant Bx,$$

then, in every case,

$$S(\kappa, N, x) = O\left(x^{\frac12 n-1+\epsilon}\right)\{(Kx-[Kx])^{\kappa} + (1+[Kx]-Kx)^{\kappa}\}.$$

NOTE BY G. H. HARDY.

Prof. Wilton points out in his footnotes to pp. 360 and 368 an error in my paper which I take the opportunity of correcting explicitly. In the formulæ (4.11) and (4.12) an additional term $O(x^{\epsilon})$ should be inserted on the right-hand side. This term is, in fact, substantially

$$-\frac{1}{\pi} r(\nu)\, sgn(\nu - x) \int_{2\pi\sqrt{x_1}\,|\sqrt{\nu}-\sqrt{\lambda}|}^{\infty} \frac{\sin u}{u}\, du,$$

when x is very near to an integer ν; and tends to zero when $x_1 \to \infty$, but not uniformly.

The error arises on p. 633, (4.24), which should read

$$\text{(4.24)} \qquad S_2 \leqq \sum_{x-\lambda}^{x+\lambda} r(\nu) = O(x^{\epsilon}\lambda + x^{\epsilon}) = O\left(\frac{x^{\frac12+\epsilon}}{\sqrt{x_1}}\right) + O(x^{\epsilon});$$

the sum is not $O(x^{\epsilon}\lambda)$ if λ is small. The application in § 4.3 to the theorem of Littlewood and Walfisz is not affected, since there λ is large.

I take this opportunity also of correcting a slip on p. 629, vol. 107. The last line but one should read

$$= J_1(N'\tau')\,J_1(\tau') + \int_{\tau'}^{\infty} J_1(N'u)\,J_0(u)\,du.$$

There are slight consequential changes in the equations at the top of p. 630, but the final expression is unchanged.

The Chemical Reactions of Carbon Monoxide and Hydrogen after Collision with Electrons.

By A. Caress and E. K Rideal.

(Communicated by T. M. Lowry, F.R S.—Received May 8, 1928.)

In a previous communication* the authors described a method of measuring rates of reaction of molecules and atoms which were being activated by electron collision in suitably constructed triode tubes. The method has since been extended to study the decomposition of carbon monoxide and its interactions with hydrogen.

Carbon monoxide has long been known to undergo decomposition, chiefly into carbon and carbon dioxide in the silent discharge.† A mixture of solid oxides containing chiefly C_3O_2 is always observed ‡ Carbon monoxide and hydrogen yield an even greater diversity of products. Thus Losanitsch and Jovitschitsch§ and de Hemptinne|| noted the production of formaldehyde and its polymers and also some formic acid. Slosse and Nowak¶ and Lob** obtained formaldehyde and methyl alcohol, while the latter also found glycollic aldehyde. M. Berthelot†† stated that excess of hydrogen favours the production of $(CH_2O)_n$, whereas excess of carbon monoxide yields $(C_3H_4O_3)_n$.

Similar reactions occur when the gases are ionised by alpha particles. Cameron and Ramsay‡‡ found that carbon monoxide was decomposed into carbon, carbon dioxide and oxygen, while Lind and Bardwell§§ observed chiefly carbon and carbon dioxide but also some suboxide; mixed with hydrogen, carbon monoxide yields a white solid.

As regards the photochemical reaction, D. Berthelot and Gaudechon|||| found traces of a solid polymer of formaldehyde when a mixture of carbon

* 'Roy. Soc. Proc.,' vol. 115, p. 684 (1927).

† See, for example, Brodie, *ibid.*, vol. 21, p. 245 (1873), etc.

‡ See M. Berthelot, 'C R.,' vol. 82, p. 1360 (1878), etc.; Crespi and Lunt, 'J. Chem. Soc.,' vol. 127, p. 2052 (1925), Ott; 'Ber. Deut. Chem. Ges.,' vol. 58, p. 772 (1925).

§ 'Ber. Deut. Chem. Ges.,' vol. 30, p. 135 (1897).

|| 'Bull. Acad. Roy. Belg.,' vol. 34, p. 269 (1897).

¶ 'Bull. Acad. Roy. Belg.,' vol. 35, p. 547 (1898).

** 'Z. Elektrochem.,' vol. 11, p. 750 (1905).

†† 'C. R.,' vol. 126, p. 609 (1898).

‡‡ 'J. Chem. Soc.,' vol. 93, p. 966 (1908).

§§ 'J. Am. Chem. Soc.,' vol. 47, p. 2675 (1925).

|||| 'C. R.,' vol. 150, p. 1690 (1910).

monoxide and hydrogen was exposed to ultra-violet light, but the existence of a direct photochemical reaction, *i.e.*, unsensitised by mercury vapour, is still in doubt.

The Research Staff of the General Electric Company* observed the disappearance of carbon monoxide in thermionic valves at pressures of about a thousandth millimetre, and potentials capable of sustaining an arc; the rate of "adsorption of ions" was shown to depend on the condition but not on the material of the surface

The object of the present investigation was to study quantitatively the chemical behaviour of the various active species. By choosing a suitable range of pressures (about one-tenth to two-tenths millimetre for the electrode dimensions used), it was possible to collect quantities of products sufficient for chemical tests; whilst the method has the advantage over discharge-tube methods that the initial energies of the colliding electrons is known with sufficient accuracy to enable the breaks in the curves showing reaction-rate as a function of grid-potential to be correlated with the definite limiting electronic energies necessary to produce the various physically active molecules by collision

Experimental

The details of the method are similar to those described in the previous paper.† The main essentials consisted of the reaction system which included a quick-reading McLeod gauge and a cylindrical triode immersed to a constant level in liquid air; the electrodes were symmetrically placed, consisting of a straight wire filament, a helical wire grid and a cylindrical platinum anode; all could be removed by a ground-joint which held a vacuum with only a very fine ring of grease. The vessel V is shown with the lift by means of which the liquid-air level was kept constant. The products of several experiments were drawn into the cooled trap T, where chemical tests were applied. For exhaust, two hard-glass mercury diffusion pumps were used, backed by a Hyvac rotary oil pump.

Hydrogen was purified by slow passage over red hot copper and palladium. Carbon monoxide was made by running pure formic acid into concentrated sulphuric acid on the water bath and was passed through potash bulbs. Phosphoric anhydride was used for drying the gases and for lining the bulbs in which they were stored. The purity of the carbon monoxide was tested by the completeness of its absorption by ammoniacal cuprous chloride.

---

* 'Phil. Mag.,' vol. 48, p. 553 (1924).

† *Loc. cit.*

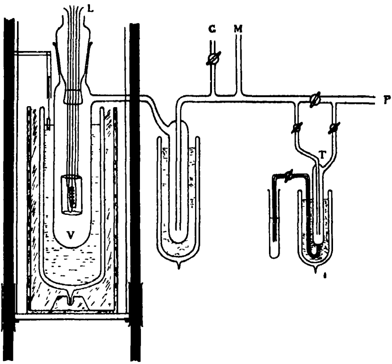

Fig. 1.—L, electrical connection. G, to gas mixtures. M, to gauge.

Measurements.

The determination of primary importance is that of reaction-rate for various voltages, *i.e.*, electron energies, the electron current being kept constant and measured. The rate is a complicated function of the gas pressure as, in addition to the effect of decreasing partial pressures of the reactants, there is the effect of the lengthening mean free path of the electrons. By plotting a series of pressure-time curves, it was possible, however, to compare the average rates over a standard range of pressure.

Measurements were also made of the initial pressure (P_1), the equilibrium pressure (P_2) after the liquid-air baths had been adjusted, the pressure (P_3) at the end of a reaction, the liquid-air baths being still in place, and the final pressure (P_4) at room temperature. The fraction $f = \frac{P_2}{P_1} \cdot \frac{P_1 - P_4}{P_2 - P_3}$ evidently gives a rough measure of the ratio of the decrease in the number of gas molecules by reaction to the number of molecules of reactants. Thus for the reactions

$$2CO \longrightarrow C + CO_2$$

$$CO + H_2 \longrightarrow HCHO,$$

f should be 0·5, while for the reaction

$$n\,\mathrm{CO} + n\,\mathrm{H_2} \longrightarrow (\mathrm{CH_2O})_n \quad \text{(solid)},$$

f should be unity.

A further measurement was made in order to calculate the "efficiencies" defined as the number of molecules removed per electron. An effective current of C milliamperes is equivalent to the passage of $60 \times \frac{\mathrm{C}}{e} \times 10^{-4}$ electrons per minute, where e is the electronic charge in e.m.u. If each electron causes the removal of n molecules, the decrease in pressure in millimetres of mercury per minute is

$$-\frac{dp}{dt} = 60 \times \frac{\mathrm{C}}{e} \times 10^{-4}\, n \times \frac{22400}{\mathrm{V}} \times \frac{760}{\mathrm{N}},$$

where N is the Avogadro number and V the volume of the system, corrected for temperature. Inserting the values $e = 1{\cdot}591 \times 10^{-20}$ e.m.u. and $\mathrm{N} = 6{\cdot}062 \times 10^{23}$, we obtain

$$n = -\,0{\cdot}0944\,\frac{\mathrm{V}}{\mathrm{C}}\,\frac{dp}{dt},$$

V being measured in cubic centimetres, C in milliamperes and $\frac{dp}{dt}$ in millimetres mercury per minute.

The Decomposition of Carbon Monoxide.

Langmuir* has shown that at very high temperatures tungsten combines with carbon monoxide to form the compound WCO. It was found, however, that the gas could be kept in the presence of glowing tungsten for several hours at a temperature high enough to give a suitable thermionic emission without appreciable decrease of pressure. Tungsten filaments were therefore used for the study of the decomposition of carbon monoxide by electrons.

On increase of the electron energy through carbon monoxide, pressure decreases were observed at potentials above the arcing potential. Carbon dioxide was shown to be a product by drawing baryta into the testing trap and comparing the cloudiness with the result of blank tests. After the tube was taken down, carbon was found on the electrodes. Traces of a grey deposit showed inside the valve after such experiment but disappeared during the baking which had to be performed between experiments. Under the conditions of experiment very little oxygen could have been left as the thinning of the filaments was extremely slow. That the main reaction can be represented by the equation

---

* 'J. Am. Chem. Soc.,' vol. 37, p. 1139 (1915).

$$2CO = C + CO_2$$

is shown by the following table of permanent pressure decreases :—

p_1.	p_2.	p_3.	p_4.	f.
mm.				
0·305	0·185	0·114	0·236	0·585
0·443	0·266	0·144	0·323	0·59
0·236	0·142	0·086	0·183	0·57
0·305	0·185	0·128	0·251	0·575

That f is slightly above 0·5 is in agreement with the production of a little solid, probably C_3O_2

Fig. 2 includes some typical pressure time curves. The rates were very

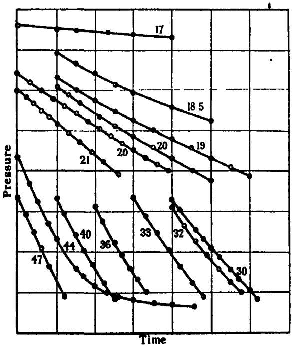

FIG. 2—The numbers represent voltages (uncorrected). For convenience of representation a shifting scale has been employed. Two divisions of the ordinate represent 0·1 mm., one division of the abscissa represents 10 minutes. For each curve the range includes 0·2 to 0·1 mm., except for the lower voltages. V for this tube = 575 c.c. Emission = 1·62 milliamp.

nearly constant over the range 0·2 mm. to 0·1 mm., and the average rates over that range have been plotted against the uncorrected voltages in fig. 3.

It will be observed that reaction commences at electron speeds equivalent to ca. 14 v., the rate remaining almost constant until ca. 19 v., when a marked rise in rate occurs. Less distinct breaks are noted at ca. 32 v. and 40 v. For the better elucidation of the changes in rate of reaction, three investigations were pursued. First, the slow rates between 14 v. and 19 v. were confirmed on several different samples of gas whose purity had been ascertained; moreover, the reaction in two cases was demonstrated to proceed almost to completion.

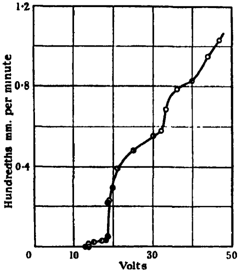

FIG. 3.—Reaction rate and electron energy in carbon monoxide.

	mm.	mm.
Initial.	0·168	0·155
Pressure after 8 hours .	0·045	0·042

The decrease in pressure in the same time with no voltage was less than one-tenth as great.

Secondly, it was confirmed that the reaction-rate scarcely rises at all between 15 v. and 18 v. but rises abruptly between 19 v. and 20 v., simultaneously with the intensification of the characteristic "sky-blue" radiation of carbon monoxide.

In the third place, attempts were made to fix the higher voltage breaks by measurements of average rates at intervals of half a volt near an apparent break, but it was found that the violent arcing prevented the repetition of results with sufficient accuracy. In the curve, rates have therefore been inserted only when they have been repeated to an accuracy of 3 to 4 per cent. Very little reliance can be placed on apparent breaks above 20 v.

The Combination of Carbon Monoxide and Hydrogen.

A. *Combination of Carbon Monoxide and Hydrogen Atoms.*—Equimolecular mixtures of the gases were mainly employed. It was found that the pressure decreased at all voltages and even with no voltage when the filament temperature was sufficiently high. That this pressure decrease was not due solely to the freezing out of hydrogen atoms formed by thermal dissociation on the hot wire was shown by the fact that the pressure fell to a value below that corresponding to the removal of all the hydrogen and that the product frozen out readily gave the resorcinol and gallic-acid tests for formaldehyde. There is thus a synthesis of formaldehyde under conditions conducive to the production of hydrogen atoms by dissociation. Formaldehyde can readily be obtained by illumination with light of $\lambda = 2537$ Å. of a gas mixture photosensitised by mercury vapour,* but it is uncertain whether hydrogen atoms are actually formed by the interaction of hydrogen and excited mercury atoms.† Since in the synthesis of ammonia from its elements it was found that hydrogen atoms combined with nitrogen molecules only in the presence of a metal catalyst or when activated by 13 v. electrons, it was of special interest to examine the formaldehyde synthesis from atoms in detail. Special precautions were taken to exclude reducible substances from the leads and glass walls, and it was found necessary to make all connections without solder and to coat the leads‡ with glass, the tube being also baked out until it fulfilled the requirement that after hydrogen atoms had been frozen out on the walls, the pressure returned to the initial pressure of hydrogen on allowing to stand at room temperature.

It was found that formaldehyde synthesis occurred readily with or without the large platinum anode, and this reaction thus differs from the ammonia synthesis in which the presence of a metal catalyst was necessary. Specimen pressure-time curves are included in fig. 6.

B. *Combination of Hydrogen Molecules with Carbon Monoxide.*—Preliminary experiments with oxide-coated filaments indicated that there was a ready reaction when the electron velocities exceeded 20 v., but after several hours use abnormally high rates were sometimes observed. Subsequent examination of the filaments showed that the oxide had become localised in spots, thus rendering a higher filament temperature necessary and consequent production of a small but effective number of hydrogen atoms by thermal dissociation. We are indebted to the Research Staff of the G.E.C. at Wembley for a fine suspension of the mixed carbonates of barium and strontium which could be deposited in extremely thin uniform layers both on platinum and (more effectively) on tungsten. As noted in the previous communication, the oxide coating is reduced by H^+ produced about 26-30 v., but these filaments (even with high rates of thermionic emission) produced in pure hydrogen scarcely any reduction of pressure below 30 v. and only a very slight reduction about 30 v. In these experiments only those emitters were employed which gave reaction rates not much greater than the mean values plotted in curve III, fig. 4

---

* Taylor and Marshall, 'J. Phys. Chem.,' vol. 29, p. 1140 (1925).

† See Compton and Turner, 'Phil. Mag.,' vol. 48, p. 360 (1924); Phillips and Taylor, 'Phys. Rev.,' vol. 29, p. 309 (1927).

‡ Any cupric oxide on the leads is easily reduced in agreement with the observations of Bonhoeffer, 'Z. Phys. Chem.,' vol. 113, p. 199 (1924).

Curve I, fig 4, was obtained by plotting the mean values of two, three or four measurements of the average rates over the range 0·2 to 0·15 mm.,

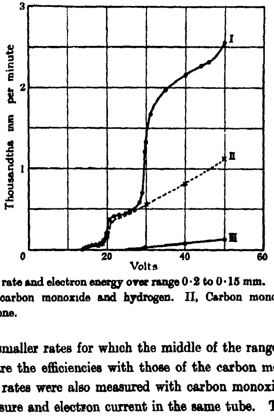

Fig. 4.—Reaction rate and electron energy over range 0·2 to 0·15 mm. I, Equimolecular mixtures of carbon monoxide and hydrogen. II, Carbon monoxide alone. III, Hydrogen alone.

except for the smaller rates for which the middle of the range was used. In order to compare the efficiencies with those of the carbon monoxide decomposition, a few rates were also measured with carbon monoxide alone at the same total pressure and electron current in the same tube. These are shown in curve II, which is similar to fig. 3, except that the latter shows more detail.

The low filament temperatures used in this tube made possible a more accurate determination of the potential breaks. Thus, under the same conditions of pressure and filament current, the arc broke in carbon monoxide at 14·0 ± 0·3 v., as shown by current-potential curves, and the double point occurred at 28·5 ± 0·2 v. This agrees well with the known ionisation potential of carbon monoxide, viz., 14·3 v. The first rise in reaction rate both for carbon monoxide alone and for its mixture with hydrogen takes place in the interval 19·5 to 20·5 v. and can therefore be attributed to a break at about 20 v. A correction of about 1 v. should therefore be applied to the curve in fig. 3.

The second rise in reaction rate with hydrogen is likewise well defined at 29·5 to 30 v.

We thus obtain three critical potentials for the interaction of carbon monoxide and hydrogen in the absence of atoms formed by thermal dissociation, viz., 14·3 v., 20 v., and 29·7 v., the first two being coincident with those necessary for the decomposition of carbon monoxide.

C. *Combination effected by Electrons in the Presence of Hydrogen Atoms.*—In order to examine the effect of firing electrons into an atmosphere of carbon monoxide and hydrogen *atoms*, measurements were made on the rates of decrease of pressure for various voltages with a tungsten filament at a high temperature as the source both of electrons and atoms. When this is done, it is useless to compare the absolute rates for a fixed emission and different voltages, since the small adjustments of temperature involve large differences in the rate of production of atoms by dissociation. Consequently, the rates with voltage on and with voltage off over short ranges of pressure were compared. The ratio of the increase of reaction-rate to the rate at zero voltage is then a measure of the effect of the electrons. These ratios are plotted in fig. 5. Sharp rises in this ratio are noted at 13–14 v. and 19–20 v. Owing to the high filament temperature there is a larger error in the voltage measurement, but that the first break corresponds to the ionising potential of the CO molecule, *i.e.*, 14·3 v., and not to the ionisation of hydrogen atoms, *i.e.*, 13·5 v., was confirmed by measurement of the total current under identical conditions for a constant filament temperature, when the first break became evident at 12 v. (corresponding to $H \longrightarrow H^+$ at 13·5 v.); and the second at 13·5 v. ($CO \longrightarrow CP^+$ at 14·3 v.). We may conclude that the combination of hydrogen atoms and CO^+ ions is more rapid or effective than the combination of the atoms with unexcited molecules, and, in addition, either H^+ ions are not appreciably more reactive than H atoms or that they are not furnished in sufficient numbers to contribute greatly to the reaction.

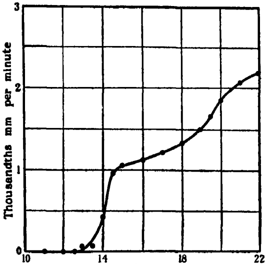

FIG. 5.—Rate of reaction of carbon monoxide and hydrogen atoms as a function of electron energy. The ordinates represent ratios of increase of rate with voltage on and rate with voltage off. Abscissæ are uncorrected voltages. Emission = 0·348 milliamp.

The Products of Reaction.

In all cases there was a permanent decrease of pressure and formaldehyde was detected in the testing trap. Neither methane, water, carbon nor methyl alcohol (as methyl salicylate) could be detected with equimolecular mixtures of carbon monoxide and hydrogen, even after the product of several experiments had been collected. It was observed further that after the product had been brought to room temperature the pressure began to decrease simultaneously with the appearance of a thin layer of white solid over the previously cooled surface of the reaction-tube. A few curves showing this "after effect" are included in fig. 6.

Eight curves examined were found to fit the formula

$$\log (p - p_0) = kt + \text{const.},$$

where p_0 = final pressure, and in every case the constant k did not differ greatly from 2×10^{-3} sec.$^{-1}$. Such a low value precludes the possibility of a true unimolecular surface reaction, even if the rate of adsorption of molecules on the walls was limited by a diffusion layer. On the other hand, from the dimensions of the apparatus and the computed value of the diffusivity of formaldehyde at experimental pressures, the rate of diffusion from the McLeod gauge into the reaction-vessel was estimated to yield a rate of reduction of pressure of from $2 \times 10^{-3}\,p$ to $4 \times 10^{-3}\,p$, on the assumption that the formaldehyde was removed (*i.e.*, by polymerisation) inside the vessel. The alternative possibility, that the pressure decrease was due to the diffusion *into* the gauge

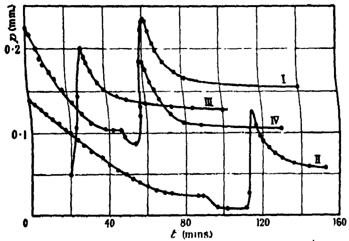

FIG. 6.—Specimen pressure-time curves. I, Reaction of hydrogen atoms with a metal catalyst. The first decrease is due to reaction, the second to cooling when the filament current was switched off, the rise is due to elevation to room-temperature, and the final lowering to polymerisation. II, Repeated with a platinum anode. III, Part of curve after reaction at 20 v. to show polymerisation. IV, The polymerisation curve after reaction at 50 v.

of a product of low vapour pressure, is precluded by the following values of the maximum and minimum pressures when the tube was immersed in liquid air and brought to room temperature a second time.

Experiment.	1.		2.	
	First.	Second.	First.	Second.
Pressure at liquid-air temperature	57	55	85	85
Highest pressure at room temperature	172	120	202	172
Lowest ,, ,, ,,	106	105	160	159

The unit pressure is 10^{-3} mm.

It would seem, therefore, that there was a definite reaction, vapour → solid, at room temperature. This in accordance with the observed behaviour of liquid formaldehyde, which condenses to trioxymethylene on warming.

Further insight is gained by an examination of the permanent pressure decreases under varying conditions.

Permanent Pressure Decreases : $CO + H_2$.

p_1.	p_2.	p_3.	p_4.	f.	Remarks.
mm					
0·178	110	38	72	0·91	Hydrogen atoms but no electron current. Mean $f = 0·915$
0·325	204	52	102	0·92	
0·278	175	57	106	0·92	
0·323	192	85	160	0·91	
0·503	303	187	322	0·94	Hydrogen atoms and electrons up to 22 v. Mean $f = 0·95$.
0·373	225	100	177	0·95	
0·325	198	89	157	0·94	
0·310	197	60	102	0·96	
0·229	136	20	67	0·83	Oxide emitter 20 v.–30 v. Mean $f = 0·83$
0·330	207	40	107	0·84	
0·345	217	125	227	0·81	
0·313	202	5	36	0·91	50 v $f = 0·91$.
0·258	157	106	186	0·86	35 v. Mean $f = 0·86$
0·340	210	96	182	0·86	

The ratio f is seen to rise from 0·8, approaching unity. This is in accordance with the observation of a solid product and some formaldehyde in the gas phase.

As regards the variation of f with the conditions of experiment, it was found that the lowest values (mean about 0·83) were obtained when atoms were not present, intermediate values (mean about 0·915) for the atom reaction without electrons and maximum values (mean about 0·95) for reactions into which atoms and electrons entered. Calling the highest pressure observed at room temperature p'_4, the ratio, $f' = p_2 (p_1 - p'_4)/p_1 (p_2 - p_3)$, was calculated for several experiments. There was a large variation in the values obtained, as is only to be expected, since the true maximum cannot be known accurately. Two important general observations were that f' was never less than 0·5, agreeing with the view that simple formaldehyde molecules are the first product; also f' was greater for the larger values of f. This would seem to indicate that there is an actual synthesis in the first place of more complex molecules, the proportion of which varies with the conditions, being greatest when hydrogen atoms react with excited carbon monoxide molecules and least when atoms do not enter into the reaction.

The Electron Efficiencies.

The efficiencies for a few voltages calculated from the rates shown in figs. 3 and 4 are given in the following table :—

Volts corrected.	Efficiency, *i.e.*, molecules removed per electron (*n*).		
	Reaction. (1)	$2CO \rightarrow C + CO_2$. (2)	$CO + H_2 \rightarrow HCHO$. (3)
17	0·013	0·016	0·018
21	0·10	0·127	0·14
31	0·19	0·21	0·61
40	0·28	0·29	0·79
50	—	0·40	0·93

Column (1) tabulates the results with a tube for which V = 575 c.c. and an emission of 1·62 milliamp., while (2) and (3) are for an emission of 0·348 milliamp. in a tube with V = 1340 c.c

The efficiencies obtained when hydrogen atoms are furnished by thermal dissociation are much higher, depending on the rate of production of atoms ; thus for fig. 4 at 20 v. under the conditions of experiment the rate of reaction was doubled by an emission of 0·348 milliamp., whilst the absolute rate was about 10 times the rate for that emission and voltage when hydrogen in the molecular form alone was present.

It must be concluded that with every ion produced, more than one molecule of carbon monoxide enters into reaction and that some type of chain or cluster mechanism is operative.

The Mechanism of the Reactions.

The synthesis of formaldehyde can be effected by a variety of processes. The simplest reaction is the direct union of carbon monoxide and hydrogen atoms produced by thermal dissociation.

$$(1)\ H_2 \longrightarrow 2H\,;$$

$$(2)\ CO + H \longrightarrow HCO\,;$$

$$(3)\ CHO + H \longrightarrow HCHO\,;\ \text{or}$$

$$(3')\ HCHO + H_2 \longrightarrow HCHO + H.$$

This reaction is similar to the sensitised photochemical reaction examined by Taylor and Marshall.* In addition there is an increase in reaction rate at

---

* 'Trans. Faraday Soc.,' March, 1926.

29·7 v., when only molecular hydrogen is originally present. This corresponds to the dissociation of hydrogen into atomic ions*

$$(4)\ H_2 \longrightarrow 2H^+ \quad (29{\cdot}7\text{ v.}).$$

Since, however, there was no break at 13·5 v. corresponding to the reaction

$$(5)\ H \longrightarrow H^+ \quad (13{\cdot}5\text{ v.}),$$

the H^+ ion does not appear to be more reactive than H and the break at 29·7 v. is merely due to the fact that this is the potential at which the actual dissociation of molecular hydrogen by electrons begins to become an efficient process.

In addition to the reactions involving modifications of molecular hydrogen, there are two others in which the excitation of the carbon monoxide alone causes combination with both molecular and atomic hydrogen. The observed critical reaction levels are 14·3 v. and 20 v. The lower level corresponds to the ionisation potential of the normal carbon monoxide molecule and we may infer either that the reaction

$$CO^+ + H_2 + \varepsilon \longrightarrow HCHO$$

proceeds with small efficiency or that the carbon monoxide ions are raised by a subsequent electron collision to the more reactive 20 v. level. The transitions of the carbon monoxide positive ion to the $1\,^2P$ and $2\,^2S$ states occur at the following levels :—

$$CO^+ \longrightarrow CO^{+\prime},\ 1\,^2P,\text{ at }16{\cdot}8\text{ v.}$$
$$CO^+ \longrightarrow CO^{+\prime},\ 2\,^2S,\text{ at }20{\cdot}0\text{ v.}\dagger$$

We note no change in reactivity of the positive ion either on transition to the $1\,^2P$ state nor on excitation to levels between 14·3 v. and 20 v. ; indeed the reaction rate rose very little in that range both in the decomposition of carbon monoxide alone and in its union with hydrogen. In striking contrast is the increase in reactivity, in both cases, of the excited positive ion in the $2\,^2S$ state. The ion in this configuration may be expected to present a larger target area than the normal ion and consequently the efficiencies may be anticipated to be greater. If, indeed, the normal ion is reactive, the target area, to hydrogen molecules, of the ion in the $2\,^2S$ state must be about eight times that of the normal ion to account for the observed increase in reaction rate. It is interesting to note that no abrupt changes in rate either of the decomposition of carbon monoxide or its union with hydrogen occur at 24 v., the approximate dissociation potential of the molecule into $C + O^+$, and, in addition, that the mean time between collisions in these experiments of the order of 10^{-6} second, an indication that the molecular ion in the $2\,^2S$ state must have a somewhat larger life than that generally attributed to excited atoms.

---

* See Compton and Mohler, 'National Research Council Bulletin,' No. 48, September, 1924.

† See Birge, 'Nature,' vol. 116, p. 170 (1925), vol. 117, p. 229 (1926) ; Duffendack and Fox, 'Science,' vol. 64, p. 277 (1926), and 'Astroph. J.,' vol. 65, p. 214 (1927).

The parallelism between the reactions of $CO^{+\prime}$ ($2\,^2S$) with normal carbon monoxide, hydrogen molecules and hydrogen atoms suggests that the various reactions may be interpreted with the aid of the theory of ionic clusters advocated by Langevin,[*] J. J. Thomson,[†] and Lind.[‡] On this view the enhanced reactivity of the $CO^{+\prime}$ in the $2\,^2S$ state would be due, not merely to its larger collision area, but also to the fact that after radiating part of its energy, it leaves a positive ion with more energy in the vibrational or " chemical " degree of freedom than the normal ion.[§] By virtue of this energy, it is enabled to form clusters with CO, H_2 and H, the clusters reacting with one another, with electrons and with the original molecules. Thus, the cluster ion $(CO \,.\, CO)^+$ yields $CO_2 + C$, $(CO \,.\, CO \,.\, CO \,.\, CO)^+$ yields C_3O_2 and CO_2, $(H_2 \,.\, CO)^+$ gives HCHO, $(CO \,.\, CO)^+ + 2H_2 + e$ could give 2HCHO and so on. The observations that $CO^{+\prime}$ ($2\,^2S$) ions combine with hydrogen atoms with great avidity, and that the first product in this case is not simple formaldehyde molecules but contains also polymers, find a ready explanation on the view that the original $(HCO)^+$ cluster is capable of forming longer clusters of the type $(H_2CO)_n$

Summary.

The decomposition of carbon monoxide into carbon and carbon dioxide (also some suboxide) and its union with hydrogen to form formaldehyde (and polymers) under excitation by electron impact have been examined. It is shown that hydrogen atoms produced by thermal dissociation react directly with carbon monoxide molecules, and also react with enhanced efficiency with carbon monoxide positive ions. It is believed that this increase in reactivity is to be attributed to either a chain or a cluster mechanism. Hydrogen molecules react with carbon monoxide positive ions, but much more readily with ions excited to the $2\,^2S$ level; this may be due either to the larger target area

---

[*] 'Ann. Chim. Phys.,' vol. 5, p. 245 (1905).

[†] 'Phil. Mag.,' vol. 47, p. 337 (1927).

[‡] 'Science,' vol. 64, p. 1 (1926).

[§] See Franck, 'Trans. Faraday Soc.,' vol. 21, p. 540 (1925); Birge, 'Nature,' vol. 117 p. 350 (1926); and Birge and Sponer, 'Phys. Rev.,' vol. 28, p. 259 (1926).

of the ion in the $2\,^2S$ state or to its greater tendency to form clusters with CO, H_2 and H. Excitation of the normal CO^+ ion and transition to the $1\,^2P$ state do not affect the reaction rate. No indication of direct decomposition into carbon and oxygen was noted at the dissociation potential. The subsequent polymerisation of formaldehyde has been shown to follow a unimolecular law, but this is due merely to slow diffusion of the simple molecules from the pressure gauge. The reaction products have been obtained in quantities sufficient for chemical tests.

Our thanks are due to the Salters' Company for a fellowship which enabled one of us (A. C.) to participate in these investigations, to the Imperial Chemical Industries for a grant out of which part of the cost of the apparatus was defrayed, and to Prof. T. M. Lowry, F.R.S., for the communication of this paper.

The Velocity Distribution of Photoelectrons produced by Soft X-Rays.

By E. Rudberg, King's College, London.

(Communicated by O. W. Richardson, F.R.S.—Received June 5, 1928.)

1.—*Introduction.*

In the literature published on the subject of soft X-rays, there are two papers* to be found, which deal particularly with the velocity of the photoelectrons produced by such rays. Both authors of these papers state, that they have found a photoelectric emission built up of homogeneous groups of electrons with characteristic velocities, giving rise to very sharp and steep jumps in the curves obtained by P. Lukirsky with retarding electric fields, and to equally sharp lines on the photographic plates in J. A. Becker's magnetic deflection apparatus. There were scarcely any electrons with low velocities present. In the autumn, 1925, the writer engaged himself in an investigation on the same problem at King's College, London, as a direct continuation of experiments which Prof. O. W. Richardson had been carrying out, chiefly in collaboration with Mr. A. A. Newbold. The electric stopping potential method was used, and a number of different tubes were designed and tested. In this way the many disturbing factors which may easily completely mask the true effects in experiments of this kind were gradually reduced, and the remaining sources of error could be allowed for. As a result of these experiments, it was quite clear, that the greater portion of the total emission from metals consists of electrons with energies of a few volts only. In addition, a small discontinuity in the current *vs* retarding voltage curves was found in the higher voltage region, the position of which at 265 volts agreed very well with the value of the K_a-quantum for carbon, the substance used for the anode, as calculated from the best critical potential determinations and confirmed at about the same time by A. Dauvillier's* first measurements using a crystal method. The curves obtained are totally different from those published by Lukirsky. From the experience gained in experiments with several different tubes the writer is inclined to think, that the shielding of the photoelectric target in Lukirsky's apparatus from the electric fields of neighbouring electrodes at high potentials may not have been sufficient to prevent a considerable distortion of the true curve. This might explain the conflicting results arrived at. As regards Becker's work, it seems to the present writer a dangerous thing to keep the photoelectric part at the same potential as the anode, for any electrons leaking out through the gauzes from the X-ray tube must inevitably have been recorded as fast photoelectrons. In a note† by Becker's collaborator, which appears to have escaped the attention of those who quote this investigator, such an effect is actually stated to have occurred

---

* Lukirsky, 'Phil. Mag.,' vol. 47, p. 466 (1924), and 'Z. f. Physik,' vol. 22, p. 351 (1924); Becker, 'Phys. Rev.,' vol. 24, p. 478 (1924).

In the stopping potential method the current between the photoelectric emitter and the surrounding electrode is always composed of two : the electrons emitted from the target against the opposing field, and a current of electrons produced by scattered radiation at the surface of the outer electrode. This current will always be present; it flows in the opposite direction to the first one and causes the total current from the emitter, as measured by the electrometer, to reverse its direction for a low value of the stopping potential. For higher stopping potentials this second current constitutes almost the whole of the measured negative current in which the changes in the small superposed current carried by fast electrons from the target must tend to disappear. Since it does not appear to be possible to get rid of the effects of scattered radiation, the stopping potential method has been abandoned for a magnetic deflection method of a special kind, described in the following.

---

* 'Journ. de Physique,' vol. 8, p. 1 (1927); 'C.R.,' vol. 182, p. 1083 (1926).

† Rose, 'Phys. Rev.,' vol. 25, p. 883 (1925).

2. *Theory of the Method.*

Several attempts were made to employ the usual arrangement based on the focussing principle first introduced by Danysz and later used in most work on the magnetic spectra of β-rays. They failed because of the difficulty to get a measurable intensity. The following method, illustrated in figs. 1 and 2, was then adopted. The photoelectrons are produced at the surface of a narrow metal rod and the current flowing to an annular collector, surrounding the rod concentrically and maintained at the same potential as this, is measured. When a magnetic field is applied, parallel to the cylinder axis of this arrangement, an electron starting from the rod will describe a helix round the direction of the field, composed of a uniform motion on a circle in the plane of the ring together with a uniform translation along the axis. The radius of the circle is given by

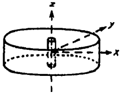

FIG. 1.

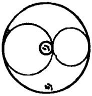

FIG. 2.

$$r = mv/e\mathrm{H}, \tag{1}$$

where v is the velocity component in the xy-plane. If the height of the whole arrangement is small, only electrons for which the direction of emission falls nearly in this plane will come into play, so that v may be taken as the resultant velocity as well in this case. If the radius of the rod can be neglected compared with r_2, the radius of the collector, all of these electrons for which $v > v_0 = r_0\mathrm{H}.e/m$, the "critical velocity" will be measured at the outer cylinder, and the rest will be returned to the rod independent of their direction of emission. Here $r_0 = \frac{1}{2}r_2$. The effect of a finite value of r_1, the radius of the rod, is to make this distinction less sharp. Thus, as will be seen from fig. 2, there will be a range of velocities Δv_0 such that of the electrons belonging to this group some will be collected and others returned, depending on the direction of expulsion from the surface of the rod. The resulting relative uncertainty in the value of the critical velocity will be:

$$\frac{\Delta v_0}{2v_0} = \frac{r_1}{2r_0}, \tag{2}$$

and in the corresponding energy in volts, since $V \backsim v^2$:

$$\frac{\Delta V_0}{2V_0} = \frac{\Delta v_0}{v_0} = \frac{r_1}{r_0} \tag{2A}$$

Inserting numerical values, the latter expression comes out a little less than 10 per cent. for the apparatus used. It will be seen that (2) and (2A) give the extreme limits of the transition interval, and that the main change in current produced by the variation of the magnetic field in the neighbourhood of the value corresponding to v_0 should occur within an interval considerably smaller than this.

The experimental procedure, then, is to measure the current flowing to the ring collector for a series of different values of the magnetic field. If the former is plotted against the latter in a diagram, the curve obtained should give the number of electrons with any given velocity as the negative derivative in the corresponding point. This method appears to have been first used by F. Paschen* in a study of the β-rays from radium; the arrangement is also very similar to the Magnetron of A. W. Hull.† The theory as outlined above is modified somewhat, when the effect of the finite height of the cylinder and of the openings in it, which it was found necessary to introduce, are taken account of. The writer has considered this point in detail, but since some of the calculations are rather lengthy and the resulting change in the formulas is practically insignificant, the matter will not be dealt with here. Only one result must be mentioned. The ring-shaped collector occupies a certain zone of the unit sphere laid round the centre of the rod. The width of this zone, which is effective in collecting electrons, is not constant for electrons with different energy, supposed great enough to carry them across, on account of the difference in the distance covered along the path of the electron during the transition, but is a function of the ratio of the energy V_0, associated with the critical velocity for the particular field in question and the energy, V_1, of the electron. This function may be shown to be:

$$g\,(V_0/V_1) = \sqrt{V_0/V_1}/\arcsin\sqrt{V_0/V_1}. \tag{3}$$

This function indicates an extreme variation from $\pi/2$ to 1 of the width of the zone, and therefore of the current to the collector due to electrons of energy V_1, as the magnetic field is raised from zero to the value corresponding to V_1. With the particular way of plotting the curves—current against log V—described below, it is possible to correct for this change. The recalculation is rather tedious but has been carried out with all curves given in the following, although the omission of this correction should not introduce any serious errors, when curves for different elements and the effects of different treatment of the target are compared

---

* 'Ann. d. Physik,' vol. 14, p. 389 (1904).

† 'Phys. Rev.,' vol. 18, p. 31 (1921).

3. *Description of Apparatus.*

The main features of the experimental arrangement finally adopted after several preliminary tests with more or less different constructions, will be seen from fig. 3, showing the whole tube from the side, and fig. 4, representing a cross section through the principal parts of it. The main body of the apparatus is formed by a cross of wide glass tubing, the " analysing chamber," where the photoelectrons are produced and measured, occupying the large central part. The X-radiation is generated in one of the side tubes, the second arm of the cross serving as a light trap for the part of the radiation, which passes to both sides of the rod and therefore is not utilised for the

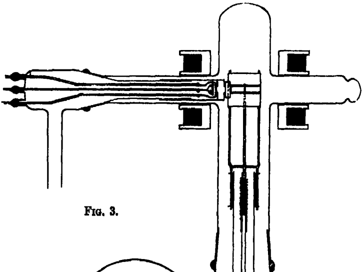

FIG. 3.

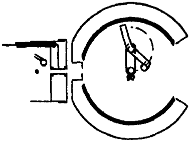

FIG. 4.—Analysing Chamber, top view.

production of electrons. Through the uniform hemispherical surface by which this trap is closed up the slits can be observed and adjusted in a line with the rod.

The anode, a small rod filed from a piece of arc carbon, and the tungsten filament, are firmly supported on quartz tubing fixed to a large glass stopper. They are completely separated from the rest of the apparatus by means of a surrounding copper cylinder, fitting tightly on a glass tube of wide bore projecting from the stopper. This cylinder is closed by two diaphragms, in which slits 1·8 × 7·5 and 1·8 × 8·5 mm. have been cut to stop the emerging X-ray beam down to the required size. The second stop has been constructed as a removable lid, so that the ion trapping device can be introduced in the space between the two slits. An arrangement of the plane condenser type was first used for this purpose, but later one single electrode has been employed, the shape of which may be seen in fig. 4 It can be described as a flat box with openings, covered with a network of very fine copper wire, on two opposite sides corresponding to the slits facing them. The whole is kept in a fixed position and well insulated from the walls by a tiny quarz framework fitting into the small space limited by the diaphragms. The whole length of this trap measured along the beam is only 8·5 mm., but when the electrode is charged to a potential about 50 volts higher than that of the anode, the trap works very satisfactorily. The lead to the trap electrode is run along the inside of the cylinder in a narrow quartz tube and finally comes out through the stopper, so that the whole X-ray tube can be taken out by removing the stopper. This is directly connected to the pumping system by a wide side tubing

The analysing chamber is built on a complicated quartz framework, which has been blown together to form one single piece in the oxygen blowpipe, thereby ensuring a very high degree of rigidity of the whole system. This framework is fixed by means of a tight-fitting copper cylinder to the upper end of a wide glass tube joined into the large stopper, which terminates the wide main tube. The outer cylindrical electrode of the chamber, 50 mm. in diameter, is 50 mm. high, but only a central strip of this, 8·5 mm. wide, constitutes the annular collector. This strip, except for a small portion containing the entrance slit for the radiation, which therefore separates the two halves of the collector, as will be seen from the diagram, is insulated from the rest of the cylinder by annular slots about 1 mm. wide and connected to the electrometer. The collector is thus an insulated part of the larger cylindrical surface, the rest of which may be looked upon as a guard ring · for the central part. This arrangement was adopted in order to reduce the effect of scattered radiation as much as possible. It was expected that the intensity of such radiation falling on the outer cylinder would not vary by any greater amount over a considerable length in the middle of a strip of this surface parallel to a generator of the cylinder. But if this is true, it is easily recognised that the total emission from the collector and the current flowing to it due to electrons emitted from the guard ring should almost completely balance each other, particularly for higher magnetic fields, when the paths are very much reduced. As a matter of fact, when the arrangement was tried the disturbance due to scattered radiation was found to have been very much diminished as compared with what was the case in an earlier tube, where this precaution had not been taken. The analysing chamber is provided with a large opening facing the light trap for the emergent radiation. The whole is surrounded by a wider cylinder, which shields the back of the collector from radiation and electric fields; this cylinder is permanently connected to the guard ring and to a short piece of wire placed on the cylinder axis some distance above the rod to enable the saturation current from the rod under an accelerating potential difference to be measured for different magnetic fields. The whole equipotential system thus formed will be referred to as the "shield."

The central rod, originally fixed to a central quartz stem, is in the final construction attached to the bent end of a narrow quartz tube, which is able to pivot round the axis obtained if the central line is displaced 10 mm. to the side, perpendicular to the X-ray beam. By this arrangement the photoelectric target can be swung into position or turned out of the X-ray beam from outside, by acting on the ground joint at the bottom of the large stopper, so that velocity measurements and blank runs can be taken alternatively in rapid succession and under identical conditions. The exact position is ensured by the contact between quartz surfaces in each case.

The magnetic field is supplied by a pair of Helmholtz coils, each consisting of 504 turns of a mean radius 80 mm. They are calculated to give 56·52 gauss per ampere with an extreme variation of 0·4 per cent. over the space utilised in the measurements.

4. *Experimental Procedure.*

The tube was exhausted by means of a set of two Volmer mercury-vapour pumps, the mercury-vapour being prevented from diffusing into the apparatus by an interposed liquid air trap. The analysing chamber was coated with lamp-black to reduce the emission of electrons, but when this coating had once been outgassed through baking at 400° C., it was never found to affect the good vacuum obtained, even after air had been admitted. The tube was run with the current to be used in the measurements for at least an hour before these were started, and no readings were taken unless the pressure was 1×10^{-6} mm. or less. Under these conditions there is no appreciable radiation from the gas residue. When the conditions were found to be satisfactory, a run was taken in which the saturation current flowing from the rod to the system-collector and shield was measured for a series of different values of the magnetic field. The rod was connected to the electrometer and was made some 140 volts negative to the shield. This has to be done, because the field, being perpendicular to the stream of bombarding electrons in the X-ray tube, will act on this like a sideward pull on an elastic string and shift the point of impact over the surface of the anode, which in turn must alter the intensity of the radiation incident on the rod. The mean of a couple of such curves was taken and later on used to correct the currents in the velocity measurements, by dividing the measured value of the current by the corresponding ordinate from the saturation curve. Since the saturation currents are much larger than the currents measured in the main experiments, the thermionic current in the first case was correspondingly reduced to give a convenient rate of deflection of the electrometer needle. That this did not alter the conditions was proved by some measurements in which the thermionic current was unaltered and the sensitivity in the current measurements reduced by adding capacity to the system, but since the condenser was less convenient to use, the first method was generally adopted. In addition to the measurement of the saturation current, a number of readings were usually taken without the magnetic field and for different potentials on the rod, including positive ones, as a control.

This done, the electrometer was connected to the collector, the rod being kept at the same potential as the shield. The thermionic current used in almost all experiments was 10 milliamps.; it could be kept sensibly constant by slightly adjusting the heating current if necessary, for which purpose this circuit was provided with three sliding resistances of different order of magnitude, all in parallel. The bombarding voltage, supplied from high-tension accumulators, was usually 700 volts, but preliminary experiments extended as far down as to 350 volts did not reveal any important differences. The ion trap was charged to 770 volts, referred to the negative end of the filament, and the metal wall of the X-ray tube was kept at − 70 volts. The high negative potential of the wall was found to be necessary to neutralise the influence on the thermions of the high positive potential on the trap electrode;

otherwise, the field from this electrode would pass through the slit and direct electrons to it, thus introducing a second anode, in which case the electrode would no longer trap the positive ions.

The analysing chamber as a whole was originally intended to be kept at the same potential as the metal wall of the X-ray tube in the experiments, since in any case it is advisable to make this part the most negative of the whole apparatus to safeguard against the influence of any traces of stray thermions. This was also done in the preliminary experiments with a fixed copper rod, of which a brief report was given in a letter to ' Nature ' in May, 1927 (vol. 119, p. 704). A more detailed study of the properties of the tube, however, lead to the adoption of a small and variable potential difference of the order of 10 volts between the chamber and the wall of the X-ray tube in the final experiments, the former usually receiving the negative charge. The object of this will become clear from the following.

When blank runs were first tried with the rod turned well out of reach of the X-ray beam, it was very puzzling in the beginning to find that there was still a small current received by the collector. Various alterations in the experimental conditions were made in the search for a possible source of this disturbance. It was then noticed, that the small residual current was very sensitive to the application of small P.Ds. between the chamber and the tube wall, and that the current could be reduced to zero, or its sign reversed, by a suitable adjustment of the applied P.D. This suggested the following explanation (compare fig. 4). The residual current is due to electrons set free from the edges of the final entrance slit by peripheral rays of the X-ray beam passing through it, and to some extent by radiation reflected from the trap electrode at grazing incidence. The number of such electrons, which is able to reach the collector through the slit, must vary with the magnetic field applied for two reasons: (1) the path is affected by the field, and (2) the amount of radiation depends on the distribution of bombarding current over the surface of the anode, which in turn is a function of the field. When the chamber is charged negatively with respect to the tube wall, the electrons are attracted by the latter, and the number entering through the slit must diminish rapidly as the negative potential is increased. The small reversal of the current, which may be produced by making the potential of the chamber too negative, must be due to a small fraction of the applied electric field, which is able to enter through the slit and catch some electrons from the nearest collector edges, which are thus lost for the balance just mentioned above. It is in good agreement with this tentative explanation that the "compensating

P.D." necessary to reduce the residual current to zero is found to be negative when there is no magnetic field, and gradually approaches zero for higher magnetic fields, the change in this quantity for a given change of the field being greatest for small fields.

In view of this, the following experimental procedure was adopted, when velocity measurements were to be taken. A blank run was first made in which the compensating P.D. was found for a series of values of the magnetic field spread over the region in question, and a smooth curve drawn through the points so obtained. The rod was then turned into position in the centre of the cylinder and the main experiment started. In this, the potential of the chamber was always set at the value given by the compensation curve just obtained, before the current to the collector was measured. This was done for all values of the magnetic field used. This method assumes, that the rest current to be balanced remains the same in the blank run as in the main experiment. There does not appear to be any serious reason to doubt that this condition is satisfactorily fulfilled, and the results may be said to justify the method.

The currents to the collector in the main experiments were not very large, in spite of the considerable input on the X-ray tube, so that they had to be measured by timing the rate of deflection of the electrometer (sensitivity 1,200 div. per volt). Since there was a large variation in the magnitude of the current over the region studied, different intervals of the scale had to be used for different parts of this region. The continuity in the measurements in changing over from one such interval to the next one was secured by taking double readings simultaneously over both intervals in the neighbourhood of the transition point and using the mean value thus obtained for the reduction factor.

In all cases where this method of applying a compensating P.D. was used, it was found that the current in the main experiment came down, as the magnetic field was increased, to a small constant value different from zero and apparently independent of the field, even for such values of this as would have stopped electrons with energy corresponding to the bombarding voltage completely. Since a very small positive potential applied to the rod reduced this current to zero, it was inferred that it must have been carried by particles of a much larger mass than electrons, and it was natural to attribute this effect to negatively charged atomic carriers, such as negative ions. For this reason, in addition to the ordinary measurements with the rod kept at the potential of the whole chamber, curves were also taken with the rod at + 3·0 volt with respect to the chamber, since this was found sufficient to make the remaining current disappear completely. Special blank runs for compensation had to be taken for these measurements as well. As a rule the compensating P.Ds. were not very different in the two cases. The potential of the chamber had usually to be kept a little more negative to the tube wall in the latter case. The difference is easily accounted for, since the presence of the charged rod inside must reduce the field in the slit due to the positive potential of the tube wall. The distance between the slit and the rod was almost the same, when the rod was turned aside, as when it was in the central position.

It may perhaps be thought to be rather rash to conclude that there are negative ions in the photoelectric emission produced by soft X-rays. It must be emphasised, however, that the current in question was always found to be very small, amounting to a few per cent. of the total emission only. It is not meant to suggest that the negative ions result directly from the action of the incident radiation; but it does not seem impossible, that a small fraction of the photoelectrons produced could become attached to traces of gas in the surface on their way out, in such a manner that the ions formed would retain a small amount of energy just sufficient to carry them away from the surface. The evidence as to the specific effects of magnetic and electric fields on this current, although perhaps not absolutely conclusive, is a strong indication of the mass of the carriers as being at least of atomic dimensions. The fact that the current in question was found to be very much reduced, and sometimes almost entirely absent, after the specimen had been degassed at 400° C. is also believed to be a good support of the explanation here proposed.

The vertical component of the earth's magnetic field, which is the only one which comes into play, is small compared with the fields mostly used in the experiments. It falls in the opposite direction to the applied field, the latter being always directed upwards in the final experiments, principally because the saturation curves showed much less variation in this case; this is easily understood, since the field tends to shift the point of impact to the front face of the anode under these circumstances (fig. 4). By means of a small test coil and a ballistic galvanometer, the current through the coils which would reduce the vertical magnetic force to zero at the centre of the Helmholtz pair was determined, and this value used to correct for the vertical component of the earth's field.

5. *Method of Plotting the Curves.*

The conclusion arrived at in the writer's earlier experiments using the electric stopping potential method was, that a considerable portion of the emission consisted of slow-moving electrons. This result has been confirmed with all the different magnetic arrangements that have since been tested, and this remarkable feature of the emission was the point particularly emphasised in the preliminary report to 'Nature.' This is well brought out by the graph in fig. 5, representing some recent results with a copper photoelectric target which had been baked at 400° C. The currents received by the collector for different fields have been plotted against the square of the current through the coils, multiplied by a numerical constant such that the abscissæ represent the equivalent volts, as shown in section 2. This curve should thus be the complete equivalent to the stopping potential ones if the errors of the latter method could be dispensed with.

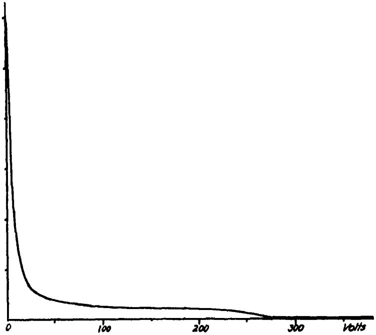

Fig. 5.—Copper, baked.

It will be seen, that with this mode of representing the results, it is not easy to give the whole region in one curve, without pushing the important part close to the axis of ordinates almost into this axis; the curve for the unbaked specimen would have been much worse in this respect. For this and several other reasons, it was chosen to plot the photoelectric currents, I, against log i, the current through the coils, which apart from a constant term and the factor $\frac{1}{2}$ is the same as log V.

Let $N(u)du$ be the number of electrons in the emission falling in the interval between u and $u+du$. Disregarding, at present, the influence expressed by the function $g(\ )$ in (3), and omitting constant proportionality factors throughout, since we are interested in the relative values only, we have :

$$I = \int_{i_0}^{\infty} N(i)\, di = \int_{H_0}^{\infty} N(H)\, dH = \int_{v_0}^{\infty} N(v)\, dv = \int_{V_0}^{\infty} N(V)\, dV \qquad (4)$$

where v, H, i and V are related to each other as set out in section 2. Bearing this in mind, we can also write :

$$I = \int_{V_0}^{\infty} N(V)\, dV = \int_{i_0^2}^{\infty} N(V)\, d\,(i^2), \qquad (5)$$

from which will be seen, that the distribution of electrons over the different values of the individual energy is determined by the negative slope of the curve giving I as a function of i^2, just as from a stopping potential curve.

There is, however, a second kind of distribution, which is of some interest. One might wish to know, how the total energy contained in the emission is distributed over the various energy units of different size, every moving electron representing such a unit. Obviously the energy carried by electrons of individual energies between V and V$+d$V is given by V N(V) d V. By transforming (4) :

$$I = \int_{V_0}^{\infty} N(V)\, dV = \int_{V_0}^{\infty} V\, N(V) \frac{dV}{V} = \int_{\log V_0}^{\infty} V\, N(V)\, d\,(\log V)$$
$$= \int_{\log i_0}^{\infty} V\, N(V)\, d\,(\log i) \qquad (6)$$

we find that the required quantity in this case is determined by the negative slope of the curves obtained when I is plotted against log i.

It has been mentioned, that the measured currents were usually represented in this way, as a function of log i. These curves may be compared directly or may be differentiated graphically to give the distribution of energy. To find the electron distribution, the values found for the slope have simply to be divided by the value in volts corresponding to the particular point of the curve. The plotting of the curves was conveniently done by the aid of special tables, computed in such a way as to give the value of log i with all corrections, including those for the ammeter, for any reading of the instrument. Other tables gave the value of log i corresponding to different V : s. In plotting the curves obtained with the rod charged to $+\,3{\cdot}0$ volts, it was assumed that the only effect of the electric field was to make the electrons start from the rod with an energy 3·0 volts less than when the field is absent. Tables for $\log i$ were then computed in which this had been accounted for and 3·0 volts added to every energy value in such a way, that the curves, when plotted, were automatically brought up into the right place, giving the distribution that would have been found had there been no field. The assumption on which this computation rests is very nearly true, when the radius of the rod is small and for the fast electrons, and only the part of the curves corresponding to such electrons has been used to correct for the current supposed to be due to negative ions. In fact, the experimental curves for 0 and 3·0 volts, when drawn in this way, were found to be parallel over a considerable range for higher fields, so that to correct the first curve the constant difference was subtracted from all ordinates.

The logarithmic representation is preferable when it is desired to correct the experimental curves for the effect expressed by the function $\mathfrak{g}$ ( ) of (3). To do this, the curve is divided into a great number of small parts, which may be treated as straight lines, corresponding to equal distances along the $\log i$ axis. Starting far out to the right, the first rise in the curve from the axis proceeding backwards is taken as a measure of the number of electrons of the corresponding energy, and the value of this rise, multiplied by the function g ( ) is marked off on each of the following lines, by which the curve had been divided. The number falling in the next interval is determined by the rise in the curve over this interval, minus the rise in the g_1 ( )-curve over the same part, due to the faster electrons. The new function, g_2, is marked off on top of g_1 on all the following lines. In the next interval, the rise in $g_1 + g_2$ is subtracted and g_3 marked off. Proceeding in this way, the whole curve is reconstructed, the rise $\Delta_k \mathrm{I}$ over the interval k of the uncorrected curve becoming $\Delta_k \mathrm{I} - \Delta_k \sum_{1}^{k-1} g_s$ after correction. The fact that g ( ) is a function of $\mathrm{V}_0/\mathrm{V}_1$ only, combined with the properties of the logarithmic plot, means that the g ( )-curve has only to be multiplied by a constant and shifted from one line to the next to give each of the subsequent corrections g_1, g_2 . . ., which is favourable for the calculation. In spite of this, the method is rather lengthy. All the final curves given in the following have been corrected in this way. In the practical case, the summation of the different g_s : s is not done graphically, but by direct calculation. The number of equal intervals chosen was twenty. In each case, the corrected curve (full line) and the same curve, but without this last correction (dotted) have been drawn. It should be mentioned that the function *g* ( ) here used is not exactly (3), since a second function of the ratio V_0/V_1, which takes account of the openings in the collector, has been included, but the extreme variation of the latter function over the whole range is only 1·7 per cent., so that the difference is insignificant.

6. *Experimental Results.*

The result of the measurements, plotted as set out in the preceding section, is collected in figs. 6 to 9. Four different elements have been tested, namely, silver, copper, aluminium, and carbon. Two curves are given for each of these elements, showing the effect obtained with the same rod previous to

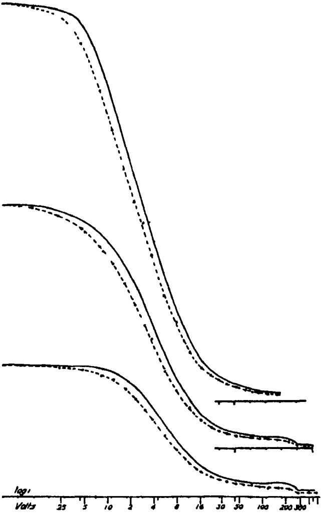

FIG. 6.—Silver. Unbaked—upper curve; baked—middle curve; film baked—lower curve.

(upper curve) and after (lower curve) heating it *in vacuo* This was done by means of an electric furnace which could be placed over the central part of the tube The temperature was raised to 400° C and maintained at this point

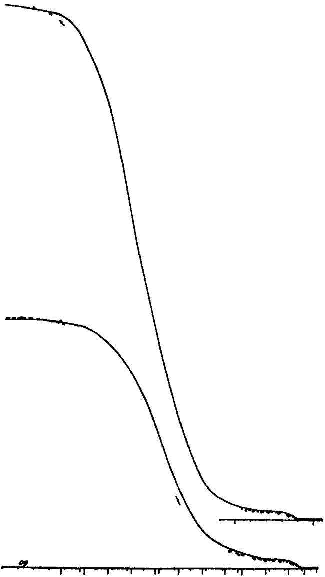

Fig 7 —Copper Unbaked—upper curve baked—lower curve

for some time—½ or 1 hour—until there was only a very slow evolution of gas The zero of the current axis has been shifted for the upper curve as indicated to the right in each case The scale is the same for all the different curves so that the ordinate to the left, corresponding to zero field, should represent the photoelectric "efficiency" for the target in question. It must be remembered, however, that the tube had to be opened up every time a new rod was inserted, and that this might easily have altered the adjustment slightly; for this reason, the efficiency could not be given with any high degree of accuracy by these curves, but they are believed to give a fair idea of the relative magnitude of this quantity.

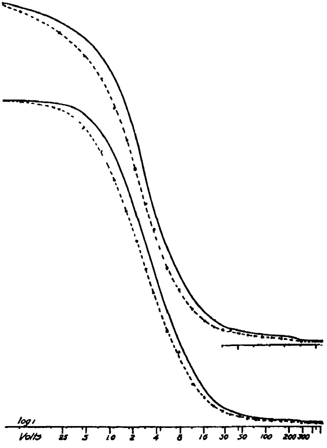

FIG. 8.—Aluminium. Unbaked—upper curve; baked—lower curve.

In all curves, except those for aluminium, the current is practically zero, and constant in the region of the highest fields. Thus, although the bombarding voltage was about 700, there is scarcely any indication of electrons having energies greater than 300 volts. As the magnetic field is reduced, there is a fairly rapid rise in the current between 280 and 200 volts followed by a small region, where the curve is again nearly horizontal. The steeper part is possibly a little exaggerated by the last correction, but it will be seen that the general shape is quite clearly indicated by the uncorrected curves as well. In almost all curves obtained, apart from those shown here, the appearance is very much the same, and the drop occurs in the measurements with 3·0 volts on the rod, as well as without any applied potential. The directly measured points are indicated in the dotted curves without the final correction and should give a fair idea of the accuracy attained in these experiments; it will be seen, that the occurrence of the steeper part for high fields in most curves could hardly be accidental.

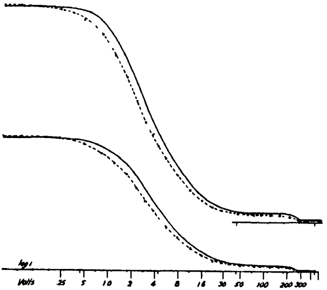

Fig. 9. Carbon. Unbaked—upper curve; baked—lower curve.

After the first rise, the curves remain nearly horizontal down to about 50 volts. Between 50 and 30 volts, the curves again turn upwards, and below 20 volts the slope rapidly increases to a maximum about 3 or 4 volts. After this, the slope gradually decreases, and below 1 volt the curves are very nearly horizontal, corresponding to an asymptotic approach to the value for zero field. The rise below 20 volts is so steep that the current is increased by a factor of from 5 to 15 in the extreme cases over the region corresponding to the last 20 volts. Thus it seems natural to speak of the whole emission as made up of two parts:—

(1) A group of electrons with low energy, mostly of the order of a few volts and scarcely exceeding 20 volts; these electrons carry at least 80 per cent. of the total current.

(2) A group of fast electrons. This group may in general be distributed over the whole region corresponding to higher fields; in the present case they appear concentrated in the part between 200 and 280 volts. There is no detectable amount of such electrons above 300 volts. The second group usually contributes only a few per cent. to the total emission.

The general appearance of the curves obtained with different photoelectric targets is very much the same in all cases. This is true for different elements as well as for the same element in different stages of degassing. It will be seen that the highest emission has been obtained with an unbaked copper target (maximum current about 2×10^{-12} amps.). The emission from an unbaked silver surface is a little less than this, and the efficiency of the carbon emitter in the unbaked state is considerably less than half the efficiency of unbaked copper. The change produced by subjecting the photoelectric target to a heat treatment, the immediate effect of which, in view of the comparatively low temperature used, must have been to reduce a surface layer of adsorbed gas, is in all three cases a considerable reduction of the emission. This is greatest for the copper target, being somewhat more than 50 per cent. In the case of silver and carbon the total emission has been diminished by about 40 per cent. through baking. The emission is thus to a considerable degree dependent on the state of the emitting substance as regards its gas content. It is not meant to suggest, that the state of the targets after baking should correspond to the pure element in question It seems fairly certain, that further degassing at much higher temperatures would produce a considerable additional reduction of the emission; the figures for the change due to heating have only been given in order to illustrate the considerable influence of the conditions as regards adsorbed gases.

There is one very important point about this influence, which is clearly exhibited in the curves. In all three cases, it is mainly the currents corresponding to small fields which are reduced by the heating. The currents for higher fields remain practically unaltered. It will also be seen, that this latter part of the curves is not much different in magnitude for different elements (although there can be little doubt that there are differences, carbon, for instance, giving smaller values than the other two). The great influence of adsorbed gas is thus confined to the first group of low velocity electrons; the number of fast electrons of the second group is not affected by a moderate heat treatment and is for different emitters essentially the same, showing much less variation than the number in the corresponding first group.

The curves for aluminium, fig. 8, differ from the others in some respects. The characteristic drop in the curves for higher fields is almost entirely absent, and the remaining current above 300 volts is perhaps a little greater than with the other elements studied. The cause of this difference is not obvious. As mentioned, the X-ray tube used in all experiments was provided with a tungsten filament and a carbon anode ; with the heavy currents which it was necessary to use sputtering of the latter could not be avoided, and no attempts were made to renew the surface by scraping the anode, when the tube was open. There is a possibility that for some reason the sputtered surface was more effective in the experiments with aluminium than with the other targets, so that the anode radiated more like a tungsten one in this particular case ; but there was nothing unusual in the behaviour of the tube in the experiments with aluminium as compared with those in which other elements were studied. Whatever the true explanation of this discrepancy, it seems justified to regard the emission as composed of two groups of electrons, in the same way as before, in this case too. The curve for unbaked aluminium differs from the others in a further respect : the slope retains a finite value also for the smallest fields employed. This peculiar shape cannot be accidental, since it repeats itself in all three curves obtained with this target previous to baking, which, as exhibited by the lower curve, restores the " normal " type of curve found for the other targets. It is possible that a small opposing contact P.D. between the unbaked target and the cylinder is responsible for this peculiar shape of the curve. The stopping potential test used to detect such P.D. : s is not accurate enough to decide about the presence of a contact P.D. of less than 1 volt, but the data obtained indicate, that the saturation is not quite complete when the applied stopping potential is zero for the unbaked target, whereas the saturation is very good under the same conditions after baking. The difference, however, is not great enough to alter the result which must be drawn from a comparison of the two curves in fig. 8 : baking the aluminium target does not produce any appreciable change in the total photoelectric emission. This also means, that the number of electrons belonging to the first group is not affected by this heat treatment. In fact, the only change produced by the baking seems to be the increased bending for the lowest velocities.

The silver target was not a solid piece of this substance as in the case of the other elements, but consisted of a quartz rod on which a thick and perfectly opaque layer of the metal had been formed by repeated deposition of silver in a Böttger solution. In view of some experimental evidence, of which the most important one will be given is the following, it is fairly certain that the low energy electrons of the first group result from a secondary process occurring in the photoelectric emitter, and it was therefore interesting to find out, if the distribution curves for very thin films as emitting substance were different from those obtained when greater thicknesses of the same material were used. It was very difficult at first to secure good contact to the thin silver films deposited on the quartz rod in these experiments. A considerable number of such films were tried and the contact was usually very satisfactory, until the tube had been baked. Different methods of making contact were tested in the attempts to find one which would stand the temperature change. The method which finally turned out successful was the following. The quartz rod, well cleaned and provided with a ring of a very fast-sticking platinum deposit at one end to which a platinum wire had been welded, first received a very thick coating of a great number of successive deposits. After this had been baked *in vacuo*—it was used as a silver target in the experiments described above—the coating was scraped off, leaving only a narrow strip at the back of the rod and the annular part close to the platinum deposit. On this the thin film was deposited in two successive baths, the rod remaining only for a short time in the solution, and after washing with distilled water the tube was put together and evacuated. The temperature was raised very slowly and was only pushed as far as 375° C. To test the contact to these perfectly transparent films, the stopping potential method could not be used, since the measured photoelectric emission current from the rod was troubled by polarisation currents, probably due to changes in the quartz exposed to the radiation, so that the current did not instantaneously respond to a change in the applied potential, which gave rise to a kind of hysteresis effect. Instead, the arrangement described by Hull was used, and the current flowing to the collectors under a fixed accelerating potential difference was measured for gradually increasing magnetic fields. Hull has shown that if the electrons are expelled with a negligible velocity this current will remain constant until a certain value of the field is reached, calculable from a knowledge of the applied P D. and the dimensions of the cylinder, beyond which the current will be zero. When the electrons have initial energy as in the present case, the drop is gradual but sets in fairly sharply very much as in the stopping potential curves. When this Hull effect could be reproduced with a film, the contact was regarded as satisfactory. As a matter of fact, many films have been tested, where it was evident for other reasons that the contact was bad, and in all these cases the sharp Hull drop was found to be replaced by a slow and gradual decrease in current extending over the greater part of the applied fields.

The results obtained with a thin film of silver after baking are represented by the bottom curve of fig. 6. The general shape of this curve is similar to that of the other curves here given, but the total emission is the lowest so far recorded, being a very little less than for the baked carbon target. Consequently, the first group of electrons is considerably reduced, but it is interesting to note that there are quite as many electrons belonging to the second group in the case of this thin film as for the thick silver coating. As a matter of fact, considering all the curves taken with this film, the currents in the region of higher fields are larger absolutely than with any of the other targets studied. This is no doubt chiefly due to the fact that, at the time when these experiments were made, the writer was not yet properly trained in the technique of using the compensation method to avoid the residual currents; for this reason, the curves obtained with 3·0 volts on the rod were not good enough to serve to correct for the small emission of negative ions—hence the high value of the constant current above 300 volts. This could not have produced any distortion of the shape of the curves. It is also interesting to note that the drop between 200 and 280 volts is very nicely developed in all six curves taken with this film, being, in fact, more striking in this case than with the other targets used. Preliminary absorption experiments with gold leaf lead to the conclusion that the absorption of the radiation in the silver film must have been nothing like complete, but it should not be necessary for this reason to assume an abnormally high absorbability of the fast electrons to account for the relatively large currents for higher fields in this case. There may have been a considerable reflection at the interface between the silver and the quartz, and it does not appear impossible that part of the fast electrons were produced in the quartz.

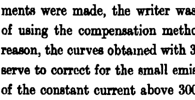

Fig. 10.—Energy Distribution.

The distribution of energy defined on p. 397, which may be obtained from the logarithmic plots by differentiation, is shown in the case of baked copper in fig. 10. This curve is thus, by definition, the complete analogy for electronic emission to the energy distribution curves for spectral emission when energy is plotted *vs.* frequency, as *e.g.*, the straight line relation of Wagner and Kulenkampff for the continuous X-ray spectrum. The two groups in the emission are fairly obvious from this graph, but it should be remarked, that the accuracy for higher voltages is not sufficient to give much detail in this region so that the second hump in this curve must be taken more as a qualitative indication of a general tendency than as a detailed representation of these things.* For this reason, the curves for the other targets shown in fig. 11 have only been

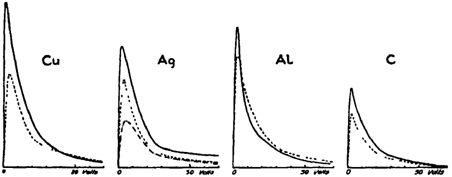

FIG. 11.—Energy Distribution. —— unbaked, ... baked, -.- -.- film baked.

given for the region below 70 volts, where the experimentally determined points fall sufficiently close to secure correct reproduction of the details. The curves drawn full are for the unbaked specimen, the dotted ones the result after baking. The curve for the silver film is included (shown thus -.-.-.-) among the curves for silver. Most of what has been said in connection with figs. 6–9 concerning the first group in the emission is also illustrated by these curves. The maximum occurring in the vicinity of 3 volts in most of the curves should be noticed. The curves after baking fall below those for the unbaked targets ; apart from this the curves are very similar in the two cases. There is some indication of a slight shift of the maximum towards higher voltages as a result of baking, except with carbon. The maximum of the curve for the silver film is also possibly shifted in this direction, and in addition is rather broad.

7. *Concerning the Nature of the Two Groups in the Emission.*

In the letter to 'Nature,' in which a first report was given of the results of the present investigation, it was pointed out, that the low average energy of the electrons must be due either to the greater part of the incident radiation being of comparatively long wave-length or to some peculiar effect taking place in the emitting substance itself. It was also suggested, that the process by which the large quanta of energy carried by the exciting electrons are transformed to small quanta of the photoelectrons might involve some kind of a compound photoelectric mechanism ; such effects should according to P. Auger* be expected to play an important part in the soft X-ray region. In fact, a little calculation shows, that if the probability of a compound effect taking place when a deeper energy level has been excited is great compared with the probability of the simple effect, the net result will be the emission of a greater number of comparatively slow-moving electrons and low-energy quanta, instead of one fast electron and one large quantum, provided there are a number of external levels to make up the chain. There might have been some doubt if the latter condition is fulfilled, particularly for the elements of low atomic weight, since there is no place for such levels in the atomic model of Bohr, but at the same time the results of critical potential experiments seemed to indicate a greater number of levels than predicted. In any case, if the compound effect plays an important part in the photoelectric target, it must necessarily do so in the anode, for the great number of low-velocity electrons is a general feature of the emission from very different elements, and the phenomenon giving rise to this distribution must be equally general ; also the compound effect must be independent of the mode of excitation, once the internal level is excited. Thus, if the compound effect is the determinating factor, the radiation from the anode must consist to a large extent of quanta corresponding to relatively long wave-lengths.

---

* From this curve a value of 15 volts for the average energy per electron may be calculated. Disregarding the second hump altogether, the value comes out 6·8 volts.

To test this, an experiment was made with a fluorite window fixed to the X-ray tube in such a way that it covered the slit in the second diaphragm completely , the rod was of copper, baked. The photoelectric emission with the window inserted was found to be 1/600 of the emission, when the radiation was allowed to fall directly on the rod. I think that even if it is admitted, that the fluorite window may not have been transparent quite down to the limit of 1200 A.U. given for good specimens, and that the photoelectric sensitivity could be less for radiation of greater wave-length than for soft X-rays, one must conclude from this result, that the amount of radiation of long wave-length was inappreciable under the conditions of these experiments, and in any case that such radiation is not responsible for the low-velocity emission.

Long before this experiment was carried out, the writer was led to reject the explanation offered by the compound photoelectric effect on the following grounds. On this theory the low-energy part of the distribution curve should be independent of the bombarding voltage for a given emitter. This is in agreement with the experimental results. Again, the complete absence of a structure in the distribution curves corresponding to low velocities is very difficult to reconcile with the idea of electrons emitted from definite energy levels with definite energies at the start. Even if such a structure, originally present, were completely wiped out due to energy losses before the electrons could escape from the surface, one would at least expect some difference, when comparing the distribution curves for different elements, since the energy levels would be different in each case. But the experimental results give very little evidence of such characteristic differences.

---

* 'Ann. de Physique,' vol. 6, p. 183 (1926).

It has occurred to the writer, that the effects set up when soft X-rays are allowed to fall on a metal should be closely related to those produced by bombardment with electrons of the corresponding energy. In both cases there is a great preponderance of low-speed electrons in the emission, and the way in which the relative amount of these electrons depends on the state of degassing of the target is at least very similar for the two. When this view is adopted, the interpretation given to the experimental results is the following.

The radiation from the anode consists chiefly of large quanta, corresponding to a few hundred volts. These quanta are absorbed in a small thickness of matter close to the surface of the photoelectric target giving rise to photoelectrons each carrying the greater part of the energy of the corresponding radiation quantum. These electrons will be referred to as the primary electrons. In the experiments on secondary emission such high-speed electrons are provided in the metal by shooting them into the target from an external source. In both cases the conditions are thus very similar, inasmuch as the immediate result is the appearance of fast primaries in the target. Experiments on electron bombardment have shown that in this case some of the primary electrons are able to escape through the surface retaining most of their initial energy, and that this escape is accompanied by a large secondary emission of low-energy electrons. The same must be expected to occur, when the primary electrons are produced by soft X-rays. From this point of view the second group in the photoelectric emission must be regarded as consisting of fast primary electrons, whilst the accompanying secondary emission constitutes the first group. (The groups have been numbered in conformity with H. E. Farnsworth's notations.)*

It has been shown that the position of the second group in the present experiments is fairly well defined with a maximum clearly indicated in the neighbourhood of 250 volts. The width of this maximum is undoubtedly greater than what would be expected if all electrons of this group had the same velocity, although it must be remembered that there is a relative uncertainty in the determination of velocities by this method as set forth in section 2 (2) and (2A). Considering all the experimental evidence on this point, however, it appears that the second group is satisfactorily accounted for by the assumption of a single monochromatic radiation giving rise to the primary electrons. The value of 275 volts for the carbon K_a-radiation as determined by J. Thibaud,* using a grating method, is in good agreement with the position of the second group. There has recently been some discussion as regards the question of the relative importance of the characteristic radiation and the continuous spectrum in the soft X-ray region. F. Holweck† concludes from his experiments, that the emission from elements of high atomic number consists almost entirely of a continuous spectrum with the same properties as the one found in the region of hard X-rays, and that most anodes must radiate in this way owing to a deposit of sputtered tungsten, at the same time he finds the K_a-radiation of carbon present in a considerable amount for higher voltages whatever the anode substance. J. Thibaud, who was unable to detect any continuous background on the plates showing an emission consisting of a few brilliant lines in his earlier experiments, has recently‡ recorded a continuous spectrum using heavy elements and very high bombarding current. H. Kurtz,§ using a platinum anticathode, concludes from absorption measurements, that the radiation is monochromatic, and consists of the carbon K_a-line. Apparently the quality of the emission depends to a great extent on the conditions, especially as regards the vacuum and the state of the anode surface; thus it appears likely that the radiation emitted 15 minutes after the tube was put together would be different from the one found after the anode has been bombarded with heavy currents for hours in a high vacuum. The question as to whether there is some radiation corresponding to the region from 50 to 200 volts under the conditions of the present experiments cannot be decided from a study of the distribution curves, but there could hardly be any great amount of such radiation. As regards the region from 300 to 700 volts, there is no evidence of electrons corresponding to radiation belonging to this region, except perhaps in the case of aluminium. It must therefore be concluded that the continuous spectrum of the type emitted in ordinary X-ray tubes, if present at all, must have been feeble in these experiments, perhaps with the exception of those in which an aluminium rod was used.

---

* 'Phys. Rev.,' vol. 31, p. 405 (1928).

---

* 'J. de Physique,' vol. 8, pp. 13, 447 (1927).

† 'Ann. de Physique,' vol. 17, p. 5 (1922); 'J. Chim. Phys.,' vol. 22, p. 311 (1925); and 'De la lumière aux rayons X,' Paris, 1927.

‡ 'C.R.,' vol. 186, p. 308 (1928).

§ 'Ann. d. Physik,' vol. 85, p. 529 (1928).

In discussing the experimental results as exhibited by the curves, figs. 6 to 9, it was pointed out, that the number of electrons emitted in the second group appeared to be fairly constant for targets in different states as regard the gas content, and also for targets made of different elements, although the total emission varied considerably in the different cases There are many factors which on the view here taken as to the nature of this group must co-operate to determine the magnitude of the corresponding current, such as the photoelectric "sensitivity"—number of electrons produced by unit energy absorbed—of the substance and the different absorption of the incident radiation and the fast electrons in the matter. It may, however, be of interest to remark that this experimental result would follow, if the sensitivity of the different elements was constant and the absorption for electrons and for radiation, which might be of different order of magnitude, varied according to the same law with the element in question. This is known not to be the case for ordinary X-rays and cathode rays.

The first group in the emission should with the interpretation of the results here proposed correspond to the secondary emission proper in experiments on electron bombardment, figs. 12 and 13, in which the experimental data given in the curves of figs. 6 to 9 have been represented in a different way are believed to lend additional support to this view. These curves have been plotted with a uniform voltage scale as the usual stopping potential curves, the unit of current in each case being the current for zero field, so that all curves start from the same ordinate corresponding to 0 volts. It will be seen that the curves are very similar, and the differences there are should be largely accounted for by the difference in the relative importance of the second group, which causes most of the spreading of the curves for higher voltages. Since, however, a separation of the currents belonging to the two groups would be liable to some arbitrariness, this has not been attempted, and the curves must be compared as they are. It will be seen that the curves obtained after baking have a tendency to fall a little higher than those for the unbaked state, also when the effect just mentioned is allowed for; the energy distribution curves showed the same kind of thing. The curve for the thin silver film falls considerably higher than the others, indicating a greater average energy of the electrons of the first group in this case. This curve also shows a considerable reduction in

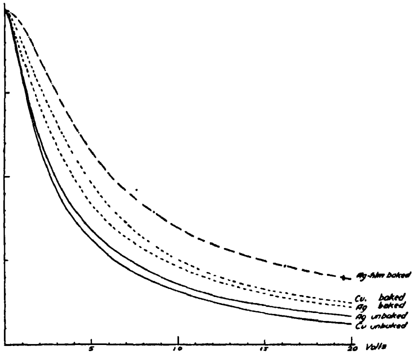
Ag-film baked
Cu. baked
Ag baked
Ag unbaked
Cu unbaked
5
10
15
20 Volts

Fig. 12.

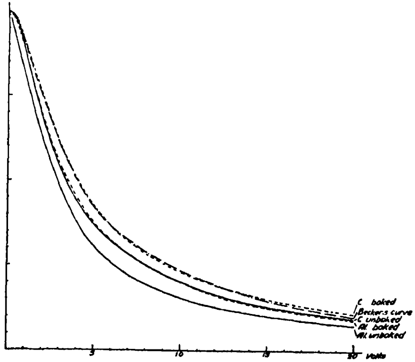
C baked
Becker's curve
C unbaked
Al baked
Al unbaked
5
10
15
20 Volts

Fig. 13.

the relative number of very slow electrons—below 1 volt—emitted from the film as compared with the curves for the other targets. I have re-examined the other curves obtained for the same film, and they seem to substantiate this result. In view of what has been said on page 404, it is probable that thee curve for unbaked aluminium would have shown the "normal" bend close to 0 volts, if the contact P.D. presumably present had been corrected for.

In fig. 13, in addition to the curves of the present investigation, a curve is given representing the distribution of the secondary emission produced by electron bombardment as measured with the stopping potential method. This curve was drawn from the upper graph of fig. 3, p. 240, of a paper by A. Becker,* and gives the distribution in the emission from a piece of metal coated with lamp black, which was bombarded with electrons of 275 volts energy. This curve was replotted in the scale of fig. 13 in such a way that the point for 20 volts would fall half-way between the curves for unbaked and baked carbon obtained in the present experiments, since the position of the corresponding zero was not indicated in the original paper. This curve, which is drawn thus, – · – · – · – · –, will be seen to fall almost exactly in the same place as the curve obtained for the photoelectric emission from baked carbon. In considering this agreement it should be remembered that there is only one adjustable parameter, namely, the position of the 20-volt point in Becker's curve. It is, perhaps, as well to state that the agreement is a little too good in view of the limited accuracy in the measurements in both cases, but, in any event, the close correspondence, such as it stands, is a definite indication of a relation between the two effects and must be said to strengthen the view here adopted as regards the nature of the emission.

A great number of investigations have been carried out on the secondary emission set up by electron bombardment of metals during the last twenty years, and recently the technique of degassing the targets under investigation has been very much improved. H. E. Farnsworth, O. Stuhlman, R. L. Petry, and H. E. Krefft† have shown that there are sudden changes occurring in the total amount of secondary emission produced by unit bombarding current for definite critical potentials as the bombarding voltage is increased; in some cases the position of these breaks in the curves appear to correspond to critical potentials of soft X-ray excitation as recorded by other observers. The distribution as regards velocities of the secondary emission in this case has been studied under what appears to have been well-defined conditions by A. Becker, C. F. Sharman, J. B. Brinsmade, and Farnsworth*; in all cases, although very different methods were employed, the result for the low-velocity electrons was similar to that exhibited by the curves in figs. 12 and 13, and no anomalies indicating the presence of groups with characteristic velocities were found in this region. Farnsworth, believed to have found evidence of such groups at first, has recently from experiments with an improved apparatus, concluded that his earlier result was erroneous, and that the true curves are quite smooth and little dependent on the bombarding voltage for higher values of this. In view of this evidence, he suggests that at least some of the critical potentials found for the total emission should be characteristic of the crystal structure of the target rather than of the energy levels of its atoms, in such a manner that the effect occurring for these bombarding voltages is an increased scattering of the primary electrons, due to the mutual reinforcement by interference of the associated de Broglie waves, as in the remarkable experiments† by C. Davisson and L. H. Germer.‡ It appears to the present writer that the fact that some of the breaks obtained by Krefft were found to be sharper for the cold metal than for the hot, is in agreement with this conception, since a rise in temperature was generally found to have the same effect on the diffraction pattern in Davisson and Germer's experiments, by these authors regarded as the analogy of the Debye temperature effect observed in the diffraction of X-rays. The present writer would like to suggest that the same phenomenon might account for some of the breaks found in critical potential work on soft X-rays, the great number§ of which has been difficult to reconcile with the theory of Bohr and with evidence recently secured in this region by grating methods. It seems natural that if increased scattering of the bombarding electrons occurs for certain voltages, an increased emission of soft X-radiation should result for these voltages, since a larger fraction of the fast electrons traverse the layer of the anode nearest to the surface three times instead of once (in any case they must finally return to the anode), and the probability for an excitation taking place in this layer, which must be the one chiefly responsible for the emission of this highly absorbable radiation, must thus be correspondingly multiplied. The results of Davisson and Germer are in agreement with the view that the scattering takes place principally in a layer a few atoms thick, and the softer rays (100 volts and less) are probably not much more penetrating. The explanation of some of the soft X-ray breaks as due to the surface arrangement of atoms, recently proposed by U. Andrewes, A. C. Davies and F. Horton,* appears to be of a kind different from the present suggestion.

---

* 'Ann. d. Physik,' vol. 78, p. 228 (1925).

† Farnsworth, 'Phys. Rev.,' vol. 25, p. 41 (1925); vol. 27, p. 413 (1926), and vol. 31, p. 405 (1928); Stuhlman, *ibid.*, vol. 25, p. 234 (1925); Petry, *ibid.*, vol. 26, p. 346 (1925), and vol. 28, p. 362 (1926); Krefft, 'Ann. d. Physik,' vol. 84, p. 639 (1927), and 'Phys. Rev.,' vol. 31, p. 199 (1928).

---

* Sharman, 'Camb. Phil. Soc. Proc.,' vol. 23, pp. 523, 922 (1927); Brinsmade, 'Phys. Rev.,' vol. 30, p. 494 (1927); and *loc. cit.*

† This interpretation is supported by the interesting results published by G. P. Thomson, 'Roy. Soc. Proc.,' A, vol. 117, p. 600 (1928).

‡ 'Phys. Rev.,' vol. 30, p. 705 (1927).

§ 'Phys. Rev.,' vol. 28, p. 601 (1926).

Several experimenters have noticed that there is a considerable resemblance between the distribution curves for the photoelectric emission excited by ultra-violet light and the curves for the thermionic emission. W. Wilson, R. Suhrmann, A. Becker, and S. C. Roy† have shown by experiments that the total photoelectric emission produced by black-body radiation obeys Richardson's law for the thermionic saturation current, T being the temperature of the radiator. A. Becker‡ has examined the distribution of velocity of the electrons emitted from metals as the result of the action of various agencies, in a series of papers. He concludes that the distribution in the secondary emission is identical with that of the δ-rays produced by bombardment with α-particles and is very similar to that of the thermions. The distribution is not quite the one which would result if the electrons had the velocities given by Maxwell's law in the metal, but the measurements are in conformity with a Maxwellian distribution of the linear velocities of the electrons striking a fixed area inside the metal. All three types of emission are accounted for quantitatively on the assumption of a distribution of this latter type if, in addition, the work done in traversing the surface is assumed to be different in the case of the thermal emission from that for the two other effects.

The remarkable persistency of the distribution curves when the bombarding potential is altered within wide limits, or when α-particles are substituted for the bombarding electrons, is undoubtedly a most interesting feature of the secondary emission, and one which needs theoretical explanation. But it appears difficult to the present writer to imagine a mechanism of emission, which would give the equilibrium distribution of the internal velocities proposed by Becker. A Maxwellian distribution of the internal velocities has been found to be in good agreement with the experimental results for the thermionic emission and for the emission due to chemical action as proved by the measurements of O. W. Richardson and M. Brotherton;[*] in this case the distribution among the electrons escaping from the surface must be independent of the magnitude of the work which has to be done by the individual electrons in crossing the surface. I have made an attempt to see how far the distribution exhibited by the curves of figs. 12 and 13 approximates to that prescribed by Maxwell's law, shifting the zero of current upwards by different amounts to correct for the contribution by electrons from the first group. In no case has the exact straight line relation been obtained which should be obtained with the method of plotting described by Richardson and Brotherton, but the points bend away from this line for higher voltages indicating a greater percentage of electrons with the corresponding energy than the theoretical curve. The slope corresponds to a temperature of the order 30,000° K. About the same temperature is indicated by the position of the inflexion in the curves of figs. 12 and 13, which should occur at a point $V = 300\ kT/e$.

---

* 'Roy. Soc. Proc.,' A, vol. 117, p. 649 (1928).

† Wilson, 'Roy. Soc. Proc.,' A, vol. 93, p. 359 (1917); Suhrmann, 'Z. f. Physik,' vol. 33, p. 63 (1925); Becker, 'Ann. d. Physik,' vol. 78, p. 83 (1925); Roy, 'Roy. Soc. Proc.,' vol. 112, p. 599 (1926).

‡ 'Ann. d. Physik,' vol. 58, p. 393 (1919); vol. 75, pp. 217, 781 (1924); and *loc. cit.*

The writer is inclined to regard the shape of the distribution curve as determined to a considerable extent by the probability of energy losses of the internal electrons before they are able to escape, in addition to the initial distribution of these electrons. These energy losses may well be such that they tend to establish a transient equilibrium corresponding to a Maxwellian distribution for a certain temperature, but the electrons have not all time to yield to this tendency, or they do not make a sufficient number of collisions to adjust themselves to the equilibrium conditions, before they escape from the metal. Thus the resulting distribution will only be similar to an equilibrium one. Although experiments on electron bombardment indicate that the collisions between electrons of a few volts' velocity and metal atoms (possibly only atoms in the surface) are mostly elastic, there is evidence that also inelastic collisions occur down to velocities corresponding to 0·1 volt.[†] The results for the silver film (fig. 12), which indicate an appreciable reduction of the number of very slow electrons in this case, receive a natural explanation on this view, but at the same time it must be born in mind that the state of the atoms in such a thin deposited film may be different to that of the atoms in a thick piece of the metal, owing to the strain which must result from the difference in the coefficient of thermal expansion for the metal and the supporting substance. No attempt has been made to measure the thickness of this film, but it is estimated that it could hardly have been greater than a few $\mu\mu$. The literature on the photoelectric emission from thin metal films is large, and the results still partly conflicting. Recently, F. Herold has published distribution curves for sputtered platinum films of gradually decreasing thickness, which show a well-marked reduction in the relative amount of very slow electrons (of the order 0·1 volt) for the thinnest films tested (1·9 $\mu\mu$); the mercury resonance line 254 $\mu\mu$ was used.

---

[*] 'Phil. Trans.,' A, vol. 222, p. 1 (1921); 'Roy. Soc. Proc.,' A, vol. 105, p. 468 (1924), and vol. 115, p. 20 (1927).

[†] Herold, 'Ann. d. Physik,' vol. 85, p. 587 (1928).

An important research on the distribution of the normal velocity components as measured by a retarding electric field has been carried out by L. Simons* in the case of the emission from thin metal films irradiated by hard X-rays. The emission is found to consist of a considerable amount of low-energy electrons, the most frequent value being 3·5 volts, in addition to the group of fast β-particles. The author points out the close resemblance with the Maxwellian distribution, and discusses several possibilities as to the origin of this emission. It is concluded that these electrons are produced by the impact of the rapid β-rays on the atoms; the limited range of velocities of this group and the remarkable independence of the speed of the primary electrons remain unexplained. It should be mentioned that the radiation used in these experiments fell in the region 0·38--0·87 A.U., so that the radiation quanta are about 100 times larger than those dealt with in the present investigation (Carbon $K_\alpha = 45$ A.U.).

8. *The Bearing of the Present Results on the Conclusions Drawn from other Experiments on Soft X-Rays.*

In view of the results secured in this investigation, some of the conclusions drawn from other measurements in the soft X-ray field may appear to require a certain modification. Such measurements are those concerned with the question of efficiency. From what has been said above it must be inferred that the quantities directly compared in experiments on the photoelectric efficiency of different substances for the same radiation is the secondary emission produced in these substances. Since the latter is determined by several factors, such as the relative penetrating power of the radiation and the primary electrons and the efficiency of the latter ones in producing secondary electrons, apart from the factor which might be termed the photoelectric "sensitivity" of the substance, it appears questionable whether any conclusions about this last factor could be drawn from such experiments. From the results reported in this paper, it would appear that the differences in the efficiency of different emitters would principally result from differences in the number of secondaries produced for one primary electron in each case, but it is possible that the other factors could vary as well.

---

* 'Proc. Phys. Soc.,' vol. 37, p. 58 (1924).

As regards the experiments in which the relative efficiency of different elements used as soft X-ray emitters is compared, it is obvious, that the fact that the measured current is due to the secondary emission, not to the primary electrons, will not have any influence on the results, at least not as long as the mean frequency of the radiation remains essentially the same for the different elements. Such measurements have been published by Richardson and F. C. Chalklin and Richardson and F. S. Robertson.[*] The evidence obtained in the experiments here reported as to the nature of the photoelectric emission does not suffice to solve the problem, discussed in these two papers, of the absolute value of the efficiency of soft X-ray production. In a preliminary test in connection with the experiments with a fluorite window previously described, it was found that a double thickness of gold leaf, $0 \cdot 16\ \mu$ in all (by weight), transmitted about 1 per cent. of the radiation. This gives an absorption coefficient $2 \cdot 9 \times 10^5$ cm.$^{-1}$ as compared with the value $5 \cdot 3 \times 10^6$ cm.$^{-1}$ for 500 volt electrons calculated from the value $\alpha/\mathrm{D} = 27 \cdot 3 \times 10^4 \dfrac{\mathrm{cm.}^{-1}}{\mathrm{g./cm.}^3}$ for nickel, recently published by A. Becker,[†] assuming mass proportionality as a first approximation. According to this author, this value would seem to apply to electrons of somewhat lower energy as well. The present writer has tried to arrive at an estimate of the total number of primary electrons E_t inside the metal in the following way.

The surface of the target is large compared with the thickness concerned in the processes dealt with. Let I be the intensity of radiation, E_1 that of the primary electron stream and S that of the stream of secondaries at a depth x below the surface, the two latter proceeding outwards. For $x = 0$ these quantities become I_0, E_0, S_0. The corresponding coefficients of absorption are α, β and γ. When unit radiation is absorbed, $2k$ primaries are formed, and $2s$ secondaries result for each unit of primaries absorbed. In addition to E_1 the current of primary electrons E_2 flowing in the opposite direction has to be considered. The differential equations

$$\left.\begin{array}{ll} d\mathrm{I} = -\alpha\mathrm{I}\,dx. & d\mathrm{E}_1 = (\beta\mathrm{E}_1 - k\alpha\mathrm{I})\,dx, \\ d\mathrm{E}_2 = (-\beta\mathrm{E}_2 + k\alpha\mathrm{I})\,dx, & d\mathrm{S} = (\gamma\mathrm{S} - s\beta\,\overline{\mathrm{E}_1 + \mathrm{E}_2)}\,dx \end{array}\right\} \quad (7)$$

---

[*] 'Roy. Soc. Proc.,' A, vol. 110, p. 247 (1926), and vol. 115, p. 280 (1927).

[†] 'Ann. d. Physik,' vol. 84, p. 779 (1927).

give
$$\left.\begin{aligned} I &= I_0 e^{-\alpha x}, \qquad E_1 = \alpha k I_0 e^{-\alpha x}/(\alpha+\beta), \\ E_2 &= \alpha k I_0 (e^{-\alpha x} - e^{-\beta x})/(\beta-\alpha), \\ S &= \frac{\alpha\beta}{(\alpha+\beta)(\alpha+\gamma)} s k I_0 e^{-\alpha x} + \frac{\alpha\beta}{\beta-\alpha} s k I_0 \left\{\frac{e^{-\alpha x}}{\alpha+\gamma} - \frac{e^{-\beta x}}{\beta+\gamma}\right\} \end{aligned}\right\} \tag{8}$$

from which, since $E_t = 2kI_0$,

$$E_0 = \tfrac{1}{2}\frac{\alpha}{\alpha+\beta}E_t, \qquad S_0 = \tfrac{1}{2}\cdot\frac{\alpha+2\beta+\gamma}{(\alpha+\gamma)(\beta+\gamma)}\cdot\frac{\alpha}{\alpha+\beta}\cdot\beta s E_t. \tag{9}$$

This is for the photoelectric case. In the experiments where the target is bombarded from outside with the primary current E_b, it is obvious that E and S will take over the part of I and E_1, in (7) with a corresponding change in the constants. This gives

$$E = E_b e^{-\beta x}, \quad S = \beta s E_b e^{-\beta x}/(\beta+\gamma), \quad S_0 = \beta s E_b/(\beta+\gamma). \tag{10}$$

For the same secondary emission in both cases, E_t and E_b will therefore stand in the relation to each other

$$E_t = \frac{\alpha+\gamma}{\alpha+2\beta+\gamma}\cdot\frac{\alpha+\beta}{\alpha}\cdot 2E_b. \tag{11}$$

Now $\beta \gg \alpha$. As regards γ, a value as low as that of α—which would make $E_t = 2E_b$—is certainly excluded. For $\gamma = \beta$, the first factor is practically $\frac{1}{2}$, and it approaches to unity for $\gamma \gg \beta$. This calculation regards the secondary electrons as produced in the interior of the substance. If instead they were excited exclusively in the surface, their number should be proportional to E_0 and E_b respectively. Hence, in this case,

$$E_t = 2E_0\frac{\alpha+\beta}{\alpha}. \tag{12}$$

But the first alternative appears more probable. Taking $\gamma = \beta$* and inserting the numerical data given above, one infers from this calculation, that the total number of primary electrons produced would be greater by a factor of the order 10 (calculated value 13·3) than the number of electrons of the same speed, which, bombarding the target from outside, would give rise to the same secondary emission. Since the latter is of the same order of magnitude as the secondary emission produced, it would appear to follow that the total current of primary electrons excited, if it could be measured, would turn out some ten times larger than the photoelectric currents actually recorded in experiments of this kind. The problem has been greatly idealised in the calculation just given, the processes actually taking place being undoubtedly much more complicated involving such effects as scattering and change in velocity due to loss of energy. It need hardly be emphasised that the present calulation must be looked upon merely as a first and very approximate attempt to estimate the quantity in question.

---

* A value of this order is indicated by some recent results of C. F. Sharman's† the much greater penetrating power found by H. E. Hartig‡ has not been confirmed by later investigators.§ A. Partzsch and W. Hallwachs‖ from measurements by K. Rubens and E. Ladenburg¶ on gold leaf using ultra-violet light calculate a value $1{\cdot}03 \times 10^6$ cm.$^{-1}$ for these electrons. (Roy† has accidentally interchanged the two coefficients for electrons and radiation given by Partzsch and Hallwachs.) This value would make $E_t = 4{\cdot}3\ E_b$.

† *Loc. cit.*

‡ 'Phys. Rev.,' vol. 26, p. 221 (1925).

§ Becker, 'Ann. d. Physik,' vol. 84, p. 779 (1927).

‖ 'Ann. d. Physik,' vol. 41, p. 247 (1913).

¶ 'Verh. Deut. Phys. Ges.,' vol. 9, p. 749 (1907).

The question whether a photoelectron is produced on each absorption of a quantum is still an open one. The surprisingly low ratio of the photoelectric to the thermionic current always observed, is probably largely due to a low efficiency of X-ray production in the anode, since the soft radiation from gases usually gives much larger currents. For hard X-rays the evidence on this point is such that absorption may be regarded as an entirely photoelectric phenomenon. B. Gudden,[*] considering the low efficiency of ultra-violet light, finds the existing evidence insufficient to decide if this is due entirely to absorption of the electrons in the substance, but admits that only a fraction of the absorption processes in metals may result in the expulsion of photoelectrons. B. Gudden and R. Pohl suggest, that photoelectric absorption only takes place in atoms which are in a special favourable condition, determined by the atom in question being in tune with the atoms surrounding it within the volume of a wave-length cube ; this leads to the result found for hard X-rays, the wave-lengths of which are small compared with the distance between neighbouring atoms and for gases, where the same thing results from the increase in the latter quantity. On this hypothesis, only a portion of all absorption processes would be expected to give rise to photoelectrons in the case of soft X-rays and solid targets. In this connexion, however, it should be mentioned that on the theory of S. C. Roy, which[†] agrees with the measurements of the extinction coefficient of silver in the ultra-violet, the absorption should be chiefly photoelectric as soon as the threshold is passed.

---

[*] 'Handbuch der Physik,' vol. 13, p. 103 (1928).

[†] 'Roy. Soc. Proc.,' A, vol. 112, p. 599 (1926).

9. *Summary.*

This paper contains an account of some experiments in which the distribution of velocity among the photoelectrons produced by the action of soft X-rays on solid conductors is studied A special method of magnetic analysis is used, in which the electrons with lower velocity emitted from the photoelectric target in the shape of a narrow rod are gradually prevented from reaching a surrounding cylindrical electrode by the application of an increasing magnetic field. The theory of this method is outlined and the final experimental design described. There is evidence of a very small fraction of negatively-charged atomic carriers in the emission, which is allowed for in special experiments.

Curves are given for the emission from silver, copper, aluminium and carbon, and from a transparent silver film deposited on a quartz rod. In all cases the emission can be described as constituted of a group of electrons with energies mostly amounting to only a few volts, and a much less prominent group having energies chiefly concentrated in the region 200–280 volts. The first group is reduced by about 50 per cent. by baking the targets at 400° C. The second group is not appreciably affected by this heat treatment. Aluminium differs from the other elements in failing to show any reduction of the first group after heating. Also, the concentration of the second group to a limited region is much less marked ; a possible reason for this is discussed. For the others, the high velocity group is of nearly the same magnitude absolutely. The relative importance of the first group is less for carbon than for silver and copper, this group is also reduced in the case of the silver film.

It is proposed that the second group consists of fast primary electrons produced directly by the incident radiation quanta, and that the first group is the secondary emission resulting from the presence of such fast primaries in the target. The energy distribution among the fast electrons is satisfactorily accounted for by the assumption of an incident radiation chiefly consisting of the carbon K_a-line. In this connection it is proved by experiments with a fluorite window that no appreciable amount of long wave-length radiation is emitted.

The curves representing the distribution of energy among the electrons of the first group are shown to compare well with such curves published by other investigators for the secondary emission produced by bombardment with electrons of the corresponding energy. They are very similar for the different targets studied.

The question as to the origin of the secondary emission is discussed. The results of the measurements on the silver film indicate that the distribution of energy in this emission is, at least to some extent, determined by the energy losses of these low-speed electrons in the target before they escape.

The bearing of the present result on the conclusions which may be drawn from some other experiments in soft X-rays is indicated, and some related problems in this field are briefly discussed. Preliminary measurements on gold leaf indicate an absorption coefficient of about 3×10^5 cm.$^{-1}$ for the radiation used in this work, which is nearly ten times less than the value recently given by A. Becker for the absorption of electrons of the same energy in nickel. A rough calculation based on these figures indicates a total amount of primary electrons some ten times greater than the resulting secondary emission.

In conclusion, the writer wishes to express his best thanks to Prof. O. W. Richardson for his continued interest and encouragement and his many valuable suggestions throughout the course of this work. It is also a pleasure to acknowledge the kind assistance received from the staff and research students of the Physics Department.

The writer is much indebted to the Ramsay Memorial Fellowships Trust for awarding him the fellowship which enabled him to carry out this investigation.

The Action of Strong Electric Fields on the Current from a Thermionic Cathode.

By N. A. DE BRUYNE, Cavendish Laboratory, Cambridge.

(Communicated by Sir Ernest Rutherford, P.R.S.—Received June 20, 1928.)

Introduction.

It is well known that the "Saturation Current" from a thermionic source rises continuously as the applied voltage is raised and in reality never reaches a saturation value. W. Schottky* predicted this rise in the saturation current on theoretical grounds and obtained a rough experimental confirmation of his theoretical formula.† The present investigation was undertaken to obtain further information about the effect and in particular to find what connection it has with the emission of electrons from cold metals under the action of intense electric fields.

If the truth of Schottky's theory be assumed it is possible to deduce the value of the electronic charge e from observations of the rise of the saturation current with the applied field. It was not the primary intention of the author to determine the value of e in this way, nevertheless the results obtained show that the method might be developed into one of some accuracy, and thus to give a value of this important constant in a way differing completely from that of Millikan (oil drop method), Perrin (Brownian movement) or of Hull and Williams (shot effect).

The Schottky Theory.

When an electron comes out of a metal it experiences a force tending to pull it back; it is this force which gives rise to the thermionic and photo-electric work functions. Very close to the surface of the metal the force is strong and due to the action of the individual atoms in the immediate neighbourhood of the electron, but at a sufficient distance away from the surface the force on the electron can be calculated, as Sir J. J. Thomson has shown, from the law of electrostatic images. An external field in the proper direction will oppose this image force and at a certain distance x_0 from the surface will be exactly equal and opposite to it. Let V be the potential of an electron at a distance x (in the neighbourhood of x_0), then

---

* 'Phys. Z.,' vol. 15, p. 872 (1914).

† Since the completion of the present investigation Pforte ['Z. f. Physik,' vol 49, p. 46 (1928)] has verified the Schottky formula more accurately up to a field of $0 \cdot 7 \times 10^6$ volts/cm.

$$V = e/4x + Xx. \tag{1}$$

where X is the external field, e is the charge on the electron. The potential V_0 at distance x_0 is obtained by differentiating (1) and equating dV/dx to zero.

$$V_0 = (eX)^{\frac{1}{2}}. \tag{2}$$

V_0 is the decrease in the work function [expressed in electron volts] produced by the action of the external field.

Schottky now assumes that all electrons striking the surface normally with kinetic energies greater than $(\chi_0 - V_0e)$ will escape and those having energies less than $(\chi_0 - V_0e)$ will return to the metal. χ_0 is the work function; it is the difference between the potential jump at the surface and the partial pressure inside. The assumption that the probability of emission of an electron is zero when its kinetic energy is less than $(\chi_0 - V_0e)$, and unity when its kinetic energy is greater than $(\chi_0 - V_0e)$, is, of course, true on classical mechanics but is not strictly true according to Nordheim's Theory* [based on wave mechanics]. On Nordheim's theory the probability of emission decreases very rapidly with the velocity of the electron when the kinetic energy is less than $(\chi_0 - V_0e)$ and reaches values of the order of unity for energies greater than the critical value. In Nordheim's paper* the probability of emission was calculated to be of the order of one half for energies greater than $(\chi_0 - V_0e)$, but later work based on a more accurate picture of the potential jump at the surface of the metal has shown that the probability is nearly unity.

The experimental interest of equation (2) is that by altering X (the external field) we can alter the opposing potential on the electrons. In this way we can investigate the velocity distribution of those electrons which ordinarily are unable to escape, and which can never be detected by the usual "Retarding Field" method of measuring a velocity distribution. It is to be noted, however, that strictly speaking all such experiments measure the product of the number of electrons with energy greater than some critical value into the average coefficient of emission for the velocities greater than the critical value. On the Classical Theory these average coefficients would be unity; from the point of view of wave mechanics this is not correct, but the error is small.

If we assume that the electrons with energies in the neighbourhood of the critical energy have a Maxwellian distribution then it is very nearly true that

---

* Nordheim, 'Z. f. Physik,' vol. 46, p. 833 (1928); Fowler and Nordheim, 'Roy. Soc. Proc.,' A, vol. 119, p. 1 (1928).

$$i = I\varepsilon^{V_0 e/KT}, \tag{3}$$

where I is the thermionic current for an infinitely weak field and i is the current in a field X.

Substituting from equation (2)

$$i = I\varepsilon^{\frac{e^{\frac{3}{2}}X^{\frac{1}{2}}}{kT}}. \tag{4}$$

Let X be measured in volts per centimetre; then on substituting numerical values for e and K and taking logarithms we get

$$\Delta \log_{10} i/\Delta X^{\frac{1}{2}} = 1{\cdot}906/T, \tag{5}$$

from which we see that $\Delta \log_{10} i/\Delta X^{\frac{1}{2}}$ should give a straight line whose slope is inversely proportional to the absolute temperature. But there is another way of considering equation (4) and one which the author believes is original. If we assume the truth of equation (4) it is possible to deduce the value of e. This is not possible in retarding field experiments which can only give the value of e/K.

Put

$$K = R/N = Re/Ne = Re/F$$

where R is the gas constant, N is Avogadro's number, F is one Faraday.

Then

$$\Delta \log_e i/\Delta X^{\frac{1}{2}} = e^{\frac{3}{2}}F/ReT = e^{\frac{1}{2}}F/RT.$$

Putting R = 8·309 joules/degrees, F = 96490 coulombs, and measuring X in volts per centimetre

$$e = 1{\cdot}311\,(T\,.\,\Delta \log_{10} i/\Delta X^{\frac{1}{2}})^2\,.\,10^{-10}\ \text{E.S.U.} \tag{6}$$

Description of Tubes.

The experimental problem to be solved was to measure the emission from a filament at a known temperature and with a known applied field at its surface, and to be able to apply as large a field as possible. Two forms of tube were designed to fulfil these conditions; type A is shown in fig. 1; it was designed for filaments of about 0·01 cm. in diameter. The filament ran through holes in rectangular nickel stampings and was kept taut by a molybdenum spring The anode and guard rings were of seamless nickel tube made by drilling out nickel rod and subsequently turning down to the required thickness; the anode and guard rings were spot-welded into rectangular nickel stampings. The nickel stampings and tube were supplied by the Cambridge Instrument

Company. The nickel stampings were slid on to the two arms of a quartz U-tube and were spaced apart by quartz tubes as shown. The filament connections were made to a four electrode pinch which was also made to support the whole assembly. The pinch was sealed into a 200 watt (gas-filled type) lamp bulb. The connections to the anode and guard rings were brought

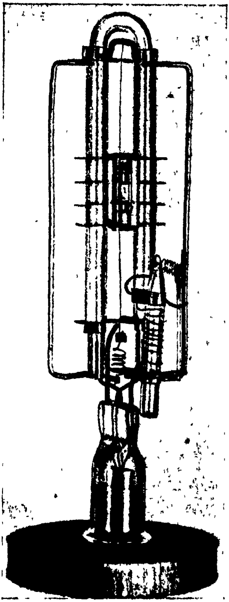

FIG. 1.

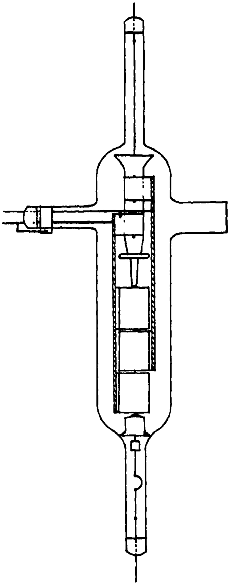

FIG. 2.

out by glass encased leads to the top of the bulb. A small quartz tube, closed at one end, was filled with magnesium; a 5 ampere tungsten filament was wound on the outside and connected to the pinch; the tube could thus be gettered as often as required by lighting the 5 ampere filament. This type of tube was sealed off from the pump before use.

The other form of tube (type B) is shown in fig. 2; this can be used with very fine filaments The main feature of the design was that the filament could easily be renewed by cutting open the top and bottom ends. The old filament was pulled out and a wire passed down through the tube from the top end, the top of a new filament assembly was then copper brazed to the bottom of this wire. The wire was then drawn up, the filament was thus pulled into position and the two ends of the tube were sealed up again The lead-in wires were of platinum sheathed wire. The filament was kept taut by a small nickel weight, this was found to be much better with fine filaments than a spring. The nickel anode and guard rings were of big diameter (1·58 cms.) so that the effect of any slight errors in centering the filament was minimised. The anode and guard rings were each 2 cms. long.

The field at the surface of the filament is given by

$$E = V/2{\cdot}303r \log_{10} R/r,$$

where R = radius of anode and r = radius of filament

Let V = 10,000 volts and $r = 0{\cdot}001$ cm,

then if R = 0·84 cm. $E = 1{\cdot}485 \times 10^6$ volts/cm.,

if R = 0·86 cm $E = 1{\cdot}479 \times 10^6$ volts/cm,

thus the radius of the anode is not the decisive factor in determining the value of the field.

Both types of tube were made of lime glass with lead glass extensions wherever lead-in seals were made. There was no difference in the results given by the two tubes; but in the final measurements, described below, type B alone was used as it was thought best to have completely comparable conditions for filaments of all diameters.

High Tension Equipment.

A high negative voltage was obtained from a full wave kenotron rectifier presented to the Cavendish Laboratory by the General Electric Company of Schenectady. The smoothing equipment consisted of a 360 henry choke shunted on each side by 0·137 mfd. condensers. The voltage was measured by a milliammeter in series with a wire wound resistance $3{\cdot}396 \times 10^6$ ohms.

The output was taken through a fuse of fine tungsten wire and a wire wound megohm resistance to the filament of the experimental tube. The filament current was supplied by accumulators carefully insulated from earth. The anode was connected to one terminal of a galvanometer, the other terminal being connected to the guard rings and to earth. The whole apparatus including pumping equipment was enclosed in an earthed cage with safety switches.

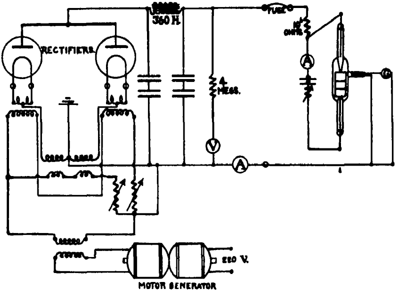

Fig. 3.—Connections.

In order to secure a steady voltage the high tension set was not run directly off the mains but through a motor generator run off direct current from the laboratory sub-station.

Pumping Equipment and Procedure.

A high vacuum is an essential condition for an investigation of this kind. No wax, grease, or ground glass joints of any kind were used on the high vacuum side of the apparatus. A three-stage hard glass diffusion pump was connected by a graded glass joint, through a mercury cut off and liquid air trap of lead glass, to the experimental tube. The diffusion pump was backed by a Hyvac two-stage pump through a large reservoir. A Pirani gauge was connected between the liquid air trap and the experimental tube, and a Macleod gauge was connected to the high vacuum side of the diffusion pump. At one period of the investigation an ionisation gauge was connected to the experimental tube and the pressure, after baking and bombarding, was found to be less than 10^{-6} mm.; but the experiments themselves soon show if the vacuum is not high by the appearance of irregularities in the observations.

The tube was first baked for an hour at 400° C.; the filament was then lit and the anode and guard rings were bombarded for half an hour. With filaments of 0·01 cm. diameter it was possible to get the anode red hot; but with smaller filaments this was not possible, but even with these there was an energy dissipation of about 15 watts so that the anode and guard rings were far hotter than during the taking of observations when the energy dissipation was of the order of a hundredth of a watt. The tube was then baked again for an hour. Tubes of type A were then sealed off quickly after first getting the glass constriction hot for a few minutes previous to sealing off. The tube was then gettered and the filament aged for an hour at 2600°. Type B was not sealed off but the filament was aged and observations were begun. All the metal parts in the tubes were heated to red heat *in vacuo* before being sealed in.

Determination of Temperature.

Probably the best method of determining the filament temperature would be by a pyrometer; but as the equipment is expensive and other methods are available it was not used. Worthing and Forsythe* have tabulated a large number of the properties of tungsten as a function of its temperature. No filament, however, is at a uniform temperature so that if the temperature is to be determined by means of the resistance, power consumed, or voltage drop these quantities must be found for the uniformly heated portion of the filament. This involves the use of fine potential leads or numerical corrections. The heating current is, however, constant throughout the length of the filament, and gives a simple method of temperature determination. It can only give the true temperature of the filament under fixed external conditions [for instance, when the temperature of the surroundings is fixed]. In the present investigation the filament was surrounded by an anode and guard rings so that reflection of heat back on to the filament, and also re-radiation, from the anode and guard rings must cause errors. The use of the thermionic emission to determine the temperature eliminates errors due to back heating; it also largely eliminates errors due to cooling at the ends, as is shown below.

Consider a filament with a non-uniform temperature distribution. Each element of the filament will give a different $\Delta \log i/\Delta X^{\frac{1}{2}}$ curve; if Schottky's relation is true each curve will be a straight line and, to a first approximation, provided that the temperature range is not too great, the resultant curve due to all the elements will be a straight line S. It is possible to find an "Effective Temperature" at which a uniformly heated filament, of the same length and diameter as that actually used, will give the same straight line S. The problem is now to deduce the effective temperature; this can be done by extrapolating the straight line S to zero field and finding to what temperature the emission at zero field corresponds. This is the effective temperature of the filament.

---

* 'Astrophys. J.,' vol. 61, p. 146 (1925).

In order to test the correctness of this conclusion a tube was made up with a molybdenum anode 2·5 cms long, without guard rings and having a filament 2·5 cms. long and 0·003 cm. in diameter. This tube was designed to accentuate end losses; the results obtained are given below

Temperature from filament heating current	2070°	2220°	2400°
Temperature from emission at zero field	1650°	1840°	2110°
Temperature from Schottky relation	1570°	1850°	2100°

It will be seen that the temperature deduced from the heating current is much higher [due to neglect of end losses] than that deduced from the emission or from the Schottky equation. The difference decreases, however, with increase of temperature.

Determination of Filament Diameter.

When the characteristics of a filament had been determined the tube was opened up and a low power microphotograph (× 62) was taken of the filament. The diameter of this image was measured on a comparator. In computing the value of the field a correction must be made for the thermal expansion of the filament, for any given temperature. The temperature was determined by plotting $\log_{10} i$ against $V^{\frac{1}{2}}$ and extrapolating to zero volts; it is not, of course, possible to draw an accurate curve of $\log_{10} i$ against $X^{\frac{1}{2}}$ until this correction for thermal expansion has been made. The expansion is of the order of 1 per cent.

Results obtained with 0·00208 *cm. Filament.*

The results obtained with a filament of 0·00208 cm. diameter are shown in fig. 4. The temperatures shown are the emission temperatures. The details for the five curves are as follows.

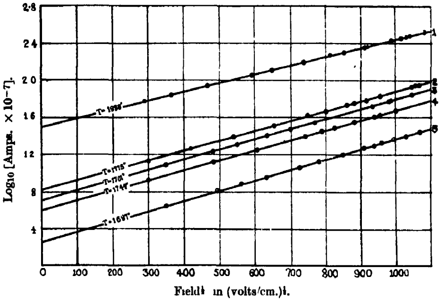

FIG. 4.—Characteristics of 0·0208 cm. Filament

Table I.

Curve	$\Delta \log_{10} i/\Delta X^{\frac{1}{2}}$	T_{em}	T_{Maxw} *	$T_{em} (\Delta \log_{10} i/\Delta X^{\frac{1}{2}})$.
1	$9·529 \times 10^{-4}$	1986°	2001°	1·892
2	$10·69 \times 10^{-4}$	1775°	1788°	1·892
3	$10·92 \times 10^{-4}$	1761°	1746°	1·923
4	$10·80 \times 10^{-4}$	1744°	1765°	1·883
5	$11·18 \times 10^{-4}$	1697°	1705°	1·897

* Maxwellian temperature calculated from Schottky equation.

The curves are good straight lines up to and above a field of 10^6 volts/cm The temperatures calculated from the slopes are in good agreement with the temperatures calculated from the emission at zero field. The slopes are inversely proportional to the temperature, although this has not been verified over a very wide range of temperature because at high temperatures gas effects become troublesome, and at lower temperatures the current becomes too small to measure.

Results obtained with Filament of 0·00339 *cm. Diameter.*

The results obtained with a filament of 0·00339 cm. diameter are shown in fig. 5. The details for the seven curves are as follows :—

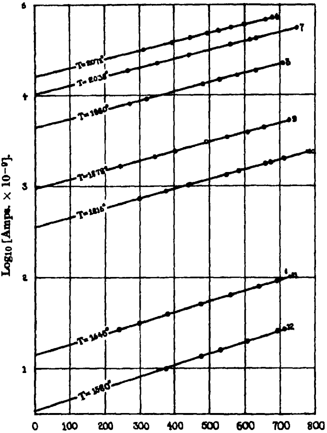

FIG. 5.—Characteristics of 0·00339 cm. Filament.

Table II.

Curve.	$\Delta \log_{10} i/\Delta X^{\frac{1}{2}}$.	T_{em}	T_{Maxw}	$T_{em}\,(\Delta \log_{10} i/\Delta X^{\frac{1}{2}})$.
6	$9 \cdot 50 \times 10^{-4}$	2071°	2006°	1·967
7	$9 \cdot 60 \times 10^{-4}$	2038°	1986°	1·956
8	$9 \cdot 87 \times 10^{-4}$	1980°	1931°	1·954
9	$10 \cdot 16 \times 10^{-4}$	1878°	1876°	1·908
10	$10 \cdot 55 \times 10^{-4}$	1816°	1811°	1·916
11	$11 \cdot 83 \times 10^{-4}$	1645°	1612°	1·946
12	$12 \cdot 00 \times 10^{-4}$	1580°	1589°	1·896

Results obtained with Filament of 0·0104 *cm. Diameter.*

The results obtained with a filament of 0·0104 cm. diameter are shown in fig. 6. Disregarding, for the time being, the sharp rise at about 250,000 volts per centimetre the details for the initial parts of the curves are as follows :—

Table III.

Curve.	$\Delta \log_{10} i/\Delta X^{\frac{1}{2}}$.	T_{em}	T_{Maxw}	$T_{em}\ (\Delta \log_{10} i/\Delta X^{\frac{1}{2}})$.
13	$9 \cdot 880 \times 10^{-4}$	1944°	1930°	1·921
14	$9 \cdot 917 \times 10^{-4}$	1900°	1920°	1·885
15	$10 \cdot 20 \times 10^{-4}$	1862°	1870°	1·900
16	$10 \cdot 40 \times 10^{-4}$	1830°	1833°	1·907
17	$11 \cdot 16 \times 10^{-4}$	1766°	1708°	1·971
18	$11 \cdot 25 \times 10^{-4}$	1748°	1694°	1·966
19	$11 \cdot 20 \times 10^{-4}$	1697°	1702°	1·901
20	$12 \cdot 40 \times 10^{-4}$	1578°	1538°	1·956

Discussion of Results.

The results obtained with the filament of 0·00208 cm. diameter shows that up to fields of 10^6 volts/cm. the Schottky relation, and therefore the Maxwellian velocity distribution, holds good. Now the results of many investigators, in particular by L. H. Germer,* show that the electrons having energies greater than 4·53 volts [the work function of Tungsten] have a Maxwellian velocity distribution. The results given above enable us to extend this limit down to about 4·2 volts since this will be the value of the work function at a field of 10^6 volts/cm. Thus we may say that not only do those electrons which are able to escape by their own energy in the absence of an external field have a Maxwellian velocity distribution, but electrons of 1/3 volt less energy than that corresponding to the work function also possess a Maxwellian velocity distribution.

The results obtained with filaments of 0·00339 and 0·0104 cm. diameter [disregarding temporarily the anomalous results above $0 \cdot 25 \times 10^6$ volts/cm.] show conclusively that it is the field at the surface of the cathode which is the decisive factor in controlling the rise in saturation current. When the slopes of the curves are multiplied by the corresponding temperatures a value is obtained which is the same for all three filaments although their radii are in the ratio 1 : 1·63 : 5·0.

But we have yet to explain the apparent departure from a Maxwellian distribution with the 0·0104 cm. filament at a field of about $0 \cdot 25 \times 10^6$ volts/cm. The results obtained with the other two filaments show that at this field strength the Schottky relation still holds good. Thus the effect is not due to a breakdown of the Schottky relation at this field strength, but must be due to some other cause. The explanation that first suggests itself is that the electrons cause ionisation of residual gas resulting in a sudden rise of current. But this explanation cannot be true, partly on the general grounds that such a process cannot take place when the mean free path is of the order of a metre or more, and partly because we should expect that the greater the thermionic current the bigger would be the sudden rise. Fig. 6 shows that when the thermionic current is big the rise of current becomes hardly noticeable and that it is only at low thermionic emissions that the sudden rise becomes important. Indeed, as curve 21 shows, the effect only becomes extremely pronounced when the filament is at room temperature This sudden rise is evidently something completely independent of, and unaffected by, the thermionic emission. Moreover on allowing air to enter the apparatus so as to bring the pressure to about 10^{-4} mm. the effect was very much reduced.*

---

* 'Phys. Rev.,' vol. 25, p. 795 (1925).

Another explanation is that the bombardment of the anode and guard rings by the thermionic electrons causes an emission of positive ions which in turn bombard the filament giving rise to delta rays. Again, however, if this explanation were correct we should expect an increasingly big rise to take place as the thermionic emission is increased. But there is another objection to such an explanation. It has been shown by Mr. M L. Oliphant, working in this laboratory, that electrons cannot be knocked out of *gas-free* metals under positive ion bombardment; the effect only takes place when the target has not been properly cleaned and out-gassed, the fact that the thermionic emission from the filament is so regular shows that it is free from gas. As a final test of the truth of such an explanation the characteristics were taken of a tube in which the anode and guard rings were not bombarded; the tube was baked for an hour, the filament [0·00339 cms] was lit and aged and readings were then taken. The resulting curve (fig 7) shows that at a certain voltage gas was probably liberated from the anode and guard rings, this gas contaminated the filament surface and decreased the emission; on decreasing the voltage another characteristic curve was obtained and the readings were not reproducible. This is a very different effect from that which we are considering.

The possibility that the rise in current is due to the emission of delta rays by the action of X-rays produced in the tube is ruled out by the fact that the rise takes place most violently of all when the filament is cold.

There seems to be only one explanation compatible with the facts of experiment. We have proved that it is the field at the surface of the cathode which is the effective agent in increasing the thermionic current, theoretically

---

* See also de Bruyne, 'Phil. Mag.,' vol. 5, p. 574 (1928).

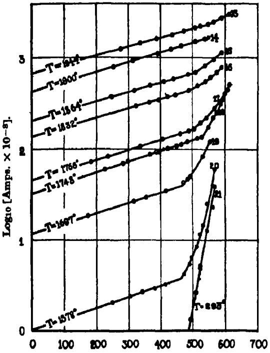

FIG. 6.—Characteristics of 0·0104 cm. Filament.

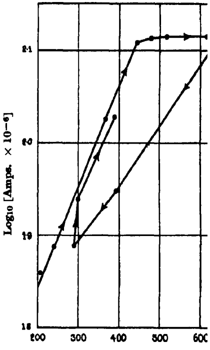

FIG. 7.

then, provided we have a big enough field, it should be possible to obtain an emission of electrons even at room temperature. Thus the most reasonable explanation is that the rise in current shown in fig. 6 is the result of a very high electric field, we know from the results obtained with the 0·00208 cm. filament that if this explanation is correct the field producing the effect must certainly be greater than 10^6 volts/cm. Such a field could be produced by a sharp submicroscopic irregularity on the surface of the 0·014 cm. filament, and this would explain why the effect was not obtained with all three filaments.

But there is one very important difference between the increase in the thermionic current produced by electric fields up to 10^6 volts/cm. and the emission of electrons produced by the very strong field.

The thermionic current definitely obeys the Schottky law, that is to say, the electrons pulled out by comparatively weak fields have a Maxwellian velocity distribution. The auto-electronic current [the current due to electrons pulled out by strong fields] definitely does not obey the Schottky law, fig. 6 shows that the rise of current with field is much quicker than according to the Schottky equation. Moreover, Gossling* and Millikan† have shown that the auto-electronic current is independent of temperature. Therefore the electrons pulled out by the strong fields cannot have the same distribution as those pulled out by weak fields. But it must be the electrons with small energies that are pulled out by strong fields; so we may say: The electrons with big energies have a Maxwellian velocity distribution, the electrons with small energies have some other distribution which is unaffected by temperature. This is in qualitative agreement with the Sommerfeld theory‡ of electrons in metals.

Determination of Electronic Charge.

We have from the results of the three filaments :—

Curve.	$T\,[\Delta \log_{10} i/\Delta X^{\frac{1}{2}}]$	$T^2\,[\Delta \log_{10} i/\Delta X^{\frac{1}{2}}]^2$.
1	1·892	3·579
2	1·892	3·759
3	1·923	3·697
4	1·883	3·514
5	1·897	3·599
6	1·967	3·869
7	1·956	3·826
8	1·954	3·819
9	1·908	3·641
10	1·916	3·673
11	1·946	3·787
12	1·896	3·594
13	1·921	3·690
14	1·885	3·552
15	1·900	3·610
16	1·907	3·637
17	1·971	3·885
18	1·966	3·865
19	1·901	3·614
20	1·956	3·826

$$\text{Mean} = 3\cdot693 \text{ degrees}^2 \times \text{cms /volts},$$

which on substitution in equation (6) gives

$$e = 4\cdot8_4 \times 10^{-10} \text{ E.S.U.}$$

---

* 'Phil. Mag.,' vol. 1, p. 609 (1926).

† 'Phys. Rev.,' vol. 27, p. 525 (1926).

‡ Sommerfeld, 'Z. f. Physik,' vol. 47, p. 1 (1928).

The author wishes to thank Dr. C. J. Smithells of the Research Laboratories of the G.E.C., Wembley, for supplying some pure tungsten wire, and Mr. C. Wilson, Director of the Osram-G.E.C. Lamp Works, for supplying bulbs and filaments. He also wishes to thank Mr. R. H. Fowler for valuable discussion of the theoretical part of this paper, and Sir Ernest Rutherford and Sir Joseph Thomson for their interest in the work.

A Further X-Ray Investigation of Long Chain Compounds (n-Hydrocarbon).

By ALEX MÜLLER.

(Communicated by Sir William Bragg, F.R.S.—Received June 20, 1928.)

(PLATES 18–19.)

Introduction.

In a previous paper* the writer has outlined the crystal structure of a number of long-chain compounds. One of the main results of this work was to show that the crystal molecules (chains) in all these substances can be represented as rods of definite cross section, the crystals being built up of bundles of these rods packed close together. A closer examination of the X-ray photographs of stearic acid gave the clue to the chain structure, and led to a general formula for the structure factor.

It was then announced that a more detailed investigation of stearic acid was to follow. The choice of stearic acid was dictated entirely by practical reasons, no other well developed crystals of other similar substances being available at that time. But as it was obviously more desirable to study first the prototype of the long chain compounds, namely, the normal hydrocarbon, efforts were first made to find single crystals of these substances. The search was unexpectedly successful, and the present paper describes an attempt to interpret the results of the X-ray examination of a single crystal of the hydrocarbon $C_{29}H_{60}$.

The writer considers himself very fortunate in having been assisted in this work by several of his colleagues at the Davy-Faraday Laboratory. Dr.

---

* 'Roy. Soc. Proc.,' A, vol. 114, p. 542 (1927).

J. M. Robertson kindly supplied a considerable quantity of a natural hydrocarbon, and Mr. W. B. Saville and Dr. H. S. Gilchrist synthesised and purified a number of these substances.

Chemical History of the Substances and their Identification.

There was no reason for giving a preference to any particular *n*-hydrocarbon. That which was chosen happened to be the only one from which sufficiently large crystals could be obtained. It was a natural product extracted from supa oil. A full description of how this hydrocarbon was found and separated is given in a paper[*] communicated to the Chemical Society by Dr. Robertson and his collaborators. Their determination of the molecular weight suggested that the substance had 30 carbon atoms. The well-known fact may be recalled here that an accurate measurement of the atomic weight of such a material by the usual methods is a very difficult matter. An error of plus or minus one carbon atom is quite possible.

One of the chief difficulties in the preliminary stages of this work was to obtain sufficiently large and well developed crystals. It was soon realised that the investigator has no real control over the crystallisation process. A large number of trials were made for which the writer is much indebted to Dr. Gilchrist, and finally a few crystals of the substance were obtained from a benzene solution. Two particularly good samples were rhomb-shaped thin flakes. The acute angle between the faces was 65°–66° (the edges were later found to coincide with the (1, 1) direction in the basal plane), the calculated value for this angle being 66° 20′. The flakes were very thin, not more than about 1/10 to 2/10 of a millimetre. The long diagonal of the flake was of the order of 1 millimetre in length Most of the X-ray photographs were obtained from these two samples.

The carbon content of the substance not being definitely settled by chemical analysis, several synthetic hydrocarbons were used for comparison purposes. One of these was taken from the batch which Mr. Saville prepared for a previous investigation. Another batch was synthesised by him using the method described in a previous paper[†] (Senderen's). The first was the $C_{31}H_{64}$, the second the $C_{30}H_{62}$. In order to be safe it seemed advisable to synthesise at least one of these standard substances by an entirely different method. The starting point for the above mentioned $C_{30}H_{62}$ were behenolic and nonoic acid, $CH_3(CH_2)_{20}COOH$ and $CH_3(CH_2)_7COOH$. For the second synthesis it was

[*] 'J. Chem. Soc.,' vol. 312, p. 3077 (1926).

[†] 'J. Chem. Soc.,' vol. 127, p. 599 (1925).

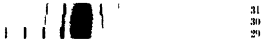

Powder Photographs of C_{31}, C_{30} and Natural Product.

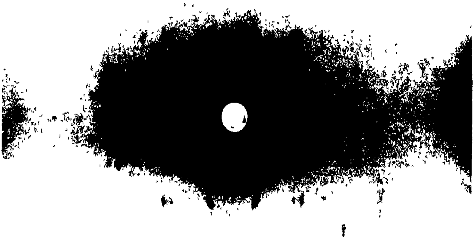

Rotation Photograph about the *a* axis.

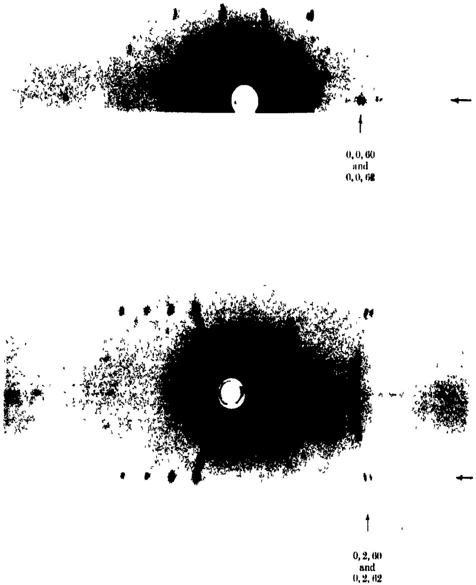

Oscillation Photograph showing high-order Reflections palmitic acid $CH_3(CH_2)_{14}COOH$. This second electrolytic method was carried out on the lines described by Peterson.* The actual work was done by Dr. Gilchrist.

A series of experiments was made in order to test the purity of the $C_{30}H_{62}$. A small distillation apparatus was built in which minute quantities of the substance could be distilled in a vacuum on to a polished metal surface. The various fractions gave within the limits of experimental errors the same melting point and identical X-ray photographs. No differences could be found in the melting points and the X-ray photographs when samples of the differently prepared $C_{30}H_{62}$ were compared.

A series of melting points was then taken for the three substances C_{31}, C_{30} and the natural product, and the long spacings were determined very carefully. The following table gives the numerical data :—

Table I.

M P.	Long spacing.	Difference long spacing.
°	A.U.	
C_{31} 68–69	41·2	1 2
C_{30} 66–67	40·0	1 4
Nat. pr. 64–65	38·6	

(Plates 18, 19 show the long spacing reflections of the three samples.)

The deviation from a constant difference of the long spacings being within the limits of experimental error, it was concluded that the natural hydrocarbon had 29 carbon atoms. This value was used in all the further calculations.

X-ray Technique used in dealing with the Single Crystal.

The crystal was attached to a thin glass fibre with a trace of shellac. The free end of the fibre could then easily be fixed to the goniometer head of an X-ray spectrometer. A series of complete rotation and oscillation photographs was taken with copper rays $\lambda = 1 \cdot 539$ A.U. The diameter of the camera was such as to make 1 millimetre of length (measured on the equator) equal to 2° of arc. Some of these photographs are shown on Plates 18 and 19.

Dimensions of the Cell, Number of Molecules and Space Group.

The following data were obtained for the cell size :—

$$a = 7 \cdot 45 \text{ A.U.}, \qquad b = 4 \cdot 97 \text{ A.U.}, \qquad c = 77 \cdot 2 \text{ A.U.},$$

---

* 'Z. f. El. Chem.,' vol. 12, p. 144 (1906).

the error being of the order of $\frac{1}{2}$ per cent. The cell was found to be a rectangular prism. This point was tested carefully. The crystal was first set with its surface normal to the collimator axis (by optical reflection) and one of the short axes was set parallel to the axis of the spectrometer by means of X-rays. The crystal was then turned until one of the strong reflections appeared on a fluorescent screen and the range of visibility of the reflections read on the spectrometer table, this range being of the order of 1°. This was repeated by turning the crystal face into the symmetric position relative to the direct beam. It was found that the two angles of setting for which reflection occurred were the same. Identical results were found for the second setting of the crystal, which showed that the "*c*" axis was perpendicular to the surface. This important point was further brought into evidence when oscillation photographs were taken Starting from a position in which the crystal surface was normal to the incident beam, it was found that the right and left side photographs were identical. Laue photographs taken with the beam perpendicular to the "*c*" plane showed very few and rather ill-defined spots. All the planes which can reflect with sufficient strength and at moderate angles are not in a reflecting position for this particular setting of the crystal

A density determination using the flotation method gave 0·95. This combined with the known atomic weight gave four molecules to the unit cell.

The crystal was expected to be not less symmetrical than stearic acid, which according to previous investigations belongs to the monoclinic prismatic system. No general halvings were found for the hydrocarbon crystal, but the (h, o, l) reflections were absent when h was odd. No signs of any of the odd orders of the (0, 1, 0) plane could be detected on the photographs. This proved indeed that the crystal had at least monoclinic symmetry. It was further found that not only the (0, 1, 0) plane but all the $(0, k, l)$ planes were halved when $k + l$ was odd (with the exception of the curious phenomenon of the occasional very faint (0, 1, 30) line which is described later). This suggested that the crystal belonged to the orthorhombic system (an inspection of the model given at the end of this paper shows that the crystal belongs to the orthorhombic space group Q_h^{16}).

It is interesting to point out here already that the cross section of the cell is $37 \cdot 0 \times 10^{-16}$ sq. cms. This coincides very nearly with the average of the cross sections found in the previous paper ($36 \cdot 6 \times 10^{-16}$ sq. cms.) and is a fact which was anticipated.

Characteristic Features of the Intensity Distribution.

The chief interest of this paper lies in the interpretation of the very peculiar intensity distribution among the spots observed on the photographs. The general outline of this interpretation has already been given in the previous paper.

A complete survey of the observable spots showed that the indices could all be written in one of the following forms: $(h, k, 0/1)$; $(h, k, 30/31)$; $(h, k, 60/61/62)$ ...; or in other words, unless a reflection belonged to these groups, it was either extremely faint or not observable at all. Here again, just as in the previous case, the connection between these "characteristic l" values and the number of carbon atoms in the chemical molecule is striking.

The Geometrical Structure Factor.

A systematic discussion of these facts can best be done with the aid of the geometrical structure factor. Before proceeding to work out this factor for the crystal we are dealing with here, we shall first discuss the properties of the simplest possible model of a long chain crystal.

This hypothetical crystal is assumed to have only one molecule to the unit cell (axis a, b, c) the molecule itself consisting of "n" identical atoms or scattering centres of scattering power 1. These atoms are placed at equal distances along one axis of the crystal, say, the "c" axis. If "s" is the distance between two successive atoms, and c_0 the co-ordinate of the first atom—this last quantity being expressed as a fraction of the "c" axis—then the co-ordinates of the pth atom are :—

$$x_p = 0\,;\; y_p = 0\,,\; z_p = c_0 \,.\, c + (p-1) \,.\, s.$$

The geometrical structure factor for this single chain is then :—

$$\begin{aligned} S_n &= \left| \sum_{p=1}^{p=n} \exp\left[2\pi i\,(x_p h/a + y_p k/b + z_p \,.\, l/c)\right] \right| \\ &= \left| \sum_{p=1}^{p=n} \exp\left[2\pi i\,\{c_0 + (p-1) \,.\, s/c\} \,.\, l\right] \right| \\ &= \left| \exp\left[\pi i\,\{2c_0 + (n-1) \,.\, s/c\} \,.\, l\right] \,.\, \frac{\sin \pi n \frac{s}{c} \,.\, l}{\sin \pi \frac{s}{c} \,.\, l} \right| \\ &= \left| \frac{\sin \pi n \,.\, \frac{s}{c} \,.\, l}{\sin \pi \frac{s}{c} \,.\, l} \right|. \qquad (1) \end{aligned}$$

The two vertical lines in (1) mean that the absolute values of these expressions have to be taken.

We shall call this particular structure factor the "chain factor" in accordance with the notation in the previous paper.

s/c and "n" being constant for a given arrangement of the crystal, this S_n* is a function of the index "1." This function has the well-known property of oscillating between zero and "n," and shows very sharp maxima provided "n" is large, as we assume it to be in our case. These maximum values of S_n appear when $\frac{s}{c} . l$ is an integer or in the neighbourhood of an integer; "l" can only vary in steps of a unit. We get therefore a very marked increase of the numerical value of our function at constant intervals of "l," but we still do not know how this interval is connected with the number of atoms in the molecule. In order to find this connection we have to settle the size of "s" We now make the further assumption that the molecule stretches right across the cell leaving only a relatively small gap at each end. This gap we take to be of the order of the distance between two consecutive molecules in the chain, that is to say nearly equal to "s." The distance between the centre of the first and the last atom in the chain is $(n - 1) . s$. We therefore assume that $s . n$ is approximately equal to c, or

$$s/c \sim 1/n. \tag{2}$$

The maxima of S_n therefore occur when "l" is equal or near to zero, n, $2n$, $3n$, . . ., *i.e.*, our chain factor is in general accord with the observed intensity distribution.

The very simple model from which these facts can be derived cannot be expected to give more than a general explanation of the observations. First we have to remember that our $C_{29}H_{60}$ crystal has four molecules to the unit cell. The only reasonable assumption which we can make when trying to build up a model of this crystal, is to put two of our long chain molecules end to end alongside the "c" axis. There are therefore 58 atoms in the length of the cell. If therefore we find a maximum when $l = 30$, we conclude that alternate carbon atoms are situated differently. The pattern is repeated, not every atom, but every second atom. This is in accord with the design of the molecule which previous work has already shown to be probable: it is shown in the lower part of fig. 1A. It can be described as consisting of two rows in parallel, their distance apart remaining to be discovered. It is not yet necessary to assume that the rows are so placed with respect to each other as to give the zigzag a perfectly regular form, though the fact will appear presently.

---

* The notation S_n will be used instead of S_c in the previous paper. "n" indicates the number of atoms in the row.

It can easily be seen that no other arrangement of the scattering centres, such as a true spiral, or a double periodic zigzag will give the intensity distribution observed in this particular case. This does not exclude such arrangements being possible under different circumstances.

We now proceed to form the structure factor for the unit cell of the hydrocarbon crystal under investigation. Our previous argument relates only to a single molecule consisting of a zigzag chain of a single type of atom. We have now to take into account first that there are hydrogens as well as carbon atoms, and, secondly, that there are four molecules in the cell. As regards the former point it is convenient and justifiable to link up with each carbon atom the two hydrogens that belong to it, and to assume that the group can be represented by a single scattering centre. If also we neglect one hydrogen at each end of the chain we can suppose the structure to be represented by the zigzag arrangement of centres already discussed, all the centres being now alike.

Experiment shows, as already stated, that all the (h, o, l) planes are halved if h is odd, and that the $(0, 1, 0)$ plane is halved. This implies that we can represent the arrangement of the molecules in the crystal by the following group of co-ordinates .—

$$\left.\begin{array}{ll}
(a) & x_p, \quad y_p, \quad z_p, \\
(b) & x_p + \tfrac{1}{2}, \quad -y_p + \beta_0, \quad z_p; \\
(c) & -x_p + \alpha_0, \quad y_p + \tfrac{1}{2}, \quad -z_p + \gamma_0; \\
(d) & -x_p + \tfrac{1}{2} + \alpha_0, \quad -y_p + \tfrac{1}{2} + \beta_0, -z_p + \gamma_0
\end{array}\right\}. \qquad (3)$$

Were x_p, y_p, z_p are the co-ordinates of the pth scattering centre of the first molecule, and the position of the corresponding centres of the other three molecules represented by (b), (c), (d) respectively. (The symbols all represent fractions of the axes a, b, c : α_0, β_0, γ_0 are parameters yet to be determined.) The second set of co-ordinates (b) represents a molecule obtained by reflecting (a) across a plane parallel to "xz" and afterwards translating it parallel to the "x" axis through a distance $a/2$. The third (c) is obtained by a diagonal rotation about an axis parallel to the "y" axis followed by a translation $b/2$ along that axis. The molecule (d) is centrosymmetrical with (a).

If the axis of "z" is not taken to be perpendicular to the plane of "xy," the supposed arrangement is c_{2h}^5. But if the "z" axis is perpendicular to the plane "xy" and the molecule has symmetry of its own—and it certainly is extremely near to doing so—the additional symmetry given to the cell makes it orthorhombic, the space group being known as Q_h^{16}. For the moment it is not necessary to suppose that the higher condition of symmetry are absolutely fulfilled.

It is further convenient to use two different notations when referring to the two rows of atoms in each molecule. Our molecule has an odd number of scattering centres. We call $n + 1$ the number of atoms in the first row and n the number in the second row, the numbers being therefore 15 and 14 in our case. Remembering that the distances between consecutive atoms are the same for either row, and calling x, y, z the co-ordinates of the first atom in the first row of the first molecule and $\bar{x}$, $\bar{y}$, $\bar{z}$ the corresponding co-ordinates for the second row, we have :—

co-ordinates of the pth atom, 1st molecule, 1st row—

$$x_p = x\,;\ y_p = y\,;\ z_p = z + (p-1)\,.\,s/c \tag{4}$$

co-ordinates of the pth atom, 1st molecule, 2nd row—

$$\bar{x}_p = \bar{x}\,;\ \bar{y}_p = \bar{y}\,;\ \bar{z}_p = \bar{z} + (p-1)\,.\,s/c. \tag{4A}$$

The corresponding values for the three other molecules are obtained by applying the transformations (3) to the above expressions.

The calculation of the structure factor involves a sum over all the scattering points in the unit cell. This operation is done best by splitting it into three parts.

In the first part the sum is taken over the four possible positions (3) leaving the general co-ordinates in the expressions.

In the second part the expressions so obtained are summed over the $n + 1$ atoms of the first row of the molecule.

Lastly, the same operation is performed for the second row of n atoms. The result for the two rows are then added together. Owing to (4) and (4A) these two sums can be written in a fairly compact form.

It is unnecessary to write down here the still rather long expressions for S, which we are able to simplify by making a very plausible assumption with regard to the parameter β_0. We put $\beta_0 = \frac{1}{2} + y + \bar{y}$, *i.e.*, we place the reflection molecule (3B) in the middle of the four surrounding neighbours and choose the most convenient zero for our co-ordinates by making $\overline{y} = -y$. The structure factor can then be written as follows :—

$$\left.\begin{array}{ll} \mathrm{S} = \left| 4a_{\mathrm{CH}_2} . \cos 2\pi yk . \{\mathrm{S}_{n+1} . \cos \pi \mathrm{A} + \mathrm{S}_n . \cos \pi \overline{\mathrm{A}}\} \right| , & h \text{ even} ;\ k \text{ even} \\ \mathrm{S} = \left| 4a_{\mathrm{CH}_2} . \sin 2\pi yk . \{\mathrm{S}_{n+1} . \sin \pi \mathrm{A} - \mathrm{S}_n . \sin \pi \mathrm{A}\} \right| ; & h \text{ even} ,\ k \text{ odd} \\ \mathrm{S} = \left| 4a_{\mathrm{CH}_2} . \sin 2\pi yk . \{\mathrm{S}_{n+1} . \cos \pi \mathrm{A} - \mathrm{S}_n . \cos \pi \mathrm{A}\} \right| , & h \text{ odd} ;\ k \text{ even} \\ \mathrm{S} = \left| 4a_{\mathrm{CH}_2} . \cos 2\pi yk . \{\mathrm{S}_{n+1} . \sin \pi \mathrm{A} + \mathrm{S}_n . \sin \pi \mathrm{A}\} \right| , & h \text{ odd} ;\ k \text{ odd} \end{array}\right\} , \quad (5)$$

where

$$\mathrm{A} = (2x - \alpha_0) . h + (2z - \gamma_0 + n\, s/c) . l$$

$$\overline{\mathrm{A}} = (2\overline{x} - \alpha_0) . h + (2\overline{z} - \gamma_0 + [n - 1]\, s/c) . l$$

$$a_{\mathrm{CH}_2} = \text{scattering weight of the } \mathrm{CH_2}\text{-group.}$$

$$\mathrm{S}_{n+1} = \sin (\pi (n + 1)\, s/c . l)/\sin (\pi\, s/c . l) ;$$

$$\mathrm{S}_n = \sin (\pi n . s/c . l)/\sin (\pi\, s/c . l).$$

Determination of the Constants and Parameters.

Some of the parameters in (5) can now be determined quite easily. First we make use of the fact of the constant differences in the length of the "c" axes of the three substances C_{31}, C_{30} and C_{29}, and secondly of the observation that none of the odd orders of the (0, 0, l) planes show on the photographs.

The first fact suggests that the two rows of atoms in each of our crystal molecules are placed in such a way that each scattering centre in one of the two rows is at equal distance from its two next neighbours on the other row, or

$$\overline{z} = z + s/2c.$$

The structure factor for the (0, 0, l) planes takes then the following simple form

$$\mathrm{S}_{(0,\,0,\,l)} = 4a_{\mathrm{CH}_2} \times \cos \pi\, (2z - \gamma_0 + n . s/c) \quad l \times [\mathrm{S}_{n+1} + \mathrm{S}_n].$$

According to the second observation this expression has to vanish for all the odd orders of l. We therefore must have

$$2z - \gamma_0 + n . s/c = \tfrac{1}{2}.$$

The constants A and $\overline{\mathrm{A}}$ in (6) can accordingly be written in the following form

$$\mathrm{A} = (2x - \alpha_0) . h + \tfrac{1}{2} . l ; \quad \overline{\mathrm{A}} = (2\overline{x} - \alpha_0) . h + \tfrac{1}{2} . l. \qquad (7)$$

These values will be substituted in all the further calculations involving (5).

We can now go one step further and try to get a numerical value for our fundamental constant s/c. The structure factor of the $(0, 0, l)$ planes reduces now to the following expression.

$$S'_{(0,0,l)} = 4a_{CH_2} \cdot \cos\frac{\pi}{2}l \cdot [S_{n+1} + S_n] = 4a_{CH_2} \cdot \cos\frac{\pi}{2}l \cdot \frac{\sin\left(\pi\frac{2n+1}{2}\cdot\frac{s}{c}\cdot l\right)}{\sin\left(\frac{\pi}{2}\cdot\frac{s}{c}\cdot l\right)}. \tag{8}$$

The only unknown constant left is s/c. This suggests the use of intensity measurements in the $(0, 0, l)$ set of planes for a determination of this fundamental constant.

It is well known that the intensity of X-ray reflection from a crystal depends upon many, and very often partly unknown factors. Certain relative measurements can, however, be performed whereby most of these unknown quantities do not enter into the calculations.

The expression for the intensity can be split into two factors.[1] One of these, the geometrical structure factor is a rapidly changing, oscillating function of the three indices h, k, l; whereas the other, also depending upon the indices (temperature factor) or the reflecting angle (polarisation factor, atomic scattering factor) changes slowly compared with the first. If we calculate therefore the intensities of two planes which not only have nearly the same spacing but also nearly the same position in the crystal, we can assume that the slowly varying factor is very nearly the same for the two reflections. The knowledge of the geometrical structure factor will then suffice to calculate the intensity ratio of the two reflections.

The crystal under investigation is in some ways particularly suited for this type of intensity ratio evaluation. One of the cell dimensions being very large compared with the other two, it is possible to get sets of planes, which, without having too small a spacing, differ very little both in spacing and position.

We still have to determine the function which connects the ratio of the two values of the geometrical structure factor, and the observable ratio of the integrated intensities of the two reflections. We know this function in two limiting cases, *i.e.*, for the ideally perfect, and for the ideally imperfect or mosaic crystal.

To which type our crystal belonged had, of course, to be settled by experiment.

Considering the almost complete absence of any tendency of the substance to crystallise, it seemed very unlikely that these hydrocarbon crystals approach the ideally perfect type. When comparing the intensity ratios of certain particularly strong high order reflections on single crystal photographs and on photographs from " powders " of this hydrocarbon, no difference could be found. These powders were, of course, not powders in the ordinary sense, the substance being far too soft to form any sort of fine grain. It was, however, very unlikely that smearing the substance on to a glass surface, and compressing it afterwards into convenient shape should not have had the effect of bringing the mass into the " imperfect crystalline " state

A word may be said here about the identification of the high order reflections which are constantly used in this work.

The reflections of the (o, o, l) planes could be observed right up to the 30th order by using long exposures. Between the 30th and the 60th order was a gap which had to be calculated. The accuracy of the measurements of the long spacing was quite sufficient to give an unequivocal determination of the (0, 0, 60) and (0, 0, 62) reflection. These two reflections were afterwards used as standards for the measurements of their neighbours.

My colleague Mr. W. T Astbury has been so kind as to determine the intensity ratio of the (0, 0, 60) and (0, 0, 62) reflection, using a method developed by him* which gives directly the integrated intensities. As a result of repeated measurements on different photographs this ratio was found to be 1·83 ± 0·036. A small correction was applied to this figure to allow for the variation of the intensity with the angle of reflection, and use was made of Ponte's† F-curves for the scattering of the carbon atom in diamond (the variation of the temperature factor being unknown in this case, the corresponding correction had to be neglected). It was found that·

$$(S_{(0,\,0,\,60)}/S_{(0,\,0,\,62)})^2 = 1\cdot 66.$$

With this numerical value we can now with the aid of (8) calculate our fundamental constant s/c. We know that it must be in the neighbourhood of 1/30. The following table gives a few of the ratios in function of s/c ·—

s/c	0·03284	0·03285	0·03286	0·03287
$(S_{(0,0,60)}/S_{(0,0,62)})^2$	1·42	1·51	1·63	1·74

It is interesting to note that a small variation of s/c produces a comparatively large change in the numerical value of the square of the ratio of the structure factor. In other words, a relatively rough estimate of the intensity ratio is quite sufficient to give an accurate numerical value for our fundamental constant. It has, however, to be borne in mind that in deriving the structure factor we have been assuming that the chain is absolutely uniform. For this we have at the present stage of this work no direct proof. But apart from the discontinuity at the ends of the crystal molecules there is hardly any other factor present which is likely to upset the uniformity of the chain, and this "end effect" is not likely to make itself felt over a big range. The assumption of strict uniformity seems therefore not unreasonable.

---

* 'Roy. Soc. Proc.,' A, vol. 115, p. 640 (1927).

† 'Phil. Mag.,' vol. 3, p. 195 (1927).

If we assume the correction due to the temperature factor to be of the same order of magnitude as the one already applied, we conclude, using the data from Table II that

$$s/c = 0 \cdot 03286 \pm 0 \cdot 00002.$$

For comparison it may be mentioned here that if s/c were calculated under the assumption that the crystal belonged to the ideally perfect type, its numerical value would be approximately 2½ per cent. smaller than the figure given above.

We now proceed to calculate other parameters in our structure factor. It is useful to write our fundamental equation (5) in a slightly different form. Taking for example the first equation and introducing the following abreviations:

$$\alpha = (x + \bar{x} - \alpha_0)\,; \quad \beta = 2\pi y\,; \quad \gamma = \pi(\bar{x} - x),$$

we have

$$\mathrm{S} = 4a_{\mathrm{CH}_2} \,.\, \cos \beta k \,.\, \Big\{ \mathrm{S}_{n+1} \,.\, \cos\Big[(\alpha - \gamma)\, h + \frac{\pi}{2}\, l\Big]$$

$$+ \,\mathrm{S}_n \,.\, \cos\Big[(\alpha + \gamma)\, h + \frac{\pi}{2}\, l\Big]\Big\}$$

or

$$= 4a_{\mathrm{CH}_2} \,.\, \cos \beta k \,.\, \cos\Big(\alpha h + \frac{\pi}{2}\, l\Big) \,.\, \cos \gamma h \,.\, [\mathrm{S}_{n+1} + \mathrm{S}_n]$$

$$\times \Big\{1 + \frac{\mathrm{S}_{n+1} - \mathrm{S}_n}{\mathrm{S}_{n+1} + \mathrm{S}_n} \,.\, \tan\Big(\alpha h + \frac{\pi}{2} l\Big) \,.\, \tan \gamma h\Big\}.$$

This, and the three other corresponding expressions can be written in a more compact form by using the symbols which are introduced in the following table. The numerical data are calculated by using $s/c = 0 \cdot 03286$.

Table III.

l.	S_{15}.	S_{14}.	$\bar{S}$	Δ.
0	+15·0	+14·0	14·5	+0·035
1	+ 9·81	+ 9·63	9·7	+0·009
29	+ 5·45	− 5·95	5·7	−0·043
30	+13·90	−13·11	13·5	+0·029
31	+13·12	−12·47	12·8	+0·025
32	− 4·04	+ 4·74	4·4	−0·080
60	+10·95	+10·65	10·8	+0·014
61	+14·9	+13·9	14·4	+0·035
62	+ 8·35	+ 8·50	8·4	−0·009

$$\bar{S} = \tfrac{1}{2}(|S_{15}| + |S_{14}|); \quad \Delta = (|S_{15}| - |S_{14}|)/(|S_{15}| + |S_{14}|).$$

With the notations of Table III and using the transformations indicated in (9) we can now write our fundamental expressions for the structure factor S in the following form :—

Table IV.

	S/Sa_{CH_2}, $S =$	
	when $l = 0; 1; 60; 61; 62$	when $l = 29; 30; 31$
h even and k even	$\cos\beta k . \cos(ah + \frac{1}{2}\pi l) . \cos\gamma h$ $\times \{1 + \Delta . \tan(ah + \frac{1}{2}\pi l) . \tan\gamma h\}$	$\cos\beta k . \sin(ah + \frac{1}{2}\pi l) . \sin\gamma h$ $\times \{1 + \Delta . \cot(ah + \frac{1}{2}\pi l) . \cot\gamma h\}$
h even and k odd	$\sin\beta k . \cos(ah + \frac{1}{2}\pi l) . \sin\gamma h$ $\times \{1 - \Delta . \tan(ah + \frac{1}{2}\pi l) . \cot\gamma h\}$	$\sin\beta k . \sin(ah + \frac{1}{2}\pi l) . \cos\gamma h$ $\times \{1 - \Delta . \cot(ah + \frac{1}{2}\pi l) . \tan\gamma h\}$
h odd and k even	$\sin\beta k . \sin(ah + \frac{1}{2}\pi l) . \sin\gamma h$ $\times \{1 + \Delta . \cot(ah + \frac{1}{2}\pi l) . \cot\gamma h\}$	$\sin\beta k . \cos(ah + \frac{1}{2}\pi l) . \cos\gamma h$ $\times \{1 + \Delta . \tan(ah + \frac{1}{2}\pi l) . \tan\gamma h\}$
h odd and k odd	$\cos\beta k . \sin(ah + \frac{1}{2}\pi l) . \cos\gamma h$ $\times \{1 - \Delta . \cot(ah + \frac{1}{2}\pi l) . \tan\gamma h\}$	$\cos\beta k . \cos(ah + \frac{1}{2}\pi l) . \sin\gamma h$ $\times \{1 - \Delta . \tan(ah + \frac{1}{2}\pi l) . \cot\gamma h\}$

Δ is small compared with "1." The whole term multiplied with Δ can under certain conditions become small, and will in this case either be neglected or treated as a small correction. We shall use the word "correction term" as an abbreviation for the whole of the second term in the curved bracket in the above expressions.

Calculation of the Remaining Constants and Discussion of Intensities.

With the aid of Table IV we can here already predict the absence or extreme weakness of a certain number of reflections (apart from those whose absence follows from the space group). The indices of these planes are given in the following table:—

Table V.

Indices of planes which according to Table IV ought to be extremely weak or unobservable.	Observations.
(0, 0, 30/31); (0, 1, 1); (0, 1, 60/61/62) (0, 2, 30/31); (0, 3, 1), (0, 3, 60/61/62) (0, 4, 30/31), (0, 5, 1), (0, 5, 60/61/62)	All these planes are either unobservable or very weak compared with their neighbours.

A striking observation which leads to the determination of a further constant is the fact that the (0, 4, 0) reflection is completely absent. The (0, 0, 60) plane whose spacing differs only from the (0, 4, 0) by a small percentage lies almost on the same spot where the (0, 4, 0) reflection ought to appear when the crystal is rotated round the "*a*" axis. The (0, 0, 60) and the (0, 0, 62) reflections show both very strongly even on short exposures, whereas no reflection appears from the (0, 4, 0) plane even when the crystal is oscillated over a small range containing the reflecting position.

In order to make the (0, 4, 0) plane disappear we have according to Table IV to give β a definite value. We must have

$$\cos 4\beta = 0 \text{ or } 4\beta = m \,.\, \pi/2 \quad (m \text{ odd}); \text{ or } \beta = 22\tfrac{1}{2}^\circ,\ 67\tfrac{1}{2}^\circ,\ 112\tfrac{1}{2}^\circ, \text{ etc.}$$

When we introduce any of these numerical values of β in the equations in Table IV we must expect again a whole series of planes to be absent. This is shown by the next table.

Table VI.

Indices of planes which ought to vanish if $\beta = 22\tfrac{1}{2}^\circ \,.\, m$ (m. odd).	Observations.
(0, 4, 0/1), (2, 4, 0/1); (4, 4, 0/1) (see Table V); (2, 4, 30/31), (4, 4, 30/31), (0, 4, 60/61/62), (2, 4, 60/61/62)	All absent on oscillation photographs.

In the form given in Table IV our expressions for the structure factor are relatively easy to handle. We proceed to put the theory to a further test. From Table IV we find:

Table VII.

Theoretical.	Observations.
For all values of "k," $\left(\frac{S_{(0,\,k,\,60)}}{S_{(0,\,k,\,62)}}\right)^2 = \left(\frac{\bar{S}_{(l\,=\,60)}}{\bar{S}_{(l\,=\,62)}}\right)^2 = 1{\cdot}66,$ also for all values of "h" and "k" provided the correction term is small $\left(\frac{S_{(h,\,k,\,60)}}{S_{(h,\,k,\,62)}}\right)^2 \sim \left(\frac{\bar{S}_{(l\,=\,60)}}{\bar{S}_{(l\,=\,62)}}\right)^2 = 1{\cdot}66.$	The following pairs of planes are found to have approximately the same intensity ratio as (0, 0, 60)/(0, 0, 62) · (0, 2, 60)/(0, 2, 62) (2, 2, 60)/(2, 2, 62) (1, 1, 60)/(1, 1, 62) (2, 0, 60)/(2, 0, 62)

On Plate 19 samples of oscillation photographs are reproduced which show two of these "doublets" very clearly. One pair is the (0, 0, 60/62), the other pair on the second photograph is the (0, 2, 60/62).

Mr. Astbury measured also the ratio (2, 0, 60/62) by his method, and found it to be the same as the ratio (0, 0, 60/62). He further found the intensity of the (2, 0, 61) to be between three to four times larger than the (2, 0, 62). This result will now be used for an evaluation of the constant α.

Neglecting the "correction term" which means assuming that neither 2α nor 2γ are very close to zero or 90°, we find from Table IV

$$(S_{(2,\,0,\,61)}/S_{(2,\,0,\,62)})^2 \sim (\bar{S}_{(l=61)}/\bar{S}_{(l=62)})^2 \,.\, \tan^2 2\alpha = 2{\cdot}9_4 \,.\, \tan^2 2\alpha.$$

The left side of this equation is equal to the observed intensity ratio (the small temperature and angle corrections being within the limits of accuracy can be neglected) and is according to observation between 1/3 and 1/4. The calculation gives :—

$$\left.\begin{array}{l}\text{For the ratio } 1/3:\ \alpha = 22\tfrac{1}{2}^\circ \pm m \,.\, 90^\circ \\ \text{For the ratio } 1/4:\ \alpha = 25^\circ \pm m \,.\, 90^\circ\end{array}\right\}\ m = \text{zero or } 1.$$

Thus α is approximately either $23\tfrac{3}{4}^\circ$ or $66\tfrac{1}{4}^\circ$.

The ratio (1, 1, 0)/(1, 1, 1) is according to observation between ½ and ⅓. Again neglecting the "correction term" we find that from Table IV :

$$(S_{(1,\,1,\,0)}/S_{(1,\,1,\,1)})^2 \sim (\bar{S}_{(l=0)}/S_{(l=1)})^2 \,.\, \tan^2\alpha = 2{\cdot}23 \,.\, \tan^2\alpha.$$

For $\alpha = 23\tfrac{3}{4}^\circ$ we get

Intensity ratio (1, 1, 0)/(1, 1, 1) ~ 0·43.

For $\alpha = 66\tfrac{1}{4}^\circ$ we get

Intensity ratio (1, 1, 0)/(1, 1, 1) ~ 11·5.

We therefore assume that $m = 0$ and adopt

$$\alpha = 24^\circ$$

for the following calculations.

So far we have been on relatively safe ground with regard to the determination of our constants. They have been derived from relative intensity measurements, the reflections being chosen from planes which, in each case, differed very little from each other in their spacings and their relative positions in the crystal.

We now go one step further and try to compare the intensities of reflections from planes which are not far apart in their spacings but which may differ widely with regard to their relative positions in the crystal lattice. If we still try to calculate our intensity ratios from the geometrical structure factor alone, we assume that the temperature factor is a function of the spacing, and that the position of the individual reflecting plane does not matter. This would certainly lead to wrong conclusions if any finer details were to be considered. No such attempt will be made in the present paper, and so long as only approximate estimates are made, this neglect of the temperature factor is not likely to be serious.

We now try to find an estimate for the limits between which the last constant γ has to lie. One of the low-index reflections which is strikingly weak compared with its neighbours is the group composed of the (1, 2, 0) and (1, 2, 1) reflections. The average spacing of this group is slightly smaller than the (0, 2, 0) spacing; the intensity of the group is about equal to the intensity of the β line of the (0, 2, 0) reflection, *i.e.*, about 1/6 of (0, 2, 0).

Before calculating γ we have first to settle the definite value for the constant β in the structure factor. The photographs show that the intensity of the (1, 2, 0/1) group is between 1/6 and 1/3 of the (1, 1, 30/31) reflections. The two spacings differ little from each other. We assume therefore that the observed ratio is approximately equal to the square of the calculated ratio of the structure factors.

The value of the observed ratio is obtained from a photograph with the crystal rotated round the "*a*" axis. The reflections appear both on the first layer line. During one revolution of the crystal the following reflections in the (1, 2, 0/1) group appear:

$(1, 2, 0)$; $(1, \bar{2}, 0)$; $(1, 2, 1)$; $(1, 2, \bar{1})$; $(1, \bar{2}, 1)$; $(1, \bar{2}, \bar{1})$.

In the (1, 1, 30/31) group:

$(1, 1, 30)$; $(1, 1, \overline{30})$; $(1, \bar{1}, 30)$; $(1, \bar{1}, \overline{30})$; $(1, 1, 31)$; $(1, 1, \overline{31})$
$(1, \bar{1}, 31)$; $(1, \bar{1}, \overline{31})$.

These reflections have to be taken into account in the calculations. Neglecting again the " correction term " we have ·

$$\left(\frac{S_{(1,\,2,\,0/1)}}{S_{(1,\,1,\,30/31)}}\right)^2 \sim \frac{\sin^2 2\beta\,.\,\sin^2\gamma\,.\,[\tfrac{1}{2}\,.\,\bar{S}^2_{(l=0)}\,.\,\sin^2\alpha + \bar{S}^2_{(l=1)}\,.\,\cos^2\alpha]}{\cos^2\beta\,.\,\sin^2\gamma\,.\,[\bar{S}^2_{(l=30)}\,.\,\cos^2\alpha + \bar{S}^2_{(l=31)}\,.\,\sin^2\alpha]}$$

$$\sim 2{\cdot}16\,.\,\sin^2\beta.$$

From observation we find

$$1/3 > 2{\cdot}16\,.\,\sin^2\beta > 1/6.$$

Only the smallest of the possible values of β on p. 450 satisfies this equation, *i.e.*, we have

$$\beta = 22\tfrac{1}{2}^\circ.$$

The constant γ can now be calculated by making use of the already mentioned ratio of the (1, 2, 0/1) and (0, 2, 0) groups

$$\left(\frac{S_{(1,\,2,\,0/1)}}{S_{(0,\,2,\,0)}}\right)^2 \sim \frac{2\ \ \sin^2 2\beta\,.\,\sin^2\gamma\,.\,[\tfrac{1}{2}\,.\,\bar{S}^2_{(l=0)}\,.\,\sin^2\alpha + S^2_{(l=1)}\,.\,\cos^2\alpha]}{\cos^2 2\beta\,.\,S^2_{(l=0)}}$$

$$1/6 \sim 0{\cdot}91_5\,.\,\sin\gamma \quad \text{or} \quad \gamma \sim 25^\circ.$$

The two following observations lead to two further independent calculations of γ. It is found that the (0, 0, 62) reflection is about as strong as the (2, 0, 61) reflection, shown on rotation photographs with "*a*" and "*b*" settings. This gives

$$\gamma \sim 28^\circ.$$

The (1, 1, 61) reflection is about twice as strong as the (0, 0, 60) on rotation photographs about the "*a*" or "*b*" axis. The resulting value for γ is

$$\gamma \sim 36^\circ.$$

The three values for γ differ considerably from each other. This is not surprising. We can hardly expect to get more than a rough estimate of the cross dimensions of our simple chain molecule at the present stage of this work.

Although we cannot hope to account for all the intensity ratios of the weaker reflections in this part of the investigation, we are nevertheless able to predict the indices of the strongest reflections. Our structure factor can be written in the following form

$$S = |\bar{S}\,.\,\phi_1 + \bar{S}\,.\,\Delta\,.\,\phi_2|.$$

ϕ_1 and ϕ_2 are functions which oscillate between + 1 and − 1, and which depend upon the indices *h*, *k*, *l*. Δ is, as we know from Table III, small compared with $\overline{S}$. If we want to find the strongest reflections we can neglect the second term in the expression above, and have simply to find those values of h, k, l for which ϕ_1 is near to its limits, *i.e.* ± 1. We are then able to test our theory in the following way. Supposing we have found a set of indices for which ϕ_1 is equal or at least near to ± 1. Among all the reflections which have ϕ_1 not equal or near to ± 1 we take those which lie close to the first mentioned reflection. If the theory is correct we should find the intensity of all those reflections smaller than the one for which ϕ_1 is ± 1.

From Table IV we can easily see that the strongest reflections must be found among those in the $l \sim$ zero and $l \sim 60$ group for which $h + k$ is even and small, *i.e.*,

(0, 0, 60); (0, 0, 62); (1, 1, 0/1); (1, 1, 61).

This is in excellent agreement with the observed facts. Owing to the fact that $\beta = \pi/8$ we expect to find (0, 3, 31); (0, 5, 31) and also (1, 4, 30) to be strong. This again is found to be correct. The crystal model of the hydrocarbon which has been built up in this paper seems therefore to be correct at least in its essential features.

Before going on to the discussion of the results, an observation may be mentioned for which no explanation has yet been found.

A slight fogging was noticed between the relatively strong (0, 1, 31) and the faint (0, 1, 29) reflections. The spots being close together, this fog was first thought to be due to overlapping of the two. Special photographs were afterwards taken with a very fine slit. Under these circumstances both the (0, 1, 31) and the (0, 1, 29) reflections appeared as well defined sharp lines on the films. The fog however had not disappeared. The (0, 1, 30) reflection was expected to be absent according to the structure factor, and indeed no trace of it could be found on a whole series of photographs which was taken to test this point. On a certain number of these pictures, however, an extremely faint line could be seen quite distinctly between the (0, 1, 29) and the (0, 1, 31) reflection. The fog was there whether the line appeared or not. The (0, 1, 30) line could only have been found, theoretically, if the crystal molecules showed polarity. In this case the (0, 0, 61) reflection would have appeared as well as the other. No trace of such a reflection or of a fogging was found between the (0, 0, 60) and the (0, 0, 62) line on any of the many photographs which were taken in the course of this work. The only uncontrolled factor which was likely to produce this curious phenomenon was the temperature. This point will have to be cleared in the continuation of this work.

Discussion of the Model.

With the numerical data at hand we are now able to complete the picture of our hydrocarbon crystal. Our constants are:

$$\alpha \sim 24^\circ ; \quad \beta \sim 22\tfrac{1}{2}^\circ ; \quad 36^\circ > \gamma > 25^\circ ,$$

and since

$$\pi (x + \bar{x} - \alpha_0) = \alpha ; \quad 2\pi y = \beta ; \quad \pi (\bar{x} - x) = \gamma ,$$

we find

$$\bar{x} + x - \alpha_0 \sim 1/7 \cdot 5 ; \quad y \sim 1/16 ; \quad 1/5 > \bar{x} - x > 1/7 .$$

It is convenient to introduce two quantities the meaning of which can be seen in fig. 1; w and ϕ can be expressed in terms of $\bar{x} - x$ and y, as follows:

$$w = \sqrt{a^2 (\bar{x} - x)^2 + 4b^2 y^2} , \qquad \tan \phi = 2by / a (\bar{x} - x)$$

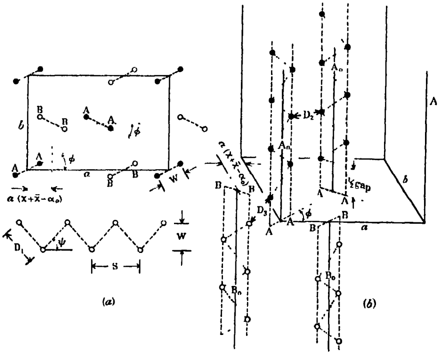

FIG. 1.

Substituting the numerical data

$$a = 7 \cdot 45 ; \quad b = 4 \cdot 97 \text{ Å.U.} ; \quad 1/5 > (\bar{x} - x) > 1/7 ; \quad y \sim 1/16 ,$$

we find

$$1 \cdot 62 > w > 1 \cdot 23 \text{ Å.U.} \qquad 30^\circ > \phi > 23^\circ .$$

We shall further want the distance "s"

$$s/c = 0{\cdot}03286\,; \quad c = 77{\cdot}2 \text{ Å.U.}$$

and

$$s = 2{\cdot}54 \text{ Å U.}$$

Fig. 1 (*a*) which is drawn to scale represents the cross section of the unit cell. A, A, B, B, ... are the projections of the scattering centres upon the plane of the cross section. It is interesting to see that the bulk of the scattering mass is concentrated near parallel lines A_0, A_0, ... B_0 ... (chain axes), fig. 1 (*b*), and that these axes are relatively wide apart.

The following figures will give another illustration of this fact. We compare the distance D_2 of nearest approach of a scattering centre in one chain to a centre in a neighbour molecule, with the distance D_1 of two successive scattering centres in the same chain.

$$D_2 = \sqrt{a^2\,[\tfrac{1}{2} - (\bar{x} - x)]^2 + b^2/4 + s^2/4}$$

$$D_1 = \sqrt{w^2 + s^2/4.}$$

Introducing the figures gives

$$3{\cdot}9 > D_2 > 3{\cdot}6 \text{ Å U.} \qquad 2{\cdot}0 > D_1 > 1{\cdot}8 \text{ Å U.}$$

The distance D_2 of nearest approach is therefore about twice as big as the distance between two successive centres in the zigzag chain. D_2 being of the order of 3·7 Å.U. there is ample space between the chains for even comparatively large molecules. A substitution of hydrogen atoms by other atoms should therefore have little or no effect upon the cell dimensions.

This appears to be true. It is found that the ketone

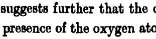

$$\underset{\displaystyle O}{CH_3(CH_2)_{20}C(CH_2)_7CH_3}$$

has, within the limits of experimental error, exactly the same cell dimensions as the hydrocarbon

$$CH_3(CH_2)_{28}CH_3,$$

which has the same number of carbon atoms as the ketone. The fact that certain characteristic intensity ratios are the same on both the ketone and the hydrocarbon photographs suggests further that the continuity of the carbon chain is not broken by the presence of the oxygen atom. There are, of course, certain modifications of the relative intensities in a number of other reflections.

The influence of substituted atoms upon the chain structure opens an interesting field for research and will be the subject of further investigations.

The crystal molecule in our hydrocarbon appears, at least to a first approximation, as a zigzag arrangement of single scattering centres. The angle between the centre lines, fig. 1, is given by

$$\tan \psi = 2w/s,$$

or using the numerical data

$$52^\circ > \psi > 44^\circ.$$

The average of these two angles is about 48°, which is approximately 13° larger than the angle which would be observed if the scattering centres were mutually spaced as are the carbon atoms in diamond. The angle which is found in the chain structure of the centres and which corresponds to the tetrahedral angle in diamond is $180^\circ - 2 \times 48^\circ = 84^\circ$, whereas the tetrahedral angle is 109° 20′. The zigzag angle in our crystal is therefore about 25° smaller than the tetrahedral angle. Suppose that we calculate the distance between two successive centres in a chain which has the same s ($= 2 \cdot 54$ Å.U.), but in which the zigzag angle is equal to the tetrahedral angle. We find for this distance $s/2 \cos 35^\circ 20' = 1 \cdot 55$ Å.U., *i.e.*, almost exactly the diameter of the carbon atom in diamond. This is very significant and suggests that the carbon centres in our crystal form a tetrahedral chain. The distance between the two rows of scattering centres in such a chain is

$$\tfrac{1}{2}s \tan 35^\circ 20' = 0 \cdot 89 \text{ Å.U.},$$

whereas the corresponding average value for our chain is about 1·4 Å U. The two rows of scattering centres in the actually observed chain are therefore about 0·5 Å U further apart than those in the tetrahedral carbon chain. This observation is easily explained if we remember that the scattering centres in our chain represent CH_2-groups. The addition of two hydrogen atoms to each carbon atom would have the effect of shifting the rows of the resulting CH_2-centres further apart.

For the gap between the ends of two successive chains in our crystal (measured in the direction of the "c" axis) we should expect to find something of the same order as the distance of nearest approach D_2. The gap can be calculated as follows

$$\text{gap} = c \,.\, (\tfrac{1}{2} - 14 \,.\, s/c) = 3 \cdot 09 \text{ Å.U.}$$

($14 \,.\, s/c$ is the length of our crystal molecule, measured from between the extreme centres of the chain, and expressed as a fraction of the long axis "c.")

This figure is indeed not very different from $D_2 \sim 3 \cdot 7$ Å.U. Approximately the same figure as D_2 is found for the distance D_3 of nearest approach of two molecules in the " end on " position. Fig. 1B. We have

$$D_3 = \sqrt{(\text{gap})^2 + b^2/4 + a^2([x + \bar{x} - \alpha_0] - [\bar{x} - x])^2}.$$

$x + \bar{x} - \alpha_0$ being very nearly equal to $\bar{x} - x$ in our case, we can neglect the last term under the square root and find

$$D_3 \sim \sqrt{3{\cdot}09^2 + 2{\cdot}486^2} \sim 4 \text{ Å.U.}$$

Considering the two figures $D_2 \sim 3{\cdot}7$ and $D_3 \sim 4{\cdot}0$ Å.U. we may therefore say that the distance of nearest approach of these chain molecules is between 3·7 and 4·0 Å.U.

Summary of the Numerical Data.

(1) Cell of the $C_{29}H_{60}$ crystal :

$a = 7{\cdot}45$ Å.U. ; $b = 4{\cdot}97$ Å.U. ; $c = 77{\cdot}2$ Å.U. (error approx. ½ per cent.) ;

angles between the faces of the unit cell, all 90°.

Area of the base or " cross section "

$$37{\cdot}0 \times 10^{-6} \text{ sq. cms.}$$

Cross section area occupied by one molecule

$$18{\cdot}5 \times 10^{-16} \text{ sq. cms.}$$

(2) Size and position of the molecules :

Distance between two consecutive scattering centres on either row of the crystal molecule—

(*a*) Measured as a fraction of " *c* "

$$s/c = 0{\cdot}03286 \pm 0{\cdot}00002.$$

(*b*) Absolute

$$s = 2{\cdot}537 \text{ Å.U. (error approximately } \tfrac{1}{2} \text{ per cent.).}$$

Distance between two consecutive centres in the chain

$$2{\cdot}0 > D_1 > 1{\cdot}8 \text{ Å.U.}$$

Distance between the two rows in the molecule

$$1{\cdot}6 > w > 1{\cdot}2 \text{ Å.U.}$$

Zigzag angle $(180° - 2\psi)$

$$76° < (180° - 2\psi) < 92°.$$

Angle between the plane of the two rows and the symmetry plane in the crystal

$$23^\circ < \phi < 30^\circ.$$

Gap between the ends of two consecutive molecules in the crystal (measured in the direction of the "*c*" axis)

$$\text{Gap} = 3 \cdot 09 \text{ Å U.}$$

Distance of nearest approach between two centres on two neighbouring molecules (placed sideways)

$$3 \cdot 6 < D_2 < 3 \cdot 9 \text{ Å.U.}$$

Distance of nearest approach between two centres on two neighbouring molecules (placed end to end)

$$D_3 \text{ approximately } 4 \cdot 0 \text{ Å.U.}$$

In conclusion the author wishes to express his sincerest thanks to Sir William Bragg for his friendly and encouraging interest which he has taken in this work. He also wishes to thank all his colleagues for their most valuable help and to the managers of the Royal Institution for the splendid opportunities given to him for carrying out this work at the Davy-Faraday Laboratory.

Steam Tables and Equations, extended by Direct Experiment to 4,000 lb./sq. in. and 400° C.

By Prof. H. L. CALLENDAR, F.R.S.

(Received August 9, 1928.)

Summary of the Original Equations.

The original Steam Tables and Equations published in 1900* represented the first thermodynamically consistent system devised for the tabulation of the properties of water and steam. They were based on direct experimental measurements by the following methods, which were specially devised for the purpose :—

(1) The adiabatic relation between P and T for dry steam, was obtained by direct observation of its changes of temperature in adiabatic expansion and compression over the range 200° to 800° F. with a very sensitive platinum thermometer, thus eliminating a variety of errors to which the old PV method was liable. The results showed the adiabatic equation to be of the simple form,

$$P/T^{13/3} = \text{constant}, \qquad (1)\dagger$$

and proved that the specific heat of steam at zero pressure, denoted by S_0, must be very nearly constant and equal to 0·477, or $13R/3$ over this range, assuming that steam approximated to the ideal state represented by the gas equation $P(V - b) = RT$ at low pressures.

(2) The variation of the specific heat of water was measured over the range 32° to 212° F. by the continuous electric method devised for this purpose, and was found to be consistent above 100° F. with a thermodynamic equation for the total heat h of water at saturation, namely,

$$h = s(t - 32) + vL/(V - v), \qquad (2)\ddagger$$

in which s is the minimum specific heat of water at 100° F., L the latent heat of vaporisation, and V and v the volumes of saturated steam and water at t F.

(3) The specific heat S of steam was measured by a slight modification of the same method at atmospheric pressure and 108° C. and found to be 0·497, which agreed very closely with the value of S_0 required by (1), allowing for

---

* 'Roy. Soc. Proc.,' vol. 67, p. 266 (1900); 'Ency. Brit.,' 1902; 'Phil. Mag.,' vol. 5, p. 48 (1903).

† Verified by Makower at 108° C., 'Phil. Mag.,' vol. 5, p. 226 (1903).

‡ 'Phil. Trans.,' A, vol. 200, p. 147 (1902).

the variation of S with pressure, thus affording independent verification of equation (1).

(4) It followed from (1), by the application of the two laws of thermodynamics that the expression for the total heat H of the vapour must be of the form

$$\mathrm{H} - \mathrm{B} = (13/3)\, a\mathrm{P}\,(\mathrm{V} - b) + ab\mathrm{P}, \tag{3}$$

in which B and b are constants, and a is the factor reducing PV to heat units.

It also followed that the expression for V must be of the general type,

$$\mathrm{V} - b = \mathrm{RT}/a\mathrm{P} - c, \tag{4}$$

in which the defect of volume c, due to molecular coaggregation, must be such that $c\mathrm{P}/\mathrm{T}$ remained constant along any adiabatic, or was some function of $\mathrm{P}/\mathrm{T}^{13/3}$. Accordingly, the first term in the expansion of c in powers of P should be of the form $c_0 = c_1\,(373\cdot1/\mathrm{T})^{10/3}$, where c_1 is the value at 100° C. This was verified by experiments with a differential throttling calorimeter, designed to eliminate errors due to wetness or heat-loss, and the value of c_1 was found to be 26·30 c.c./gm. (0·4213 cu. ft./lb.). It appeared that the second term in the expansion of c was probably of the form $kc^3\,(\mathrm{P}/\mathrm{T})^3$, or that c was a function of the temperature only to the *second* order of small quantities. The first approximation would amply suffice for practical purposes at moderate pressures, or even at high initial pressures with sufficient superheat. It would be useless to attempt a second approximation on these lines without accurate experimental data at very high pressures. Moreover, equation (4) was obviously inconsistent with the universally accepted theory of the critical state, and could not be extended to represent the phenomena in the critical region, unless the existing theory could be disproved by new experimental evidence of a very striking character.

Extension beyond the Critical Point.

The required evidence has now been obtained from three distinct methods of experiment, showing that equations (1), (2) and (3) remain accurate in the critical region without any modification, and that equation (4), when the higher degrees of coaggregation are taken into account, is capable of representing the critical phenomena with much greater accuracy than any equation of the van der Waals type. The first observations suggesting such a possibility were made in verifying the critical temperature at 374° C. (705·2° F.) as determined by Traube and Teichner by the meniscus method in a capillary tube of quartz glass. With improved apparatus on a larger scale, using very pure water free from air, it was observed that the densities of liquid and vapour did *not* become equal at 374° C. when the meniscus vanished, but that a visible difference of density persisted beyond this point, and could be traced nearly up to 380° C. under favourable conditions. The expansion of the liquid could be determined with considerable accuracy by using different quantities of water sealed in tubes of quartz glass, and observing the temperature at which the meniscus just reached the top of the tube. The expansion could also be traced beyond the critical point, though with rapidly diminishing accuracy, by making similar observations on the line of demarcation between liquid and vapour due to difference of density. The volume of the saturated vapour was similarly determined, by using smaller quantities of liquid, and observing the temperature at which the last trace of liquid disappeared. This observation could not be extended beyond the critical point at 374° C., but it was inferred by producing the curve that the densities would become equal and the latent heat would vanish a little above 380° C. Above 374° the liquid and vapour were capable of mixing in all proportions, and appeared to be in somewhat unstable state of equilibrium, which was easily upset by small traces of impurity, such as air or gas, which promoted ebullition and caused rapid mixing.

Density of Water and Steam.

The observed variation of density for water and steam near the critical point is illustrated by the experimental curves shown in the annexed figure, 1. A portion of Amagat's density parabola for CO_2, with a scale of "corresponding" temperatures, is included in the figure to illustrate the procedure for finding the critical density on the orthodox theory. The cardinal feature of this theory, as exemplified in the van der Waals equation, is that the densities become equal and the latent heat vanishes at the critical point, where the meniscus disappears. The observations on CO_2 appear to be the most accurate available for comparison with steam, but all observers have found great difficulty in obtaining stable values of the volume near the critical point by the methods usually employed, in spite of the relatively low critical pressure and temperature of CO_2. The usual practice has been to draw the diameter representing the mean of the densities observed at lower temperatures, and to produce it to the critical temperature to estimate the critical density. A similar method has often been applied to steam by calculating a formula of the Thiesen type to represent the latent heat, on the assumption that it vanishes at the critical point. The volume of the vapour is then obtained from Clapeyron's equation, and the diameter of the corresponding density curve (shown dotted in the figure) is produced to the critical point. The curve thus obtained did not agree at all well with the direct observations, and required an excessively rapid variation for both liquid and vapour in *opposite* directions

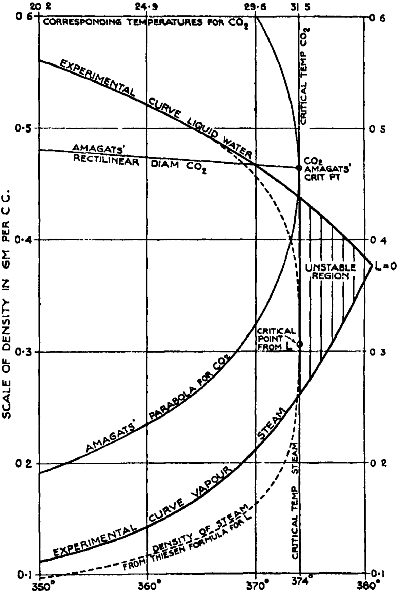

FIG. 1.—Density of Water and Steam, gm./c.c.

at the critical point, where their properties should be approaching identity in all respects.

In the absence of any reasonable explanation of this disagreement with the universally accepted theory, it was impossible to publish the direct observations of the volumes, unless some confirmation could be obtained from measurements of the latent heat, more especially when the very accurate observations of Holborn and Baumann (1910) (on the saturation pressures of steam in a steel cylinder by a static method, with platinum thermometers and a dead-weight gauge) verified the critical temperature at 374° C. by showing that there was no saturation pressure beyond this point, but a continuous change of pressure with volume at constant temperature, thus confirming the orthodox theory of the critical state in the case of steam.

Direct Measurements of the Total Heat of Water and Steam.

The method finally employed for the direct measurement of the total heat of water or steam at any temperature or pressure was devised about this time, but was first employed for verifying the variation of the total heat of water between 0° and 100° C., as determined by the continuous electric method.*

In applying the same method to water and steam at high pressures, the only modification required was the introduction of a throttle between the high-pressure pocket and the condenser to reduce the steam to atmospheric pressure before condensation. This does not alter the total heat to be measured, but makes it possible to employ the same condenser in all cases, whatever the initial temperature or pressure of the steam Unfortunately, the observations were interrupted by the War at an early stage, and remained in abeyance for some years later, until the British Electrical and Allied Industries Research Association became interested in the work and undertook the greater part of the expense involved in the provision of special apparatus and assistance for the completion of the research. The progress of the work, and the evolution of the apparatus employed, has been described and illustrated in various interim reports, published in 'World Power,' May and June, 1924, June, 1925, August and September, 1926, and 'Howard Lectures, Roy. Soc. Arts,' November, 1926. It remains only to summarise the results obtained in the critical region from 2000 to 4000 lb. pressure, which are of primary importance in testing the theory, and in determining the form of the equations required for representing the properties of steam and water over the whole experimental range.

The Importance of using Air-Free Water.

Great pains had been taken in the experiments by the continuous electric method (1902), and in the later experiments (1912) with the jacketed condenser at low pressures, to use only air-free water, since the presence of even 1 in 10,000 by weight of air interfered seriously with the accuracy of the results It was thought that such a small trace of air would be immaterial at high pressures, but the reverse was soon found to be the case. With a steady flow calorimeter capable of reading to 1 in 5000 of the total heat, and subject to a heat-loss of less than 1 per cent., it was possible to keep a continuous check on the purity of the water, and to investigate systematic errors of this kind. Besides greatly increasing the tendency to corrosion at high temperatures, the presence of air appeared to retard the attainment of true equilibrium between the complex molecules at high pressures, exaggerating the errors due to time-lag and nuclear condensation in the neighbourhood of saturation. An automatic apparatus was accordingly installed for supplying the pump with air-free distilled water, and a special form of air-cushion was devised for the experiments on the total heat of water, in which the water was completely protected from contact with the compressed air. In the case of steam this complication was unnecessary, because the steam itself acted as a perfect cushion. But without this device, it was impossible to obtain steady readings of pressure with water, and, if an ordinary air cushion were employed, the air dissolved so rapidly at 3000 lb. that no consistent values of the total heat near saturation could be obtained. Observations taken near the critical point with ordinary distilled water, containing from a tenth to a twentieth of its *volume* of air at atmospheric pressure, afforded a very striking illustration Values found for the total heat near saturation were much too low in the case of steam owing to nuclear condensation, and much too high in the case of water owing to ebullition promoted by the dissolved air. These errors were somewhat irregular, owing to accidental variations in the quantity of air in the water, but when the apparent values of H and h at saturation were plotted against P, as in Amagat's familiar PV − P curve for CO_2, they gave a remarkably good parabola, with its vertex at $H = h = 945$ B.Th.U. (525 cals. C.) at a temperature of 705° F. (374° C.), and appeared to give the most complete confirmation of the orthodox theory that could be desired.

---

* Bakerian Lecture, 'Phil. Trans.,' A, vol. 212, p. 1 (1912).

On the other hand, when air-free water was employed, the observations both of H and h became incredibly more concordant, and gave the entirely different results shown in the annexed H − P diagram, fig. 2, for steam near the critical point. Instead of the familiar condition $H = h$, with $L = 0$, and $V = v$, commonly assumed at the point where the meniscus vanished, namely, 374° C. or 705·2° F., the value found for H was 554·2 cals. C. (997·6, B.Th.U./lb.) and that for h only 481·8 cals. C. (867·3 B.Th.U./lb.), showing a latent heat L = 72·4 cals. C. or 130·3 B.Th.U./lb. Moreover, the saturation lines could be traced for both liquid and vapour up to 380° C. (716° F.),

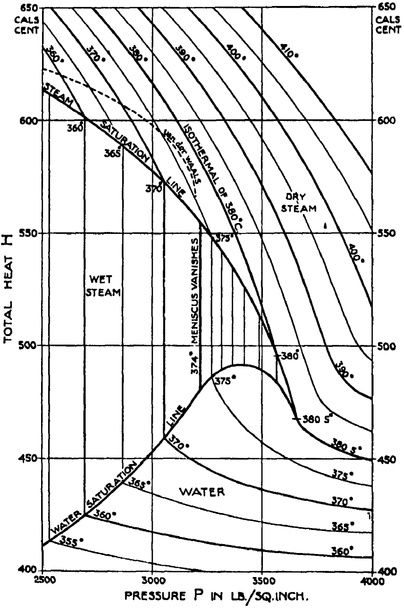

Fig. 2.—H — P Diagram for Steam.

where the latent heat was still appreciable. They appeared to meet at 717° F., where a very good observation was obtained, and the mixture was found to be entirely in the state of water, with all the steam condensed, and a sudden flattening of the isothermal. This is exactly what should happen on the coaggregation theory, but is quite irreconcilable with the van der Waals equation. It was found, in fact, that the observations on the total heat of air-free water showed the most minute agreement in every detail with the old observations on the saturation volumes of water and steam in quartz-glass tubes as illustrated in the previous figure. The water sealed in these tubes had been carefully deprived of air in order to prevent boiling of the liquid and disturbance of the meniscus during heating. The qualitative agreement of the two figures is obvious on inspection, but the quantitative agreement with equation (2) for the liquid is easily verified by reference to Clapeyron's equation, which gives in conjunction with (2) the simple relation,

$$V/v = (H - st)/(h - st). \tag{5}$$

Taking the values of v from the experimental curve for the liquid in fig 1, the values of h could easily be calculated, and were found to agree very closely with the observed values along the saturation line for water, thus verifying equation (2) up to the critical point with remarkable precision. Beyond this point the law changes, owing to the vanishing of the surface tension at 374° C, but equation (5) still appears to hold, and gives values of V, deduced from the observed values of H and h, continuous with the experimental curve for $1/V$ in fig. 1. The values thus found apply to an intimate mixture of water and steam in varying proportions, starting with dry saturated steam at 374° C. and $H = 554$ cals. and finishing with water at 380·5° C.

Extension of the Equations.

The H — P diagram, as shown in fig. 2, could be completed directly from the observations of H and h. More than 100 complete observations were available between the limits 370° to 380° C alone, so that it was comparatively easy to draw the isothermals. This applies particularly to the curves for water below the saturation line, for which no equations were available, except (2) for the saturation line itself. But it was most important from a theoretical standpoint to see whether the observed values of H and V for steam could be represented satisfactorily by equations of the type (3) and (4), consistent with the adiabatic equation (1), and to deduce the corresponding equations for the entropy and the saturation pressure, in order to make the verification complete.

Many attempts had already been made in 1908 to represent the observed values of V near the critical point by using a series for c including the higher degrees of coaggregation. The best and most promising of these was a simple geometrical series with first term c and common ratio Z^2, the sum of the series being represented by the expression $c/(1-Z^2)$, in which $Z = kcP/T$, as required by the adiabatic equation (1). Retaining the original values of c and b, and taking the saturation pressure p from an empirical formula giving $p = 3158$ lb. at 374° C., it was found that the value $k = 2 \cdot 39$ for the constant in the expression for Z gave a very good approximation to the experimental curve for V. This form of equation gave perfect agreement with the adiabatic, and reduced exactly to the original equation for V at low pressures; but there were no experimental values of H available for the verification of equation (3) at high pressures, and equation (4) could not be reconciled with the subsequent observations of Holborn and Baumann on the saturation pressures by a static method.

The case was completely altered when the direct observations of H and h showed that the saturation line for steam extended beyond 374° (as illustrated in fig. 2), and supplied accurate measurements of saturation pressures by a steady flow method affording a continuous check on the purity of the fluid. The values of H could be determined with greater precision than those of V, and extended over a much wider range, from 1000 to 4000 lb., thus permitting a far more exact verification of any proposed formula. Retaining the same value of c as in the original equations, the value of b could be calculated as well as that of k in the expression for Z. Thus, taking the value $H = 554 \cdot 2$ cals at 374° C., and 3222 lb. as observed on the saturation line, the value of k was found to be $2 \cdot 229$ (in place of $2 \cdot 39$ as previously found at 3158 lb.), the value of b being determined from the experimental value of V at this point. There are many alternative methods of procedure, but the above is the easiest to follow.

Substituting for $P(V-b)$ in (3) from (4), the expression for H becomes,

$$H - B = S_0T - (13/3)\,acP/(1-Z^2) + abP, \tag{6}$$

in which the second term on the right represents the latent heat of coaggregation, corresponding to the term $c/(1-Z^2)$ representing the coaggregation volume, which replaces the term c in the original expression (4) for V.

The expression for the entropy Φ is deduced from (4) and (6) by integrating the general relation $d\Phi = dH/T - a\,(V/T)\,dP$. The terms representing the entropy of coaggregation, and replacing the term $(10/3)acP/T$ in the original expression, to which they reduce at low pressures, are as follows:

$$(3/130)\log_e (1+Z)/(1-Z) - (13/3)\,acP/T\,(1-Z^2). \tag{7}$$

In taking the difference $\Phi - H/T$ to find the Gibbs' function G/T, the second of these terms disappears, leaving only the first, which reduces to the form acP/T at low pressures, as in the original equation for G/T.

Equation of Saturation Pressure

This is obtained in the usual way by equating the value of G/T found for the vapour to that similarly obtained for the liquid from equation (2). Using common logarithms and collecting the terms, we thus obtain the numerical formula for the logarithm of the saturation pressure p, on the Centigrade scale,

$$\log p = \text{const.} - 2903\cdot 4/\mathrm{T} - 4\cdot 7174 \log \mathrm{T} \\ + 0\cdot 20956 \log \{(1 + \mathrm{Z})/(1 - \mathrm{Z})\} + 0\cdot 001138\, p/\mathrm{T}, \quad (8)$$

in which the constant is found from the standard value $p = 760$ mm. at 100° C. This equation is easily solved by trial and interpolation, taking the experimental values of p as a first approximation in the small terms. But the values found at each point agreed so closely with the experimental values that a second approximation was seldom required. Equation (8) also agreed within 0·3° C. on the average over the whole range from 0° to 374° C. with the observations of Henning and of Holborn and Baumann, though it would not have been surprising if the steady flow method had shown larger systematic differences from their static methods The closeness of this agreement affords independent confirmation of the whole system of equations based on the adiabatic (1), because all the coefficients in (8) are obtained from direct observations of H, h, and V, and are not deduced from the saturation pressures themselves.

Thus the value of the first coefficient in (8) is deduced from the experimental value of the latent heat at 100° C., and remains unaltered since none of the fundamental constants has been changed. The coefficient of log T in the next term represents $(s - \mathrm{S}_0)/\mathrm{R}$, and is also the same as in the original equation for p. The next term represents the effect of the coaggregation on the value of G/T for the vapour, and the last term represents the effect of the small constant b. The value of b could not be determined experimentally in the original equations, because it was so small as compared with V at low pressures. It was therefore estimated on the lines of the van der Waals theory, in which it plays a very important part. It has now been determined in accordance with equation (4) from the observed value of V, namely, 3·79 c.c./gm. at 374° C., and found to be only $-0\cdot 175$ c.c./gm., which is much smaller than the value

1 c.c./gm. originally assumed. It could also be determined from equation (8) by assuming p to be 3222 lb. at 374° C., but this gave the same value. The exact theoretical interpretation of this constant remains doubtful, and is of little importance in the coaggregation theory, but it was most satisfactory to find that the old experimental values of V agreed so well with the new equation of saturation pressure based on observations of H and h.

It would not have been very surprising if equation (8) had failed to represent the saturation pressures observed beyond 374° C. It was found, however, that the agreement with experiment continued up to 380·5° C, at which point the saturation line became tangential to the isothermal and the equation automatically ceased to give any further solution for p at higher temperatures. The somewhat abrupt flattening of the isothermal of 380·5° C. beyond this point, indicating that all the single molecules of the type H_2O are condensed, and that the mixture has acquired the properties of water, was verified by measurements of h at higher pressures. But since water, according to equation (2), contains its own volume of steam, this is the most natural way in which the conditions, $H = h$, $V = v$, and $L = 0$ can be satisfied. The complete interpretation of these equations raises many other points of interest, which must be reserved for some future occasion. Many other substances, when sufficiently stable and capable of adequate purification, show similar phenomena, but the difficulties of accurate measurement are very great, and such cases are beyond the scope of this paper. There are many possible modes of coaggregation, and it is doubtful whether an equally simple form of adiabatic would apply to other substances.

The van der Waals Equation.

To compare the results with an equation of the van der Waals type, an equation for P as a cubic function of $1/V$ has been constructed in such a way as to be consistent with the adiabatic (1). If $P(V - b)/T$ is constant along any adiabatic as in (4), it follows, by dividing it by $P/T^{13/3}$ that $(V - b)T^{10/3}$ will also be constant. Thus the adiabatic condition will be satisfied by equating $P(V - b)/T$ to any function of $(V - b)T^{10/3}$, as in the following example,

$$P(V - b)/RT = 1 - c/(V - b) + c^2/3(V - b)^2, \qquad (9)$$

provided that c varies as $1/T^{10/3}$. This makes P a cubic function of $1/(V - b)$, and gives a critical point of the usual type defined by the conditions, $V - b = c = RT/3P$. If the critical pressure is 3200 lb. at 374° C., the value of c at the critical point differs little from that given by (4), and the values of H and V show a rough agreement with those of the vapour. But no equation of the van der Waals type is capable of representing the properties of the *liquid* satisfactorily, as assumed in the van der Waals theory, and (9) gives hopeless results for the saturation pressure if Maxwell's theorem is assumed. When, however, (9) is combined with equation (2) for the liquid, it gives the saturation line shown dotted in fig. 2. The agreement with observation could be improved by taking a higher value such as 3400 for the critical pressure, and a lower value such as 2·5 for the index of T in the expression for c. But this would upset the agreement with the adiabatic, and the equation would in any case be most inconvenient for practical calculations. It could never show the many coincidences in points of detail which appear to follow with such effortless precision from the coaggregation theory.

The H — P diagram is employed in these comparisons, in preference to the H — Φ diagram, which is more familiar to engineers, for the following reasons:—(1) All the temperature and pressure lines run together near the critical point on the H — Φ diagram so that no detail can be shown in this region; (2) the H — P diagram, on the other hand, permits the observed quantities H, P, and t to be very easily and clearly plotted; (3) the entropy Φ cannot be observed directly but is merely calculated from H and V; (4) in virtue of equation (3), the H — P diagram shows a very close correspondence with the PV — P diagram employed by Amagat and other observers in this region, and facilitates comparison with their observations and with the van der Waals theory.

Practical Applications.

The chief interest of these results for steam engineers is that the properties of steam can be represented by comparatively simple equations which are exactly consistent with the adiabatic equation (1), even at the critical point, which had previously been considered to be impossible according to the universally accepted theory of the critical state. It follows that the formulæ previously given for the adiabatic heat-drop, and for the discharge through a nozzle, which are so important in the theory of the turbine, can be applied with confidence in all cases for dry steam; and that equation (3), giving a most useful expression for V in terms of H and P at any point, is equally valid. All these relations are considerably simplified in practice by the discovery that the small constant b is actually more than five times smaller than was previously supposed, so that it may safely be neglected in almost all cases.

Since equation (4) satisfies the condition that $P(V - b)/T$ is constant along any adiabatic, equation (1) may be put in either of the equivalent forms,

$$(V - b)\,T^{10/3} = \text{const}: \quad \text{or} \quad P\,(V - b)^{1\cdot 3} = \text{const}, \tag{10}$$

which remain valid and are useful for many purposes.

The verification of equations (2) and (5) for water and wet steam up to and beyond the critical point confirms all the previous expressions for wet steam, including those for the entropy of water and the Gibbs' function G, as well as those for the volume in terms of H and p, and for the reheat factor.

One of the chief experimental difficulties found in dealing with steam at high pressures near saturation was the comparative sluggishness of the complex molecules in reaching a state of equilibrium. Steam when rapidly heated up to a given temperature and pressure showed lower values of H than when rapidly cooled to same point. These effects were accentuated by the presence of impurities, such as air, and great pains were taken to avoid them. The results now published represent *equilibrium* states, as nearly as possible, and are applicable to initial states in which the steam is maintained at a steady temperature for a sufficient time. It appears that, in very rapid expansion from a high superheat, the more complex molecules included in the series $c/(1 - Z^2)$ would have no time to form. The Enlarged Steam Tables (1924) were designed for the case of rapid expansion, and are probably more accurate for this purpose than the new extension, though they would not apply satisfactorily to initial states.

Extended Tables for the equilibrium states of steam up to 4000 lb. pressure have been calculated on the basis of the new expression for the coaggregation, and have been forwarded to the British Electrical and Allied Industries Research Association, as being the body primarily interested in the research, and mainly responsible for its successful completion.

A special debt of gratitude is due to the members of the Committee on the Properties of Steam for their support and encouragement in the face of difficulties which appeared at first insurmountable. I have also to thank the Governors of the Imperial College for providing accommodation and workshop facilities, with free use of all the valuable apparatus in the Physics Department. Many essential parts of the apparatus were constructed entirely in the Physics workshop, and owe much to the experience of the superintendent, Mr. W. J. Colebrook, and the skill of the assistant, Mr. E. White, who constructed the electric boilers and most of the accessories. My thanks are due to Dr. H. Moss for assistance in some of the intricate calculations, and to my son, G. S. Callendar, who acted as research assistant throughout the investigation, and acquired an almost uncanny facility in running the apparatus without a hitch, and in reproducing any desired conditions.

The Structure of Thin Films. Part XII.—*Cholesterol and its Effect in Admixture with other Substances.*

By N. K. Adam and G. Jessop.

(Communicated by J. B. Leathes, F.R.S.—Received June 20, 1928.)

In 1923, Leathes* showed that cholesterol, when mixed with certain fatty acids in monomolecular films on water or dilute hydrochloric acid, caused a diminution of the area occupied by the fatty acids. Under conditions when the acid, if present alone in the film, would be an expanded film, in the presence of fairly small amounts of cholesterol, the film was found to have the area of a condensed film.

This paper gives a further analysis of this action of cholesterol. The only means which appear available for attack on the problem, are (*a*) the examination of mixtures of cholesterol with suitable substances forming expanded films, measuring the degree to which the area is reduced by various proportions of cholesterol; (*b*) the comparison of the action of cholesterol with that of other substances which might be expected to have a similar effect.

Advance along these lines is rather slow, and the cause of the phenomenon is not yet fully ascertained; but publication at the present stage seems desirable, as many data have been accumulated, and a partial analysis of the problem accomplished.

The conclusion is that there is probably no special attraction between the cholesterol molecules and the fatty acids; but that the cholesterol molecules are large enough, and have sufficient inertia, to obstruct the tilting motions of the fatty acid molecules mechanically. These tilting motions are probably the cause of the expanded state.

The constitution of cholesterol is partially known: Windaus† gives it as—

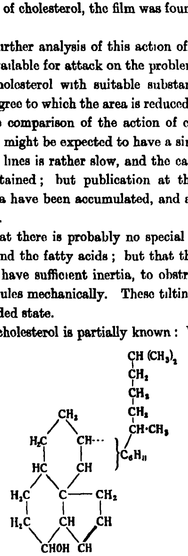

---

* 'Physiol. Soc. Proc.,' November, 1923. † 'Z. f. Physiol. Chem.,' vol. 130, p. 113 (1923).

Films of Cholesterol and Simple Derivatives.

Cholesterol forms a stable film, liquid at room temperature, of area 39 sq. Å. at no compression (*fig.* 1, right-hand curve). The films remain condensed up to 80°. Cholesteryl formate and acetate form films indistinguishable from cholesterol, and also remain condensed up to 80°.

The palmitate and benzoate do not form stable films. These facts show unmistakably that the molecule is held to the water by the adhesion of the hydroxyl group, which is spoiled by the presence of the bulky palmityl and benzoyl groups. The acetyl and formyl groups do not, in other cases where the attachment is by the hydroxyl group, very seriously impair the attachment to the water, but bulky groups such as palmityl and benzoyl have been found to render films unstable, when the attachment is by hydroxyl or carboxyl.

It is also clear that the complex ring system is oriented perpendicular to the water, or nearly so. There are two rings (with two common carbons) next the water, and probably two rings above these. Since the area of one benzene ring, standing perpendicular to the water, is 24 sq. Å., 39 sq Å. is about right for the condensed double ring. But the four rings tilted over at any considerable angle would require much more space.

Further, there is an exceptionally strong lateral attraction between adjacent molecules, the greater part of which must be due to adhesion between the complex ring systems of adjacent molecules. This is shown by the persistence of the condensed state up to high temperatures; even with the acetate, no expansion takes place up to 85°. Eicosyl acetate expands at about 49°; the acetate of the straight chain alcohol series which would expand at 85° would be that of the alcohol with about 25 carbon atoms. Probably the side chain of cholesterol has only eight carbons; hence the adhesion between the ring systems of adjacent molecules in cholesterol seems to be not less than that between closely packed straight chains of 17 carbons, and is possibly much greater than this.

Cholesterol Mixed in Liquid Expanded Films.

Fig. 1 shows the curves relating the area of myristic acid (on N/50 HCl at 15°) in films containing various proportions of cholesterol. The ratios are of the number of molecules of each, myristic being the first figure; the areas are found by subtracting the area of the cholesterol present, assuming it to be the same as in the pure state, from the whole film, and dividing by the number of molecules of myristic acid present. The assumption that the cholesterol occupies the same area as in the pure film of that substance, is probably unobjectionable, since the molecule cannot occupy less area than it does in the

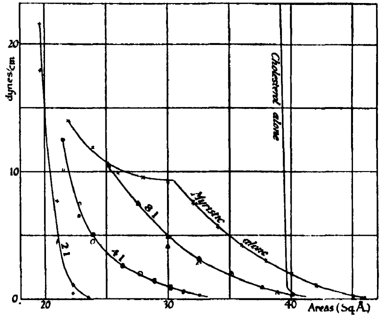

FIG. 1.—Cholesterol-Myristic Acid Mixtures.

(condensed) film of the pure substance, and the alteration of area in the mixture is simply a contraction.

The myristic acid alone is an expanded film below 9 dynes per centimetre. Even one molecule in eight of cholesterol causes appreciable contraction of the film, while with one in two, the acid is completely reduced to the state of a condensed film.

Nearly identical results, qualitatively and quantitatively, were obtained with palmitic nitrile, and dodecyl alcohol, in place of the myristic acid. These substances are all within about 10° of their expansion temperatures, below which they form condensed films. Lauric acid, which has an expansion temperature some 28° below room temperature, was also condensed to some extent, but less than myristic acid. The 4 : 1 mixture with lauric acid gave a curve practically identical with the 8 : 1 with myristic; the 2 : 1 curve of lauric resembled the 4 : 1 of myristic.

Oleic acid, which is a coherent liquid expanded film of quite small surface vapour pressure, but expands at about − 30°, is still less condensed, the 1 : 1 mixture being far from completely condensed. Fig. 2 shows that there is nevertheless some action.

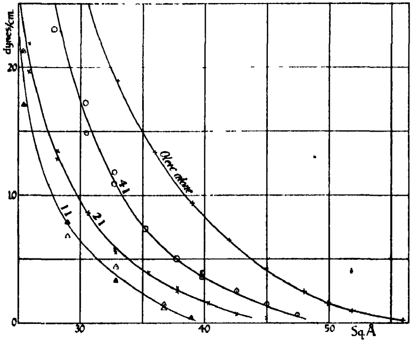

FIG. 2.—Cholesterol-Oleic Acid.

Nonyl phenol (fig. 3) was exceptionally strongly condensed, although the expansion temperature is about $-11°$. The 16 : 1 mixture shows decided condensation: even the 32 : 1 mixture shows a trace of contraction, although

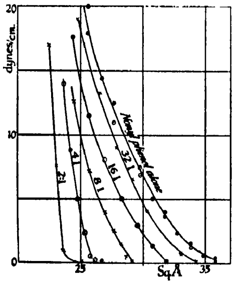

FIG. 3.—Cholesterol-Nonyl Phenol.

this may be within the experimental error. Corroborative evidence that the molecules of the nonyl phenol are brought together in much the same way as in a condensed film, is afforded by the elastic after-working, strongly shown in the 2 : 1 mixture, and slightly in the 4 : 1 mixture.

In both these mixtures, the complete response to sudden compression and de-compression was delayed by several minutes; this was a striking feature of the films of dodecyl phenol (Part X).*

Cholesteryl formate and acetate have an almost exactly similar effect to cholesterol: the mixtures tried were the formate with nonyl phenol and palmitic nitrile; the acetate with myristic acid, dodecyl alcohol and tetradecyl alcohol (at 32°), and palmitic nitrile.

Cholesterol and Vapour Expanded Films.

With ethyl palmitate (fig. 4) there is some condensing action in the 1 : 1 mixtures, but with two molecules of ethyl palmitate to one of cholesterol,

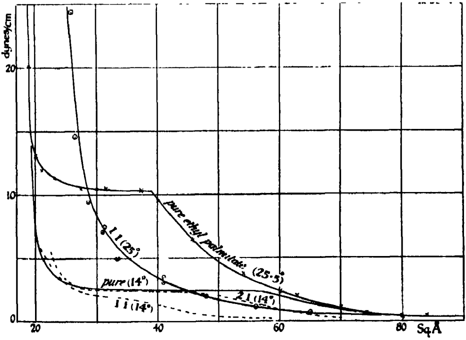

FIG. 4.—Cholesterol–Ethyl Palmitate.

there is a barely detectable contraction. Similar results were obtained with other esters, including the acetates of cetyl and octadecyl alcohols. The action was in all cases very much less than with the liquid expanded films. In some cases the acetate and formate of cholesterol had a slightly greater condensing action than cholesterol itself, but this was not invariably observed. There is no doubt that a sharp distinction must be drawn between the action of cholesterol on the liquid expanded, and the vapour expanded films. It will be seen later than other condensing substances (*e.g.*, tripalmitin) have a much more marked effect on a vapour expanded film than cholesterol.

---

* 'Roy. Soc. Proc.,' A, vol. 117, p. 532 (1928).

Discussion.

The structure of the expanded films needs to be remembered; it is probably an aggregate of tilted molecules, in rapid motion through a variety of angles of tilt. In the liquid expanded films, there is sufficient cohesion to keep the molecules together as a coherent film; in the vapour expanded films there is not; and there is some evidence that the greater attraction between the molecules in the liquid expanded state resides largely in the end groups nearest the water. These points have been brought forward in earlier papers, and must be regarded not as finally proved, but as the most probable theory at the present time.

The cholesterol may act in either of two ways: (*a*) by exerting a special attraction on the smaller molecules; (*b*) by impeding mechanically the thermal motions which cause the molecules to tilt over to form the expanded state. Molecules of great size and inertia may well form obstacles in the film sufficient to damp the thermal motions considerably, so that a higher temperature will be necessary to cause expansion. And if there is a strong lateral adhesion between any cholesterol molecules in contact, the size of the obstacles may be increased and the restraining effect on expansion also increased.

The suggestion (*a*) may be tested directly. If there is a special attraction between the cholesterol and the smaller molecules, this should appear in a restraint of the tendency of these molecules to escape outwards from the coherent film along the surface. This is measured by the "surface vapour pressure" exerted by the coherent film in equilibrium with a gaseous film (Part VII).* We should expect that, in the absence of any specific attraction between the cholesterol and the smaller molecules, the surface vapour pressure would be reduced in the proportion of the cholesterol molecules present, just as the three dimensional vapour pressure of solutions obeys Raoult's Law in the absence of special attractions. The surface vapour pressure can be measured with an accuracy of about 0·02 dyne per centimetre with the sensitive apparatus, and the following table shows that in no case does the observed depression of surface vapour pressure exceed the theoretical by more than the experimental error. It was ascertained that the cholesterol and other large molecules employed had a negligible surface vapour pressure.

---

* 'Roy. Soc. Proc.,' A, vol. 110, p. 426 (1926).

Mixture.	Vapour pressure of pure film of smaller molecules, dyne per cm.	Approximate depression.	Theoretical depression (Raoult's Law).
Cholesterol and myristic acid. 1 : 2	0·18	0·05*	0·06
Cholesterol and ethyl palmitate. 1 : 2	ca. 0·2*	0·04*	0·07
Cholesteryl acetate and myristic acid. 1 : 4	0·18	0·025	0·036
Cholesteryl formate and palmitonitrile. 1 : 2	0·14	ca. 0·05	0·047
Behenic acid and myristic acid. 1 : 2	0·18	negligible	0·06
Bromostearic acid and myristic acid. 1 : 4	0·18	0·05	0·036
Octadecyl phenol and myristic acid. 1 : 2	0·18	0·01	0·06

* These substances have not strictly a "vapour pressure," as the pressure is not constant anywhere. Over a large region of areas, however, the slope is so small that the depression caused by the admixture can be measured fairly accurately.

The evidence thus indicates that the cholesterol does not exert a specific attraction on the smaller molecules sufficient to restrain their translatory motions along the surface to a serious extent. It is therefore *unlikely that there is a special attraction binding the smaller molecules to the cholesterol, large enough to reduce their thermal motions and tendency to tilt within the film.*

Cholesterol is a strongly condensed film, and if there were no special adhesion between the cholesterol molecules and the smaller ones, there might be a general effect due to the strong general adhesion of the cholesterol molecules. In that case, other strongly condensed films ought to show the effect to a greater or less degree. Behenic acid and octadecyl phenol, in 1 : 1 mixtures, do not, however, have a detectable condensing effect on myristic acid. Hence the condensing effect on cholesterol is not due to a strong *general* attraction round the molecule.

The possible explanation (*a*) has therefore no evidence in support. The explanation (*b*) that the great size and inertia of the cholesterol molecule obstructs the tilting motions of the smaller molecules, receives some support from the fact that the effect of cholesterol can be imitated by other large molecules.

Condensing Effect of other Large Molecules.

Tripalmitin, in 1 : 1 and 2 : 1 mixtures, gives wholly condensed films of myristic acid. As the mixtures are made weaker in tripalmitin, the effect falls off more rapidly than with cholesterol, the 4 1 mixture being about as much condensed as the 8 1 mixture with cholesterol With palmitic nitrile, tripalmitin has about the same effect as cholesterol A few experiments with tristearin gave similar results

Penta erythritol tetrapalmitate (Part VI)* has four chains which are oriented upwards in the film, and are bound together at the base near the water The film is fairly stable and has an area about 100 sq Å at no compression This has an effect on myristic acid intermediate between that of cholesterol and tripalmitin, and practically the same effect as these substances on palmitic nitrile

With nonyl phenol however tripalmitin has no condensing effect and pentaerythritol tetrapalmitate a very slight effect only This substance was condensed more strongly than any other by cholesterol

These large molecules occupy a greater area on the surface than cholesterol, but they are much less compact, the three or four long chains being free to vibrate and bend individually and only connected at the base A possible explanation of the absence of condensing action on nonyl phenol is that, in the expanded films of nonyl phenol, the molecules stand with the benzene rings more or less upright and only the long chains tilted The long chain in nonyl phenol would, in this case begin some 6 Å above the base of the other molecules, at a point where these large molecules are probably quite flexible Cholesterol, with its ring system which has two stories of rings one above the other would be quite rigid at this height This view is little more than speculation at present however

Monomyristin (Part X)* is a liquid expanded film of 70 sq Å U at no compression The head of the molecule consists of three carbons with oxygen atoms attached to each, there is every opportunity for the head of the molecule to lie flat on the surface in the expanded film of this substance, and possibly that is the reason why the area of this expanded film is unusually large, it was found in Part XI that the benzene derivatives in which there was a tendency for the benzene head of the molecule to lie flat on the water, had an unusually large area in the expanded state We should therefore expect that penta erythritol tetrapalmitate and tripalmitin will condense this film to some extent Fig 5 shows that there is a considerable condensing action in the 2 1 mixtures cholesterol has a greater effect than the other two molecules, producing complete condensation above 10 dynes per centimetre The 4 : 1 mixtures also show some condensation

---

* 'Roy Soc Proc,' A, vol 106, p 707 (1924)

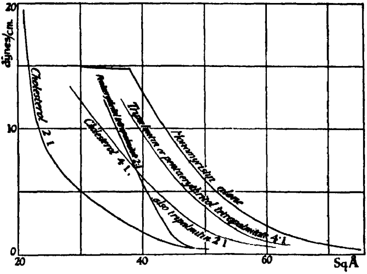

FIG. 5.—Monomyristic Mixtures.

Vapour Expanded Films and Tripalmitin, etc.

Ethyl palmitate is much more strongly condensed by tripalmitin and pentaerythritol tetrapalmitate, than by cholesterol. Fig. 6, which may be com-

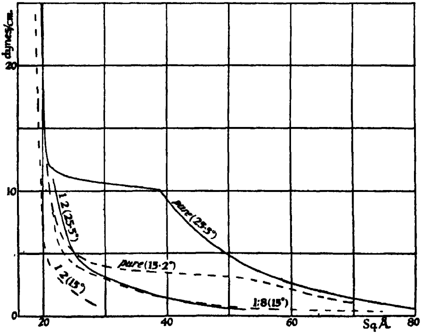

FIG. 6.—Ethyl Palmitate and Tripalmitin or Pentaerythritol Tetrapalmitate.

pared with fig 4 shows that at 15° (some 3° above the expansion temperature the 8 1 mixtures are more condensed than the 2 1 mixtures with cholesterol) while the 2 1 mixtures are completely condensed

A full explanation cannot be given of these differences without much more data on vapour expanded films The explanation may possibly be found in the fact that the molecules of tripalmitin and pentaerythritol tetrapalmitate are extremely rigid near the base and it is probably just at the base where the molecules of ethyl palmitate require most restraint or support in order to keep them in the condensed state The liquid expanded films seem to have more mutual attraction at the base than the vapour expanded films A fuller investigation of the condensation of the vapour expanded films by large molecules must be left for the future

Summary

Cholesterol and some simple derivatives form condensed surface films of area 39 sq Å The ring systems are probably closely packed and adhere very strongly to each other

Mixed with substances which form liquid expanded films in concentrations one molecule of cholesterol to two of the smaller molecules the expanded films are reduced in area completely to the state of condensed films provided the temperature is not too high Even in one to eight molecular concentrations there is appreciable condensation

Since the cholesterol does not produce an abnormal lowering of the surface vapour pressure there is probably no special attraction between the cholesterol molecules and the smaller molecules Since the condensing effect of cholesterol can be imitated by other large molecules such as tripalmitin and pentaerythritol tetrapalmitate it is probable that the condensation is due to mechanical obstruction of the tilting oscillations of the smaller molecules by the bulky and massive large molecules these tilting oscillations are probably the cause of the expanded state

There are minor differences between the action of different large molecules on films of different smaller molecules which are probably due to the varying degrees of rigidity of the large and small molecules at different distances from the anchoring and group at the base of the molecules Vapour expanded films behave somewhat differently from liquid expanded in the cases examined cholesterol does not condense the vapour expanded films to more than a small extent but tripalmitin and pentaerythritol tetrapalmitate do so fairly strongly

The "Action" of an Electromagnetic Field.

By S. R. Milner, D.Sc., F.R.S., Professor of Physics, The University, Sheffield.

(Received June 7, 1928.)

Variation Principles in Dynamics and in the Electromagnetic Field.—In the dynamics of a material system the name "action" is given to two different quantities. One of these is

$$S = \sum_r \int_{q'_r}^{q''_r} p_r \, dq_r = \sum_r \int_{t'}^{t''} p_r \dot{q}_r \, dt, \tag{1}$$

q_r, p_r being the co-ordinate and momentum associated with the rth degree of freedom, and the integral being extended from one definite set of values of the q_r's, to another. The other is

$$A = \int_{t'}^{t''} \Big(\sum_r p_r \dot{q}_r - H \Big) dt, \tag{2}$$

where H (except in special circumstances) is in conservative systems the total energy, and the integral is taken between two definite times t' and t''. Corresponding to S and to A, there are two distinct principles of "least action." Among the group of imaginary systems produced by varying the p_r and q_r under specified conditions in each case, on the one hand the S and on the other the A, of the "natural" system which obeys the laws of dynamics, possesses an extreme value. Thus

$$\delta S = 0 \tag{3}$$

subject to

$$\delta H = 0, \qquad \delta q'_r = 0, \qquad \delta q''_r = 0$$

(Maupertuis' or Euler's Principle), and

$$\delta A = 0 \tag{4}$$

subject to

$$\delta t' = 0, \qquad \delta t'' = 0, \qquad \delta q'_r = 0, \qquad \delta q''_r = 0.$$

(Hamilton's Principle.)

The first deduction of a corresponding stationary principle for the electromagnetic field was made in 1900 by Sir Joseph Larmor,* who showed that the integral of the difference between the magnetic and electric energy densities, extended over all space free from charges and between two definite times, possesses a stationary property analogous to some extent to equation (4). Larmor's demonstration of the principle

---

* 'Aether and Matter,' p. 82, Camb. Univ. Press (1900).

$$\delta \int_{t}^{t'} \int \tfrac{1}{2} (h^2 - e^2)\, dV\, dt = 0 \tag{5}$$

consisted in proving that if the one half of Maxwell's equations*

$$\dot{\mathbf{e}} = \operatorname{curl} \mathbf{h}, \qquad \operatorname{div} \mathbf{e} = 0 \tag{6A}$$

be assumed, essentially as a definition of e, then the other half

$$\dot{\mathbf{h}} = -\operatorname{curl} \mathbf{e}, \qquad \operatorname{div} \mathbf{h} = 0 \tag{6B}$$

is deducible directly from (5).† Larmor assumed that the magnetic energy of the field was equivalent to the kinetic energy T, and the electric to the potential energy U, of a mechanical medium in motion, so that (5) became identical with the old classical form of Hamilton's principle ,

$$\delta \int_{t}^{t'} (\mathrm{T} - \mathrm{U})\, dt = 0. \tag{7}$$

As a result of this and subsequent work, $\mathfrak{A}$, where

$$\mathfrak{A} = \iint \tfrac{1}{2} (h^2 - e^2)\, dV\, dt \tag{8}$$

extended over a definite region of space-time, is now usually called the " action " of this region of the field, and $\mathfrak{L}$, where

$$\mathfrak{L} = \int \tfrac{1}{2} (h^2 - e^2)\, dV, \tag{9}$$

its Lagrangian function.

There does not appear to be a sound justification for the assumption that (8) and (9) are the correct electromagnetic equivalents of the action and of the Lagrangian function of a mechanical system. The idea that magnetic energy can be fully identified with kinetic energy has been long abandoned, as a result of all attempts to formulate completely a theory of the field as a moving medium on the lines of classical mechanics having come to grief in one respect or another. On modern dynamical theory we may note that there is another reason why the assumed identification is not possible. (7) is an *approximate* form of Hamilton's principle, valid only in classical mechanics, in which masses are assumed constant; in the mechanics of the special relativity theory it is not true, the correct form being (4). The identifications which are called for are in any case not those of $\frac{1}{2}h^2$ with kinetic, and $\frac{1}{2}e^2$ with potential, energy densities. It appears, moreover, that, except in the special case in which e and h are perpendicular to each other, an identification of the integrands of (8) and (2) is not possible.

---

* Heaviside units are used with $c = 1$ throughout this paper.

† In four-dimensional theory it is preferable to invert this procedure and take (6B) as the equation of definition, since (6B) is a purely geometrical consequence of the existence of a four-potential. (6A) is then deducible from the principle. The independent variables are now the components ϕ_i of the four-potential, and the integration in (5) may be extended over any definite region of space-time subject to $\delta\phi_i = 0$ at the boundary of the region. *Cf.* W. Pauli, 'Relativitätstheorie,' p. 642 (Teubner, 1921).

It is, however, possible to derive the functions of e and h which correspond strictly with the definitions (1) and (2) in the mechanical system. To do this and to show that the electromagnetic actions so obtained satisfy variation principles which are the exact equivalents of the mechanical ones (3) and (4), is the object of the present communication.

Hamiltonian Action of the Field.—Writing (2) in vector form

$$\mathrm{A} = \int_{t'}^{t''} \Big(\sum_{n} \mathbf{g}\mathbf{v} - \mathrm{H}\Big)\, dt, \tag{10}$$

where $\mathbf{g}$ is the momentum of one of the n particles, $\mathbf{v}$ its velocity, and we take H as the total energy of the system, we see that if we can localise the momentum and energy in the instantaneous space field,* we can also localise the action in flat space-time by postulating that each element $d\mathrm{V}\,dt$ of space-time contains the action

$$d\mathrm{A} = (\mathbf{G}\mathbf{v} - \mathrm{W})\, d\mathrm{V}\, dt \tag{11}$$

where $\mathbf{G}$ and W are the momentum and energy space-densities at the element. Now Hamiltonian action is invariant to Lorentz transformations. Consequently if a transformation is made such that the transformed $\mathbf{G}$ is zero over the infinitesimal region $d\mathrm{V}\,dt$ (11) may be written

$$d\mathrm{A} = \mp \mathrm{W}_0\, d\mathrm{V}_0\, dt_0, \tag{12}$$

where the suffix indicates the "rest" or "proper" values of the variables which would be seen by an observer to whom the element $d\mathrm{V}_0$ appears to contain no momentum. An element of action can be defined by this equation in the same way in the dynamical and in the electromagnetic case. Apart from sign* it appears as the proper energy—Δw_0, associated with a particle, or $W_0\, dV_0$ with a space element—extended over a proper time dt_0.

---

* This cannot ordinarily be done in the applications of the principle of least action made in dynamics, because the potential energy that usually has to be introduced is an artificial concept which cannot be localised; the conditions are, however, satisfied for an electromagnetic field.

To express it in the electromagnetic field, we have, using the ordinary formula for energy density

$$dA = \mp \tfrac{1}{2}(e_0^2 + h_0^2)\, dV_0\, dt_0 \tag{13}$$

where e_0, h_0 are the values of e and h when the field at the point is transformed to zero momentum. They are therefore parallel. (13) gives, on re-writing it so that the content of each bracket is an invariant,

$$\begin{aligned} dA &= \mp \tfrac{1}{2}\{(e_0^2 - h_0^2)^2 + 4(e_0 h_0)^2\}^{\frac{1}{2}}(dV_0\, dt_0) \\ &= \mp \tfrac{1}{2}\{(e^2 - h^2)^2 + 4(\mathbf{eh})^2\}^{\frac{1}{2}} d\,V\, dt. \end{aligned} \tag{14}$$

We may conclude that the coefficient of the differentials in (14) expresses the space-time density of the Hamiltonian action of the field in regions which are free from charge.

Canonical Form of the Laws of Motion of Field Elements.—In the ordinary form of the electromagnetic equations e and h are conceived as quantities which vary with the time *at a fixed point* in the observer's space. It is evident from the presence of v in (11) that the attribution of *action* to the field requires that another view can be taken, in which e and h are conceived as being *in motion* in the observer's space. These views are not inconsistent with each other, as I have proved in a previous paper.† In this section it is proposed to show that the so-called "mechanical relations" derived from Maxwell's equations can be transformed into equations which express the laws of motion of elements of the field in Hamilton's canonical form.

In a region which does not contain electric charges the electromagnetic mechanical relations are completely expressed by the tensor equation

$$\frac{\partial S^{ik}}{\partial x_i} = 0. \tag{15}$$

Here i, k stand for the numbers 1, 2, 3, 4 representing x, y, z, t, and in accordance with the usual convention a summation over all four numbers is understood when the same index occurs twice in one term. S^{ik} represents any contravariant component of the "energy-stress-momentum" tensor, given by the following scheme:

---

* The two signs are the result of the fact that the velocity of transformation (which is found to be identical with v) has two possible values, one less and one greater than the velocity of light. $Gv - W$ is negative if $v < c$, and positive if $v > c$. In relativity theory action is considered as being an entity filling a region of space-time, so that it should be essentially a positive quantity when observed along a real time axis ($v < c$). The fact that it is actually negative in these conditions is merely a matter of the definition, inherited from classical theory, of action density as $Gv - W$ instead of as the positive quantity $W - Gv$.

† 'Roy. Soc. Proc.,' A, vol. 114, p. 23 (1927).

$$S^{ik} = \left.\begin{array}{c|cccc} {}_{i\downarrow}\overset{k}{\rightarrow} & 1 & 2 & 3 & 4 \\ \hline 1 & \Pi_{xx} & \Pi_{yx} & \Pi_{zx} & G_x \\ 2 & \Pi_{xy} & \Pi_{yy} & \Pi_{zy} & G_y \\ 3 & \Pi_{xz} & \Pi_{yz} & \Pi_{zz} & G_z \\ 4 & G_x & G_y & G_z & W \end{array}\right\}. \qquad (16)$$

In (16) Π_{xx}, , are the components of Maxwell's stress system Π, G_x, .. , those of the momentum density G, and W is the energy density. In terms of e and h,

$$\left.\begin{aligned} \Pi_{xx} &= \tfrac{1}{2}(e^2+h^2) - e_x^2 - h_x^2 \\ &\quad . \quad . \quad . \quad . \\ \Pi_{xy} &= \Pi_{yx} = -(e_x e_y + h_x h_y) \\ &\quad . \quad . \quad . \quad . \\ G_x &= e_y h_z - e_z h_y, \quad W = \tfrac{1}{2}(e^2+h^2) \\ &\quad . \quad . \quad . \quad . \end{aligned}\right\}. \qquad (17)$$

In the equations developing (15) further we must separate the terms involving space and time. It makes a great simplification to retain the tensor notation (including the summation convention) for the x, y, z components; thus Maxwell's stress will be written Π_{ik} $(i, k = 1, 2, 3)$, etc. (15) then resolves into the two equations (18) which state (A) that the rate of increase of the momentum in a fixed unit volume is given by the resultant force on that volume due to Maxwell's stress, and (B) that the rate of increase of the energy in the volume is measured by the convergence there of the momentum density, which, when $c = 1$, is the same as Poynting's energy flux:

$$\left.\begin{aligned} \frac{\partial G_k}{\partial t} &= -\frac{\partial \Pi_{ik}}{\partial x_i} & & \text{(A)} \\ & & (i, k = 1, 2, 3) & \\ \frac{\partial W}{\partial t} &= -\frac{\partial G_i}{\partial x_i} & & \text{(B)} \end{aligned}\right\}. \qquad (18)$$

Consider now two quantities v_i and P_{ik}, defined by the equations

$$\left.\begin{aligned} P_{ik} + v_i G_k &= \Pi_{ik} \quad \text{(A)} \\ v_k P_{ik} + v_i W &= G_i \quad \text{(B)} \end{aligned}\right\}. \qquad (19)$$

The extent to which their *values* are determined by (19) will be considered later. At present we are concerned only with their physical meaning and their substitution in (18) which gives:

$$\left.\begin{aligned}\frac{\partial G_k}{\partial t}+\frac{\partial}{\partial x_i}(v_iG_k)&=-\frac{\partial P_{ik}}{\partial x_i} \qquad \text{(A)}\\ \frac{\partial W}{\partial t}+\frac{\partial}{\partial x_i}(v_iW)&=-\frac{\partial}{\partial x_i}(v_kP_{ik}) \qquad \text{(B)}\end{aligned}\right\}. \qquad (20)$$

Equations (20) are identical in form with the mechanical equations for an ordinary material medium moving at each point with the velocity v_i and subject to a system of internal stress P_{ik}.

The electromagnetic field, however, obviously is not an ordinary material medium, and it is necessary to enquire what is the precise meaning of the statement that it can be considered to be in motion. Consider a region of space surrounded by a closed boundary. If there are electrons in it we shall imagine each surrounded by an "internal" boundary, as near the charge as we please; the space between these internal and external boundaries is then the region V under consideration. At a given instant let V be divided into an infinite number n of "space elements" $dx\,dy\,dz$ (written shortly $d\mathrm{V}$) by planes perpendicular to x, y, z; and by "field element" let us mean not only a space element, but in addition that part of the electromagnetic field which is included in the space element. The term motion of the field can only have a useful meaning if (1) these elements possess features by which they can be identified as having moved to other places at a later time, and (2) if the time-alterations of the field are expressible in terms of the changes in position, size, shape, orientation, and velocity which the elements undergo. We shall assume, deferring till later the verification, that these conditions can be satisfied if the v_i given by (19) represents the velocity of a field element at each of its points.

If now we write

$$g_k = G_k d\mathrm{V}, \qquad w = W d\mathrm{V} \qquad (21)$$

for the k-momentum and the energy of any moving element $dx\,dy\,dz$, and if d/dt stands for the time rate of change of a property of a given element as it moves, we have, by purely kinematical considerations based on the interpretation of v_i,

$$\frac{dG_k}{dt}=\frac{\partial G_k}{\partial t}+v_i\frac{\partial G_k}{\partial x_i}, \qquad \frac{d}{dt}(d\mathrm{V})=\frac{\partial v_i}{\partial x_i}\,d\mathrm{V},$$

whence

$$\frac{dg_k}{dt}=\left\{\frac{\partial G_k}{\partial t}+\frac{\partial}{\partial x_i}(v_iG_k)\right\}d\mathrm{V},$$

with a similar equation for dw/dt. Hence (20) may be written

$$\left.\begin{aligned} \frac{dg_k}{dt} &= -\frac{\partial}{\partial x_i}(\mathrm{P}_{ik})\,d\mathrm{V}, \\ \frac{dw}{dt} &= -\frac{\partial}{\partial x_i}(v_k \mathrm{P}_{ik})\,d\mathrm{V}. \end{aligned}\right\} \tag{22}$$

The right-hand sides of (22) represent respectively the k-resultant force and activity of a stress system P_{ik} acting on and moving with the element $d\mathrm{V}$. These are respectively equal to the time rate of increase of the element's k-momentum and energy.

From the two equations of (22) we deduce

$$\begin{aligned} \frac{dw}{dt} - v_k \frac{dg_k}{dt} &= \left\{ -\frac{\partial}{\partial x_i}(v_k \mathrm{P}_{ik}) + v_k \frac{\partial}{\partial x_i}(\mathrm{P}_{ik}) \right\} d\mathrm{V} \\ &= -\mathrm{P}_{ik}\frac{\partial v_k}{\partial x_i}\,d\mathrm{V}; \end{aligned}$$

and since by our assumption

$$v_k = \frac{dx_k}{dt}, \tag{23}$$

we get, multiplying throughout by dt,

$$dw = v_k\,dg_k - \mathrm{P}_{ik}\frac{\partial}{\partial x_i}(dx_k)\,.\,d\mathrm{V}, \tag{24}$$

dw here is the alteration of energy which the element $d\mathrm{V}$ actually undergoes with the lapse of an infinitesimal time. We now assume that this is but one of a class of conceivable alterations δw, which would be the results of displacements δx_k, and alterations of momentum, δg_k, given to the element. The δx_k thus defined are not, however, entirely arbitrary displacements, since they must be supposed subject to the condition that there is to be continuity between adjacent elements, after, as well as before, a displacement.

Writing

$$\mathrm{H} = \sum_n w \tag{25}$$

for the total energy of the field in V, this condition will clearly be satisfied if in the variation

$$\delta\mathrm{H} = \sum_n v_k\,\delta g_k - \int \mathrm{P}_{ik}\frac{\partial}{\partial x_i}(\delta x_k)\,.\,d\mathrm{V}, \tag{26}$$

the summation being over the total number of elements, and the integration over all the region V. The integral, when expressed more fully by writing $dx_1\,dx_2\,dx_3$ for $d\mathrm{V}$, splits up into three triple integrals, such as

$$\int_{x'_2}^{x''_2}\int_{x'_3}^{x''_3} dx_2\,dx_3 \int_{x'_1}^{x''_1} \mathrm{P}_{1k}\frac{\partial \delta x_k}{\partial x_1}\,dx_1,$$

in which the integrations are taken along the lines of elements parallel to x_1, x_2, x_3 respectively. These can be integrated by parts giving for the whole

$$-\iiint \frac{\partial}{\partial x_i}(\mathrm{P}_{ik})\,\delta x_k\,dx_1\,dx_2\,dx_3 + \iint\Big[\mathrm{P}_{1k}\,\delta x_k\Big]_{x'_1}^{x''_1} dx_2\,dx_3$$

$$+ \iint\Big[\mathrm{P}_{2k}\,\delta x_k\Big]_{x'_2}^{x''_2} dx_1\,dx_3 + \iint\Big[\mathrm{P}_{3k}\,\delta x_k\Big]_{x'_3}^{x''_3} dx_1\,dx_2.$$

The square brackets here indicate the difference of the values of the expressions, taken at the two ends, *e.g.*, x''_1 and x'_1, formed by the boundary A, of the line of elements parallel to x_1. In the further integrations $dx_2\,dx_3$ is an element of the boundary surface at the ends of this line, and may be called $d\mathrm{A}_1$, etc. We may thus, putting $dx_1\,dx_2\,dx_3/dx_i \equiv d\mathrm{A}_i$, so as to include the three boundary terms in one by the summation convention, express (26) in the form

$$\delta\mathrm{H} = \sum_n v_k\,\delta g_k + \int \frac{\partial}{\partial x_i}(\mathrm{P}_{ik})\,\delta x_k\,d\mathrm{V} - \iint\Big[\mathrm{P}_{ik}\,\delta x_k\Big]_{x'_i}^{x''_i} d\mathrm{A}_i.$$

The last term here represents the total work done by the stress P_{ik} in the variation at the boundary. In consequence of (22) and (23) we have, replacing the first integral by a summation over the elements,

$$\delta\mathrm{H} = \sum_n \dot{x}_k\,\delta g_k - \sum_n \dot{g}_k\,\delta x_k - \iint\Big[\mathrm{P}_{ik}\,\delta x_k\Big]_{x'_i}^{x''_i} d\mathrm{A}_i. \qquad (27)$$

The energy of the field in V is thus seen to be a function of two sets of variables, the positions x_k and the momenta g_k of the individual elements. For an element in the interior

$$\frac{\partial\mathrm{H}}{\partial g_k} = x_k, \qquad \frac{\partial\mathrm{H}}{\partial x_k} = -\dot{g}_k, \qquad (28\text{A})$$

while for one at the surface the second of these becomes

$$\frac{\partial\mathrm{H}}{\partial x_k} = -\dot{g}_k + \mathrm{P}'_{ik}\,d\mathrm{A}_i \quad \text{or} \quad -\dot{g}_k - \mathrm{P}''_{ik}\,d\mathrm{A}_i, \qquad (28\text{B})$$

according to whether the element is at the beginning x'_i or the end x''_i of the x_i line.

Since (27) is of Hamilton's canonical form we may conclude that all the theorems of mechanics applicable to a moving fluid subject to a stress, hold, when properly interpreted, for the electromagnetic field moving with the velocity v_k.

Principle of Least Action in the Field.—Consider now a "natural" change in the field which takes place between two instants t' and t'', fixed for a given observer. We have assumed that in it the time variations of e and h at each point can be envisaged as due to the motion of identifiable field elements along certain paths and with certain velocities from their positions at t' to those at t''. These paths and motions will be subject to the conditions (28). The time variation of the boundary A, if this is not at infinity, will have to be considered in this connection. It will in general have to change in position in order that the same elements shall be enclosed by it throughout the interval. It should be observed that the change will include that due to the motion of charges present in the field; these will be represented by corresponding displacements of the "internal" boundaries which closely surround the charges. Having defined a natural change, we are in a position to imagine the change between t' and t'' to take place in other ways, by the elements traversing paths and having velocities infinitesimally different by δx_k and $\delta \dot{x}_k$ from the natural ones. In any such variation, if L stands for the quantity

$$\mathrm{L} = \sum_n g_k x_k - \mathrm{H}, \tag{29}$$

we shall have by (27)

$$\begin{aligned} \delta\mathrm{L} &= \sum_n g_k\, \delta \dot{x}_k + \sum_n g_k\, \delta x_k + \iint \Big[\mathrm{P}_{ik}\, \delta x_k \Big]_{x'_i}^{x''_i} d\mathrm{A}_i \\ &= \sum_n \frac{d}{dt}(g_k\, \delta x_k) + \iint \Big[\mathrm{P}_{ik}\, \delta x_k \Big]_{x'_i}^{x''_i} d\mathrm{A}_i, \end{aligned} \tag{30}$$

and consequently

$$\int_{t'}^{t''} \delta\mathrm{L}\, dt = \sum_n \Big[g_k\, \delta x_k \Big]_{t'}^{t''} + \int_{t'}^{t''} \iint \Big[\mathrm{P}_{ik}\, \delta x_k \Big]_{x'_i}^{x''_i} d\mathrm{A}_i\, dt.$$

If we suppose that the time is not varied, the δ on the left-hand side can be taken outside the integral sign, if, further, the variations in x_k vanish in the initial and final states the Σ term disappears, if finally they also vanish at the boundaries,* the last term is zero, and we get, subject to these conditions, the variational equation

$$\delta \int_{t'}^{t''} \mathrm{L}\, dt = 0 \tag{31}$$

---

* This restriction appears formally as though it excluded variations in the paths of electrons present, since electrons have been excluded from the region V by the "internal" boundaries. The assumption of internal boundaries, however, was only made for simplicity, and is not strictly necessary. If the singularities of the field which form the charges have a vanishing volume, for example, if an electron is supposed to be a charged infinitely thin disc, these internal boundaries enclose zero volume and can be dispensed with. A variation of the path of an electron produces a corresponding variation of the elements of the whole (resultant e, h) field, to which the action principle of course applies. If, on the other hand, the electron is supposed to be a singularity of the Lorentz kind, for example a charged spheroid, a finite region, which varies with the electron's path and velocity, has to be excluded from V by the internal boundary. In this case we have to take account of the

satisfied for the electromagnetic quantity defined by (29). This is identically Hamilton's principle.

Electromagnetic Values of v and L.—The value of L depends on that of v, and the latter is obtainable from (19), by eliminating P_{ik} from the two equations, in terms of the electromagnetic quantities G, W and Π_{ik}. We get

$$v_k\Pi_{ik} - v_i v_k G_k + v_i W - G_i = 0 \tag{32}$$

which gives three equations for v_i, one for each value of i. The simplest way of solving these is to take at the point considered axes parallel to the three principal directions of Maxwell's stress. These may be obtained as follows: If two vectors **p** and **q** are defined by the equations

$$\left.\begin{aligned} \mathbf{p} &= \mathbf{e}\cos\alpha + \mathbf{h}\sin\alpha \\ \mathbf{q} &= -\mathbf{e}\sin\alpha + \mathbf{h}\cos\alpha \end{aligned}\right\}, \tag{33A}$$

where α is the smallest positive angle* satisfying the equation

$$\alpha = \tfrac{1}{2}\tan^{-1}\frac{2\,(\mathbf{eh})}{e^2 - h^2}, \tag{33B}$$

then **p**, **q**, and their vector product [**pq**] are mutually perpendicular and lie along the principal axes of the stress system Π_{ik} at each point.

The use of this special system of axes produces great simplifications for the present purpose. Henceforward up to p. 497 x, y, z will be understood to mean

---

"internal" energy of the Lorentz electron, which it is well known has to be assumed present in the space enclosed by the charge, in order that the dynamical scheme may be consistent. The total energy H′ of the region V must consequently be written as

$$H' = H + \Sigma w_e,$$

where H is the previous value given by (25) and Σw_e is the internal energy of all the electrons. The corresponding Lagrangian function is

$$L' = L - \Sigma w_e.$$

When the position or shape of an electron alters, the internal energy by the principle of conservation must be supposed to alter in amount by the work done on the surface (*i.e.*, on the corresponding internal boundary of V) by the stress P_{ik}. The additional term $-\Sigma\,\delta w_e$ of $\delta L'$ then cancels with the term

$$+\int\Big[P_{ik}\,\delta x_k\Big]_{x_i}^{x'_i} dA_i$$

of (30) so far as this represents the work done by the stress on the variation of the internal boundaries surrounding the electrons. Consequently, the principle (31) when applied to cases which include variations in the paths of electrons of the Lorentz type still remains valid, if the L of (29) is replaced by the L′ defined above.

* This stipulation is necessary to fix uniquely the directions of **p** and **q**. The use of the next larger value of α satisfying (33B) interchanges the defining equations of **p** and **q**.

components parallel to p, q *and* [pq] *respectively* at the point of the field considered.

It can then readily be shown from (17) that

$$\left.\begin{aligned} -\Pi_{xx} &= +\Pi_{yy} = \tfrac{1}{2}(p^2 - q^2) \\ \Pi_{zz} &= \tfrac{1}{2}(p^2 + q^2) = \mathrm{W}, \quad \Pi_{ik} = 0 \ (i \neq k) \\ \mathrm{G}_x &= \mathrm{G}_y = 0, \quad \mathrm{G}_z = pq = \mathrm{G} \end{aligned}\right\}. \tag{34}$$

Substituting these values in (32) for $i = x, y, z$ respectively we get, after a little reduction,

$$v_x(q^2 - v_z pq) = 0,$$

$$v_y(p^2 - v_z pq) = 0,$$

$$v_z^2 - v_z \frac{p^2 + q^2}{pq} + 1 = 0,$$

as the equations determining the components of v.

They are satisfied by two values of v,

either

$$\left.\begin{aligned} &v_x = \text{arbitrary}, \quad v_y = 0, \qquad\quad v_z = q/p, \quad (\text{A}) \\ \text{or}\quad &v_x = 0, \qquad\quad v_y = \text{arbitrary}, \quad v_z = p/q. \quad (\text{B}) \end{aligned}\right\}. \tag{35}$$

To fix ideas, we shall suppose in the following that $p > q$, so that solution (A) represents a value of v_z less than 1, *i.e.*, than the velocity of light, and (B) a value greater than 1.

Although both values of v are to a certain extent arbitrary, by reason of their x- (or y-) components, the value of the Lagrangian function is quite definite. (29) may be written, after replacing the summation by an integral over the region V,

$$\mathrm{L} = \int (\mathrm{G}_k v_k - \mathrm{W})\, d\mathrm{V},$$

and since the x- and y- components of G are zero, $\mathrm{G}_k v_k$ is the same as $\mathrm{G}v_z$, whatever v_x and v_y may be. On using the values of G, v_z and W from (34) and (35), we get

$$\mathrm{L} = \mp \int \tfrac{1}{2}(p^2 - q^2)\, d\mathrm{V}, \tag{36}$$

the upper or lower sign being taken according as v_z is given the smaller or the greater of its two values.

L may be expressed in terms of e and h by using (33). The equation (31) expressing the variational principle then becomes

$$\delta \int_{t'}^{t''} \int \mp \tfrac{1}{2}\{(e^2 - h^2)^2 + 4(eh)^2\}^{\frac{1}{2}}\, d\mathrm{V}\, dt = 0, \tag{37}$$

under the conditions (1) that the space integral is extended over a region V which comprises the same individual elements throughout the interval, (2) that t' and t'' and the initial and final configurations of the field elements, and the boundaries of V are not varied. The integrand of (37) is the same as the expression for the action density deduced on p. 486 in another way.

Correlation of Displacement Variations with Changes of the Field Vectors.—In the variation principle (31) or (37) δ refers to infinitesimal changes in the positions x_k and velocities x_k of each point of the field. In order that the variation may represent a comprehensible process, x_k and x_k have to be understood also as expressing the positions and motions of the centres of individual and permanent field elements, and, when this is done x_k and g_k, the positions and momenta of the elements, form an equivalent set of variables. Again, for the variation theorem to have any useful meaning the variations symbolised by δ must be correlated with recognisable changes of the field variables e and h, or preferably for the present purpose, with those of p and q, which are directly connected with e and h.

Consider a variation as it affects a single element. For such we have from (26) by omitting the summations

$$\delta w = v_k \delta g_k - \mathrm{P}_{ik} \frac{\partial \delta x_k}{\partial x_i} \, dx \, dy \, dz, \tag{38}$$

the x_k being here regarded, as just explained, as the k-co-ordinate of the position of the centre of the element. This equation states generally the relation which must exist between the variations in the energy, momentum and position of an individual element in order that the action of the whole field shall be stationary.

As before we take special axes along the principal directions of Maxwell's stress at the point, and we suppose that the element is initially rectilinear with dx, dy, dz, parallel to these axes. Further, consider only the case where the motion is given by the solution (35A) in which $v_z < 1$. The corresponding value of P_{ik} is obtained by substituting this value of v in (19). We thus get the following values of the variables for the element in question:

$$\left.\begin{aligned} w &= \tfrac{1}{2}(p^2 + q^2) \, dx \, dy \, dz, \\ g_x &= g_y = 0, \qquad g_z = pq \, dx \, dy \, dz, \\ -\mathrm{P}_{xx} &= +\mathrm{P}_{yy} = +\mathrm{P}_{zz} = \tfrac{1}{2}(p^2 - q^2), \\ \mathrm{P}_{zx} &= -\mathrm{G}_z v_x. \end{aligned}\right\} . \tag{38A}$$

It will be observed that P_{zx} involves the arbitrary velocity v_x. All the other components of P_{ik} (including P_{xz}) are zero.

The substitution of these values in (38) now gives the following somewhat complex relation, which can, however, be considerably simplified:

$$\delta\{\tfrac{1}{2}(p^2+q^2)\,dx\,dy\,dz\} = v_x\delta g_x + \frac{q}{p}\,\delta\,(pq\,dx\,dy\,dz)$$
$$+\tfrac{1}{2}(p^2-q^2)\left\{\frac{\partial\delta x}{\partial x}-\frac{\partial\delta y}{\partial y}-\frac{\partial\delta z}{\partial z}\right\}dx\,dy\,dz$$
$$+\,\mathrm{G}_z v_x\,\frac{\partial\delta z}{\delta x}\,dx\,dy\,dz. \qquad (39)$$

By simple geometry, in virtue of the considerations on the continuity of the elements referred to on p. 486, we have here

$$\frac{\partial\delta x}{\partial x}\,dx = \delta\,(dx),\ \text{etc.,}\quad \frac{\partial\delta z}{\partial x} = \delta\theta_{zx}. \qquad (40)$$

In the term on the left the field is considered as a continuum which is varied, on the right $\delta\,(dx)$ is the variation in the length of the side parallel to Ox of an individual element and $\delta\theta_{zx}$ is the angle in the plane of xz through which the element is turned in the variation. This latter alteration of orientation involves a change

$$\delta g_x = -\,\mathrm{G}_z\,dx\,dy\,dz\,\delta\theta_{zx}$$

in its x-momentum, which was zero initially. The last term of (39) therefore cancels with $v_x\,\delta g_x$, and the arbitrary component v_x of the velocity disappears from the equation. By using the geometrical relations (40), (39) can be still further reduced to the simple result

$$\delta\,(p\,dy\,dz) = 0. \qquad (41\text{A})$$

We see that in the variation the flux of the vector p over the cross section $dy\,dz$ of each element remains constant. This fact throws a clear light on the nature of the variation itself. In the first place the constancy of its p-flux gives to each element the individuality which enables it to be recognised in a displaced position, in the second it connects the variation symbolised by δx_k directly with a corresponding variation of the field vector p. Further, since $\delta\dot{x}_z = \delta\,(q/p)$, δx_k and δx_k together determine a definite variation of p and q, and consequently one of e and h, so far as these are expressible in terms of p and q.

The meaning of the variation can perhaps be seen best by considering the simple case of an electrostatic field, which corresponds to $p = e$, $v_z = 0$. The tubes of force here determine the field at each point through the fact that the flux of e over the cross-section of a tube is a fixed quantity. Imagine the bounding lines of each tube to be displaced to infinitely near positions, and assume that in the displacement the flux of each tube remains unchanged ($\delta\,(e\,dy\,dz) = 0$). The new cross-sections then determine the varied field and the theorem (37), after omitting the integration in t, here unnecessary since the field is independent of the time, becomes

$$\delta \int \tfrac{1}{2} e^2\, d\mathrm{V} = 0.$$

This is Kelvin's theorem of minimum energy, and we observe that it holds for any displacement of the lines of force subject to constancy of the flux of e over the cross-sections of the tubes. The theorem (37) is the extension of the same conception to the electromagnetic field. The corresponding lines, however, are neither those of e nor of h, but of p, a derived vector which is a composite of both e and h, and for which a constant flux condition corresponding to that of the electrostatic case holds in the variation. Further, the lines being in motion, an integration over the time, and the replacement of energy by the Lagrangian function is necessary.

The constant p-flux condition (41A) only holds for the set of values of v given by (35A). For the second set (35B), in which $v_s > 1$, it may be proved in a similar way that a constant q-flux condition holds in the variation which gives (31):

$$\delta\,(q\,dx\,dz) = 0. \qquad \text{(41B)}$$

Mass and Potential and Kinetic Energy of the Field.—A natural time alteration of the field, forming as it does a possible variation, is also subject to the constant flux condition.* This fact enables expressions for the mass, and the potential and kinetic energy, of a field element to be deduced which, since the flux theorem and the canonical expression for the energy are in reality the same equation, necessarily are in full agreement with dynamical principles.

Take the case of motion in which $v_s < 1$, and call it u_1, so that

$$u_1 = q/p.$$

Writing in accordance with (41A)

$$p\,dy\,dz = \mathrm{C}_1$$

(constant with the time or in any variation) we get from (38A)

$$g = \mathrm{C}_1^2\,\frac{dx}{dy\,dz}\,.\,u_1.$$

---

* The equation $\frac{d}{dt}(p\,dy\,dz) = 0$ expressing this fact may be deduced directly from the fundamental equations. (Milner, *loc. cit.*, p. 38.)

The coefficient of the velocity in this expression for the momentum forms the mass m_1 of the element defined in the usual dynamical way. Hence

$$m_1 = C_1^2 \frac{dx}{dy\,dz}. \tag{42A}$$

While it may be given an arbitrary value when the elements are constructed, the mass of each remains a determinate quantity through the subsequent history of the field. It depends, however, on the *shape* which the element takes up at later times, the electromagnetic field contrasting in this respect with a material fluid.

The energy w when expressed in terms of m_1, becomes

$$w = \tfrac{1}{2}m_1(1 + u_1^2).$$

The part $\frac{1}{2}m_1$ (really $\frac{1}{2}m_1c^2$) depends only on the shape of the element, and the other part $\frac{1}{2}m_1u_1^2$ depends on the velocity as well. In dynamical theory these would be called potential and kinetic energy respectively. If we do so here they allow the Lagrangian function of an element to be expressed in the classical form as the difference between its kinetic and potential energies, thus

$$dL = gu_1 - w = \tfrac{1}{2}m_1u_1^2 - \tfrac{1}{2}m.$$

The corresponding values of the kinetic and potential energies of the whole field are

$$T_1 = \tfrac{1}{2}\int q^2\,dV, \qquad U_1 = \tfrac{1}{2}\int p^2\,dV. \tag{42B}$$

These may be translated into terms of e and h by (33).

This method of splitting the whole energy into kinetic and potential is not, however, the only possible one. If we take the second solution for v_z,

$$v_z = p/q = u_2, \text{ say},$$

we have to write

$$\left.\begin{array}{c} q\,dx\,dz = C_2, \qquad m_2 = C_2^2 \dfrac{dy}{dx\,dz} \\ w = \tfrac{1}{2}m_2(1 + u_2^2) \end{array}\right\}, \tag{43A}$$

from which we get

$$T_2 = \tfrac{1}{2}\int p^2\,dV, \qquad U_2 = \tfrac{1}{2}\int q^2\,dV, \tag{43B}$$

so that what was previously called the kinetic energy becomes now the potential energy, and *vice versa*.

Elements of Action and Extension of the Variation Principle.—The variation principle (37) can be given a more general form by four dimensional analysis, because when we consider the electromagnetic field as an entity in the manifold of space-time the equations are symmetrical in all four variables. The formulæ can be considerably simplified without loss of generality, and their meaning made clearer, by using special axes for x, y, z, t, chosen in such a way that they follow out the lines of simplest structure of the field. We shall take at a given point the axes of x and y as the lines of those two principal directions of Maxwell's stress which lie in the plane of e and h in the instantaneous hyperplane of an arbitrary observer. These are identical with the special x- and y-axes adopted previously. The axis of t will be chosen at the point so that it coincides with the proper time axis of an observer to whom there appears to be no momentum in the field there. This allocation of the x-, y-, and t-axes fixes that of z, which is (analytically) perpendicular to each of them. If, starting from the given point, each of these four axes be extended through space-time, by adding a succession of infinitesimal lengths always oriented in accordance with the definitions given above, it will form a continuously curved line, which, unless it is a closed curve, can extend to the boundary of any region of the field (four-dimensional volume $= \Phi$) considered. The whole of Φ can be marked out with such x-, y-, z-, t-lines, forming a curved co-ordinate system, one line of each kind passing through each point.* We can now construct a *curved* space-time element by taking infinitesimal lengths x_1, y_1, z_1, t_1 of the lines passing through a given point to form its four adjacent edges, the remaining edges being formed by corresponding lines passing through the other ends of x_1, y_1, z_1, t_1. At, *e.g.*, the x-end of this element, another element, x_2, y_2, z_2, t_2, can be formed in a similar way, and the whole of Φ ultimately can be filled by ∞^4 elements which may be considered indifferently as arranged along any one of four sets of curved four-dimensional tubes, whose axes are x-, y-, z-, t-lines respectively.

I have proved in a previous paper† that if x_r, y_r, z_r, t_r stand for the lengths of the corresponding lines passing through any point of one of these elements, and d/dx represents "axial" differentiation along the curved x-line, etc., then the following four equations, each of which expresses a constant flux relation characteristic of the element, can be deduced directly from the fundamental equations:

---

* The x-, y-, z-, t-lines defined in the above way are not *uniquely* fixed in space-time, they vary with the time axis of the initial arbitrary observer. Strictly it is only the xt and yz planes at each point that are fixed by the definitions, and the t-axis may have any arbitrary direction in the fixed xt plane. This fact explains the result in the three-dimensional calculation, rather puzzling at first sight, of the arbitrariness of the component v_x of the motion of the field elements. In a material medium the world lines of the moving particles are uniquely laid down in space-time; the four-dimensional structure consists of world-*lines*. In the electromagnetic field the structure is more closely (though not accurately, as their differential equations are not in general unconditionally integrable) represented by *surfaces*, on which arbitrary world-lines can be drawn. The two values of v_x are also explainable as the result of the complete symmetry in the four-dimensional equations of x with y and z with t.

† 'Phil. Mag.,' vol. 44, p. 705 (1922).

$$\left.\begin{aligned} \frac{d}{dx}(\mathrm{R}y_r z_r) = 0, \qquad \frac{d}{dt}(\mathrm{R}y_r z_r) = 0 \\ \frac{d}{dy}(\mathrm{R}x_r t_r) = 0, \qquad \frac{d}{dz}(\mathrm{R}x_r t_r) = 0 \end{aligned}\right\}, \tag{44}$$

where

$$\mathrm{R} = \{(e^2 - h^2)^2 + 4\,(\mathrm{eh})^2\}^{\frac{1}{4}}.$$

This space-time element with the action

$$d\mathrm{A} = \tfrac{1}{2}\mathrm{R}^2\, x_r y_r z_r t_r \tag{45}$$

included in it represents an *element of action** constructed in the simplest possible way, *i.e.*, with its curved edges drawn along lines which mark out as it were the natural structure of the four-dimensional field. It possesses the properties that the flux

$$\mathrm{R}y_r z_r = \Delta_1\mathrm{F} \tag{46A}$$

is constant over every possible yz two-dimensional section of the four-dimensional element, and the flux

$$\mathrm{R}x_r t_r = \Delta_2\mathrm{F} \tag{46B}$$

is constant over every xt section.

Let us now imagine that, the whole field in the region Φ having been divided into elements of action in the way described, the co-ordinates x, y, z, t of every point are varied in any possible way, such that the elements after the variation still fill without discontinuity the space-time region. Here again the variation can have no meaning unless something remains constant to render the displaced elements identifiable. We shall prove that if *either* of the fluxes $\Delta_1\mathrm{F}$ or $\Delta_2\mathrm{F}$ be supposed to remain constant in the variation then the total action in Φ, when the variation vanishes at its boundary, is stationary for the natural field which is subject to the electromagnetic laws (44).

To simplify the proof we will consider only one component displacement at a time, and take this in the direction z, *i.e.*, we suppose that every point of each element is displaced by the arbitrary amount δz along the curved z-lines. Let further each displaced and distorted element be subject to the constant flux condition

$$\delta\,(\mathrm{R}y_r z_r) = 0.$$

---

* The $\mp$ sign is omitted, action being considered here as a positive entity, *vide* p. 486.

Suppose that there are n elements in one of the z-tubes, and m z-tubes, and that our typical element is the rth in order in its z-tube. Then

$$\delta\mathrm{A} = \sum_m \sum_n \delta(\tfrac{1}{2}\mathrm{R}^2 x_r y_r z_r t_r).$$

Eliminating $\delta\mathrm{R}$ from the two equations we get

$$\delta\mathrm{A} = \sum_m \sum_n \tfrac{1}{2}(\mathrm{R}y_r z_r)^2\, \delta\left(\frac{x_r t_r}{y_r z_r}\right).$$

Now since the elements when displaced along z must fill completely the z-tubes in which they lie, and these latter are not changed in shape by the variation, we have

$$\delta\left(\frac{x_r t_r}{y_r}\right) = \frac{d}{dz}\left(\frac{x_r t_r}{y_r}\right)\delta z.$$

Further, it can readily be seen that, when z is considered as a function of the continuous pure number r whose integral value stands for the number of the typical element, then the following identities may be made use of:

$$\sum_n z_r \equiv \int_0^n \frac{dz}{dr}\,dr$$

$$\frac{d}{dr} \equiv z_r \frac{d}{dz}.$$

We can consequently write

$$\delta\mathrm{A} = \sum_m \sum_n \tfrac{1}{2}\mathrm{R}^2 y_r^2 z_r \frac{d}{dz}\left(\frac{x_r t_r}{y_r}\right)\delta z - \sum_m \int_0^n \tfrac{1}{2}\mathrm{R}^2 x_r y_r t_r\, \delta\left(\frac{dz}{dr}\right) dr.$$

On integrating by parts the second term and assuming that δz vanishes at both ends of the z tube, we get for it

$$+\sum_m \sum_n \tfrac{1}{2} z_r \frac{d}{dz}(\mathrm{R}^2 x_r y_r t_r)\,\delta z.$$

Consequently

$$\delta\mathrm{A} = \sum_m \sum_n \mathrm{R}y_r z_r \frac{d}{dz}(\mathrm{R}x_r t_r)\,\delta z,$$

which is zero by (44).

The same zero value results when x, y, or t is taken as the co-ordinate varied or $\Delta_2\mathrm{F}$ as the flux which is kept constant. The variation principle consequently holds for *any* displacement in which the varied elements, defined by either of the fluxes (46), fill without discontinuity the fixed space-time region Φ.

Euler's Principle.—The equivalent of Euler's principle (3) for the electromagnetic field may be deduced in a similar way to that of Hamilton's principle.

Reverting to the conception of moving three dimensional elements of the field, we have generally, when the integral is extended over the interval between given unvaried initial and final states of the field,

$$\delta \int_{t'}^{t''} \sum_{n} g_k x_k \, dt = \sum_{n} \int_{t'}^{t''} (x_k \, \delta g_k + g_k \, \delta x_k) \, dt$$

$$= \sum_{n} \int_{t'}^{t''} (x_k \, \delta g_k - \dot{g}_k \, \delta x_k) \, dt.$$

Consequently, by equation (27) under the conditions that (1) the total energy of the field is constant ($\delta \mathrm{H} = 0$)*, and (2) the variations of x_k vanish at the boundary, it follows that

$$\delta \int_{t'}^{t''} \sum_{n} g_k v_k \, dt = 0.$$

Translated into terms of e and h by (33), (34) and (35), this gives

$$\left.\begin{aligned} \delta \mathrm{S} &= 0 \\ \text{where} \quad \mathrm{S} &= \int_{t'}^{t''} \int \left[\tfrac{1}{2}(e^2 + h^2) \mp \tfrac{1}{2}\{(e^2 - h^2)^2 + 4\,(\mathrm{eh})^2\}^{\frac{1}{2}}\right] d\mathrm{V} \, dt = 0 \end{aligned}\right\}, \quad (47)$$

the upper or lower sign being taken according as the smaller or greater of its two values is chosen for v_s. (47) is the electromagnetic equivalent of Euler's principle.

S denotes the type of action with which the quantum theory is concerned. For a periodic orbit, assuming that a solution of Maxwell's equations for a field representing it has been found for which the total energy is constant, when the time integral is extended over a complete period τ the quantum theory requires that S should be an integral number of times Planck's quantum. H. S. Allen† has shown that for simple cases of periodic electronic orbits, as an approximation based on the identification of the magnetic with the kinetic energy of the system, the action in a complete period is

$$\mathrm{S} = \int_{t}^{t+\tau} \int h^2 \, d\mathrm{V} \, dt.$$

The more complex expression (47) reduces to this when the upper sign is taken and the scalar product of e and h is considered negligible.

---

* For Lorentz electrons $\delta \mathrm{H}' = 0$, *vide* footnote pp. 491-492.

† 'Phil. Mag.,' vol. 48, p. 429 (1924).

Summary.

The electromagnetic equations in their usual form express the rates of variation of the field vectors along the time axis of an arbitrary observer. The consideration of the rates of variation along other lines in space-time, in particular along the lines which mark out the simplest structure of the field, leads to the equally legitimate conception of the field as being in motion. In this way expressions for the Hamiltonian and Eulerian *actions* of the field are obtained which form strict equivalents to those for the actions of a dynamical system. The electromagnetic Hamiltonian action thus determined is

$$A = \mp \iint \tfrac{1}{2} \{(e^2 - h^2)^2 + 4\,(\mathbf{eh})^2\}^{\frac{1}{2}}\, d\mathrm{V}\, dt,$$

the integral extending over a given region of space-time. This quantity is proved to possess a stationary value in the electromagnetic field subject to conditions equivalent to those characterising Hamilton's principle in dynamics.

The Zeeman Effect for the Spectrum of Tantalum.

By Prof. J. C. McLennan, F.R.S., and A. M. I. A. W. Durnford, M.A.*

(Received June 28, 1928.)

[Plates 20–23.]

Introduction.

Among the elements whose arc spectrum has not as yet been analysed, one of some interest is Tantalum. Of atomic number 73, it occurs between Hafnium and Tungsten in the atomic table, and according to Bohr it is a homologue of Uranium X. As one of the most powerful methods we have available for investigating the structure of a spectrum is a study of the Zeeman effect shown by its constituent wave-lengths, we decided to use it with tantalum. The magnetically resolved components of over 50 of the more important wave-lengths of its arc spectrum were determined, and the results, together with an account of the investigation, are given in what follows.

---

* Holder of Studentship from the National Research Council of Canada.

Apparatus.

The light source used consisted of a modified form of vacuum arc and the arc chamber formed an integral part of an electro-magnet, which was of the Du Bois type. The grating, a 4-inch concave one with 15,000 lines per inch, had a radius of 3 metres and was used with an Eagle mounting. The photographs taken were those of second order spectra.

A detailed consideration of the vacuum arc assembly follows.

The pole pieces (Plate 20, fig. 1) were 5 cms in diameter, tapered on the ends at 55° to give an end-face diameter of 1·3 cms. Threaded brass shoulders carried the pole pieces in the assembly and a vacuum-tight seal was maintained by using well-vaselined paper gaskets Cylindrical pole caps were screwed on to the pole pieces, the latter being drilled and tapped. The pole caps had a thickness of 3 mm. and in the assembly were separated by 4 mm.

Tantalum was used in the form of ⅛-inch rod and formed the negative electrode by being inserted directly into one of the pole caps. The tantalum projection was limited to 2 mm.

The positive electrode (Plate 20, fig. 2) consisted of a copper plate 1 mm. thick, soldered to a copper U-tube of 1 mm. bore, through which a stream of cold water was passed. The U-tube was rigidly attached to the top structure that carried the water leads, the latter being insulated from the outer brass cylinder by means of a hard rubber sleeve. Since the pole pieces and the arc chamber were kept at the same potential as the negative electrode, it was necessary to insulate the lower portion of the positive electrode from the adjacent pole cap. This was done by attaching a thin sheet of mica to the copper plate and having the pole cap carry a ring of hard rubber Adjustments in the position of the electrode were made possible by the use of an outer brass sleeve having a set of knife edges that rested on a brass tube attached to the vacuum arc chamber. A short length of thin-walled rubber hose furnished a flexible vacuum-tight connection between the brass sleeve and the chamber.

The positive electrode was capable of a to-and-fro motion parallel to the magnetic field, this motion being produced by an electro-magnetic trembler that was operated off the arc circuit. The trembler was connected with the lower portion of the positive electrode and had a flexible vacuum-tight connection with the chamber.

The operation of the trembler was made to depend upon the mutual attraction between two small electro-magnets, one stationary and the other attached to the trembler. The stationary one was firmly attached to the base of the Du Bois magnet. A light coil spring, fastened to the upper portion of the positive electrode, kept the arc closed when no arc current was passing. When the arc switch was closed, part of the arc current passed through the magnets, and as a result of their mutual attraction, opened the arc. It was found that normally an arc was hard to maintain in a magnetic field, but with the above device, as soon as it was extinguished, the mutual attraction of the electro-magnets ceased and the spring caused a fresh contact to be made. The effect was that the arc was self-sustaining.

The vacuum arc in a magnetic field is most easily maintained at certain pressures, so that with unsuitable conditions only a to-and-fro motion of the positive electrode results. The above device therefore gave a means of finding the most suitable conditions for the maintenance of the arc, and also allowed for its operation under any desired conditions. The vacuum arc current was supplied by a 110-volt D.C. circuit, and in the case where tantalum was the metal used the lines were most easily obtained by employing a current of 4 amperes with one-half of an atmosphere of air in the chamber.

Plate 20, figs. 3 and 4, give a longitudinal and transverse view of the vacuum arc assembly. On account of the number of wax and vaseline joints used in the assembly, cooling tubes carrying water were inserted in the chamber.

The light, produced in the centre of the magnetic field, passed through a window in the side of the chamber and was focussed on the slit of the spectrograph by means of a lens placed immediately outside of the window. A second window was provided for observation purposes during exposures. The second electrode outlet was not used as the method of inserting the element in the pole cap permitted exposures of sufficient duration to be made.

As already stated, a large Du Bois electro-magnet was used for producing the magnetic field. The soft iron core, 8 cms. in diameter, was in two sections, each section being firmly held to the base by two large bolts Further, each section could be moved parallel to the field so that the two end faces of the core could be brought into contact with the outer faces of the pole pieces. Alignment of the vacuum arc assembly was secured by meant of a ½-inch bolt attached to one of the pole pieces and fitted into a corresponding cavity in the core.

The windings of the electro-magnet consisted of 10 V-shaped sections which fitted over the curved core, and had a total resistance of 5·25 ohms (68° F.). Current was supplied by a separate 100-volt D.C. circuit. Preliminary experiments indicated that the field intensity changed by less than 1 part in

400, for a period slightly less than two hours, provided the current was kept constant. This condition was realised by gradually lessening the amount of the auxiliary resistance in the circuit as the resistance of the magnet coils increased through heating. Exposures of 1 hour duration sufficed to give the Zeeman patterns of the wave-lengths under investigation.

Experimental Procedure.

The wave-lengths of many of the most prominent lines in the arc spectrum of tantalum fall in the region λλ 6700–5500 Å. They are shown grouped together in Table I. In operating with the vacuum arc, a few of the weaker lines and some of the spark lines were observed to give prominent Zeeman patterns, and the wave-lengths of these are grouped together in Table II.

Table I.—Wave-Lengths of the Stronger Lines occurring in the Arc Spectrum of Tantalum. From Exner and Haschek Values; H. Kayser, 'Handbuch der Spectroscopie,' vol. 6, p. 567.

Wave-length Å.U.	Intensity.	Wave-length Å.U.	Intensity.	Wave-length Å U	Intensity.
6675·78	5	6356·38	5	5944·27	4
73·98	3	46·20	3	40 00	3
21 53	5	41·37	3	19·19	3
12·20	5	33·11	3	16·75	2
6575·08	5	25·30	4	02·15	3
61·82	3	12·45	2	5882 53	3
16 40	10	09·80	5	77 61	4
14·68	10	09·30	2	49·89	2
05 79	4	6289·60	3	11 33	8
02·77	3	88·17	3	5780 00	3
6485·60	15	81 59	3	76·97	4
60·11	3	78·54	3	68·10	3
56·02	2	68·90	5	66·76	2
50·59	10	56·93	5	56 03	2
46·10	3	50 00	3	15·51	2
44·85	3	6154·69	3	5699 47	2
31·02	8	44·77	2	65·11	4
28·28	4	01·83	2	46·10	4
6392·40	3	6047·49	2	40 40	2
89·68	5	45·62	4	20·89	2
73·29	3	20·92	3	5519·11	3
61·06	5	5997·49	5		

Two settings of the grating sufficed to cover the region indicated above, since each setting included about 600 Å. Ilford (10 inch by 2 inch) thin glass panchromatic plates were used. The neon spectrum, supplemented by the iron arc spectrum for wave-lengths less than λ 5850 Å., furnished a convenient set of standards for dispersion purposes. From the set of wave-lengths obtained, a dispersion wave-length curve was secured for each setting

Table II.—Wave-Lengths of Tantalum, not listed in Table I, but of which Zeeman patterns have been secured.

Wave-length.	Intensity.	Wave-length.	Intensity.	Wave-length.	Intensity.
6152·70	1	5746·02	1	5599·47	1
5844·21	1	06·50	1	99·03	1 spk.
44 06	1	04·96	1	84·25	1
16·68	1	04·50	1	48·50	1
5752·0	1 spk.	5635·95	1		

of the grating and the dispersion at any point on the plates was ascertained from it. The value of the dispersion varied over the entire region, from 2·67 to 2·56 Å. per millimetre.

The spectrograms A and B of Plate 21 give the arc wave-lengths over the region λλ 6700–5548 Å. and for purposes of comparison these are matched with the spectrograms giving Zeeman patterns. Measurements of the separation of the components of the different Zeeman patterns were taken directly from the plates by means of a travelling microscope. Because of the small value of the separation, in each case, a set of readings was taken, from which a mean value was secured. The Zeeman pattern of the zinc line λ 6362 Å. was secured on the same plates as the tantalum Zeeman patterns, and as the magnetically resolved components of this wave-length were known, it was possible from measurements on one of the best plates, Z 37, to evaluate the field strength. Its value was found to be 21,500 gauss. The Zeeman pattern for Zn λ 6362 Å. is shown in fig. 5 and a Moll tracing of the pattern in fig. 6.

In addition to the above, some plates were also secured that gave the known patterns of two other wave-lengths, Sn λ 6453 Å and Pb λ 6660 Å., together with that of the zinc triplet. One of the best of these, Z 35, was used for measurements. Since $d\lambda_n/\lambda^2$ was dependent only on H, the field strength, it followed that it should have a constant value for each plate. By taking each of the three patterns as standards, the values of $d\lambda_n/\lambda^2$ obtained were found to be identical. This indicated that a true value for $d\lambda_n/\lambda^2$ for any plate could always be obtained from the value of the $2d\lambda_n$ separation given by the zinc triplet, λ 6362 Å. The measurements that led to this conclusion are given in Table III. This table, it will be seen, includes the number of readings used, in each case, to determine a mean value for the separation of the components and also the average deviation of the set of observations from the mean. The latter is measured in ten thousandths of a millimetre and applies to the value given for the mean.

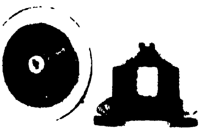

FIG. 1.

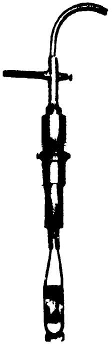

FIG 2.

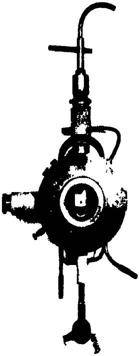

FIG. 3.

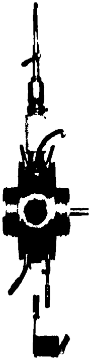

FIG. 4.

(*Facing p* 508.)

A.

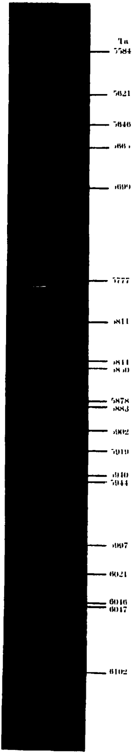
Ta
5584
5621
5646
5661
5699
5777
5811
5844
5850
5878
5883
5902
5919
5940
5944
6007
6021
6046
6047
6102

B

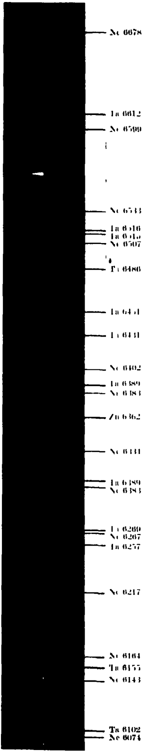
Ne 6678
Ta 6612
Ne 6599
Ne 6533
Ta 6516
Ta 6515
Ne 6507
Ta 6486
Ta 6451
Ta 6431
Ne 6402
Ta 6389
Ne 6383
Zn 6362
Ne 6334
Ta 6289
Ne 6304
Ta 6260
Ne 6267
Ta 6257
Ne 6217
Ne 6164
Ta 6155
Ne 6143
Ta 6102
Ne 6074

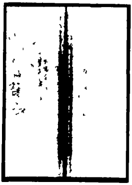

Fig 5
Zn λ 6362.

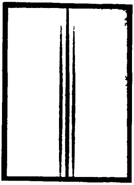

Fig 7
Ta λ 6102.

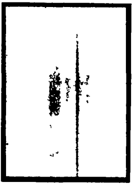

Fig 9
Ta λ 6516 and λ 6515

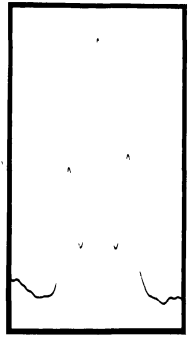

Fig 6
Zn λ 6362.

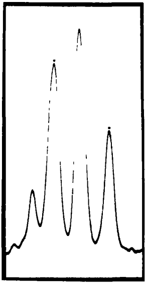

Fig. 8.
Ta λ 6102

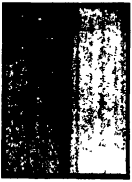

FIG. 11
Ta λ 6257

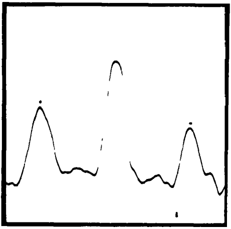

FIG. 10
Ta λ 5844

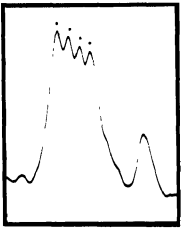

FIG. 12
Ta λ 6257.

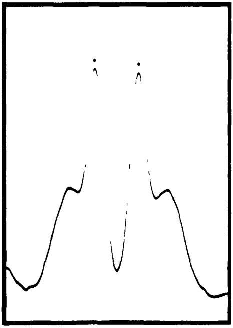

FIG. 14.
Ta λ 6431.

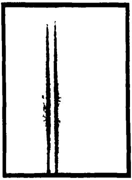

FIG. 13.
Ta λ 6431 and λ 6429

Table III.

Element.	Wave-length.	Plate.	Separation.	No. of observations.	Mean.	Average deviation	$d\lambda_n/\lambda^2$.
					mm.		cm^{-1}
Zn .	6362	Z 35	$2\,d\lambda_n$	12	0·313	18	1·009
Sn .	6453	Z 35	$2/3\,d\lambda_n$	7	0·108	27	
			$2\,d\lambda_n$	7	0·323	16	1·009
Pb	6660	Z 35	$4/3\,d\lambda_n$	7	0·232	29	
			$8/3\,d\lambda_n$	7	0·470	13	
	(from mean	of above)	$2\,d\lambda_n$		0·350		1·009
Zn .	6362	Z 37	$2\,d\lambda_n$	14	0·316	21	(*a*)
			$2\,d\lambda_n$	9	0·314	17	(*b*)
	(from mean	of above)	$2\,d\lambda_n$		0·315		1·014
Ta	6102	Z 37	$2\,d\lambda$	9	0·384	20	(*a*)
			$2\,d\lambda$	13	0·383	29	(*b*)
		Mean :	$2\,d\lambda$		0·3835		1·014
Ta ...	6102	Z 41	$2\,d\lambda$	7	0·378	13	(*a*)
			$2\,d\lambda$	7	0·377	13	(*b*)
		Mean ·	$2\,d\lambda$		0·3775		0·9815

Note.—

Ta, 6102, Z 37, $2d\lambda = (0{\cdot}3835)(2{\cdot}645) = 1{\cdot}014$ Å.U.

Ta, 6102, Z 41, $2d\lambda = (0{\cdot}3775)(2{\cdot}600) = 0{\cdot}9815$ Å.U

Since two settings of the grating were used, it was necessary to have a standard pattern for the second region. One of our plates, Z. 41,* gave the Zeeman patterns for wave-lengths between λ 5545 Å. and λ 6165 Å. and the tantalum triplet λ 6102 Å. occurred on plates of both settings. As pointed out above, the zinc triplet λ 6362 Å. gave a very good means of securing the constants of the plates for the region λλ 6700–6075 Å., and in consequence the constants of plates for the lower region were secured from the zinc triplet through the intermediary of the tantalum triplet λ 6102 Å. The results involved in this conversion are given in Table III. It was found that measuring the triplets in one operation gave a value less than that obtained when the measurement was made in two operations as a result of setting on the central component. Measurements obtained in this way are designated (*a*) and (*b*).

Results.

In all, 55 Zeeman patterns were measured up for wave-lengths of tantalum between λ 5548 Å. and λ 6700 Å. The results of the investigation are given in Table IV. As a number of the patterns included components which were

---

* The Spectrograms A and B of Plate 21 include Plates Z 41 and Z 37.

Table IV.

Wave-length	$d\lambda_n$ Å U	$d\lambda_n$ mm.	$2d\lambda$ mm.	Average deviation.	$d\lambda/d\lambda_n$.
Section I.					
6515	0·4303	0·1664	0·592	19	1·778
6390	0·4140	0·1590	0·323	27	1·016
6310	0·4036	0·1544	0·437	34	1·415
6102	0·3774	0·1427	0·3835	10	1·343
5944	0·3468	0·1323	0·358	23	1·353
5883	0·3397	0·1294	0·335	15	1·294
5811	0·3309	0·1256	0·350	19	1·393
5756	0·3253	0·1232	0·326	27	1·323
5705	0·3196	0·1209	0·260	16	1·075
5665	0·3150	0·1187	0·260	9	1·095
Section II					
6516	0·4305	0·1665	0·214*	40	0·643
6446	0·4213	0·1620	0·385	50	1·188
6445	0·4211	0·1619	0·285	20	0·880
6373	0·4117	0·1581	0·310	46	0·980
6346	0·4083	0·1564	0·278*	50	0·889
6341	0·4078	0·1563	0·376	16	1·203
6155	0·3842	0·1455	0·346	38	1·189
6153	0·3839	0·1454	0·396	22	1·362
5917	0·3439	0·1310	0·392	22	1·496
5817	0·3315	0·1258	0·363	32	1·442
5747	0·3241	0·1227	0·335	44	1·365
5716	0·3207	0·1213	0·235	33	0·968
5706	0·3197	0·1209	0·304	60	1·258
5584	0·3060	0·1147	0·322*	40	1·404
Section III					
6612	0·4482	0·1725	0·684*	80	1·983
6309	0·4035	0·1544			
5844	0·3352	0·1275	0·766	45	3·004
5636	0·3118	0·1172	0·196*	50	1·672
5600	0·3078	0·1153	0·272*	80	1·179
5599	0·3077	0·1153	0·360*	80	1·562
Section IV.					
6676	0·4519	0·1762	0·265*f*	16	0·755
6674	0·4516	0·1761	0·291	40	0·826
6486	0·4266	0·1647	0·273*f*	22	0·829
6451	0·4221	0·1624	0·196*	40	0·603
6431	0·4194	0·1613	0·219*f*	30	0·629
6325	0·4055	0·1551	0·291	27	0·938
			0·082	17	0·264
6209	0·3985	0·1521	0·500*	40	1·643
6257	0·3970	0·1516	0·180	14	0·594
			0·060	36	0·198
6047	0·3588	0·1380	0·148*	40	0·536
6046	0·3587	0·1380	0·207	10	0·750
6021	0·3558	0·1367	0·207	18	0·757
			0·640*	40	2·340
5940	0·3463	0·1322	0·215	17	0·813
5919	0·3440	0·1310	0·279	48	1·064
			0·152	28	0·580
5777	0·3275	0·1241	0·409	31	1·648
			0·273	27	1·100
5752	0·3249	0·1230	0·142	50	0·577
Section V.					
5997	0·3580	0·1352	0·36		1·33
5902	0·3419	0·1302	0·05		0·19
5878	0·3390	0·1292	0·13		0·50
5850	0·3359	0·1277			
5646	0·3130	0·1177	0·09		0·38

too indefinite to allow for accurate measurement, micro-photometer curves were secured for all the patterns. Measurements were made on these curves, and with them we were able to check up the measurements on the original plates. The results have been classified into various sections.

Section I gives information concerning triplets that had strong and unique components. One of these, Ta λ 6102 Å, is shown in fig. 7 and a micro-photometer curve of another, Ta λ 6310 Å, in fig. 8 (Plate 22).

Section II also deals with triplets but differs from Section I in that the components are of lower intensity and in general broader. With these triplets no fine structure was indicated. A few of the results in this section have very low average deviations, and for such cases it is the central component that is broad. Illustrations of the types of Zeeman patterns dealt with in Sections I and II are given in fig. 9 (Plate 22).

Section III deals with triplets that differ from the above in that their micro-curves indicate a finer structure. A curve illustrating this type of resolution is that of Ta λ 5844 Å. It is shown in fig. 10 (Plate 23). The separation to which the measurement refers is indicated by two dots on the curve

Section IV deals with Zeeman patterns other than triplets. In many instances only one pair of components could be measured. One of these, a quartet, Ta λ 6257 Å., is shown in figs. 11 and 12 (Plate 23)

In some cases where the Zeeman pattern was not measurable and the micro-photometer curves showed definite peaks, measurements were made from the curves. Results obtained in this manner are indicated by an asterisk. The letter *f* is used to denote a doublet with fuzzy sides, *e g*, Ta λ 6431 Å. (figs. 13 and 14). Where a single result is given without any distinguishing mark, the pattern appeared as a doublet. As only one reading was taken in the case of asterisked measurements, the value of the average deviation was estimated from a comparison between the two methods of measurements as applied to a number of patterns in Section I.

Section V deals with a few patterns that are included for their qualitative value.

It remains to point out the error involved in the determination of the normal separation, $d\lambda_n$, for the various wave-lengths.

(i) Justification for taking the $2d\lambda$ separation of the zinc triplet (6362) as a true measure of $2d\lambda_n$ has been considered above.

(ii) Measurements on the zinc triplet, involving 23 observations, gave as the value of the double normal separation, $2d\lambda_n = 0{\cdot}315 \pm 0{\cdot}001$ mm. It follows that any calculation involving this value would possess a maximum error of 0·3 per cent. As this error would carry the same sign throughout, all calculations would be affected in the same way. In consequence, this type of error is excluded from the considerations that follow.

(iii) Since the calculation of $d\lambda_n$ (Å U.) involves λ^2 and λ is taken to the nearest Å U., the greatest possible error in $d\lambda_n$ (Å U.) is less than $\frac{2\,(0\cdot5)}{5000}$. We therefore have the accuracy $d\lambda_n$ (Å U.) ± 0·02 per cent.

(*iv*) *In securing the dispersion for each wave-length from the dispersion* wave-length curves, the greatest possible error was less than $\frac{0\cdot0025}{2\cdot500}$, *i.e.*, less than 0·1 per cent.

Combining (iii) and (iv) we have, therefore, $d\lambda_n$ (mm.) ± 0·12 per cent. with a residual error of 0·3 per cent.

(v) The values for the various separations possess varying percentage errors, the magnitude of which may be determined by combining the average deviation with the value of the mean. The latter values involve the magnitude of the separation and the sharpness of the components and indicate that the value of $d\lambda_n$ (mm.) as obtained is sufficiently accurate. It is intended that the value of the average deviation may be used to indicate the worthiness of the final calculation, viz., $d\lambda/d\lambda_n$.

Conclusion.

Recent work on atomic states and spectral terms* gives the lowest spectral term for tantalum as $^4F_2$, thus indicating a quartet system for the arc spectrum. Several of the Zeeman patterns confirm this statement, but in the present communication no attempt has been made to reduce the values of $d\lambda/d\lambda_n$ to Runge fractions. The analysis of the arc spectrum will be given in another communication.

---

* McLennan, McLay and Smith, 'Roy. Soc. Proc.,' A, vol. 112, p. 76 (1926).

Motion of Electrons in Gases.

By J. S. Townsend, F.R.S.

(Received July 7, 1928.)

1. In order to find an explanation of many of the ordinary electrical phenomena in gases it is necessary to consider the effects that occur in collisions between electrons and molecules or atoms of the gas. Collisions may be divided into two classes, those in which the electrons move with a small velocity and lose or gain a small amount of energy in collisions with molecules, and those in which the velocity is large and the electrons may lose a large proportion of their energy. In collisions of the latter type the kinetic energy of the electron is of the order of the energy which corresponds to the ionising potentials.

Many of the original investigations of phenomena where these effects predominate have been made at the Electrical Laboratory, Oxford, and this work is accepted by several authors* as being of importance in the theory of the electrical properties of gases.

Other authors, who are more interested in models of atoms, do not refer to this work or do so in order to criticise it adversely.

In a paper by Atkinson† an attempt is made to show that there are many errors throughout the whole of this work. In some cases in order to explain experiments which conflict with the theories which he advocates, Atkinson finds it necessary to assume that electrical properties of monatomic gases are principally due to impurities which are not removed by any known process of purification. But in other cases his criticisms are less speculative, and he claims to have found that our results conflict with simple dynamical principles and that they must involve very grave errors. These criticisms are strongly emphasised, and as the principles involved are elementary it is possible to deal with them in a simple manner.

2. The errors, to which special attention is drawn, are said to occur in the investigations of the average loss of energy of electrons in collisions with molecules when the electrons move with small velocities. According to

---

* Schumann, 'Electrische Durchrückfeldstärke von Gasen' (1923); Stücklen, 'Handbuch der Physik,' vol 14, chap. 1 (1927); Warburg, *ibid.*, vol. 19, chap. 7 (1927), Przibram, *ibid.*, vol. 22, chap. 4 (1926); Darrow, 'Introduction to Contemporary Physics' (1927); Whitehead, 'Dielectric Phenomena, Electrical Discharges in Gases' (1927).

† 'Roy. Soc. Proc.,' A, vol. 119, p. 335 (1928).

Atkinson the method we have adopted for finding the average loss of energy of electrons in collisions is obscure; in argon and helium losses of energy have been found which are about half a certain theoretical value, and he concludes that "The exact cause of the error need not be inquired into here, but the fact that such a serious error has been overlooked cannot but create a suspicion that in more obscure cases also, such as the calculations of the mean free paths, agitation energies, and so on, equally essential considerations have been omitted."

Also according to Atkinson there appears no way at all of accounting for an average loss of energy which is smaller than $2\ m/M$, m being the mass of the electron and M that of the atom.

This statement and others of a similar nature reveal the fact that in the method of investigation adopted by Atkinson, as in that of Hertz,* no account is taken of the motion of agitation of the gas in finding the loss of energy in the simplest cases where the molecules or atoms of the gas are supposed to be perfectly elastic spheres. The constant $2m/M$ is the mean value of the proportion of the energy of an electron lost in a collision when the spheres are at rest. This constant is thus obtained on the supposition that there are no collisions in which electrons gain energy and the maximum loss of energy in a collision is $4\ m\mathrm{E}/\mathrm{M}$, E being the energy of the electron.

3. An elementary calculation shows that if the kinetic energy E of an electron were about the same as the energy acquired under the action of one volt, it would gain energy in amounts of the order $60\ m\mathrm{E}/\mathrm{M}$ in some collisions with atoms of helium at 15° C, and in amounts of the order $200\ m\mathrm{E}/\mathrm{M}$ in collisions with atoms of argon if the atoms were perfectly elastic spheres. It is plain from the outset that it is necessary to investigate very carefully to what extent these gains are balanced by losses. This problem was first solved by Pidduck for the case of steady motion of electrons in a uniform electric field. The formulæ which he gives lead to very interesting conclusions, but the results of some of the experiments may be explained by considering the well-known properties of mixtures of two gases.

An example occurs in the case of helium where large changes have been found in the proportion of the energy of an electron which is lost in the collisions with atoms. The results obtained with this gas have not been overlooked, but no particular attention has been drawn to them, as they may be explained in a very simple manner which has occurred to physicists who are familiar with the ordinary dynamical theory of gases.

---

* 'Verh. D. Phys. Ges.,' vol. 19, p. 368 (1917).

When electrons move in a gas with kinetic energy which is large compared with the energy of agitation of the gas, they lose more energy than they gain in the collisions with molecules. In the average of a large number of collisions the proportion of the energy of an electron which is lost in a collision diminishes with the energy of agitation of the electron, and when there is no electric force acting on the electrons, they continue to lose energy until thermal equilibrium is established When equilibrium is attained the average loss of energy of an electron in collisions with molecules is zero, as the losses of energy in some collisions are balanced by the gains in others. It is quite plain that the proportion of the energy of an electron which is lost in a collision is not constant, and the average loss diminishes as the kinetic energy of the electron approaches the mean energy of agitation of the molecules of the gas, when the molecules are taken as being perfectly elastic spheres. This is shown by the results of the experiments with helium which are given below in section 8.

4. The investigations of the motion of electrons which have been made in the Electrical Laboratory, Oxford, are not more obscure than the ordinary investigations in the kinetic theory of gases. The experimental part of the work consists in finding the mean velocity of agitation U of the electrons and the velocity W in the direction of the electric force Z, by methods which do not involve a previous knowledge of the mean free path.

The principle of the method of finding U is described in the explanation which was given of the first experiments* on the lateral diffusion of a stream of ions in the corpuscular state (*i.e.*, electrons). The experiments showed that "The velocity of translation† of the ions increases under the electric force, and when collisions with molecules occur they do not in general lose all the energy they acquire but continue to move in all directions with increased energy after several collisions." When the stream has traversed a distance of a few centimetres in the direction of the electric force a steady state of motion is attained in which the mean velocity of agitation remains constant while the stream continues to move in the direction of the electric force. In this stage of the motion the average loss of energy of an electron in a collision is equal to the average gain in moving between two consecutive collisions under the electric force, but this loss is small compared with the average kinetic energy of the electrons. Maxwell's equations of motion for the interdiffusion of gases may be applied to electrons in a steady state of motion, and the mean velocity of agitation U may be found from determinations of the lateral diffusion of a stream of electrons moving in a uniform electric field.

---

* 'Roy. Soc. Proc.,' A, vol. 81, p. 464 (1908).

† The term "velocity of agitation" was subsequently used for "velocity of translation."

What is actually found is the coefficient k which gives the ratio of the mean energy of agitation ($m\mathrm{U}^2/2$) of an electron to the mean energy of agitation ($\mathrm{M}\,\Omega^2/2$) of a molecule of a gas at 15° C Thus the velocity U is $1\cdot 15 \times 10^7 \sqrt{k}$ cm. per second.

Several experiments* were made to find the values of k for different gases, and to determine the form of apparatus which could be used to obtain accurate measurements of the velocities U and W since no reliable estimate of the proportion of energy lost in a collision, or of the coefficient of elasticity, can be made without finding W as well as U These were the first experiments which showed definitely that electrons moving with small velocities lose only a small proportion of their energy in collisions with molecules. It is noticeable that Atkinson following the example of Franck and Hertz, does not refer to them.

5. The first complete sets of experiments† in which both W and U were determined with the same electric forces and gas pressures, were made with air at low pressures.

In order to determine what values may be attributed to the dimensions of molecules, the coefficients of elasticity, the proportion of the energy of an electron which is lost in a collision, or the mean free path of an electron, it is necessary to define a collision. This involves some hypothesis with regard to the law of force between an electron and a molecule, but there is no *a priori* reason for supposing that a hypothesis which is adopted with a view to simplifying mathematical calculations will lead to results that agree with any theory of molecular structure.

It may be supposed that collisions between electrons and molecules are of the same nature as those which would occur between small particles and elastic spheres. On this hypothesis a formula is obtained connecting the mean free path with the velocities W and U which is of the form,

$$\mathrm{W} = \frac{\mathrm{Z}}{p} \times \frac{e}{m} \times \frac{\mathrm{L}}{\mathrm{U}} \times 0\cdot 813, \qquad (1)$$

where p is the pressure of the gas in millimetres, and L the mean free path of an electron in the gas at 1 mm. pressure when the electrons are moving with the velocity U.

---

* 'Roy. Soc Proc.,' A, vol. 85, p. 25 (1910); Haselfoot, 'Roy. Soc. Proc ,' A, vol. 82, p 18 (1909), and vol. 87, p. 350 (1912); Townsend and Tizard, 'Roy. Soc. Proc.,' A, vol. 87, p 357 (1912).

† Townsend and Tizard, 'Roy. Soc. Proc ,' A, vol 88, p. 336 (1913).

The exact value of the numerical coefficient depends on the distribution of the velocities of agitation about the mean, but as far as this discussion is concerned it is unnecessary to consider the degree of accuracy of the numerical coefficients which occur in the formulæ. The approximate values which have been found for the coefficients may be taken in order to indicate the main features of the experimental results.

Since W and U are functions of Z/p, the above formula may be examined by substituting the values of the velocities which are found experimentally. With air the formula was found to be nearly correct for certain values of Z/p when L is taken as the mean free path obtained from the coefficient of viscosity ($L = 0 \cdot 032$ cm.). But for other values of Z/p there was a discrepancy which could not be attributed to experimental error. The value of L required to satisfy the formula diminishes as U increases. It was concluded* that "The nature of the collisions between electrons and molecules may not resemble the collisions between elastic spheres to the same extent for different values of U."

From the values of k and W obtained experimentally, Pidduck† found the coefficient of elasticity for collisions between electrons and molecules of air. His results are the first quantitative estimate of the degree of elasticity in collisions of electrons with molecules of a gas. The following are some of the numbers which he obtained:—

k	1·9	21	56
f	0·9993	0·9988	0·99

where $f = \frac{1}{2}(1+e)$, e being the coefficient of restitution. The following relation between k and W was obtained for perfectly elastic collisions:

$$k - 1 = 1 \cdot 2 \times W^2/\Omega^2 \text{ approximately,} \tag{2}$$

which gives for the ratio of W^2/U^2

$$\frac{W^2}{U^2} = \frac{1}{1 \cdot 2}\left(1 - \frac{1}{k}\right) \times \frac{m}{M} \text{ approximately.} \tag{3}$$

---

* Townsend and Tizard, *loc. cit.* (1913).

† 'Roy. Soc. Proc.,' A, vol. 88, p. 296 (1913), and 'Proc. Lond. Math. Soc.,' vol. 15, p. 89 (1916).

Thus in air when the energy of agitation of the electrons is equal to the energy corresponding to 2 volts [$k = 54$], the coefficient of elasticity f is about 1 per cent. less than unity, which is the value for perfect elasticity.

For many years these experiments were viewed with suspicion. The idea that the mean free path of an electron should increase as the velocity diminishes was considered to be a physical impossibility, and even up to the present many physicists believe that electrons lose most of their energy in collisions with molecules of oxygen, and that in air the coefficient of elasticity cannot be near the value corresponding to perfect elasticity.

6. The average loss of energy in a collision may be found by dividing the energy $Z.e.z.$ gained by an electron in moving a distance z in the direction of the electric force, by the number of collisions which it makes with molecules In estimating the number of collisions [Uz/Wl] it is assumed that for each value of U there is a certain molecular radius such that the mean free path l is the same as the value of L/p obtained from equation (1).

This means that although the radius of the sphere changes with U the loss of energy and the change in the direction of motion of an electron in a collision are assumed to have reference to the same sphere

With this specification of a collision the average loss of energy in a collision is $1 \cdot 23 \times mW^2$, and the proportion λ of the energy of an electron lost in a collision is $\lambda = 2 \cdot 46\ W^2/U^2$

One of the advantages of estimating the loss of energy of an electron in a collision by this method, where U and W refer to a stream in steady motion under the action of an electric force, is that all the electrons are kept moving with an energy of agitation which is very near the mean value. Equation (1) shows that if the value of U for any group of electrons diminishes below the mean value the velocity W increases The rate at which the electrons in this group gain energy in moving in the direction of the force is thus increased, and the energy of agitation is brought back to the mean value. A similar effect operates in checking any tendency of an increase in U above the mean equilibrium value. This feature of the motion is accentuated when the mean free path L increases as U diminishes, since a further increase in W is thereby obtained when the velocity of agitation drops below the mean value.

In the calculations of the average loss of energy in collisions with perfectly elastic spheres the spheres are also supposed to be perfectly smooth, and it is assumed that there is no force perpendicular to the line joining the centre of the sphere and the electron. In this case the ratio W^2/U^2 is given approximately by equation (3), so that if the molecules were perfectly smooth elastic spheres the value of λ should be $\lambda = 2m(k-1)/Mk$ approximately.

7. It would be difficult to obtain any such results, on ordinary dynamical principles, with an atomic model in which electrons move with high velocities in orbits round a nucleus. The average loss or gain of energy of another electron when it collides with this atom would depend on the kinetic energy of the electrons in the atom. Thus when electrons and atoms of the gas are in thermal equilibrium the energy of agitation of the electrons would be much greater than that of the atoms, and it would be impossible to account for the small values of k obtained in the experiments where the electrons move under an electric force.

In argon,* and to a lesser extent in helium, the values of k are, in some cases, above the exact value corresponding to perfectly elastic spheres, which may be taken as being due to some motion in the atom which has a very small effect on the transference of energy in a collision with an electron, but it is impossible to arrive at a very definite conclusion on this point owing to the probable error in the determination of k

8. The values obtained experimentally for the coefficient of elasticity, and the loss of energy of electrons in collisions with atoms of monatomic gases, are nearly the same as the calculated values for smooth elastic spheres The experiments are therefore in general agreement with the hypothesis of an atomic structure which is spherically symmetrical, and may harmonise with Schroedinger's conception of an atom.

The agreement is very remarkable in the case of helium as the experiments† extend over a large range of values of k. In the following table the loss of energy λ $(2\cdot46\,W^2/U^2)$ obtained experimentally for different values of k is given in the third line, and the loss calculated from the formula for elastic spheres in the fourth line. The experimental error in measuring W was about 3 per cent., and a similar error may occur in the measurement of k, so that the experimental error in $\lambda = 2\cdot46\,W^2/U^2$ may be as much as 8 or 10 per cent.‡

---

* 'J. Franklin Inst.,' vol. 200, p. 563 (1925).

† Townsend and Bailey, 'Phil. Mag.,' vol. 46, p. 657 (1923).

‡ With the smaller values of z/p, the error in the experiments with argon is greater than in those with helium.

Helium.

Z/p	0·013	0·02	0·05	0·20	1·0	1·5	2·5	5·0
k	1·77	2·12	3·68	11·3	53·0	79·0	124·0	172·0
$\lambda \times 10^4$	1·3	1·56	2·3	2·55	2·4	2·6	3·4	9·8
$\frac{2m}{M}\left(1-\frac{1}{k}\right) 10^4$	1·19	1·45	1·99	2·48	2·68	2·7	2·72	2·73

Thus there is a good agreement between the results of the experiments and the theoretical value of the loss of energy, for values of Z/p from 0·013 to 1·5 and values of k from 1·77 to 79.

For larger values of Z/p, λ is much greater than the theoretical values, which is due to large losses of energy in some collisions. With these values of Z/p ionisation by collision begins to be appreciable. The coefficient of ionisation α/p is 0·02 for $Z/p = 2{\cdot}5$ and 0·14 for $Z/p = 5{\cdot}0$.

9. It is possible that Atkinson may have found some ground for his suspicion of our methods in a paper by Compton,* quoted by him. Compton treated the relation of k and W theoretically, and arrived at results which he considered to be essentially different from ours. He wrote $e\,\Omega$ for the molecular kinetic energy which we have called $\frac{1}{2}M\,\Omega^2$, eU for the energy of agitation $\frac{1}{2}kM\,\Omega^2$, and his W^2 bears to our W^2 a ratio $0{\cdot}666MU/e$. He found an equation, equation (33) of his paper, which when squared becomes, in our notation,

$$k\,(k-1) = 0{\cdot}666\;W^2/e\,.\,2ek/\,\Omega^2,$$

or

$$k - 1 = 1{\cdot}33\;\;W^2/\,\Omega^2 \tag{4}$$

which is nearly the same as equation (2). The factor 1·33 is a little higher than the most probable value for elastic spheres, but this is unimportant since Compton himself described his calculations as approximate. What is surprising, is that Compton did not realise the close relation of his formula to those that had been published before, but drew attention to a difference of analytical form which does not, in fact, exist. Compton wrote down another equation, equation (34) of his paper, which when squared differs from his equation (33) by having $(k-1)^2$ in place of $k\,(k-1)$, and is therefore in our notation

$$(k-1)^2/k = 1{\cdot}33\;W/\,\Omega^2, \tag{5}$$

which does not appear to be correct.

10. In a paper on the transfer of energy in collisions between electrons and molecules I criticised some statements made by Jeans and Bloch in connection

---

* K. T. Compton, 'Phys. Rev.,' vol. 22, p. 333 (1923).

with an application of the Quantum Theory to electrical phenomena. According to Atkinson my objection is based on misapprehension as to the exact claims of the Quantum Theory, and he endeavours to show that no misunderstanding should arise from the statements made by Franck and Hertz. The following are examples of statements to which I made two objections.

Referring to the experiments made by Franck and Hertz, Jeans states, " Electrons were projected with ever-increasing velocity into a mass of mercury vapour. At first it was found that the electrons rebounded from the mercury atoms without any loss of energy whatever, precisely as though the mercury atoms were perfectly elastic spheres,"* and according to Bloch, " La discussion des résultats de Franck et Hertz conduit à la conclusion que, dans l'hélium pour les voltages inférieures à une dizaine de volts, tous les chocs sont parfaitement élastiques La perte d'énergie accompagnant la réflection est absolument négligeable."

My first objection was that in a perfectly elastic collision with a molecule supposed to be at rest an electron loses a small proportion of its energy which is not absolutely negligible

My second objection was to the effect that the experimental evidence on which the statements are based is not convincing.

The authors must have considered that their statements represented the general truth of the theory they advocated, but evidently they did not realise that in the accounts that Franck and Hertz have given of their work the phrase " collisions without loss of energy " referred to experiments which claimed to show with an accuracy then estimated at from 1/3rd to 1/10th of a volt that at low potentials " no loss " occurred on reflection Atkinson also points out that " the loss involved in an elastic collision, however, is of the order of 1/1000 volt, so that it is immediately evident that these experiments were concerned only with possible inelastic losses."

11. In 1917, Hertz (*loc cit.*) gave a theoretical estimate of the loss of energy of electrons in the experiment† with helium at 1·3 mm. pressure where the electrons moved from a filament to a grid with a potential difference of 18 volts. The electrons collide with a large number of electrons in which they lose energy so that on reaching the grid their kinetic energy V expressed in volts was less than 18. In order to determine V a plate electrode was fixed near the grid opposite the filament in the ordinary manner, and the potential difference P between the plate and the grid was adjusted so that after passing through the

---

* Jeans, ' Report on Radiation and the Quantum Theory,' second edition, p. 48 (1924).

† Franck and Hertz, ' Verh. D. Phys. Ges.,' vol. 15, p. 930 (1913).

grid the electrons moved in a retarding field towards the plate and a small proportion of the total number reach the plate. The current i to the plate diminishes as P increases and the curve representing i in terms of P shows that the current i is nearly zero at the point where P is 17 volts. If the potentials are measured to an accuracy of 1/5th of a volt the experimental error in determining the loss of energy in the collisions (18 — V) is about 20 per cent.

In the theoretical investigation an expression is obtained for the current i in terms of P assuming a certain angular distribution in the direction of motion of the electrons as they pass through the grid, the kinetic energy of each electron being V. For values of P corresponding to the smaller currents the equation connecting i and P is of the form

$$i = \mathrm{I}\,(1 - \sqrt{\mathrm{P}/\mathrm{V}}).$$

The agreement of this formula with the experimental results shows that a suitable angular distribution of velocity was assumed. As far as V is concerned the equation only shows that the constant V is the value of P at which $i = 0$. But the corresponding point on the experimental curve is not determined accurately owing to the fact that all the electrons have not the same energy when they arrive at the grid.

Having thus found the total loss of energy (18 — V), the loss in one collision is found by equating the potential (18 — V) to an estimated value of the total loss of energy of an electron in all the collisions it makes with atoms in passing through the accelerating field. This estimate involves a previous knowledge of the mean free path of an electron. The proportion of the energy of an electron lost in collision with an atom of helium was thus found to be $2{\cdot}7 \times 10^{-4}$ which agrees with the number $2{\cdot}73 \times 10^{-4} = 2m/\mathrm{M}$). According to Atkinson this investigation proves that "at all actual (not average) energies below about 20 volts in helium the collisions were strictly elastic."

If the problem be examined carefully it will be found that, apart from the difficulty of finding the total loss of energy (18 — V) from the experiments, this method of finding the average loss of energy in a collision is very unreliable. In fact the experiments would have been more in agreement with the theory of perfect elasticity, if the proportion of energy lost in a collision had been found to be less than $1{\cdot}3 \times 10^{-4}$, instead of $2{\cdot}7 \times 10^{-4}$.

In the theoretical investigation Hertz assumes that the total loss of energy of all electrons in collisions with atoms is the same (18 — V). This might be assumed to be sufficiently accurate for a first approximation if the atoms were perfectly elastic spheres at rest, as in this case the maximum loss of energy in a collision is $4m\mathrm{E}/\mathrm{M}$, which is only twice the average loss. But if the motion of the atoms be taken into consideration it is found that there are such large differences in the amounts of energy passing between electrons and atoms that all the electrons have not lost the same amount of energy in collisions while passing from the grid to the filament.

Even if each electron collided with the same number of atoms (say 200), a considerable proportion of them would arrive at the grid having lost on an average the amount $m\mathrm{E}/\mathrm{M}$ instead of $2m\mathrm{E}/\mathrm{M}$ in a collision. Since the small currents received by the plate are due to the electrons which have the largest energies in passing through the grid, the loss to be expected from these experiments, assuming the collisions to be perfectly elastic, should be as low as $m\mathrm{E}/\mathrm{M}$.

12. The interchange of energy in collisions depends on the ratio of the kinetic energy $m\mathrm{U}^2/2$ of the electrons to the energy of agitation $\mathrm{M}\,\Omega^2/2$ of the gas. In Franck and Hertz's experiments the temperature of the gas may be taken at about 70° C., since the gas is heated by the filament. Also the principal losses of energy occur with the large values of U so that the average kinetic energy of the electrons may be taken as about 15 volts, when they lose energy in collisions.

The interchange of energy may therefore be considered for the case in which

$$m\mathrm{U}^2 = 320\mathrm{M}\,\Omega^2.$$

In the collisions with atoms moving with the velocity Ω in the same direction as U the maximum loss of energy of an electron is $23m\mathrm{E}/\mathrm{M}$, and the maximum gain of energy when the atoms move in the opposite direction is $15m\mathrm{E}/\mathrm{M}$.

It is difficult to find an average effect taken over all kinds of collisions, but for the purpose of an approximate estimate it may be supposed that in all collisions the electrons either lose energy in the amounts $10m\mathrm{E}/\mathrm{M}$ or gain energy in the amounts $6m\mathrm{E}/\mathrm{M}$, and that these two types of collision are equally probable.

The case of a stream comprising a large number 8N electrons may be considered. After each electron has made 60 collisions the average loss of energy in a group of 4N is $70m\mathrm{E}/\mathrm{M}$, and in the remainder the average loss is $170m\mathrm{E}/\mathrm{M}$. Thus after 180 collisions there would be one group of N electrons in which the average loss is $210m\mathrm{E}/\mathrm{M}$ and another group of N in which the average loss is $510m\mathrm{E}/\mathrm{M}$.

This constitutes a cause of inequality in the energy V of the electrons arriving at the grid, which must be considered in any theoretical explanation of the experimental results obtained with a retarding potential.

13. Atkinson suggests that the purpose of the experiments made by Franck and Hertz in 1913 was to disprove a part of the hypothesis which I adopted* in explaining the action of electrons moving under a large electric force.

In this case the electrons lose a large proportion of their energy in collisions in which molecules are ionised, and in some other collisions also.

The following [three statements] contain the version of this Theory given by Franck and Hertz† .- ·

(1) The mean free path of electrons moving in the gas is given by the kinetic theory.

(2) Electrons lose all their energy at every impact with gas molecules.

(3) Ionisation by collision occurs when the energy of the impacting electron exceeds a definite value.

It cannot be considered that it was necessary to make experiments in 1913 to disprove the idea conveyed in the statements (1) and (2) as several experiments‡ had been made from 1908 to 1913 which showed that with the smaller velocities the energy of the electrons is not lost in collisions. Also the statements (1) and (2) never formed part of the theory referred to. The following statement explaining the action of negative ions (electrons) was given in my book on 'Ionisation by Collision,' p. 28 (1910):—

"It has been assumed that one effect of a collision is to reduce the velocity of the ion to a relatively small value, an assumption which seems reasonable when the velocities are so large that the ions tend to produce changes in the molecules by impact. In these cases a large proportion of the energy of an ion would be absorbed by the molecule, so that after the collision the ion would begin to move under the electric force with a small velocity. But when the velocities on impact are much below that which is required to ionise the molecule there is no reason for supposing that a large proportion of the kinetic energy of the ion is lost on collision; it may thus acquire the critical velocity more frequently than is shown by the calculations for the smaller forces."

In this theory N represents the number of collisions in which the electron loses a large proportion of its energy while moving through a distance of 1 cm. in the direction of the electric force, when the gas is at 1 mm. pressure. In a certain number α of these collisions, depending on the electric force the molecules are ionised.

---

* 'Theory of Ionisation by Collision' (1910).

† Franck and Hertz, 'Phys. Z.,' vol. 17, p. 411 (1916); Hertz, 'Verh. D. Phys. Ges.,' vol. 19, p. 268 (1917).

‡ Townsend, Haselfoot, Tizard, *loc. cit.*

It was pointed out that 1/N is not the mean free path of the electron obtained from the kinetic theory of viscosity. The value of N given for air at 1 mm pressure was 14·6, so that $1/N = 0 \cdot 07$ cm., whereas the mean free path obtained by the kinetic theory is 0·032 cm. A table of figures was given from which it may be seen that 1/N is more than double the mean free paths obtained by the kinetic theory for different gases

This theory contains the principles on which it is possible to obtain a rational explanation of the phenomena which occur when the electric force is increased and ionisation by collision is obtained It explains ionisation by collision and accounts for large losses of energy in other collisions ($N - \alpha$) where changes in the molecules are produced by the impacts of electrons, as are required in order to dissociate molecules of diatomic gases or excite radiation. The total number of collisions as estimated by the kinetic theory is much larger than N, and in all these (excepting the number N) the loss of energy of an electron is small.

Researches on the Chemistry of Coal. Part V.—The Maturing of Coal considered from the Standpoint of its Benzene-Pressure-Extraction.

By William A. Bone, D.Sc., F.R.S., Laurence Horton, Ph.D., and Louis J. Tei, B.Sc.

(Received July 4, 1928.)

Introduction

In Part III of this series* it was shown that on extraction with benzene under "soxhlet" conditions, at pressures between about 18 and 48 atmospheres (corresponding with temperatures between 240° and 285° C.), the coal substance of some typical coking bituminous and non-coking sub-bituminous† coals yielded between about 5 and 12 per cent. of its weight of an extract which, on treatment, successively, with light petroleum and ethyl alcohol, could be fractionated into four portions, as follows :—

---

* 'Roy. Soc. Proc.,' A, vol. 105, p. 608 (1924).

† It should be understood that the term "sub-bituminous" in this and previous papers refers to coals of maturity intermediate between bituminous coals and lignites proper.

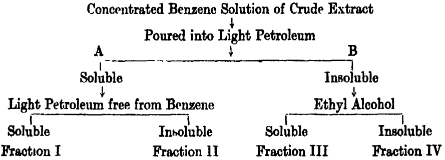

Fraction I consisted of neutral, yellowish-brown, non-nitrogenous, viscous oils or vaseline-like substances containing

$$C = 83{\cdot}3 \text{ to } 89{\cdot}7,\ H = 8{\cdot}1 \text{ to } 10{\cdot}8,\ O = 2{\cdot}3 \text{ to } 5{\cdot}5 \text{ per cent.}$$

Fraction II was a reddish-brown solid, softening about 25° C., and more difficult to characterise than the others.

Fraction III consisted of reddish-brown brittle "resinous" substances, weakly acidic, softening about 60° C., substantially free from nitrogen and sulphur, containing

$$C = 76{\cdot}25 \text{ to } 86{\cdot}6,\ H = 6{\cdot}6 \text{ to } 7{\cdot}8,\ O = 8{\cdot}8 \text{ to } 16{\cdot}5 \text{ per cent.}$$

Fraction IV was a neutral, amorphous, cinnamon-brown, nitrogenous, "humic" powder, softening between 185° and 230° C., and containing

$$C = 79{\cdot}9 \text{ to } 88{\cdot}5,\ H = 5{\cdot}4 \text{ to } 7{\cdot}7,\ N = 0{\cdot}8 \text{ to } 1{\cdot}5,\ S = \text{nil to } 0{\cdot}9, \text{ and}$$
$$O = 3{\cdot}50 \text{ to } 9{\cdot}25 \text{ per cent.}$$

It was also found that (i) whereas the first and second of these four fractions were quite devoid of "binding" qualities (when suitably heated in intimate admixture with powdered coke), and had no influence upon the coking propensities of coals, the third and fourth possessed them in a high degree, and (ii) provided that the last named exceeded about 2 per cent., below which limit the coals were non-coking, the coking propensities of coals could be approximately correlated with their yields of Fraction IV.

Other notable features of the investigation were that (1) in each case the pressure-extraction process had a definite "end-point," the extracted "residues" always being quite devoid of coking properties; (2) the oxygen-content of each of the four fractions diminished, and its carbon-content correspondingly increased, with the maturity of the coal substance; and (3) typical non-coking "semi-bituminous" coals, yielding between 10 and 18 per cent. of "volatiles" at 900° C., gave but little (0·5 to 1·25 per cent. only) crude extract, a circumstance which could be ascribed to the seam from which these coals were obtained having been subjected to the influence of "igneous intrusion" subsequent to their formation, whereby the benzene-extractable substances had been in greater part expelled from them.

It was also found that the immature brown coal occurring in the uppermost bed of the famous Morwell Deposit in the Gippsland Region of the State of Victoria in Australia yielded as much as 15 per cent. of crude extract. And while this extract in part comprised substances analogous to those constituting Fractions I and II from the much maturer "sub-bituminous" and bituminous coals, it also contained, instead of Fractions III and IV, a considerable quantity of alkali-soluble acidic and phenolic bodies as well as resene-like esters.

Altogether, a considerable body of weighty evidence was forthcoming of these benzene-extractable substances having played an important rôle in the maturing of the coal substance, especially in regard to the development of coking propensities; and it seemed desirable to continue their investigation, especially in regard to their occurrence in immature brown coals and lignites, with a view to tracing back (if possible) their origin in brown coals and the early stages of their subsequent development in lignites.

Fortunately in 1924 one of us (W. A. B.) had the opportunity, whilst visiting Canada with the British Asseciation, of seeing something of the important cretaceous Western Canadian Coalfield, which, stretching from the province of Saskatchewan in the east, through Alberta, to the Rockies in the west, shows in general a gradual maturing of the coals in an east to west direction; and, thanks to the co-operation of Drs. Charles Camsell, D. B. Dowling and R. E. Gilmore of the Canadian Department of Mines, he was afterwards supplied with properly-taken composite samples of typical coals from various parts of the field. Also, on representing the scientific importance of the matter to the Fuel Research Board, grants were placed at his disposal for maintaining a group of research assistants for its systematic investigation, which has been proceeding continuously since the beginning of 1925. The present paper embodies its principal results up to date.

An Experimental Examination of some Recent Criticisms.

Whilst the investigation was proceeding, however, the benzene pressure-extraction process has been the subject of certain criticisms which it will now be convenient to deal with in the light of our further experience.

(1) It has been asked, for example, how can there be any assurance of the substances comprising the "crude extract" having been originally present as such in the coal substance, seeing that during the benzene-pressure-extraction it is necessarily subjected to temperatures between 240° and 285° C.? Dr. H. G. Colman put the point to us quite clearly and fairly in the course of a discussion on the subject about a year after the appearance of our previous paper; he said that, whilst agreeing that the use of benzene is much preferable to that of pyridine as a "solvent" in the investigation of the coal substance, he was "not yet altogether convinced that even with benzene a partial resolution of the complex molecules did not take place at temperatures of 200° or over. In that case the benzene extract would not consist entirely of substances originally present in the coal, but would contain, perhaps in large proportion, less complex substances formed by the early action of heat upon some of the original coal substance"[*]

There are two experimental grounds on which the question thus raised may be answered decidedly in the negative.

In the first place (as previously recorded), in extracting a great variety of bituminous coals in no case have we ever observed any gas evolution at all, and only in one or two cases could any sign of water-elimination from the coal substance be detected, and then only of the slightest. The same also has applied generally to the sub-bituminous coals and black lignites examined. Indeed, it has been only in cases of very immature brown coals or brown lignites, whose "cellulosic" constituents admittedly begin to undergo "internal condensation" with simultaneous elimination of water and carbon dioxide at temperatures below 250° C., that we have ever detected any sign of gas-evolution or marked water-elimination; moreover, even in such cases, the implied "internal condensation" does not involve any breakdown of, or deep alteration in, the essential molecular structure of the coal substance.

Secondly, at Dr. Colman's suggestion, two typical bituminous coking coals—namely, (*a*) the South Wales hard-coking coal F. (yielding 22·6 per cent. of "volatiles" at 900° C. on the dry-ashless coal substance), referred to in our previous paper,[†] and (*b*) a rather weakly coking coal from the Shafton Seam of the Grimthorpe Colliery near Barnsley (Yorks), yielding 35·5 per cent. of "volatiles" on the dry-ashless coal substance at 900° C.—have been examined experimentally in the following manner: Each coal was pulverised to a suitable degree, and then dried in a vacuum oven. Two equal portions of each were then taken, one of which was immediately benzene-extracted in six successive stages at 18 to 55 atmospheres pressure, whilst the other was first of all maintained at between 220° and 270° C. for 7 days in a current of nitrogen, and afterwards benzene-extracted in similar manner.

---

[*] 'J. Soc. Chem. Ind.,' vol. 44, p. 299 (1925).

[†] *Ibid.*, p. 614.

In each case it was found that, concurrently with a marked diminution in the coking propensities, the effect of such heat-treatment was rather to diminish than to increase the percentage of benzene-extract, as the following figures show :—

	Percentage of total benzene-pressure-extract.		Percentage of Fractions III and IV.	
	From original coal.	From coal after 7 days heat-treatment at 240° to 270° C.	From original coal.	From coal after 7 days heat-treatment.
Welsh hard coking coal F.	7·8	6·5	5·4	3·85
Shafton coal	10·62	6·75	5·0	3·00

It should be added that, in each case, careful ultimate analyses of corresponding fractions obtained from the coal *before* and *after* the heat-treatment referred to showed no material difference between their compositions. Therefore, whilst in each case the heat-treatment diminished the amounts both of the total extract and of Fractions III and IV obtained therefrom, it did not materially alter in any way the chemical character of the several fractions. From this it may be reasonably inferred that the substances removed by benzene-pressure-extraction were not produced by thermal decomposition (in the sense of any real breakdown of the coal substance) but were pre-existent in it, either as such, or more probably in some loose molecular association with the coal complex.

(2) The conclusion put forward in Part III of this series that the nitrogenous "humic" bodies comprising our Fraction IV of the benzene-pressure-extract are "mainly responsible for the coking propensities of bituminous coals" has been questioned by F. Fischer and his colleagues of the Kaiser Wilhelm-Institut for Kohlenforschung in Mulheim-Ruhr. These investigators—who originated the method—extract coals with benzene at about the same pressure (55 atmospheres = 283° C.) as we employ, but for a shorter period; and whereas we divide our crude extract into four fractions, they divide theirs into two only—characterising these as "Oelbitumen" and "Festbitumen"

respectively—according as they are soluble or otherwise in a mixture of three parts petroleum ether and one part of benzene. And while in general confirming our experimental observations,* they consider that the "coking" propensities of coals really reside in their "Oelbitumen," although their "swelling" properties may be ascribed to their "Festbitumen." Also they have suggested that the proportion of "Oelbitumen" in a given coal increases with its maturity.

It may here be recalled that in 1925 Messrs. J. D. Davis and D. A. Reynolds of the U.S. Bureau of Mines in Pittsburgh, Pa., reported that, having (i) first extracted Mesa Verda and Pittsburgh Coals by benzene at 285° C. under a pressure of 55 atmospheres, (ii) then resolved their crude extract into "oils" and "solid" fractions by means of petroleum-ether, according to Fischer's method, and (iii) subsequently tested their "bitumens" both on the extracted residues and on a coke, their results were "*in substantial agreement with those of Bone as opposed to those of Fischer,*" and that "*contrary to the findings of Fischer and in agreement with those of Bone, the oily bitumen possessed little agglutinating power, whereas that of the solid bitumen was strong.*"†

In this connection, be it noted, we have never held that the coking propensities of coals can be *wholly* ascribed to the presence, or production in them, of the substances comprising our Fractions III and IV; on the contrary, in our previous paper we specially directed attention to the circumstance that on mixing the benzene-extracted coal-residues intimately with Fraction IV, in proportions corresponding with those found in the original coals, nothing like the strongly coking propensities of the latter were reproduced; from which it would seem "*as though some factor other than the mere intimate association of the chief coking constituents with the residues is required to develop fully the coking propensities of the coals.*"‡ The matter is doubtless more complicated than would appear at first sight, and further patient investigation may be needed to clear up all its aspects.

In comparing results obtained by Fischer's procedure with those given by ours, it should be remembered that, whereas throughout his pressure-extraction the coal is kept in contact with the *whole* of the benzene-solvent *plus* extract, in ours the soxhlet principle is used, whereby contact between the extracted substance and the residual mass is avoided. And for this reason we consider our procedure preferable to his.

---

* 'Brenstoff Chemie,' vol. 6, pp. 33 and 349 (1925). "Wir haben nunmehr sowohl unsere früheren Versuche wiederholt als auch den von Bone beschrittenen Weg nachgearbeitet und konnten unsere früeren Angaben ebenso wie die Angaben von Bone bestätigen" (*ibid.*, p. 351).

† 'Ind. Eng. Chem.,' vol. 18, p. 838 (1926).

‡ *Ibid*, p. 617.

Desirous of clearing up matters, we have recently made a comparison between our extraction method and his, using a strongly coking Durham coal from the "Busty" seam (volatiles at 900° C. = 25·5 per cent. of the dry-ashless coal substance[*]), and then resolving the crude extract into fractions by our method (in each case our Fraction I was further resolved into two portions I (*a*) and I (*b*), according as it was volatile in steam or not) with the following suggestive results:—

Extraction method	Total extract.	Fraction				
		I.		II.	III	IV.
		(*a*).	(*b*).			
	Per cent.	Per cent.	Per cent.	Per cent.	Per cent.	Per cent.
Fischer .	12·44	1·27	2·99	1·68	0·04	6·46
Bone .	15·60	1·33	1·96	3·03	0·04	9·24

It would thus seem as though the extraction according to Fischer's method was less complete than in ours, especially in regard to Fraction IV, although his method yielded more of Fraction I (*b*) than ours. Contrary to our former experience, we have also found that in the case of *some* (though by no means all) coking coals, our Fraction II (which would be contained in Fischer's "Oelbitumen") does contribute as well as Fractions III and IV to the binding properties. It therefore seems possible that the apparent differences between Fischer's observations and ours may be in part due to this seeming inconstancy in the properties of our Fraction II. Indeed, from the outset of our work, we have never regarded Fraction II as so clearly representing a distinct type of substance as do the other three of our fractions. This is a matter which will be again referred to later.

With regard to Fraction I, however, we can only say that, having now examined a large number of different coals of all classes (black lignites, sub-bituminous, bituminous, etc.) covering a wide range of properties, we have never once found that it has *per se* any influence upon the coking propensities; nor have we ever found it possible to correlate the two in any way. In this conclusion we are supported by the observations of Mr. Harold Nielsen, who isolated a neutral oil of the same character and composition as our Fraction I from the oils resulting from his process for the low-temperature carbonisation of coals by direct contact with hot gases; and he confirmed our observations as to its non-binding propensities.

---

[*] The ultimate composition of this coal substance was C = 87·75, H = 5·00, N = 1·55, S = 0·75 and O (by diff.) 4·95 per cent.

(3) More recently C. Cockram and R. V. Wheeler have criticised our correlation of coking propensities with the yields of Fraction IV by our method on the grounds that this fraction is not homogeneous but can be resolved further into two parts, soluble and insoluble in ether respectively, each of which they regard as "resin" or "resin-like," notwithstanding their nitrogenous characters, high softening points, and other clearly non-resinous characteristics. Whilst it may be true that our Fraction IV is not entirely homogeneous—(indeed, it is hardly possible by any method yet proposed to resolve any coal "extract" into a *limited* number of typical fractions each one of which shall be in *all* respects homogeneous)—we have found that such further resolution of Fraction IV by ether-treatment has no effect either upon the chemical composition or the binding properties of the soluble and insoluble portions respectively, as the following results obtained by resolving Fraction IV from the strongly coking Durham "Busty" coal will show.

Fraction IV from Durham "Busty" Coking Coal.

Ultimate composition.	(*a*). Ether-soluble portion.	(*b*). Ether-insoluble portion.
	Per cent	Per cent.
C	86·60	87·65
H	5·75	5·50
N	1·80	1·60
S	0·75	0·70
O (by diff.)	5·10	4·55
	100·00	100·00

Moreover, apart from the close similarity thus shown between the ultimate compositions of the ether-soluble and insoluble portions of Fraction IV, other evidence was forthcoming of their identity as regards chemical type, and they were indistinguishable as regards binding properties. We regard the difference between Fraction IV (*a*) and (*b*) as merely what might be expected in the case of a mixture of colloidal substances of the same chemical type but different molecular aggregations. From such standpoint the criticism referred to seems insubstantial.

The Extraction of Morwell Brown Coal.

We may appropriately commence the discussion of the main problem—namely, how the various typical substances comprised in the benzene-pressure-extract from a bituminous coal have originated and been developed—by considering the character of those derived from the immature tertiary brown coal occurring in the uppermost bed of the Morwell Deposit in Victoria (Australia).

The Raw Coal.—The sample of raw coal investigated contained rather more than 50 per cent. of water and about 4 per cent. of mineral matter, whilst the dry-ashless coal substance contained C = 64·9, H = 4·8, N and S = 0·8, and O = 29·5 per cent., and at 900° C. yielded 53·3 per cent of "volatiles." This composition is characteristic of an earthy brown coal in a very early stage of development.

Its Extraction.—Contrary to all our experience with the well-matured sub-bituminous and bituminous coals previously examined, during the benzene-pressure-extraction of the dried Morwell coal, at pressures between 40 and 48 atmospheres (corresponding with temperatures between 250° and 280° C.), a small quantity of water, together with some gas containing 85 per cent. of carbon dioxide and 15 per cent. of carbon monoxide, was eliminated from the coal substance, whose "cellulosic" constituents had evidently undergone some "internal condensation," without breakdown of the prime molecular structure.

Phenolic Constituents of the Crude Extract.—It was immediately evident that the crude extract differed materially from any of those hitherto obtained from sub-bituminous or bituminous coals. Indeed, between 50 and 60 per cent. of it was phenolic in character and soluble in alkali. A detailed examination of this alkali-soluble fraction resulted in the isolation of the following :—

(i) *Phenol*—probably up to about 60 per cent. of the whole—identified by conversion into phenyl 3 : 5 dinitrobenzoate melting at 146° C.

(ii) *p-Cresol*—probably up to about 25 per cent. of the whole—identified by conversion into *p*-tolyl 3 : 5 dinitrobenzoate melting at 180° C.

(iii) *Catechol*—in small amount—melting at 104° C., and further identified by conversion into its diphenylurethane melting at 167° to 168° C.

Other unidentified phenolic bodies were also present.

Basic Constituents.—The crude benzene-extract also yielded basic substances, soluble in dilute hydrochloric acid, but in too small proportion to permit of their identification.

Neutral Oils.—After removal of the foregoing acidic and basic constituents, the remaining 40 per cent. of the crude benzene-extract consisted of a dark reddish-brown, neutral oil, resolvable into four different portions, as follows :—

(i) *A very small portion volatile in steam*—consisting principally of the hydrocarbons *diphenyl* and *mesitylene*.

(ii) *Saponifiable phenolic esters*, in all about one-seventh of the total neutral oil.

(iii) *Dark brown, vaseline-like, non-nitrogenous substances, soluble in light petroleum*, and containing C = 81·8, H = 9·7, and O = 8·5 (S in traces only) per cent. These substances constituted at least 60 per cent. of the total neutral oil, or (say) about 3·5 per cent. of the original dry-ashless coal substance, and were in all essentials comparable with the Fraction I of the benzene-pressure-extract from sub-bituminous and bituminous coals.

(iv) *A non-nitrogenous, amorphous, chocolate-brown powder, insoluble in light petroleum*, and containing C = 73·2, H = 7·9, and O = 18·7 (S less than 0·2). This constituted about 25 per cent. of the total neutral portion of the crude benzene-pressure-extract, and in many respects resembled the Fraction II of the crude extracts obtained from sub-bituminous and bituminous coals.

Summary.—Neglecting constituents present in small proportions only, the crude benzene-pressure-extract from this Morwell brown coal had thus been resolved into four principal fractions as follows :—

Crude Extract = 15 per cent. of Original Coal Substance.

	I. Neutral oils soluble in light petroleum.	II. Neutral amorphous, chocolate-brown powder insoluble in light petroleum.	III Phenolic esters.	IV. Phenols.
Approximate percentage of original coal substance	3·5	1·5	1·0	9·0
	Characters resembling those of Fractions I and II respectively from bituminous coals.		No resemblance to fractions from bituminous coals.	

The extraction of so large a quantity of phenolic bodies from the coal substance of an immature brown coal is a remarkable circumstance. And the question naturally arose, were these bodies pre-existent as such in the original coal substance, or had they been produced from it by incipient thermal decomposition during the extraction process? Accordingly, experiments were carried out from which it was inferred that, although not present in the free state, these phenols were pre-existent in the coal substance in some loose "molecular association," rather than in firm chemical union, with the main coal-complex. So that, on fractionally extracting the dry coal substance with benzene under pressure in successive periods of about 2½ hours each, the earlier fractions contained much larger proportions of phenols than did the later ones.

Extraction of Coals from the Western Canadian Coalfield.

The Canadian coals investigated in this connection comprised:—

(i) A typical tertiary brown lignite from Estevan in Saskatchewan.

(ii) A series of four black lignites or non-coking sub-bituminous coals of cretaceous origin from various places in Alberta.

(iii) A non-coking semi-bituminous coal—also of cretaceous origin—from Canmore, Alberta. Their proximate and ultimate analyses are shown in Table I, where the coals are arranged in order of their maturities, beginning with the least mature of them.

Table I.—Proximate and Ultimate Analyses of the Western Canadian Coals.

Coal.	Per cent. water in raw coal as received.	Per cent. ash on dry coal.	Per cent. "volatiles" at 900° C. in dry-ashless coal.	Ultimate composition of dry-ashless coal.				
				C.	H.	N.	S.	O.
1. Estevan	37 8	7 65	44 9	67 75	4 3	0 95	0·6	26·4
2. Cardiff	18 0	11 7	41 3	71 2	4 3	1·7	0·5	22 3
3. Rose Deer	16 0	9 0	40 3	72 6	4·2	2·0	0·6	20·6
4. Pembina	15·2	15 0	38·1	73·8	4·3	1·4	0 4	20 1
5. Harlech	6·9	8·8	36·0	76·0	4 3	1·2	0·5	18·0
6. Canmore	1·6	6·2	14·1	89 7	4·0	1·4	1·0	3·9

Further particulars about them are as follows:—

(1) "*Estevan*," from the top 7-ft. seam of tertiary brown lignite with a 25-ft. "overburden" of clay shale belonging to the Estevan Coal and Brick Company, S. Saskatchewan.

(2) "*Cardiff*," from a seam near Edmonton just under the surface at the base of the Edmonton formation, a brackish water deposit 700 feet thick, at the top of the cretaceous.

(3) "*Rose Deer*," from a seam at Drumheller of the same horizon as the "Cardiff," but having had a 400-ft. cover since late Miocene times.

(4) "*Pembina*," from a seam near Pembina, under a 100-ft. cover mostly of sandstones.

(5) "*Harlech*," from a seam of horizon near that of "Cardiff" but, being nearer the mountains, the series of sediments enclosing the seams is much thicker, so that the "overburden" is much greater, and consequently the coal is much more matured, than in the "Cardiff" seam.

(6) "*Canmore*," from a seam in the lower cretaceous formation which has passed through the stress of mountain building. In the Crow's Nest Pass the coals are coking, but in the seam at Canmore the coal is semi-bituminous.

All the coals were comparatively lean as regards benzene-extractable constituents and absolutely devoid of coking properties.

Extraction of the Estevan Brown Lignite.—On extracting 425 grams of the dry coal with benzene in three stages at 17 to 50 atmospheres, small amounts of gas ($CO_2 = 80 \cdot 4$, $CO = 11 \cdot 5$, $H_2 = 0 \cdot 1$, $CH_4 = 0 \cdot 8$, $N_2 = 6 \cdot 5$ per cent.) and water were eliminated during the first stage, but not thereafter, much as had been observed with the Morwell Brown Coal, and indicative of a similar "internal condensation" of part of the coal substance. Although the total amount of crude extract obtained when the "end-point" had been reached was only 4·5 per cent. of the dry-ashless coal substance (as compared with the 15 per cent. yielded by the Morwell brown coal), the character and composition of the two extracts were practically the same, save that whereas the proportion of phenolic to neutral portions in the case of the Morwell coal was about 60/40, with Estevan coal it was as nearly as possible 50/50.

The phenols isolated from the acidic portion of the Estevan extract (phenol, *p*-cresol, and catechol) were the same, and nearly in the same proportions, as in the Morwell extract (*q.v.*). The neutral portion likewise comprised very similar substances—namely, diphenyl, mesitylene (volatile in steam), phenolic esters, and non-nitrogenous, non-volatile, neutral oils (partly soluble and partly insoluble in light petroleum) containing $C = 83 \cdot 14$ to $84 \cdot 16$, $H = 9 \cdot 3$ to $9 \cdot 4$, $O = 7 \cdot 5$ to $6 \cdot 4$, but mere traces of sulphur—to those contained in the corresponding portion of the Morwell extract. And, save that the Estevan non-volatile oils contain much less oxygen, and correspondingly more carbon and hydrogen, than the corresponding Morwell oils, the similarity of the two was very close. Both of the crude extracts likewise contained small amounts of basic substances. Altogether, then, the only difference between the two crude extracts lay in the less oxygenated character of the Estevan non-volatile neutral oil fraction, which is only what might be expected from the greater maturity of the Estevan coal.

The following shows how the 4·5 per cent. (referred to the dry-ashless coal-substance) yield of crude extract from the Estevan coal was distributed among the four principal fractions into which it had been resolved, namely :—

I. Neutral oils soluble in light petroleum.	II. Neutral solids insoluble in light petroleum.	III. Phenolic esters	IV. Phenols.
Percentage of coal substance.			
1·65	0·30	0 30	2 25

It is remarkable how closely, in nearly all respects, the extract obtained from this Canadian brown lignite resembled that obtained from the Australian brown coal; indeed, but for the yield in the latter case being more than three times greater than in the former, and for the less oxygenated character of the Estevan non-volatile neutral constituents, the difference between the two extraction-results was so small as to suggest a close similarity in the chemical aspects of the brown coal formation from the original vegetable débris in the two cases. It is our intention, in future work, to examine typical brown coals from other localities with a view to finding whether or not the similarity referred to can be regarded as pertaining to brown coals generally.

Extraction of the Black Lignites from Alberta.—Each of the four "lignitic" coals ("Cardiff," "Rose Deer," "Pembina" and "Harlech")—ground so as to pass a 20- but to remain on a 40-mesh sieve—was first of all dried and then extracted with benzene under pressure in 400- to 500-gram batches, usually in two stages, namely, first for about 50 hours at 33 atmospheres pressure and then for another similar period at 40 to 48 atmospheres pressure, under "soxhlet" conditions in the special apparatus described in our previous paper (*q.v.*).* In each case a complete extraction was thus effected; moreover, it is important to note that *in no case was there either any evolution of gas or sign*

---

* *Ibid.*, p. 610.

of water-elimination from the coal, a circumstance which may be regarded as rebutting any suggestion of decomposition (in the sense of breakdown) of the coal substance during the extraction process. The total extract so obtained varied in the different coals between 3·15 and 4·30 per cent. of the dry coal substance.

It was immediately evident, from subsequent examination of the crude extracts, that they differed from those obtained from either of the two brown coals (Morwell and Estevan) examined in being non-phenolic in character, and resembled more those obtained from sub-bituminous and bituminous coals. Indeed, it became clear that, while the *amount* of "total" extract obtained was not materially altered, the transition from the Estevan brown lignite to the Alberta black lignites had involved a profound change in at least the phenolic and phenolic-ester constituents (*i.e.*, Fractions IV and III) of the former, causing their complete disappearance as such.

Indeed, the benzene-extracts had acquired such a likeness to those normally obtainable from bituminous coals that not only could they be resolved into four "fractions" by the same solvent treatment with light petroleum and ethyl alcohol as had been employed in the case of bituminous coals (*q.v.*), but also the characters of resulting fractions resembled the corresponding fractions of a typical sub-bituminous or bituminous coal-extract.

The results of the benzene-pressure-extraction of these four coals, and of the resolution of their respective "crude extracts" into four fractions by means of light petroleum-ether and ethyl alcohol (as outlined in the introduction hereof), as well as the ultimate composition of each of the four fractions so obtained, are detailed in Tables II and III.

Table II.—Results of the Benzene-Pressure-Extractions of the Western Canadian Coals expressed as Percentages on the Dry Coal Substance.

Coal.	Total extract.	Fraction.			
		I.	II.	III.	IV.
1. Estevan	4·5	1·65	0·3	0·3†	2·25*
2. Cardiff	3·15	1·55	1·10	0·35	0·15
3. Rose Deer	3·85	2·20	0·70	0·75	0·20
4. Pembina	3·85	1·50	1·45	0·60	0·30
5. Harlech	4·30	1·3	1·3	1·20	0·50
6. Canmore	1·35	1·2	0·1	0·02	0·03

† Phenolic esters and * Phenols not found in any of the other maturer coals.

Table III.—Ultimate Compositions of the Fractions and Residues from the Western Canadian Coals.

Coal.	Fraction I.					Fraction II.					Fraction III.				
	C.	H.	N	S.	O.	C.	H.	N.	S.	O.	C.	H.	N.	S.	O.
Cardiff	83·3	10·1	Nil	Trace	6·6	77·45	8·7	Trace	0·25	13·6	74·65	6·35	Nil	Trace	19·0
Rose Deer	81·7	9·85	Nil	Trace	8·45	77·0	9·3	Nil	0·20	13·5	75·65	5·6	1·5	0·45	16·8
Pembina	82·75	9·95	Nil	Trace	7·30	78·0	8·95	Trace	0·15	12·9	78·3	6·0	Trace	0·3	15·4
Harlech	84·85	9·0	Nil	Trace	6·15	80·0	6·5	0·95	0·30	12·25	80·0	6·2	Trace	Trace	13·8
Canmore	86·45	9·15	Nil	Trace	4·4	83·4	5·6	Trace	Trace	11·0	78·25	6·2	Nil	Trace	15·5
General description	Neutral semi-solid dark red-brown waxes. (Canmore = oil.)					Chocolate-brown solids.					Brittle red-brown "resinous" solids.				

Coal.	Fraction IV.					Residue.					
	C.	H.	N.	S.	O.	C.	H.	N.	S.	O.	Per cent. volatiles at 900° C.
Cardiff	77·0	6·55	0·5	0·2	15·75	71·1	3·65	1·6	0·35	23·25	42·0
Rose Deer	78·4	5·8	0·5	0·2	15·1	70·0	3·45	1·85	0·55	24·15	37·8
Pembina	79·15	6·05	Nil	0·2	14·6	73·7	3·75	1·25	0·35	20·95	37·8
Harlech	79·1	5·5	Nil	0·05	15·35	75·45	4·0	1·25	0·35	18·95	35·2
Canmore	81·9	5·15	0·5	0·2	12·25	88·75	3·85	1·35	0·80	5·25	14·6
General description	Very dark brown powders.										

Fraction I (the yield of which varied between 1·3 and 2·2 per cent. of the original dry coal substance) was in each case a semi-solid (or vaseline-like) non-volatile, dark red-brown, non-nitrogenous substance of neutral reaction with comparatively high carbon and hydrogen, but low oxygen, contents, thus :—

$$C = 81{\cdot}8 \text{ to } 84{\cdot}85,\ H = 9{\cdot}0 \text{ to } 10{\cdot}1,\ O = 6{\cdot}15 \text{ to } 8{\cdot}45.$$

Except for its greater oxygen content, this fraction closely resembled, both in ultimate composition and general character, the corresponding Fraction I obtained from sub-bituminous or bituminous coals. Indeed, the whole evidence of the investigation irresistibly compels us to the conclusion that these "neutral oils" are contained in coals of all ages and maturities from brown coals up to bituminous, as the following data regarding their ultimate compositions will (we think) sufficiently indicate :—

Coal.	Percentage compositions of non-nitrogenous neutral oils (Fraction I).		
	C.	H.	O.
1. Morwell brown coal	81·8	9·7	8·5
2. Estevan brown lignite	83 to 84	9·3 to 9·4	6·4 to 7·5
3. Four Alberta black lignites	81·7 to 84·45	9·0 to 10·1	6·15 to 8·45
4. Two sub-bituminous coals	83·3 to 85·3	10·1 to 10·8	4·6 to 5·6
5. Four bituminous coking coals	87·9 to 89·0	8·0 to 9·2	2·3 to 3·2

Another characteristic and constant feature of these neutral oils is that they are quite devoid of "binding power" [*e.g.*, when slowly heated up to 900° C. in suitable intimate (10/90) admixture with either powdered coke or benzene-extracted coal "residues"] a circumstance which (*inter alia*) confirms our conclusion that *per se* they have no direct influence upon the coking propensities of coals.

Fraction II (the yield of which was between 0·7 and 1·45 per cent. of the dry coal substance) was always a chocolate-brown, amorphous solid and (except in one case) non-nitrogenous, or practically so. Its ultimate composition lay between the limits :—

$$C = 77{\cdot}0 \text{ to } 80{\cdot}0,\ H = 6{\cdot}5 \text{ to } 9{\cdot}3,\ N = \text{nil to } 0{\cdot}95,\ O = 12{\cdot}25 \text{ to } 13{\cdot}6 \text{ per cent.}$$

In many respects, including chemical composition, it resembled the Fraction II similarly obtained from sub-bituminous and bituminous coals; indeed, we think that, as is undoubtedly the case with Fraction I, the type of bodies composing it persist through coals of all maturities, as the following figures relating to ultimate composition indicate :—

Coal.	Percentage composition of Fraction II.		
	C.	H.	O.
Morwell brown coal	73·2	7·9	18·7
Four Alberta black lignites	77·0 to 80·0	6·5 to 9·3	12·25 to 13·6
Two sub-bituminous coals	78·8 to 82·7	9·75 to 11·75	8·0 to 8·5
Three bituminous coking coals	81·3 to 87·8*	6·25 to 6·90	4·1 to 10·25

* In two out of these three coking coals C = 81·3 to 82·8 and O = 8·5 to 10·25.

As will be seen later, the characterisation and interpretation of this fraction are, however, less clear and certain than with any of the others ; thus, whereas in the two brown coals and three of the black lignitic coals, it was non-nitrogenous (or practically so), in the "Harlech" coal (as in most bituminous varieties hitherto examined) it contained nearly 1 per cent. of nitrogen.

Fraction III was always a reddish-brown amorphous brittle substance of resinous appearance, and (save in one case) substantially non-nitrogenous. Its ultimate composition varied between the following limits :—

$$C = 74 \cdot 65 \text{ to } 80 \cdot 0, \; H = 5 \cdot 6 \text{ to } 6 \cdot 35, \; O = 13 \cdot 8 \text{ to } 19 \cdot 0 \text{ per cent.}$$

In nearly all respects (save greater oxygen- and smaller carbon-contents) this fraction resembled that of the corresponding Fraction III from bituminous coals , and, taken as a whole, the evidence of the investigation so far strongly supports the supposition that the type of substance comprising this fraction first appears during what may be termed the "black lignitic" stages of coal-formation, and persists (and in some cases even increases) during its later stages.

Fraction IV, which was present in small proportion only, was composed of amorphous, chocolate-brown solids (sometimes containing up to 0·5 per cent. of nitrogen, sometimes none at all) which in most respects resembled the corresponding Fraction IV from semi-bituminous and bituminous coals. And there is little doubt in our minds that the two are generically connected.

The question naturally arises as to what connection or significance (if any) there is between the disappearance of the phenolic esters and phenols found in the two brown coals and the appearance of these foregoing two fractions III and IV when the "black-lignitic" stage is reached ; but at present we can only direct attention to the circumstance, leaving the query to be answered after further knowedge has accrued.

The Extraction of Canmore Semi-Bituminous Coal.—This non-coking semi-bituminous coal from the extreme western part of the W. Canadian Coalfield yielded only 1·35 per cent. of benzene-pressure-extract, which was almost entirely composed of the neutral oil Fraction I. Apparently, under "the stress of mountain building" subsequent to the formation of the seam, the coal had lost nearly all the bodies contained in the Fractions II to IV found in the other Alberta coals, a circumstance which recalls our former observations in regard to Welsh and Spanish semi-bituminous coals (*q.v.*).*

Also, on steam distilling Fraction I, besides a trace of diphenyl (m.p. 69° C.), about a quarter of it passed over as a lemon-yellow, pleasantly odorous mobile oil, leaving a non-volatile, reddish-brown oil from which a trace of solid separated on long standing. In this respect the "Canmore" Fraction I, while differing from the corresponding fractions obtained from the four Alberta lignitic coals, behaved similarly to Fraction I from most of the bituminous coals examined; thus we obtained:—

	Percentage on dry-ashless coal.	Ultimate composition.		
		C.	H.	O.
Fraction I—		Per cent.	Per cent.	Per cent.
(*a*) Steam-volatile.	0·33	82·95	8·40	8·65
(*b*) Non-volatile	0·83	86·45	9·15	4·40

It will be observed how, save for a *slightly* higher oxygen content, the ultimate composition of the non-volatile Fraction I (*b*) fell within the limits already found for the non-volatile neutral oil Fraction I obtained from fully developed bituminous coals. These features of our results rather suggest some thermal resolution of the non-volatile neutral oils found in the brown coals and black lignites into (*a*) volatile and (*b*) non-volatile portions during the transition from the "black lignite" to the "bituminous" stage in the maturing process.

The Extraction of Bituminous Coals.

During the course of our further investigations, a number of bituminous coals, other than those previously examined, have been extracted with results generally confirming our former conclusions. We think it desirable, however, now to describe in some detail the results obtained with three of these newly examined bituminous coals, because of their special interest in relation to the matters now under discussion. These coals were as follows:—

---

* Part III, *loc. cit.*, p. 617.

(1) *Shafton Coal.*—A weakly coking variety from a seam, not very far below the surface, in the Grimthorpe Colliery of the Carlton Main Colliery Company near Barnsley (Yorks). As received by us, it contained about 10 per cent. of moisture, the *dry* coal having 5·45 per cent. of ash. Its interest was that, while giving good yields of oils and a "semi-coke" of satisfactory quality, it swelled considerably between 300° and 600°, and on carbonisation at 900° yielded a weak coke. The dry-ashless coal substance contained,

$$C = 77\cdot35,\ H = 4\cdot95,\ N = 2\cdot00,\ S = 2\cdot00,\text{ and }O = 13\cdot7\text{ per cent.},$$

and at 900° C. yielded 35·45 per cent. of "volatiles."

(2) *Busty Coal.*—A typical Durham hard-coking coal from the "Busty" seam in Langley Park Colliery belonging to the Consett Iron Company (Co. Durham). The dry coal contained 3·45 per cent. of ash, while the dry-ashless coal substance contained,

$$C = 87\cdot75,\ H = 5\cdot00,\ N = 1\cdot55,\ S = 0\cdot75,\text{ and }O = 4\cdot95\text{ per cent.},$$

and at 900° C. yielded 25·5 per cent. of "volatiles."

(3) *A South African Coal.*—A non-coking coal from the upper portion of No. 2, or the main-working, seam in the Coronation Colliery, Witbank, E. Transvaal, South Africa. There are altogether five seams in this coalfield, all more or less horizontal, the coals being considered as of permo-carboniferous age. No. 2 seam lies about 100 feet below the surface, but about 5250 feet above sea-level. The dry coal (as received by us) contained 10·35 per cent. ash; and the dry-ashless coal substance contained,

$$C = 81\cdot75,\ H = 4\cdot50,\ N = 2\cdot00,\ S = 0\cdot55,\text{ and }O = 11\cdot2\text{ per cent.},$$

and at 900° C. it yielded 27·6 per cent. of "volatiles," the residue being an absolutely non-coherent powder.

From our point of view, the interest of coals (2) and (3) lies in the fact that, while (3) is obviously a less matured coal than (2) and devoid of coking porperties, both yielded at 900° C. nearly the same percentage of "volatiles" (namely, 25·5 and 27·6 respectively). According to the Regnault-Grüner classification of bituminous coals, both of them should be strongly

Table IV.—Showing Results of Extractions of Bituminous Coals

Coal	Shafton					Busty					South African				
Total yield* of crude extract	10 6					15 6					7 5				
Yields* of fraction	I (*a*)	I (*b*)	II	III	IV	I (*a*)	I (*b*)	II	III	IV	I (*a*)	I (*b*)	II	III	IV
	1 22	2 28	2 14	2 30	2 68	1 33	1 96	3 03	0 04	9 24	0 56	1 16	1 97	0 60	3 20
Ultimate composition C	80 20	85 85	83 50	79 25	80 55	83 25	87 40	89 20	74 60	85 50	76 95	86 00	83 15	78 55	83 40
H	9 40	8 85	7 05	6 20	5 55	11 55	8 85	6 40	6 70	5 30	9 20	9 00	6 55	6 10	5 80
N	Nil	Nil	Nil	Trace	Trace	Nil	Nil	1 00	Nil	1 60	Nil	Nil	1 35	1 90	1 50
S	Nil	Trace	Trace	Trace	Nil	Nil	Trace	1 05	Nil	0 70	Trace	0 20	0 30	0 30	0 40
O	10 40	5 30	9 45	14 50	13 90	5 70	3 75	2 35	18 70	6 90	13 85	4 80	8 65	13 15	8 90

* All these yields are expressed as percentages on the dry ashless coal substance

coking coals; but whereas the Durham coal is such, the South African coal is absolutely without any coking propensities at all.

Broadly speaking, the results of our benzene-pressure-extractions of these coals—which were all carried out to completion in our usual manner—as shown in Table IV, support our previous conclusions as to the coking propensities of coals being bound up with their yields of Fractions III and IV (but chiefly IV) rather than with those of the neutral oil Fraction I. For, whereas the hard-coking Durham ("Busty") coal gave the largest yield of Fraction IV ever obtained by us (namely, no less than 9·24 per cent. referred to the "dry-ashless coal-substance") the combined yields of Fractions III and IV from the weakly coking Shafton Coal amounted to just under 5 per cent, and from non-coking South African coal to 3·8 per cent. only. The corresponding yields of the neutral Fraction I—namely 3·3 ("Busty"), 3·5 ("Shafton") and 1·72 (S. African); or 1·96 ("Busty"), 2·28 ("Shafton") and 1·16 (S. African), if the non-volatile portion thereof be regarded as the more proper criterion—were, however, in no relation to the coking propensities of the coals. Generally speaking, also, the ultimate compositions and characteristics of the several fractions were in line with those previously found in the case of bituminous coals.

One or two new points, however, emerged from these further experiments, namely, (1) Fraction I could now always be resolved into two portions (I (*a*) and I (*b*)) volatile and non-volatile in steam, respectively, of which I (*a*) had a naturally higher oxygen content than I (*b*); the latter probably comprised what may be regarded as the true "neutral oils" of the original coals; (2) in the case of the hard-coking "Busty" (Durham) coal, Fraction II (as well as Fractions III and IV) had binding properties and, therefore, contributed to the coking propensities; and (3) Fraction IV from the "Shafton" coal (according to oxygen-content the least mature of the three examined) was, practically speaking, non-nitrogenous.

Summary and Conclusions.

For convenience of reference the general results of our benzene-pressure-extracts up to date of coals of greater maturity than the Morwell brown coal and Saskatchewan brown lignite are now summarised in Table V. The principal results, and conclusions therefrom, of these our further investigations are summarised in the following paragraphs :—

(1) Broadly speaking, the results of our previous work have been confirmed and extended, except it is now shown that in some cases Fraction II

Table V.—Summarising all Benzene-Pressure-Extraction Results to Date (excepting those with the Brown Coals).

Coal.	Coking propensity.	Per-centage oxygen on dry-ashless coal	Per-centage volatiles on dry-ashless coal.	Percentage yield of Fractions—				
				I.		II.	III.	IV.
Canadian black lignites.								
"Cardiff"	Nil	22 3	41 3	1·55		1 10	0 35	0·15
"Rose Deer"	Nil	20 6	40·3	2·20		0·70	0·75	0·20
"Pembina"	Nil	20 1	38·1	1·50		1 45	0·60	0 30
"Harlech"	Nil	18·0	36·0	1·30		1·3	1·20	0·50
Sub-bituminous.								
New Zealand	Nil	21 2	45·4	2 9		1·7	2·4	1·2
Nigerian	Very feeble	12 55	45 0	1·8		0 3	0 8	2 1
Bituminous.								
				I (a).	I (b).			
South African	Almost nil	11·22	27 58	0·56	1 16	1·97	0 60	3 20
Shafton	Weak	14·6	35 5	1 22	2·28	2·14	2·30	2·68
				I.				
Barnsley	Fairly strong	7·93	33 1	2 20		0·6	0 4	5 1
Spanish	,,	6 61	21 7	3 9		0 2	0 7	4·6
Welsh	Strong	7·8	22 6	1 3		1·1	0·3	5·1
Durham (Langley Park)	Very strong	7·6	27 0	1 9		1·7	0 8	7·0
				I (a).	I (b)			
Durham (Busty)	,,	4·95	25·5	1·33	1 96	3·03	0 04	9·24
Semi-bituminous.								
Spanish	Nil	4·13	17·9	Total extract 0·48 per cent.				
Welsh	Nil	5·67	10 2	Total extract 1·25 per cent.				
				I.				
Canadian (Canmore)	Nil	3·9	14·1	1·2		0 1	0·02	0 03

(as well as Fractions III and IV) may contribute to the coking propensities of bituminous coals, which, however, while chiefly bound up with their yields of Fraction IV, are quite unrelated to their yield of the "neutral oils" comprised in Fraction I.

(2) The residues from such benzene-pressure-extraction are always quite devoid of coking propensities.

(3) The substances removed from the coal by our benzene-pressure-extraction process are pre-existent in (either as such, or in some loose molecular association with) the original coal-complex, and are not derived from it by thermal decomposition in the sense of any real breakdown in the essential structure of coal substance.

(4) Both Fractions I and II of the benzene-extract from bituminous and sub-bituminous coals have their similitudes and counterparts in corresponding fractions obtained from both brown coals and lignites.

(5) Whereas Fractions III and IV of the benzene-extracts from bituminous and sub-bituminous coals could also be traced through their counterparts in the laminated black lignites examined, nothing like unto them was found in either the Morwell brown coal or the Saskatchewan brown lignite examined.

(6) In the Morwell brown coal and the Saskatchewan brown lignite, however, the places of Fractions III and IV of the maturer coals referred to were taken by phenolic esters and phenols, respectively.

(7) Therefore, it seems probable that the Fractions III and IV invariably found in the laminated black lignites, sub-bituminous and bituminous coals examined, and which are closely related to the coking propensities of bituminous coals, have originated in the phenols and phenolic esters found in the brown coals referred to.

(8) Also, the general effect of "maturing" has been progressively to diminish the oxygen contents of the substances comprised in each and all the various fractions of the benzene-pressure-extracts as well as of the benzene-extracted residue.

In conclusion our best thanks are due first of all to the Fuel Research Board of the Department of Scientific and Industrial Research for their generous grants in aid of these researches, which have enabled two of us to devote the whole of our time to them; also to Drs. Charles Camsell, D. V. Dowling and R. E. Gilmore of the Canadian Department of Mines in respect of the samples which they so kindly obtained and sent us of various typical coals from the Western Canadian Coalfield; and finally to the Carlton Main Colliery Company, near Barnsley, and the Consett Iron Company (Co. Durham) for furnishing us with samples of their "Shafton" and "Busty" seams respectively.

Gaseous Combustion at High Pressures. Part XI.—*Further Experiments on the Influences of Hydrogen and Steam on the Explosion of Carbonic Oxide-Air, &c., Mixtures.*

By William A. Bone, D.Sc., F.R.S., Donald T. A. Townend, Ph.D., D.I.C., and Gordon A. Scott, B.Sc., D.I.C.

(Received July 31, 1928.)

In Part II of this series* were described the results obtained in the year 1920 by the late W. A. Haward and one of us by exploding isothermic $2(mH_2 + nCO) + O_2 + 4N_2$ mixtures (where $m + n = 1$) in our spherical bomb No. 2 at an initial pressure of 50 atmospheres, from which it was concluded (*inter alia*) that, in such circumstances, not only had hydrogen exerted a peculiar influence in accelerating the rise of pressure, disproportionate to the amount of it present, but also that it is more potent than its equivalent of steam as a promoter of the combustion of carbonic oxide.

Since the results referred to were published, not only have certain new facts affecting their interpretation been discovered, but also new questions relating thereto have been propounded for discussion. Among the new facts should be mentioned the peculiar radiation-absorbing rôle played by nitrogen in CO-Air explosions at high initial pressures; also that, in such circumstances, carbonic oxide is directly oxidised without any chemical intervention of steam at all.

During recent discussions of the subject, the question whether hydrogen or steam is the more potent promoter of the combustion of carbonic oxide has been raised anew by R. V. Wheeler and Payman, who have maintained that "moisture is more effective than hydrogen in promoting the combustion of carbon monoxide."†

Apart altogether from the importance of settling this question, we thought it desirable to repeat and extend the Bone–Haward experiments with a view to finding whether or not in any other circumstances the effects of successive CO by H_2 replacements might become "additive," which most certainly they had not been in those referred to.

While not pretending to have exhausted the subject, we think the new experiments described herein, besides clearing up some of the old issues, will also suggest new points for further investigation. These, however, will be dealt with in discussing the experimental results.

---

* 'Roy. Soc. Proc.,' A, vol. 100, p. 67 (1921).

† 'Trans. Chem. Soc.,' vol. 123, p. 1256 (1923).

Experimental.

It should be understood that all the explosions described herein were carried out in our No. 2 nickel-steel bomb with a 242 c.c. spherical explosion cavity, generally as described in our previous papers (but more particularly in Part III hereof)* except that, in all but the first series, the body of the bomb, instead of being at room temperature, was kept at 100° C. in order to facilitate the introduction of steam into the explosive mixture fired. Any other variation from our usual procedure will also be indicated in the text.

In tabulating the new experimental results,

P_i = the initial pressure in atmospheres at which each mixture was fired.

P_m obs. = the observed maximum pressure in atmospheres attained in the explosion.

P_m corrd. = the same, but "corrected" for cooling in respect of any t_m exceeding 0·005 sec.

t_m = the time in seconds taken for the attainment of maximum pressure after the commencement of the pressure rise.

θ = temperature of bomb when the mixture was filled in and ignited.

1st Series.—*Repetition and Extension of the Bone–Haward Experiments with Isothermic* $2\ (mH_2 + nCO) + O_2 + 3\cdot76\ N_2$ *Mixtures at* $P_i = 50$ *atmospheres and Bomb at Room Temperature* (17° *C.*).

In the Bone–Haward experiments, a series of isothermic $2\ (mH_2 + nCO) + O_2 + 4N_2$ mixtures (where $m + n = 1$) were exploded in our No. 2 Bomb at an initial pressure of 50 atmospheres, the bomb being at room temperature in each case. Immediately before each experiment the spherical explosion chamber of the bomb (capacity = 242 c.c.) had been well dried out in a current of $CaCl_2$-dried hot air; and, in making up the explosive mixture, each constituent was passed into the bomb from a storage cylinder in which its pressure was 50 atmospheres or more. Hence the moisture content of each mixture fired would certainly not have exceeded, and probably would have been substantially less than, 0·045 per cent. The ratio H_2/CO in the mixtures fired in different experiments were approximately 0/28·6, 1·25/25·5, 2·1/24·7,

---

* 'Roy. Soc. Proc.,' A, vol. 103, p. 205 (1923).

3·6/22·5, 6·7/19·9, 13·5/14·0 and 28·2/0, respectively, the *lowest* hydrogen content (except in the case where it was not present at all) being actually 1·10 per cent.

In repeating the experiments, it was thought desirable always (i) to make the N_2-content of each $2(mH_2 + nCO) + O_2 + 3\cdot76\,N_2$ mixture the same as that in a theoretical CO-Air mixture, (ii) to introduce each constituent slowly into the spherical explosion chamber (which had been previously thoroughly dried out by means of a $CaCl_2$-dried hot air blast, followed by a 30 minutes-evacuation with a "Hyvac" pump) from a storage cylinder at 100 atmospheres, passing it *en route* through a 20-inch column of redistilled and purified phosphoric anhydride, so as to ensure each mixture being fired at 50 atmospheres and room temperature (about 17° C.) in a uniformly "well-dried" condition corresponding with a moisture content of less than 0·02 per cent, and (iii) particularly to study the influence of smaller proportions of hydrogen than had been introduced in the Bone–Haward experiments. It should be noticed also that the Petavel gauge used in the new experiments was rather more sensitive than in the Bone–Haward series, so that probably the new "t_m's" are somewhat more reliable than the old.

The repeat experiments comprised (i) seven in which the hydrogen-content of the mixture fired was raised in stages from nil up to 0·8 per cent., or by less than in any of the Bone–Haward experiments, and (ii) four in which it always exceeded 1 per cent. (namely 1·4, 3·4, 5·4 and 29·4 per cent., respectively), as in the Bone–Haward series.

The results (see Table I), while substantially confirming those of Bone and Haward, also showed that the peculiar effect observed by them required a H_2-content exceeding 0·65 per cent. in the mixture fired. For it has transpired that, although the effect of the first few successive small CO by H_2-replacements was approximately proportional to the hydrogen so introduced, with a H_2-content of 0·65 per cent. or more it became abruptly so exceedingly great that for most of the pressure rise the combustion was practically instantaneous. Also, after passing the said 0·60 limit, the explosions were always accompanied by a peculiar sharp "click," which before had been absent, as though they had become abruptly much more violent.

The general character of the results may be judged from Table I and the series of pressure-time curves (for the explosion periods only) shown in fig. 1. Special attention is directed to the following characteristics, namely :—(i) the abrupt change, already referred to, at or about 0·65 per cent. H_2-content, (ii) the fact that, as shown in fig. 1, with all higher H_2-contents, and except

Table I.—Experimental Results (1st Series) with Isothermic 2 ($mH_2 + nCO$) $+ O_2 + 3\cdot76\ N_2$ Mixtures at $P_i = 50$ Atmospheres and $\theta = 17°$ C.

Percentage composition of mixture exploded.			t_m sec.	$1/t_m$	P_m		P_m/P_i corrected.	Pressure fall in 1 sec after t_m.	
H_2.	CO.	Air.			Observed.	Corrected.		Atmospheres	Per cent.
Nil	29·9	70·1	0·22	4·45	413	453	9·06	98	23·7
0·20	28·8	71·0	0·085	11·8	425	447	8·94	102	24·0
0·45	29·5	70·05	0·07	14·3	424	444	8·89	110	26·0
0·50	28·8	70·7	0·07	14·3	428	448	8·96	106	24·8
0·60	28·6	70·8	0·06	16·7	429	448	8·96	111	25·9
*									
0·65	29·0	70·35	0·025	40·0	431	439	8·78	150	34·8
0·80	29·0	70·2	0·02	50·0	440	447	8·94	150	34·1
1·40	28·1	70·5	0·015	67·7	432	438	8·76	157	36·4
3·40	25·3	71·3	0·010	100	440	444	8·88	155	35·3
5·40	24·4	70·2	0·010	100	422	425	8·50	154	36·6
29·40	Nil	70·6	0·005	—	404	404	8·01	229	56·8

* Note the abrupt change in the character of the explosion at this point.

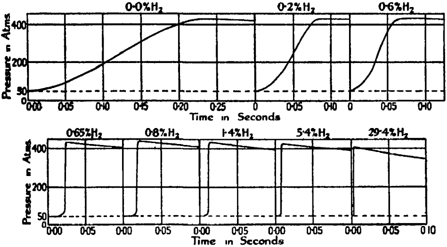

FIG. 1.—$2(mH_2 + nCO) + O_2 + 3\cdot76\ N_2$. $P_i = 50$ atmos. $\theta = 17°$ C.

for an extremely short interval after ignition, the pressure-rise curves all became parallel and almost vertical, showing the practical instantaneous character of the main combusion in each case, and (iii) that, simultaneously with the abrupt change in the character of the explosions referred to, the observed rates of cooling during the first second after P_m also abruptly became faster.

Having thus confirmed the Bone-Haward observations in regard to "theoretical" H_2-CO-Air mixtures with H_2-contents between 0·65 and 5·4 per cent., it hardly seemed necessary to follow up the matter any further; because it may be regarded as certain that the effect of further progressive CO by H_2 replacements in the mixtures referred to would have been the same as those previously observed.

2ND SERIES.—*Explosions of Isothermic* $2\,(m\mathrm{H}_2 + n\mathrm{CO}) + \mathrm{O}_2 + 3{\cdot}76\,\mathrm{N}_2$ *Mixtures at* $\mathrm{P}_i = 64{\cdot}4$ *Atmospheres and Bomb at* 100° *C.*

It next occurred to us to repeat the previous series of explosions, with the same charge-density as before, but keeping the bomb at 100° C. (instead of at room temperature) throughout. Accordingly, in this series of experiments, by means of a simple heating device, which need not be detailed, the body of the bomb was kept at 100° C., and the initial firing pressure was raised to 64·4 atmospheres so as to secure the same charge-density as in the previous series.

Immediately before each experiment, the bomb being at 100° C., the explosion chamber was thoroughly dried out by means of a current of hot $CaCl_2$-dried air followed by 30 minutes evacuation with a "Hyvac" pump. Each constituent of the explosive mixture was then successively filled into the bomb from a cylinder at 100 atmospheres, through a 20-inch column of redistilled and purified phosphoric anhydride *en route*, so as to ensure the mixture being fired in a uniform "well-dried" condition (*i.e.*, with certainly less than 0·02 per cent. steam present).

Table II.—Experimental Results (2nd Series) with Isothermic $2\,(m\mathrm{H}_2 + n\mathrm{CO}) + \mathrm{O}_2 + 3{\cdot}76\,\mathrm{N}_2$ Mixtures at $\mathrm{P}_i = 64{\cdot}4$ Atmospheres and $\theta = 100°$ C.

Percentage composition of mixture exploded.			t_m sec.	$1/t_m$	P_m.		$\mathrm{P}_m/\mathrm{P}_i$ corrected.	Pressure fall in 1 sec. after t_m.	
H_2.	CO.	Air.			Observed.	Corrected.		Atmospheres.	Per cent.
Nil	29·2	70·8	0·19	5·3	425	460	7·14	95	22·4
0·3	28·7	71·0	0·085	11·8	435	455	7·065	105	24·2
0·8	28·8	70·4	0·06	16·7	435	450	6·99	108	24·8
1·1	27·8	71·1	0·05	20·0	430	441	6·85	108	25·2
1·5	27·2	71·3	0·04	25·0	430	439	6·82	109	25·4
2·0	27·5	70·5	0·035	28·6	441	450	6·99	125	28·4
2·8	26·6	70·6	0·02	50·0	444	448	6·96	137	30·9
10·4	19·2	70·4	0·015	66·6	430	435	6·75	155	36·1
29·5	Nil	70·5	<0·005*	—	415	415	6·44	175	42·2

* Although it is hardly possible to make t_m measurements from our Petavel-gauge records with greater accuracy than 0·005 sec., it may be regarded as certain that in this case t_m was rather *less than* 0·005 sec.

The experimental results, which are summarised in Table II, differed from those of the previous series in that none of them exhibited the characteristic features of the Bone-Haward explosions, namely, the practically instantaneous character of the main pressure development. On the contrary, while the accelerating influence of successive CO by H_2 replacements upon the pressure-rise were well marked (*vide* the curves shown in fig. 2), the reciprocals of t_m, which are plotted as ordinates against percentages of hydrogen as abscissæ in the upper curve reproduced in fig. 3, show that after the first 1 per cent.

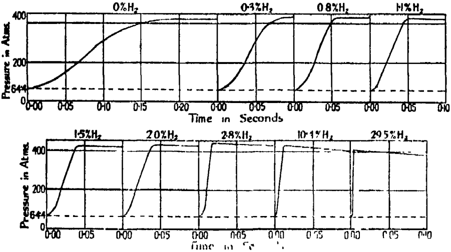

FIG. 2.—$2(mH_2 + nCO) + O_2 + 3\cdot76\,N_2$. $P_i = 64\cdot4$ atmos. $\theta = 100°$ C.

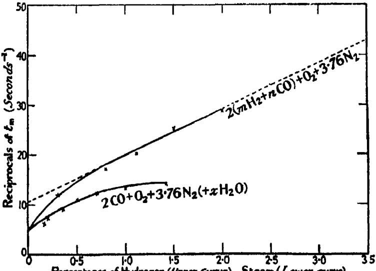

FIG. 3.—$P_i = 64\cdot4$ atmos. $\theta = 100°$

(or so) of hydrogen had definitely catalysed the CO-combustion up to a certain velocity (about twice that of the well-dried $2CO + O_2 + 3\cdot76$ mixture), further amounts of it produced merely an "additive" accelerating effect, which is not at all surprising seeing that, in the circumstances referred to, the rate of combustion of a theoretical H_2-air is at least 50 times faster than that of a well-dried theoretical CO-air mixture.

It is not easy to account for the striking contrast between the results of these experiments and those of the previous series with H_2-contents exceeding about 0·65 per cent. in the mixtures fired, although there can be no doubt about the facts actually being as recorded in each of the two series. The explosion chamber, the charge-density, and the means and position of ignition were the same in both, the only difference in conditions being that the bomb and its charge were at room temperature (17° C.) throughout the first, but at 100° C. throughout the second series. The fact that, in the first series, with the relatively cold bomb, a "knock" effect always supervened when the H_2-content of the explosive medium exceeded 0·65 per cent., but never in the second series with the bomb at 100° C., possibly may have been due to some shortening of the pre-flame period in the second case; or it may have been that the hotter walls of the explosion chamber in the second may have "de-activated" something responsible for the "knock" in the first series. Obviously it is a matter requiring further investigation, which we propose undertaking.

3rd Series.—*Experiments showing the Influence of Steam upon the Rate of Pressure Development in Theoretical* CO-*Air Explosions at* $P_i = 32\cdot2$ *and* 64·4 *Atmospheres respectively with* $\theta = 100°$ *C.*

In this series of experiments (divided into two groups, A and B) we measured the acceleration by successive additions of steam of the rate of pressure-development observed in the explosion of a "well-dried" theoretical CO-air mixture ($2CO + O_2 + 3\cdot76\ N_2$) at initial firing pressures of 32·2 and 64·4 atmospheres, respectively, the bomb temperature being 100° C. throughout. The "charge densities" would thus be the same as if the bomb temperature had been 17° C. but the initial firing pressure 25 or 50 atmospheres respectively.

To ensure exactly the desired amount of steam being introduced into the gaseous mixture before firing it in each experiment, the special device shown in fig. 4 was screwed on to the admission valve of the bomb so as to come immediately between it and the usual filling-in system. It consisted of a hexagonal nut, about 2¼ inches long, bored out so as to accommodate a small copper boat containing the weighed quantity of water which it was desired to introduce into the bomb with the gaseous mixture. Before starting the filling-in operation, however, the explosion cavity of the bomb (whose temperature was 100° C.) was first of all thoroughly exhausted; the copper boat containing the weighed amount of water was then slipped into the bore of the hexagonal nut in question, after which the filling-in of the gas from cylinders at 100 atmospheres was proceeded with, the nut being sufficiently heated by means of a Bunsen flame so as to ensure complete evaporation of the water in the boat and its homogeneous incorporation (as steam) with the gaseous explosive mixture subsequently fired in the bomb.

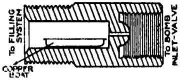

FIG. 4.

Starting with a "well-dried" theoretical CO-air mixture made up from compressed gases in cylinders at 100 atmospheres, without any addition of steam *en route* to the bomb, the device referred to enabled us to study experimentally the effect of adding to it successive and known quantities of steam nearly up to "saturation," which at 100° C. and $P_i = 32 \cdot 2$ atmospheres would mean the presence of about 3, but with $P_i = 64 \cdot 4$ atmospheres of about 1·5 per cent. of steam by volume.

Group A. With a $2CO + O_2 + 3 \cdot 76 N_2$ *Mixture at* $P_i = 32 \cdot 2$ *Atmospheres and* $\theta = 100°$ *C.*—The results, as regards the effects of steam upon t_m and P_m respectively, are summarised in Table III as follows:—

Table III.—$P_i = 32 \cdot 2$ Atmospheres. $\theta = 100°$ C.

Percentage of steam added to mixture.	Percentage composition of mixture		t_m sec	$1/t_m$.	P_m observed.	Pressure fall in 1 sec. after t_m.	
	CO.	Air				Atmospheres.	Per cent.
<0·02*	28·6	71·4	0·14	7·15	198	62	31·3
0·35	29·2	70·8	0·065	18·2	205	75	35·0
0·70	29·2	70·8	0·05	20·0	203	74	34·8
1·40	29·0	71·0	0·05	20·0	205	76	37·1
2·80	28·8	71·2	0·045	22·2	203	79	39·0

* Mixture made up of compressed gases from storage cylinders at 100 atmospheres, after slow passage through a column of purified phosphoric anhydride in each case, and without any addition of steam *en route*.

Group B. With a $2CO + O_2 + 3 \cdot 76 N_2$ *Mixture at* $P_i = 64 \cdot 4$ *Atmospheres and* $\theta = 100°$ *C.*—In this group, we started with (1) P_2O_5-dried gases from cylinders at 100 atmospheres, then passed on to (2) a mixture containing just about 0·02 per cent. of steam, made up from compressed gases each stored in cylinders at 100 atmospheres, but without any steam addition *en route*, and finally (3) to experiments in which known and successively increasing amounts of steam were so added up to "super-saturation." The results are summarised in Table IV and plotted (reciprocals of t_m as ordinates against percentage of steam as abscissæ) in the upper of the two curves shown in fig. 5.

Table IV.—$P_t = 64 \cdot 4$ Atmospheres. $\theta = 100°$ C.

Percentage of steam added to mixture.	Percentage composition of mixture.		t_m sec.	$1/t_m$.	P_m.		P_m/P_t corrected.	Pressure fall in 1 sec. after t_m.	
	CO.	Air.			Observed.	Corrected.		Atmospheres.	Per cent
<0·02*	29·1	70·9	0·19	5·3	428	464	7·20	94	22·0
0·02	29·4	70·6	0·17	5·9	425	458	7·13	95	22·3
0·16	29·3	70·7	0·155	6·5	420	450	7·00	94	22·4
0·18	29·2	70·8	0·14	7·15	420	448	6·97	93	22·2
0·35	29·3	70·7	0·11	9·1	420	442	6·88	90	21·4
0·50	29·4	70·6	0·09	11·1	428	448	6·97	95	22·2
0·70	28·6	71·4	0·08	12·5	426	444	6·90	94	22·0
1·00	29·2	70·8	0·075	13·4	430	447	6·94	97	22·6
1·40 (saturation)	28·8	71·2	0·07	14·3	424	440	6·85	95	22·4
1·90	29·3	70·7	0·065	15·4	428	443	6·87	102	23·7

* Mixtures made up of compressed gases from storage cylinders at 100 atmospheres, after slow passage through a column of purified phosphoric anhydride in each case, and without any addition of steam *en route*.

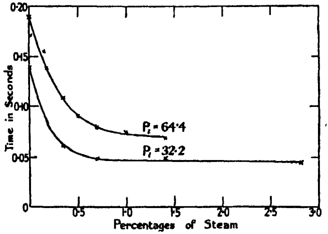

Fig. 5.—$2CO + O_2 + 3 \cdot 76 N_2 (+ xH_2O)$. $\theta = 100°$ C. $P_t = 64 \cdot 4$ and $32 \cdot 2$ atmos.

Considering the results of the two groups of experiments as a whole, it is abundantly clear that, whereas the first small successive addition of steam to a "well-dried" theoretical CO-air mixture markedly accelerated the rate of pressure-rise during the explosion-period, a point (at about 1 per cent. of steam in each case) was soon reached when further successive additions produced very little further effect. This is brought out very well in the two curves (ordinates $= t_m$, and abscissæ percentage of steam present in the gaseous medium fired) shown in fig. 5. And while it would perhaps hardly be correct to say that in either of the two groups of experiments "optimum" combustion conditions had been fully attained, undoubtedly in each case they had been nearly so, with no more than 1 per cent. of steam in the medium. When it is recalled that, according to both H. B. Dixon* and W. Payman and R. V. Wheeler† optimum combustion conditions for a theoretical CO-oxygen or CO-air mixture at atmospheric pressure are not attained until between 5 and 6 per cent. of steam are present in the system, while R. W. Fenning‡ found that about 2·38 per cent. sufficed at 5 atmospheres, it may be inferred from their results and ours that the amount of steam required for optimum conditions in such explosions decreases rather rapidly as the initial pressure rises.

In this connection it may be stated that, during the course of these investigations, our colleague Dr. D. M. Newitt has obtained abundant spectrographic evidence—namely, the entire absence of steam lines in the spectrograms of the explosion flames with "moist" (even up to "saturation") theoretical CO-air mixtures at initial pressures of 32·2 and 64·4 atmospheres ($\theta = 100°$ C.)—proving that, whatever the rôle of steam may be in such circumstances it is not chemical, in any sense of involving its alternating decomposition and regeneration. And it is perhaps significant that in the Group B experiments of this series successive additions of moisture up to saturation neither increased any of the corrected P_m values (indeed, they tended to diminish as steam was added) nor yet affected the rate of pressure-fall after the attainment of maximum pressure. Therefore it would not appear that addition of steam to the "well-dried" theoretical CO-air mixtures in the circumstances referred to has any effect in increasing the liberation of "kinetic" at the expense of "radiant" energy on explosion.

Another interesting circumstance to which attention may be drawn, is that the "corrected" P_m value for the "well-dried" $2CO + O_2 + 3{\cdot}76\,N_2$ mixture in Group B of this series was 464 atmospheres as compared with a "corrected," value of 478 atmospheres for a similarly "well-dried" $2CO + O_2 + 3{\cdot}76\ CO$ mixture under precisely the same conditions, the difference being wholly attributable to the suppression in the latter case of the 5 per cent. CO_2-dissociation at P_m occurring in the former.

---

* 'Phil. Trans.,' vol. 184, p. 187 (1893).

† 'Trans. Chem. Soc.,' vol. 123, p. 1254 (1923).

‡ 'Phil. Trans.,' A., vol. 225, p. 331 (1926).

4TH SERIES.—*Comparison between the Effects of Hydrogen and Steam respectively.*

From the results already detailed in the second and third series of our present experiments it may be inferred (see fig. 3) that, quite apart from what may be termed the mere flame-speeding-up effect of successive small additions of a theoretical H_2-air to a theoretical CO-air mixture in explosions at the high initial pressures under consideration, hydrogen is a more potent promoter than its equivalent of steam of CO-combustion.

With a view of investigating the matter further, however, it was decided to carry out comparative groups of experiments under precisely the same conditions—namely, at $P_i = 64{\cdot}4$ atmospheres and $\theta = 100°$ C.—with $2CO + O_2 + 6R$ (where $R = N_2$, CO or Ar) mixtures in which *either* (i) successive small amounts of water up to "saturation" were added *or* (ii) an equivalent part of the CO had been replaced by H_2. In this way, without materially altering the amounts of total energy Σ developed in the successive explosions, comparable small amounts of steam were either originally introduced, or formed during explosion, in the system.

The results of these experiments—which are summarised in Tables V, VI and VII, and (so far as the reciprocals of the t_m's are concerned) are plotted in the curves shown in figs. 6, 7 and 8, respectively—confirm our previous conclusion that hydrogen is a more potent promoter than its equivalent of steam of CO-combustion at high initial pressures. Apparently also from these curves, the relatively greater H_2-effect was much more marked with 6CO than with either $6N_2$ or 6Ar as the "diluent." And, if anything, it was rather greater with $6N_2$ than with 6Ar as diluent.

Table V.—P_i = 64·4 Atmospheres. θ = 100° C.

$2CO + O_2 + 6N_2 + xH_2O$.

Percentage of steam added to mixture.	Percentage composition of mixture.			t_m sec.	P_m observed.	Pressure fall in 1 sec. after t_m	
	CO.	O_2.	N_2.			Atmospheres.	Per cent
Nil	21·8	11·5	66·7	0·97	338	76	22·5
0·4	22·4	11·25	66·35	0·41	377	95	25·2
0·7	22·5	11·3	66·2	0·33	378	98	26·0
1·4	22·6	10·9	66·5	0·29	380	103	27·1

$2(mH_2 + nCO) + O_2 + 6N_2$.

Percentage composition of mixture.				t_m sec.	P_m observed.	Pressure fall in 1 sec. after t_m.	
H_2.	CO.	O_2.	N_2.			Atmospheres.	Per cent.
Nil	21·8	11·5	66·7	0·97	338	76	22·5
0·7	21·5	11·1	66·7	0·20	382	106	27·8
1·8	20·3	11·0	66·9	0·13	400	118	29·5
3·2	19·5	11·1	66·2	0·085	410	126	30·8

Table VI.—P_i = 64·4 Atmospheres. θ = 100° C.

$2CO + O_2 + 6CO + xH_2O$.

Percentage of steam added to mixture.	Percentage composition of mixture.			t_m sec.	P_m observed.	Pressure fall in 1 sec. after t_m.	
	CO.	O_2.	N_2.			Atmospheres.	Per cent.
Nil	87·0	11·1	1·9	0·27	400	102	25·5
0·5	86·7	11·5	1·8	0·085	414	97	23·4
0·7	86·6	11·3	2·1	0·060	410	98	23·9
1·4	86·8	11·3	1·9	0·055	410	111	27·1

Table VI (continued).

$2\,(mH_2 + nCO) + O_2 + 6CO$.

Percentage composition of mixture.				t_m sec.	P_m observed.	Pressure fall in 1 sec. after t_m.	
H_2	CO.	O_2.	N_2.			Atmospheres.	Per cent.
Nil	87·0	11·1	1·9	0·27	400	102	25·5
0·7	86·5	11·3	1·5	0·035	400	99	24·8
1·4	85·5	11·4	1·7	0·025	417	111	26·6

Table VII.—$P_i = 64 \cdot 4$ Atmospheres. $\theta = 100°$ C.

$2CO + O_2 + 6Ar + xH_2O$.

Percentage of steam added to mixture.	Percentage composition of mixture.			t_m sec.	P_m observed.	Pressure fall in 1 sec. after t_m.	
	CO.	O_2.	Ar.			Atmospheres.	Per cent
Nil	22·4	11·0	66·6	0·12	472	154	32·6
0·7	22·0	11·3	66·0	0·05	473	161	34·0
1·4	22·8	11·0	66·2	0·045	476	159	33·4

$2\,(mH_2 + nCO) + O_2 + 6Ar$.

Percentage composition of mixture.				t_m sec.	P_m observed.	Pressure fall in 1 sec. after t_m.	
H_2.	CO.	O_2.	Ar.			Atmospheres.	Per cent.
Nil	22·4	11·0	66·6	0·12	472	154	32·6
1·5	21·1	11·2	66·2	0·03	480	174	36·3

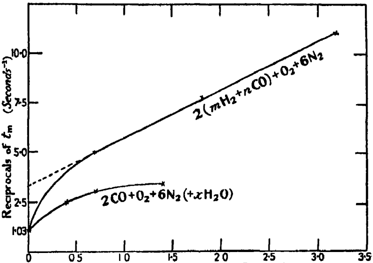

FIG. 6.—P_i = 64·4 atmos. θ = 100° C.

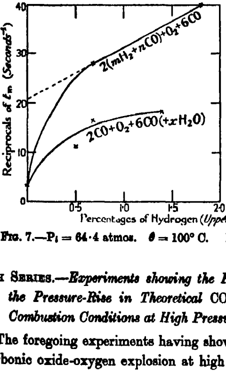

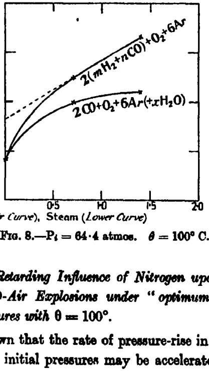

FIG. 7.—P_i = 64·4 atmos. θ = 100° C. FIG. 8.—P_i = 64·4 atmos. θ = 100° C.

5TH SERIES.—*Experiments showing the Retarding Influence of Nitrogen upon the Pressure-Rise in Theoretical CO-Air Explosions under "optimum" Combustion Conditions at High Pressures with* θ = 100°.

The foregoing experiments having shown that the rate of pressure-rise in a carbonic oxide-oxygen explosion at high initial pressures may be accelerated by the presence of steam up to a certain point, irrespective of the nature of the "diluent" present—*i.e.*, whether nitrogen, argon, or excess combustible gas, it remained now to show that the "lag" in the pressure rise observed in such theoretical CO-air explosions is due principally to nitrogen, quite apart from the (relatively speaking) " dryness " of the system.

It may be recalled that in former experiments, and particularly in those described in Part V[*] hereof, it was shown that, whereas on exploding a " well-dried " theoretical CO-air mixture in our spherical bomb at room temperature the rate of pressure-development progressively diminished as the initial firing pressure increased, thus :—

$P_i =$	3,	10,	25,	50,	75,	100,	125,	150,	175	Atms.
$t_m =$	0·07,	0·10,	0·15,	0·19,	0·32,	0·40,	0·47,	0·53,	0·56	Secs.

The substitution for nitrogen of an equivalent of either argon or excess carbonic oxide as the " diluent " always had the opposite effect at all initial pressures above 10 amtospheres. Hence there could be no doubt about " nitrogen-activation " being the principal cause of the peculiarity referred to in CO-air explosions.

Seeing, however, that in the said experiments the explosive medium had always been in a fairly uniform condition of " dryness "—having been made up in a well-dried-out explosion chamber at room temperature from gases which had been slowly admitted into it from storage cylinders at high pressures through a 10-inch column of redistilled phosphoric anhydride—it now seemed of interest to make further experiments at two different initial pressures, in each case under " optimum " conditions as regards steam-content of the explosive medium.

With this object in view, groups of comparative experiments were carried out at initial pressures of 32·2 and 64·4 atmospheres, respectively, with the following mixtures, namely :—

$$2CO + O_2 + 3{\cdot}76 \text{ and } 6N_2,$$

$$2CO + O_2 + 3{\cdot}76 \text{ and } 6CO$$

$$\text{and } 2CO + O_2 + 3{\cdot}76 \text{ and } 6Ar,$$

each containing 1·4 per cent. of steam, the bomb being kept at 100° C. throughout, and the steam being introduced as described in p. 552. Such conditions may be regarded as " optimum " for CO-combustion at each of the initial pressures concerned (*vide* 3rd Series hereof).

From the results of these experiments, which are summarised in Table VIII, it will be observed that (i) not only in every case did the replacement of nitrogen by its volume equivalent of either carbon monoxide or argon considerably

---

[*] 'Roy. Soc. Proc.,' A., vol. 108, p. 393 (1925).

Table VIII.—Experiments (5th Series) on the Explosion of $2CO + O_2 + 3\cdot76$ R and 6R Mixtures containing 1·4 per cent. Steam at Initial Pressures of 32·2 and 64·4 Atmospheres respectively, and $\theta = 100°$ C.

Diluent.	P_i.	Percentage composition of mixture.			t_m sec.	P_m observed.	P_m/P_i observed.	Pressure fall in 1 sec. after t_m.	
		CO.	O_2.	N_2 or Ar.				Atmospheres	Per cent.
$3\cdot76\ N_2$	32·2	29·0	14·6	56·4	0·05	205	6·37	76	37·1
	64·4	28·8	14·8	56·4	0·07	424	6·60	95	22·4
$6N_2$	32·2	22·0	11·4	66·6	0·20	176	5·47	80	45·5
	64·4	22·6	10·9	66·5	0·29	380	5·90	103	27·1
3·76 CO	32·2	83·6	14·6	1·8	0·015	230	7·14	124	53·8
	64·4	83·8	14·4	1·8	0·005	478	7·44	190	39·7
6CO	32·2	86·6	11·3	2·1	0·055	185	5·75	89	48·0
	64·4	86·8	11·3	1·9	0·055	410	6·37	111	27·1
3·76 Ar	32·2	29·1	14·2	56·7	0·02	266	8·25	152	57·2
	64·4	28·9	14·5	56·6	0·02	546	8·49	230	42·0
6Ar	32·2	21·7	11·0	67·3	0·05	220	6·83	122	55·5
	64·4	22·8	11·0	66·2	0·045	476	7·40	159	33·4

more than halve t_m, but also (ii) whereas a doubling of the initial pressure always materially increased t_m in the nitrogen-diluted mixtures, in all other cases it was either unaltered or shortened. It is, therefore, abundantly clear that nitrogen is the principal cause of the peculiar "lag" in the pressure-rise always observed in theoretical CO-air explosions at high initial pressures irrespective of the hygroscopic condition of the medium.

In this connection attention may be directed to the fact that, whereas in our former explosions of relatively "dry" $2CO + O_2 + 4Ar$ mixtures the value of t_m at $P_i = 50$ atmospheres and $\theta =$ room temperature was 0·025 seconds, which, with the same charge density ($P_i = 64\cdot4$ atmospheres, and $\theta = 100°$ C.) and 1·4 per cent. of steam present now became 0·020 second (or only 0·005 second shorter), in the corresponding $2CO + O_2 + 4N_2$ experiments, the t_m values were 0·19 and 0·07 second respectively. This suggests that steam may have a less influence on t_m with argon than with nitrogen as diluent in our explosions, a point which is reserved for further investigation.

Summary.

The principal facts brought to light during the foregoing investigation may be summarised as follows :—

(1) While the peculiar influence of successive CO by H_2 replacements observed in the Bone-Haward experiments on the explosion of theoretical $2(mH_2 + nCO) + O_2 + 4N_2$ mixtures at initial pressures of 50 atmospheres and room temperature have been confirmed, it is now shown to come in abruptly when the H_2-content of the mixture exceeds about 0·65 per cent., and then to be of the nature of a "knock" effect which may be eliminated by raising the bomb temperature to 100° C. without altering the charge-density.

(2) When such "knock" effect has been eliminated by the means referred to, effects of successive CO by H_2 replacements upon explosions of the mixtures in question were twofold, namely, initially and up to a certain point, which is reached when about 1·0 per cent. of hydrogen is present, definitely "catalytic," but afterwards purely "additive" only, the second phase being attributable merely to a speeding-up of the flame propagation resulting from the concurrent combustions of a relatively fast-burning theoretical H_2-air and a relatively slow-burning theoretical CO-air mixture, the oxygen supply being always sufficient for complete combustion in the system.

(3) The effects of successive small additions of steam to a theoretical CO-air mixture on explosion at initial pressures of 32·2 and 64·4 atmospheres, respectively, and with the bomb chamber at 100° C. was to promote combustion, but without the steam intervening chemically in the sense of its being continuously decomposed and regenerated, "optimum" conditions being nearly reached in each case when but 1 per cent. only of steam was present. It is the initial *small* addition of steam which most matters in such circumstances.

(4) Actually, and apart altogether from the "knock" effect referred to under (1), the addition of a small quantity of hydrogen had a greater effect than its equivalent of steam in speeding up the explosion of a CO-air mixture at high pressures; which of the two H_2-influences referred to in (2) was most responsible for this result is perhaps not yet altogether certain, though the evidence seems distinctly in favour of the view that what may be termed the purely "catalytic" effect of hydrogen exceeds that of steam in like circumstances. Certainly, the reverse is not the case.

(5) Apart altogether from any influence which mere "dryness" may have during the explosion of a theoretical CO-air mixture at high initial pressures, the progressively increasing "lag" in t_m observed as the initial pressure rises is principally, and for the most part, a nitrogen-effect, because it is not observed at all when the nitrogen is replaced by its volume equivalent of either carbonic oxide or argon.

In conclusion, we desire to tender our grateful thanks to the Government Grant Committee, the Department of Scientific and Industrial Research, and Imperial Chemical Industries, Limited, for generous grants out of which the heavy expenses of the investigations have been defrayed.

Gaseous Combustion at High Pressures. Part XII.—*The Influences of Steam and Temperature, respectively, upon the "Explosion Limits" of Carbonic Oxide-Air Mixtures.*

By William A. Bone, D.Sc., F.R.S., D. M. Newitt, Ph.D., D.I.C., and C. M. Smith, B.Sc., D.I.C.

(Received July 31, 1928.)

In Part IX* of this series, experiments were described showing (*inter alia*) that, under the usual firing conditions, the explosion range of "well-dried" CO-air mixtures becomes progressively narrower as the initial pressure increases. In each case the components of the experimental mixtures had been slowly passed into the bomb (at room temperature) from cylinders at 100 to 150 atmospheres, through an 8-inch long column of freshly distilled and specially purified phosphoric anhydride, so that they would all be fired at room temperature in a uniformly very dry condition.

Under such conditions, the "explosion ranges" found for CO-air mixtures at various initial pressures were as follows:—

Initial pressure.	Per cent. CO in CO-air "limit mixtures."		Explosion range. $L_2 - L_1$.
	L_1.	L_2.	
1·0	14·2	71·0	56·8
5·0	15·4	67·5	52·1
10·0	17·8	62·8	45·0
30·0	20·3	58·8	38·5
50·0	20·6	56·8	36·2
125·0	20·7	51·6	30·9

---

* 'Roy. Soc. Proc.,' A, vol. 117, p. 553 (1928).

It will be observed that, whereas an increase in P_i beyond 50 atmospheres hardly affected the lower limit, where the oxygen was present in great excess, the upper limit, when it was always in considerable defect, continued to fall, so that the " explosion range " continued to contract with increasing pressure.

It was impossible to say, from the information then available, how far such progressive contraction in the " explosion range " with increasing high pressures was attributable either to the presence of nitrogen or to some possible slight increase in the dryness of the explosive medium. That it could not wholly (if at all) be due to nitrogen was evident from the fact that the substitution of argon for nitrogen in the medium did not eliminate, though it reduced, the contraction in question between 10 and 50 atmospheres, thus :—

Initial pressure atmospheres.	Per cent. CO in CO-" argon-air " limit mixture.		Explosion range, $L_2 - L_1$.
	L_1.	L_2.	
10	14·0	66·0	52·0
50	15·3	60·4	45·1

On the other hand, when CO-" helium-air "* mixtures were employed, there was but little contraction in the " explosion range " on similarly increasing the pressure, thus :—

Initial pressure atmospheres.	Per cent. CO in CO-" helium-air " limit mixture.		Explosion range, $L_2 - L_1$.
	L_1.	L_2	
10	13·9	67·3	53·4
50	15·1	66·2	51·1

Since the experiments in question were carried out, further evidence has come to hand in our laboratories of the sensitiveness as regards explosion time of theoretical CO-air explosions to slight changes in hygroscopic conditions at high initial pressures, even though the moisture actually present in the system be less than 0·04 per cent. And, seeing that the increasing compression of a gas progressively dries it, it is especially necessary in work of this kind always to ensure that the hygroscopic state of the gaseous explosive mixture is well under control and accurately known. Hitherto it has been our regular practice to introduce the constituents of our mixtures slowly and successively into the bomb (the explosion chamber of which is always thoroughly dried out in a current of hot $CaCl_2$-dried air) from cylinders where they had been stored at pressures somewhere between 100 and 200 atmospheres, *en route*, through an 8- to 10-inch column of redistilled and purified phosphoric anhydride, a procedure which ensures the mixture being fired in a state of fairly uniform "dryness" corresponding with something substantially more than "$CaCl_2$-dryness," namely, with a moisture content probably below 0·02 per cent.

---

* The expressions " argon-air " and " helium-air " as used in this and other papers of the series always mean air in which the nitrogen has been wholly replaced by its volume equivalent of either argon or helium, respectively (*i.e.*, $O_2 + 3 \cdot 76$ He or Ar).

Experimental.

It being the object of the further experiments described herein to determine the influence of steam upon the limits of explosion of CO-air mixtures at high initial pressures, arrangements were made whereby the temperature of our cylindrical bomb No. 4 (explosion chamber 75 cm long × 5 cm. diameter, capacity 2 litres) could be maintained at 100° C. throughout so as to permit of the gaseous mixtures being fired at either 32·2 or 64·4 atmospheres initial pressure, as required, either (i) in a "well-dried" (moisture certainly below 0·02 per cent) or (ii) in an 80 per cent. saturated condition, such that the moisture content would be either 2·24 or 1·12 per cent. respectively, according to whichever of the two initial mixtures referred to was employed. Reference to the third series of experiments described in Part XI hereof will show that as nearly as possible "optimum" combustion conditions (as regards moisture content) would be attained in such "moist" experiments at each of the two initial pressures in question.

It should be particularly noted that (i) the bomb now being always at a constant temperature of 100 ± 0·5° C., instead of at room temperature as formerly, the present initial pressures of 32·2 and 64·4 atmospheres, respectively, would give the same "charge-densities" as the former initial pressures of 25 and 50 atmospheres, respectively; (2) before each experiment the hot explosion chamber was well dried out by means of a current of $CaCl_2$-dried air, followed by a 15 minutes exhaustion by means of a Hyvac pump; and (3) in the "dry" experiments the components of the gaseous explosive mixtures were slowly and successively introduced into the bomb from storage cylinders at 150 atmospheres pressure, through an 8-inch column of redistilled and purified phosphoric anhydride *en route**; and in the "wet" experiments, the predetermined amount of steam was introduced into the gases as they passed into the bomb by means of the special device described and illustrated in p. 552 of the preceding paper (Part XI hereof).

The same criterion for judging the actual "limit mixture" was employed as formerly (*vide* p. 557 of Part IX hereof) for CO-air mixtures, namely, an abrupt change in the "percentage combustion" when mixtures of slightly varying CO-content in the neighbourhood of each limit mixture were fired in the bomb, as shown in each case by the intersection of the horizontal and vertical portions of the "percentage combustion" diagrams accompanying the text.

The clearest way in which the experimental results can be summarised is by means of a series of tables with corresponding graphs specially designed to show up the "explosion limits" in each case, from which the reader will readily see how they were determined. This will be done in Tables I to IV and the corresponding figs. 1 to 4. In what follows—

θ = the temperature of the bomb explosion chamber.

P_i = the initial firing pressure in atmospheres.

P_m = the observed maximum pressure in atmospheres.

t_m = the time in seconds required for the attainment of t_m after commencement of the pressure-rise.

---

* The mixtures would thus be fired in much the same hygroscopic condition as in our former "limit" experiments, *i.e.*, with moisture content well below 0·02 per cent.

1st Series.—*All with* $P_t = 32 \cdot 2$ *Atmospheres and* $\theta = 100°$ *C.*

Table I.—Group A: With "dry" CO-air Mixtures (*i e.*, Moisture below 0·02 per cent.).

($P_t = 32 \cdot 2$ Atmospheres and $\theta = 100°$ C.)

Per cent. CO in mixture	P_m observed atmospheres.	t_m seconds	Percentage combustion	
17·1	60	—	11·0	
17·6	128	1·26	50·5	
18·0	—	—	90·0	Lower
19·2	150	0·80	95·1	← limit
23·8	177	0·47	97·1	
25·2	192	0·32	98·4	
55·2	160	0·75	97·5	
61·1	140	0·80	95·2	
61·8	140	0·85	95·5	Upper
62·8	—	--	92·1	← limit.
63·1	—	—	66·1	
63·4	—	—	59·0	
64·4	would not fire			

Per cent CO.

N.B. { Lower limit from curve (fig 1) = 18·1
Upper limit from curve (fig 2) = 62·7

Table II.—Group B: With "moist" CO-air Mixtures (*i.e.*, 80 per cent. "saturated" $H_2O = 2 \cdot 4$ per cent.).

($P_i = 32 \cdot 2$ Atmospheres and $\theta = 100°$ C.)

Per cent. CO in mixture.	P_m atmospheres.	t_m seconds.	Percentage combustion.	
14·9	35	—	6·0	
15·3	40	—	32·0	Lower
15·8	80	1·10	90·1	limit.
16·0	100	0·85	95·4	
17·6	111	0·56	96·6	
26·4	150	0·15	98·1	
50·0	149	0·18	98·4	
62·5	112	0·61	96·5	
64·1	100	0·63	94·9	Upper
65·9	70	1·10	88·4	limit.
66·3	70	1·00	81·1	
67·5	50	—	61·0	
68·6	would not fire			

Per cent. CO.

N.B. Lower limit from curve (fig. 1) = 15·7

N.B. Upper limit from curve (fig. 2) = 65·7

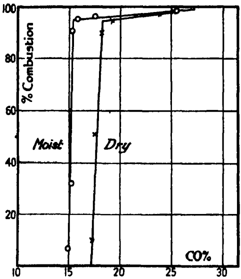

Fig. 1.
$P_i = 32 \cdot 2$ atmospheres.

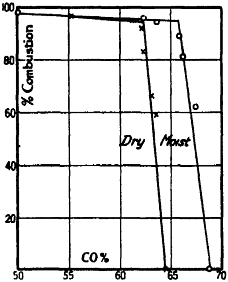

Fig. 2.
$P_i = 32 \cdot 2$ atmospheres.

2ND SERIES.—*All with* $P_i = 64{\cdot}4$ *Atmospheres and* $\theta = 100°$ *C.*

Table III.—Group C: With "dry" CO-air Mixtures (*i.e.*, Moisture below 0·02 per cent.).

($P_i = 64{\cdot}4$ Atmospheres and $\theta = 100°$ C.)

Per cent CO in mixture	P_m atmospheres	t_m seconds	Percentage combustion	
17·9	103	0·60	27·9	
18·6	118	0·80	28·5	Lower ←
19·2	263	1·60	96·8	limit.
19·7	—	—	96·1	
20·1	270	1·40	97·3	
20·7	279	1·22	96·7	
53·1	320	0·75	96·5	
57·1	299	0·78	95·0	
59·1	243	1·77	78·3	Upper ←
59·5	125	0·90	70·4	limit
59·8	110	0·75	32·9	
60·9	did not ignite			

Per cent. CO.

N.B. {Lower limit from curve (fig. 3) = 18·9
Upper limit from curve (fig. 4) = 59·3

Table IV.—Group D: With "moist" CO-air Mixtures (*i.e.*, 80 per cent. "saturated" $H_2O = 1 \cdot 2$ per cent.).
($P_i = 64 \cdot 4$ Atmospheres and $\theta = 100°$ C.)

Per cent. CO in mixture	P_m atmospheres.	t_m seconds.	Percentage combustion.
15·5	would not ignite		
15·7	ignited but flame soon died out		10·7
16·0	190	2·00	88·7 ← Lower limit.
16·8	208	1·08	93·5
18·7	300	0·70	96·5
26·6	365	0·22	98·8
62·9	271	0·76	95·3
65·1	240	1·01	95·3
66·1	205	1·60	94·5
66·6	211	1·80	95·1
66·7	200	2·00	95·5 ← Upper limit.
66·8	120	—	62·2
67·8	would not ignite		—

Per cent. CO.
N.B. { Lower limit from curve (fig. 3) = 16·0
Upper limit from curve (fig. 4) = 66·7

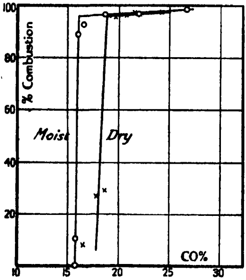

FIG. 3.
$P_i = 64 \cdot 4$ atmospheres.

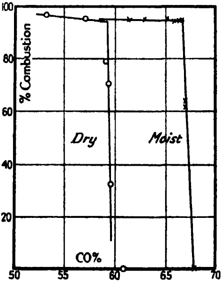

FIG. 4.
$P_i = 64 \cdot 4$ atmospheres.

Summary.

(1) The new experimental results show quite clearly that the mere drying of CO-air mixtures narrows their explosion ranges at the high initial pressures employed, as follows :—

P_i atmospheres.	Hygroscopic condition of mixtures	Percentage CO in limit mixtures.		Explosion range, $L_2 - L_1$
		L_1.	L_2	
32·2	" Dry "	18·1	62·7	44·6
	80 per cent. saturated at 100° C.	15·7	65·7	50·0
64·4	" Dry "	18·9	59·3	40·4
	80 per cent. saturated at 100° C.	16·6	66·7	50·1

(2) In the case of the " moist " mixtures the influence of increasing pressure (charge density) was slightly to shift each limit downwards without narrowing the " explosion range " at all, but with the " dry " mixture, the " explosion range " was definitely narrowed by doubling the initial pressure (see fig. 5).

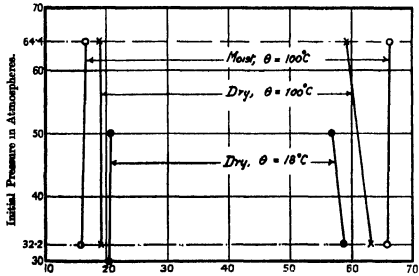

Percentage CO in Limit Mixture.

FIG. 5.

(3) By comparing the results of the present " dry " experiments at 100° C. and at 32·2 and 64·4 atmospheres initial pressure, respectively, with those of our former " dry " experiments (*vide* Part IX hereof) at 18° C. and initial

pressures of 25 and 50 atmospheres, respectively, we can see at once that the influence of temperature *per se* is to widen the "explosion range," because the charge density at 18° C. and 25 atmospheres is the same as at 100° C. and 32·2 atmospheres, while at 18° C. and 50 atmospheres it is the same as at 100° C. and 64·4 atmospheres. The results of such "corresponding experiments" compare as follows:—

P_i atmospheres.	θ ° C.	Percentage CO in limit mixture.		Explosion range $L_2 - L_1$.
		L_1.	L_2.	
(1) 25·0	18	20·3	58·8	38·5
32·2	100	18·1	62·7	44·6
(2) 50·0	18	20·6	56·8	36·2
64·4	100	18·9	59·3	40·4

In conclusion, we desire to tender our grateful thanks to the Government Grant Committee, the Department of Scientific and Industrial Research, and Imperial Chemical Industries, Limited, for generous grants out of which the heavy expenses of the investigations have been defrayed.

A Theory of Partial Osmotic Pressures and Membrane Equilibria, with special reference to the application of Dalton's Law to Hæmoglobin Solutions in the presence of Salts.

By G. S. Adair, Fellow of King's College, Cambridge.

(Communicated by Sir William Hardy, F R S—Received October 10, 1927)

1. Introduction.

Dalton's Law of Partial Pressures affords a point of departure for the discussion of the osmotic pressure of colloidal solutions. The observed osmotic pressure of a solution of a protein such as hæmoglobin is essentially a property of the protein system as a whole, and a knowledge of the partial pressures of the various components is of service in a systematic study of the properties of the solution.

It will be shown that many of the difficulties in the interpretation of such systems can be overcome by the application of Dalton's Law in the form used by Gibbs.

The osmotic pressures of aqueous solutions of hæmoglobin have been discussed in a previous communication (Adair (1925), 3) * The removal of the salts associated with a protein under natural conditions may cause fundamental changes in its properties, and therefore it is necessary to investigate the osmotic pressures of solutions of proteins in the presence of salts.

Measurements of the osmotic pressures of hæmoglobin and of the membrane equilibrium of diffusible salts, recorded below, show that there are deviations from the theoretical formulæ of Donnan (1911) and of Loeb (1922)

The magnitude of the deviations is so great that it is necessary to investigate systems with a wide range of concentrations of hydrogen ions, of salts and of the protein, in order to find out what assumptions can be considered justifiable in correcting osmotic pressure measurements for the effects due to diffusible ions and in calculating the size of protein particles in the presence of salts.

The experiments recorded in this work indicate that within certain limits of hydrogen ion and salt concentrations, including the range that obtains in the blood, it is legitimate to interpret the observed osmotic pressures of hæmoglobin by the modified form of Dalton's Law of Partial Pressures given in Section 5.

---

* For Literature and references, see p. 602.

2. METHODS.

The thermodynamic activities of the components of the protein systems which have been studied in this work have been deduced from the results of experiments in which protein solutions contained inside collodion sacs have been allowed to reach equilibrium with solutions of diffusible crystalloids

The apparatus used and the criteria for osmotic equilibrium have been described in a previous communication (Adair (1925), 2). In general, equilibration has been continued for at least seven days at a temperature of 0° C, in order to ensure a close approximation to a true thermodynamic equilibrium. After equilibration, the potential difference across the membrane has been measured with saturated calomel electrodes as described by Loeb (1922), Taylor (1924), Northrop and Kunitz (1926) and Bjerrum (1924)

Samples of the inner and outer fluids have been taken for measurements of the densities and for chemical analyses, which include determinations of the bases (Stadie and Ross (1925)), chlorides (Van Slyke (1923)), phosphates (Briggs (1922)). The protein content of pure protein solutions has been determined by drying at 103° C, but in the case of mixtures of proteins and salts, the protein content has been calculated from Kjeldahl nitrogen determinations or from the differences in densities of the inner and outer fluids, or from the differences in refraction of the inner and outer fluids

The hydrogen ion concentrations have been determined with the Clark hydrogen electrode in certain cases, but in general the colorimetric method has been used for the "outer fluids" which are free from protein. (Ref. Clark, 1923.)

3. THE STABILITY AND THE NUMBER OF COMPONENTS AND DEGREES OF FREEDOM OF PROTEIN SYSTEMS.

Before applying the theory of membrane equilibrium to protein systems, it is necessary to establish their stability and the number of components and degrees of freedom by experimental methods.

It has been shown in a previous paper that solutions of one of the proteins—namely, hæmoglobin—are practically stable at 0° C. (Adair (1925), 2) in respect of their osmotic properties.

Theoretically the number of components may be changed by the formation of reduced hæmoglobin, met-hæmoglobin and other derivatives of oxy-hæmoglobin.

Comparative studies of fresh and of old preparations and of pure met-hæmoglobin prepared by the ferricyanide method, and reduced hæmoglobin prepared by Stokes' reagent, have shown that under certain conditions it is possible to obtain differences of 5 per cent. between the osmotic pressures of different preparations, and slightly larger variations in the membrane potentials and the distribution of ions, but in the calculations of partial pressures and molecular weights given below, the error due to changes in the hæmoglobin seems too small to require detailed discussion in this paper.

The possibility that the osmotic equilibrium of hæmoglobin is influenced by enzymes or by traces of lipoids, globulins, stroma protein and other colloidal impurities requires experimental investigation, because Planck (1917) has shown mathematically that it is impossible entirely to eliminate impurities, and therefore all of the substances present in the corpuscle must be considered as components

In this work hæmoglobin has been purified by fractional crystallisation.

A comparative study of the osmotic pressures of preparations subjected to three different degrees of purification (Adair (1925), 2) yielded results so nearly identical that, for the purposes of this work, it seems legitimate to omit the colloidal impurities in calculating the number of degrees of freedom of the system under normal conditions.

The osmotic pressure of hæmoglobin equilibrated with distilled water shows a range of variation which suggests that traces of ammonia and carbon dioxide, and other crystalloidal impurities, must be included in calculations of the number of degrees of freedom (Adair (1925), 3).

The smooth curves obtained when the protein is equilibrated with a salt solution of well-defined composition (fig. 6) indicate that under these conditions it is legitimate to assume that the number of components is $1 + N$ where N is defined by the composition of the salt solution.

4. THE DIFFUSIBLE COMPONENTS OF A PROTEIN SYSTEM.

The general theory of the thermodynamic properties of the diffusible substances present in natural protein-systems is beyond the scope of a paper concerned mainly with the analysis of the osmotic pressures of proteins in the presence of salts, but there are a number of special points in which measurements of the "thermodynamic activities" or the effective concentrations of diffusible substances are essential for the interpretation of the osmotic pressure measurements.

In the first place, the simple theoretical formulæ for the osmotic pressure due to the unequal distribution of ions across membranes (Donnan (1911), Sorensen (1917), Loeb (1922), Wilson (1925)) have been based on the assumption that the ideal solution laws are applicable.

In solutions of finite concentration it is possible to estimate the margin of error in the theoretical assumptions by means of measurements of the activities and activity coefficients of the ions, which are correlated with their osmotic pressures by thermodynamic formulæ (Bjerrum (1918, 1923))

The experimental evidence given in Tables I, II, III and IV shows that even if the concentration of diffusible ions is as small as 0·01 equivalents per litre, the margin of uncertainty in the partial pressures of the diffusible ions is of the same order of magnitude as the observed osmotic pressures of the protein recorded under the same experiment numbers in Tables VI, VIII and X.

The tables published by Loeb (1922) prove that even if the concentration of diffusible ions is as small as 0·001, there is a risk that Donnan's equations may give results of the wrong order of magnitude if they are applied for the purpose of calculating the part of the observed osmotic pressure which is due to diffusible ions, and the part which is due to the protein itself.

In the second place, the direct experimental proof (Tables I, II, III, IV) that the protein causes appreciable changes in the activity coefficients of the diffusible salts associated with it supports the hypothesis, developed in this paper, that certain variations in the osmotic pressure, formerly attributed to actual changes in the aggregation of the protein (Roaf (1910), Barcroft and Hill (1910)), are really due to deviations from the ideal solution laws.

(i) *The Application of Gibbs' Equations for Membrane Equilibrium*

Crystalloidal non-electrolytes and salts can diffuse across collodion membranes without restriction, and therefore it is possible to apply the equation of Gibbs, which has been re-stated below in the activity notation (Gibbs (1876), Formula 77)—

$$a_n' = a_n'' \tag{1}$$

a_n' = the activity or effective concentration of a diffusible substance in the protein solution, or "inner fluid." a_n'' = the activity of this substance in the "outer fluid" in diffusion equilibrium with the protein solution. The convention that a single accent as in a_n' refers to the inner fluid and two accents, as in a_n'', refers to the outer fluid has been applied to the concentrations in mols per litre (c_n' and c_n'') and other symbols used in this paper.

Since a_n'' can be calculated from the concentration in a pure solution of crystalloids (Lewis and Randall (1923)), formula 1 shows that a_n' can be determined by measurements of the distribution of the diffusible substance. The activity of water can be determined by equation 1 if the freezing-point of the outer fluid has been measured.

Charged ions can diffuse across the membranes in equivalent proportions The equations of Gibbs, and the corresponding formulæ in the activity notation given by Donnan and Allmand (1914), show that the products of the activities of the ions of a salt must be equal on both sides of the membrane.

The activities of individual ions inside and outside the membrane are related to the membrane potentials by formulæ 2 and 3—

$$\mathrm{E}' - \mathrm{E}'' = \frac{-\mathrm{RT}}{n\mathrm{F}} \, ln \, \frac{a_1'}{a_1''}. \tag{2}$$

$\mathrm{E}' - \mathrm{E}''$ = potential difference in volts between the protein solution, or inner fluid, and the outer fluid.

F = 96,494 coulombs per equivalent.

R = 8·316 volt coulombs or joules per degree.

T = 273·1 at 0° C.

a_1' = activity of a diffusible ion in the protein solution.

a_1'' = activity of a diffusible ion in the outer fluid.

n = valence of the ion.

$$a_1' = f_1'' c_1'' \left(\text{anti log} - \frac{n\mathrm{E}}{54 \cdot 193}\right). \tag{3}$$

c_1'' = concentration of the ion in the outer fluid, a pure solution of strong electrolytes.

f_1'' = activity coefficient of the ion in the outer fluid.

$f_1'' = a_1''/c_1''$.

f_1'' has been obtained from the tables and formulæ published by recent workers on pure solutions of strong electrolytes, reviewed by Bronsted (1927).

E = membrane potential in millivolts at 0° C.

$$54 \cdot 193 = \text{constant for } 0^\circ \text{ C.} = 1000 \times 2 \cdot 303 \times \mathrm{RT/F}.$$

Rona and Petow (1923) have raised the question whether the theory of membrane equilibrium applies to all of the ions in protein solutions, but it has been pointed out (Adair, 1923) that the general equations are supported by the authority of Gibbs.

The extensive researches of Loeb proved that formula 2 represents the relationship between the hydrogen ion activities and the membrane potentials, if the concentration of electrolytes is not too small for the application of electro-metric methods.

(ii) *Experimental Investigations of the Activities of Diffusible Ions in Protein Solutions.*

(*a*) *Activities of Chloride Ions in Dilute Solutions.*—Table I shows that even in dilute solutions there is a considerable reduction in the activity coefficient of the chloride ion in the presence of proteins

This reduction might be due to the formation of an unionised protein chloride, as suggested by Pauli and Schon (1924) and Northrop and Kunitz (1926).

In more recent work Pauli and Wit (1926) and Frisch, Pauli and Valkó (1925) have adopted the hypothesis that the protein chlorides are fully ionised.

It is possible to attribute the fall in the activity coefficient to the electrical forces due to the multivalent protein ions, which may lead to an accumulation of diffusible ions in the neighbourhood of the protein and a diminution of their effective concentration in the bulk of the fluid, even if the protein chloride is fully ionised

The agreement between the observed values and those calculated by the formula of Debye and Huckel (1923) and Hückel (1925) shows that the interionic forces may be great enough to account for the fall in the activity coefficient.

(*b*) *Activities of Chloride Ions in Concentrated Solutions.*—In protein solutions which are not very dilute it is impossible to apply the equations of Debye and Hückel in their original form.

One factor that must be allowed for is the volume of the natural protein. Van Slyke, Wu and McLean (1923) found by experiment that if the concentrations of ions are expressed in mols per 1000 grammes of water, the results for blood and serum are in good agreement with the ideal solution laws.

In extensions of the work to more concentrated salt solutions, referred to below, it appears that the corrected activity coefficients of the chloride ions are abnormally high, if it is assumed that the loss of weight in drying the solution represents the mass of free water under natural conditions.

A part of the loss in weight may be attributed to the decomposition of the protein. From the thermodynamic point of view, water which is produced by an irreversible reaction should not be treated as a component of the system in its original state. In the circumstances, an allowance has been made for the effects of the volume of the natural protein by the empirical formula stated below:

$$m_1' = c_1'/(1 - V_p) = c_1'/(1 - 0\cdot01\alpha C), \tag{4}$$

c_1' = gramme mols of an ion per litre of protein solution.

V_p = effective volume of the protein.

f_1' the corrected activity coefficient $= a_1'/m_1'$.

m_1' = corrected concentration in mols per litre of "dispersion medium."

C = the protein concentration in grammes of dry matter per 100 c.c. of solution.

The data for the more concentrated solutions recorded in Table II show that if $\alpha = 0\cdot965$, the corrected activity coefficient f_1' is practically equal to f_1'', the activity coefficient of the chloride ions in the outer fluid. It seems probable that the empirical constant α is approximately equal to the volume of natural protein which yields 1 gramme of dry matter. The specific volume of dry protein is about 0·75 c.c., and therefore the loss of water by denaturation appears to be about 0·21 c.c. per gramme of dry material. Theoretically, a more exact estimate of α can be obtained by formula (5), which includes an empirical correction for the adsorption or combination of the salt or non-electrolyte used in the distribution experiment:

$$c_n' = c_n''\,(1 - 0\cdot01\alpha C) + 10b\,.\,C \tag{5}$$

b = mols of diffusible substance adsorbed per gramme of protein.

Table I.—Activities of Chloride Ions in Dilute Solutions.
(Edestin chloride + hydrogen chloride.)

f_{Cl}' Observed.	f_{Cl}' Calculated.	[Cl]′ Concentration.	[H]′ Concentration.	c_p	J
0·86	0·81	0·0125	0·0094	0·000126	0·10
0·89	0·80	0·0128	0·0090	0·000145	0·12
0·80	0·74	0·0178	0·0085	0·000353	0·27
0·62	0·66	0·0361	0·0064	0·00127	0·74
0·65	0·64	0·0404	0·0060	0·00141	0·84
0·59	0·63	0·0405	0·0070	0·00132	0·90

f_{Cl}' = observed activity coefficient of chloride ions in a solution of edestin chloride equilibrated with approximately 0·01 Molar HCl.

[Cl]′ = mols of Cl per litre, determined by analysis.

[H]′ = hydrogen ion concentration, assuming.

[H]′ = a_H'/f_{Cl}' (not exact).

c_p = protein concentration — provisional estimates (assuming Mol. Wt. 17,000).

J = $[\mathrm{Cl}] + [\mathrm{H}] + c_p n_p^2$. ($n_p$ is about 24.)

f_{Cl}' (calculated) has been obtained by applying the formula of Debye and Hückel, re-stated below (Hückel, 1925):

$$\log f_1 = 0{\cdot}344\ n_1^2\ \mathrm{J}^{\frac{1}{2}}/(1 + \kappa\alpha_1). \tag{6}$$

n_1 = valence of the ion.

J = the sum of the ion concentrations multiplied by the square of their valences.

$\kappa = 0{\cdot}229.10^8 \cdot \mathrm{J}^{\frac{1}{2}}$., α_1 = an empirical constant which depends upon the radius of the chloride ion and the mean radii of other ions. In this case $\alpha_1 = 3 \times 10^{-8}$.

Table II.—Activity Coefficients at Different Salt Concentrations.
(Hæmoglobin + sodium chloride.)

Experiment No.	CHb	$[\mathrm{Cl}]'$	m_{Cl}'	$[\mathrm{Cl}]''$	$\frac{a_{\mathrm{Cl}}'}{a_{\mathrm{Cl}}''}$	$\frac{f_{\mathrm{Cl}}'}{f_{\mathrm{Cl}}''}$
246	20·4	0·098	0·122	0·125	0·903	0·93
245	19·6	0 391	0·482	0·495	0·967	0·99
259	19·7	1·62	2·00	2·02	1·00	1·00
244	19·1	3·34	4·09	4·04	1·00	0·99
243	20·7	3 24	4·05	4 04	1·00	1·00

$[\mathrm{Cl}]'$ = concentration in mols. per litre of protein solution.

m'_{Cl} = corrected concentration (formula 4).

$[\mathrm{Cl}]''$ concentration of NaCl in outer fluid, buffered at pH 8·3 by 0·025 Molar $\mathrm{NaHCO_3}$.

$$f_{\mathrm{Cl}}' = a_{\mathrm{Cl}}'/m_{\mathrm{Cl}}' \cdot f_{\mathrm{Cl}}'' = a_{\mathrm{Cl}}''/[\mathrm{Cl}]''.$$

CHb = grammes dry hæmoglobin per 100 c.c. solution.

f_{Cl}' is distinctly less than f_{Cl}'' if the concentration $[\mathrm{Cl}]'' = 0{\cdot}125$.

This observation is not inconsistent with formula 6, if the term $c_p n_p^2$ (approximately $0{\cdot}003 \times 10^2$) is included in the calculation of J for the inner fluid.

The suggestion has been made that the charges on protein ions are so far apart that they can exert only slight effects on f_{Cl}. If this is the case, the reduction in the ratio $f_{\mathrm{Cl}}'/f_{\mathrm{Cl}}''$ must be due to some unknown factor.

(*c*) *Activities of Chloride and Phosphate Ions at Different Protein Concentrations.*

Table III illustrates a number of points of theoretical interest.

A 34 per cent. hæmoglobin solution diminishes the ratio of the (corrected) activity coefficients to 0·87 in a membrane equilibrium experiment. Van Slyke, Hastings, Murray and Sendroy (1925) have shown that the ratio of the coefficients for Cl in corpuscles and plasma is about 0·77.

f_{Cl}' and f_{HPO_4}' are so much reduced by the protein that there is an excess of Cl and PO_4 ions inside the membrane, although the protein is acting as an anion.

The differences between the results obtained with different preparations with different proportions of oxidised and reduced hæmoglobin are comparatively small.

Table III.—Activity Coefficients at Different Protein Concentrations. [Hæmoglobin + KCl + Na_2HPO_4 + KH_2PO_4] *p*H 7·8.

Ion Species.	Experiment No.	CHb	c_1'	m_1'	c_1''	Ratio a_1'/a_1''	Ratio f_1'/f_1''
Cl	203	19·0	0·0890	0·109	0·101	0·970	0·90
Cl	298	24·0	0·0806	0·105	0·1022	0·956	0·93
Cl	205	28·0	0·081	0·111	0·102	0·944	0·87
Cl	299	34·4	0·0714	0·107	0·1017	0·919	0·87
$[HPO_4]_t$	250	19·4	0·0533	0·066	0·0639	0·94	0·91
$[HPO_4]_t$	298	24·0	0·0514	0·0667	0·0668	0·919	0·92
$[HPO_4]_t$	205	28·0	0·0545	0·0746	0·0271	0·896	0·87
$[HPO_4]_t$	299	34·4	0·044	0·066	0·0674	0·853	0·87
$(Na^+]_t$	298	24·0	0·2043	0·2659	0·229	1·046	0·90
$[Na^+]_t$	299	34·4	0·175	0·262	0·237	1·088	0·98

Experiment No. Ref. Table X (membrane potentials).

c_1' = gramme mols per litre of protein solution.

m_1' = corrected concentration (formula 4).

c_1'' = gramme mols per litre of outer fluid.

a_1'/a_1'' = activity ratio.

(For phosphates a correction has been introduced for the 10 per cent. of H_3PO_4.)

f_1' = corrected activity coefficient = a_1'/m_1' (mean value for phosphates).

$[HPO_4]_t$ denotes total phosphate.

$[Na]_t$ denotes total base (Na + K).

The measurements of total base are subject to much larger errors than chloride or phosphate determinations.

Measurements of the activity coefficients of ions in approximately isoelectric hæmoglobin solutions (Table IV) show that the condition of the isoelectric protein is much more complex than was formerly supposed.

There is a large excess of ions inside the membrane, which does not agree with Loeb's (1922) application of the Donnan theory. Moreover, the excess of anions much exceeds the excess of cations, an observation which does not agree with Pauli's theory that both ions of a salt combine with the protein.

Sörensen, Linderstrom-Lang and Lund (1927) have pointed out that theoretically there may be a difference between I, the true isoelectric point where the net charge of the protein is zero, and I_A' the "isoionic point," where the charge due to combination with hydrogen and hydroxyl ions is zero, if the protein combines with other ions.

Unfortunately, it is impossible to determine I in terms of Sörensen's definition, but if the true isoelectric point is defined as suggested below, I is distinctly on the acid side of I_A'.

Proposed Definition of the True Isoelectric Point.

The isoelectric point I of a protein in equilibrium with a buffer mixture is the activity of hydrogen ions a_H', at which a_H' would be equal to a_H'', which is the same as the point of zero membrane potential.

Table IV.—Activity Coefficients at Hydrogen Ion Concentrations near the Isoelectric Point.

Ion Species.	Experiment No.	CHb	c_1'	m_1'	c_1''	a_1'/a_1''	$_pH''$	f_1'/f_1''
Cl	253	19 3	0·109	0·134	0·121	0·98	6·85	0·88
$[HPO_4]_t$	253	19·3	0·0612	0·0753	0·0637	0 97	6·85	0·82
$[HPO_4]_t$	304	17·5	0·0134	0·0158	0·00965	1·0	6·95	0·61
$[HPO_4]_t$	313	17 5	0·0120	0·0144	0·00988	0·93	6 9	0·64
NH_4	313	17·5	0·014	0·0165	0·0142	1 05	6·9	0·90

5. THE PARTIAL OSMOTIC PRESSURE OF THE PROTEIN IONS.

In order to determine the partial osmotic pressure and the molecular weight of a protein in the presence of diffusible salts, it is necessary to analyse the "observed osmotic pressures" defined by formula 7 in terms of the pressure due to the excess of ions inside the membrane and the pressure due to the protein ions themselves:

$$p_{obs.} = P' - P'' \qquad (7)$$

p_{obs} = the observed osmotic pressure, or the pressure measured with a membrane permeable by water and salts, but impermeable by the protein.

P' = total osmotic pressure of the protein solution or "inner fluid."

P'' = total osmotic pressure of the "outer fluid," a solution of salts in diffusion equilibrium with the protein solutions.

The determinations of partial pressures of proteins in the presence of an excess of diffusible ions may be invalidated by relatively small errors in the theoretical assumptions concerning the diffusible ion pressures and by the deviations from Dalton's Law of Partial Pressures investigated by Abegg (1893) and Cernatescu (1920).

The risk of error is so great that it has been found necessary to modify the theoretical assumptions* made by Donnan (1911) and by Loeb (1922), as suggested under the heading Method I, or even to treat the problem from a different point of view suggested by the theory of membrane equilibrium referred to in a previous communication (Adair, 1927).

The accumulation of the experimental data required for the application of the more accurate Method II is not yet complete,† but it shows that under certain conditions, where the ion pressure difference (defined below) is a small fraction of the observed osmotic pressure, Method I is a useful approximation for the special purpose of calculating the partial pressure of the protein ions.

Method I. Application of Dalton's Law of Partial Pressures.—The data required for the application of this method include a determination of the observed osmotic pressure and the membrane potential of a protein solution in equilibrium with a solution of diffusible salts, the concentration of which must be within the range of application of the modification of Dalton's Law stated in formula 8 :

$$p_{\text{obs.}} = \Sigma p_p' + \Sigma p_i' + \Sigma p_n' - \Sigma p_i'' - \Sigma p_n''. \qquad (8)$$

$\Sigma p_p'$ = sum of partial pressures of the protein ions.

$\Sigma p_i'$ = sum of partial pressures of the diffusible ions (in the inner fluid).

$\Sigma p_n'$ = sum of partial pressures of the unionised molecules (in the inner fluid).

$\Sigma p_i''$ = sum of partial pressures of the diffusible ions (in the outer fluid).

---

* Abnormalities in the osmotic pressures of diffusible ions in protein systems have been demonstrated by Hammarsten (1924), Linderström-Lang (1926), Bjerrum (1924).

† The detailed thermodynamical treatment of the partial pressures of protein ions in equilibrium with salt solutions of constant composition, and the activities of protein ions will be published later.

$\Sigma p_n''$ = sum of partial pressures of the diffusible unionised molecules (in the outer fluid).

Formula 8 is an empirical modification of the equation suggested by Gibbs in his work on the theory of ideal gas mixtures (Gibbs, 1876).

He defined the partial pressure of a gas in a mixture as the pressure which would be exerted by the gas in the pure state at the same temperature and potential. The equations referred to in Section 4 show that the potential of a non-electrolyte is the same inside and outside the membrane, and it follows from Gibbs' definition that the terms $\Sigma p_n'$ and $\Sigma p_n''$ cancel out, even if the solutions are not ideal.

Formula (8) is therefore equivalent to formula (9).

$$p_{\mathrm{obs.}} = \Sigma p_s' + \Sigma p_i' - \Sigma p_i''. \tag{9}$$

As a first approximation $\Sigma p_i'$ and $\Sigma p_i''$ have been evaluated by applying formulæ (10) and (11)—

$$p_1'' = \mathrm{RT}gc_1''. \tag{10}$$

$$p_1' = [\mathrm{RT}gc_1'']\, e^{-nu}, \tag{11}$$

c_1'' = the concentration of an ion in the outer fluid.

g = the mean osmotic coefficient of the outer fluid, or the observed freezing point divided by the theoretical freezing point.

n = the valence of the ion (negative for anions).

u = a symbol representing the expression $(\mathrm{E}' - \mathrm{E}'')\ \mathrm{F/RT}$.

$\mathrm{E}' - \mathrm{E}''$ = membrane potential. (Ref. formulæ (2) and (3).)

If E is expressed in millivolts at 0° C., $u = \mathrm{E}/23{\cdot}535$.

Formula (11) is the same as Nernst's equation for a concentration cell, quoted below—

$$\mathrm{E}' - \mathrm{E}'' = \frac{-\mathrm{RT}}{n\mathrm{F}}\, ln \frac{p_1'}{p_1''}.$$

It has been applied to the membrane potentials of glass electrodes by Haber and Klemensiewicz (1909). This formula has been employed rather than the formula (12) $p_1' = \mathrm{RT}\ c_1'$ (Donnan, 1911), or the formula (13) $p_1' = \mathrm{RT}a_1'$ (Loeb, 1922), because the osmotic coefficients of ions are different from their activity coefficients.

If the formulæ (10) and (11) are applied to all of the diffusible ions, it is possible to make *provisional* calculations of the "ion pressure difference" defined by formula (14) and the partial osmotic pressure of the protein by formula (15).

$$p_i = \Sigma p_i' - \Sigma p_i'', \tag{14}$$

$$p_{\text{obs.}} = p_p + p_i. \tag{15}$$

p_i = ion pressure difference,

p_p = partial osmotic pressure of the protein ions.

If the membrane potentials are small—less than 3 millivolts—the computations can be shortened by the use of the exponential series formula No. (16), resembling that applied by Bjerrum (1924) in his treatment of ideal solutions.

$$\Sigma p_i' = \text{RT}\,\Sigma\,[gc_i''\,(1 - n_i u + \tfrac{1}{2}n^2{}_i u^2)]. \tag{16}$$

Since terms of the form $gc_i''\,n_i u$ for anions and cations cancel out, it follows that

$$\Sigma p_i' = \text{RT}g\,\Sigma c_i'' + \text{RT}g\,(\tfrac{1}{2}u^2)\,\Sigma c_i'' n_i^2. \tag{17}$$

If pressures are measured in mms. of mercury at 0° C

$$\Sigma p_i' = 17{,}033g\,\Sigma c_i'' + [15{\cdot}4\ g\,.\,r\,.\,\Sigma c_i'']\,\text{E}^2 \tag{18}$$

r = a valence factor — a constant for any given salt = $\Sigma c_i'' n^2{}_i / \Sigma c_i''$.

$$p_i = 15{\cdot}4\,.\,g\,.\,r\,.\,\Sigma c_i''\,\text{E}^2 = k_1\text{E}^2. \tag{19}$$

k_1 = a constant for a given outer fluid.

Under certain conditions a provisional estimate of the order of magnitude of the ion pressure difference can be obtained by applying the formula (20) derived from formula (17), by the substitution of the value of "u" given by formula (21)

$$p_i = \text{RT}g\,.\,\tfrac{1}{2}\,(c_p n_p)^2 / r\Sigma c_i'', \tag{20}$$

$c_p n_p$ = equivalent concentration of protein. n_p = valence of protein ion, defined by the formula $c_p n_p = -\,\Sigma c_i' n_i$. Formula (21) has been derived from the series in formula (16).

$$c_p n_p = u\Sigma c_i'' n_i^2 = ur\Sigma c_i''. \tag{21}$$

In order to compute n_p at 0° C it is necessary to know the molecular weight of the protein (Section 7), the amounts of acid or base bound at a definite *p*H, the temperature coefficient of ionisation, and, in addition, it is necessary to investigate the degree of ionisation of protein chlorides, sodium proteinates and similar salts, a subject which will be discussed in a later communication.

The acid and base binding power of hæmoglobin at 38° C. has been studied by Van Slyke and his colleagues (Hastings, Van Slyke, Neill, Heidelberger and Harington (1924), Hastings, Sendroy, Murray and Heidelberger (1924)). Some rough provisional estimates have been given in Table V.

Table V.—Provisional Estimates of the Valence of Hæmoglobin Ions.

pH	2	6	6·8	7·4	8	9·5
n_p	+ 40	+ 6	0	− 6	− 9	− 20

It has been stated that the formula (15), $p_p = p_{obs.} - p_i$, yields a "provisional value" for the partial osmotic pressure. The next step is to find out whether there is a range of concentrations of hydrogen ions, salts, and of the protein in which the "provisional value" is approximately correct.

The experimental evidence bearing upon this question can be discussed from the standpoint of formula (23), which has been derived from formula (22).

$$p_{obs.} = p_i + \mathrm{RT}g_pc_p, \tag{22}$$

g_p = osmotic coefficient of the protein. c_p = molar concentration of the protein.

$$p_{obs.} = p_i + \mathrm{RT}\,(\phi_h\phi_s\phi_p)\left(\frac{10\mathrm{C}}{\mathrm{M}_a}\right). \tag{23}$$

ϕ_h = a function which has been introduced to represent the variations in the osmotic coefficient caused by hydrogen ions, in systems where the protein concentration and the salt concentrations have been kept constant.

ϕ_s = a function representing the effects of diffusible salts (s = equivalent concentration of salts in the outer fluid).

ϕ_p = a function representing the variations in the osmotic coefficient at different protein concentrations.

C = grams of protein per 100 c.c. of solution.

M_a = molecular weight of the protein. (If the protein is a mixture of polymers, M_a is the average value of the mass of the particles.)

Formula (23) shows that the application of Dalton's Law to protein systems can be verified by determinations of the molecular weight of a protein.

If the calculations of molecular weights at different concentrations of hydrogen ions, salts, and of the protein are not concordant, the discrepancy might be due to three causes:

(i) The "provisional values" of the partial osmotic pressure may be different from the real value, if Dalton's Law is not applicable, or if the approximate formulæ for ion pressure differences are in error.

(ii) The osmotic coefficient $(\phi_h\phi_s\phi_p)$ may be very different from unity even at low protein concentrations.

(iii) M_a may be altered by changes in the hydrogen ion and salt concentrations.

It will be shown in Section 7 that the calculated values of the molecular weight of hæmoglobin in a number of different solvents are in close agreement. The evidence in Section 6 makes it seem improbable that the agreement is due to an accidental compensation of deviations from Dalton's Law by variations in $\phi_h\phi_s\phi_p$ or the degree of aggregation, and therefore it may be inferred that the agreement in the calculated molecular weights is evidence in favour of the application of Dalton's Law within a limited range of hydrion, salt and protein concentrations.

Outside this range the problem is more complicated, there are many relationships between osmotic pressure and one other variable which are consistent with the hypothesis that there are great deviations from Dalton's Law, and there are other relationships consistent with the theory of A. V. Hill (Barcroft and Hill (1910), Brown and Hill (1923)), which has been supported by Roaf (1910) According to Hill's theory, the degree of aggregation of hæmoglobin is a function of the concentration of hydrogen ions and salts.

If, however, the observations are visualised as a model, or a series of models, in which the " provisional value " of the partial osmotic pressure is represented as a function of the hæmoglobin concentration and the concentrations of hydrogen, potassium, sodium, chloride phosphate and bicarbonate ions and the temperature, the relationships which are consistent with the aggregation theory appear to have a different interpretation.

The hypothesis suggested in this paper is that over the wide range covered by the experiments in Section 6, the degree of aggregation is a constant, and the apparent variations are accounted for by the functions $\phi_h\phi_s\phi_p$.

It seems probable that with the exception of a few experiments in which p_t is relatively large or the diffusible salt concentration is abnormally great, the deviations from Dalton's Law do not cause serious differences between the partial osmotic pressure of the protein and the provisional values defined by formula (15) in the experiments referred to below.

6. THE ANALYSIS OF THE OBSERVED OSMOTIC PRESSURES OF HÆMOGLOBIN.

(*a*) *Osmotic Pressures at Different Hydrogen Ion Concentrations.*

Condition (*I*).—Hæmoglobin 1 per cent. Salts, Mixtures of $M/15 . KH_2PO_4 + M/15 . Na_2HPO_4$. (Clark, 1923.)

The points marked by squares in fig. 1 show that under these conditions, where the concentration of diffusible salts is so much larger than the equivalent concentration of the protein that the value of p_t is reduced to a fraction of a millimetre (formula (20)), the observed osmotic pressure of the protein and the provisional value of its partial osmotic pressure are practically constant over a wide range of hydrogen ion concentrations.

Two explanations of these observations may be considered. The hydroxyl ions may diminish the degree of aggregation of the protein, and the variations in the molecular weight may be masked by deviations from Dalton's Law of Partial Pressures.

The explanation adopted in this paper is that the degree of aggregation is a constant over a wide range of hydrogen ion concentrations, and that Dalton's Law is at least approximately correct (Adair, 1926).

The provisional values of the partial osmotic pressures are in fairly close agreement with the line AB, calculated on the assumptions that $\phi_\lambda\phi_s\phi_p = 1\cdot0$ under these conditions, and that the molecular weight equals 67,000, as suggested in Section 7.

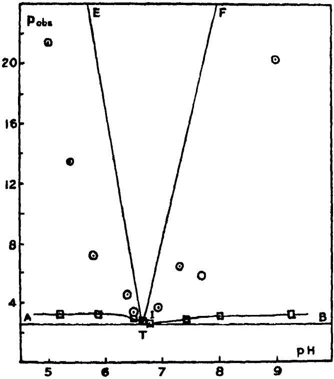

Fig. 1.—$p_{obs.}$ (ordinate) = observed osmotic pressure of 1 per cent. hæmoglobin solutions (in millimetres of mercury at 0° C.). pH (abscissa) = − log hydrogen ion concentration of the "outer fluid." Circles: Outer fluids, very dilute solutions of NH_4OH and H_2CO_3. Squares: Outer fluid, mixtures of M/15 Na_2HPO_4 + M/15 KH_2PO_4. EIF = Theoretical value of the osmotic pressure of a protein salt. RT C_p $(1 + n_p)$. AB = Theoretical value of osmotic pressure of the protein ion RT C_p.

Condition (II).—Hæmoglobin 1 per cent., equilibrated with very dilute solutions of ammonia or of carbonic acid.

The circles in fig. 1 show that hydrogen ions cause great variations in the observed osmotic pressure, $p_{\text{obs.}}$, if the " outer fluid " is a very dilute solution. Under these conditions $p_{\text{obs.}}$ is practically the same as the total osmotic pressure of the protein salt, minus a small correction term $\Sigma p_i''$, as stated in formula (24). (Formula (8))

$$p_{\text{obs.}} = \mathrm{RT} g_s c_p (1 + n_p) - \Sigma p_i''. \qquad (24)$$

The osmotic coefficients of protein salts (g_s) or their apparent degree of ionisation, calculated by the classical theory, may range from 0·5 to 0·8 or more under these conditions, according to the observations of Adair (1925, 1) and Austin, Sunderman and Camack (1926).

The partial pressures of the protein under these conditions have not been discussed because the outer fluids were too dilute for the application of the membrane potential method and formula (11). It may be observed, however, that in all cases the osmotic pressures are smaller than the estimates of the total osmotic pressure of the ammonium hæmoglobinate or the hæmoglobin bicarbonate (Curve EIF), assuming $g_s = 1 \cdot 0$.

Condition (III).—Protein concentration 20 per cent. Salts, 0·23 equivalents per litre.

The data given in Table VI and fig 2 show that over the range from pH = 6·8 to pH 7·8, the " provisional value " of the partial osmotic pressure defined by Method I is a constant, and it is probable that the degree of accuracy of the provisional values is great enough to justify the assumption that the degree of aggregation is constant. Calculations based on Method II indicate that the function ϕ_h is diminished as the pH is increased from 6·8 to 8·3. This function will be discussed in a later communication.

Table VI.—Osmotic Pressures at Different Hydrogen Ion Concentrations. Hæmoglobin + Phosphates and Bicarbonates.

Experiment No.	pH″	E	$p_{\text{obs.}}$	p_i	p_p	CHb
253*	6 8	−0*	101·1	1·7	99·4	19·33
250	7·9	−0·75	103·6	4·4	99·2	19·42
252	8·0	−0·87	110·9	5·7	105·2	20·00
246	8·3	−2·40	126·8	24·7	102·1	20·40

* No. 253 (E). Measurement inaccurate—probable range 0− to −0·5.
CHb = grammes dry hæmoglobin per 100 c.c. solution.

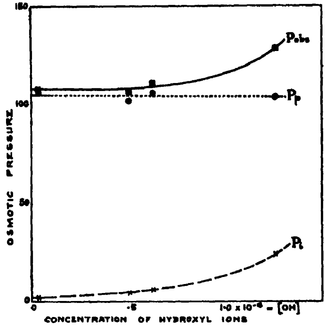

Fig. 2.—$p_{obs.}$ (ordinate) = observed osmotic pressures of 20 per cent. hæmoglobin solutions (in millimetres of mercury at 0° C.). [OH] = concentration of OH ions in the outer fluids (mixtures of chlorides, phosphates and bicarbonates) (Tables VI and VII). p_i = diffusible ion pressure difference = $15 \cdot 4\, g.r.\, 2c_i'' E^2$ (Equation 19). p_p = partial osmotic pressure of protein (provisional value).

Table VII.—Densities and Ion Concentrations.

Experiment No.	Density, Inner.	Density, Outer.	[K]″	[Na]″	[Cl]″	[HPO$_4$]″	[H$_2$PO$_4$]″
253	1·0593	1 0124	0·153	0·064	0·121	0·0319	0·0319
250	1·0596	1·0128	0·104	0 119	0·100	0·0597	0·0042
252	1 0596	1·0125	0·103	0·127	0·100	0·0633	0·0033
246*	1·0562	1 0052	0·000	0·150	0·125	0·000	0 000*

* No. 246 (0·025). Buffered by bicarbonate 0·025 Molar (HPO$_4$ absent).

(b) *Osmotic Pressures at Different Salt Concentrations.*

The relationship between the "observed osmotic pressure" of hæmoglobin and *s*, the concentration of diffusible salts in the fluid in diffusion equilibrium with the protein solution, has been shown by the curves in figs. 3 and 4, and by Table VIII.

The analysis of the pressure in terms of p_i and p_p, given in Table VIII, shows that the initial fall in osmotic pressure is due to the diminution in p_i, and the rise in pressure at higher salt concentrations must be due to the term p_p.

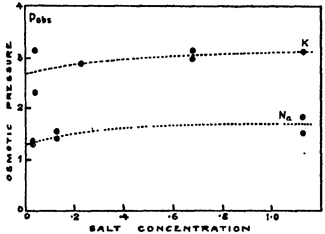

FIG. 3.—$p_{obs.}$ = observed osmotic pressure in millimetres of mercury at 0° C. In this range $p_{obs.}$ is equal to the provisional value of p_p. Salt concentration (abscissa) in gramme equivalents per litre of the outer fluid. Curve K: 1 per cent. hæmoglobin + potassium salts at pH 7·8. Curve Na: 0·5 per cent. hæmoglobin + sodium salts at pH 8·8 (mixtures of phosphates and chlorides).

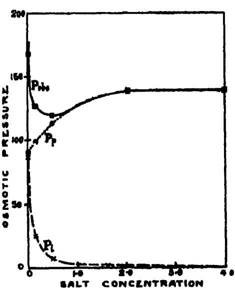

FIG. 4.—$p_{obs.}$ = observed osmotic pressure of 20 per cent. hæmoglobin solutions. p_i = diffusible ion pressure difference. p_p = partial osmotic pressure of protein ions (provisional value). Salt concentration, gramme equivalents of sodium salts (NaCl buffered by 0·025 Molar NaHCO$_3$) per litre of outer fluid (Table VIII).

Table VIII.—Osmotic Pressures and Membrane Potentials of Hæmoglobin Equilibrated with Sodium Chloride Solutions, Buffered by 0·025 Molar $NaHCO_3$ (pH″ = 8·3).

No.	CHb	[Na]″	E	p_{obs}	p_i	p_p	p_p (corr.)	ϕ_s
247	19·1	0·0268	−10·55	167·6	87	80·6	88·5	1·03
246	20·4	0·1504	− 2·4	126·8	24·7	102·1	98·0	1·14
245	19·55	0·520	− 0·65	115·8	6·2	109·6	114·7	1·38
259	19·70	2·045	0	138·5	0	138·5	140·6	1·63
244	19·08	4·064	0	127·4	0	127·4	139·0	1·62
243	20·65	4·067	0	148·1	0	148·1	139·0	1·62

CHb = grammes dry hæmoglobin per 100 c.c. solution (inner liquid). [Na]″ = gramme mols Na per litre of outer fluid (NaCl + $NaHCO_3$). p_p (corr.) = p_p for CHb = 20, corrected by estimates of ϕ_p. ϕ_s = p_p (corr.)/86. (86 mm. = extrapolated pressure for [Na]″ = 0.) Cl = concentration (see Table II).

Measurements at very low protein concentrations showed that as a first approximation $p_{obs.}$ (and the provisional value of p_p) are independent of the salt concentration over the range from 0·01 to 4·0 equivalents per litre (fig. 3).

It is here suggested that the state of aggregation of hæmoglobin is constant over a wide range of salt concentrations, and that if the protein concentration is low the deviation from Dalton's Law does not exceed 15 per cent.

The theory that salts increase the degree of aggregation (Barcroft and Hill (1910), Roaf (1910)) cannot be reconciled with the observations for dilute protein solutions without postulating great deviations from Dalton's Law.

At higher protein concentrations the problem is more complicated, but in view of the relationships between osmotic pressure and protein concentration demonstrated in Tables X, XI, XII, XIII, it is difficult to explain the results by changes in aggregation, and the variations in osmotic pressure may be attributed to the function ϕ_s.

If this hypothesis is correct, the function ϕ_s defined by formula (25) is of *significance in calculations of the molecular weights of proteins in the presence* of salts.

$$p_p = \phi_s [p_p]_0. \tag{25}$$

p_p = partial osmotic pressure of the protein.

$[p_p]_0$ = theoretical value of the partial pressure (at the same hydrogen ion and protein concentration) at zero salt concentration.

The range of variation in ϕ_s is from 1 to 1·09 under the conditions represented in fig. 3. At higher protein concentrations the range is much larger. It will be observed that a 2 Normal solution of sodium chloride gives the value

1·63 in Experiment No. 259, Table VIII, and under similar conditions ammonium sulphate gave 1·48, magnesium chloride 1·83, and potassium chloride 1·63, the same as sodium chloride.

(*c*) *Osmotic Pressures at Different Protein Concentrations.*

Condition I.—Concentrations of hydrogen ions and salts in the physiological region.

It has been shown that if the hæmoglobin of the horse is in equilibrium with a neutral decinormal solution of sodium chloride, the observed osmotic pressures can be represented by the formula given below (Adair, 1924).

$$p_{\text{obs.}} = k_m\text{C}/(1 - \text{K}_b\text{C}), \tag{26}$$

$p_{\text{obs.}}$ = observed osmotic pressures, measured at room temperature (18° to 20° C.) reduced to millimetres of mercury at 0° C. by Gay Lussac's Law.

k_m = an empirical constant—approximately 2·55.

K_b = an empirical constant—approximately 0·033.

C = grammes of anhydrous protein per 100 c.c. of solution.

Similar results with a slightly smaller value for K_b have been obtained with human hæmoglobin and horse hæmoglobin, equilibrated the mixture of ions found in the red corpuscle, namely, K = 0·116, Na = 0·03, Ca = 0·0014, Mg = 0·001, Cl = 0·0725, HCO_3 = 0·026, H_2PO_4 = 0·006, HPO_4 = 0·022, SO_4 = 0·0011 mols per litre of water.

Application of van't Hoff's Law at Low Protein Concentrations.

The preliminary experiments carried out in 1921 indicated that van't Hoff's Law applies to the osmotic pressure of hæmoglobin if the concentration of *the protein is less than 3 per cent. In view of the importance of this conclusion* from the point of view of molecular weight determinations, the observations have been repeated by more exact methods at 0° C., and with the "outer fluid" defined in Table IX, in which the hydrogen ion concentration could be reproduced with much greater exactness than is practicable with solutions of sodium chloride or the salts of blood.

The observations recorded in fig. 5 confirm the provisional conclusion that the osmotic pressure is proportional to the concentration in dilute solutions, but they show that there are appreciable deviations in solutions containing more than 1 per cent. of protein.

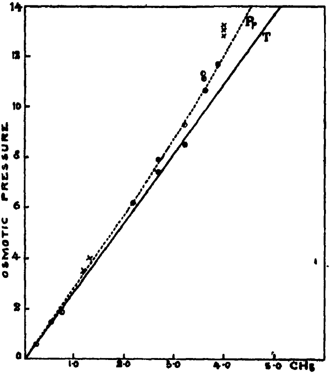

Fig. 5.—Osmotic pressures of dilute solutions of hæmoglobin equilibrated with phosphates (Table IX). p_p = theoretical curve calculated by formula (29). T = theoretical curve calculated by formula (27). CHb = grammes dry hæmoglobin per 100 c.c. solution. Circles, sheep's hæmoglobin. Crosses, human hæmoglobin.

Table IX.—Composition of "Outer Fluid" pH 7·8 in Experiments Recorded in Figs. 5 and 6 and Table X.

KCl = 0·10 mols = 7·546 grammes per litre of solution (density 1·013).
KH_2PO_4 = 0·00533 mols = 0·726 grammes per litre.
$Na_2HPO_4 . 12 H_2O$ = 0·06133 mols = 21·98 grammes per litre.

Note.—The pH of the phosphate mixture (7·8 at 0° C.) is greater than the pH of blood (about 7·4 at 38° C.), a condition which compensated for the diminution in the dissociation constant of the protein with fall of temperature referred to by Warburg (1922) and Stadie and Martin (1924).

Application of the Equations of Hirn and van der Waals in Concentrated Protein Solutions.

The observations recorded in Table X and fig. 6 show the observed osmotic pressures and also the partial osmotic pressures of the protein ions, in solutions equilibrated with the mixture of potassium chloride and phosphates at *p*H 7·8, defined in Table IX.

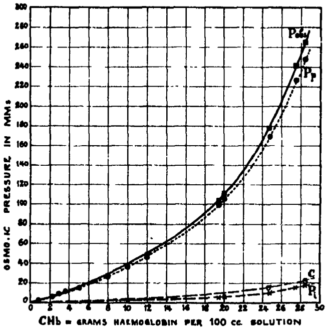

FIG. 6.—p_{obs} = observed osmotic pressure of hæmoglobin in millimetres of mercury at 0° C. p_p = partial pressure of the protein ions. p_i = diffusible ion pressure difference calculated by formula (34). C = diffusible ion pressure difference calculated by formula (35). CHb = grammes dry hæmoglobin per 100 c.c. protein solution, in equilibrium with phosphate buffer mixture at *p*H 7 8 (Table X).

It is possible to represent the observations by means of a number of simple empirical formulæ, which have been stated below, with their range of application and numerical constants.

$$p_{obs.} = k_m\mathrm{C}\,; \quad p_p = k_m\mathrm{C}. \tag{27}$$

Range C = 0 — 0·8 (in grammes dry protein per 100 c c. solution), $k_m = 2{\cdot}67$.

$$p_{obs} = k_m\mathrm{C} + k_m k_b \mathrm{C}^2 + k_i\mathrm{C}^2. \tag{28}$$

$$p_p = k_m\mathrm{C} + k_m k_b \mathrm{C}^2. \tag{29}$$

$$p_i = k_i\mathrm{C}^2.$$

Range C = 0·8 — 4·0, $k_m = 2{\cdot}72$, $k_m k_b = 0{\cdot}066$, $k_i = 0{\cdot}018$.

$$p_{obs.} = k_m\mathrm{C}/(1 - \mathrm{K}_b\mathrm{C}). \tag{30}$$

$$p_p = k_m\mathrm{C}/(1 - k_b\mathrm{C}). \tag{31}$$

Range C = 1·0 – 20·0, $k_m = 2{\cdot}72$, $\mathrm{K}_b = 0{\cdot}0254$, $k_b = 0{\cdot}0242$.

$$p_{obs.} = p_i + \mathrm{RT}/(\mathrm{V} - \beta\mathrm{V}_m). \tag{32}$$

Range General.—V = volume in litres of solution per mol of protein. V_m = volume of one mol of protein. β = a variable factor defined by this formula. β diminishes from 3·4 at C = 8·0 to 2·26 at C = 34·4, and, as a first approximation, the variation can be represented in a formula with three empirical constants of the form stated below—

$$p_p\,[V - V_m\,(\beta_1 - \beta_2 e^{-ap})] = RT. \tag{33}$$

The term V_m, the product of the molecular weight (about 68,000), and the effective volume per gramme (α in formula (4) is approximately 0·965 c.c.) is 66 litres.

The term p_i has been calculated by two methods. The curve marked p_i in fig. 6 has been calculated from membrane potentials by formula (19), quoted below.

$$p_i = 15{\cdot}4\,g\,.\,r\,\Sigma c_i''\,E^2 = 15{\cdot}4\,(0{\cdot}87)\,(1{\cdot}48)\,(0{\cdot}395)\,E^2 = 7{\cdot}74\,E^2. \tag{34}$$

The curve marked C has been calculated from entirely different data, by formula (20) quoted below, assuming that the valence of the protein equals 8.

$$p_i = \tfrac{1}{2}RTg\,(m_p n_p)^2/r\Sigma c_i'' = 0{\cdot}018\,(c\text{Hb})^2. \tag{35}$$

$m_p n_p$ = equivalent concentration of protein (formula (4)). (cHb) = grammes protein per 100 c.c. of solvent.

$$c\text{Hb} = C/1 - 0{\cdot}00965\,C. \tag{36}$$

For certain purposes equation 30 must be re-stated in the forms given below—

$$p_{\text{obs}}\,(V - b_1) = \phi_s RT. \tag{37}$$

$$p_{\text{obs}}\,(v - b) = \phi_s RT. \tag{38}$$

V = litres of solution per mol of protein.
v = litres of solvent or " dispersion medium."
b_1 = 173·4 litres.
b = 107·5 litres ($b = b_1 - V_m$).
ϕ_s = empirical correction factor = 1·09.

The formulæ (33), (37) and (38) resemble the gas equations of Hirn and van der Waals and the equations for the osmotic pressure of non-electrolytes developed by Sackur (1910) and Porter (1917), in that they contain a correction for the volume of the molecules. The data in Tables XI, XII, XIII show that this correction is of significance at different salt concentrations, because g_p', the corrected osmotic coefficient, defined by formula (39), increases with the protein concentration; but there is no strict analogy between the term βV_m

in formula (32) and van der Waals' b, because βV_m is a function of the concentration of diffusible salts.

$$p_p = RTg_p' \left(\frac{10C}{M}\right)\left(\frac{1}{1 - 0\cdot00965C}\right). \qquad (39)$$

The value of M, the molecular weight, has been discussed in Section 7.

Table X.—Osmotic Pressures at Different Protein Concentrations. Hæmoglobin plus KCl 0·1 Molar, Na_2HPO_4 0·0613 Molar, KH_2PO_4 0·00533 Molar.

Experiment No.	C	$p_{obs.}$	p_i	p_p	p_p (calc.)	pH''	E
225	0·68	1·9	0·00	1·9	1·9	7·8	0·02*
184	2·21	6·2	0·04	6·2	6·2	8·0	0·07
258	2·90	8·6	0·07	8·5	8·5	7·9	0·10
211	3·58	11·2	0·07	11·1	10·7	7·75	0·10*
256	5·00	14·9	0·31	14·6	15·4	7·8	0·20
207	8·00	28·2	0·50	27·7	27·0	7·75	0·24*
300	8·12	28·8	0·61	28·2	27·5	7·7	0·28*
255	10·00	40·2	2·00	38·2	35·9	7·9	0·50
204	12·00	48·7	1·20	47·5	46·0	7·75	0·40*
297	15·50	67·4	2·80	64·6	67·6	7·7	0·60*
250	19·40	103·6	4·40	99·2	99·3	7·9	0·75
202	19·80	104·2	3·80	100·4	103·4	7·75	0·70
252	20·00	110·9	5·70	105·2	105·3	8·00	0·87
298	24·00	155·0	8·50	146·5	156·2	7·70	1·05
201	25·00	179·0	9·50	169·5	172·2	7·75	1·10
205	28·00	242·0	14·20	227·8	236·2	7·75	1·35*
200	29·00	264·6	16·50	248·1	264·5	7·75	1·45
299	34·40	382·8	30·60	352·2	558·8	7·65	1·98

C = grammes of sheep's hæmoglobin per 100 c.c. solution.

$p_{obs.}$ = observed osmotic pressure in millimetres of mercury at 0° C.

p_i = diffusible ion pressure difference (formula (34)).

p_p = partial osmotic pressure of protein = $p_{obs} - p_i$.

p_p = (calc.) = pressure computed by formula (31).

pH'' = pH of the "outer fluid" (Table IX).

E = membrane potential in millivolts (inner fluid negative). Those marked with an asterisk are calculated values.

The activities of diffusible ions in the protein solution have been given in Table III.

Table XI.—Osmotic Pressure of Carbon Monoxide Hæmoglobin.* In equilibrium with Ammonium Phosphate at pH 6·7 (Isoelectric). Concentration $(NH_4)\,H_2PO_4$, 0·006 Molar $(NH_4)_2\,HPO_4$, 0·004 Molar.

C	1·98	4·24	7·13	14·1	18·2	23·5	27·7
$p_{obs.}$	5·28	12·55	23·3	58·1	90·3	138·4	175·7
g_p'	1·03	1·14	1·19	1·39	1·68	1·80	1·82

Table XII.—Osmotic Pressure of Reduced Hæmoglobin In equilibrium with Phosphate Mixture 6·8 (approximately Isoelectric). Concentrations

KH_2PO_4, $\frac{1}{30}$ Molar, Na_2HPO_4 $\frac{1}{30}$ Molar, KCl $\frac{1}{10}$ Molar

C	1·15	1·83	7·89	14·75	19·33
$p_{obs.}$	3·02	4·93	29·3	61·7	101·1
g_p'	1·04	1·06	1·37	1·44	1·70

Table XIII—Osmotic Pressures of Reduced Hæmoglobin. In equilibrium with 2 Molar NaCl + 0·025 Molar $NaHCO_3$ (pH 8·3).

C	4·7	8·46	16·32	19·7
$p_{obs.}$	19·0	41·6	104·7	138·6
g_p'	1·58	1·80	2·16	2·28

* p_i is practically negligible under the conditions referred to in Tables XI, XII, XIII.

7. DETERMINATION OF THE MOLECULAR WEIGHT OF A PROTEIN IN THE PRESENCE OF SALTS.

It has been shown (Adair, 1925, 3) that in the absence of salts, the mass of the hæmoglobin molecule is four times the equivalent weight 16,666, determined by iron analyses. This result has been confirmed by Svedberg and Fåhreus (1926), and Svedberg and Lysholm (1927).

In calculations of the mass of the particles in the presence of salts, a number of different factors must be taken into account, as stated in formula (23) (quoted below).

$$M_s = \phi_h \phi_s \phi_v \, RT \,.\, 10C/(p_{obs} - p_i) \tag{40}$$

It has been shown that under certain conditions the term p_i is relatively small, and the osmotic pressure is approximately proportional to the concentration, as stated in formula (27).

If it is assumed that the functions ϕ_h and ϕ_s are equal to unity, under these conditions it follows that

$$M_a = \frac{10RT}{k_m} = \frac{10 \times 760 \times 22 \cdot 414}{k_m} = \frac{170,330}{k_m}. \tag{41}$$

Extrapolation—Method I.

The first method of determining k_m in formula (41) depends upon the observation that when dilute solutions (less than 3 per cent. of protein) are equilibrated with certain salt solutions of constant composition, the osmotic pressures can be represented by an empirical formula like equation 28, re-stated below:

$$\pi = p_{obs}/C = k_m + k_m k_b C + k_i C. \tag{42}$$

The relationship between π defined by equation (42) and C, the concentration in grammes of dry protein per 100 c.c. of solution, appears to be approximately linear in very dilute solutions, and therefore k_m (or π for $C = 0$) can be determined with considerable accuracy by extrapolation.

Results obtained by this method have been stated in Table XIV.

Extrapolation—Method IA.

This method differs from Method I in that it depends upon measurements of osmotic pressures at higher protein concentrations. Theoretically, the correction for the deviations from van't Hoff's Law is not quite so accurate, but from the technical point of view Method IA is simpler because measurements of osmotic pressure below 5 mm. require exceptional precautions, and may take many days to reach equilibrium (Adair, 1925, 2).

In applying Method IA p_p (or $p_{obs.}$ if p_i is small) has been plotted as ordinate and C as abscissa, and the ratio k_m has been determined by extrapolation (Adair, 1924, fig. 1).

The value $2 \cdot 55 \pm 0 \cdot 2$ for k_m has been obtained by this method for hæmoglobin equilibrated with a solution of the ions present in the red corpuscle.

Method II.

The measurements recorded in Section 6 and Table X show that if the concentration of salts is great enough to reduce the term p_i to a small fraction of the observed osmotic pressure, and not great enough to cause large variations in ϕ_s, the observed osmotic pressures can be represented by an equation of the type stated below—

$$\frac{1}{C} = \frac{K_m}{p_{obs.}} + K_b = \frac{K_m}{p_p} + k_b. \tag{43}$$

In the case of hæmoglobin solutions in the range from 4 per cent. to 20 per cent., $K_m = 2 \cdot 72$ if the solvent is a phosphate mixture. This figure differs by less than 10 per cent. from the value of that obtained by extrapolation methods, and therefore Method II may be of service in the case of a series of observations on concentrated protein solutions, in which the data required for the application of Methods I and IA are not available.

In the case of the serum proteins the provisional estimates given by equation (43) are of the same order of magnitude as these calculated by Sorensen's formula (Sörensen, 1925), which gave the figures 45,000, 80,000 and 140,000 for serum albumin, pseudoglobin and euglobulin. Formula (43) gives uniformly higher values—namely, 68,000, 147,000 and 170,000. Differences between the function ϕ_s and unity may be of importance in these calculations.

In the case of hæmoglobin, experiments have been carried out (fig. 3) which make it possible to correct for the salt effect by extrapolation, and it appears that under the conditions referred to in the determination of K_m, $\phi_s = 1 \cdot 09$, and by applying this correction, the following formula can be obtained—

$$M_a = 10RT\phi_s/K_m = 68{,}260. \qquad (44)$$

A small correction for the unequal distribution of a protein in a gravitational field reduces this result to 68,000.

Table XIV.—Values of k_m and Provisional Values of the Molecular Weight of Hæmoglobin (M_a) at Different Salt Concentrations.

k_m	M_a	pH	Salts.
2·62	65,000	6·8	0·001 Molar $Na_2HPO_4 + KH_2PO_4$ mixture.
2·54	67,000	6·7	0·01 Molar $(NH_4)_2\ HPO_4 + (NH_4)\ H_2PO_4$.
2·55	66,800	6·8	0·22 Normal $Na_2HPO_4 + KH_2PO_4 + KCl$.
2·67	63,800	7·8	0·23 Normal $Na_2HPO_4 + KH_2PO_4 + KCl$.

M_a = grammes of dry protein (dried at 103° C.) per gramme mol. The molecular weight in terms of undenatured protein is probably 82,000, about 22 per cent. greater than M_a. The first three values have been obtained by extrapolation Method I, the last by Method IA.

The measurements on serum proteins show that in general the determination of the size of protein particles in the presence of salts is a difficult problem, but in the case of hæmoglobin it seems justifiable to accept the provisional value obtained by Methods I and IA.

A brief summary of the experimental evidence bearing on this question has been given below. In a previous paper (Adair, 1925, 2) it has been shown that (1) the osmotic pressures remain constant for long periods, (2) the results for preparations of different degrees of purification are in close agreement, (3) the results for human, horse, ox and sheep's hæmoglobins are in agreement. In this work it has been found that (4) the results for oxyhæmoglobin, reduced hæmoglobin, met-hæmoglobin and carbon monoxide hæmoglobin are in agreement; (5) the crystalline fractions give the same pressure as "total hæmoglobin," and therefore it is probable that hæmoglobin is a pure substance; (6) the osmotic pressures at 0°, 11° and 22° C. are proportional to the absolute temperature (Martin, 1896); (7) the agreement of the provisional values of M_a at different salt concentrations makes it probable that the corrections for the ion pressure difference, p_i, and the osmotic coefficient of the protein are at least approximately correct.

Summary.

The osmotic pressures of hæmoglobin solutions in equilibrium with solutions of diffusible salts have been measured and correlated with determinations of the membrane potentials, and the distribution of diffusible ions.

Although the relationships between the activities of diffusible ions and the membrane potentials are in accordance with Donnan's theory, his assumptions concerning osmotic pressures are not applicable to the protein solutions of finite concentration which have been studied in this work.

Within certain ranges of hydrion, salt and protein concentrations, a modified form of Dalton's Law of Partial Pressures appears to be applicable for the purpose of analysing the observed osmotic pressures in terms of p_i, the diffusible ion pressure difference, and p_p, the partial osmotic pressure of the protein ions.

Systematic experimental investigations of the partial pressures indicated that certain variations formerly attributed to changes in aggregation are due to the existence of great deviations from the law of van't Hoff.

In solutions with hydrogen ion concentrations from 10^{-5} to 10^{-9}, and with sodium chloride concentrations from 0·01 to 4 mols per litre, and in solutions with different species of ions, including K, Na, NH_4, Mg, Cl, HCO_3, SO_4, H_2PO_4, HPO_4, the degree of aggregation of hæmoglobin appears to be constant.

Methods for determining the molecular weight of proteins in non-ideal solutions containing salts have been developed.

The value 67,000 obtained for hæmoglobin in physiological salt solutions agrees with that previously determined for hæmoglobin in distilled water.

In conclusion, I wish to thank Sir William Hardy, F.R.S., for the support that he has given to this work.

LITERATURE.

Abegg, R. (1893). 'Z. Phys. Chem.,' vol. 11, p. 248.

Adair, G. S. (1923). 'Science,' vol. 58, p. 13.

Adair, G. S. (1924). 'Proc. Camb. Phil. Soc.' (Biol.), vol. 1, p. 75.

Adair, G. S. (1925) 1. 'J. Biol. Chem.,' vol. 63, p. 493.

Adair, G. S. (1925) 2. 'Roy. Soc. Proc.,' A, vol. 108, p. 627.

Adair, G. S. (1925) 3. 'Roy. Soc. Proc.,' A, vol. 109, p. 292.

Adair, G. S (1926). 'Skandinav. Arch.,' vol. 49.

Adair, G. S. (1927). 'Trans. Faraday Soc.,' vol. 23, p. 536.

Austin, J. H., Sunderman, F. W, and Camack, J. G (1926). 'J. Biol. Chem.,' vol. 70, p. 427.

Barcroft, J., and Hill, A. V. (1910). 'J. Physiol.,' vol. 39, p. 411.

Bjerrum, N. (1918), 'Z. Elektrochem.,' vol 24, p. 321.

Bjerrum, N. (1923). 'Z. Phys. Chem.,' vol. 104, p. 406.

Bjerrum, N. (1924). 'Z. Phys. Chem.,' vol. 110, p. 656.

Briggs, A. B. (1922). 'J. Biol. Chem.,' vol. 53, p. 13.

Brönsted, J. N. (1927). 'Trans. Faraday Soc.,' vol. 23, p. 416.

Brown, W. E. L., and Hill, A. V. (1923). 'Roy. Soc. Proc.,' B, vol. 94, p. 297.

Cernatescu, R. (1920). 'Ann. Sci. Univ Jassey,' vol. 10, p 259.

Clark, W. M. (1923). "The Determination of Hydrogen Ions," Baltimore.

Debye, P., and Hückel, E. (1923). 'Physik. Z.,' vol. 24, p. 185.

Donnan, F. (1911). 'Z. Elektrochem.,' vol. 17, p. 572.

Donnan, F., and Allmand, A. J. (1914) 'Trans. Chem. Soc.,' vol. 105, p. 1941.

Frisch, J., Pauli, W., and Valkó, E. (1925). 'Biochem. Z.,' vol. 164, p. 401

Gibbs, J. W. (1876). 'Trans. Conn. Acad.,' vol. 3, p. 108.

Gibbs, J. W. (1878). 'Amer. J. Sci.,' vol. 46, p. 441.

Haber, F., and Klemensiewicz, Z. (1909). 'Z. Phys Chem.,' vol. 67, p. 385.

Hammarsten, E. (1924). 'Biochem. Z.,' vol. 144, p. 383.

Hardy, W B. (1905). 'J. Physiol.,' vol. 33, p. 251.

Hastings, A. B., van Slyke, D. D., Neill, J. M., Heidelberger, M., and Harington, C. R. (1924). 'J. Biol. Chem.,' vol. 60, p. 89.

Hastings, A. B., Sendroy, J., Murray, C. D., and Heidelberger, M. (1924). 'J. Biol. Chem.,' vol. 61, p. 317.

Hückel, E (1925). 'Kolloid. Z.,' vol. 36, p. 204.

Lewis, G. N., and Randall, M. (1923). 'Thermodynamics,' New York.

Linderström-Lang, K. (1926). 'C.R. lab. Carlsberg,' vol. 16.

Loeb, J. (1922). 'Proteins and the Theory of Colloidal Behaviour,' New York.

Martin, C. J. (1896). 'J. Physiol.,' vol. 20, p. 364.

Northrop, J. H., and Kunitz, M. (1926). 'J. Gen. Physiol.,' vol. 9, p. 351.

Pauli, W., and Schön, M. (1924). 'Biochem. Z.,' vol. 153, p. 253.

Pauli, W., and Wit, H. (1926). 'Biochem. Z.,' vol. 174, p. 308.

Planck, M. (1917). 'Treatise on Thermodynamics,' p. 233, London.

Porter, A. W. (1917). 'Trans. Faraday Soc.,' vol. 13, p. 123.

Roaf, H. E. (1910). 'Q. J. Expt. Physiol.,' vol. 3, p. 75.

Rona, P., and Petow, H. (1923). 'Biochem. Z.,' vol. 137, p. 356.

Sackur, O. (1910). 'Z. Phys. Chem.,' vol. 70, p. 477.

Sörensen, S. P. L. (1917) 'C R. lab. Carlsberg,' vol. 12.

Sörensen, S. P. L. (1925). 'Proteins.' The Fleischmann Company, New York.

Sörensen, S. P. L., Linderström-Lang, K., and Lund, E. (1927). 'J. Gen. Physiol,' vol. 8, p. 543.

Stadie, W. C., and Martin, K. A. (1924). 'J. Biol Chem,' vol. 60, p 191.

Stadie, W. C., and Ross, E. C. (1925). 'J. Biol. Chem.,' vol. 65, p 735.

Svedberg, T, and Fåhreus, R. (1926). 'J. Amer. Chem. Soc.,' vol. 48, p. 430.

Svedberg, T., and Lysholm, A. (1926). 'Nova Acta R Soc. Sci. Uppsal.'

Taylor, H. (1924). 'Roy. Soc. Proc.,' B, vol. 96, p. 383.

Van Slyke, D. D. (1923). 'J. Biol. Chem.,' vol. 58, p. 523.

Van Slyke, D D., Wu, H., and McLean, F. C. (1923). 'J. Biol Chem.,' vol 56, p. 765.

Van Slyke, D. D., Hastings, A. B., Murray, C. D., and Sendroy, J. (1925). 'J. Biol. Chem.,' vol. 65, p. 701.

Warburg, E. J. (1922) 'Biochem. J.,' vol. 16, p. 153.

Wilson, H. C. (1925). 'Biochem. J.,' vol. 19, p. 80.

Photographic Study of Detonation in Solid Explosives. Part I.—The Development of a Photographic Method for measuring Rates of Detonation.

By Elwyn Jones.

(Communicated by J. F. Thorpe, F.R.S.—R[illegible]ay 15, 1928)

[Plates 24–[illegible]

Introductio[illegible]

On detonation, a solid explosive undergoes extremely rapid chemical change with the liberation of a large amount of energy. The rate at which this energy is liberated is governed chiefly by the rate at which the explosive detonates. It is known, however, that the rate of detonation varies with the conditions under which the explosive is fired and is, therefore, presumably dependent on the rate at which the energy liberated on detonation is used up in doing work. It appears, therefore, that the behaviour of, and the results to be obtained from, a detonating explosive under given conditions are intimately connected with its rate of detonation under those conditions, and that an exact knowledge of the latter is of considerable importance in the study of detonating explosives and their power.

The rate of detonation of a solid explosive is usually measured either by the method devised by Mettegang,[*] or by that due to Dautriche.[†] The former is generally used for lengths of about a metre of explosive. The latter is capable of being used for shorter lengths, but is not an absolute method, as it is dependent on a preliminary determination of the rate of detonation of T.N.T. fuse by the Mettegang method.

Detonation rarely starts uniformly, so that the above methods give no indication of the rate of detonation over the first few inches of the explosive cartridge, a portion of the cartridge which is of considerable interest, since only small quantities are normally used in other explosive tests.

The author[‡] has previously described an absolute method for measuring rates of detonation wherein use is made of the partial discharge of a condenser during the time taken by the detonation pulse to break two electrical circuits. Although this method can be used to measure still shorter time intervals, it is evidently limited in its application owing to the fact that it gives only the average rate of detonation between two points in a cartridge. It was consequently decided to attempt to develop a photographic method which would be absolute, and in which a continuous and permanent record would be obtained in each experiment.

A photographic method has been used on many occasions to determine rates of combustion and detonation in gaseous mixtures, but its application to the study of detonation in solid explosives has not been extensive. Laffitte[§] used a rotating camera to measure the velocities of detonation of certain explosives c [redacted] tubes and also to observe the disturbance
travelling out fro under given conditions. More recently,
Perrott and Gawth lished an account of rather similar work,
the explosive in th confined in paper.

In a photographic method, where a luminous phenomenon travelling along a cartridge is recorded on a moving film, the sharpness of the resulting photograph will depend on the extent to which the stationary image of the cartridge approximates to a straight line. The image of the cartridge must therefore be reduced in thickness as much as possible, and this can be brought about in a number of ways. The method adopted in the present work has many advantages, and, in view of the particular nature of the work, is considered the most suitable. The explosive is fired behind a narrow slit in a steel screen, so that the cartridge is obscured with the exception of a narrow central strip, the width of which is adjusted so as to give an image about 0·007 cm. thick. By this means the thickness of the image can be made as small as desired without limiting any dimension of the cartridge and, as it permits the explosive to be fired very much closer to the lens and camera, there is a corresponding increase in the intensity of an image of similar magnification, thus making it possible to obtain photographs where otherwise the light might have been insufficient to affect the sensitised film.

---

[*] 'V. Internationaler Kongress für angewandte Chemie,' Berlin, vol 2, p 322 (1903)

[†] 'C. R., vol. 143, p. 641 (1906).

[‡] 'Safety in Mines Research Board Paper,' No. 22.

[§] 'Ann. de Chim. et de Phys.,' vol. 4, p. 587 (Phys.) (1925).

[||] 'J. Franklin Inst.' (1) January, 1927; (2) March, 1927.

All evidence goes to show that, in a cylindrical cartridge of uniform composition, detonated axially, the detonation front is symmetrical about the axis of the cartridge so that the progress of detonation along any narrow longitudinal strip of the cartridge correctly reproduces the progress of detonation along the whole surface of that cartridge. This has been verified on several occasions by firing the cartridge with its axis vertical and at right angles to the slit, and thus observing the arrival of detonation at points on the surface of the cartridge in a plane perpendicular to the axis.

Description of the Apparatus

The camera (A, fig. 1) used in the present work is of a special design, capable of giving very high speeds of rotation. In order to attain these speeds, it was necessary to curtail the width of the film, thus restricting the length of the image obtainable. In view of this fact, it was decided to limit the length of cartridge under observation to about 15 cm., but in consequence of the high speeds attainable and the nearness of the explosive, it has nevertheless been possible to use a higher magnification of the image than has been obtainable hitherto. This magnification factor is directly determined with the film in motion by exposing an illuminated scale in the position usually occupied by the explosive cartridge. The actual speed of the film is determined in each experiment by measuring on the film itself the distances between successive markings made by allowing light from a bright source to fall on the film at definite short-time intervals, the exposure of the film to these time-markings being made to coincide with the detonation of the explosive.

The lens (B, fig. 1) used to focus the image of the explosive cartridge on the film is a Cooke lens of 25·4 cm. focal length and aperture f 2·5, and is fitted with an iris diaphragm with which to vary the amount of light allowed through, according as the intensity of the illumination given out by the explosive demands. It is placed in such a position that its axis is horizontal and is at right angles to and level with the axis of the camera. The lens is

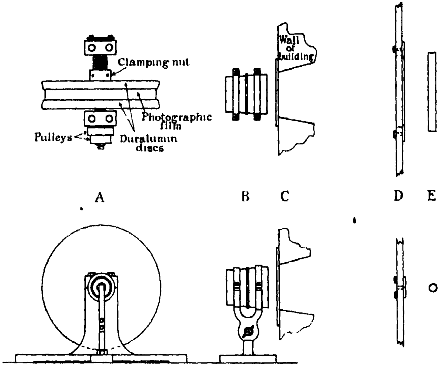

FIG. 1.

protected from projected solid particles by a plate-glass screen (C, fig. 1) placed immediately in front of it.

The explosive is fired behind a vertical steel screen (D, fig 1) which is 2·5 cm. thick. This screen is placed parallel to the axis of the camera and at a distance of about 210 cm. from the lens. A horizontal slit, 1·3 cm. wide and 17·8 cm. long, is cut in this screen, such that its centre is in line with the axis of the lens. Over this slit a steel plate 0·64 cm. thick is bolted, and in this there is a similarly placed but much narrower slit. In most of the earlier experiments the width of this slit was 0·16 cm., but it has since been reduced to 0·08 cm., with improved definition in the photographs. The advantage of having the narrow slit in a separate steel place is that it can readily be taken down for repair.

Procedure.

In the early stages of the work, the explosive cartridge was usually unwrapped before firing. It was then suspended in a horizontal position at a definite distance from the slit, such that the axis of the cartridge was parallel to the slit and at the same level. The reasons for firing the explosive a short distance away from the slit will appear later.

When the explosive is mounted in this position, the image formed on the film is that of a very narrow central strip on the surface of the cartridge, and is exactly at right angles to the direction of motion of the film and parallel to the direction of motion of detonation in the cartridge. On firing the explosive, it thus follows that a photograph is obtained which gives the position of detonation on the surface of the cartridge at any instant after initiation. A typical photograph obtained with the above procedure is that reproduced in Plate 24.

General Remarks.

It will be observed that Plate 24, fig. 1, in common with all the other photographs given later, shows the presence of two separate luminous phenomena That appearing first is due to the passage of detonation along the cartridge, this giving rise to a narrow bright band on the photograph. As the explosive cartridge is detonated on the remote side of a slit, this trace always has definite boundaries governed by the length of this slit. Shortly after this, another luminous effect becomes evident. In this case, however, the bright portion projects beyond the boundaries of the slit, showing that this phenomenon occurs between the slit and the camera. It was found experimentally that the time interval elapsing between the appearances of these two luminous phenomena increases with the distance between the explosive and the slit. This shows that the secondary illumination is due to the presence of the screen or slit, or both. In general, the photographic record of this secondary illumination shows three successive bright bands, and, as a section of the slit used shows three reflecting surfaces at A, B, and C (fig. 2), it is likely that the phenomenon is connected with reflection at these surfaces of the disturbance sent out from the detonated explosive* Such reflection gives rise to an increase in temperature which may cause greater luminosity in the products of detonation either directly or, indirectly, as a result of increased chemical action amongst those products. On the other hand, it has been

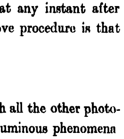

FIG. 2.

---

* A later change in the shape of the slit modified the photographic record of the secondary illumination in accordance with this supposition.

shown by Liveing and Dewar*, Dixon,† and Laffitte‡ that the spectrum of such a reflected disturbance exhibits, in a marked degree, lines corresponding to the elements found in the reflecting surface, so that it is also possible that the increased luminosity may be due to minute incandescent solid particles torn from the sides of the slit. The present paper, however, is not directly concerned with this secondary illumination, and, by firing the explosive at a short distance from the slit, its appearance has been delayed slightly so as to ensure the separation of the photographic record of the detonation phenomenon from that of this secondary illumination.

It should be borne in mind that detonation is photographed as it appears on the surface of the opaque explosive cartridge and, except in the case of nitro-glycerine, it has not been possible to determine directly the manner of propagation inside the cartridge

From the practical point of view this surface rate of detonation is of importance, as the initial shock experienced by a body when placed near an explosive cartridge is due to impulses received from the effective surface of the cartridge.

In general the explosive is initiated by means of a detonator placed axially and entirely buried at one end of the cartridge. When the detonator is inserted in this way, the explosive is initiated in the region of the end of the detonator, and detonation spreads out from this point. Assuming the surface of the detonation zone to be spherical, it will be seen that, when detonation first appears at the surface of the cartridge at B (fig 3), it will have travelled along the axis to C, a distance equal to the radius of the cartridge. From the point B detonation will travel in both directions along the surface of the cartridge. A short time later the detonation front will occupy such a position as B′C′, and, since BB′ is greater than CC′, the rate of detonation measured along the surface of the cartridge will be greater than that along the axis. Under these

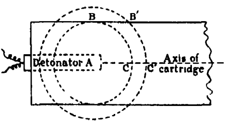

Fig. 3.

---

* 'Roy. Soc. Proc.,' vol. 36, p. 471 (1883).

† 'Phil. Trans.,' A, vol. 200, p. 319 (1902).

‡ *Loc. cit.*

conditions detonation as observed on the surface of the cartridge will start from B in both directions with a very high initial rate, but this will fall off until eventually it has much the same value as that along the axis of the cartridge. Thus the photographic record has a hooked shape at the end corresponding to the detonator-end of the cartridge.

It has been assumed above that the cartridge is initiated at a point, but actually it is initiated by a detonator which has a definite shape and volume. Thus the detonation front in the explosive will start with an initial shape depending on the detonator used, and this will influence the initial form of the photographic record obtained. In the early stages the surface rate of detonation is also influenced by the manner in which detonation in the particular explosive varies in speed from the initiation value to the steady final velocity. Thus the photographic record generally consists of an initial curved portion, governed partly by the detonator used and partly by the properties of the explosive, and a straight portion which corresponds to the stable velocity of detonation of the explosive in a cartridge of the diameter used

Effect of the Surrounding Medium.

Most of the earlier work with the photographic method was carried out with gelatinous explosives on account of their rigidity and the consequent ease with which the bare cartridges could be mounted in position. The photographs obtained with a number of these explosives were characteristic, typical examples being reproduced in Plate 24, figs. 1, 2. The former was obtained with a cartridge of 58 per cent. N.S. gelignite and shows that the rate of detonation becomes uniform at a distance of 7 cm. from the end of the detonator, this uniform rate of detonation being 2290 metres per sec The latter was obtained with a cartridge of "Arctic" gelignite No. 2 and shows that the rate of detonation is increasing during the first 15 cm. of the cartridge.

The application of the method to the determination of the velocities of detonation of powder explosives presented some difficulty. In dealing with these explosives it was necessary to enclose the cartridge in a rigid transparent container, and it was decided to use thin-walled glass tubes for this purpose. The photographs obtained under these conditions appeared distorted and the changed appearance aroused suspicion. In consequence, a cartridge of a powder explosive was mounted in position without removing the ordinary wrapper. A narrow strip was cut out of the paper wrapper in such a way that the bare explosive was exposed to the camera through the slit in the steel screen. With this arrangement a photograph (Plate 24, fig. 3) was obtained which had the same characteristics as those obtained with the bare gelatinous explosives. The effect observed on using a glass container is shown in Plate 24, fig. 4, which reproduces one of two identical photographs obtained on firing liquid nitroglycerine in a thin-walled glass tube by means of a No. 6 service detonator. This photograph, obtained with a transparent explosive, shows the primary flash due to the detonator and the later arrival of detonation at the surface where it encounters the glass walls of the container. A pressure pulse is thus initiated in the glass and this travels out with the velocity of sound, namely, about 5300 metres per sec. These extremely high pressures cause deformation of the medium in which they are travelling, so that the passage of the pulse along the tube is accompanied by shattering of the glass. Thus, if the rate of detonation of the explosive is less than the velocity of sound in glass, it appears that the shattering of the glass may proceed ahead of the detonation of the explosive The whole tube, however, is not shattered by the passage of the initial pulse, because the shattering of the glass causes degradation of this pulse and the pressure soon falls to a value which is transmitted without deformation. The pulse, however, is continuously maintained by the advancing detonation, so that the boundary of the shattered section of the tube advances correspondingly. The pulverised glass remains relatively stationary until it is dispersed later by the expanding products of detonation. Thus the powdered glass, illuminated by the very intense light from the detonation reaction in the transparent explosive, appears in the photograph as a bright band with parallel sides, the slope of which giving the rate of detonation of the explosive. Within this bright band appears a still brighter line, probably indicating where the detonation front is in contact with the pulverised glass, an effect similar to that observed on photographing a cartridge wrapped in white paper. With the above assumptions the low velocity of detonation of nitroglycerine appears to be about 1590 metres per sec., a value which agrees closely with those obtained by other methods.*

If the foregoing explanation were correct, it should be possible to obtain a clear photograph of the detonation front provided its velocity were greater

---

* Another interesting feature of the photograph is the evidence therein of a disturbance which leaves the point at which detonation first reaches the glass and travels forwards at a speed approximating to that of sound in glass. This, on reflection at the far end, appears to become the origin of a number of bright lines running approximately parallel to the direction of motion of the film. Whether or not these lines correspond to illuminated cracks caused by the reflection of the pressure as a tension, this parallelism to the direction of motion of the film indicates that relatively little movement of the glass takes place during this stage.

1

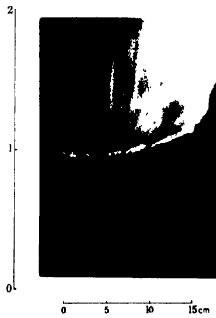
×10⁻⁴sec
2
1
0
0
5
10
15cm

2

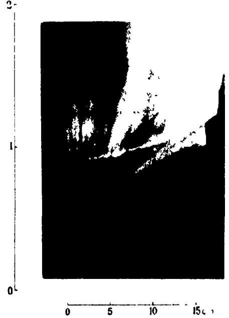
×10⁻⁴sec
2
1
0
0
5
10
15cm

3

×10⁻⁴sec.
2
1
0
0
5
10
15cm

4

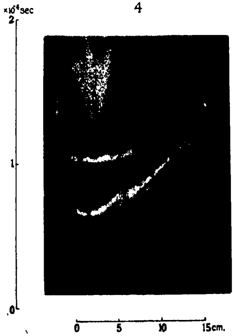
×10⁻⁴sec
2
1
0
0
5
10
15cm.

5

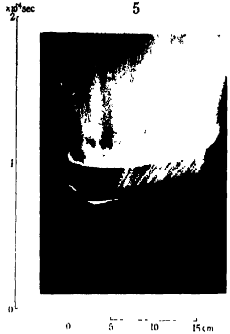
×10⁻⁴sec
2
1
0
0
5
10
15cm

6

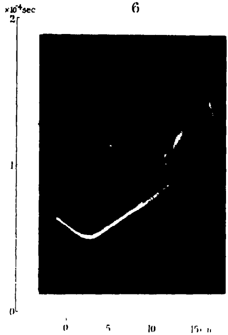
×10⁻⁴sec
2
1
0
0
5
10
15cm

7

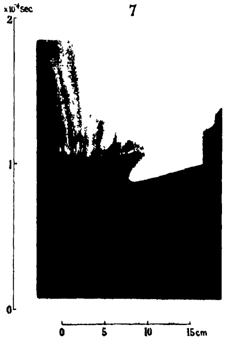
×10⁻⁴sec
2
1
0
0
5
10
15cm

8

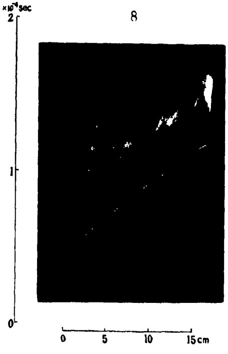
×10⁻⁴sec
2
1
0
0
5
10
15cm

9

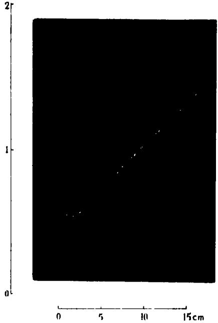
×10⁻⁴sec
2
1
0
0
5
10
15cm

10

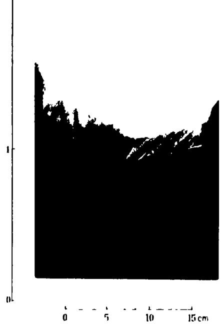
×10⁴sec
2
1
0
0
5
10
15cm

11

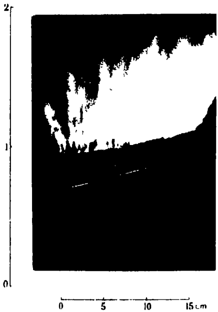
×10⁴sec
2
1
0
0
5
10
15cm

12

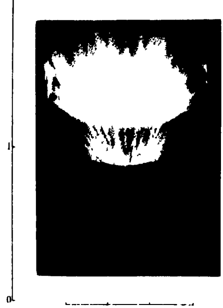
×10⁴sec
2
1
0
0
5
10
15cm

than that of the pressure pulse through glass which is about 5300 metres per sec * The high velocity of detonation of nitroglycerine is considerably in excess of this figure and by the use of a suitable initiator it was hoped to set up this high velocity A No 8 Briska detonator was used and the resulting photograph is reproduced in Plate 25 fig 5 This photograph obtained with a transparent explosive shows the progress of detonation along the axis of the cartridge where it is most advanced Detonation travels laterally from the detonator and reaches the surface of the explosive where it encounters the glass and initiates the pressure pulse in it In this case detonation travels along the surface of the explosive faster than a pressure pulse travels in glass so that the initial shattering of the glass accompanies the surface detonation pulse and does not precede it as in the previous case Meanwhile the detonation front inside the cartridge is in advance of that on the surface so that the former is photographed through glass which has experienced no shock and is therefore transparent The front edge of the narrow bright band on the photograph thus gives the rate of detonation along the axis of the cartridge and shows that in this particular instance the high velocity was established immediately The other edge of the narrow bright band corresponds to the surface detonation and in consequence takes the hooked form characteristic of all surface detonation records In this case however the hook at the locus of initiation is very obtuse on account of the extremely high velocity of detonation The high velocity of detonation of nitroglycerine determined from this photograph is 7820 metres per sec and agrees with a later value 7810 metres per sec obtained with the nitroglycerine contained in a thin transparent shell of cellophane in which the velocity of a pressure wave is much lower than in glass

The foregoing results indicate that when the explosive is in contact with a transparent medium in which the disturbance set up by the explosion travels faster than the detonation zone in the explosive the photograph of the detonation may be distorted The author in common with Comey † Laffitte ‡ Perrott § and Holmes || finds that, under certain conditions and in certain directions the disturbance outside a cartridge of solid explosive detonated in

---

* This conclusion was later verified with a number of other explosives, and it was found that in all cases where the velocity of detonation was above 5480 metres per sec the photographic record was quite clear whereas with velocities of 4700 metres per sec or under the photographs were distorted

† Seventh Int Cong Appl Chem London, 1909

‡ *Loc cit.*

§ 'J Franklin Inst March, 1927

|| 'J Franklin Inst., April, 1927

a gaseous medium can have a considerably higher speed than that of the detonation phenomenon in the cartridge itself. It thus appears possible that, even in the case of a naked explosive cartridge freely suspended in air, there may be special circumstances under which this disturbance may obscure the detonation of the cartridge. Such a possible case is illustrated in fig. 4, which represents a section through the cartridge in a horizontal plane passing through the slit in the steel screen. At a particular instant the surface detonation zone, which it is desired to photograph, occupies the position AB, but if the front of an opaque disturbance takes some such form as BCD, no light from AB can reach the lens. If this disturbance is luminous, a photographic record will be obtained which simply gives the rate of progress in the direction of the cartridge of the most advanced point C of this disturbance. Since it is the luminosity of the disturbance that is being photographed, the resulting record will correspond to the visible portion CD of its surface between C and the steel screen. Thus the photograph will not exhibit the characteristic narrow bright band associated with detonation, and will be easily recognisable.

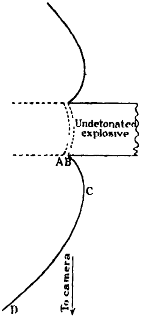

Fig. 4.

Under normal conditions the disturbance outside a cartridge does not often take up the form assumed above, but it has been possible to produce this result in two ways. In one case it was produced by using an unwrapped cartridge made up of two explosives of the same type, but with different rates of detonation The first half-cartridge had a rate of detonation of 2600 metres per sec., while that of the second half was 1710 metres per sec. The photograph obtained is reproduced in Plate 25, fig. 6. On passing from one explosive to the other there is a comparatively sudden change in the rate of detonation, but the disturbance caused by the first half-cartridge proceeds unabated and is thus able to gain on the retarded detonation. In this case the products of detonation are much less luminous than the detonation zone, so that the two can easily be distinguished. The front of the advancing disturbance is plainly recorded by its own luminosity, and, as it gets farther ahead of the detonation zone, the latter appears to diminish gradually in intensity, being obliterated by the increasing amount of opaque material between the cartridge and the steel screen. A similar result was obtained by initiating a bare cartridge of a gelatinous explosive by means of a very strong detonator. Under the influence of the detonator the front portion of the cartridge detonated at a much faster rate than the normal, but the initial rate of detonation set up is not sustained and rapidly falls to the stable value for the explosive. It will be seen, therefore, that the conditions are essentially the same as in the previous case.

It has been stated that this abnormal shape of the disturbance due to a detonating cartridge is very seldom encountered, but a somewhat similar effect is observed in the case of explosives detonating with a high velocity. In general, it has been observed that as the velocity of detonation increases, the luminosity of the resulting products also increases It thus occurs that with the very high velocity explosives the products of detonation are sufficiently luminous to make it difficult to distinguish between the photographic records left by the two causes This effect is illustrated in the photograph reproduced in Plate 25, fig. 7. This was obtained with a bare cartridge of ' Arctic " gelignite, and shows that over the first 8 cm. of the cartridge the rate of detonation is comparatively low, with the result that a normal photograph of the detonation zone is obtained About half-way along the cartridge there is a sudden increase in the rate of detonation, the high velocity set up being accompanied by a very luminous disturbance outside the cartridge Beyond the point at which the change in velocity takes place, it is almost impossible to judge from the photograph itself whether the front of the photographic record corresponds to the front of the detonation zone or to the most advanced point of this disturbance, which may or may not coincide with the front of the detonation zone Owing to the high velocity of detonation, it is unlikely that the disturbance can proceed faster in this direction, but it was considered advisable to test this conclusion in the case of an explosive cartridge which would favour the formation of an extremely rapid disturbance. For this purpose, a rough determination was made of the actual contour of the disturbance sent out from an unconfined cartridge of this high velocity explosive The explosive chosen was high-grade TNT pressed into cartridge form under a pressure of 10 tons per square inch, the cartridges being 6·1 cm. long and 3·2 cm. diameter. The behaviour of these cartridges under different tests led to the conclusion that it could be assumed that each cartridge detonated in a very similar way. The average rate of detonation over the latter part of this cartridge was found to be 6200 metres per sec., but the disturbance leaving the end of the unconfined cartridge was found to have an initial speed of about 7000 metres per sec. Cartridges were detonated in various known positions with reference to the slit, the axis of each cartridge being kept in a vertical plane parallel to and at a fixed distance from the steel screen. Assuming that the disturbance sent out from the explosive cartridge is symmetrical about the axis of the cartridge, the photograph obtained in any one experiment shows the progress of the front of this disturbance along the line of intersection of the horizontal plane through the slit and the vertical plane through the axis of the cartridge. Thus, if fig. 5 represents the position of the cartridge in one experiment, the resulting photograph gives the position of the front of the disturbance at different times on a line making an angle θ with the axis of the cartridge and meeting the surface of the cartridge at a point A distant x from the end. The times were all measured from the instant at which detonation first appeared on the surface of the cartridge, allowance being made in each case for the time required for detonation to reach the point A at which the disturbance is observed to leave the cartridge.

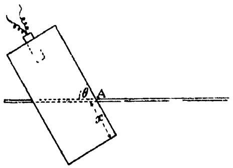

Fig. 5.

From these readings the position of the disturbance was determined at intervals of 10^{-6} sec., and plotted on a graph, a smooth curve being drawn through corresponding points to give the approximate contour at certain definite intervals. The results of these experiments are contained in fig. 6, which shows the instantaneous contour of the disturbed region surrounding this cartridge at intervals of 10^{-6} sec. from the instant at which the disturbance was initiated. The results tended to show that whereas the front and sides of the disturbed region were well defined, the portion in between appeared to have an irregular surface. The dotted portions of the curves shown in fig. 6 indicate means positions derived from a series of observations.

As far as the present work is concerned it is sufficient to point out that, even with this high velocity and high density explosive, the disturbed zone is not of the abnormal form to which reference has previously been made.

In spite of the confirmation afforded by these experiments it was decided to attempt to separate the luminosity due to other causes from that due to

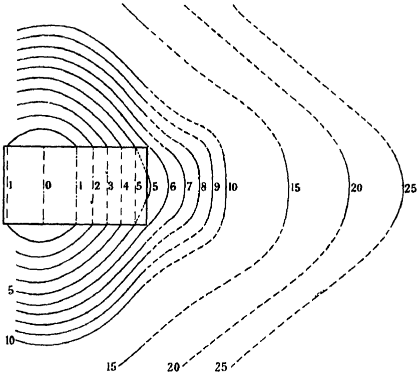

FIG. 6.

detonation, and thus arrive at a characteristic record of the detonation phenomenon even with high velocity explosives. If the explosive is in contact with a solid medium, the pressure pulse must travel through this first before the products of detonation can expand appreciably. Thus, by enclosing the explosives in a container of a suitable material, the expansion of the explosion products may be delayed, and by the use of a suitable thickness of this material it is possible to delay this for a sufficient length of time to separate the record of the detonation phenomenon from the luminosity due to the reaction products. The experiments carried out have shown that the material chosen must be transparent and remain so under very high pressures. In addition, a pressure-wave once set up in the material should die away rapidly, and its velocity of propagation should be as low as possible. Cellophane, a gelatinised and transparent form of cellulose, has been found to be quite suitable for this purpose, and in general the powder explosives are cartridge in sheet cellophane, 0·05 mm. thick, the usual waxed paper wrapping being dispensed with. Plates 25, fig. 8, and 26, fig. 9 show typical photographs obtained on using the same powder explosive with and without cellophane respectively. In the case of the high velocity explosives rather thicker material is used, the thickness of the shell surrounding the cartridge being about 0·2 mm. An illustration of the photographs obtainable is given in Plate 26, fig. 10, which was obtained with the same explosive as was used for fig. 7, the only difference being that in fig. 10 the cartridge was wrapped in cellophane It will be seen that the characteristic form of the photographic record of the detonation zone reappears on using a cellophane container. This is also shown in Plate 26, fig. 11, which was obtained with three short cartridges of compressed TNT, placed end to end and wrapped in the usual thickness of cellophane. A constant velocity of detonation of 6350 metres per sec is quickly established in this explosive.

Results.

The two methods generally used to determine the velocity of detonation of an explosive are those devised by Mettegang and Dautriche By means of the latter method, the average velocity of detonation can be determined over a length of 15 cm. of explosive, and, as this is the length of cartridge under observation in the photographic method, it is evident that the Dautriche method is suitable for comparison with the photographic method. A series of tests was therefore carried out to compare directly the results obtained by the photographic method with those obtained by the Dautriche method. In these tests determinations were made on the same 15-cm length of the same cartridge by the two methods, three explosives of a similar type being chosen to give a wide range of velocities. The results are given in Table I, and show that velocities of detonation given by the two methods are in substantial agreement.

The values given by the Dautriche method are based on a preliminary determination of the velocity of detonation of TNT fuse obtained by the Mettegang method, so that all three methods are involved in this comparison.

Table I.—Comparison of the Photographic with the Dautriche Method.

Explosive.	Velocity of detonation in metres per second	
	Photographic method.	Dautriche method.
Glasgow dynamite, 12 per cent. N/G	1710	1660
" " 28·5 " N/G	3240	3240
" " 60 " N/G	5120	5180

The velocities of detonation of several other explosives have been determined by the photographic method, some determinations of general interest appearing in Table II. These results illustrate the two velocities at which detonation is capable of propagation in the gelatinous explosives and the change in velocity on storage. The results also show the effect of the nitroglycerine content of a particular type of powder explosive on its velocity of detonation.

The cartridges of explosive were cylindrical in shape and 3·2 cm diameter, that being the diameter of cartridge most generally used in practice.

Table II.

Nature.	Explosive	Nitro-glycerine	Condition.	Velocity of detonation in metres/sec.
		Per cent.		
Gelatines	N.S. gelignite, 50 per cent N/G	49·9	Fresh	Low 3010
				High 6800
			Old	Low 2200
	N.S. gelignite, 58 per cent. N/G	57·9	Fresh	Low 3050
			Old	Low 2290
	Arctic gelignite No. 2	38·0	Fresh	High 5720
			Old	Low 2540
	Blasting gelatine	90·3	Old	Low 2010
				High 7590
Liquid	Nitroglycerine	—	—	Low 1590
				High 7820
Powders	Glasgow dynamite	11·0	—	1600
	" "	12·0	—	1710
	" "	18·5	—	2120
	" "	28·5	—	3240
	" "	40·0	—	3790
	" "	60·0	—	5120

Duration of Detonation Phenomenon.

It has been shown that the portion of the photographic record directly associated with the detonation of the explosive is characteristic and, unless distorted, always appears as a narrow well-defined band. If it is assumed that this band is due to luminous radiation emitted during the extremely violent reactions taking place in the detonation zone, then it is possible to determine the time of duration of these reactions from measurements of the photographs.

If d = thickness of the slit

and x = thickness of the detonation zone in the cartridge

(*i e.*, the length of cartridge undergoing reaction at a given instant), then the instantaneous image of the detonation zone is a rectangle having sides mx and md, where m = magnification factor (see fig 7). Both detonation zone and film are moving, however, and the resulting negative will be a dark band bounded by the lines AA′ and BB′. If at any point the thickness of this band in the direction of motion of the film be y, we see that.—
$\tan \theta = mx/(y - md)$, x = thickness of the detonation zone on the surface of the cartridge,

$$x = (y - md) \tan \theta/m = (y - md) \mathrm{V}/v,$$

where θ = angle made by the tangent to the curve at the chosen point,
V = velocity of detonation at that point,
v = velocity of film.

The duration of the phenomenon is given by

$$t = (y - md)/v.$$

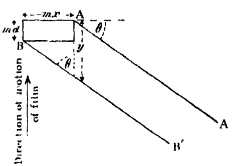

Fig. 7.

On measuring the photographs, it appears that the detonation zone passes a point on the surface of the cartridge in approximately 10^{-6} sec, the length of cartridge undergoing reaction at any instant being about 0·3 cm. It is uncertain whether or not halation has been completely eliminated, so that these figures may be slightly high.

The duration of detonation over a plane section perpendicular to the axis of a cartridge is influenced both by the thickness of the detonation zone and by its curvature Owing to the fact that detonation is most advanced on the axis of a cylindrical cartridge, it first arrives at the centre of a transverse section and appears to travel outwards from this point. By firing a cartridge of explosive with its axis horizontal and at right angles to the slit, so that an image is obtained on the film of a very narrow strip of explosive along a diameter of the end section of the cartridge, a photograph was obtained which gave the outward movement of detonation from the centre of this end section. The explosive used was a modified Glasgow dynamite detonating at 1750 metres per sec., and the cartridge was long enough to ensure that the steady condition had been reached. This photograph, Plate 26, fig 12, gives the relative times at which detonation arrives at points at different distances from the centre of a transverse section of the cartridge In the steady state the detonation front assumes a definite shape which travels uniformly along the cartridge, and as this uniform velocity was known, the actual form of the detonation front inside the cartridge could be derived from measurements of the photograph.

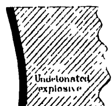

FIG. 8.

The stable form of the detonation front in a 7·6 cm. diameter cartridge of this explosive is shown in fig 8, which represents a longitudinal section of the cartridge in a plane passing through the axis In this case the detonation front on the axis of the cartridge is 0 65 cm in advance of that on the surface. It thus appears that in this particular case the duration of the detonation phenomenon over a transverse section of this cartridge is AB divided by the velocity of detonation of the explosive, or 6×10^{-6} sec In the case of a cartridge of 3 2 cm diameter the difference in position is usually about 0·3 to 0·4 cm. and the time of duration of detonation over a transverse section is about 3×10^{-6} sec This figure varies slightly from one explosive to another

Summary

A photographic method for studying detonation in solid explosives has been developed and applied to the measurement of rates of detonation.

Photographic records give the rate of movement of the detonation zone along the surface of an explosive cartridge and differences existing between the "surface" and "axial" rates of detonation are considered.

It has been shown that, under certain conditions, the disturbance set up in the surrounding medium may cause distortion of the photographic records of the detonation phenomenon and a method of overcoming this is described.

It is confirmed that under certain circumstances the disturbance set up

outside an explosive cartridge placed in a gaseous medium travels faster than the detonation phenomenon in the cartridge.

The contour of the disturbed region surrounding a particular cartridge of explosive has been approximately determined at definite intervals from the instant at which the disturbance is first initiated.

Photographic determinations of velocities of detonation are found to agree with those obtained by the Dautriche method.

Some results are tabulated to illustrate the two stable velocities of detonation peculiar to the gelatinous explosives and the effect of the nitroglycerine content of a powder explosive on its velocity of detonation.

A method is given for determining the approximate duration of the detonation phenomenon over a transverse section of a cartridge.

The stable form assumed by the detonation front inside a 7·6-cm. diameter cartridge of a certain explosive has been determined.

This work was undertaken on behalf of the Explosives in Mines Research Committee at the Research Laboratories of Nobel's Explosives Co., Ltd. The author wishes to thank the Committee, in particular Mr. W. Rintoul, Research Manager, Nobel Industries, Ltd, under whose direction the work was carried out, for permission to publish the results.

On the Magnetic Moment of the Electron.

By Prof. C. G. Darwin, F R S.

(Received July 21, 1928.)

1. In a recent paper[‡] the present writer discussed Dirac's new formulation[§] of the quantum mechanics of the electron from the point of view of the wave theory. In the course of that work formulæ were obtained for the electric density and current associated with any type of electron wave. These formulæ link the electron with the æther, so that to a first approximation (that is, excluding such questions as the reaction of its own emitted radiation on the electron) we have a complete expression of the state of affairs, which is suitable for use in the classical electromagnetic theory. But there are certain problems in which it is *convenient* to attribute part of the magnetic field of a moving electron to an electric convection current and part to its intrinsic magnetisation; for example, this would be so in discussing the Stern-Gerlach effect for free electrons In the earlier paper a separation of this kind was carried out for an electron in an atom and a short account was given of the corresponding case for an electron moving freely. As the paper was intended to cover a much wider field, these matters were only reviewed rather briefly, and the purpose of the present note is to elaborate them somewhat more fully. The process is one of pure classical theory, for the establishment of current and density is the only appeal that need be made to the quantum theory. We shall exhibit directly the magnetic moment of the electron, working it out in the first instance for slow motions, as it is easy to generalise this case by relativity principles. It would no doubt be possible to develop the whole result in one step, but the purely classical problem of the fields of a swiftly moving magnet is quite troublesome, even though the principles have been fully mastered, so that it would be an unnecessary and profitless exercise to follow this procedure.

It may be recalled that Dirac's equations[||] were easily shown to be invariant for any space or relativity transformation,[‡] even though their form is quite unsymmetrical. The associated density-current functions[§] naturally have the property of covariance, though also quite unsymmetrical in appearance. We shall here meet other tensors, also quadratic in the ψ's, and having the same unsymmetrical appearance. Their construction is by no means obvious, and the only process seems to be a direct application of all the transformations of the group to each component—a straightforward but laborious method. Before Dirac's equations were found one would have said without hesitation that the correct procedure in such a case would be to reduce the equations themselves to tensor form, for then the associated tensors should become obvious It is not hard[||] to throw the equations into space-vector form, but if the relativity transformation is to be included, they obstinately refuse to go into any but a very clumsy form and nothing is gained , this being so, it seems not worth while to use the space-vector either I have the hope that this subject may interest some analytical geometer and may tempt him to investigate these curiously unsymmetrical invariant properties. As we shall see, they appear to be connected with the stereographic projection of a sphere and perhaps with the homographic transformations of a complex variable, subjects with which I am not very familiar.

[‡] 'Roy. Soc. Proc.,' A, vol. 118, p. 654 (1928). As I shall have to refer to many formulæ in this paper, I shall denote them by a †. Thus (2.2)† denotes the four fundamental equations.

[§] 'Roy. Soc. Proc.,' A, vol. 117, p. 610 (1928).

[||] With his matrix methods, Dirac never actually writes down these equations, but they are extracted from his work and given in (2.2)†.

The purpose of the present note is illustration rather than proof, as it makes no new demands on the quantum theory, but is in effect pure electro-dynamics. It arose out of an investigation given in the immediately following paper, which aims at seeing whether any magnetic polarisation of electrons could arise when they are diffracted, say by a crystal. The results there obtained made it necessary to consider somewhat more deeply the interpretation of the wave equations and led to the present work.

2. There are two different ways in which magnetic moment can be observed, which may be called the internal and the external, typified respectively by the Stern-Gerlach method and the magnetometer. In the internal method we expose the magnet to a magnetic field and find its changed energy, in the external we isolate it and observe the magnetic field at a distance. As long as the electromagnetic equations are satisfied, the two methods must be equivalent and we may choose whichever is most convenient. There can be no question but that the external method is much simpler. for even if we avoid

---

[‡] See p 656†, (1), (2) and (3).

[§] The expressions (3.3)†

[||] See (2.3)†. Dirac uses a somewhat similar process, by splitting his matrices into pairs of factors one set of which is a space vector, but the work is still very unsymmetrical.

the troublesome non-uniform field of the Stern-Gerlach experiment, we still have to use something equivalent to the ponderomotive force of Lorentz in order to find the energy, whereas the external moment can be calculated from Maxwell's equations directly.

We therefore first consider how in the classical theory magnetic moment would exhibit itself externally. The general electromagnetic equations may be written

$$\left.\begin{aligned} \frac{1}{c}\frac{\partial \mathrm{E}}{\partial t} + 4\pi\frac{j}{c} &= \operatorname{curl}\mathrm{H}, \qquad \operatorname{div}\mathrm{E} = 4\pi\rho \\ -\frac{1}{c}\frac{\partial \mathrm{H}}{\partial t} &= \operatorname{curl}\mathrm{E}, \qquad \operatorname{div}\mathrm{H} = 0 \end{aligned}\right\}, \tag{2.1}$$

where ρ and j are density and current. As long as no single magnetic poles are allowed, these equations can describe any system. In Lorentz's theory the current is attributed to the convection of electricity so that $j = \rho v$, but this must now be changed so as to allow for the magnetic moment. The change is simple and brings the equations to the form they have in the elementary theory of magnetism. Let μ be the magnetisation (density of magnetic moment), then B the magnetic induction is given by $\mathrm{B} = \mathrm{H} + 4\pi\mu$ and the last two equations must be replaced by

$$-\frac{1}{c}\frac{\partial \mathrm{B}}{\partial t} = \operatorname{curl}\mathrm{E}, \qquad \operatorname{div}\mathrm{B} = 0$$

Eliminating H from the first equation we have

$$\frac{1}{c}\frac{\partial \mathrm{E}}{\partial t} + 4\pi\left(\rho\frac{v}{c} + \operatorname{curl}\mu\right) = \operatorname{curl}\mathrm{B} \tag{2.2}$$

At the distant point of observation we need not distinguish between H and B and so can attribute the effects to a current

$$j = \rho v + c\operatorname{curl}\mu. \tag{2.3}$$

We shall therefore show that part of j is proportional to the electron's velocity and part is the curl of a certain vector, and from this we shall deduce the magnetisation of the electron.

3. The magnetisation of the electron can only be observed by supposing that the electron wave is confined to a limited region of space. If it is observed by a Stern-Gerlach experiment, slits must be used, or if by a magnetometer, the electron wave must be somewhere away from the instrument. Moreover, if part of the magnetic field is to be attributed to the convection of electricity,

we must be able to assign a definite velocity to that convection. All these conditions are fulfilled if we take the electron as a "wave-packet." The accurate form of such a packet can be set down by the use of Fourier integrals, but, unlike the case of Schrodinger's equation, the integrals cannot be worked out, so that the distribution of the wave in space is not made explicit. However, by taking low velocity an approximate solution can be found, and this is all that is needed.

The accurate solution of Dirac's equations in the form of plane waves is

$$\left.\begin{aligned} \psi_3 &= \mathrm{A}\,.\,\mathrm{S} & \psi_4 &= \mathrm{B}\,.\,\mathrm{S} \\ \psi_1 &= \frac{-\mathrm{A}r - \mathrm{B}(p - iq)}{mc + \mathrm{W}/c}\,.\,\mathrm{S} & \psi_2 &= \frac{-\mathrm{A}(p + iq) + \mathrm{B}r}{mc + \mathrm{W}/c}\,.\,\mathrm{S} \end{aligned}\right\}, \tag{3.1}$$

where $\mathrm{S} = \exp i\,\frac{2\pi}{h}\,(px + qy + rz - \mathrm{W}t)$

and

$$\mathrm{W}/c = \sqrt{\{m^2c^2 + p^2 + q^2 + r^2\}}.$$

If the velocity is small, we have $\mathrm{W} = mc^2 + (p^2 + q^2 + r^2)/2m$, and the equations for ψ_3, ψ_4 reduce practically to Schrodinger's. In order to construct a wave packet we replace A by

$$\mathrm{A}\left(\frac{\sigma}{h}\sqrt{2\pi}\right)^3 \exp - \tfrac{1}{2}\left(\frac{2\pi\sigma}{h}\right)^2 [(p - mu)^2 + (q - mv)^2 + (r - mw)^2],$$

and taking the new A as a constant we now integrate over all values of p, q, r. As was shown in an earlier paper[‡], the result will be a packet initially round the origin, moving with velocity u, v, w and spreading somewhat as it goes. The initial value, which is all that we need here, is

$$\psi_3 = \mathrm{AP}, \qquad \psi_4 = \mathrm{BP}, \tag{3.2}$$

where

$$\mathrm{P} = \exp - \frac{1}{2\sigma^2}(x^2 + y^2 + z^2) + i\frac{2\pi}{h}m\,(ux + vy + wz).$$

To evaluate ψ_1, ψ_2 approximately we may replace W/c in the denominator by mc and the integrations can then be done. For our purpose we only want the initial values, and these can be found alternatively by the use of (4.1)[†]. We have

$$\left.\begin{aligned} \psi_1 &= -\frac{1}{2mc}\left\{\mathrm{A}\left[mw + \frac{ih}{2\pi\sigma^2}z\right] + \mathrm{B}\left[m\,(u - iv) + \frac{ih}{2\pi\sigma^2}(x - iy)\right]\right\}.\,\mathrm{P} \\ \psi_2 &= -\frac{1}{2mc}\left\{\mathrm{A}\left[m\,(u + iv) + \frac{ih}{2\pi\sigma^2}(x + iy)\right] - \mathrm{B}\left[mw + \frac{ih}{2\pi\sigma^2}z\right]\right\}.\,\mathrm{P} \end{aligned}\right\} \tag{3.3}$$

[‡] 'Roy. Soc. Proc.,' A, vol. 117, p. 258 (1927).

These four quantities express the instantaneous wave form at time $t = 0$ for a packet moving with small velocity u, v, w.

Next form the density and current by the use of (3.3)[†]—apart from a constant factor the four expressions are given below in (4.2). Then approximately

$$\rho = -e(\mathrm{AA}^* + \mathrm{BB}^*) \exp -(x^2 + y^2 + z^2)/\sigma^2 \tag{3.4}$$

$$\begin{aligned} j_1 &= e\left\{-\mathrm{AA}^*\left(u - \frac{h}{2\pi\sigma^2 m}y\right) - \mathrm{BB}^*\left(u + \frac{h}{2\pi\sigma^2 m}y\right)\right. \\ &\qquad \left. - \mathrm{AB}^*\frac{ih}{2\pi\sigma^2 m}z + \mathrm{A}^*\mathrm{B}\frac{ih}{2\pi\sigma^2 m}z\right\} \exp -(x^2+y^2+z^2)/\sigma^2 \\ &= \rho u + \frac{eh}{4\pi m}\left\{(\mathrm{BB}^* - \mathrm{AA}^*)\frac{\partial}{\partial y}\right. \\ &\qquad \left. - (i\mathrm{A}^*\mathrm{B} - i\mathrm{AB}^*)\frac{\partial}{\partial z}\right\} \exp -(x^2 + y^2 + z^2)/\sigma^2. \end{aligned} \tag{3.5}$$

In the same way we find

$$\begin{aligned} j_2 &= \rho v + \frac{eh}{4\pi m}\left\{(-\mathrm{A}^*\mathrm{B} - \mathrm{AB}^*)\frac{\partial}{\partial z}\right. \\ &\qquad \left. -(\mathrm{BB}^* - \mathrm{AA}^*)\frac{\partial}{\partial x}\right\} \exp -(x^2 + y^2 + z^2)/\sigma^2. \\ j_3 &= \rho w + \frac{eh}{4\pi m}\left\{(i\mathrm{A}^*\mathrm{B} - i\mathrm{AB}^*)\frac{\partial}{\partial x}\right. \\ &\qquad \left. -(-\mathrm{AB}^* - \mathrm{A}^*\mathrm{B})\frac{\partial}{\partial y}\right\} \exp -(x^2 + y^2 + z^2)/\sigma^2. \end{aligned}$$

These are of the form required by § 2, and so we may say that there is a magnetisation with components

$$\left.\begin{aligned} \mu_1 &= \frac{eh}{4\pi mc}(-\mathrm{A}^*\mathrm{B} - \mathrm{AB}^*) \exp -(x^2 + y^2 + z^2)/\sigma^2 \\ \mu_2 &= \frac{eh}{4\pi mc}(i\mathrm{A}^*\mathrm{B} - i\mathrm{AB}^*) \exp -(x^2 + y^2 + z^2)/\sigma^2 \\ \mu_3 &= \frac{eh}{4\pi mc}(-\mathrm{AA}^* + \mathrm{BB}^*) \exp -(x^2 + y^2 + z^2)/\sigma^2 \end{aligned}\right\} \tag{3.6}$$

To describe a single electron the constants A, B must be so normalised, that

$$(\mathrm{AA}^* + \mathrm{BB}^*)\iiint \exp -(x^2 + y^2 + z^2)/\sigma^2\, dx\, dy\, dz = 1, \tag{3.7}$$

and it follows that the magnetic moment is $eh/4\pi mc$, as it should be. The expressions (3.6) are, of course, a special case of (4.6)† according to which

$$\left.\begin{aligned}\mu_1 &= -\ \psi_3{}^*\psi_4 - \psi_3\psi_4{}^* \\ \mu_2 &= i\psi_3{}^*\psi_4 - i\psi_3\psi_4{}^* \\ \mu_3 &= -\ \psi_3\psi_3{}^* + \psi_4\psi_4{}^*\end{aligned}\right\}. \tag{3.8}$$

If we take an infinite plane wave, the direct observation of the moment is not possible, but it is easy to extend the process so as to cover this case. Experimentally we may imagine a screen to intercept all but a small pencil of the wave, which thus becomes amenable to observation; theoretically we can adopt (3.8) as a definition of the magnetisation. In discussing such questions as the diffraction of a stream of electrons, we want to be able to describe how the magnetic moment will be affected by the diffracting system, and it is thus necessary to find how the direction of the magnetisation is correlated with A and B If the direction of magnetisation has colatitude χ and longitude ω with reference to the z-axis, it is easy to show that $-$ B/A $= \cot \frac{1}{2}\chi\, e^{i\omega}$ Now if we project stereographically‡ from the positive pole of a sphere on a plane, at unit distance, the point χ, ω has co-ordinates $\cot \frac{1}{2}\chi \cos \omega$, $\cot \frac{1}{2}\chi \sin \omega$ Thus the ratio $-$ B/A bears to the direction of magnetisation the same relation as that borne by a point ζ in the complex plane to the direction in a sphere that corresponds by stereographic projection In any diffraction problem the diffracted wave must bear a linear relation to the incident, that is to say, $A' = \alpha A + \beta B$, $B' = \gamma A + \delta B$, and so the new direction of magnetisation, described by $-$ B′/A′, is related by a homographic transformation to the old.

4. The expressions (3 8) are easily verified to be components of a vector by applying the transformations (2) and (3) of p 656†, but they have only been worked out for low velocities and need modification for high. At low velocities ψ_1, ψ_2 are negligible, so that we are at liberty to add terms in them to the μ's, and by doing so we can find six expressions forming an antisymmetric tensor of the second rank which obey exactly the same rules of transformation for (1), (2) and (3) as do the electric and magnetic *forces* for any relativity transformation. The process is quite easy though laborious, for in view of the unsymmetrical appearance of the components, each of the six has to be tested

---

‡ The stereographic projection was first used in this connection by Jordan, 'Z. f. Physik,' vol. 44, p. 292 (1927). Though his purpose was rather different, his work covers much of the matter discussed here.

with each transformation, making 18 operations in all. In giving the components we use subscripts *xyzt* for the tensor, to avoid confusion with the numerical subscripts of the ψ's, which have not a vector meaning. Then

$$\left.\begin{aligned}
\mu_{xt} &= -\psi_3\psi_4^* - \psi_4\psi_3^* + \psi_1\psi_2^* + \psi_2\psi_1^* \\
\mu_{yt} &= -i\psi_3\psi_4^* + i\psi_4\psi_3^* + i\psi_1\psi_2^* - i\psi_2\psi_1^* \\
\mu_{zt} &= -\psi_3\psi_3^* + \psi_4\psi_4^* + \psi_1\psi_1^* - \psi_2\psi_2^* \\
\mu_{yz} &= i\psi_1\psi_4^* - i\psi_4\psi_1^* + i\psi_2\psi_3^* - i\psi_3\psi_2^* \\
\mu_{zx} &= -\psi_1\psi_4^* - \psi_4\psi_1^* + \psi_2\psi_3^* + \psi_3\psi_2^* \\
\mu_{xy} &= i\psi_1\psi_3^* - i\psi_3\psi_1^* - i\psi_2\psi_4^* + i\psi_4\psi_2^*
\end{aligned}\right\}. \tag{4.1}$$

These expressions are, of course, all real, because we have not followed the practice of expressing relativity transformations with the use of imaginary time. The first three components are the magnetic moment, as we have seen, and the last three are therefore the electric moment. Before applying the formulæ, we may consider, quite inconclusively, some more mathematical questions that they raise.

In addition to the moment tensor, it is possible to construct other invariants which are quadratic in the ψ's and their conjugates. Thus we have the density-current vector of (3.3)†, which we may repeat here with the omission of a constant factor,

$$\left.\begin{aligned}
c\rho &= -\psi_1\psi_1^* - \psi_2\psi_2^* - \psi_3\psi_3^* - \psi_4\psi_4^* \\
j_x &= \psi_1\psi_4^* + \psi_2\psi_3^* + \psi_3\psi_2^* + \psi_4\psi_1^* \\
j_y &= i\psi_1\psi_4^* - i\psi_2\psi_3^* + i\psi_3\psi_2^* - i\psi_4\psi_1^* \\
j_z &= \psi_1\psi_3^* - \psi_2\psi_4^* + \psi_3\psi_1^* - \psi_4\psi_2^*
\end{aligned}\right\}. \tag{4.2}$$

Moreover we can see that in (3.1)† the coefficient of *mc* must be (and of course is verified to be) invariant

$$\mathrm{I} = -\psi_1\psi_1^* - \psi_2\psi_2^* + \psi_3\psi_3^* + \psi_4\psi_4^*, \tag{4.3}$$

and another invariant can be formed

$$\mathrm{J} = i\psi_1\psi_3^* + i\psi_2\psi_4^* - i\psi_3\psi_1^* - i\psi_4\psi_2^*. \tag{4.4}$$

These are not all independent, for the following relations may be verified :—

$$c^2\rho^2 - j_x^2 - j_y^2 - j_z^2 = \mathrm{I}^2 + \mathrm{J}^2. \tag{4.5}$$

$$\mu_{xt}^2 + \mu_{yt}^2 + \mu_{zt}^2 - \mu_{yz}^2 - \mu_{zx}^2 - \mu_{xy}^2 = \mathrm{I}^2 - \mathrm{J}^2. \tag{4.6}$$

The relation (4.5) is a familiar one in relativitiy theory and (4.6) was used by

Frenkel‡ in his paper on the spinning electron. I do not know if this is a complete list of quadratic covariants, but it seems probable, and indeed it is rather surprising, that there should even be as many as this.

It would be a problem of some mathematical interest to make a systematic method of dealing with these formulæ. I should certainly have expected that the tensor calculus would prove convenient, and it may be so, for I can only say that a good many trials have been unsuccessful. Dirac himself has pointed out that the equations are not final and may need modification later, but that hardly affects the question; for whether right or wrong they conform to relativity and yet seem most unwilling to obey the tensor discipline which has succeeded with ease in ruling all other phenomena.

It may be noted in this connection that a similar set of invariants can be developed for light waves. If the electromagnetic equations for free space are combined by introducing the complex quantities

$$\left.\begin{array}{ll} \psi_1 = -i\mathrm{H}_z, & \psi_2 = \mathrm{H}_y - i\mathrm{H}_x \\ \psi_3 = \mathrm{E}_z, & \psi_4 = \mathrm{E}_x + i\mathrm{E}_y \end{array}\right\}, \qquad (4.7)$$

we get four equations which are identical with Dirac's, when *m* and *e* are equated to zero. The only difference is that here E_z is real, whereas for the electron ψ_3 is necessarily complex; though at present the distinction is important, it will probably disappear when we understand the meaning of negative energy. The quantities (4.7) must obey the same rules of transformation as Dirac's, but, of course, with other axes the ψ's no longer stand for the same functions of the forces. The associated invariants must also exist, though they do not look like invariants when expressed in terms of the forces, because, if this is done, two different rules of transformation are being mixed together. Allowing for this peculiarity (4.2) represents the energy and momentum, and (4.1) depends on the polarisation, vanishing, for example, for circularly polarised light. The stereographic relation between the "magnetic moment" and the elliptic polarisation of the wave is that given by Jordan. If we turn over to the language of particles, we can describe the relation of light to electricity by saying that a light-quantum is simply an electron without charge or mass.

5. We now consider the free motion of an electron moving at any speed, and shall first take the motion in the *z*-direction. If the particle-velocity is $c \tanh \beta$, the momentum is $mc \sinh \beta$ and energy $mc^2 \cosh \beta$. We then have

$$\left.\begin{array}{ll} \psi_1 = -\mathrm{A} \sinh \tfrac{1}{2}\beta \,.\, \mathrm{S} & \psi_2 = \mathrm{B} \sinh \tfrac{1}{2}\beta \,.\, \mathrm{S} \\ \psi_3 = \mathrm{A} \cosh \tfrac{1}{2}\beta \,.\, \mathrm{S} & \psi_4 = \mathrm{B} \cosh \tfrac{1}{2}\beta \,.\, \mathrm{S} \end{array}\right\}, \qquad (5.1)$$

---

‡ 'Z. f. Physik,' vol. 37, p. 243 (1926).

where $S = \exp i \frac{2\pi}{h} mc\,(z \sinh \beta - ct \cosh \beta)$. We can reduce the electron to rest by applying the transformation (1) p. 656† and the solution becomes

$$\psi_1 = \psi_2 = 0, \quad \psi_3 = A \,.\, S_0, \quad \psi_4 = B \,.\, S_0, \text{ where } S_0 = \exp - i \frac{2\pi}{h} mc^2 t.$$

Thus in (5.1) the ratio $- B/A$ determines the direction of the magnetisation for the system of co-ordinates in which the electron is at rest. In this system we may write

$$\mu_x{}^0 = - A^*B - AB^*, \quad \mu_y{}^0 = iA^*B - iAB^*, \quad \mu_z{}^0 = - AA^* + BB^*. \tag{5.2}$$

These quantities, which may be called the "null moments," are really more important than the actual moments, for example, in an unpolarised beam the null moments would be distributed in all directions equally, whereas the actual moments, as we shall see, are condensed towards the equator of the motion.

Now substitute (5.1) in (4.1) and we have

$$\left.\begin{array}{lll} \mu_{xt} = \mu_x{}^0 \cosh \beta, & \mu_{yt} = \mu_y{}^0 \cosh \beta, & \mu_{zt} = \mu_z{}^0 \\ \mu_{yz} = \mu_y{}^0 \sinh \beta, & \mu_{zx} = - \mu_x{}^0 \sinh \beta, & \mu_{xy} = 0 \end{array}\right\}. \tag{5.3}$$

Thus at high speeds the transverse component of magnetisation increases, while the longitudinal is unchanged, and so the moment tends towards the equatorial plane The electric moment is transverse to the motion and can be expressed as vector product of the magnetisation and the velocity (not the velocity dx/dt, but that usually denoted dx/ds).

We have treated of the motion along the z-direction first because we had available the transformation which would reduce the electron to rest. But we can show that the same result applies for any other direction of motion. In (3.1) take $p = mc \sinh \beta \,.\, l_x$, $q = mc \sinh \beta \,.\, l_y$, $r = mc \sinh \beta \,.\, l_z$, $W = mc^2 \cosh \beta$ and substitute in (4.1). As there is no point in normalising an infinite wave, we divide out all the expressions by a common factor‡ and have

$$\mu_{xt} = \mu_x{}^0 \cosh \beta - l_x\,(l\mu^0)\,(\cosh \beta - 1), \tag{5.4}$$

etc., and

$$\mu_{yz} = - (l_y \mu_z{}^0 - l_z \mu_y{}^0) \sinh \beta, \tag{5.5}$$

etc. Here $\mu_x{}^0$, etc., are defined by (5.2) and as we now have vector formulæ we can see by comparison with (5.3) that they are the null moments. Thus the method of stereographic projection gives for all plane waves just what is usually required, the direction of magnetisation for the system of co-ordinates in which the associated particle-velocity is zero.

---

‡ If it should be desired to normalise, the appropriate quantity is $AA^* + BB^*$, which is the invariant I when the same factor is taken out.

The vector product relation of electric to magnetic moment was introduced by Frenkel—for the particle electron; but there is a difference in the way it arises. In Frenkel's work the relation was taken as a kinematical constraint, necessary in order that the electron should have no electric moment when at rest. This constraint made his system non-holonomic, whereas we have a purely holonomic system. To make a very elementary analogy, the motion of a rolling body is non-holonomic, but happens to become holonomic for a cylinder; Dirac has shown that Frenkel's rolling body really was a cylinder. In a more recent paper Frenkel‡ has attempted to extend his kinematical condition to the wave theory, but with less success, because he applies it to the amplitudes ψ, whereas we have seen that it is quadratic in the ψ's. It is, in fact, a dynamical, not an undulatory relation.

The electron wave can be specified by its electric moment just as well as by its magnetic, and this has the convenience that the direction is always transverse. At first sight it would appear that one less element is needed, but this is not so, because the electric moment is arbitrary in magnitude, whereas the magnetic is fixed by the total intensity of the wave. The only defect in using the electric moment is that though it fixes the magnitude of the longitudinal magnetic component, it leaves it arbitrary whether it is forwards or backwards. We may liken this to the specification of elliptically polarised light, which can be described by means of the position of the major axis and the ratio of the axes, but still requires the statement of the sense in which the ellipse is traversed.§

In conclusion, we should consider the character of an unpolarised beam of electrons. When two beams of elliptically polarised light of the same frequency are superposed, the resultant is again elliptically polarised light, and in the same way two superposed polarised electron waves compound into a third polarised wave. To represent an unpolarised wave we have to proceed in the same way as for light. There (though it is perhaps physically rather meaningless) it is the case that rigorously monochromatic light must have a definite polarisation, and unpolarised light can only arise by occasional chance changes of phase, which imply a departure from monochromatism. So when the electron wave has its wave-length given precisely, the magnetic moment must be in a definite direction, and an unpolarised wave can only be represented by supposing occasional changes of phase. It is a curious, though unpractical, result that if the velocity of an electron is absolutely precise, it must have a definite direction of magnetisation.

---

‡ 'Z. f. Physik,' vol. 47, p. 786 (1928). This work was composed before the appearance of Dirac's paper.

§ Compare Jordan, *loc. cit.*

Summary.

Starting from the wave equations for an electron and the associated electric density and current, it is shown how the electromagnetic fields of a moving electron can be attributed partly to the convection of electricity and partly to an intrinsic magnetisation. A geometrical construction shows the relation between the wave constants and the magnetisation. The formulæ, first worked out for slow motion, are easily generalised by relativity for high speeds, and in this case there are electric as well as magnetic moments, and various invariant properties are given. A comparison is made between an electron wave and a light wave, and the resemblance may be loosely expressed by saying that a light-quantum is an electron without charge or mass.

On the Diffraction of the Magnetic Electron.

By Prof. C. G. DARWIN, F.R.S.

(Received July 21, 1928.)

1. As soon as it was appreciated that the phenomenon of the "spinning electron" was to be attributed to the existence of *simultaneous* wave functions,[‡] the question naturally arose as to how far there would be an analogy with the polarisation of light, and in particular whether in diffraction by a slit or grating or in reflexion from a mirror, electrons would be selected having a preferential direction of magnetisation. Dynamical conceptions suggest that it would require a magnetic force to produce a change in the polarisation, so that the general indication was rather strongly negative, and it seemed hardly worth while to verify the fact by direct solution. I believe, however, that recently experiments have been undertaken to search for such an effect (by means of successive diffractions from two crystals), and in view of this I have examined

---

[‡] 'Roy. Soc. Proc.' A, vol. 116, p. 227 (1927).

the question more closely. The result, broadly speaking, bears out the first conjecture that no effect could be observed in practice, but in certain cases (of a rather hypothetical kind) an effect might be found and the whole problem is interesting as an example of the wave theory.

The essence of the matter is sufficiently represented by taking a line grating instead of a crystal, and, furthermore, by limiting the electric and magnetic forces of the grating in such a way that there shall only be first order spectra on each side, two reflected and two transmitted. The grating is supposed made out of a periodic distribution of electric or magnetic material. Actual crystals will consist of almost purely electric material, but the magnetic case is as easy to treat and, though unpractical, gives rise to interesting results. It will appear that when a polarised electron wave falls on such a grating, the direction of magnetisation may be changed in the diffracted rays. It is a true polarisation effect in that the change in direction is independent of the strength of the field in the grating, which only determines the total intensity. In the case of pure electric forces and of some magnetic forces, the change of direction of magnetisation can be represented by a rotation about an axis through a definite angle, both axis and angle depending only on the directions of the incident and diffracted rays and on the speed of the electrons. It follows that a stream of electrons which are initially unpolarised cannot become polarised by diffraction, since the grating merely rotates all the components like a solid body. In cases where there are simultaneous electric and magnetic fields this might not be so, but the calculation becomes rather heavy, and I have only examined its outline sufficiently to see that some polarisation would occur. The matter is quite unpractical, for not only are the electric forces of atoms far stronger than the magnetic, but even if they were equal the electric would be much more effective in controlling the polarisation. I should conjecture also that it would not be practically possible to make a stream of electrons get anywhere near a powerfully magnetised iron crystal; and for all these reasons it would seem fairly safe to say that no polarisation effect will be detected.

2. The passage of electrons through a grating is a special case of a general problem discussed by Dirac‡ under the title "The Transition to States of Equal Energy." His process is, of course, indisputably correct, but it calls for some comment. Suppose that an incident Schrödinger wave (to avoid the complication of having several wave functions) falls on a grating, which is represented by a weak perturbing electric field of potential V. Let the incident

---

‡ 'Roy. Soc. Proc.,' A, vol. 114, p. 234 (1927).

wave be represented by ψ_0 and one of the diffracted waves by ψ_1. Then he shows that the strength will depend on $\iiint V\,\psi_0\,\psi_1{}^*\,dx\,dy\,dz$. Now ψ_1, like ψ_0, is a solution of the wave equation with V omitted and so represents a wave extending to infinity on both sides of the grating, incident as well as emergent. What we want is only the half of this wave which emerges from the grating, and it is not clear that this is legitimately represented by ψ_1. A second difficulty will be clear to anyone who has ever tried to apply the general formula to a special case. When the integral is set down it is nearly always found to be infinite, and to find the appropriate normalisation for such a divergent integral is troublesome. The difficulty can, of course, be overcome, but the sort of process that must be used is to limit the size of grating and of incident beam. But these limitations imply that we are to solve a more complicated problem than before, for they imply some sort of discussion (perhaps quite indirect) of the resolving power of the grating, a matter having really nothing to do with the initial problem. Yet a third difficulty arises when we come to polarisation, for with the method under discussion we take any ψ_1 as a trial solution, and when $\int V\,\psi_0\,\psi_1{}^*$ does not vanish we say that it represents a diffracted wave. Now, in fact, the diffracted wave has a perfectly definite direction of polarisation, but if we make a trial solution with a ψ_1 representing magnetisation in some other direction, the integral will only vanish if this direction happens to be perpendicular to the true magnetisation. So merely to obtain a non-vanishing integral is not enough, it is also necessary to verify that any wave with perpendicular magnetisation would make the integral vanish. I do not wish to contend that these difficulties cannot be overcome, but only that they all have to be considered if the method is to be used, whereas there is a perfectly simple direct attack on the problem which raises none of them. I do not know how far this would be true in other problems, but certainly in many the difficulty of fitting the correct normalisation to a general formula (which is, in fact, a divergent integral) is quite as great as the difficulty of direct solution from first principles.

It will make the procedure clearer if we first solve the simpler problem of diffraction for Schrodinger waves by the method afterwards to be used in the more complicated case. The grating is represented by a weak electric potential

$$V = 2f(z)\cos \alpha x,$$

where $f(z)$ is supposed to vanish except for values near zero. Throughout the present work we shall simplify the formulæ by taking the quantum h as 2π. Then the wave equation is

$$-\frac{1}{2m}\Delta\psi + eV\psi = i\frac{\partial\psi}{\partial t}. \tag{2.1}$$

The incident wave is

$$\psi = A \exp i\,(p_0 x + q_0 y + r_0 z - Wt), \tag{2.2}$$

and to satisfy the null equation (without V) we must have

$$W = (p_0^2 + q_0^2 + r_0^2)/2m.$$

When V is introduced we shall evidently need new terms in the solution which will involve $\exp i\,[(p_0 \pm \alpha)\,x + q_0 y - Wt]$ and so we take as trial solution

$$\psi = A \exp i\,(p_0 x + q_0 y + r_0 z - Wt) + \phi\,(z) \exp i\,[(p_0 + \alpha)\,x + q_0 y - Wt] \\ + \chi\,(z) \exp i\,[(p_0 - \alpha)\,x + q_0 y - Wt], \tag{2.3}$$

where the functions ϕ and χ, which are small of the order V, are to be determined. Substitute in (2.1), neglecting the order V^2, and the terms involving $\exp i\,[(p_0 + \alpha)\,x + q_0 y - Wt]$ must vanish by themselves; that is,

$$-\frac{1}{2m}\left\{\frac{d^2\phi}{dz^2} - [(p_0 + \alpha)^2 + q_0^2]\,\phi\right\} + eA\,f(z)\,e^{ir_0 z} = W\phi. \tag{2.4}$$

There is a similar relation for χ, but the whole argument goes in exactly the same way right through and we need not discuss it at all.

We shall write p for $p_0 + \alpha$ and q for q_0 and take r as the positive solution of $r^2 = 2mW - p^2 - q^2$. Then

$$\frac{d^2\phi}{dz^2} + r^2\phi = 2meA\,f(z)\,e^{ir_0 z}. \tag{2.5}$$

This is a standard type of equation and the solution is

$$\phi = \frac{meA}{ir}\int^z f(\zeta)\,e^{ir_0\zeta - ir(\zeta - z)}\,d\zeta - \frac{meA}{ir}\int^z f(\zeta)\,e^{ir_0\zeta + ir(\zeta - z)}\,d\zeta. \tag{2.6}$$

and by taking different arbitrary values for the two lower limits of integration this solution is general. To fix them we introduce the condition that the effect must be a wave emerging in both directions from the grating, without any part incident on it; in fact, the particular solution we need must have asymptotic value e^{irz} for positive z and e^{-irz} for negative. Since $f(\zeta)$ vanishes except near the origin, this is accomplished by taking the first lower limit as $-\infty$ and the second as $+\infty$. Then on the positive side the asymptotic value becomes

$$\phi = \frac{me\mathrm{A}}{ir} e^{irz} \int_{-\infty}^{\infty} f(\zeta)\, e^{i(r_0-r)\zeta}\, d\zeta, \tag{2.7}$$

and on the negative

$$\phi = \frac{me\mathrm{A}}{ir} e^{-irz} \int_{-\infty}^{\infty} f(\zeta)\, e^{i(r_0+r)\zeta}\, d\zeta.$$

In either case we have a quantity proportional to the general formula $\int \mathrm{V}\psi_0\psi_1^*$, but its magnitude has been determined without trouble and without the objection that the general formula does not directly imply which half of the wave has physical reality.

In what follows we take the theorem that if

$$\frac{d^2\phi}{dz^2} + r^2\phi = \mathrm{F}(z), \tag{2.8}$$

where F vanishes except near the origin, then the asymptotic value for positive z is to be taken as

$$\phi = \frac{e^{irz}}{2ir} \int_{-\infty}^{\infty} \mathrm{F}(\zeta)\, e^{-ir\zeta}\, d\zeta. \tag{2.9}$$

3. We now apply the same process to the magnetic electron. The grating is supposed to contain both electric and magnetic forces, all periodic in the same length and of small strength. The electric forces are due to a potential

$$\mathrm{V} = f(z)\, e^{i\alpha x} + f^*(z)\, e^{-i\alpha x}. \tag{3.1}$$

The vector potentials must satisfy div A = 0, so that we take them as

$$\left.\begin{aligned} \mathrm{A}_x &= g'(z)\, e^{i\alpha x} + g^{*\prime}(z)\, e^{-i\alpha x} \\ \mathrm{A}_y &= h(z)\, e^{i\alpha x} + h^*(z)\, e^{-i\alpha x} \\ \mathrm{A}_z &= -i\alpha g(z)\, e^{i\alpha x} + i\alpha g^*(z)\, e^{-i\alpha x} \end{aligned}\right\}, \tag{3.1}$$

where $g'(z) = dg/dz$. The functions f, g, h are complex, and by a suitable alteration in their arguments we can imagine the magnetic forces shifted along the direction of x relative to the electric. In the case where g and h vanish the forces are purely electrical, and we call this an "electric grating." If f and h vanish there are only magnetic forces along the lines of the grating and this we call a "longitudinal magnetic grating"; while if f and g vanish we have a "transverse magnetic grating." In these three cases, as we shall see the results are specially simple.

As we are mainly concerned with qualitative results, we simplify Dirac's equations‡ by taking $h = 2\pi$ and $e = c$, so that the operator $\frac{h}{2\pi i}\frac{\partial}{\partial x} + \frac{e}{c}\mathrm{A}_x$ becomes $-i\frac{\partial}{\partial x} + \mathrm{A}_x$, etc.; if required, the absolute values can easily be restored from dimensional principles. The whole motion is periodic in the time, so that we can omit the factor $\exp - i\mathrm{W}t$ throughout. Then the equations are

$$\left.\begin{aligned}
&(\mathrm{W}/c + mc)\,\psi_1 - i\left(\frac{\partial}{\partial x} - i\frac{\partial}{\partial y}\right)\psi_4 - i\frac{\partial}{\partial z}\psi_3 \\
&\qquad\qquad + \mathrm{V}\psi_1 + (\mathrm{A}_x - i\mathrm{A}_y)\,\psi_4 + \mathrm{A}_z\psi_3 = 0 \\
&(\mathrm{W}/c + mc)\,\psi_2 - i\left(\frac{\partial}{\partial x} + i\frac{\partial}{\partial y}\right)\psi_3 + i\frac{\partial}{\partial z}\psi_4 \\
&\qquad\qquad + \mathrm{V}\psi_2 + (\mathrm{A}_x + i\mathrm{A}_y)\,\psi_3 - \mathrm{A}_z\psi_4 = 0 \\
&(\mathrm{W}/c - mc)\,\psi_3 - i\left(\frac{\partial}{\partial x} - i\frac{\partial}{\partial y}\right)\psi_2 - i\frac{\partial}{\partial z}\psi_1 \\
&\qquad\qquad + \mathrm{V}\psi_3 + (\mathrm{A}_x - i\mathrm{A}_y)\,\psi_2 + \mathrm{A}_z\psi_1 = 0 \\
&(\mathrm{W}/c - mc)\,\psi_4 - i\left(\frac{\partial}{\partial x} + i\frac{\partial}{\partial y}\right)\psi_1 + i\frac{\partial}{\partial z}\psi_2 \\
&\qquad\qquad + \mathrm{V}\psi_4 + (\mathrm{A}_x + i\mathrm{A}_y)\,\psi_1 - \mathrm{A}_z\psi_2 = 0
\end{aligned}\right\}. \tag{3.2}$$

The incident wave is given in direction and wave-length by

$$\mathrm{S} = \exp i\,(p_0x + q_0y + r_0z),$$

so that

$$\mathrm{W}^2/c^2 = m^2c^2 + p_0^2 + q_0^2 + r_0^2.$$

The polarisation is given by taking

$$\psi_3 = \mathrm{A}\,.\,\mathrm{S}, \qquad \psi_4 = \mathrm{B}\,.\,\mathrm{S}, \tag{3.3}$$

and these determine

$$\left.\begin{aligned}
\psi_1 &= \frac{-\mathrm{A}r_0 - \mathrm{B}\,(p_0 - iq_0)}{\mathrm{W}/c + mc}\,.\,\mathrm{S} = \mathrm{C}\,.\,\mathrm{S} \\
\psi_2 &= \frac{-\mathrm{A}\,(p_0 + iq_0) + \mathrm{B}r_0}{\mathrm{W}/c + mc}\,.\,\mathrm{S} = \mathrm{D}\,.\,\mathrm{S}
\end{aligned}\right\}. \tag{3.3}$$

The symbols C and D will be used in the earlier stages to save writing the rather clumsy expressions for which they stand.

---

‡ See references at beginning of preceding paper, p. 621.

It will suffice to study only one of the four lateral spectra, and we shall take that for which

$$\left.\begin{aligned} p = p_0 + \alpha, \qquad q = q_0 \\ \text{and} \qquad r = \sqrt{\{p_0^2 + q_0^2 + r_0^2 - p^2 - q^2\}} \end{aligned}\right\}. \tag{3.4}$$

Omitting the terms corresponding to $p_0 - \alpha$, we take as solution

$$\begin{aligned} \psi_3 &= \mathrm{A} \,.\, \mathrm{S} + \phi_3(z) \exp i\,(px + qy), \\ \psi_4 &= \mathrm{B} \,.\, \mathrm{S} + \phi_4(z) \exp i\,(px + qy), \\ \psi_1 &= \mathrm{C} \,.\, \mathrm{S} + \phi_1(z) \exp i\,(px + qy), \\ \psi_2 &= \mathrm{D} \,.\, \mathrm{S} + \phi_2(z) \exp i\,(px + qy). \end{aligned}$$

If we now substitute these in (3.2) and pick out the terms involving $\exp i\,(px + qy)$, we have

$$\left.\begin{aligned} (\mathrm{W}/c + mc)\,\phi_1 + (p - iq)\,\phi_4 - i\phi_3' + e^{ir_0z}\,[f\mathrm{C} + (g' - ih)\,\mathrm{B} - i\alpha g\,\mathrm{A}] = 0 \\ (\mathrm{W}/c + mc)\,\phi_2 + (p + iq)\,\phi_3 + i\phi_4' + e^{ir_0z}\,[f\mathrm{D} + (g' + ih)\,\mathrm{A} + i\alpha g\mathrm{B}] = 0 \\ (\mathrm{W}/c - mc)\,\phi_3 + (p - iq)\,\phi_2 - i\phi_1' + e^{ir_0z}\,[f\mathrm{A} + (g' - ih)\,\mathrm{D} - i\alpha g\mathrm{C}] = 0 \\ (\mathrm{W}/c - mc)\,\phi_4 + (p + iq)\,\phi_1 + i\phi_2' + e^{ir_0z}\,[f\mathrm{B} + (g' + ih)\,\mathrm{C} + i\alpha g\mathrm{D}] = 0 \end{aligned}\right\} \tag{3.5}$$

Next, to eliminate ϕ_1 and ϕ_2, operate on the first with id/dz, multiply the second by $-(p - iq)$ and the third by $(\mathrm{W}/c + mc)$ and add. The result automatically eliminates ϕ_4 also, and gives $\phi_3'' + r^2\phi_3$ equal to a function of z, which is rather long to write down, but easily seen from the above. By (2.9) the asymptotic value of ϕ_3 for positive z is $\mathrm{A}'e^{irz}$, where

$$\begin{aligned} \mathrm{A}' = -\frac{1}{2ir}\int_{-\infty}^{\infty} dz\, e^{-irz} \Big\{ i\frac{d}{dz}\, e^{ir_0z}\,[f\mathrm{C} + (g' - ih)\,\mathrm{B} - i\alpha g\mathrm{A}] \\ - (p - iq)\, e^{ir_0z}\,[f\mathrm{D} + (g' + ih)\,\mathrm{A} + i\alpha g\mathrm{B}] \\ + (\mathrm{W}/c + mc)\, e^{ir_0z}\,[f\mathrm{A} + (g' - ih)\,\mathrm{D} - i\alpha g\mathrm{C}] \Big\}. \end{aligned}$$

This can be simplified by partial integration, and writing

$$\left.\begin{aligned} \mathrm{F} &= \int_{-\infty}^{\infty} f e^{-irz + ir_0z}\, dz \\ \mathrm{G} &= \int_{-\infty}^{\infty} g e^{-irz + ir_0z}\, dz \\ \mathrm{H} &= \int_{-\infty}^{\infty} h e^{-irz + ir_0z}\, dz \end{aligned}\right\} \tag{3 6}$$

we have

$$\begin{aligned}\mathrm{A}' = \frac{i}{2r}\Big\{&\mathrm{F}[-r\mathrm{C} - (p - iq)\,\mathrm{D} + (\mathrm{W}/c + mc)\,\mathrm{A}] \\ &+ i\mathrm{G}\,[\,(r - r_0)\{-r\mathrm{B} - (p - iq)\,\mathrm{A} + (\mathrm{W}/c + mc)\,\mathrm{D}\} \\ &\qquad + \alpha\,\{r\mathrm{A} - (p - iq)\,\mathrm{B} - (\mathrm{W}/c + mc)\,\mathrm{C}\}] \\ &+ i\mathrm{H}\,[r\mathrm{B} - (p - iq)\,\mathrm{A} - (\mathrm{W}/c + mc)\,\mathrm{D}]\Big\}.\end{aligned}$$

Substituting for C and D, and using (3.4), we have

$$\begin{aligned}\mathrm{A}' = \frac{i\mathrm{F}}{2r}\Big\{&\mathrm{A}\,(\mathrm{W}/c + mc) \\ &+ \frac{\mathrm{A}\,[rr_0 + (p - iq)\,(p_0 + iq_0)] + \mathrm{B}\,[r\,(p_0 - iq_0) - r_0\,(p - iq)]}{\mathrm{W}/c + mc}\Big\} \\ &+ \frac{\mathrm{G}}{2r}\{2\mathrm{A}\,(rp_0 - r_0p) + \mathrm{B}\,[(p - p_0)^2 + (r - r_0)^2]\} \\ &- \frac{i\mathrm{H}}{2r}\{\mathrm{A}\,[q + q_0 + i\,(p - p_0)] - \mathrm{B}i\,(r - r_0)\}. \qquad (3.7)\end{aligned}$$

Proceeding in exactly the same way for ψ_4 we find

$$\begin{aligned}\mathrm{B}' = \frac{i\mathrm{F}}{2r}\Big\{&\mathrm{B}\,(\mathrm{W}/c + mc) \\ &+ \frac{\mathrm{A}\,[r_0\,(p + iq) - r\,(p - iq)] + \mathrm{B}\,[rr_0 + (p + iq)\,(p_0 - iq_0)]}{\mathrm{W}/c + mc}\Big\} \\ &+ \frac{\mathrm{G}}{2r}\{-\mathrm{A}\,[(p - p_0)^2 + (r - r_0)^2] + 2\mathrm{B}\,(rp_0 - r_0p)\} \\ &- \frac{i\mathrm{H}}{2r}\{-\mathrm{A}i\,(r - r_0) + \mathrm{B}\,[q + q_0 - i\,(p - p_0)]\}. \qquad (3.7)\end{aligned}$$

These formulæ can be expressed more geometrically. If the particle-speed is $c \tanh \beta$, we have $\mathrm{W} = mc^2 \cosh \beta$, and if the direction of the incident wave is $l_0 : m_0 : n_0$, and of the diffracted $l : m : n$ (the two meanings of m will not cause confusion), we have $p_0 = l_0\,mc \sinh \beta$, etc. If the angle of deviation is ϵ, we have $pp_0 + qq_0 + rr_0 = m^2c^2 \sinh^2 \beta \cos \epsilon$, and if $l_1 : m_1 : n_1$ is the direction perpendicular to both rays, $qr_0 - q_0r = m^2c^2 \sinh^2 \beta \,.\, l_1 \sin \epsilon$, etc. Then

$$\begin{aligned}\mathrm{A}' = \frac{i\mathrm{F}}{2n \sinh \beta}\{&\mathrm{A}\,(\cosh \beta + 1) + (\cosh \beta - 1)\,[\mathrm{A}\,(\cos \epsilon + in_1 \sin \epsilon) \\ &\qquad + \mathrm{B} \sin \epsilon\,(m_1 + il_1)]\} \\ &+ \frac{\mathrm{G}mc \sinh \beta}{2n}\{\mathrm{A}\,2m_1 \sin \epsilon + \mathrm{B}\,2\,(1 - \cos \epsilon)\} \\ &- \frac{i\mathrm{H}}{2n}\{\mathrm{A}\,[(m + m_0) + i\,(l - l_0)] - \mathrm{B}i\,(n - n_0)\}, \qquad (3.8)\end{aligned}$$

$$
\begin{aligned}
\mathrm{B}' = \frac{i\mathrm{F}}{2n \sinh \beta} \{\mathrm{B} (\cosh \beta + 1) + (\cosh \beta - 1) [\mathrm{A} \sin \varepsilon (-m_1 + il_1) \\
+ \mathrm{B} (\cos \varepsilon - in_1 \sin \varepsilon)]\} \\
+ \frac{\mathrm{G}mc \sinh \beta}{2n} \{-\mathrm{A}\, 2 (1 - \cos \varepsilon) + \mathrm{B}\, 2m_1 \sin \varepsilon\} \\
- \frac{i\mathrm{H}}{2n} \{-\mathrm{A}i (n - n_0) + \mathrm{B} [(m + m_0) - i (l - l_0)]\}. \qquad (3.8)
\end{aligned}
$$

The diffracted wave is then

$$\psi_3 = \mathrm{A}' \exp i (px + qy + rz),\ \psi_4 = \mathrm{B}' \exp i (px + qy + rz),$$

and ψ_1, ψ_2 could be deduced if we required them.

4. In the preceding note it was shown how the coefficients A, B are connected with the magnetisation of the electron wave. The important quantity is the *null moment*, that is, the magnetisation in the system of co-ordinates for which the particle speed is zero; the actual magnetic and electric moments follow from this by a simple application of relativity. The components of the null moment are $-\mathrm{A}^*\mathrm{B} - \mathrm{A}\mathrm{B}^* : i\mathrm{A}^*\mathrm{B} - i\mathrm{A}\mathrm{B}^* : \mathrm{B}\mathrm{B}^* - \mathrm{A}\mathrm{A}^*$. These are connected with A, B by the relation that if the direction of magnetisation is marked by a point on a unit sphere, and if this point is projected stereographically on to a plane represented by a complex variable ζ in the usual way, that variable is $-\mathrm{B}/\mathrm{A}$. We now quote a relation, well known in geometry. Suppose that an axis L : M : N is taken in the sphere, and that the sphere is rotated through angle Ω about this axis, it is required to find the relation between ζ' and ζ, the stereographic representations of a point of the sphere after and before the rotation. The result is

$$\zeta' = \frac{(\cos \tfrac{1}{2}\Omega + i\mathrm{N} \sin \tfrac{1}{2}\Omega)\, \zeta + \sin \tfrac{1}{2}\Omega\, (-\mathrm{M} + i\mathrm{L})}{(\cos \tfrac{1}{2}\Omega - i\mathrm{N} \sin \tfrac{1}{2}\Omega) + \sin \tfrac{1}{2}\Omega\, (\mathrm{M} + i\mathrm{L})\, \zeta}. \qquad (4.1)$$

Thus, if we have any homographic transformation $\zeta' = (\alpha\zeta + \beta)/(\gamma\zeta + \delta)$, it corresponds to a pure rotation if $\delta = \alpha^*$, $\gamma = -\beta^*$.

Whatever the diffractive effect of the grating, it is evident from the nature of the equations that $\mathrm{A}' = \alpha\mathrm{A} + \beta\mathrm{B}$, $\mathrm{B}' = \gamma\mathrm{A} + \delta\mathrm{B}$, so that the transformation of $-\mathrm{B}/\mathrm{A}$ is always homographic. If it should correspond to the form (4.1), then the magnetisation of the diffracted ray is given by a pure rotation. If the incident beam is unpolarised, all its incoherent components will be rotated just like a rigid body and the diffracted beam must also be unpolarised. We can see from (3.8) that this is so for each set of terms in F, G and H separately, so that no polarisation is produced in any of these cases. We may examine the axis and angle of rotation for these special types of grating.

(1) Electric grating, $G = H = 0$.

Forming $-B'/A'$ in terms of $-B/A$, we have

$$\left.\begin{aligned}(\cosh\beta+1)+(\cosh\beta-1)\cos\varepsilon &= K\cos\tfrac{1}{2}\Omega\\ -(\cosh\beta-1)\,n_1\sin\varepsilon &= KN\sin\tfrac{1}{2}\Omega\\ -(\cosh\beta-1)\,m_1\sin\varepsilon &= KM\sin\tfrac{1}{2}\Omega\\ -(\cosh\beta-1)\,l_1\sin\varepsilon &= KL\sin\tfrac{1}{2}\Omega\end{aligned}\right\}, \tag{4.2}$$

where K is a constant of proportionality. The axis of rotation is evidently $l_1 : m_1 : n_1$, perpendicular to both rays. The amount of rotation is given by

$$\tan\tfrac{1}{2}\Omega = -\frac{\sin\varepsilon}{\coth^2\tfrac{1}{2}\beta+\cos\varepsilon}. \tag{4.3}$$

For low speeds this vanishes and the direction of magnetisation is unchanged. This is the principal practical result we set out to establish. For very high speeds $\coth\frac{1}{2}\beta \sim 1$ and $\Omega \sim \varepsilon$, so that the direction of polarisation makes the same angle with the ray after diffraction as before. The actual magnetic moment is flattened down towards the equator by relativity, and its azimuth is given by the rotation about $l_1 : m_1 : n_1$.

(2) Longitudinal magnetic grating, $F = H = 0$.

A similar comparison gives $L = N = 0$, $M = 1$, so that the rotation is about the grating lines, as we should expect. The angle is best found by taking

$$\left.\begin{aligned}l_0 : m_0 : n_0 &= \sin\kappa\sin\lambda_0 : \cos\kappa : \sin\kappa\cos\lambda_0\\ l\ :\ m\ :\ n\ &= \sin\kappa\sin\lambda\ :\ \cos\kappa : \sin\kappa\cos\lambda\end{aligned}\right\}, \tag{4.4}$$

so that $\frac{\pi}{2} - \lambda_0$ is the angle made by the plane of the grating with the plane containing the incident ray and the grating lines, and similarly for λ. Then we find that $\Omega = \lambda - \lambda_0$. In projection on a plane perpendicular to the grating lines the moment makes the same angle with the ray for both incident and diffracted wave.

(3) Transverse magnetic grating, $F = G = 0$.

Here $M = 0$, and in terms of (4.4) the axis is at angle $\frac{1}{2}(\lambda + \lambda_0)$ to the grating normal. The angle of rotation is given by

$$\tan\tfrac{1}{2}\Omega = -\tan\kappa\sin\tfrac{1}{2}(\lambda-\lambda_0).$$

For the special case (which would usually be employed) when $\kappa = \frac{\pi}{2}$, the rotation is through angle π.

These results have been discussed generally, but they are much simplified if the incidence is perpendicular to the grating, and they are epitomised in the following diagrams, in which the incident beam and both the transmitted lateral spectra are shown, each crossed by an arrow to show the direction of *magnetisation.*

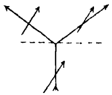

Electric Grating.
Slow Electron.

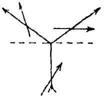

Electric Grating
Swift Electron.

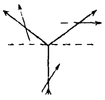

Longitudinal
Magnetic Grating.

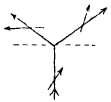

Transverse
Magnetic Grating.

In the general case, when both electric and magnetic forces are present, the matter becomes more complicated. It must not be forgotten that F, G and H may be complex constants, and it is only for special conditions of distribution that the diffracted rays will fit into the formula (4.1). In other cases there is a partial polarisation of an initially unpolarised wave. It is not hard to express its amount, but the result leads to rather complicated integrals. It is probable that some one familiar with the theory of homographic transformations could treat the whole matter simply, and the direct integrations which I have carried out are not of sufficient practical interest to give here. The process goes as follows: we assign probability $\sin\chi\,d\chi d\omega$ for initial value $\cot\frac{1}{2}\chi e^{i\omega}$ of $-\mathrm{B}/\mathrm{A}$. Transforming from χ, ω to $\xi\eta$, where $\xi + i\eta = \zeta = -\mathrm{B}/\mathrm{A}$, we have

$$\sin\chi\,d\chi\,d\omega = 4\,d\xi\,d\eta/(1+\xi^2+\eta^2)^2.$$

The diffracted beam is given by $-\mathrm{B}'/\mathrm{A}' = \zeta' = (\alpha\zeta+\beta)/(\nu\zeta+\delta)$ and the associated moment has components

$$\frac{\zeta'+\zeta'^*}{\zeta'\zeta'^*+1},\quad \frac{-i\zeta'+i\zeta'^*}{\zeta'\zeta'^*-1},\quad \frac{\zeta'\zeta'^*-1}{\zeta'\zeta'^*+1}.$$

We thus work out μ_x', the mean moment of the diffracted wave in the x direction by integrating

$$\mu_x' = \int_{-\infty}^{\infty} \int_{-\infty}^{\infty} \frac{4\,d\xi\,d\eta}{(1+\xi^2+\eta^2)^2} \frac{\zeta' + \zeta'^*}{\zeta'\zeta'^* + 1}.$$

The evaluation of the three integrals is quite practicable, and I have worked them out; but they are not very simple, and as they are quite unimportant in practice there is no need to give them.

Summary.

The problem is solved of the diffraction of an electron wave by a line-grating exerting periodic electric or magnetic forces; this represents the essential features of diffraction by a crystal. The incident wave is supposed to be magnetised in a definite direction, and it is shown that when the grating exerts only electric forces, the effect is to rotate the direction of magnetisation through a definite angle about an axis perpendicular to the incident and diffracted rays, and no polarisation can be produced by the diffraction. For some magnetic forces a similar rotation occurs, but in general the simultaneous action of electric and magnetic forces may produce a partial polarisation, though the case is too remote from experiment to be worth treating in detail.

The First Spark Spectrum of Krypton.

By P. K. Kichlu, D.Sc , Demonstrator in Physics, Science College, Patna.

(Communicated by M. N. Saha, F.R S.—Received June 4, 1928.)

The earliest investigation of the spark spectra of krypton is due to E. C. C Baly.* Later L. Bloch, E. Bloch and Dejardin† made the first careful arrangement of these lines in different groups according to the stages of excitation. These authors also measured several new lines, especially in the red, not observed before. This list has recently been supplemented by some very exact observations in the Schumann region by J. H. Abbink and H. B. Dorgelo.‡ With the aid of these data I have been able to effect an analysis of the spark spectrum of krypton. A preliminary note was published by the present writer in 'Nature,' October 15, 1927.

Table I gives the electronic configurations in Kr^+ with corresponding theoretical terms, and the nomenclature of terms adopted in this paper. Here the ^2D and ^2S terms originating from the configuration $4N_2O_1$ are based upon ^1D and ^1S states of the $4N_2$ core, and, with the exception of ^2P terms from $5N_2$, all the rest are based upon the ^3P state of the $4N_2$ core.

Table I.

Electronic configurations.	Terms (theoretical).	Present nomenclature.
$5N_2$	^2P	$a\,^2P$
↓ $4N_2O_1$	$^4\overline{P}$, $^2\overline{P}$, ^2D, ^2S	$b\,^4\overline{P}$, $b\,^2\overline{P}$, $b\,^2D$, $b\,^2S$
$4N_2N_3$	$^4\overline{F}$, ^4D, $^4\overline{P}$, $^2\overline{F}$, ^2D, $^2\overline{P}$	
↓ $4N_2O_2$	$^4\overline{D}$, ^4P, $^4\overline{S}$, $^2\overline{D}$, ^2P, $^2\overline{S}$	$c\,^4\overline{D}$, $c\,^4P$, $c\,^4\overline{S}$, $c\,^2\overline{D}$, $c\,^2P$, $c\,^2\overline{S}$
↓ $4N_2O_3$	$^4\overline{F}$, ^4D, $^4\overline{P}$, $^2\overline{F}$, ^2D, $^2\overline{P}$	d_1, d_2, , d_{17}
$4N_2P_1$	$^4\overline{P}$, $^2\overline{P}$, ^2D, ^2S	

The doublet P-terms obtained from $5N_2$ and $4N_2O_2$ form a Rydberg sequence, and from this the fundamental $^2P_2$ term is calculated to be about 214000. The values of all the other terms are given in Table II.

---

* 'Phil. Trans.,' vol. 202, p. 183 (1904).

† 'Ann. de Physique,' vol. 2, p. 461 (1924).

‡ 'Z. f. Physik,' vol 47, p. 221 (1928).

Table II.

Term designation.	J.	Term value.
$a\,{}^2P_2$	2	214000
$a\,{}^2P_1$	1	208629
$b\,{}^4P_3$	3	101170
$b\,{}^4P_2$	2	98906
$b\,{}^4P_1$	1	96396
$b\,{}^2P_2$	2	95525
$b\,{}^2P_1$	1	92997
$b\,{}^2D_3$	3	93572
$b\,{}^2D_2$	2	92220
$b\,{}^2S_1$	1	86409
$c\,{}^4P_3$	3	80074 3
$c\,{}^4P_2$	2	79711·5
$c\,{}^4P_1$	1	78826 7
$c\,{}^4\bar{S}_2$	2	78217 0
$c\,{}^4\bar{D}_4$	4	?
$c\,{}^4\bar{D}_3$	3	77929 1
$c\,\overline{{}^4D}_2$	2	75618 5
$c\,{}^4D_1$	1	74896·5
$c\,{}^2D_3$	3	73880 9
$c\,{}^2\bar{D}_2$	2	72277·3
$c\,{}^2\bar{P}_2$	2	73862 8
$c\,{}^2\bar{P}_1$	1	72004 3
$c\,{}^2\bar{S}_1$	1	71636 4
d_1	3	56920 8
d_2	3	56114 7
d_3	3	52714 9
d_4	3	52590 6
d_5	3	52548 1
d_6	2	52198 0
d_7	2	52122 5
d_8	2	51940 7
d_9	2	51433·7
d_{10}	3	50641·6
d_{11}	2	49560 3
d_{12}	3	48922 4
d_{13}	3	48858·1
d_{14}	1	46998 4
d_{15}	2	46480·9
d_{16}	2	46086 8
d_{17}	1	44295 0
p'	1	37373·4
p''	1	39411 0

It will be seen that no terms from the $4N_2N_3$ combination have been observed, and it is probable that the combination is either very weakly represented or not present at all. In the case of Ne^+, there being no L_3 level, the question of the identification of these terms does not arise, but it will be interesting to know if they occur in A^+. The assignment of the azimuthal quantum numbers in the case of the terms obtained from $4N_2O_2$ state is in certain cases not without ambiguity, and remains to be confirmed from Zeeman effect data. The terms designated as d_1, d_2 . . . d_{17} evidently come from $4N_2O_3$, $4N_2P_1$ states, but beyond fixing their inner quantum numbers no progress has been made in their proper identifications. Here also Zeeman effect might prove helpful.

A few typical multiplets which the terms given in Table II give rise to are shown below.—

The Multiplets.

	$b\,{}^4\overline{P}_3$	(2264)	$b\,{}^4\overline{P}_2$	(2511)	$b\,{}^4\overline{P}_1$	$b\,{}^2\overline{P}_2$	(2528)	$b\,{}^2\overline{P}_1$
$a\,{}^2P_2$	112830		115095		117604	118475		121007
(5371)	(10)		(3)		(2)	(6)		(3)
$a\,{}^2P_1$			109722		112233	113105		115636
			(4)		(5)	(3)		(5)
$c\,{}^4P_3$	21094 9		18831 3			15449		
(362·8)	(7)		(3)			(1)		
$c\,{}^4P_2$	21457 7		19194·0		?			
(884 8)	(5)		(5)					
$c\,{}^4P_1$			20078 8		17568 1			
			(1)		(2)			
$c\,{}^2P_2$	27306 1		25042·5		22531·5	21660 3		?
(1858·5)	(1)		(6)		(5)	(3)		
$c\,{}^2P_1$			26901 0		24390 0	23518·6		20991·1
			(1)		(5)	(3)		(3)
$c\,{}^4\overline{S}_2$	22951·1		20688 5		18177·7			
	(12)		(4)		(1)			

Table III contains all the lines classified by the present analysis. The wave-length measurements by the previous workers were given on Rowland scale. They are here converted into International units.

Table III.

λ.	I.	ν (vac.).	Combination.
783·72	2	127597	$a\,{}^2P_2 - b\,{}^2S_1$
818·11	5	122233	$a\,{}^2P_1 - b\,{}^2S_1$
821·11	1	121786	$a\,{}^2P_2 - b\,{}^2D_2$
826·40	3	121007	$a\,{}^2P_2 - b\,{}^2\overline{P}_1$
830·30	4	120430	$a\,{}^2P_2 - b\,{}^2D_3$
844·06	6	118475	$a\,{}^2P_2 - b\,{}^2\overline{P}_2$
850·31	2	117604	$a\,{}^2P_2 - b\,{}^4\overline{P}_1$
859·04	4	116409	$a\,{}^2P_1 - b\,{}^2D_2$
864·78	5	115636	$a\,{}^2P_1 - b\,{}^2\overline{P}_1$
868·85	3	115095	$a\,{}^2P_2 - b\,{}^4\overline{P}_2$
884·13	3	113105	$a\,{}^2P_1 - b\,{}^2\overline{P}_2$
886·29	10	112830	$a\,{}^2P_2 - b\,{}^4\overline{P}_3$
890·99	7	112235	$a\,{}^2P_1 - b\,{}^4\overline{P}_1$
911·39	4	109722	$a\,{}^2P_1 - b\,{}^4\overline{P}_2$
2960·80	1	33764·8	$b\,{}^2\overline{P}_2 - p''$
3008·45	0	33230·0	$c\,{}^4P_2 - d_{15}$
3139·58	2	31842·2	$c\,{}^4\overline{D}_3 - d_{18}$
3150·93	5	31727·5	$b\,{}^2\overline{P}_2 - p'$
3200·40	2	31237·1	$b\,{}^2\overline{P}_1 - p''$
3202·54	1	31216·2	$c\,{}^4P_2 - d_{13}$
3282·07	1	30459·8	$b\,{}^2D_2 - p''$
3315·66	1	30151·2	$c\,{}^4P_2 - d_{11}$
3379·04	1	29585·7	$c\,{}^2\overline{D}_3 - d_{17}$
3381·10	2	29567·7	$c\,{}^2P_2 - d_{17}$
3385·21	1	29531·8	$c\,{}^4\overline{D}_2 - d_{16}$
3396·58	3	29432·9	$c\,{}^4P_2 - d_{10}$
3405·14	4	29359·0	$c\,{}^4\overline{S}_2 - d_{19}$
3423·73	2	29199·6	$b\,{}^2\overline{P}_1 - p'$
3427·70	3	29165·7	$b\,{}^4P_2 - c\,{}^2P_1$
3431·01	1	29137·6	$c\,{}^4\overline{D}_2 - d_5$
3446·52	3	29006·5	$c\,{}^4\overline{D}_3 - d_{12}$
3460·09	4	28892·7	$b\,{}^4\overline{P}_2 - c\,{}^2\overline{D}_2$
3470·04	3	28809·9	$c\,{}^4\overline{D}_1 - d_{16}$
3488·59	7	28656·7	$c\,{}^4\overline{S}_2 - d_{11}$
3493·01	3	28620·4	$c\,{}^4\overline{D}_2 - d_{14}$
3517·37	0	28422·2	$b\,{}^2\overline{D}_2 - p'$
3535·33	3	28277·8	$c\,{}^4P_2 - d_9$
3553·46	2	28133·6	$c\,{}^4P_2 - d_4$
3572·67	1	27982·3	$c\,{}^2\overline{D}_2 - d_{17}$
3586·25	0	27876·3	$c\,{}^4P_3 - d_6$
3599·20	5	27776·0	$c\,{}^2P_2 - d_{18}$
3599·90	5	27770·6	$c\,{}^4P_2 - d_6$
3607·87	4	27709·3	$c\,{}^2P_1 - d_{17}$
3623·59	2	27589·1	$c\,{}^4P_2 - d_7$
3631·87	5	27526·2	$c\,{}^4P_2 - d_8$
3637·48	2	27483·7	$c\,{}^4P_3 - d_6$
3648·59	2	27400·1	$c\,{}^2\overline{D}_2 - d_{18}$
3651·1	2	27381	$c\,{}^2P_2 - d_{18}$

Table III (continued).

λ.	I.	ν (vac)	Combination.
3653·96	6	27359 8	$c\,^4P_3 - d_2$
3661·00	1	27307 2	$b\,^4\overline{P}_3 - c\,^2P_3$
3663 42	2	27289·1	$b\,^4\overline{P}_2 - c\,^2D_3$
3666·00	0	27269 9	$b\,^4\overline{P}_3 - c\,^2\overline{S}_1$
3680·37	4	27163 5	$c\,^4P_3 - d_5$
3686·15	4	27120·0	$c\,^4P_3 - d_4$
3716·13	1	26902 1	$b\,^4\overline{P}_3 - c\,^2P_1$
3721·35	3	26864·3	$c\,^2P_2 - d_{16}$
3732·62	3	26783 2	$c\,^4\overline{S}_2 - d_9$
3735·76	3	26760·7	$c\,^4\overline{D}_3 - d_{13}$
3744·80	4	26696 1	$c\,^4\overline{D}_3 - d_{12}$
3754 20	5	26629·3	$b\,^4\overline{P}_3 - c\,^2\overline{D}_2$
3804·65	2	26276 2	$c\,^4\overline{S}_2 - d_3$
3817·08	1	26190 6	$c\,^2\overline{D}_2 - d_{16}$
3836 49	1	26058 1	$c\,^4\overline{D}_3 - d_{11}$
3842·25	1	26010 1	$c\,^4\overline{S}_2 - d_6$
3846·84	2	25988 0	$c\,^4\overline{D}_3 - d_8$
3857·29	1	25917 6	$c\,^2P_1 - d_{16}$
3875 41	7	25796 4	$c\,^2\overline{D}_3 - d_{15}$
3894·68	2	25668 8	$c\,^4S_2 - d_3$
3901·13	0	25626 4	$c\,^4\overline{S}_2 - d_4$
3912·54	5	25551 6	$b\,^4P_3 - c\,^4\overline{D}_2$
3912·86	1	25549·5	$c\,^2\overline{S}_1 - d_{16}$
3920·14	7	25502 1	$c\,^4S_2 - d_8$
3938 83	1	25381·1	$c\,^4D_3 - d_5$
3945·45	0	25338 5	$c\,^4\overline{D}_3 - d_4$
3954 75	4	25278 9	$c\,^2\overline{D}_2 - d_{14}$
3964 87	2	25214 4	$c\,^4\overline{D}_3 - d_3$
3975	0	25150	$c\,^2S_1 - d_{15}$
3991·93	6	25043 5	$b\,^4P_3 - c\,^2P_2$
3994·83	6	25025 3	$b\,^4\overline{P}_3 - c\,^2\overline{D}_3$
3997·95	3	25005 8	$c\,^2P_1 - d_{14}$
4002·58	2	24976 9	$c\,^4\overline{D}_3 - d_{16}$
4005·55	1	24958 3	$c\,^2D_3 - d_{12}$
4008 45	2	24940 3	$c\,^2P_2 - d_{12}$
4098 74	5	24390·9	$b\,^4\overline{P}_1 - c\,^2P_1$
4145·13	2	24117 9	$b\,^4P_1 - c\,^2\overline{D}_2$
4172·47	2	23959 9	$c\,^4P_3 - d_2$
4185 13	2	23887·4	$b\,^2\overline{P}_2 - c\,^2\overline{S}_1$
4222·20	1	23677 7	$c\,^4D_2 - d_3$
4236·65	3	23596·2	$c\,^4P_3 - d_2$
4250·60	3	23519 5	$b\,^2\overline{P}_2 - c\,^2P_1$
4254·82	2	23496 2	$c\,^4\overline{D}_3 - d_7$
4268·56	4	23420 5	$c\,^4\overline{D}_3 - d_8$
4268·81	4	23419 2	$c\,^2\overline{D}_2 - d_{12}$
4292·94	6	23287·5	$b\,^4\overline{P}_2 - c\,^4\overline{D}_2$
4300·51	4	23246·5	$b\,^2\overline{P}_2 - c\,^2\overline{D}_2$
4301·55	4	23240·9	$b\,^4\overline{P}_3 - c\,^4\overline{D}_3$

Table III (continued).

λ.	I.	ν (vac.).	Combination.
4305·21	2	23221·2	$c\,^2P_2 - d_{10}$
4317·82	4	23153·3	$c\,^4P_3 - d_1$
4333·34	1	23070·4	$c\,^4\overline{D}_3 - d_4$
4354·97	2	22955·8	$c\,^4\overline{D}_1 - d_5$
4355·50	12	22953·0	$b\,^4\overline{P}_2 - c\,^4\overline{S}_2$
4386·52	3	22790·7	$c\,^4P_2 - d_1$
4389·70	0	22774·2	$c\,^4\overline{D}_2 - d_7$
4400·81	2	22716·7	$c\,^2\overline{D}_2 - d_{11}$
4404·30	1	22698·7	$c\,^4\overline{D}_1 - d_6$
4436·81	5	22532·4	$b\,^4\overline{P}_1 - c\,^2P_2$
4454·38	3	22443·5	$c\,^2P_1 - d_{11}$
4457·25	2	22429·1	$c\,^2\underline{P}_2 - d_4$
4523·15	4	22102·3	$c\,^4S_2 - d_2$
4556·60	3	21940·0	$c\,^2\overline{D}_3 - d_5$
4582·86	4	21814·3	$c\,^4\overline{D}_2 - d_3$
4598·46	2	21740·3	$c\,^2P_2 - d_7$
4610·81	3	21682·1	$c\,^2D_3 - d_6$
4614·49	3	21664·8	$c\,^2P_2 - d_8$
4615·28	3	21661·1	$b\,^2\overline{P}_2 - c\,^2P_2$
4619·13	5	21643·0	$b\,^2\overline{P}_2 - c\,^2\overline{D}_2$
4650·15	2	21498·7	$b\,^4\overline{P}_1 - c\,^4\overline{D}_1$
4658·86	5	21458·5	$b\,^4P_2 - c\,^4P_2$
4680·39	4	21359·8	$b\,^2\overline{P}_1 - c\,^2\overline{S}_1$
4686·25	1	21333·1	$c\,^2\overline{D}_3 - d_3$
4694·41	4	21296·0	$c\,^4\overline{S}_2 - d_2$
4695·64	4	21290·4	$c\,^2\overline{D}_2 - d_4$
4699·64	1	21272·3	$c\,^2P_2 - d_4$
4738·98	7	21095·7	$b\,^4\overline{P}_3 - c\,^4P_3$
4762·42	3	20991·9	$b\,^2\overline{P}_1 - c\,^2\underline{P}_1$
4765·72	5	20977·3	$b\,^4P_2 - c\,^4\overline{D}_3$
4796·30	2	20843·6	$c\,^2\overline{D}_2 - d_9$
4811·73	3	20776·8	$b\,^4\overline{P}_1 - c\,^4\overline{D}_2$
4825·19	3	20718·8	$b\,^2\overline{P}_1 - c\,^2\overline{D}_2$
4832·08	4	20689·3	$b\,^4\overline{P}_2 - c\,^4\overline{S}_2$
4846·58	5	20627·4	$b\,^2\overline{P}_2 - c\,^4\overline{D}_1$
4857·18	2	20582·3	$b\,^2D_2 - c\,^2\overline{S}_1$
4915·93	1	20336·4	$c\,^2\overline{D}_2 - d_8$
4945·57	3	20214·5	$b\,^2\underline{D}_3 - c\,^2P_1$
4948·49	0	20202·6	$c\,^2\overline{S}_1 - d_9$
4960·26	1	20154·6	$c\,^2\overline{D}_3 - d_7$
4978·82	1	20079·5	$b\,^4\overline{P}_3 - c\,^4P_1$
4982·77	0	20063·6	$c\,^2P_1 - d_8$
5013·24	1	19941·6	$b\,^2D_2 - c\,^2\overline{D}_2$
5022·39	3	19905·3	$b\,^2\overline{P}_2 - c\,^4\overline{D}_3$
5028·30	0	19881·9	$c\,^2P_1 - d_7$
5072·53	1	19708·5	$b\,^2D_3 - c\,^2\underline{P}_2$
5077·19	1	19690·5	$b\,^2D_3 - c\,^2\overline{D}_3$
5123·17	3	19513·7	$c\,^2\overline{S}_1 - d_7$

Table III (continued)

λ.	I	ν (vac).	Combination.
5125·70	3	19504 1	$c\,{}^4\overline{D}_2 - d_2$
5143·07	1	19138 2	$c\,{}^2\overline{S}_1 - d_6$
5208·33	5	19194 7	$b\,{}^4\overline{P}_2 - c\,{}^4P_2$
5308 66	3	18831·9	$b\,{}^4\overline{P}_2 - c\,{}^4P_3$
5446 30	2	18356 0	$b\,{}^2D_2 - c\,{}^2P_2$
5499 52	1	18178 4	$b\,{}^4\overline{P}_1 - c\,{}^4\overline{S}_2$
5523·53	2	18099·4	$b\,{}^2\overline{P}_1 - c\,{}^4\overline{D}_1$
5568·62	2	17952 8	$b\,{}^2D_3 - c\,{}^4\overline{D}_2$
5632·95	2	17747 8	$c\,{}^2P_2 - d_2$
5681·93	4	17594 8	$b\,{}^2P_2 - c\,{}^4D_3$
5690·34	2	17568 8	$b\,{}^4\overline{P}_1 - c\,{}^4P_1$
5752 97	1	17377 5	$b\,{}^2\overline{P}_1 - c\,{}^4\overline{D}_2$
5771 38	2	17322 1	$b\,{}^2D_2 - c\,{}^4\overline{D}_1$
6391	1	15643	$b\,{}^2D_3 - c\,{}^4\overline{D}_3$
6471	1	15448	$b\,{}^2P_2 - c\,{}^4P_2$
6512	3	15352	$b\,{}^2D_3 \quad c\,{}^4\overline{S}_2$
6708	2	14771	$b\,{}^2\overline{P}_1 - c\,{}^4\overline{S}_2$

Ionisation Potential of Kr^+.

The ionisation potential of Kr^+, as we have calculated above, comes out to be 26·4 volts. The measurement of Dejardin* with three and four electrode tubes indicates a value of 28·25 volts. The discrepancy is perhaps due to the fact that we have calculated the ionisation potential by taking only the first two members of a Rydberg sequence, and, as is well known, such a calculation can only give a rough estimate of the actual value.

I wish to thank Prof. M. N. Saha, F R.S , for the kindly interest he has taken in this work My thanks are also due to Prof. A. T. Mukerji, M.A., for affording me facilities to continue this investigation.

---

* 'C. R.,' vol. 178, p. 1069 (1924).

The Absorption Spectrum of Cæsium.

By Irene Maud Mathews, Assistant Lecturer in Physics, The University, Sheffield.

(Communicated by S. R. Milner, F.R.S.—Received June 6, 1928—Revised July 23, 1928.)

[Plate 27]

Measurements of the wave-lengths of the lines in the absorption spectrum of cæsium were first made by Prof. P. V. Bevan* in 1912. He produced the vapour of cæsium in a steel tube by heating the anhydrous chloride with metallic lithium, and analysed the light of a carbon arc passed through the vapour with a Hilger quartz spectrograph giving the spectrum from λ 6000—λ 2200 on a 10-inch plate The wave-length of 31 lines of the principal series were given to two places of decimals. His estimated error, however, in most of the lines amounted to 0·2 A.U. These appear to be the only measurements extant of the principal series in the absorption spectrum of this element.

In the present research an attempt has been made to obtain more accurate values by photographing the spectrum, using a Rowland grating of 10 feet radius of curvature and 20,000 lines to the inch. The ruled surface was 8 × 5 cm., but of the 8 cm. it was found that three had to be covered up to obtain the best definition. The spectrum used was the first order, and in the region of the series photographed the dispersion was about 43 A U. per centimetre, and the theoretical resolving power 0·08 A.U.

The cæsium vapour was prepared *in situ* in a steel tube 3 feet 6 inches long by heating pure dried cæsium carbonate in the presence of powdered magnesium.† The heating was done electrically by a battery of 32 cells; 8 metres of nichrome wire 0·05-inch diameter, resistance 8 ohms, were wound in two layers insulated with asbestos paper on a steel tube 2 feet long, the whole being thermally insulated by many layers of asbestos rope. The heating coil could be slipped into position over the first tube, into which a mixture of 20 grammes of cæsium carbonate and 4·5 grammes of magnesium was introduced. The ends of this tube were closed with quartz plates, sealing-waxed on, and kept cool by continuously dripping water. A side tube, brazed on at one end, was in connection with a phosphorus pentoxide tube, McLeod gauge and mercury pump. Light from a carbon arc, rendered parallel by a quartz lens, was passed down the tube, and focussed by another quartz lens on the slit of the grating. As the tube was heated a considerable amount of moist vapour had to be pumped off. At about a red heat the vapour of cæsium gave a sudden increase of pressure, and showed a fluorescent green light. The pressure of the vapour could be regulated, to a certain extent, by the heating current and the pump, but it partly depended on how much cæsium had condensed near the quartz windows. When these were removed, the mixture in the tube invariably exploded when in contact with air, so that it was considered unsafe to attempt to dislodge the cæsium near the windows before dismantling the apparatus.

---

* 'Roy. Soc. Proc.,' A, vol. 86, p. 320 (1912).

† Graefe and Eckhardt, 'Z. Anorg. Chem.,' vol. 22, p. 158 (1899).

For the measurement of the wave-lengths the carbon arc was replaced by an iron arc, and a part of the plate covered by an opaque shutter.

Three satisfactory plates were obtained showing as absorption lines the principal series (with the exception of the first two members), but the earlier lines were rather dense, and the last six lines appeared on only one of the plates.* They were measured on a comparator reading to 0·001 mm., Burns'† measures of the iron lines being used in the reduction. It was discovered that there were strong indications of a small periodic error in the comparator screw, consequently each line was measured either two or three times with different settings, and a quadratic formula was employed for the interpolations, use being made of two iron lines on each side of the cæsium line measured—first two of longer wave-length and one of shorter, then two shorter and one longer. The effect of a periodic error in the comparator screw was thus minimised. It is believed that the wave-lengths determined are in general accurate to about 0·02 A.U.

In the following table the first column gives the connotation of the line in the formulæ.‡

$$\left.\begin{aligned} \mathrm{P}_1(m) &= s(1) - p_1(m) \\ \mathrm{P}_2(m) &= s(1) - p_2(m) \end{aligned}\right\}(m = 1, 2, 3 \ldots).$$

---

* For this exposure the pressure of the vapour was about 47 mm. Hg, and for the other two the pressure was smaller, about 15 mm.

† Burns, Meggers, Merrill, 'Bull. Bur. Stand.,' vol. 274, p. 245 (1916).

‡ The modern usage in which the suffix of P represents the inner quantum number has been adopted in the notation used in the paper. This requires the shorter wave-length and stronger component of the doublet to be denoted by P_2, instead of by P_1, as used to be the case. To avoid confusion with the older tables it should be observed that, *e.g.*, the line denoted by $\mathrm{P}_2(3)$ in the text is called $\pi_1(3)$ in Fowler's Report and $1s-4p_1$ in the tables of Paschen-Götze, a different choice of the term number m having also been made in the latter case.

Beyond $m = 8$ the doublets show single lines only. For the first few lines, however, this is not due to lack of resolving power, but to the weakness of the fainter component P_1. That this is so is shown by the easy resolution of the doublet Na 3303, which appears as an impurity, and the separation of which is practically the same as that of Cs 9. Measures from $m = 8$ to $m = 16$ have accordingly been referred in the table to the brighter component $P_2(m)$. The series could not be traced beyond $m = 32$.

In the second column the mean wave-length in air in I.A. is given, and in the third the corresponding wave number *in vacuo*. In order to make the table into a complete list of the principal lines, the first two members ($m = 1, 2$), measured by Meggers* and Ramage,† are included, although they were not measured on my plates. In the fourth column is an estimate of the error in the wave-length made from three plates, except the last four, which were from two plates. Where the estimate is missing the line appeared on one plate only.

The wave-lengths of the lines measured by Bevan are given in the last column for comparison. The present measurements taken with bigger dispersion, and extending the accuracy to another decimal place, agree closely with his, and indicate that he obtained a remarkable accuracy under the conditions of his small dispersion.

In the column marked O—C, the observed values of the P_2 lines are compared with those calculated from the Hicks' formula, the constants of which were determined from the lines $m = 1, 2, 3$:

$$P_2(m) = 31406 \cdot 20 - \frac{N}{(m + 1 \cdot 448955 - 0 \cdot 087840/m)^2},$$
$$N = 109679 \cdot 2.$$

The results for the last few lines tend to show that a more probable value of the limit is S (1) = 31406·1 The O—C values vary fairly regularly, except in the cases of P (21) and P (27). In these two cases there are close emission lines in the comparison spectrum blotting out the base of the absorption line. The emission lines have wave-lengths 3205·401 (Burns) and 3196·96 approximately, and the effect of these would be to tend to make the observed λ too big and ν too small, as appears to be the case from the comparison with the formula.

---

* 'Bull. Bur. Stand.,' vol. 14, p. 384 (1919).

† 'Roy. Soc. Proc.,' A, vol. 70, p. 304 (1902).

Cæsium Principal Series.

—	λ (I.A.)	ν (vac.)	Δλ	ν (O−C)	λ (Bevan).
P_1 (1)	8943·46	11178 3	—	—	—
P_2 (1)	8521·12	732 33	—	0	—
P_1 (2)	4593·16	21765 4	—	—	—
P_2 (2)	55·26	946·42	—	0	—
P_1 (3)	3888·622	25708·79	0 02	—	3888·65
P_2 (3)	76 184	791·28	0 02	0	76·39
P_1 (4)	3617·296	27637·11	0 02	—	3617·41
P_2 (4)	11·448	81·86	0 02	−0·38	11·52
P_1 (5)	3480·106	28726 56	0 04	—	3480·13
P_2 (5)	76·825	53·67	0 03	−0 99	76·88
P_1 (6)	3399·979	29403·54	0·01	—	3400·00
P_2 (6)	97·996	20·70	0·02	−1·04	398·14
P_1 (7)	3348 720	29853·61	0 04	—	3348·72
P_2 (7)	47·549	64·05	0·03	−1·13	47 44
P_1 (8)	3314·125	30165 22	—	—	3314·04
P_2 (8)	13·149	74·11	0·04	−0·78	13·16
P_1 (9)	—	—	—	—	3289·13
P_2 (9)	3288 605	30399·30	0·02	−0 48	88·56
P_2 (10)	3270 499	30567·59	0 02	−0·58	3270·44
P_2 (11)	56·696	697·15	0·02	−0·43	56·66
P_2 (12)	45·881	799·43	0·02	0·27	45·91
P_2 (13)	37·354	880·54	0 02	0·18	37 47
P_2 (14)	30·46	946·45	0·05	0·17	30·58
P_2 (15)	24·838	31000·39	0·01	0·16	25·00
P_2 (16)	20 065	046·34	0 02	0·60	20·23
P (17)	16·133	084·29	0 02	0 51	16·34
P (18)	12·831	116·24	0 02	0 27	12 91
P (19)	09·960	144·08	0·03	0·29	10·07
P (20)	07·509	167·86	0 03	0·16	07 67
P (21)	05·457	187·82	0·02	−0·66	05·53
P (22)	03·478	207·08	0·02	0·42	03·69
P (23)	01·820	223 25	0·02	0·59	02 02
P (24)	00·411	236·99	0·02	0·19	00·60
P (25)	3199·124	249·55	0·03	0·18	3199·34

Cæsium Principal Series—continued

—	λ (I A)	ν (vac)	Δλ	ν (O—C)	λ (Bevan)
P (26)	96 014	260 41	0 02	—0 18	8 14
P (27)	97 027	270 05	—	—0 60	7 17
P (28)	96 046	279 64	—	—0 06	6 09
P (29)	95 217	287 76	—	—0 12	5 31
P (30)	94 455	295 24	—	—0 04	4 48
P (31)	93 794	301 70	—	—0 22	3 83
P (32)	93 172	307 80	—	—0 35	—

Sowerby and Barratt * from the observation of some combination *s*—*d* absorption lines have suggested that the term values for cæsium may require revision but as far as the *s* and *p* terms are concerned the constants of the Hicks formula obtained above are not materially different from those given by Hicks† and Fowler ‡

A reproduction of the spectrum showing the absorption lines from λ 3900 to 3100 is given in Plate 27 A rubidium and a sodium doublet appear on the negative

A number of satellites to the earlier lines of the series were shown on a plate made from an earlier preparation of cæsium They could not unfortunately be measured very accurately as there were indications of a shift in the comparison spectrum and the series lines themselves were too broad to use in its place The following approximate measurements were however made —

Satellites λ *P* (4) 3610 P (5) 3484 3475 P (6) 3402 P (7) 3351

I am very grateful to Prof S R Milner for his kind help and encouragement in the course of this work

---

* Roy Soc Proc A vol 110 p 192 (1926)

† Hicks Analysis of Spectra, p 316

‡ A Fowler Report on Series in Line Spectra, p 106

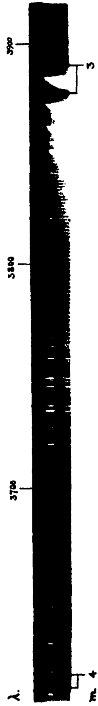
3900
3800
3700
3
4
λ.
m.

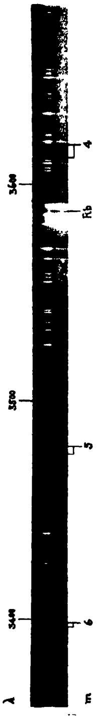
3600
3500
3400
4
Rb
5
6
λ
m

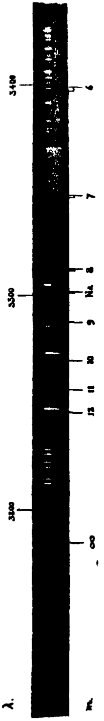
3400
3300
3200
6
7
8
Na
9
10
11
12
∞
λ.
m.

(*Facing p.* 654.)

The Effect of Ozone on the Temperature of the Upper Atmosphere.

By Edward H. Gowan.

(Communicated by F. A. Lindemann, F.R.S.—Received June 13, 1928.)

Some interesting papers have recently been published concerning the temperature of the atmosphere above 11 km. It is known experimentally from "ballon sonde" observations that up to 25 or 30 km. the temperature is nearly constant at about 220° K., possibly rising slightly. There are several sources of indirect evidence that above this height the temperature rises again till it is about the same as, or even higher than, at ground level. Lindemann and Dobson[*] have calculated the density of the atmosphere from observations of meteors. From the abnormally high values obtained they conclude that the temperature above 60 km. is of the order of 300° K. They further showed that if the temperature were 220° K., as generally supposed, there would be insufficient heating effect for meteors of less velocity than 19 km. per second to appear, whereas if the temperature were 300° K. the critical velocity would be 12 km. per second. A considerable number of observations give velocities less than 19 km. per second. The author's suggested explanation of the occurrence of a high temperature at such heights was the strong absorption of solar energy in the ozone which has been observed. Whipple[†] refers to the zones of audibility which occur at some distance around big explosions. Assuming a reasonably sharp transition of temperature from 220° to 280° K. at a height of about 60 km., he makes a rough estimate of the minimum radius of the outer zone of audibility. This agrees very well with observations that have been made. Chapman[‡] has determined the height and ion concentration of the Heaviside layer by day and by night, and Hulburt[§] claims that the required number of ions would be supplied above 130 km. if the density as calculated on the isothermal hypothesis were multiplied by a factor of 1000. This factor would bring the density into agreement with the results of Lindemann and Dobson.

---

[*] 'Roy. Soc. Proc.,' A, vol. 102, p. 411 (1922).

[†] 'Nature,' vol. 111, p. 187 (1923).

[‡] 'Q.J.R. Met. Soc.,' vol. 52, p. 219 (1926).

[§] 'Nature,' vol. 120, p. 187 (1927).

Continuing with the explanation suggested by Lindemann and Dobson, it is proposed in this paper to consider the radiative equilibrium of the upper part of the atmosphere, taking into account the effects, with selective absorption, of water-vapour and ozone. It will be shown that this also leads to a region of high temperature in the neighbourhood of, and above, 60 km.

General Treatment.

The problem of the radiative equilibrium of the atmosphere has been thoroughly treated from a general point of view. Humphreys[*] has pointed out that if the effective radiating power of the earth and the lower layers of the atmosphere were the same as that of a black body at temperature T_1, the effect on any radiating and absorbing matter near enough to the earth for the radiating surface to be regarded as an infinite plane would be to keep the matter at a constant temperature, such that the radiation from it would be one-half the radiation from it at T_1. If the matter admitted the application of Stefan's Law, its temperature would be T, where $T^4 = \frac{1}{2}T_1^4$. If one uses for T_1 the value 256° K estimated by Abbot and Fowle[†] from observations of the solar constant (regard being paid to that portion of the solar energy which is reflected and does not contribute to heating the earth or lower layers of the atmosphere), the resulting value of T agrees very well with the actual temperature of the stratosphere as far as observations go. This treatment does not consider the possibility of there being absorption of solar radiation in the upper layers.

Gold[‡] developed the radiation theory more fully, and showed that the temperature of the stratosphere must lie between certain limits. His interpolated value between those limits agrees fairly well with the results of the balloon ascensions. He, however, does not take full account of selective absorption, and also rejects the possibility of solar radiation being important in the higher regions of the stratosphere.

In a non-convective region any layer of air is dependent for its average temperature on solar radiation, radiation from the solid earth, and radiation from the atmosphere above and beneath it. The loss or gain of heat by conduction is infinitesimal. On the average loss and gain horizontally may be neglected in this region, for the layer is assumed homogeneous in that direction, and at the same average temperature in all parts. Hence there is a horizontal equilibrium which does not affect that in the vertical direction.

---

[*] 'Astrophys. J.,' vol. 29, p. 14 (1909).

[†] 'Ann. Obs. Smithson. Inst.,' vol. 2, p. 166 (1908).

[‡] 'Roy. Soc. Proc.,' A, vol. 82, p. 43 (1909).

In such a region, then, let at wave-length λ, $R_{\lambda T}$ be the radiation from any layer at temperature T, X'_λ and Y'_λ be the absorbed portions of the atmospheric radiations from above and below the layer, E'_λ and S'_λ be the portions of the terrestrial and solar radiations absorbed in the layer. Then the equation of equilibrium, considering only vertical radiation, is

$$\int R_{\lambda T}\,d\lambda = \int (X'_\lambda + Y'_\lambda + E'_\lambda + S'_\lambda)\,d\lambda$$

An analytical solution of this equation can be found when the coefficient of absorption does not vary with the wave-length. *i.e.*, when the atmosphere is assumed grey. When selective absorption is used a graphical solution is possible, though laborious, and it is such a solution, by successive approximation, that is obtained in this paper.

Particular Treatment.

Consider a disc-shaped element of the atmosphere, with faces horizontal. The loss or gain of heat from the edges is negligible, for the element is in horizontal radiative equilibrium with adjacent elements as mentioned above. Hence in what follows only vertical radiation is considered

The element receives normally on its upper face radiation from the sun and from the higher layers of the atmosphere, and on its lower face radiation from the earth and lower layers of the atmosphere In the case of the solar radiation, suppose day and night are averaged out by considering it to fall continuously on the cross-section of the earth, instead of intermittently and at various angles over the surface of a sphere. Then the actual solar energy at the distance of the earth must be divided by 4.

A certain portion of the solar radiation is known to be reflected from the earth's atmosphere, and to take no part in the heating of the earth. The reflection is probably a gradual process, taking place at no definite height, but the energy reflected is certainly available for heating the layers through which it has to pass on its way out, provided parts of it can be absorbed by the material in the layers. For the purposes of this calculation, 30 per cent. of what reaches the tropopause is assumed reflected vertically for all wave-lengths.

It is assumed that water-vapour and ozone are the principal gases in the upper atmosphere which absorb solar and terrestrial energy. The contribution of the air itself is very small at any height. Carbon dioxide has an appreciable absorption in the infra-red, but in the stratosphere, being a heavy gas, it rapidly becomes unimportant, and has here been neglected.

Let K_{λ_s} and K_{λ_w} be the fractions absorbed by ozone and water-vapour respectively from energy passing normally through the element, at wave-length λ. Then the total energy absorbed is given by

$$\int_0^\infty K_{\lambda_s}(S_\lambda + s_\lambda + E_\lambda + X_\lambda + Y_\lambda)\,d\lambda + \int_0^\infty K_{\lambda_w}(S_\lambda + s_\lambda + E_\lambda + X_\lambda + Y_\lambda)\,d\lambda,$$

where

S_λ is that portion of the sun's radiation which reaches the element.

s_λ is that portion of the reflected solar radiation which reaches the element.

E_λ is that part of the earth radiation which reaches the element.

X_λ and Y_λ are the atmospheric radiations from above and below which reach the element.

It is obvious that the element absorbs partly from above and partly from below, but radiates equally in both directions. Thus the surface of radiation is effectively double the surface of absorption, and the condition of equilibrium is

$$\int_0^\infty R_{\lambda T_0}\,d\lambda = \tfrac{1}{2}\int_0^\infty K_{\lambda_s}(S_\lambda + s_\lambda + E_\lambda + X_\lambda + Y_\lambda)\,d\lambda$$
$$+ \tfrac{1}{2}\int_0^\infty K_{\lambda_w}(S_\lambda + s_\lambda + E_\lambda + X_\lambda + Y_\lambda)\,d\lambda,$$

where $R_{\lambda T_0}$ is the energy of a black body at temperature T_0 multiplied by the sum of K_{λ_s} and K_{λ_w}.

The use of an absorption coefficient for parallel radiation traversing a layer normally is supposing a very much idealised case. Actually the radiation is diffuse in the atmosphere and travels through layers in which the absorbing material and the temperature are continuously variable. This case is considered mathematically by Gold, by Milne, and by Emden,* and it appears that as a first approximation the absorption coefficient for parallel rays must be doubled. Actually the factor is unity when the absorption is practically complete, and approaches 2 when the absorption is small. For the coefficients used in the various layers of the stratosphere the factor, including the difference in what gets through each layer, may be taken as 1·6.

A curve showing the actual spectral distribution of the energy in $E_{0\lambda}$, the outgoing radiation at 11 km. has been obtained, using the amounts of water-vapour given by Simpson[*] and the appropriate absorption coefficients tabulated by Gold On the average over the absorbing regions a black body curve at 260° K. is slightly more than 50 per cent. too high. Over the transparent regions it is too low, as the energy emerging is practically that from the surface of the earth. The total energy is, of course, the same in both cases.

---

* Gold, *loc. cit.*; Milne, 'Phil. Mag.,' vol. 44, p. 872 (1922); Emden, 'Sitzb. bayer. Akad. Wiss.,' vol. 100, p. 100 (1913).

The terrestrial energy absorbed by any layer is $E_0 e^{-t}(1 - e^{-t_1})$ where $E_0 = \int E_{0\lambda}\,d\lambda$, t represents the absorbing material between 11 km. and the layer, and t_1 represents the absorbing material in the layer itself. It is more convenient to use the absorption coefficient for parallel rays, as then the same coefficient can be applied to both terrestrial and solar radiation It is evident from the foregoing paragraphs that the assumption of E_0 as black at 260° K. brings in a factor which practically compensates for the absorption coefficient in the case of this radiation Such simplifying assumptions were felt to be justified in this preliminary investigation of the possibilities of the problem.

Material.

(*a*) The distribution of energy in the solar spectrum has been investigated by Abbot,[†] and the curve used in this work is substantially that obtained by him. In the region of short waves, however, up to 0·4 μ, Abbot's curve is unsatisfactory. It cuts off at 0·3 μ, and this ultra-violet limit of the solar spectrum has been shown to be due to ozone [‡] The very strong absorption of this gas in that region makes the observations rather uncertain. Fabry and Buisson, in a later paper,[§] have measured by a photographic method the energy in the solar spectrum down to 2920 Angstrom units They conclude that one quarter of the energy is of wave-length less than 4000 Angstroms, and show that in this region the solar energy curve may be taken as black at 6000° K. From 0·4 to 1·2 μ the values were taken direct from Abbot's curve, and from 1·2 to 6 μ there is a negligible difference between the observed curve and that of a black body at 6200° K. All values were divided by 4 to get the average over the earth.

(*b*) The average radiation from the earth and the moisture-laden atmosphere below 11 km. has been taken as black at 260° K. This is practically the temperature found by Abbot's and Fowle's work on the solar constant, and by Humphreys' approximate theory.

---

[*] 'Mem. R. Met. Soc.,' vol. 2, p. 88 (1928).

[†] 'Ann. Obs. Smithson. Inst.,' vol. 3, p. 200 (1913).

[‡] Fabry and Buisson, 'J. de Physique,' vol. 21, p. 197 (1921).

[§] 'C.R.,' vol. 175, p. 156 (1922).

(*c*) The total amount of ozone present in the atmosphere varies from place to place and from day to day, but has been taken as constant at 0·300 cm. of the pure gas at N.T.P. This is, of course, the equivalent thickness measured vertically through the layer.* The distribution of this ozone is unknown, but the height of its centre of gravity has been determined by several investigators. Cabannes and Dufay† and Lambert, Dejardin and Chalonge‡ agree in the determination of this height as between 40 and 50 km.

(*d*) The absorbing fraction for ozone, $K_{\lambda x}$, is given by

$$K_{\lambda x} = \frac{I_0 - I}{I_0} = 1 - 10^{-\alpha x},$$

where I_0 and I are the intensities before and after the radiation has passed through x cm of pure ozone at N.T.P. or its equivalent. The coefficient α is defined by the relation

$$\frac{I}{I_0} = 10^{-\alpha x}.$$

Fabry and Buisson§ have determined the value of α in the ultra-violet for the ozone band whose centre is at 2550 Angstroms In the visible Colange‖ has determined α, and his values were used as a basis. It was not thought worth while to consider the fine structure that he gives, and a smooth average curve was therefore drawn.

Ladenburg and Lehmann¶ give values of the per cent. absorption for the most important infra-red bands in ozone. Humphreys, in his "Physics of the Air," has already noted the fact that they do not give the exact pressures at which the measurements were taken. It appears, from correspondence with Dr. Lehmann, that pressures of 50, 100 and 200 mm. of mercury were used. The ozone was practically pure, being obtained from the boiling liquid. Using this information the values of $K_{\lambda x}$ at the maxima and minima of the bands in this region were found.

(*e*) A report containing the absorbing fractions of water-vapour is published by Fowle.[*] He gives a graph of percentage transmissions from 1 to 9 μ (p. 23), and a table of collected results from 3 to 60 μ (p. 51). Both contain bands due to impurities, carbon dioxide and probably ozone. The values of α to be used in this computation were chosen by consideration of both the table and the graph, and as far as possible the effects of the impurities were eliminated [†]

---

* Cabannes and Dufay, 'J. de Physique,' vol. 7, p. 257 (1926); Dobson and Harrison, 'Roy. Soc. Proc.,' A, vol. 110, p. 660 (1926); and vol. 114, p. 521 (1927).

† 'C.R.,' vol. 181, p. 312 (1925).

‡ 'C.R.,' vol. 183, p. 800 (1926).

§ 'J. de Physique,' vol. 5, p. 196 (1913).

‖ 'J. de Physique,' vol. 8, p. 254 (1927).

¶ 'Ann. d. Physik,' vol. 21, p. 305 (1906).

(*f*) As a starting point from which to calculate the amount of water-vapour in the various absorbing layers of the stratosphere, saturation at 11 km. at a temperature of 219° K. was assumed.

As mentioned above, the actual distribution of the ozone is unknown. It is believed that one of the factors responsible for the ozone layer is the ultra-violet light from the sun. There are probably other agencies, but whatever they may be the ozone cannot well be less than proportional to the oxygen from 45 km., the centre of gravity of the layer, upwards. Below 45 km. the amount probably decreases rather rapidly to the very small proportions found near the surface. Such a distribution has, then, been assumed as a basis. It gives the smallest possible amounts of ozone in the top layers, and hence a minimum temperature there.

As a starting point for the computation of the amount of oxygen present at different heights, the value of 35·3 mm of mercury has been taken as the partial pressure at 11 km.[‡]

Method

In radiative equilibrium the temperature of the air is determined by equating the amount of energy emitted to the amount absorbed. These amounts depend, of course, primarily upon the amounts of water-vapour and ozone present; but the amount of water vapour depends upon the temperature. The only method of attack, therefore, is to assume a distribution of temperature, determine the proportion of water-vapour at various heights, and on this basis calculate what the temperature would be. If one has assumed the right temperature curve, the final temperatures calculated will agree with the original assumptions. If the original assumptions were faulty, the calculated temperatures will differ from those assumed, and one must assume a fresh distribution and start the process over again. In this way, by a series of approximations, it is possible to arrive at a curve in which the temperatures initially assumed agree with those calculated.

---

[*] 'Smithson. Misc. Coll.,' vol. 68, pp. 23, 51 (1917).

[†] Hettner ('Ann. d. Phys.,' vol. 55, p. 476 (1918)) has measured the absorption coefficients of water-vapour, and his results differ somewhat from Fowle's. The latter were chosen, however, because Fowle took such particular care to eliminate stray light, which is the greatest source of error in extreme infra-red measurements where the energy is small.

[‡] Humphreys, 'Physics of the Air,' p. 69.

In principle, of course, one should divide up the atmosphere into a large number of layers in order to carry out this process. Since, however, these calculations are excessively laborious, the non-convective part of the atmosphere was divided into nine layers as follows: 11–30, 30–40, 40–50, 50–60, 60–70, 70–80, 80–100, 100–130, 130–150 km.

An average temperature, T_0, for each layer was assumed, and the water-vapour pressure at the boundaries calculated This is given by the following equation :—

$$-\,dp = p\,\frac{dh}{H}.$$

H is the height of the homogeneous atmosphere, or the height it would have if everywhere at the same temperature and pressure. It is by Boyle's Law independent of the actual value of the pressure.

Integrating between limits p and p_0, h and h_0 gives

$$\log_{10} p = \log_{10} p_0 - \frac{0\cdot434\,(h - h_0)}{H},$$

where p and p_0 are the pressures at h and h_0 metres respectively and $0\cdot434$ converts from hyperbolic to common logarithms.

$H = b\,\frac{\delta_m}{\delta_a}$ for normal gravity where δ_m = density of mercury and δ_a = density of air at 273° K., and pressure represented by barometer reading b.

For any other gas whose density is δ, at temperature T_0

$$H = 7991 \times \frac{\delta_a}{\delta} \times \frac{T_0}{273}$$

the factor 7991 being the value of H for air under standard conditions of the atmosphere.

The difference of pressure between the boundaries gives the pressure due to the water-vapour in the layer. The amount of absorbing vapour is stated as so much precipitable water, meaning the depth of liquid water which, if evaporated into a column of the same cross-section, would produce the absorbing layer of vapour. This gives x in the equation for $K_{\lambda w}$ and, knowing a, values over the desired part of the spectrum, from 1 to 50 μ, can be calculated. For parallel radiation passing normally through the layer—

$$K_{\lambda w} = 1 - 10^{-ax}.$$

The partial pressures of oxygen at the boundaries were calculated as for the water-vapour, δ in this case being the density of oxygen. The differences, as before, give the pressure due to the oxygen in the layer. From 40 km. upwards the ozone was distributed proportionally to the oxygen. In the 30–40 layer the same amount as in the 50–60 layer was assumed, and below that none. The total, of course, made up the average thickness of 0·300 cm. at N.T.P.

α and x being known, the values of K_{λ_s} were found in the ultra-violet from 0·23 to 0·34 μ, in the visible from 0·45 to 0·65 μ, and in the infra-red from 1 to 12 μ.

The radiation from the layer occurs altogether in the infra-red. For simplicity in calculating it the absorbing fractions of ozone and water-vapour in this region were added together. This sum, represented by $K_{\lambda(s+w)}$, multiplied by the black body curve for the assumed temperature, T_0, gives the energy radiated from the layer. The area under the curve of this energy plotted against λ is

$$\int_0^\infty R_{\lambda T_0}\, d\lambda.$$

All the integrations were carried out from 0 to 50 μ, where radiation becomes negligible.

In computing the total energy absorbed by each of the layers, the energy of any particular radiation is decreased successively as it passes through the layers, the decrement in each case being the incident energy multiplied by K_λ for whatever absorbing agent is being considered The sum of the decrements in each layer gives, of course, the total of the energy absorbed in the layer. In both cases, water-vapour and ozone, this procedure was followed for the direct solar radiation inwards, and for the reflected solar, and the terrestrial radiations outwards. These three items were totalled and plotted as one curve for each absorbing agent for each layer In treating the water-vapour and ozone as separate absorbing agents there is little danger of appreciable overlapping of energies. For either when the ozone absorption is large that of the water-vapour is small, and *vice versa*, or else they are both small over the same region In either case the error introduced is negligible.

The areas under these curves of energy against wave-length give respectively the values, for ozone

$$\int_0^\infty K_{\lambda_s}(S_\lambda + s_\lambda + E_\lambda)\, d\lambda,$$

and for water-vapour

$$\int_0^\infty K_{\lambda_w}(S_\lambda + s_\lambda + E_\lambda)\, d\lambda.$$

Now the correction for the radiation from the atmosphere itself must be considered. Each layer absorbs something from the radiation of every other layer, either from above or below. Using $K_{\lambda(s+w)}$ and the radiations calculated above, an analogous system of decrements gives the required items for each layer. The totalling, plotting and measuring of this curve gives the value of

$$\int_0^\infty K_{\lambda(s+w)}\,(X_\lambda + Y_\lambda)\,d\lambda.$$

The areas under all the curves were measured by means of a planimeter, and reduced to gramme calories per square centimetre per minute. One half the total of the absorbed energies thus found should be equal to the energy radiated. If it is not a different assumption of the average temperatures of the layers must be made, and the whole computation recommenced from the beginning.

As an interpolation formula, and to give a certain amount of guidance in the choice of new values for the temperatures, Stefan's law may be used in the following form :—

$$T = T_0\,(E/E_0)^{\frac{1}{4}},$$

where E is one half the energy absorbed by any layer and E_0 is the energy radiated by the layer at the assumed temperature T_0.

This formula was tested and found to give consistent values when applied to the radiation of one layer at a number of different temperatures. It was accurate within 2 per cent. over ranges up to 40°, and was therefore most useful in estimating the corrections to be applied to the temperatures initially assumed in each step of the successive approximation.

Results.

Km.	11–30.	30–40.	40–50.	50–60.	60–70.	70–80.	80–100.	100–130.	130–150.
II	220 (224)	210 (213)	207 (209)	205 (204)	205 (204)	205 (204)	205 (203)	←—205	(201)—→
III	220 (224)	220 (222)	250 (256)	270 (268)	305 (304)	305 (308)	290 (290)	240 (237)	220 (217)
IV	220 (225)	220 (220)	250 (255)	270 (271)	300 (292)	300 (300)	300 (310)	←—300	(312) —→

The table and figure give the results of three sets of approximations. In the table the temperatures assumed are given first. Following them, in brackets, are the values obtained by calculation. Ideally, of course, these figures should coincide, but the calculations are so laborious that the above approximation was considered sufficiently close.

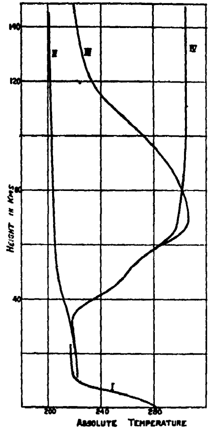

In practice the production of one of these curves entailed the calculation of about four approximations, but the temperatures assumed for the first of the four were the result of several preliminary estimates. Leaving aside the ground work of collecting the material and arranging it in convenient form for use, one approximation required about fifty hours' work for completion. Thus it is clear that one had to be content with the above accuracy. It is greater than the 5 per cent. which, from the data, can be allowed to the method in general.

Curve I shows an average of the balloon observations given by Sir Napier Shaw in Part II of his "Manual of Meteorology."

Curve II was obtained by considering the absorption and radiation of water-vapour alone. This curve was intended for use as a basis of comparison.

Curve III is the result when the observed amount of ozone is distributed so as to be proportional to the oxygen down to 40 km. From 30 to 40 there is the same amount as in the layer from 50 to 60, and below that no appreciable amount is assumed.

In computing Curve IV an attempt was made to see how much ozone would be necessary in the upper layers to keep the temperature in the neighbourhood of 300° K. up to 150 km. at least One arrives at this curve if one assumes that the amount of ozone in the top four layers is greater than it would be if it were proportional to the oxygen by the following factors · 100 to 150 km , 10·3 ; 80 to 100 km , 2·16 ; 70 to 80 km., 1·10 ; and 60 to 70 km., 1·05. The excess in the uppermost layers is balanced by reducing the amount in the layer from 40 to 50 km. to 0·985 of what it would be if proportional to the oxygen The other layers are left as they would have been.

Examination of Assumptions and Results.

The actual amount of water-vapour present in the part of the atmosphere considered in this paper has an important bearing on the temperatures obtained. The assumption of saturation at 11 km gives the greatest amount possible, but Gold* adduces strong arguments in favour of this. Suppose it should be less than saturated. The energy due to water-vapour will be reduced in the same ratio on both sides of the equation, but for any layer in which there is also absorption by ozone the proportionate effect on the total will be greater on the radiation side than on the absorption side. To maintain equilibrium therefore, the temperature of the gas would have to be higher. Thus, Curves III and IV are lower limits as far as this variable is concerned. The upper part of Curve III has already been mentioned as a lower limit in connection with the ozone distribution. If the relative humidity were 30 per cent. at 11 km. instead of 100 per cent. as has been assumed, the calculated temperature at about 70 km would be over 350° K. Similar reasoning holds for any change in the absorption coefficient.

The question of variation of the absorption with temperature and pressure next arises. In the case of ozone nothing seems to be known. Miss Eva von Bahr† has investigated the effects in water-vapour. She found that the absorption decreased with the total pressure. A comparison of results using steam, with those taken under atmospheric conditions, indicates that less absorption would be expected at the lower temperatures. Following up Curves

* 'Geophys. Mem. No. 5,' p. 129.

† 'Ann. d. Physik,' vol. 29, p. 780 (1909); and vol. 33, p. 585 (1910).

III or IV, the temperature and pressure effects would tend to balance each other, and so they cannot have led to any great error.

The assumed value of the Albedo, 0·30, is rather lower than the value 0·337 obtained by Abbot,* and still lower than Aldrich's value, 0·43. Owing, however, to the fixing of the height of reflection at 11 km., and the necessary inclusion of all wave-lengths without discrimination, it may still be effectively too high. If, as is probable, a great part of the reflection is from cloud banks which are below 11 km., the 30 per cent will be reflected in the spectral regions for which water-vapour is relatively transparent, but much less than 30 in the regions, all-important in this instance, where it is highly absorbing. The net result is that too much energy will have been included from this source, and the effect will be the more noticeable the lower the layer. This may partly explain the high values that have been obtained by calculation for the 11–30 km. layer. Neglecting the whole of the energy due to the reflection brings the temperature of this layer two to three degrees nearer the assumed value.

It was mentioned above that the assumption of E_0 as black at 260° K., and the use of the parallel ray absorption coefficient for the low temperature radiation introduced practically compensating errors. Strictly, the absorption of the re-radiation from the layers of the stratosphere itself is also of sufficient importance to correct. In the several approximations the energy from this source was from 10 to 30 per cent. of the total absorption in any layer. The use of the absorption coefficient for diffuse radiation would have increased this proportion and have raised the temperature slightly.

Dr. Dobson has recently been making some measurements on the height of the ozone layer The average of some fifty values (as yet unpublished) is nearly 10 km. lower than the average obtained in France. Tentative results indicate that the layer is higher in spring than in autumn—that is, the height increases with increase in the amount of ozone From this it appears probable that the lower boundary remains nearly stationary, the change in effective height taking place by increased concentration in the upper parts of the ozone layer. This would suggest that between, say, 30 and 60 km. the temperature will change very little with variation in the ozone, but that important changes might take place above 60 km. The general effect on the calculations of making the change to 35 km. on the average would be to decrease the temperatures and lower the height at which the increase of temperature occurs. The difference in both cases would probably be small, but it is impossible to make any reliable estimate without going into the matter fully, and completing another set of approximations.

---

* *Loc. cit.*, p. 145.

It was mentioned early in the paper that the air itself and carbon dioxide were being neglected, but that the carbon dioxide might have a small effect in the lower layers up to about 40 km. It is here mentioned again only to point out that any effect would be such as to raise slightly the temperature of those layers

Apart from the possible corrections mentioned, the curves bear out very well the explanation of the results from sound ranging. It was pointed out that near 60 km. a temperature of about 280° K. was to be expected, and, if found, would explain satisfactorily the refraction of the sound waves. The agreement is fairly good.

The temperature is also in good agreement with that obtained from the meteor observations The height at which the maximum is reached is important in this connection It has been observed that very few meteors disappear at heights round about 60 km The explanation put forward by Lindemann and Dobson is that a drop occurs in the rate of heating due to the passing of the meteor from a warm layer into a colder one below, delaying the time of final evaporation of the material If Curves III or IV represent a fair approximation to the true gradient, it is easy to see that this would happen.

It must be remembered that these curves are all averages over the surface of the earth. One can make a rough estimate, however, of the difference between night and day temperatures from the figures of the computations.

A total pressure at 40 km. of 1·94 mm. of mercury gives the mass of gas above this height on each square centimetre as 2·64 gm. The heat lost per degree by this mass of gas is $0 \cdot 24 \times 2 \cdot 64 = 0 \cdot 63$ calories, assuming the specific heat does not change much with whatever alteration in composition there may be.

The total energy radiated by all the layers above 40 km. is 0·0215 cal./cm.^{2}/min Therefore if all sources of radiation were cut off from this region, it would fall in temperature at the rate of 1° C. in $\frac{0 \cdot 63}{0 \cdot 0215} = 29$ minutes, say half an hour. Thus during a 12-hour night the temperature would fall 24°.

To get an estimate of the day temperature in temperate latitudes, the value of the solar energy used in these computations must be multiplied by about 2·5. Roughly, this would have the effect of shifting Curve IV over to 320° K.

These estimates of the night and day temperatures have been made from the mean, and though they are very rough, it would appear that the total variation in temperature is nearly 40°. Actually the change will be rather less than this. In the above estimates of the departures from the mean during the night and day, the value 0·0215 was used for the radiation $\int R_{\lambda T_0}\, d\lambda$. As this is, of course, not a constant the deviation on either side of the mean tends to be smaller than the estimates show. Prof. Lindemann has suggested another agency tending to reduce the change. As the temperature begins to drop when the solar radiation is cut off, the gas contracts and falls in the gravitational field. The potential energy thus lost can only appear as heat, and will be greatest in the upper layers which fall the farthest. Hence the compensation is greatest in the layers which tend to cool the most. The converse would be true when the gas is heating up during the day The effect of both these agencies will be, therefore, always to reduce the amplitude of the daily variation.

The factors materially affecting the general average of the temperature obtained are now summarised A decrease in the relative humidity at 11 km. raises the temperature. More ozone in the upper layers than is proportional to the oxygen raises the temperature above 80 km., but below that lowers it slightly The additional correction for diffuse re-radiation from the stratosphere would raise the temperature. If the centre of gravity of the ozone layer should be 35 instead of 45 km., the temperature would be lowered. The application of the changes suggested in all these factors would probably raise the temperature, but not greatly, as is suggested by the near coincidence of calculated and observed values below 30 km., and no one of them alone can cause Curves III or IV to approach Curve II. Thus, given the ozone in the upper atmosphere, a theoretical consideration of the radiative equilibrium leads to a warm region agreeing very well as regards both temperature and height with the results of indirect observations.

It is realised that this paper covers but the first step in a possible series of interesting computations by the same or a slightly modified method. The variation of the average temperature with the amount of ozone, the determination of the day and night temperatures at different latitudes with constant ozone, and the effect of changing the relative humidity are all worth investigating carefully. It is hoped that some, if not all, of these may be attempted at a later date.

In conclusion, I wish to thank Prof. F. A. Lindemann for suggesting the problem, and for many valuable criticisms during the course of the work.

The Steady Motion and Stability of a Helical Vortex.

By Prof H. Levy, M.A, D.Sc., and A. G. Forsdyke, A.R.C.S., B.Sc., Beit Scientific Research Fellow.

(Communicated by S Chapman, F.R S.—Received June 21, 1928.)

§ 1. *Introductory.*—This is the third of a series of papers dealing with the stability or instability of certain forms of vortex motion associated with the wake of a body moving in a fluid. In the earlier papers[*] we examined the case of a system of equal vortex rings in parallel planes, as they might form in the rear of a sphere in steady motion. Nisi and Porter[†] have shown that the lowest speed at which the vortex ring forms is $8 \cdot 14\ \nu/d$ where ν is the kinematic viscosity of the fluid and d is the diameter of the sphere. Such a system of vortices has been proved[*] to be only partially stable, and it is therefore to be inferred that their production occurs at a transition stage to a more stable type of flow.

Now it is well known that in the case of two dimensional flow past a cylinder of any cross-sectional shape, eddies are formed in symmetrical pairs at low values of Reynolds' number, whereas at higher values asymmetry sets in and the eddying is formed alternately at one side of the cylinder and then at the other with regular periodicity. This latter stage occurs over a range of values of Reynolds' number extending from about[†] 70 to 10^5. Detailed explorations of the field for some distance behind the cylinder have established that the centres of eddying approximately assume the stable formation which has come to be known as the "Kármán vortex street."[‡]

A corresponding systematic study of the flow in the case of three dimensional motion at high values of Reynolds' number has unfortunately not yet been conducted, although it has now been commenced. Some photographs of the state of flow in the wake of a flat plate[§] indicate, however, that in certain circumstances a vortex filament spirally unwinds itself from the body and travels down stream. A measurement of the pitch of this helix gives roughly a value of 0·3. In R and M, No. 332, Adv. Cmtee. for Aeronautics, Naylor and Fraser in studying the formation of eddy centres in the wake of a circular cylinder in a water channel draw particular attention to the occurrence of some form of screw motion, and note that the axes of the eddies appear to be skewed out of the vertical.

---

[*] 'Roy. Soc. Proc.,' A, vol. 114, p. 594 (1927), and vol. 116, p. 352 (1927).

[†] 'Phil. Mag.,' vol. 46, p. 754 (1923); 'Rep. Advis. Comm. Aeronaut.,' No. 332 (1917); Levy, 'Phil. Mag.,' vol. 2, p. 844 (1926); Relf and Simmonds, 'Phil. Mag.,' vol. 49, p. 509 (1925); Prandtl, 'Aeronaut. J.,' Aug., 1927.

[‡] Fage and Johansen, 'Roy. Soc. Proc.,' A, vol. 116, p. 170 (1927).

[§] Eden, 'Rep. Advis. Comm. Aeronaut.,' No. 31 (1911).

On this as a basis it is possible to construct a tentative rational picture of the probable nature of the flow in the more general case. The circular vortices produced in the rear of a body such as a sphere, for example, at low values of Reynolds' number, appear to be analogous to the symmetrical production of eddy pairs in the case of two dimensional motion If, varying the latter case slightly, the body be a plate or cylinder, finite in length but long in proportion to its breadth, then at large enough values of Reynolds' number the vortex filament formed at one long edge (AB, say) and moving down stream may be expected to continue over a short end (AA′, say) to the parallel vortex filament in process of formation at the opposite edge, A′B′, and as this reaches maturity and is discharged the filament would continue over the remaining short edge (BB′) to a new vortex forming at the first long edge: and so on. Thus we are naturally led to a picture of a spiral-shaped vortex (in this case elongated in the direction of the length of the plate or cylinder) continuously unwinding itself from the edge of the body and passing down stream into the wake. This picture is consistent not only with the direct evidence of Naylor and Frazer but with that from Eden's photographs and, in the limiting case of two dimensional flow, with the very conclusive evidence of the "Kármán vortex street."*

If the foregoing discussion is, in its broad outline, correct, the next stage of our investigation must concern itself with a discussion of the steady motion of a right helical vortex of uniform strength, and an examination of the conditions in which such a motion will be stable. It will be seen that such a vortex will move forward in the direction of its axis with steady speed, and in general rotate about that axis with uniform angular velocity.

The conception of stability that will be here adopted will be similar to that of the previous papers: the helical vortex will be presumed stable in form if it can maintain certain steady fundamental modes of vibration of its filament of small amplitude.

§ 2. *Nature of Disturbances to Filament.*—The vortex filament in question has, for its central curve, the right circular helix whose equations with respect to axes fixed relatively to it are

$$x = a\cos\psi, \qquad y = a\sin\psi, \qquad z = a\psi\tan\alpha, \tag{1}$$

---

* Kármán and Rübach, 'Phys. Z.,' vol. 13, p. 49 (1912).

the azimuthal angle ψ being measured from the point at which the helix crosses the axis of x. Due to its own vorticity, the helical vortex possesses a uniform velocity of spin about its axis, and a uniform velocity of translation V along the direction of its axis. Considering a right-handed system of axes, and supposing that the spin is positive, of magnitude w, we shall have, with respect to stationary axes, coincident with our moving system at time $t = 0$,

$$x = a\cos(\psi + wt), \quad y = a\sin(\psi + wt), \quad z = \mathrm{V}t + a\psi\tan\alpha. \qquad (2)$$

It will be found convenient in the subsequent analysis of the motion to write $\phi = \psi + wt$. Then

$$x = a\cos\phi, \qquad y = a\sin\phi, \qquad z = \mathrm{V}t + a\psi\tan\alpha, \qquad (3)$$

give the position at time t of the point ψ on the central curve of the helix.

Denoting the component velocities of the fluid element situated at the point ψ by x, y, z, we have, in the undisturbed state of the system,

$$x = -aw\sin\phi, \qquad y = aw\cos\phi, \qquad z = \mathrm{V}. \qquad (4)$$

We now proceed to find the corresponding expressions for these component velocities when the central line of the vortex filament is distorted out of its normal form. Let the fluid element at the point ψ undergo small displacements $\rho\cos r\psi$ along the radius drawn from the axis of the helix to the point ψ, $\sigma\cos r\psi$ parallel to the axis, and $a\beta = a\gamma\cos r\psi$ "circumferentially," *i.e.*, in a direction perpendicular to the radius to the point ψ and perpendicular to the axis

Consequently in (2) we must write $(a + \rho\cos r\psi)$ for a, and $(\psi + \gamma\cos r\psi)$ for ψ. Putting these values in (3) we have

$$\begin{aligned} x &= (a + \rho\cos r\psi)\cos(\phi + \gamma\cos r\psi) \\ &= (a + \rho\cos r\psi)(\cos\phi\cos.\overline{\gamma\cos r\psi} - \sin\phi\sin.\overline{\gamma\cos r\psi}) \\ &= (a + \rho\cos r\psi)(\cos\phi - \gamma\cos r\psi.\sin\phi), \end{aligned}$$

on expanding as far as first order terms in γ. Therefore, to the first order,

$$x = a\cos\phi + \rho\cos r\psi\cos\phi - a\gamma.\cos r\psi\sin\phi. \qquad (5)$$

Similarly

$$y = a\sin\phi + \rho\cos r\psi.\sin\phi + a\gamma.\cos r\psi.\cos\phi \qquad (6)$$

and

$$z = a\psi\tan\alpha + \mathrm{V}t + \sigma\cos r\psi. \qquad (7)$$

These equations give

$$\dot{x} = -aw \sin\phi + \rho \cos r\psi \cos\phi - \rho w \cos r\psi \,.\, \sin\phi$$
$$\qquad - a\,\dot{\gamma} \cos r\psi \sin\phi - aw\gamma \cos r\psi \,.\, \cos\phi, \qquad (8)$$

$$\dot{y} = aw \cos\phi + \rho \cos r\psi \sin\phi + \rho w \cos r\psi \cos\phi$$
$$\qquad + a\gamma \cos r\psi \cos\phi - aw\gamma \cos r\psi \,.\, \sin\phi, \qquad (9)$$

$$\dot{z} = \mathrm{V} + \sigma \cos r\psi. \qquad (10)$$

These equations give, with respect to fixed axes, the components of velocity of the fluid element at the point ψ. We resolve this velocity radially, circumferentially and axially. Denoting these components by ξ, η and $\dot{\zeta}$ we have

$$\dot{\xi} = \dot{x} \cos(\phi + \gamma \cos r\psi) + \dot{y} \sin(\phi + \gamma \cos r\psi),$$

which becomes, on substitution of the values of $\dot{x}$ and $\dot{y}$ from (8) and (9), and expansion of $\cos(\phi + \gamma \cos r\psi)$ and $\sin(\phi + \gamma \cos r\psi)$ as far as terms of the first order in γ,

$$\dot{\xi} = \rho \cos r\psi.$$

Similarly

$$\eta = aw + \rho w \cos r\psi + a\gamma \cos r\psi, \quad \zeta = \mathrm{V} + \sigma \cos r\psi \qquad (11)$$

The analysis of the motion of the helical vortex under the postulated form of disturbance shows that an exactly similar disturbance proportional to $\sin r\psi$ is induced on the vortex. In order, therefore, that our disturbance may be a normal mode, we must consider, in addition, a disturbance whose radial component is $\rho' \sin r\psi$, with corresponding circumferential and axial components. But this disturbance has the same wave form as the first, the only difference being in the phase; for putting $r\tau = r\psi - \frac{1}{2}\pi$, the disturbance proportional to $\sin r\psi$ is also proportional to $\cos r\tau$. Hence as a result of the complete disturbance

$$\rho \cos r\psi + \rho' \sin r\psi \,\ldots,$$
$$\rho \cos r\psi + \rho' \cos r\psi \,\ldots,$$

we obtain, instead of equations (11),

$$\left.\begin{aligned} \dot{\xi} &= \rho \cos r\psi + \rho' \sin r\psi \\ \eta &= aw + \rho w \cos r\psi + \rho' w \sin r\psi + a\dot{\gamma} \cos r\psi + a\dot{\gamma}' \sin r\psi \\ \dot{\zeta} &= \mathrm{V} + \sigma \cos r\psi + \sigma' \sin r\psi \end{aligned}\right\}. \qquad (12)$$

§ 3. We proceed in the first place to an analysis of the motion of the particle at the point ψ on the helix, under a wave disturbance of the form $\rho \cos r\psi$, $a\gamma$

$\cos r\psi$, $\sigma \cos r\psi$. Denote by θ a variable point on the helix and by R the distance between this point and ψ (x, y, z), taking (x', y', z') as the co-ordinates of θ. If κ is the strength of the vortex the component velocities u, v, w of the fluid element situated at (x, y, z) are given by

$$u = \frac{\kappa}{4\pi}\int\left\{\frac{dz'}{d\theta}(y-y') - \frac{dy'}{d\theta}(z-z')\right\}\frac{d\theta}{\mathrm{R}^3}, \qquad {}^*(13)$$

with corresponding formulæ for v and w, the integration extending over the complete length of the vortex. The value of R is given by the usual formula

$$\mathrm{R}^2 = (x-x')^2 + (y-y')^2 + (z-z')^2.$$

In connection with this formula and its subsequent use in this paper, a note of explanation is necessary and may conveniently be inserted here. We are supposing the cross section of the vortex filament to be circular in form, of radius ϵ which is small compared with a. Then without appreciable error we may take both the points (x, y, z) and (x', y', z') to lie on the central line of the vortex, unless the two points closely approach one another. In the latter case the radius of cross section ϵ is no longer negligible in comparison with R, and formula (13) has therefore to be modified; for if we consider (x, y, z) and (x', y', z') to lie on the central line of the vortex, R^{-3} will become infinite for $\theta = \psi$, and the expressions for u, v, w will become indeterminate.

The difficulty arises because we have wrongly assumed that (13) holds for all points ψ, and in particular, for points inside the vortex filament for which ψ is nearly equal to θ. In this case we have to consider a point ψ, not on the central line of the vortex, but lying just outside it.

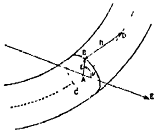

FIG. 1.

Fig. 1 illustrates a portion of the vortex filament, where A corresponds to the point ψ and D to θ, both on the central line. The circle BC is a normal cross section through A; B a point on this circle whose polar angle, measured from the principal normal AE, is ν.

If AD is large compared with ϵ, and (x, y, z), (x', y', z') are the co-ordinates of A and D respectively,

$$\mathrm{R}^2 = (x-x')^2 + (y-y')^2 + (z-z')^2.$$

When D approaches A, we consider not A but B, and obtain for R^2

$$(x-x')^2 + (y-y')^2 + (z-z')^2 + \epsilon^2 + f\{\nu, (x-x'), (y-y'), (z-z')\}\,.\,\epsilon,\dagger$$

---

* Lamb, 'Hydrodynamics,' 5th ed., § 149.

† See Nicholson, 'Phil. Mag.,' vol. 19, p. 77 (1910).

where ν is involved in f in the form of circular functions multiplied by terms linear in the small quantities $(x - x')$, $(y - y')$, $(z - z')$, so that $f \cdot \epsilon$ is small compared with ϵ^2. Clearly the part of R^2 involving ν arises from local disturbances which vary round the vortex filament, and are not to be taken account of in a consideration of the motion of the vortex as a whole. All points B lying on the circle AC share this motion; in addition they possess a local motion depending on the polar angle ν. We shall therefore obtain the motion of A by neglecting this latter part of the motion of B; that is, in the expression for R^2 we shall include the term ϵ^2 which is independent of ν, but neglect the terms linear in ϵ. Moreover, when A and D are remote from each other, ϵ^2 will be negligible in comparison with R^2, and its inclusion in the formula for R^{-3} over the whole of the range of integration will be immaterial. Similarly in the expressions $\frac{dz'}{d\theta}(y - y')$, etc., there enter terms linear in ϵ and involving ν. These again depend on the local motion and will be neglected in the investigation.

It can, indeed, be shown, by a complete analysis of the motion, that the terms neglected do arise solely through local disturbance, *i.e.*, a change of shape of the cross section of the vortex filament. It has, however, been shown by Thomson and others* that so long as the radius of cross section of a vortex filament is small compared with the radius of curvature of its central line the cross section will remain approximately circular under the self-influence of the whole vortex. It is, then, impossible that the local disturbances should bring about any appreciable changes in the motion of the vortex under the type of disturbance we propose to consider; they may therefore be neglected.

To justify this procedure in detail it would be necessary to give the laborious complete analysis of the motion, a great part of which has little bearing on the present problem and would finally be rejected. We shall obtain results sufficient for the solution required by neglecting, at the outset, the terms which arise only through local or "cross-sectional" disturbances.

Writing $\chi = \theta + wt$ we obtain for the co-ordinates of the point θ, after disturbance,

$$\left.\begin{aligned} x' &= a\cos\chi + \rho\cos\chi\cos r\theta - a\gamma\sin\chi\cos r\theta \\ y' &= a\sin\chi + \rho\sin\chi\cos r\theta + a\gamma\cos\chi\cos r\theta \\ z' &= a\theta\tan\alpha + Vt + \sigma\cos r\theta \end{aligned}\right\} . \qquad (14)$$

---

* J. J. Thomson, 'Motion of Vortex Rings'; Bassett, 'Hydrodynamics,' vol. 2, p. 88; Lamb, 'Hydrodynamics,' 5th ed., p. 213.

These forms are analogous to (5), (6) and (7), consequently

$$\left.\begin{aligned}(x - x') &= a(\cos\phi - \cos\chi) + \rho(\cos\phi\cos r\psi - \cos\chi\cos r\theta)\\ &\qquad + a\gamma(\sin\chi\cos r\theta - \sin\phi\cos r\psi)\\ (y - y') &= a(\sin\phi - \sin\chi) + \rho(\sin\phi\cos r\psi - \sin\chi\cos r\theta)\\ &\qquad + a\gamma(\cos\phi\cos r\psi - \cos\chi\cos r\theta)\\ (z - z') &= -a(\chi - \phi)\tan\alpha + \sigma(\cos r\psi - \cos r\theta)\end{aligned}\right\} . \quad (15)$$

Writing $\lambda = (\theta - \psi) = (\chi - \phi)$ we therefore have

$$\begin{aligned}R^2 = {} & 2a^2(1 - \cos\lambda) + a^2\lambda^2\tan^2\alpha + \epsilon^2\\ & + 2a\rho\{(1 - \cos\lambda)(1 + \cos r\lambda)\cos r\psi - \sin r\lambda\sin r\psi(1 - \cos\lambda)\}\\ & + 2a^2\gamma\{\sin\lambda(\cos r\lambda - 1)\cos r\psi - \sin\lambda\sin r\lambda\sin r\psi\}\\ & + 2a\sigma\tan\alpha\{\lambda(\cos r\lambda - 1)\cos r\psi - \lambda\sin r\lambda\sin r\psi\}. \qquad (16)\end{aligned}$$

The reason for the introduction of the term ϵ^2 has already been explained.

It is found convenient to write

$$a^2J = 2a^2(1 - \cos\lambda) + a^2\lambda^2\tan^2\alpha + \epsilon^2,$$

$$\left.\begin{aligned}M_1 &= (1-\cos\lambda)(1+\cos r\lambda), \quad M_2 = -\sin\lambda\sin r\lambda, \quad M_3 = -\lambda\sin r\lambda\\ N_1 &= -\sin r\lambda(1-\cos\lambda), \quad N_2 = \sin\lambda(\cos r\lambda-1), \quad N_3 = \lambda(\cos r\lambda-1)\end{aligned}\right\}, \quad (17)$$

so that R^2 may now be written in the form

$$\begin{aligned}R^2 = a^2J & + 2a\rho \,.\, \cos r\psi \,.\, M_1 + 2a\rho\sin r\psi \,.\, N_1\\ & + 2a^2\gamma\cos r\psi \,.\, N_2 + 2a^2\gamma\sin r\psi \,.\, M_2\\ & + 2a\sigma\tan\alpha \,.\, \cos r\psi \,.\, N_3 + 2a\sigma\tan\alpha\sin r\psi \,.\, M_3. \qquad (18)\end{aligned}$$

It has been mentioned that our presupposed disturbance proportional to $\cos r\psi$ initially induces a second disturbance proportional to $\sin r\psi$, *i.e.*, to $\cos r\tau$ where $r\tau = r\psi - \pi/2$. Since, further, $\sin r\tau = -\cos r\psi$ we may account for the effect of this second disturbance by adding to (18) terms $\rho'\sin r\psi$, $-\rho'\cos r\psi$ for every term that occurs of the form $\rho\cos r\psi$ or $\rho\sin r\psi$. Extending this to include the circumferential and axial disturbances we have

$$\begin{aligned}R^2 = a^2J & + 2a\rho\cos r\psi \,.\, M_1 + 2a\rho'\sin r\psi\, M_1\\ & + 2a\rho\sin r\psi \,.\, N_1 - 2a\rho'\cos r\psi \,.\, N_1\\ & + 2a^2\gamma\cos r\psi \,.\, N_2 + 2a^2\gamma'\sin r\psi \,.\, N_2\\ & + 2a^2\gamma\sin r\psi \,.\, M_2 - 2a^2\gamma'\cos r\psi\, M_2\\ & + 2a\sigma\tan\alpha\cos r\psi \,.\, N_3 + 2a\sigma'\tan\alpha \,.\, \sin r\psi \,.\, N_3\\ & + 2a\sigma\tan\alpha\sin r\psi \,.\, M_3 - 2a\sigma'\tan\alpha \,.\, \cos r\psi \,.\, M_3. \qquad (19)\end{aligned}$$

This is conveniently written as

$$a^2\mathrm{J} + \mathrm{K},$$

where K includes all the first order terms in (19). Then

$$\mathrm{R}^{-3} = (a^2\mathrm{J} + \mathrm{K})^{-3/2} = 1/a^3\,\mathrm{J}^{-3/2} - 3/a^5\,.\,\mathrm{K}\,.\,\mathrm{J}^{-5/2}, \tag{19A}$$

on expansion as far as the first order terms. This is the form in which R^{-3} is required in formula (13). In the integration the variable is changed from θ to λ, since the velocity components can be more simply expressed in terms of the latter. Since $\lambda = \theta - \psi$, $d\theta = d\lambda$, and, the limits of θ in the integration being $\pm\infty$, so also are the limits in the integration with respect to λ. Let

$$\left.\begin{aligned} \mathrm{V}_x &= \frac{dy'}{d\theta}(z - z') - \frac{dz'}{d\theta}(y - y') \\ \mathrm{V}_y &= \frac{dz'}{d\theta}(x - x') - \frac{dx'}{d\theta}(z - z') \\ \mathrm{V}_z &= \frac{dx'}{d\theta}(y - y') - \frac{dy'}{d\theta}(x - x') \end{aligned}\right\}. \tag{20}$$

Taking account only of the cosine wave disturbance, we have, from (14),

$$\left.\begin{aligned} \frac{dx'}{d\theta} &= -a\sin\chi - \rho\sin\chi\cos r\theta - r\rho\cos\chi\sin r\theta \\ &\qquad - a\gamma\cos\chi\cos r\theta + r\,.\,a\,.\,\gamma\,.\,\sin\chi\,.\,\sin r\theta \\ \frac{d\theta}{dy'} &= a\cos\chi + \rho\cos\chi\cos r\theta - r\rho\sin\chi\sin r\theta \\ &\qquad - a\gamma\,.\,\sin\chi\cos r\theta - ra\gamma\cos\chi\sin r\theta \\ \frac{dz'}{d\theta} &= a\tan\alpha - r\sigma\sin r\theta \end{aligned}\right\}. \tag{21}$$

We then find, using (15), (20), and (21), that

$$\begin{aligned} \mathrm{V}_z = {} & a^2\tan\alpha\,(-\sin\phi + \sin\chi - \lambda\cos\chi) \\ & + a\rho\tan\alpha\,(\sin\chi\cos r\theta - \sin\phi\cos r\psi \\ & \qquad + \lambda r\sin\chi\sin r\theta - \lambda\cos\chi\cos r\theta), \\ & + a^2\gamma\tan\alpha\,(\cos\chi\cos r\theta - \cos\phi\cos r\psi \\ & \qquad + \lambda\,.\,r\,.\,\cos\chi\sin r\theta + \lambda\sin\chi\cos r\theta) \\ & + a\sigma\,(\cos\chi\cos r\psi - \cos\chi\cos r\theta \\ & \qquad + r\,.\,\sin r\theta\sin\phi - r\sin r\theta\,.\,\sin\chi), \end{aligned} \tag{22}$$

$$\begin{aligned} V_y = {} & a^2 \tan\alpha\,(\cos\phi - \cos\chi - \lambda\sin\chi) \\ & + a\rho\tan\alpha\,(\cos\phi\cos r\psi - \cos\chi\cos r\theta \\ & \qquad - \lambda\sin\chi\cos r\theta - \lambda\,.\,r\,.\,\cos\chi\sin r\theta) \\ & + a^2\gamma\tan\alpha\,(\sin\chi\cos r\theta - \sin\phi\cos r\psi \\ & \qquad - \lambda\cos\chi\cos r\theta + \lambda\,.\,r\,.\,\sin\chi\sin r\theta) \\ & + a\sigma\,(\sin\chi\cos r\psi - \sin\chi\cos r\theta \\ & \qquad - r\sin r\theta\,.\,\cos\phi + r\sin r\theta\,.\,\cos\chi). \end{aligned} \tag{23}$$

The component velocities u and v of the fluid at the point ψ will then be given by

$$u = \frac{\kappa}{4\pi}\int_{-\infty}^{\infty} V_x\,.\,R^{-3}\,.\,d\lambda; \quad v = \frac{\kappa}{4\pi}\int_{-\infty}^{\infty} V_y.\ R^{-3}\,d\lambda.$$

The radial and circumferential components of this velocity, $\dot{\xi}$ and $\dot{\eta}$, are given by

$$\left.\begin{aligned} \dot{\xi} &= u\cos(\phi + \gamma\cos r\psi) + v\sin(\phi + \gamma\cos r\psi) \\ \dot{\eta} &= v\cos(\phi + \gamma\cos r\psi) - u\sin(\phi + \gamma\cos r\psi) \end{aligned}\right\}. \tag{24}$$

If then we put

$$\left.\begin{aligned} V_r &= V_x\cos(\phi + \gamma\cos r\psi) + V_y\sin(\phi + \gamma\cos r\psi) \\ V_\theta &= V_y\cos(\phi + \gamma\cos r\psi) - V_x\sin(\phi + \gamma\cos r\psi) \end{aligned}\right\}, \tag{25}$$

we shall have

$$\dot{\xi} = \frac{\kappa}{4\pi}\int_{-\infty}^{\infty} V_r\,.\,R^{-3}\,.\,d\lambda, \qquad \eta = \frac{\kappa}{4\pi}\int_{-\infty}^{\infty} V_\theta\,.\,R^{-3}\ \ d\lambda. \tag{26}$$

In the integration the first order terms in V_r and V_θ have to be multiplied by $1/a^3\ J^{-3/2}$ which is an even function of λ. Hence all terms of odd degree in λ in the first order parts of V_r and V_θ will vanish on integration. We may neglect such terms at the outset, and denote the remaining parts of V_r and V_θ by V_r' and V_θ' respectively. It is then found that

$$\begin{aligned} V_r' = {} & a^2\tan\alpha\,(\sin\lambda - \lambda\cos\lambda) \\ & + a\rho\tan\alpha\,(-\sin\lambda\,.\,\sin r\lambda\,.\,\sin r\psi + \lambda\,.\,r\,.\,\sin\lambda\cos r\lambda\sin r\psi \\ & \qquad + \lambda\sin r\lambda\,.\,\cos\lambda\sin r\psi) \\ & + a^2\gamma\tan\alpha\,(-\cos r\psi + \cos\lambda\cos r\lambda\cos r\psi \\ & \qquad + \lambda\,.\,r\,.\,\cos\lambda\,.\,\sin r\chi\cos r\psi + \lambda\sin\lambda\cos r\lambda\cos r\psi) \\ & + a\sigma\,(-r\sin\lambda\sin r\lambda\cos r\psi + \cos\lambda\cos r\psi \\ & \qquad - \cos\lambda\,.\,\cos r\lambda\cos r\psi). \end{aligned}$$

Write

$$\begin{aligned}
\mathrm{R}_a &= \sin\lambda - \lambda\cos\lambda, \\
\mathrm{R}_1 &= \tfrac{1}{2}\cos(r+1)\lambda - \tfrac{1}{2}\cos(r-1)\lambda \\
&\qquad + \tfrac{1}{2}\lambda(r+1)\sin(r+1)\lambda - \tfrac{1}{2}\lambda(r-1)\sin(r-1)\lambda, \\
\mathrm{R}_2 &= -\cos\lambda - \lambda\sin\lambda + \tfrac{1}{2}\cos(r+1)\lambda + \tfrac{1}{2}\cos(r-1)\lambda \\
&\qquad + \tfrac{1}{2}\lambda(r+1)\sin(r+1)\lambda + \tfrac{1}{2}\lambda(r-1)\sin(r-1)\lambda, \\
\mathrm{R}_3 &= \cos\lambda + \tfrac{1}{2}(r-1)\cos(r+1)\lambda - \tfrac{1}{2}(r+1)\cos(r-1)\lambda. \qquad (27)
\end{aligned}$$

Inserting the terms in V_r' due to the sine wave disturbance, we finally obtain

$$\begin{aligned}
\mathrm{V}_r' &= \mathrm{R}_a \,.\, a^2\tan\alpha + a\rho\tan\alpha \,.\, \sin r\psi \,.\, \mathrm{R}_1 - a\rho'\tan\alpha\cos r\psi \,.\, \mathrm{R}_1 \\
&\quad + a^2\gamma\tan\alpha \,.\, \cos r\psi \,.\, \mathrm{R}_2 + a^2\gamma'\tan\alpha\sin r\psi \,.\, \mathrm{R}_2 \\
&\quad + a\sigma \,.\, \cos r\psi \,.\, \mathrm{R}_3 + a\sigma'\sin r\psi \,.\, \mathrm{R}_3. \qquad (28)
\end{aligned}$$

Proceeding in a similar way we find

$$\begin{aligned}
\mathrm{V}_\theta' &= \Theta_a \,.\, a^2\tan\alpha + a\rho\tan\alpha \,.\, \cos r\psi \,.\, \Theta_1 + a\rho'\tan\alpha \,.\, \sin r\psi \,.\, \Theta_1 \\
&\quad + a^2\gamma \,.\, \tan\alpha\sin r\psi \,.\, \Theta_2 - a^2\gamma'\tan\alpha\cos r\psi \,.\, \Theta_2 \\
&\quad + a\sigma\sin r\psi \,.\, \Theta_3 - a\sigma'\cos r\psi \,.\, \Theta_3, \qquad (29)
\end{aligned}$$

where

$$\left.\begin{aligned}
&\Theta_a = 1 - \cos\lambda - \lambda\sin\lambda, \qquad \Theta_1 = \Theta_a - \mathrm{R}_2, \qquad \Theta_2 = \mathrm{R}_1, \\
&\Theta_3 = -r\cos r\lambda + \tfrac{1}{2}(r+1)\cos(r-1)\lambda + \tfrac{1}{2}(r-1)\cos(r+1)\lambda
\end{aligned}\right\}. \quad (30)$$

Further,

$$\begin{aligned}
\mathrm{V}_z' &= a^2 Z_a + a\rho\cos r\psi \,.\, Z_1 + a\rho'\sin r\psi \,.\, Z_1 \\
&\qquad + a^2\gamma\sin r\psi \,.\, Z_2 - a^2\gamma'\cos r\psi \,.\, Z_2, \qquad (31)
\end{aligned}$$

where

$$\left.\begin{aligned}
\mathrm{Z}_a &= (1 - \cos\lambda), \\
\mathrm{Z}_1 &= 2\cos r\lambda - \cos\lambda - \tfrac{1}{2}(r+1)\cos(r+1)\lambda + \tfrac{1}{2}(r-1)\cos(r-1)\lambda, \\
\mathrm{Z}_2 &= -r\cos r\lambda + \tfrac{1}{2}(r+1)\cos(r+1)\lambda + \tfrac{1}{2}(r-1)\cos(r-1)\lambda
\end{aligned}\right\} \quad (32)$$

§ 4. To find the radial and circumferential velocities at the point ψ, we make use of the relations (26) and (19A). Then

$$\dot{\xi} = \frac{\kappa}{4\pi a^3}\int_{-\infty}^{\infty} \mathrm{V}_r' \{\mathrm{J}^{-3/2} - 3/a^2\mathrm{J}^{-5/2} \,.\, \mathrm{K}\}\, d\lambda.$$

Now K is given by equation (19). Observing that J, M_1, M_2, M_3 are even functions of λ while N_1, N_2, N_3 are odd functions, we obtain

$$\left.\begin{aligned}\dot{\xi} = {} & 1/a^2 \,.\, \rho \sin r\psi \,.\, \tan\alpha\,\{R_1 J^{-3/2} - 3R_a \,.\, N_1 J^{-5/2}\} \\ & + 1/a^2 \,.\, \rho' \cos r\psi \tan\alpha\,\{- R_1 J^{-3/2} + 3R_a N_1 J^{-5/2}\} \\ & + 1/a^2 \,.\, a\gamma \cos r\psi \tan\alpha\,\{R_2 J^{-3/2} - 3R_a N_2 J\}^{-5/2} \\ & + 1/a^2 \,.\, a\gamma' \sin r\psi \,.\, \tan\alpha\,\{R_2 \,.\, J^{-3/2} - 3R_a N_2 J^{-5/2}\} \\ & + 1/a^2 \,.\, \sigma \cos r\psi\,\{R_3 J^{-3/2} - 3\tan^2\alpha R_a N_3 J^{-5/2}\} \\ & + 1/a^2 \,.\, \sigma' \sin r\psi\,\{R_3 J^{-3/2} - 3\tan^2\alpha \,.\, R_a N_3 J^{-5/2}\} \\ = {} & 1/a^2 \,.\, \tan\alpha\,\{R_1 J^{-3/2} - 3R_a N_1 J^{-5/2}\}\,(\rho \sin r\psi - \rho' \cos r\psi) \\ & + 1/a^2 \,.\, \tan\alpha\,\{R_2 J^{-3/2} - 3R_a N_2 J^{-5/2}\}\,(a\gamma \cos r\psi + a\gamma' \sin r\psi) \\ & + 1/a^2 \,.\, \{R_3 \,.\, J^{-3/2} - 3\tan^2\alpha \,.\, R_a \;\; N_3\} J^{-5/2}\}\,(\sigma \cos r\psi \\ & \qquad\qquad\qquad\qquad\qquad\qquad - \sigma' \sin r\psi)\end{aligned}\right\} . \quad (33)$$

Similarly

$$\begin{aligned}\dot{\eta} = {} & 1/a \,.\, \Theta_a \tan\alpha J^{-3/2} \\ & + 1/a^2 \,.\, \tan\alpha\,\{(\Theta_a - R_2)\, J^{-3/2} - 3\Theta_a M_1 J^{-5/2}\}\,(\rho \cos r\psi + \rho' \sin r\psi) \\ & + 1/a^2 \,.\, \tan\alpha\,\{R_1 J^{-3/2} - 3\Theta_a M_2 J^{-5/2}\}\,(a\gamma \sin r\psi - a\gamma' \cos r\psi) \\ & + 1/a^2 \,.\, \{\Theta_3 J^{-3/2} - 3\tan^2\alpha\, \Theta_a M_3 J^{-5/2}\}\,(\sigma \sin r\psi - \sigma' \cos r\psi),\end{aligned} \qquad (34)$$

and

$$\begin{aligned}\dot{\zeta} = {} & 1/a \,.\, Z_a J^{-3/2} \\ & + 1/a^2 \,.\, \{Z_1 J^{-3/2} - 3Z_a M_1 J^{-5/2}\}\,(\rho \cos r\psi + \rho' \sin r\psi) \\ & + 1/a^2 \,.\, \{Z_2 J^{-3/2} - 3Z_a M_2 J^{-5/2}\}\,(a\gamma \sin r\psi - a\gamma' \cos r\psi) \\ & + 1/a^2 \,.\, \{- 3\tan\alpha \,.\, Z_a M_3 J^{-5/2}\}\,(\sigma \sin r\psi - \sigma' \cos r\psi).\end{aligned} \qquad (35)$$

In these formulæ the factor $\kappa/4\pi$ and the sign of integration have been omitted for convenience in writing. Their presence should, however, be remembered, wherever they are omitted in the remainder of this paper.

§ 5. *The Vibrational Equations.*—Comparing the coefficients of $\sin r\psi$, $\cos r\psi$ in (33), (34) and (35) with the three equations (12) we obtain the equations of motion of the system. The angular velocity ω and the velocity of advance V along the axis of the helical vortex are also determined, and we have

$$\begin{aligned}\omega & = \frac{\kappa}{4\pi a^3}\int_{-\infty}^{\infty} \tan\alpha \,.\, \Theta_a J^{-3/2} \,.\, d\lambda \\ & = \frac{\kappa}{2\pi a^3} \tan\alpha \int_0^{\infty} \frac{1 - \cos\lambda - \lambda \sin\lambda}{\{2\,(1 - \cos\lambda) + \lambda^2 \tan^2\alpha + \epsilon^2/a^2\}^{3/2}}\, d\lambda,\end{aligned} \qquad (36)$$

and

$$V = \frac{\kappa}{2\pi a}\int_0^\infty \frac{1-\cos\lambda}{\{2(1-\cos\lambda)+\lambda^2\tan^2\alpha+\varepsilon^2/a^2\}^{3/2}}\,d\lambda. \tag{37}$$

Substitute the value of ω given by (36) in the second of equations (12). Then equating coefficients in the respective equations we obtain the set of six linear differential equations, the equations of motion of the system. These are of the form

$$\left.\begin{aligned} \rho &= \mathrm{A}\rho' + \mathrm{B}a\gamma + \mathrm{C}\sigma, & \rho' &= -\mathrm{A}\rho + \mathrm{B}a\gamma' + \mathrm{C}\sigma' \\ a\dot{\gamma} &= \mathrm{E}\rho + \mathrm{F}a\gamma' + \mathrm{G}\sigma', & a\dot{\gamma}' &= \mathrm{E}\rho' - \mathrm{F}a\gamma - \mathrm{G}\sigma \\ \dot{\sigma} &= \mathrm{H}\rho + \mathrm{J}a\gamma' + \mathrm{K}\sigma', & \sigma' &= \mathrm{H}\rho' - \mathrm{J}a\gamma - \mathrm{K}\sigma \end{aligned}\right\}, \tag{38}$$

where

$$\left.\begin{aligned} \mathrm{A} &= \frac{\kappa\tan\alpha}{2\pi a^2}\left\{-\int_0^\infty \mathrm{R}_1\mathrm{J}^{-3/2}\,d\lambda + 3\int_0^\infty \mathrm{R}_a\mathrm{N}_1\mathrm{J}^{-5/2}\,d\lambda\right\} \\ \mathrm{B} &= \frac{\kappa\tan\alpha}{2\pi a^2}\left\{\int_0^\infty \mathrm{R}_2\mathrm{J}^{-3/2}\,d\lambda - 3\int_0^\infty \mathrm{R}_0\mathrm{N}_2\mathrm{J}^{-5/2}\,d\lambda\right\} \\ \mathrm{C} &= \frac{\kappa}{2\pi a^2}\left\{\int_0^\infty \mathrm{R}_3\mathrm{J}^{-3/2}\,d\lambda - 3\int_0^\infty \mathrm{R}_a\mathrm{N}_3\tan^2\alpha\ \ \mathrm{J}^{-5/2}\,d\lambda\right\} \\ \mathrm{E} &= -\frac{\kappa\tan\alpha}{2\pi a^2}\left\{\int_0^\infty \mathrm{R}_2\mathrm{J}^{-3/2}\,d\lambda + 3\int_0^\infty \Theta_a\mathrm{M}_1\mathrm{J}^{-5/2}\,d\lambda\right\} \\ \mathrm{F} &= \frac{\kappa\tan\alpha}{2\pi a^2}\left\{-\int_0^\infty \mathrm{R}_1\mathrm{J}^{-3/2}\,d\lambda + 3\int_0^\infty \Theta_a\mathrm{M}_2\mathrm{J}^{-5/2}\,d\lambda\right\} \\ \mathrm{G} &= \frac{\kappa}{2\pi a^2}\left\{-\int_0^\infty \Theta_3\mathrm{J}^{-3/2}\,d\lambda + 3\int_0^\infty \tan^2\alpha\,\Theta_a\mathrm{M}_3\mathrm{J}^{-5/2}\,d\lambda\right\} \\ \mathrm{H} &= \frac{\kappa}{2\pi a^2}\left\{\int_0^\infty \mathrm{Z}_1\mathrm{J}^{-3/2}\,d\lambda - 3\int_0^\infty \mathrm{Z}_a\mathrm{M}_1\mathrm{J}^{-3/2}\,d\lambda\right\} \\ \mathrm{J} &= \frac{\kappa}{2\pi a^2}\left\{-\int_0^\infty \mathrm{Z}_2\mathrm{J}^{-3/2}\,d\lambda + 3\int_0^\infty \mathrm{Z}_0\mathrm{M}_2\mathrm{J}^{-5/2}\,d\lambda\right\} \\ \mathrm{K} &= \frac{\kappa\tan\alpha}{2\pi a^2}\left\{3\int_0^\infty \mathrm{Z}_a\mathrm{M}_3\mathrm{J}^{-5/2}\,d\lambda\right\} \end{aligned}\right\}. \tag{39}$$

The six equations of motion (38) can be reduced to three equations if we put

$$\mathrm{X} = \rho + i\rho', \qquad \mathrm{Y} = a\gamma + ia\gamma', \qquad \mathrm{Z} = \sigma + i\sigma'. \tag{40}$$

The three resultant equations are

$$\left.\begin{aligned} \dot{X} &= -iAX + BY + CZ \\ Y &= EX - iFY - iGZ \\ \dot{Z} &= HX - iJY - iKZ \end{aligned}\right\}, \tag{40}$$

where the coefficients A ... K are all real and defined by (39). If D represents the operator d/dt, and ϕ any one of the variables X, Y, Z, the solution of (40) is determined from

$$\begin{vmatrix} D + iA & -B & -C \\ -E & D + iF & iG \\ -H & iJ & G + iK \end{vmatrix} \phi = 0,$$

which reduces to

$$\{D^3 + iP \, . \, D^2 + QD + iR\} \phi = 0, \tag{41}$$

where

$$\left.\begin{aligned} P = A + F + K, \qquad Q &= JG - FA - KA - KF - EB - HC \\ R &= JGA - FAK - EBK + ECJ + BHG - HCF \end{aligned}\right\}. \tag{41A}$$

Regarding (41) as an algebraic equation in D, with roots μ_1, μ_2, μ_3, the solution is

$$\phi = \Delta_1 e^{\mu_1 t} + \Delta_2 e^{\mu_2 t} + \Delta_3 e^{\mu_3 t}, \tag{42}$$

where Δ_1, Δ_2, Δ_3 are constants, in general complex.

We can now determine the condition for stability or instability of the vortex system. Put x for D in (41) and we have

$$x^3 + iPx^2 + Qx + iR = 0 \tag{43}$$

or

$$z^3 + Pz^2 - Qz - R = 0, \quad \text{where } x = iz. \tag{44}$$

Equation (44) is a cubic in z, with real coefficients. Its roots may therefore be

(*a*) all real;

(*b*) one real, and two of the form $(a \pm ib)$.

The corresponding forms of the roots of (43) are

(*a*) all purely imaginary;

(*b*) one purely imaginary, and two of the form $\pm b + ia$.

In the former case, μ_1, μ_2, μ_3 are purely imaginary; in the latter case, the real part of one of the roots must be positive, in which event the system will be unstable.

The necessary and sufficient condition for stability in the general case is, therefore, that the roots of the cubic equation

$$z^3 + Pz^2 - Qz - R = 0 \tag{45}$$

shall be all real.

§ 6. *The Conditions for Stability.*—To investigate the stability or instability of the helical vortex under the general type of disturbance is a matter involving considerable labour, owing to the complicated set of equations of motions and the nature of the definite integrals which occur as coefficients in these equations. A method has been used which will allow of the investigation being made for any particular pitch of helix. The details of the method and the results obtained in five different cases are given later in this paper.

The special case of the rectilinear vortex, which is the limiting form of the helix as $\tan\alpha$ increases indefinitely, can be solved immediately. It has been shown by Sir. W. Thomson* that the rectilinear vortex whose cross section is a circle is stable to "columnar disturbances," *i.e.*, disturbances affecting the shape of the cross section. The present investigation relates to a rectilinear vortex column, when the disturbance consists of a displacement of its central line.

In the equations of motion, J is of the order $\tan^2\alpha$ If we neglect all terms of a higher order than $1/\tan^2\alpha$, and put

$$p = \frac{\kappa}{2\pi a^2}\int_0^\infty \tan\alpha \quad R_1 J^{-3/2} \,.\, d\lambda, \qquad q = \frac{\kappa}{2\pi a^2}\int_0^\infty \tan\alpha \; R_2 J^{-3/2}\, d\lambda,$$

the equations of motion reduce to

$$X = ipX + qY, \quad Y = -qX + ipY, \tag{46}$$

where

$$X = \rho + i\rho', \quad Y = a\gamma + ia\gamma'$$

The terms involving σ do not appear in these equations. Clearly since this disturbance is parallel to the axis, it would have no significance in the case of a rectilinear vortex.

The determinant of (46) is

$$\begin{vmatrix} D - ip & -q \\ q & D - ip \end{vmatrix} \phi = 0.$$

Therefore

$$(D^2 - 2ipD + q^2 - p^2)\,\phi = 0. \tag{47}$$

The auxiliary equation clearly has both its roots imaginary and we conclude that the rectilinear vortex is stable to disturbances involving a displacement of its central line.

---

* 'Phil. Mag.,' vol. 10, p. 155 (1880).

§ 7. *Evaluation of the Functions.*—We have seen that for any form of disturbance the character of the subsequent motion depends upon the nature of the roots of the cubic equation (44). These roots are themselves dependent upon the coefficients P, Q, R, which quantities are derived from the definite integral expressions given in (39). Our problem, then, is to evaluate these integrals in any particular case, and from them to form the cubic equation (44), which provides the criterion for stability or instability. It is evident that the definite integrals in (39) cannot be evaluated by ordinary methods, neither are any tables of these functions known to be in existence. The method adopted in the present investigation was one of mechanical quadrature, by means of a planimeter. The hitherto exact character of the work is now lost, but it may be assumed that the error of the final results is no greater than about 2 per cent. This error does not affect the final conclusions to be drawn regarding the stability of the vortex system.

The fundamental mode of oscillation is that characterised by $r = 1$. The method now adopted is, however, perfectly general in its application, and may be used taking any value of r.

With $r = 1$, the functions R_1, R_2, Θ_1, etc., given in (27)–(32) take specially simple values. They may be expressed in terms of ten of their number, which we have denoted by $Q_1 \ldots Q_{10}$, thus :—

$$R_1 = Q_1, \quad R_2 = Q_2, \quad R_3 = -Q_5, \quad \Theta_1 = -Q_1, \quad \Theta_2 = Q_2, \quad \Theta_3 = Q_5,$$
$$Z_1 = Q_{10}, \quad Z_2 = -Q_{10}, \quad R_a = Q_3, \quad \Theta_a = Q_4, \quad Z_a = Q_5,$$

and from (17)

$$M_1 = Q_6, \quad M_2 = -Q_6, \quad M_3 = Q_7, \quad N_1 = Q_8, \quad N_2 = -Q_8, \quad N_3 = Q_9, \tag{48}$$

where

$$\left.\begin{aligned} &Q_1 = \lambda \sin 2\lambda - \sin^2 \lambda, \quad Q_2 = Q_4 + Q_1, \quad Q_3 = \sin \lambda - \lambda \cos \lambda, \\ &Q_4 = Q_5 + Q_7, \quad Q_5 = 1 - \cos \lambda, \quad Q_6 = \sin^2 \lambda, \quad Q_7 = -\lambda \sin \lambda \\ &Q_8 = -\sin \lambda\,(1 - \cos \lambda), \quad Q_9 = -\lambda\,(1 - \cos \lambda), \quad Q_{10} = \cos \lambda - \cos 2\lambda \end{aligned}\right\}. \tag{49}$$

Our aim is to obtain the values of the quantities A, B, . . . K in (39). Each of these quantities consists of two parts, one involving $J^{-3/2}$ and the other involving $J^{-5/2}$. Let us indicate these parts by suffixes 1, 2 respectively, *e g.*, $A = A_1 + A_2$. Further, let us write

$$\left.\begin{array}{llll} P_1 = Q_1J^{-3/2}, & P_2 = Q_3Q_8J^{-3/2}, & P_3 = Q_2\,J^{-3/2}, & P_4 = Q_5J^{-3/2}, \\ P_5 = Q_3Q_9J^{-5/2}, & P_6 = Q_4Q_6J^{-5/2}, & P_7 = Q_4Q_7J^{-5/2}, & \\ P_8 = Q_5Q_6J^{-5/2}, & P_9 = Q_5Q_7J^{-5/2}, & P_{10} = Q_{10}J^{5/2} & \end{array}\right\}. \quad (50)$$

Putting also

$$\left.\begin{array}{ll} S_1 = -\tan\alpha\int_0^\infty P_1\,d\lambda, & S_2 = 3\tan\alpha\int_0^\infty P_2\,d\lambda, \\ S_3 = \tan\alpha\int_0^\infty P_3\,d\lambda, & S_4 = -\int_0^\infty P_4\,d\lambda, \\ S_5 = -3\tan^2\alpha\int_0^\infty P_5\,d\lambda, & S_6 = -3\tan\alpha\int_0^\infty P_6\,d\lambda, \\ S_7 = 3\tan^2\alpha\int_0^\infty P_7\,d\lambda, & S_8 = -3\int_0^\infty P_8\,d\lambda, \\ S_9 = 3\tan\alpha\int_0^\infty P_9\,d\lambda, & S_{10} = \int_0^\infty P_{10}\,d\lambda, \end{array}\right\} \quad (51)$$

we have

$$\left.\begin{array}{llllll} A_1 = S_1, & B_1 = S_3, & C_1 = S_4, & E_1 = -S_3 & F_1 = S_1, & G_1 = S_4, \\ H_1 = S_{10}, & J_1 = S_{10}, & K_1 = 0. & A_2 = S_2, & B_2 = S_2, & C_2 = S_5, \\ E_2 = S_6, & F_2 = S_6, & G_2 = S_7, & H_2 = S_8, & J_2 = S_8, & K_2 = S_9. \end{array}\right\} \quad (52)$$

Then clearly

$$\left.\begin{array}{lll} A = S_1 + S_2, & B = S_3 + S_2, & C = S_4 + S_5, \\ E = S_6 - S_3, & F = S_1 + S_6, & G = S_4 + S_7, \\ H = S_{10} + S_8, & J = S_{10} + S_8, & K = S_9. \end{array}\right\}. \quad (52\text{A})$$

The process of evaluating A, B, ... K, now consists essentially in evaluating the definite integrals in (51) where $P_1 \ldots P_{10}$ are given by (50) and (49). The integrations in (51) are conveniently divided into two parts. The first consists of approximating to the value of the integral over the range $0 < \lambda < \pi/6$; the second gives the value of the integral from $\pi/6$ upwards. Denote the two parts by S_r' and S_r'' ($r = 1 \ldots 10$). Then

$$S_r' = \int_0^{\pi/6} P_r\,d\lambda, \qquad S_r'' = \int_{\pi/6}^\infty P_r\,d\lambda,$$

and $S_r = (S_r' + S_r'')\, f_r$, where f_r is the factor multiplying the integral in question in (51).

Consider first the evaluation of S_r''. This is carried out by plotting the function P_r against λ, and integrating by means of a planimeter. Clearly P_r is a convergent function · the process of quadrature is therefore terminated at any convenient value of λ for which P_r has become of smaller magnitude than the error we are allowing.

For the purpose of approximating to the integral S_r' we must take a definite value of ϵ/a. This is conveniently taken to be 1/10 as in a former paper.* The upper limit for λ is $\pi/6$, so that we may expand the cosine in

$$J = 2\,(1 - \cos\lambda) + \lambda^2 \tan^2\alpha + \epsilon^2/a^2$$

and obtain

$$J = \sec^2\alpha\,(\lambda^2 + m^2), \tag{53}$$

where $m = \epsilon/a \sec\alpha = \frac{1}{10}\cos\alpha$. The maximum error involved is given by $\left(\frac{\lambda^4}{24}\right)_{\lambda = \pi/6}$, which is within our limits of accuracy.

The Q-functions can also be expanded in powers of λ; these we expand as far as λ^6.

It is found that the functions $S_1', \ldots S_{10}'$ depend upon the five integrals given below:

$$\left.\begin{array}{c} I_1 = \displaystyle\int_0^{\pi/6} \frac{\lambda^2}{\sec^3\alpha\,(\lambda^2 + m^2)^{3/2}}\, d\lambda, \qquad I_2 = \int_0^{\pi/6} \frac{\lambda^4\, d\lambda}{\sec^3\alpha\,(\lambda^2 + m^2)^{3/2}}\, d\lambda, \\ I_3 = \displaystyle\int_0^{\pi/6} \frac{\lambda^6\, d\lambda}{\sec^3\alpha\,(\lambda^2 + m^2)^{3/2}}\, d\lambda, \\ I_5 = \displaystyle\int_0^{\pi/6} \frac{\lambda^4 \,.\, d\lambda}{\sec^5\alpha\,(\lambda^2 + m^2)^{5/2}}\, d\lambda, \qquad I_6 = \int_0^{\pi/6} \frac{\lambda^6 \,.\, d\lambda}{\sec^5\alpha\,(\lambda^2 + m^2)^{5/2}}\, d\lambda \end{array}\right\} . \tag{54}$$

The process is best illustrated by an example; we consider the evaluation of S_1':

$$S_1' = \int_0^{\pi/6} Q_1 J^{3/2}\, d\lambda = \int_0^{\pi/6} (\lambda \sin 2\lambda - \sin^2\lambda)\, J^{-3/2}\, d\lambda,$$

which becomes, on expansion,

$$\frac{1}{\sec^3\alpha} \int_0^{\pi/6} (\lambda^2 - \lambda^4 + \tfrac{2}{9}\lambda^6)\,(\lambda^2 + m^2)^{-3/2}\, d\lambda = I_1 - I_2 + \tfrac{2}{9} I_3. \tag{55}$$

---

* Levy and Forsdyke, 'Roy. Soc. Proc.,' A, vol. 116, p. 352 (1927).

The integrals $I_1 \ldots I_6$ are easily evaluable, giving

$$\left.\begin{aligned} I_1 &= \cos^3\alpha\,\{z - \tanh z\} \\ I_2 &= m^2 \cos^3\alpha\,\{\tfrac{1}{4}\sinh 2z - \tfrac{1}{2}z + \tanh z\}, \\ I_3 &= m^4 \cos^3\alpha\,\{\tfrac{1}{32}\sinh 4z - \tfrac{1}{2}\sinh 2x + \tfrac{15}{8}z - \tanh z\} \\ I_5 &= \cos^5\alpha\,\{z - \tanh z - \tfrac{1}{3}\tanh^3 z\} \\ I_6 &= m^2\cos^5\alpha\,\{\tfrac{1}{4}\sinh 2z - \tfrac{5}{2}z + 2\tanh z + \tfrac{1}{3}\tanh^3 z\} \end{aligned}\right\}, \quad (56)$$

where $z = \sinh^{-1}.\dfrac{\pi}{6m}$ and $m = \dfrac{\sec\alpha}{10}$.

Proceeding as in (55) we obtain

$$\left.\begin{aligned} &S_1' = I_1 - I_2 + \tfrac{3}{5}I_3, \quad S_2' = \tfrac{1}{6}I_6, \quad S_3' = \tfrac{1}{2}I_1 - \tfrac{7}{8}I_2 + \tfrac{11}{24}I_3, \\ &S_4' = \tfrac{1}{2}I_1 - \tfrac{1}{24}I_2 + \tfrac{1}{720}I_3, \quad S_5' = -\tfrac{1}{6}I_6, \quad S_6' = -\tfrac{1}{2}I_5 = \tfrac{7}{24}I_6, \\ &S_7' = \tfrac{1}{2}I_5 - \tfrac{5}{24}I_6, \quad S_8' = \tfrac{1}{2}, I_5 - \tfrac{5}{24}I_6, \quad S_9' = -\tfrac{1}{2}I_5 + \tfrac{1}{8}I_6, \\ &S_{10}' = \tfrac{3}{5}I_1 - \tfrac{3}{8}I_2 + \tfrac{7}{80}I_3. \end{aligned}\right\}. \quad (57)$$

For any given value of $\tan\alpha$, it has been shown how to obtain numerical values of S_r', S_r'' and therefore of $S_r = f_r(S_r' + S_r'')$ These lead at once to A, B, ... K by (52) and (52A), and the cubic equation (41) can then be found by using equations (41A). The solution of our problem for the particular disturbance characterised by $r = 1$ is then complete.

Apart from the case of the rectilinear filament the process detailed above has been carried through for four different values of $\tan\alpha$, viz.,

$$\tan\alpha = 1\cdot25, \quad 1\cdot132, \quad 1\cdot00, \quad 0\cdot25.$$

The second of these was chosen because at this value of α the intersection of a plane through the axis of the helix with the latter gave a series of points having the precise spacing that Kármán had found corresponded to stability in the two dimensional case, and it was thought possible that the change from stability to instability would occur somewhere in this region. Hence also values of $\tan\alpha$ were taken at $\tan\alpha = 1\cdot25$ and $\tan\alpha = 1$ in this neighbourhood. The fourth case ($\tan\alpha = 0\cdot25$) was chosen as a result of measurement of the photograph obtained by Eden,* which gave the approximate value $\tan\alpha = 0\cdot3$.

---

* *Loc. cit.*

The calculated values of A, B, . . . K in these four cases are shown in the following table :—

Tan α.	1·25.	1·132.	1·00.	0·25.
A	−0·584	−0·627	−0·662	−0·322
B	0·0675	0·057	0·039	−0·050
C	−0·657	−0·775	−0·935	−2·789
E	0·226	0·284	0·361	0·116
F	−0·120	−0·080	−0·006	0·278
G	0·0979	+0·065	−0·001	−1·111
H	0·577	0·612	0·668	0·156
J	0·577	0·612	0·668	0·156
K	−0·462	−0·544	−0·659	−0·606

The cubic equations, upon the nature of whose roots depends the stability or instability, are, in the respective cases,

$$\left.\begin{array}{ll} z^3 - 1{\cdot}166\ z^2 - 0{\cdot}0245\,z + 0{\cdot}1207 = 0 & (\tan\alpha = 1{\cdot}25) \\ z^3 - 1{\cdot}251\ z^2 - 0{\cdot}0631\,z + 0{\cdot}1592 = 0 & (\tan\alpha = 1{\cdot}132) \\ z^3 - 1{\cdot}327\ z^2 - 0{\cdot}1655\,z + 0{\cdot}2168 = 0 & (\tan\alpha = 1{\cdot}00) \\ z^3 - 0{\cdot}6501\,z^2 - 0{\cdot}3560\,z - 0{\cdot}0773 = 0 & (\tan\alpha = 0{\cdot}25) \end{array}\right\}. \quad (59)$$

The first three of these equations have each three real roots, while the last has only one real root, so that in the former cases the vortex is stable and in the latter case unstable.

Our results may be given a wider interpretation if we consider the discriminants of the cubic equations (59). If all the roots of any cubic equation

$$z^3 + 3b_1z^2 + 3b_2z + b_3 = 0 \qquad (60)$$

are real, then its discriminant

$$\Delta = 3b_1^2b_2^2 + 6b_1b_2b_3 - b_3^2 - 4b_2^3 - 4b_1^3b_3$$

is positive, while if the equation has two complex roots, then Δ is negative.

The following table gives the value of Δ in each case :—

Tan α.	b_1.	b_2.	b_3.	Δ
1·25	−0·3887	−0·0082	0·1207	$1{\cdot}61\,.\,10^{-2}$
1·132	−0·417	−0·021	0·159	$2{\cdot}95\,.\,10^{-2}$
1·00	−0·442	−0·055	0·217	$6{\cdot}20\,.\,10^{-2}$
0·25	−0·217	−0·119	−0·077	$-1{\cdot}23\,.\,10^{-2}$

Fig. 2 (2) shows the discriminant Δ plotted against tan α.

The value of tan α corresponding to the transition from stability to instability is given approximately by the point A at which the curve crosses the axis.

The forward velocity and the angular spin are given by (37) and (36). These integrals have been evaluated in the manner already indicated, and the results are given in the following table :— ,

Tan α.	∞	1·25.	1·132.	1·00	0·25.
$2\pi a V/\kappa$ ..	0	0·437	0·522	0·636	2·367
$2\pi a^2 \omega/\kappa$.	0	−0·331	−0·359	−0·368	0·164

In fig. 2 curves are shown drawn through the calculated values of 10Δ, $2\pi a V/\kappa$ and $2\pi a^2\omega/\kappa$, which must represent with fair accuracy the variation of these non-dimensional numbers with tan α, although, on account of the heaviness of the computation only four cases, in addition to the limiting case of a straight filament have been worked out in detail. While the curves for 10Δ and $2\pi a^2\omega/\kappa$ have been drawn to pass almost through the same point A on the axis, this has not been directly verified by computation.

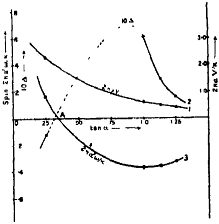

FIG. 2.

An examination of these curves suggests the following conclusions :—

1. The helical vortex is capable of maintaining the three fundamental modes of oscillation considered, provided tan $\alpha > 0 \cdot 3$. Accordingly for tan α greater than $0 \cdot 3$ the helical vortex is stable in form while for tan $\alpha < 0 \cdot 3$ it is unstable.

2. The rotational speed of the system about its central axis undergoes a reversal of sign at tan $\alpha = 0 \cdot 3$ approximately. This suggests that the helical vortex of minimum pitch which, if created, would just maintain its form

unimpaired would also move through the fluid steadily without rotation. It is significant to note that the rough measurement of tan α derived from the photograph* already referred to had this value.

§ 9. It is apparent from the calculation that there are two principal factors which determine the forward motion and the rotation of the system at any point on the filament. These are adjacent elements of the same coil, and the elements of neighbouring coils of the helix.

The torsion reaches a maximum of $0 \cdot 5/a$ at tan $\alpha = 1$ and has fallen to $0 \cdot 38/a$ at tan $\alpha = 0 \cdot 3$, at which point the effect of the neighbouring coils towards instability is more potent. Above tan $\alpha = 1$, the torsion diminishes again, but so also does the effect of the neighbouring coils, and the system remains stable until the straight filament is attained.

At first sight it appears anomalous that whereas Kármán in his investigation of two infinite rows of rectilinear vortices found a *particular* arrangement stable and all others unstable, in the present investigation helices of pitch above a certain value are stable: but in this connection it has to be remarked that in the Kármán case the effect of torsion is completely absent and he is concerned merely with the interplay of neighbouring filaments. The effect of a filament on itself is, in fact, assumed zero.

In a future paper it is proposed to show how the results of this and the preceding two papers may be utilised to provide information regarding the forces and motion in the wake of a body symmetrical about an axis in uniform motion along that axis through a fluid.

---

* Eden, *loc. cit.*

Flow in a Pipe of Rectangular Cross-Section.

By R. J. Cornish, M.Sc., Assistant Lecturer in Engineering in the University of Manchester.

(Communicated by E. A. Milne, F.R.S.—Received June 22, 1928.)

List of Symbols.

a = half width of pipe in centimetres.
b = half depth of pipe in centimetres.
m = hydraulic mean depth $= \dfrac{ab}{a+b}$.
p = pressure.
Q = quantity of water in cubic centimetres per second.
R = resistance per unit area in dynes per square centimetre.
S = average velocity in centimetres per second.
t = temperature.
w = velocity of a particle parallel to the axis of the pipe.
z = distance parallel to the axis of the pipe.
ρ = density.
μ = absolute viscosity.
ν = kinematic viscosity.

Note.—R × (area of walls) = (difference of pressure) × (area of cross-section). Hence $\mathrm{R} \,.\, 4(a+b)\,dz = -\,dp \,.\, 4ab$; or $\mathrm{R} = -\,m\dfrac{dp}{dz}$.

Object of Research.

The object of the research was to investigate the flow of water in a pipe of rectangular cross-section. Much work has been done on similar problems with pipes of circular section,* and pipes of rectangular section have been investigated by Fromm† and Davies and White.‡ Fromm worked with pipes in which the ratio of the sides was never less than 6 to 1; his report deals only with turbulent flow. In the case of Davies and White's research, the minimum ratio of the sides was 40 to 1, so that the laminar flow could be calculated from the formula for flow between infinitely wide parallel plates.

The present writer used a pipe of section 1·178 cms. by 0·404 cms. (ratio of sides = 2·92); this presents a fresh problem where stream line flow is concerned, and shows interesting results in the region of the critical velocity.

---

* See especially Stanton and Pannell, 'Phil. Trans.,' A, vol. 214, p. 199 (1914).

† 'Z. f. ang. Math. Mech.,' vol. 3, p. 339 (1923).

‡ 'Roy. Soc. Proc.,' A, vol. 119, p. 92 (1918).

Apparatus.

Fig. 1 shows a cross-section through the pipe. The two main components were two brass castings about 120 cms. long. In the lower casting a channel was cut and finished smooth with emery paper. The upper casting was a plate, planed flat and smoothed with emery paper. Three gauge-holes, α, β, γ, each 1/16 inch in diameter, were drilled in it. The distance from the entrance to α was 30·2 cms., from α to β 30·50 cms, from β to γ 36·43 cms., and from γ to the exit 22·8 cms.

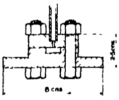

FIG. 1.

The two plates were kept together by 28 $\frac{5}{16}$-inch bolts, the surfaces in contact being covered with a thin film of vaseline to prevent leakage.

The width of the channel ($2a$) was 1·178 cms., and the depth ($2b$) was 0·404 cm. The maximum variation from these average figures was less than 0·5 per cent. in both cases.

The pressure differences were measured in three ways, according to magnitude—

(1) Very small differences, up to about 12 cms. water, were found by observing a differential water gauge with a cathetometer, which could be read to 0·001 cm. by a vernier.

(2) Up to about 30 inches water a differential water gauge, read directly, was used.

(3) For all higher pressures two mercury gauges were used.

A calibrated mercury thermometer was used for temperature, and the quantity of water was found by measuring with a stop watch (calibrated every day) the time to fill vessels whose volume was known within 0·1 per cent.

Mathematical Formula for Stream Line Flow.

The general steps of the theory are given in Appendix II.

The formula for the flow is

$$Q = -\frac{4}{3} \cdot \frac{ab^3}{\mu} \cdot \frac{dp}{dz}\left\{1 - \frac{192}{\pi^5} \cdot \frac{b}{a}\left(\tanh\frac{\pi a}{2b} + \frac{1}{3^5} \cdot \tanh\frac{3\pi a}{2b} + \ldots\right)\right\}. \qquad (1)$$

For the section under consideration, this formula gives

$$Q = -5{\cdot}08\,\frac{1}{\mu} \cdot \frac{dp}{dz}. \qquad (2)$$

Now $m = 0 \cdot 150$ cm., and $A = 0 \cdot 476$ sq. cm.; using the relations $Q = AS$ and $R = - m \,.\, dp/dz$, we easily find from (2) that

$$\frac{R}{\rho S^2} = 2 \cdot 12 \frac{\nu}{mS}. \tag{3}$$

Results.

The results have been divided into two series, and are detailed in Appendix I. Series 1 includes readings taken at gauge holes α and γ and the readings of series 2 were taken at β and γ. In fig. 2 $\log (R/\rho S^2)$ has been plotted against $\log (mS/\nu)$.

The observed equation for the stream line portion is

$$\frac{R}{\rho S^2} = 2 \cdot 10 \frac{\nu}{mS}.$$

The coefficient was found by averaging separately the first 10 readings of series 1 and the first five of series 2. In both cases the average was $2 \cdot 10$. The difference between this value and the theoretical value $2 \cdot 12$ (see equation (3)) is easily accounted for by slight errors in measuring so small a channel.

In calculating the values of $R/\rho S^2$ and mS/ν, ρ was assumed to be 1 and μ was found from the formula

$$\mu = 0 \cdot 017928/(1 + 0 \cdot 03445t + 0 \cdot 000235t^2),^*$$

where t is measured in degrees Centigrade.

Conclusions.

1. Equations (2) and (3) are confirmed by the experiments.

2 The effect of the distance of the gauge-holes from the entrance is well-marked. Even with an entrance length of 400 m, as is the case with gauge-hole β, the curve shows a departure from the stream line curve as the critical value of mS/ν is approached. The conclusions of Davies and White† from a similar result are referred to below.

3. The critical value of mS/ν for pipes of rectangular section is in the same region as that for pipes of circular section. In fig. 2, additional laminar flow curves have been drawn for a square section and for a section of infinite width. From the position of these curves one would expect the critical value of mS/ν to increase as the ratio a to b increases. This is borne out by a comparison of the author's results with those of Davies and White.

---

* Hosking, 'Phil. Mag.,' vol. 18, p. 262 (1909).

† 'Roy. Soc. Proc.,' A, vol. 119, p. 96 (1928).

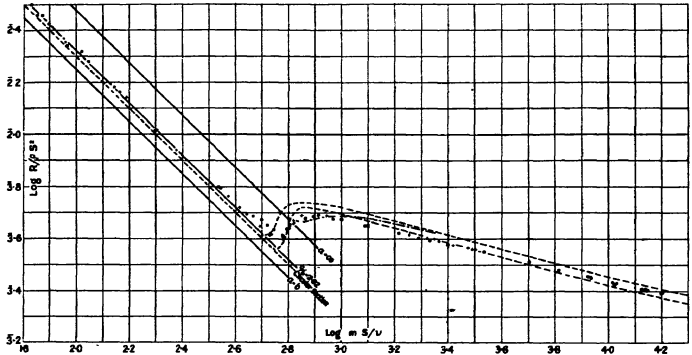

FIG. 2.—⊙ Series 1. + Series 2. Dotted lines show Stanton and Pannell's Curves for Drawn Brass Pipes. Chain-dotted lines show Davies and White's Curves for Pipes of Rectangular Section.

4. When turbulent flow is fully established, the curve connecting $R/\rho S^2$ and mS/ν approximately coincides with that for drawn brass pipes;[*] this is in agreement with the work of many investigators on smooth channels and pipes of various sections.

Note.—The conclusions of Davies and White referred to above appear to the writer to call for some discussion. They deduce a third critical value of mS/ν, below which "eddies cannot be transmitted to, or exist in, the channel."[†] There is mathematical evidence for believing that there exists a critical velocity below which "every disturbance must automatically decrease,"[‡] and above which" it is possible to prescribe a disturbance which will increase for a time."[‡] This, of course, is a very different critical velocity from that found by Davies and White, and it could not be detected by their method, the essence of which is that below a certain value of mS/ν a gauge point just inside the entrance would register steady flow under all conditions.

The experimental evidence which leads them to their conclusion is shown in figs. 3 and 4 of their paper. The present writer has been led from his own work on flow through narrow passages to consider that the dotted curves of their fig. 3 are tangential, or perhaps asymptotic, to the curve for $F/(\mu v/d)$, and the points of their fig. 3 would fit in quite well with this view. If this opinion is correct, it would seem to be difficult to find definite values from which to draw their fig. 4.

---

[*] Stanton and Pannell, *loc. cit.*

[†] 'Roy. Soc. Proc.,' A, vol. 119, p. 99 (1928).

[‡] Orr, 'Proc. Roy. Irish Acad.,' A, vol. 27, p. 77 (1907).

APPENDIX I.

Series 1.

Temperature ° F.	S.	dp.	R.	mS/ν.	$R/\rho S^2$.
57·1	5·28	0·400 cms. water	0·880	67·4	0·0316
56·9	5·54	0·401 ,,	0·882	70·5	0·0288
56·7	5·83	0·442 ,,	0·972	73·9	0·0287
56·6	6·18	0·460 ,,	1·012	78·2	0·0266
52·7	7·76	0·601 ,,	1·321	92·8	0·0220
56·3	8·29	0·648 ,,	1·425	104·7	0·0208
56·4	8·80	0·67 ,,	1·47	111·3	0·0191
56·9	10·89	0·817 ,,	1·796	138·5	0·01516
57·2	11·42	0·860 ,,	1·891	146·0	0·01452
53·1	16·57	1·290 ,,	2·837	198·9	0·01034
52·9	16·76	1·322 ,,	2·907	201	0·01036
52·4	28·9	2·399 ,,	5·276	348	0·00632
52·4	29·4	2·450 ,,	5·388	350	0·00622
51·6	39·6	3·47 ,,	7·63	465	0·00486
58·7	38·3	3·15 ,,	6·93	501	0·00472
58·7	40·2	3·29 ,,	7·23	525	0·00449
58·7	42·5	3·54 ,,	7·78	556	0·00432
49·3	54·8	5·96 ,,	13·10	621	0·00437
56·8	49·9	5·09 ,,	11·19	635	0·00450
57·0	49·9	5·10 ,,	11·22	636	0·00452
53·1	61·1	8·08 ,,	17·77	733	0·00478
49·2	69·9	10·78 ,,	23·7	788	0·00487
51·0	70·4	11·01 ,,	24·2	817	0·00491
50·0	81·1	5·56 ins. water	31·0	920	0·00473
56·1	79·4	13·52 cms. water	29·7	999	0·00472
56·4	79·4	13·54 ,,	29·8	1005	0·00473
49·8	107·5	9·21 ins water	51·4	1225	0·00446
49·8	143·9	15·45 ,,	86·3	1642	0·00418
50·5	168·5	20·32 ,,	113·5	1945	0·00401
50·5	186·3	24·25 ,,	135·4	2150	0·00391
51·0	215	31·20 ,,	174·2	2500	0·00378
49·0	304	4·33 ins. Hg	329	3430	0·00355
48·9	449	8·59 ,,	652	5050	0·00324
48·8	582	13·46 ,,	1022	6530	0·00302
48·8	742	20·81 ,,	1580	8330	0·00287
49·0	745	20·85 ,,	1583	8400	0·00285
48·8	764	21·70 ,,	1650	8580	0·00283
48·6	927	30·58 ,,	2322	10370	0·00271
48·7	939	30·91 ,,	2347	10520	0·00266
48·8	942	31·12 ,,	2363	10570	0·00267
49·1	952	32·00 ,,	2430	10740	0·00269
55·2	1074	38·7 ,,	2940	13320	0·00256
54·0	1131	43·0 ,,	3260	13760	0·00256
54·2	1150	43·9 ,,	3330	14040	0·00253
54·6	1285	53·4 ,,	4050	15810	0·00246
54·9	1290	53·9 ,,	4090	15930	0·00247

Series 2.

Temperature ° F.	S.	*dp.*	R.	*mS/ν.*	R/ρS².
55·7	7·17	0 297 cms. water	1 199	89 7	0·0235
55·5	7·32	0·299 ,,	1·208	91·4	0 0226
56·6	12·21	0·510 ,,	2·060	154·8	0·0139
54·3	18·48	0·820 ,,	3 312	238	0·00874
54 9	20·4	0·852 ,,	3 441	251	0 00831
56·3	29·6	1·261 ,,	5 093	374	0 00580
55·2	33·2	1·433 ,,	5 788	412	0 00525
54·5	35·6	1·551 ,,	6·264	438	0 00493
53·9	40·4	1·793 ,,	7 242	491	0 00445
58·9	40·8	1 696 ,,	6 850	535	0 00412
58·9	40·9	1 692 ,,	6 834	536	0 00410
59 5	41·1	1·722 ,,	6 955	544	0 00413
59 7	45 0	0·81 ins. water	8 3	598	0·00411
59 7	45 2	0·81 ,,	8 3	600	0 00407
59·7	45·5	0·82 ,,	8·4	604	0 00408
59·6	45 6	2·03 cms water	8 20	604	0 00396
59 5	48 0	2·49 ,,	10 06	635	0 00437
59·5	46·9	1·13 ins. water	11·6	659	0 00469
59·5	46·9	1·10 ,,	11·3	659	0 00457
59 5	46·6	2·84 cms. water	11·47	663	0 00458
59·1	53·8	3·50 ,,	14 13	707	0·00490
58·7	67·4	5 49 ,,	22 2	881	0 00489
59·7	94·3	9 81 ,,	39 6	1250	0 00447
49·8	110 5	5 26 ins. water	54 0	1260	0 00444
56·2	100 4	11·22 cms. water	45·3	1264	0·00451
49·4	157·8	10·00 ins. water	102 6	1789	0 00413
49·6	184·1	13·19 ,,	135·4	2096	0 00401
49·8	195 9	14·75 ,,	151·4	2240	0 00396
51·9	197·6	14·83 ,,	152·1	2330	0 00391
51·7	224	18 31 ,,	187 9	2620	0 00378
51·5	255	23 44 ,,	240 5	2990	0 00369
51·5	265	24·90 ,,	255 5	3100	0 00364
51·5	272	26 20 ,,	268 8	3190	0 00363
48 9	449	4 71 ins. Hg.	657	5050	0 00326
48·8	764	11 84 ,,	1651	8580	0·00283
48·8	942	17 01 ,,	2373	10570	0·00268

APPENDIX II.

Theoretical Formula for Stream Line Flow.

Take the origin of co-ordinates at the centre of the cross-section, Ox parallel to the longer side, Oy parallel to the shorter side, and Oz parallel to the axis of the pipe. (See fig. 3.)

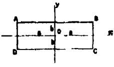

FIG. 3.

The general equations of motion reduce to

$$\frac{\partial p}{\partial x} = 0, \quad \frac{\partial p}{\partial y} = 0, \quad \frac{\partial p}{\partial z} = \mu\left(\frac{\partial^2 w}{\partial x^2} + \frac{\partial^2 w}{\partial y^2}\right). \tag{4}$$

The first two equations show that the pressure is constant over the section.

$$\text{Let } \tau = -\frac{1}{2\mu}\cdot\frac{dp}{dz}, \quad \text{and} \quad w = \chi + \tau(b^2 + y^2).$$

Substituting in (6), we have

$$\frac{\partial^2\chi}{\partial x^2} + \frac{\partial^2\chi}{\partial y^2} = 0. \tag{5}$$

The object of introducing χ is to simplify the boundary conditions

Along the boundary

$$\chi + \tau(b^2 - y^2) = w = 0. \tag{6}$$

Hence, along AB, CD,

$$\chi = 0, \tag{7}$$

and along AD, BC

$$\chi = -\tau(b^2 - y^2). \tag{8}$$

From (7) all the terms in χ must vanish when $y = \pm b$. This condition is satisfied by terms such as

$$\eta \cos\frac{(2n+1)\pi y}{2b},$$

where η is a function of x only and n is an integer.

Substitute $\chi = \eta \cos my$ in (5).

Then

$$\frac{\partial^2\chi}{\partial x^2} - m^2\eta = 0, \tag{9}$$

whence

$$\eta = A_n \cosh mx + B_n \sinh mx. \tag{10}$$

By symmetry about Oy, $B_n = 0$; hence

$$\eta = A_n \cosh mx, \tag{11}$$

and χ consists of terms like $A_n \cosh mx \cos my$, where $m = (2n+1)\pi/2b$.

These terms must now be made to satisfy the other boundary condition (equation (8)). For convenience, let

$$y = 2b\theta/\pi. \tag{12}$$

Then

$$\chi = \sum_{n=0}^{n=\infty} A_n \cosh\frac{(2n+1)\pi x}{2b}\cos(2n+1)\theta. \tag{13}$$

Substituting from (12) in (8), we have

$$\chi = \tau\,.\,4b^2(\theta^2 - \tfrac{1}{4}\pi^2)/\pi^2. \tag{14}$$

This must agree with (17) when $x = \pm a$, *i.e.*, with

$$\chi = \sum_{n=0}^{n=\infty} \mathrm{A}_n \cosh \frac{(2n+1)\pi a}{2b} \cos (2n+1)\,\theta. \tag{15}$$

Expanding (14) in a Fourier's Series, we have

$$\chi = -\frac{32\tau b^2}{\pi^3}\left\{\cos\theta - \frac{1}{3^3}\,.\,\cos 3\theta + \frac{1}{5^3}\,.\,\cos 5\theta\,\ldots\right\}. \tag{16}$$

Comparing coefficients in (15) and (16), we obtain A_0, A_1, etc., whence we find

$$\chi = -\frac{32\tau b^2}{\pi^3}\left\{\frac{\cosh(\pi x/2b)}{\cosh(\pi a/2b)}\,.\,\cos\frac{\pi y}{2b} - \frac{1}{3^3}\,.\,\frac{\cosh(3\pi x/2b)}{\cosh(3\pi a/2b)}\,.\,\cos\frac{3\pi y}{2b} + \ldots\right\} \tag{17}$$

Hence

$$w = -\frac{32\tau b^2}{\pi^3}\left\{\frac{\cosh(\pi x/2b)}{\cosh(\pi a/2b)}\,.\,\cos\frac{\pi y}{2b} - \frac{1}{3^3}.\,\frac{\cosh(3\pi x/2b)}{\cosh(3\pi a/2b)}\,.\,\cos\frac{3\pi y}{2b} + \ldots\right\} + \tau\,(b^2 - y^2). \tag{18}$$

The total flow is given by

$$\mathrm{Q} = \int_{y=-b}^{y=+b}\int_{x=-a}^{x=+a} w\,dx\,dy. \tag{19}$$

The integration of the terms in (18) is a straightforward matter, and gives finally

$$\mathrm{Q} = -\tfrac{4}{3}\,.\,\frac{ab^3}{\mu}\,.\,\frac{dp}{dz}\left\{1 - \frac{192}{\pi^5}\,.\,\frac{b}{a}\left(\tanh\frac{\pi a}{2b} + \frac{1}{3^5}\,.\,\tanh\frac{3\pi a}{2b} + \ldots\right)\right\}. \tag{20}$$

This formula is substantially equivalent to that for the torsion of a rod of rectangular section; see, for example, Prescott's "Applied Elasticity," p. 148 (1924), where approximate methods of summing the series for particular cases are given.

Two Special Cases.

(i) $a = b$.

It can easily be shown by differentiation of equation (24) that, for a given area, the square is the form of rectangular section giving the maximum flow for a given pressure difference. To find the flow in this case, put $a = b$ in (20).

Then

$$\mathrm{Q} = -\,0{\cdot}562\,\frac{a^4}{\mu}\,.\,\frac{dp}{dz}\,. \tag{21}$$

Since $\mathrm{Q} = 4a^2\mathrm{S}$, $a = m$, and $\mathrm{R} = -\,m\,.\,dp/dz$, we get

$$\frac{\mathrm{R}}{\rho\mathrm{S}^2} = 1{\cdot}78\,\frac{\nu}{m\mathrm{S}}. \tag{22}$$

(ii) "*a*" infinite; "*b*" finite.

When a is large, (24) becomes approximately

$$Q = -\tfrac{4}{3} \cdot \frac{ab^3}{\mu} \cdot \frac{dp}{dz}\left\{1 - 0{\cdot}630\frac{b}{a}\right\}, \tag{23}$$

whence

$$S = \frac{Q}{4ab} \rightarrow -\tfrac{1}{3} \cdot \frac{b^2}{\mu} \cdot \frac{dp}{dz} \text{ as } a \rightarrow \infty. \tag{24}$$

But $m = ab/(a + b) \rightarrow b$ as $a \rightarrow \infty$.

We therefore arrive at the standard formula for flow between two infinite parallel plates, viz.,

$$S = -\tfrac{1}{3} \cdot \frac{m^2}{\mu} \cdot \frac{dp}{dz} = -\tfrac{1}{3} \cdot \frac{mR}{\mu}, \tag{25}$$

or

$$\frac{R}{\rho S^2} = 3\frac{\nu}{mS}. \tag{26}$$

Flow in Open Channels.

In the case of laminar flow in an open rectangular channel of width $2a$ and depth b, the velocity gradient perpendicular to the surface is zero, if the air resistance be neglected. The flow is therefore one-half that in a pipe of rectangular section, $2a$ by $2b$, and the formula is

$$Q = -\tfrac{2}{3} \cdot \frac{ab^3}{\mu} \cdot \frac{dp}{dz}\left\{1 - \frac{192}{\pi^5} \cdot \frac{b}{a}\left(\tanh\frac{\pi a}{2b} + \frac{1}{3^5}\tanh\frac{3\pi a}{2b} + \ldots\right)\right\}. \tag{27}$$

The author acknowledges with thanks the valuable assistance he has obtained from Dr. Prescott's "Applied Elasticity," and from Prof. E. A. Milne, F.R.S., of Manchester University, in working out the above proofs.

The Velocity Distribution of β-particles after passing through Thin Foils.

By P. White, B.A., Clare College, Cambridge, and G. Millington, B.A., Clare College, Cambridge.

(Communicated by Sir Ernest Rutherford, P.R.S.—Received July 18, 1928.)

[Plate 28.]

§ 1. *Introduction.*

When a parallel beam of β-particles, homogeneous in velocity, falls upon a sheet of matter not thick enough to obstruct it completely, the stream which emerges consists of particles which in general have suffered both a loss of velocity and a change in direction of motion.

The investigation of this action accordingly falls into two parts, one directed to examining the changes in direction of motion of the particles, or scattering of the beam, the other to measuring their loss of velocity. This paper is devoted to the second of these problems.

The retardation of the particles will clearly depend upon their initial velocity and upon the thickness and composition of the sheet of matter interposed.

For initial velocities less than one half of the velocity of light ($\beta < 0 \cdot 5$) Whiddington[*] and, more recently, Terrill[†] have investigated the effect by using cathode rays and an electrical means of detection, and Becker[‡] has made use of direct deviation photographs of cathode rays. Similar observations on natural β-rays of velocities between $\beta = 0 \cdot 5$ and $\beta = 0 \cdot 96$ were made by Danysz, Rawlinson, Thibaud, and d'Espine,[§] using the photographic method with semicircular focussing.

It is well known that when β-rays from a radioactive substance such as RaB + C are analysed by a magnetic field, the velocity spectrum formed

---

[*] 'Roy. Soc. Proc.,' A, vol. 86, p. 360 (1912).

[†] 'Phys. Rev.,' vol. 22, p. 101 (1923).

[‡] 'Ann. d. Physik,' vol. 78, p. 209 (1925).

[§] Danysz, 'C.R.,' vol. 154, p. 1502 (1912) and 'J. Physique,' vol. 3, p. 949 (1913); Rawlinson, 'Phil. Mag.,' vol. 30, p. 627 (1915); Thibaud, 'J. Physique,' vol. 6, p. 334 (1925), and vol. 7, p. 277 (1927); d'Espine, 'C.R.,' vol. 182, p. 458 (1926), and 'J. Physique,' vol. 8, p. 502 (1927).

consists usually of a continuous background upon which are superimposed numerous lines each corresponding to a set of rays of one velocity; when the spectrograph used is of the semicircular-focussing type, the lines are sharply defined. If a foil is placed over the source, the rays lose velocity in passing through it and are focussed at a point corresponding to a lower velocity than in the case of an uncovered source. Following Rawlinson, the later workers used sources which were partly covered by foil and thus obtained a spectrum comprising two sets of lines due respectively to retarded and unretarded particles. Each line of the normal spectrum appeared duplicated and by measuring the distance between each corresponding pair of traces the velocity lost by each group of particles could be found.

The results obtained were in fairly good agreement with one another and with Bohr's theory of the effect (*vide infra*). No great accuracy, however, could be claimed for the observations because it was found necessary to measure the small distances involved (about 1 mm.) with the naked eye, the lines being too indefinite to admit magnification.

In addition, each worker remarked that the trace formed by particles which had passed through retarding foil was notably broadened, that is, that the emergent beam was no longer homogeneous in velocity, but had undergone a process of straggling analogous to the straggling of α-rays. In the case of α-rays the straggling is small and is only detected by refined measurements. It was therefore possible to carry the study of α-rays a long way without taking it into account. With β-rays, however, the situation is entirely different. The early cloud photographs taken by Wilson showed the great variations which occur in the history of β-particles as they pass through matter, and the study of β-rays has been held up by our ignorance of the true form of this large straggling so fundamental to the whole problem of their behaviour. The present paper is directed towards the solution of this question, and incidentally it confirms and supplements the work that has already been done on the most probable loss of velocity.

Very little attention has been paid hitherto to this dispersion of the retardations of β-particles. The photographic method of investigation outlined above illustrates the effect very clearly but seemed originally not suitable for quantitative work. Accordingly Madgwick* had recourse to an ionisation method. We have, however, been able to employ the photographic method by the application of the microphotometer.

The previous objections to the use of this method were that the characteristics of the plates for β-rays were imperfectly understood, and that no technique had been worked out for compensating the readings of the width of the trace formed by straggled particles (which we may call the straggled trace) for the finite width of the unstraggled trace. The work of Ellis and Wooster* on the photographic action of β-rays has overcome the former difficulty, while the latter is met by our method of calculation outlined below.

---

* 'Proc. Camb. Phil. Soc.,' vol. 23, p. 970 (1927).

§ 2. *Experimental Method.*

Following Rawlinson, Thibaud and d'Espine we used a radioactive source which was partly covered by a straggling foil. These workers covered half the source and d'Espine further divided his camera by a medial partition of aluminium, thus obtaining the two spectra side by side. For our purpose it was necessary to be able to control the fractions of source covered and exposed and as far as possible to distribute them evenly, and we therefore used a screen pierced at approximately equal intervals by two or three holes adjusted to give nearly equal maximum photographic densities to each of a corresponding pair of traces.

Mica was used throughout as the straggling material, and the screens were shaped as shown in fig. 1(B) and rested in slots as in 1(A) so that they touched the

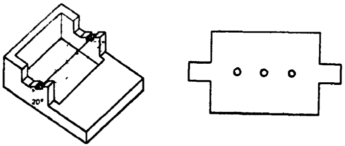

FIG. 1A. FIG. 1B.

Graphite Carriage and Mica Screen.

wire sources and made an angle of about 20° with the plane of the photographic plate. In this position they were traversed normally by all particles due to pass through the middle of the slit and reach the middle of the plate, and over the useful range of the plate the effective length in the screen of the path of the particles only varied by 2 per cent. As this is within the limits of error involved in other parts of the experiment it was neglected. The screens were prepared in the usual way by splitting up a small sheet of mica and cutting out with a razor blade sections which showed unbroken fringes in reflected sodium light. For drilling the mica was held firmly between two brass templates and the drill rotated gently with the fingers. The mica at the rims of the holes showed only slight flaking under the microscope. The surface density of the screens was found to within 2 per cent. by estimating the area and weighing.

---

* 'Roy. Soc. Proc.,' A, vol. 114, p. 266 (1927).

The source was Ra B and C initially in equilibrium with Ra A, and was deposited on a platinum wire $\frac{1}{4}$ mm. in diameter by recoil from emanation. The wire was supported by its ends in a graphite carriage, fig 1(A), and lay in two grooves so cut as to ensure its being vertically beneath and parallel to the slit.

Ilford X-ray plates were used and were developed for 5 minutes with 1 : 20 rodinal at 18° C.

The camera was of the usual design for semicircular focussing and was lined with thin plates of graphite. It gave radii of curvature between 2·1 cm. and 4·2 cm., the useful part of the plate being 5 cm. long. The pressure of residual air during the exposure was about 1/50 mm. The magnetic field was calibrated by using the values of $H\rho$ given by Ellis and Skinner* for the lines of Ra B and C. It could be kept constant usually to one part in 2000. The uniformity of the field and the values assumed for the dimensions of the camera were checked by evaluating the $H\rho$ values for all the lines on one plate in terms of one of them, the values always agreeing to 0·5 per cent. with the accepted values.

§ 3. *Measurement of Plates.*

Two typical photographs are shown in Plate 28.

By means of a microphotometer similar to those designed by Koch† and Dobson,‡ the distribution of optical density along each plate was measured and these readings were plotted as in fig. 2. In order to obtain values for the number of line-electrons which have fallen on any element of the plate, it is necessary to allow for the background due to the continuous spectrum and to chemical fog and to correct for the characteristics of the plates used.

Ellis and Wooster (*loc. cit.*) have shown that the optical density D is connected with the total exposure (I*t*) under the conditions which we used, by the equation :—

$$D = C \log_{10} (It/\tau + 1)$$

---

* 'Roy. Soc. Proc.,' A, vol. 105, p. 165 (1923).

† 'Ann. d. Physik,' vol. 39, p. 705 (1912).

‡ 'Roy. Soc. Proc.,' A, vol. 104, p. 248 (1923).

where C depends only on conditions of development and was taken as 1·27; while τ depends both upon conditions of development and velocity of the particles. Since, however, the differences in velocity involved are small, the variation in τ can be neglected and relative values of the total exposure found without knowledge of the value of τ.

In fig. 2 the background was interpolated under each trace as at A. It was frequently linear for some distance and could be ruled in. Each pair of traces with the corresponding background was then plotted on a much larger scale, and the two values of the density at each point were converted into terms of exposure and subtracted, the differences being again plotted against distance along the plate as in fig. 3.

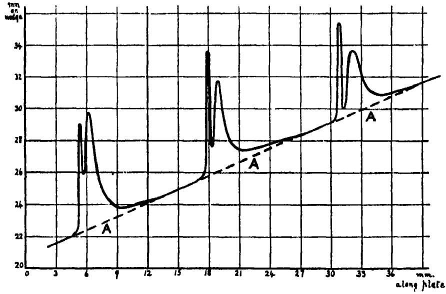

Fig. 2.

In the curves so obtained the straggled and unstraggled traces usually overlapped slightly, and it was necessary to estimate what fraction of the exposure should be attributed to each (as at B in fig. 3). In doing so we were guided by the general form of the lines obtained by taking photographs with a bare source and with an unpierced piece of mica.

The breadth of the unstraggled trace depends principally upon the following factors:—

(*a*) The geometry of the camera, including the effect of finite width and length of both source and slit (*cf.* Wooster*).

---

* 'Roy. Soc. Proc.,' A, vol. 114, p. 729 (1927).

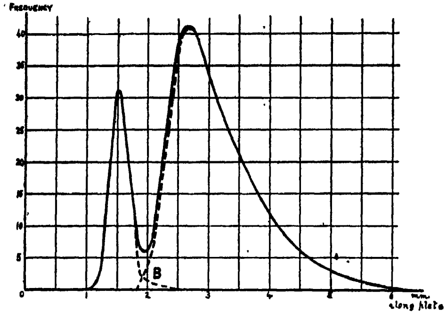

Fig. 3.

(*b*) Non-uniformity and unsteadiness of the magnetic field (*cf.* Hartree*).

(*c*) Scattering through very small angles by the residual gas.

The number of electrons falling upon any part of the plate will be governed almost entirely by these factors. The profile of the trace as measured on the photometer will show a further breadth due to :—

(*d*) Scattering of electrons in the photographic plate.

(*e*) The finite width of the photometer slit; this was effectively 1/10 mm. measured on the plate in our experiments.

All these agencies affect the electrons which have passed through the straggling material to a first approximation to the same extent as they affect the unstraggled electrons. It is shown in the Appendix that they disappear from the final result.

The additional cause of the breadth of the straggled trace is the dispersion of loss of velocity in the straggling foil itself. A procedure is necessary for computing the shape of the straggled curve which would have been obtained with an ideally fine unstraggled line. Now it can be shown (see Appendix) that if the curve of number of electrons against distance for the unstraggled

---

* 'Proc. Camb. Phil. Soc.,' vol. 21, p. 746 (1923).

A

5 72 mgms /sq cm

B

2 65 mgms /sq cm

The three important lines from left to right in both plates are $H\rho$ 1410, 1677 and 1938, A being taken with 5 72 mgm per square centimetre and B with 2 65 mgm per square centimetre The slight displacement of the lines in B relative to those in A is due to a small difference in the field used The sudden decrease in density at the right of the plates is caused by the shielding from the direct beam of β particles by the roof of the camera. The lines show up more clearly when the original plates are viewed by transmitted light, the line $H\rho$ 1410 and its straggled line on plate A standing out from the background much more than the reproduction suggests This straggled line could be measured on the photometer, but it was too diffuse to give useful results beyond an estimate of the peak-displacement

trace has the equation $y = f(x)$ and that for the straggled trace $y = F(x)$, the corresponding curve for the straggled trace in the case where the unstraggled trace is indefinitely narrow is $y = g(x)$ where the function g can be found from the (experimentally determined) functions f and F by solution of the integral equation

$$F(x) = \int_{-\infty}^{\infty} f(x_0)\, g(x - x_0)\, dx_0.$$

In the Appendix a method for doing this numerically is elaborated. This procedure was applied to the experimental curves for Hρ 1410, 1677, 1938, after correction for background and photographic effect.

The results so obtained are plotted in fig. 4. Abscissæ are losses of momentum (measured by Hρ) of the emergent particles; ordinates frequency on an arbitrary scale. It must be noted that the scale of ordinates is not the same for different curves even of the same diagram, but has been conventionally adjusted so that the area under the various curves is the same; that is, they have been drawn as if no particles had been lost from the beam (see below § 6).

The quantities measured by Danysz, Rawlinson and others are the abscissæ of the maxima of these curves or, rather, the difference between these abscissæ and the full Hρ values for the lines. In figs. 9 to 11 our values for these quantities are compared graphically with the experimental values of Becker and d'Espine (*loc. cit.*) and with the predictions of Bohr's theory.

§ 4. *Results.*

The discussion of the results falls naturally into two parts, one dealing with the general magnitudes associated with the various curves given in fig. 4 (the chief being the abscissa of the maximum); the other with the detailed form of a typical curve.

A thorough investigation was made with the three strong lines of the Ra B spectrum 1410, 1677 and 1938 Hρ, using sheets of mica of 2·25, 2·65, 3·95 and 5·72 mgm. per square centimetre (screens I to IV). Screens V, VI and VII which were of 7·92, 11·1 and 14·2 mgm. per square centimetre respectively, were also used in a brief examination of the higher lines 2256, 2980 and 5904 Hρ of Ra B and C. (See Plate 28.)

The traces of the latter three lines were much fainter than of the former; where they were so faint that no useful results could be obtained from them by means of the photometer, the distance between the maxima of the traces

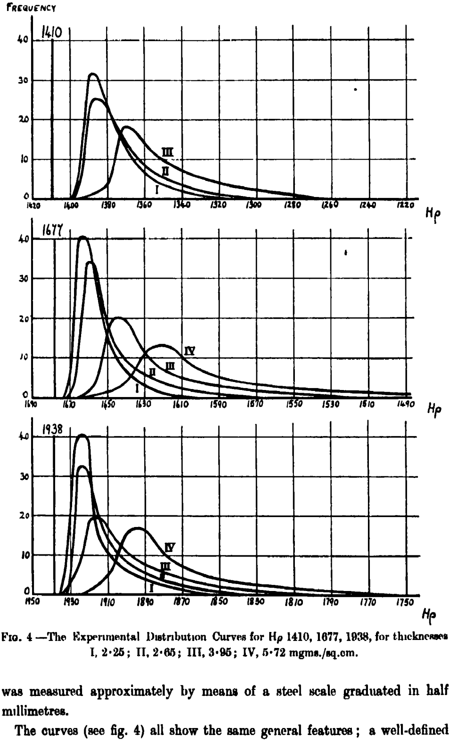

Fig. 4.—The Experimental Distribution Curves for Hρ 1410, 1677, 1938, for thicknesses I, 2·25; II, 2·65; III, 3·95; IV, 5·72 mgms./sq.cm.

was measured approximately by means of a steel scale graduated in half millimetres.

The curves (see fig. 4) all show the same general features; a well-defined peak of approximately Gaussian form, which merges on the side of greater loss of momentum into a tail which increases rapidly both in height and length relatively to the peak, as the thickness of straggling material increases or the initial velocity decreases.

§ 5. *The Fundamental Straggling Curve.*

It is important to examine whether all the curves contained in the set of curves in fig. 4 can be summarised into a single curve.

If the tangents at the two points of inflection of each of these curves are produced to cut the axis of abscissæ in F and B (as in fig. 5) and if O is the

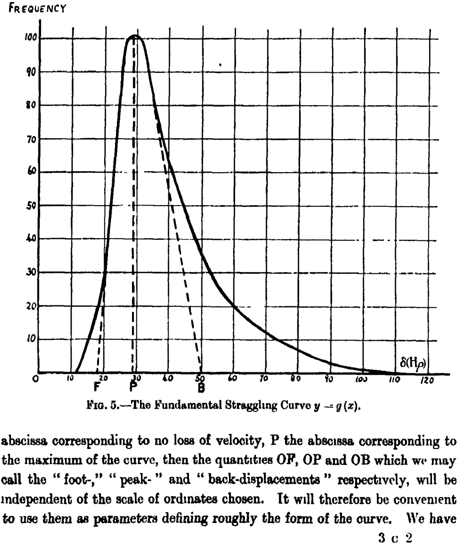

FIG. 5.—The Fundamental Straggling Curve $y = g(x)$.

abscissa corresponding to no loss of velocity, P the abscissa corresponding to the maximum of the curve, then the quantities OF, OP and OB which we may call the "foot-," "peak-" and "back-displacements" respectively, will be independent of the scale of ordinates chosen. It will therefore be convenient to use them as parameters defining roughly the form of the curve. We have to examine how these parameters depend on the thickness of straggling material and the initial velocity of the particles

In fig. 6 the quantities OF, OP, OB (l, m, n, say) are plotted for different velocities against mass per unit area of straggling material. It is clear that as the three points F, P, B move back with increasing thickness the ratios of their mutual distances apart remain approximately constant in other words, there is not only a motion of the curve as a whole but also a proportional spreading.

It is well known that the peak displacement is approximately proportional to the thickness of the foil traversed, and that the relative thicknesses required to produce equal displacements are proportional to the cube of the initial velocity Although our results show that this proportionality is not exact, we may consider that it is for the purposes of discussing the form of the curves.

Since the broadening of the curves is everywhere roughly proportional to the peak-displacement, we have the relations

$$l\beta^3/\sigma = l_0 \qquad m\beta^3/\sigma = m_0 \qquad n\beta^3/\sigma = n_0$$

where l_0, m_0, n_0 are constants, β is the ratio of the initial velocity to the velocity of light, and σ is the thickness of the foil in centigrams per square centimetre *

Corresponding to this general increase of abscissæ proportionally to σ/β^3, there must be a fall of ordinates proportional to β^3/σ, if the area of the curve is to remain constant With these suppositions, if

$$y = g(x)$$

is the equation to one of the curves for which β^3/σ is unity, x being written for $\delta(\mathrm{H}\rho)$, the equation for the general curve is

$$y = \phi(x) = \frac{\beta^3}{\sigma}\, g\left(\frac{\beta^3 x}{\sigma}\right)$$

From the curves in figs. 4 and 6, the most probable shape of the curve $y = g(x)$ was found ; the values 18, 29 and 50 were obtained for l_0, m_0 and n_0 respectively. The curve in fig. 5 represents $y = g(x)$ and in Table I are given the values of $g(x)$ for a series of values of x, when the maximum at $x = 29$ is adjusted to be 100, from which the curve $y = \phi(x)$ can be drawn for any values of β and σ. The curves in fig. 7 are drawn for $\beta = 0{\cdot}703$ ($\mathrm{H}\rho = 1677$) and for

---

* This rather unusual unit is used to simplify the subsequent discussion. If $\delta(\mathrm{H}\rho)$ is the peak displacement $\delta(\mathrm{H}\rho)/\sigma$ is usually denoted by T.

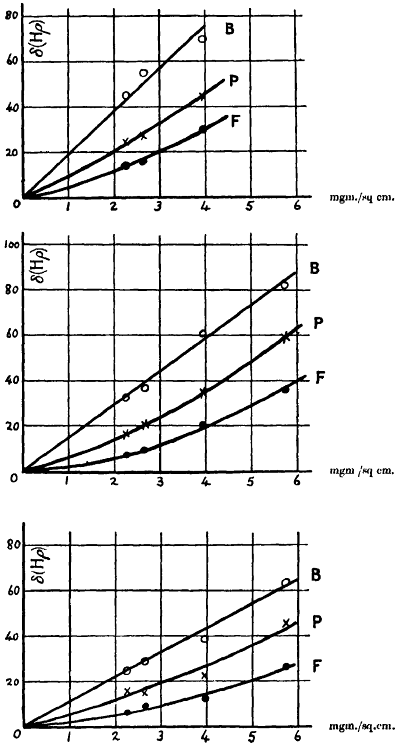

FIG. 6.—Foot-, Peak- and Back-Displacements. Curves for Hρ 1410, 1677, 1938

thicknesses I to IV. A comparison between figs. 4 and 7 shows very good agreement in the form and relative heights of the curves; fig 7 has the advantage, since in it the experimental errors are more completely averaged out, although the lack of agreement due to the assumption of exact proportionality with thickness of the foil is appreciable. The curve $y = g(x)$ may therefore be regarded as a fundamental curve expressing the form of the straggling of β-particles in passing through mica.

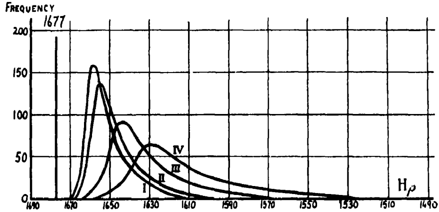

FIG. 7.—Theoretical Curves for Hρ 1677, calculated from $y = \phi(x) = \frac{\beta^3}{\sigma} g\left(\frac{\beta^3}{\sigma} x\right)$.

Table I.—Values of $g(x)$. Maximum at $x = 29$ adjusted $= 100$.

x.	$g(x)$.	x.	$g(x)$.	x.	$g(x)$.	x.	$g(x)$.
12	0	40	62·0	68	13·0	96	1·3
14	4·5	42	55·5	70	11·7	98	1·0
16	10·5	44	49·5	72	10·5	100	0·8
18	17·8	46	44·0	74	9·4	102	0·6
20	27·5	48	39·0	76	8·4	104	0·4
22	43·8	50	34·5	78	7·4	106	0·3
24	66·3	52	30·5	80	6·5	108	0·2
26	89·3	54	27·0	82	5·6	110	0·1
28	99·5	56	24·0	84	4·8	112	0·0
30	99·8	58	21·5	86	4·1		
32	96·8	60	19·5	88	3·4		
34	86·3	62	17·7	90	2·8		
36	77·3	64	16·0	92	2·2		
38	69·3	66	14·4	94	1·7		

If more complete data concerning the variation of the retardation with the thickness of the foil and the incident velocity of the particles can be obtained it may be possible to adjust the form of $\phi(x)$ to include this effect. Since the experimental values for the foot and back displacements are less reliable than the corresponding peak-displacements we can allow for this effect to the order of accuracy of the experiment by putting in the expression for $\phi(x)$ not the actual value σ of the thickness, but an effective value σ' adjusted to give the true peak displacement. From the graphs in fig. 6 it is found that within the limits of experimental error the effective thickness is independent of the initial velocity over the ranges of thickness and velocity considered. Table II gives the values of σ' for a series of values of σ from which with the modified equation $y = \frac{\beta^3}{\sigma'} g\left(\frac{\beta^3}{\sigma'} x\right)$ the straggling curve for any velocity and thickness in the given range can be computed.

Table II.—Effective thickness σ' corresponding to a thickness of foil σ in centigram per square centimetre.

σ.	σ'	σ	σ'
0·1	0·08	0·4	0·41
0·2	0·17	0·5	0·58
0·3	0·28	0·6	0·73

It is our considered opinion that this is the best method of using our results to obtain the straggling curve for any given velocity and thickness, especially for values lying between those used to obtain the curves of fig 4. Since, however, it may be important to get as near the actual experimental results as possible, and it is impossible to read values accurately off the reproduced curves, the following table is given with sufficient points to enable the curves to be constructed as originally drawn. It should be remembered that the curves so obtained are really the result of previous averaging and smoothing. In the nature of the experiment it is very difficult to estimate the errors involved. The large amount of photometering and calculating to be done limits the accuracy obtainable in the time that can reasonably be devoted to any one set of conditions.

Hρ.	Frequency ordinates for thicknesses			Hρ	Frequency ordinates for thicknesses				Hρ	Frequency ordinates for thicknesses			
1410	I	II	III	1077	I	II	III	IV.	1938	I.	II.	III.	IV.
1400	—	1·1	—	1670	4 1	—	·	- -	1930	14 2	9 3	1 8	—
1395	6 2	5 0	0 3	65	35 5	12 2	—	—	25	38·9	29 4	6 5	—
90	28 5	22 4	0·9	60	39·8	33 4	1 0	0·1	20	39·1	29 8	15 0	0 9
85	30 0	24 8	1·9	55	29 0	27 6	4 2	0 5	15	15 6	18 9	19 3	2 2
80	23·1	22 1	3 7	50	16 0	18 1	15·4	1 0	10	11·2	13 8	17 1	4 0
75	17 6	17 1	11 9	45	9 8	11 7	19 6	1·9	5	8 4	10 5	13·7	8 2
70	12 6	12 9	17·6	40	6 3	9 1	19 2	3 4	1900	6 4	8 3	11 1	14 2
65	9 2	10 0	16 6	35	4 3	7·1	15·9	6·1	1895	5 0	6 8	9 2	16·2
60	6 6	7 8	13 5	30	3 0	5 8	11 3	10 2	90	4 0	5 5	7 8	16 4
55	4 8	6 3	11 3	25	1 9	4 6	8 4	12 4	85	3·1	4·5	6 8	13·1
50	3 7	5 0	9 6	20	1 0	3 8	6 9	12 7	80	2 6	3 8	5 8	10 5
45	2 7	4 0	8·1	15	0·3	3 0	5 7	12 4	75	2 0	3 0	4 8	8 7
40	1 8	3 2	7 0	10		2 3	4 9	9 9	70	1·7	2·3	4 2	7 3
35	1 2	2 5	6 1	5		1 7	4 3	7 3	65	1 1	2 0	3 7	6 1
30	0 6	1 9	5 2	1600		1 2	3 6	6 3	60	0·9	1 6	3 1	5 3
25	0 2	1 4	4 6	1595		0 8	3 2	5 4	55	0 5	1 3	2 7	4 5
20		1 0	4 0	90		0 3	2 8	4 8	50	0·1	0·8	2 3	3·8
15		0 6	3 6	85		0 1	2 5	4 4	45		0 4	1 9	3 3
10		0 2	3·1	80			2 1	3 9	40			1 5	2 9
5			2 6	75			1 9	3·6	35			1 3	2·6
1300			2 2	70			1·6	3·2	30			1 0	2 3
1295			2·0	65			1 5	2 9	25			0 9	2 0
90			1·7	60			1 2	2 7	20			0 7	1·8
85			1·4	55			1 0	2 5	15			0 5	1 6
80			1 2	50			0 9	2 3	10			0 5	1 4
75			1 0	45			0 8	2 2	5			0 4	1 3
70			0·8	40			0 7	1·9	1800			0 2	1·1
65			0 5	35			0 6	1 9	1795				0 9
				30			0 5	1 7	90				0 8
				25			0 5	1 6	85				0 7
				20			0 4	1 4	80				0 5
				15			0 3	1 3	75				0·4
				10			0 2	1 3	70				0 3
				5			0·1	1·2	65				0·2
				1500									

Should for any purpose a very accurate curve be required for a given thickness and velocity, it might be necessary to make a special investigation under the desired conditions. Otherwise we feel that it is best to construct the curve from the formula we have deduced.

We can allow for the actual decrease in area of the curves with increase of σ/β^3 by writing

$$y = \phi(x) = \psi(\sigma, \beta) \, . \, \frac{\beta^3}{\sigma} g\left(\frac{\beta^3}{\sigma} x\right)$$

where $\psi(\sigma, \beta)$ is some function of σ and β slightly less than unity in the range in question. $\psi(\sigma, \beta)$ is the ratio of the number of electrons reaching the plate in the presence of the mica to the number which would have reached the plate from the same section of the source in the absence of the mica. That the value of $\psi(\sigma, \beta)$ may be expected to be nearly unity and to decrease slowly may be seen by considering in a general way the part played by scattering in the foil.

§ 6. *Effect of Scattering on the Observed Straggling Curve.*

In our apparatus the slit was 1 mm. wide and 3 cm. above the source, and hence in the absence of scattering all particles which eventually passed through the slit and fell on the plate, must have left the source in directions making with one another at most 2° in a plane perpendicular to the slit and 5° in a plane normal to this On account of scattering only a fraction of these remain in this solid angle, and it might at first sight be supposed that, as scattering became more pronounced, the number of particles actually reaching the plate would be considerably reduced This effect is compensated by the fact that corresponding to particles deflected out of the beam (such as λ of fig 8) there is a number of particles which will be deflected to pass through the slit, from other directions (such as μ of fig. 8). These particles have not only traversed a longer path in the foil but have in general emerged at points not normally above the source Hence they have not only an abnormally high retardation, but also fall upon the plate at a point corresponding to a different, generally lower, velocity than they actually possess The latter action causes a small spurious increase of the tail of the straggled curve. The former genuinely augments the number of heavily retarded particles and is the effect referred to by Bohr (see below, § 9).

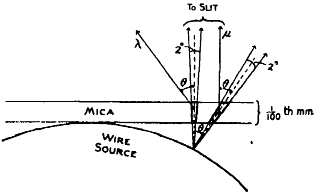

FIG. 8.—Compensation for Particles deflected from the Beam.

It is easy to see that for small angles of scattering this compensation is approximately exact, but for larger angles, θ say, the number of compensating particles is actually too great in the ratio of $\sec^2 \theta : 1$; *i.e.*, the ratio of the areas indicated in fig. 8.

Thus the beam whose velocity-distribution is measured in our arrangement comprises all particles emerging from the screen on the forward side, a slight excess of weight being given to the fractions scattered through large angles.

§ 7. *Absorption Coefficients.*

The result of the previous section suggests that it might be possible to find from our curves the total number of particles remaining in the beam by estimation of the relative areas under the straggled and unstraggled traces; that is, to make measurements of the absorption coefficient. To do so we need to know also the relative amounts of radioactive material covered and exposed. It will not be sufficient simply to measure the areas of wire-surface covered and exposed unless we can assert that the deposition by recoil from emanation is, at least macroscopically, uniform.

We made measures of the lengths of wire visible through the holes in the mica using a travelling microscope, but the values of the absorption coefficient deduced therefrom, although tending in the right direction, were more erratic than could be accounted for by experimental error The total absorption in our experiments was quite small. Even in the extreme case of the line 1410 $H\rho$ with a screen of 5·72 mgm./cm.^{2} the diminution is considerably less than half as is borne out by Madgwick's work on the Th B line $H\rho$ 1398.

It is hoped to design an apparatus which will enable the amounts of source covered and exposed to be determined accurately.

§ 8. *Variation of the Retardation with Thickness of Foil and Incident Velocity of the Particles.*

The fact that the most probable retardation (measured as $\delta(H\rho)$) is not strictly proportional to the thickness of the straggling foil is predicted by Bohr's theory, but attention has not previously been drawn to it from the experimental side.

Becker (*loc. cit.*) has, however, made measurements on cathode rays of velocity $\beta = 0{\cdot}52$ ($H\rho = 1033$) which show the variation with thickness and which are plotted in fig. 9 for comparison with our own measurements.

It is a more critical test to plot not the peak displacement itself but $I\beta^3$ against σ (see footnote, p. 710). In fig. 10 this is done for our values for $H\rho$ 1677 ($\beta = 0{\cdot}703$), taken from Table III which gives a complete list of all the peak-displacements measured by us, and Becker's values for $H\rho$ 1033

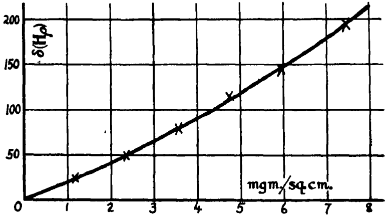

FIG. 9.—Results of Becker, showing that the retardation is not strictly proportional to thickness of foil.

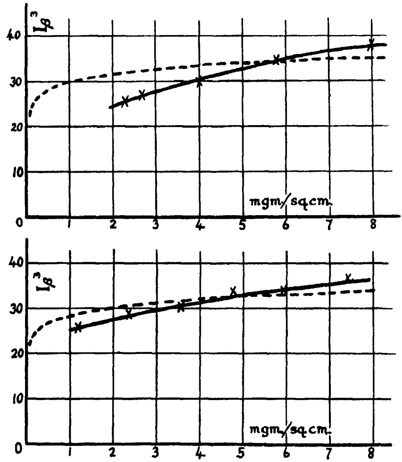

FIG. 10.—Results for $H\rho$ 1677 and $H\rho$ (1033) plotted as $1/\beta^3$ against thickness. Broken curves calculated from Bohr's theory with $c = 40 \cdot 6$.

Table III.

Line ($H\rho$).	Thickness of screen in mgm./cm.^{2} = 10σ.	($H\rho$).	$I = \delta(H\rho)/\sigma$.	Average I.	β^2.	$I\beta^2$.	$I/H\rho$.
1410	2·25	23·6*	105	105·5	0·2615	27·6	0·075
	2·65	25·0* 28·8	94·3 107				
	3·95	41·6* 46·2	105 117				
1677	2·25	16·3*	72·4	89·2	0·3478	30·9	0·053
	2·65	19·4* 21·1	73·6 79·4				
	3·95	33·6*	85·0				
	5·72	58·5*	99·5				
	7·92	85·5	108				
	11·1	117	105				
1938	2·25	16·4*	94·3	78·0	0·4265	33·3	0·040
	2·65	16·4* 17·5	61·4 65·9				
	3·95	23·8*	60·3				
	5·72	45·5* 46·2 49·8	79·9 80·8 87·1				
	7·92	63·8	80·5				
	11·1	87·2 98·0 92·3	78·5 86·1 83·1				
2256	5·72	36·3 40·0	63·4 70·0	67·5	0·5112	34·5	0·030
	11·1	75·9 75·7	68·4 68·1				
2980	5·72	31·8 32·1 37·7	55·6 56·1 65·8	55·8	0·6566	36·6	0·0187
	11·1	56·6 56·1*	51·0 50·6				
4866	14·2	62·4†	44·0	44·0	0·8426	37·0	0·0090
5904	14·2	62·0*	43·6	43·6	0·8880	38·8	0·0074

* These measured on photometer. † Only one doubtful reading for this line.

Complete table of peak-displacements δ ($H\rho$).

($\beta = 0{\cdot}52$); the broken lines are calculated on Bohr's theory putting $c = 40{\cdot}6$ (see § 9). The drop in the value of $I\beta^3$ for small thicknesses of foil is more pronounced than is indicated by theory.

Table IV.

Line (Hρ)	$I = \delta(H\rho)\,\sigma$	$I\beta^3$.	$1/H\rho$
1410	105·5	27·6	0·0750
1677	89·1	31·0	0·0531
1938	78·3	33·4	0·0404
2256	67·6	34·7	0·0300
2980	54·4	35·7	0·0182
4866	44·9	37·8	0·0092
5904	43·6	38·7	0·0074

Although the values of I given in Table III vary among themselves for each value of the initial velocity, the average values of $I\beta^3$ when plotted against Hρ (as in fig. 11) show the increase with Hρ to be expected. The broken line

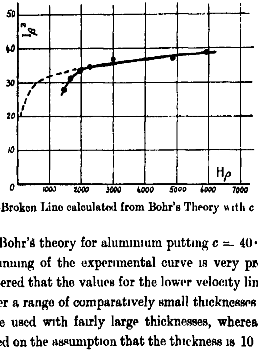

FIG. 11.—Broken Line calculated from Bohr's Theory with $c = 40{\cdot}6$.

is calculated on Bohr's theory for aluminium putting $c = 40{\cdot}6$ (see § 9). The drop at the beginning of the experimental curve is very pronounced, but it must be remembered that the values for the lower velocity lines were obtained by averaging over a range of comparatively small thicknesses of foil, while the higher lines were used with fairly large thicknesses, whereas the theoretical curve is computed on the assumption that the thickness is 10 mgm. per square centimetre. The variation due to thickness would therefore account for at least part of the initial drop.

In Table IV are given some values of I interpolated from the graph in fig. 11

with the corresponding values of $I/H\rho$, and fig. 12 shows the graph of $I/H\rho$ against $H\rho$. The values may be compared with the most probable values for

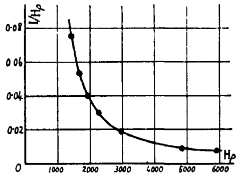

Fig. 12

aluminium given by d'Espine ('Journal de Physique'). It may be remarked that if d'Espine's values are plotted in the form $I\beta^3$ against $H\rho$ they do not lie on a smooth curve, probably because they were obtained from a graph of $I/H\rho$ against $H\rho$ which is somewhat insensitive to small changes of I.

Comparison between the work of Rawlinson on mica and d'Espine and others on aluminium suggests that there is a considerable disparity in the respective values of $I\beta^3$, but from a comparison of Table IV and fig. 12 with the table and graph given by d'Espine it will be seen that our work indicates that the two substances are approximately equivalent as is to be expected on general grounds (*cf.* Kohlrausch, 'Phys. Z.,' vol. 29, p. 153 (1928)).

§ 9. *Discussion.*

We have investigated the nature of the straggling of β-particles and have shown that to a first approximation it obeys simple laws. In addition we have made measurements on the most probable loss of energy, and have obtained results which agree in general with those of previous workers and give some definite information on some of the more detailed points. It is therefore a matter of great interest to compare our results with those derived from theoretical considerations.

The general method of attacking the problem of the scattering and straggling of α- and β-particles by classical dynamics is well known, and it is only necessary in outlining Bohr's theory* to stress the assumptions upon which it depends. The most fundamental of these is the one introduced to provide an upper limit to the distance of approach of the β-particle to an electron for which energy can be transferred, and this involves the concept of characteristic frequencies with which the electrons in the atom vibrate when they are disturbed by the passage of a β-particle. It is assumed that energy can only be transferred provided that the free period of the electron is large compared with the time of collision, which is defined somewhat indefinitely as the time taken by the particle to travel a distance equal to the distance of approach. In the case of β-particles there is the additional difficulty that for those particles which make close collisions the probability laws used in the theory for α-particles cannot be applied The criterion adopted for deciding when the laws break down is more or less arbitrary, but Bohr has shown that by considering separately the particles which make close collisions and those to which the probability laws can be applied, the analysis yields not the average loss of energy but a value which must be very near to the most probable loss of energy. This is fortunate in as much as it is this quantity which is usually determined experimentally. Finally, there are some minor assumptions involved in the application of the relativity correction for the high speed of the β-particles.

---

* 'Phil. Mag.,' vol. 30, p. 581 (1915).

The formula obtained by Bohr may be written

$$I\beta^3 = 5\cdot 10\frac{Z}{A}\left| 96\cdot 1 - \log_e\frac{A}{Z} - 2C + \log_e \sigma - f(\beta) \right|$$

where $I = \Delta(H\rho)/\sigma$.

$\Delta(H\rho)$ being the diminution in $H\rho$ corresponding to the most probable loss of energy, *i e.*, the peak displacement and σ is the surface density of the foil in centigrams per square centimetre, Z and A are the atomic number and atomic weight of the material of the foil,

$$f(\beta) = \log_e\left(\frac{1-\beta^2}{\beta^2}\right) + \beta^2,$$

and $c = \frac{1}{Z}\sum_{1}^{Z} \log_e \nu$, a summational term involving the characteristic frequencies for the various electrons in the atom.

It was from this expression that the theoretical curves in figs. 9 and 11 were computed, using the value $c = 40\cdot 6$ chosen to give the best agreement, and the value of Z/A for aluminium. In making the comparison the point which is most striking is that the agreement is so good, and when we realise that the theory gives values of the right order both for α- and β-particles and for the ranges in various stopping materials, we are tempted to follow up the agreement in more detail. But it must be remembered that in doing so we shall be testing just those features of the theory which are known to be doubtful.

It has long been recognised that $I\beta^3$ should vary slightly with β on account of the term $f(\beta)$, and Kohlrausch* has pointed out that there should be a small variation with σ due to the presence of the term $\log_e \sigma$. These variations are in the same direction as those found experimentally but noticeably smaller. Our experiments indicate quite definitely that there is a residual effect left unexplained by the theory. The agreement is not quite so good as we have made it seem, since we have adjusted c to be $40 \cdot 6$, whereas Bohr finds $c = 39 \cdot 0$ for aluminium by using the experimental evidence of Marsden and Taylor for the thickness of aluminium required to cut down the velocity of α-particles of known speed to one half, and Kohlrausch by assuming that the characteristic frequency of an electron is the frequency corresponding to the ionising potential for the level in which it is situated obtains the value $c = 39 \cdot 6$. It is difficult to see any justification for the latter method, and it is not surprising in view of the assumptions involved that the former should not fit exactly for β-particles. An alteration in the value of c merely raises or lowers the values of $I\beta^3$ as a whole, and does not explain or produce the discrepancies found in the variations with β and σ.

Considering now in more detail the shape of the straggling curves, it is found that although the peaks occur approximately in the predicted positions and the curves rise steeply on the high velocity side for small thicknesses, there is much more straggling than would be expected from the theory, that is to say, far more β-particles lose large amounts of energy than the theory accounts for. In view of the difficulties involved in studying theoretically the straggling, partly owing to the failure of the probability laws for close collisions, and partly to the complications introduced by deflections of the particles by nuclei and electrons which make the actual path traversed greater than the thickness of the foil, it is only possible to describe the *form* of the *straggling curve* in very general terms.

It is obvious therefore that a new theory, or possibly a modification of the old, is needed to solve the problem of the close collisions and to set the method of fixing the upper limit to the distance of approach on a firmer basis. Gaunt† has worked out the problem for α-particles assuming the previous results for close collisions by means of the new quantum theory, and obtains effectively the same result as Bohr, but the complete problem including the effect of the close collisions and for β-particles has not yet been solved. Our experiments give some definite information of the order of the effects to be explained, and should form a test of any new theory which may be proposed.

---

* 'Phys. Zeits.,' vol. 29, p. 153 (1928).

† 'Proc. Camb. Phil. Soc.,' vol. 23, p. 732 (1927).

Summary.

1. The velocity distribution of β-rays (Hρ 1410 to 1938) which have passed through sheets of mica (2 to 6 mgm. per square centimetre) has been found by photometry of a magnetic spectrum and the results expressed in terms of a fundamental straggling curve.

2. The relation between most probable loss of velocity and thickness of stopping material has been investigated for Hρ 1410 to 5904, and surface density 2 to 14 mgm. per square centimetre, and has been found to show a small systematic divergence from Bohr's theory which is beyond the limits of experimental error.

3. The same has been found of the relation between initial velocity and most probable loss of velocity.

It is a pleasure to have this opportunity of thanking Sir Ernest Rutherford and Dr. C. D. Ellis for suggesting this problem and for their continual advice and encouragement, and also Mr. G A. R Crowe for the preparation of numerous sources. One of us (G.M) is indebted to the Department of Scientific and Industrial Research for a maintenance grant.

APPENDIX I

Derivation of the Integral Equation on p 707.

If there are N particles in the unstraggled trace, a number N $f(x)\,dx$ of them fall in the element distant between x and $x + dx$ from some arbitrary origin. Moreover if in the absence of straggling foil P particles would fall in a small region about the point P, then when straggling occurs, a number P $g(\xi)\,d\xi$ fall in the element distant between ξ and $\xi + d\xi$ from P These are the definitions of f and g. F is defined by saying that in the straggled trace there fall between X and X + dX from the origin of f, a fraction F (X) dX of the whole number of particles.

This group comprises a fraction $g(\mathrm{X} - x_1)\,d\mathrm{X}$ of the N $f(x_1)\,dx$ particles which in the absence of straggling would have fallen at x_1 plus a fraction $g(\mathrm{X} - x_2)\,d\mathrm{X}$ of the N $f(x_2)\,dx$ otherwise fallen at x_2, and so on ; the whole of the unstraggled trace being divided into elements about x_1, x_2, etc. Summing and proceeding to the limit, we have

$$\mathrm{N}\,.\,\mathrm{F}(\mathrm{X})\,d\mathrm{X} = \int_{-\infty}^{\infty} \mathrm{N} f(x)\,.\,g(\mathrm{X} - x)\,dx\,.\,d\mathrm{X}.$$

which is equivalent to the quotation on page 707.

Actually $f(x)$ and $g(X - x)$ are zero for negative values of the argument, but it is convenient to leave the lower limit as $-\infty$ for the simplification of the proof in Appendix III.

APPENDIX II.

Solution of the Equation.

A method of trial and error was used.

A good approximation to the function $g(x)$, say $g'(x)$, is formed by replotting $F(X)$ with the scale of abscissæ so reduced that the sum of the squares of the half-breadths of $f(x)$ and $g'(x)$ is equal to the square of the half-breadth of $F(X)$. This procedure is suggested by the properties of the Gaussian Error Function.

From $g'(x)$ and $f(x)$ we evaluate a number of points on the curve for

$$\int_{-\infty}^{X} f(x)\, g'(X - x)\, dx,$$

which we may call $F'(X)$, and by comparing these points with the observed curve for $F(X)$ we adjust $g(x)$ to give a good agreement. After a little practice we found that one correction gave a sufficiently accurate result.

To compute points on $F'(X)$ we divide $f(x)$ and $g'(x)$ into strips by a number of equidistant ordinates, say, $f_1, f_2 \ldots$ and $g_1, g_2, \ldots$ and to find $F'(s)$ we form the sum of products

$$f_1 g_s + f_2 g_{s-1} + f_3 g_{s-2} + \cdots + f_{s-1} g_2 + f_s g_1$$

The quantity so formed, however, misrepresents the curves of f and g as having the form of a flight of steps, as in fig. 13A. We may improve this considerably by treating each curve as a set of chords between the points used as in fig. 13B. This can be done by replacing either each f_r by $\frac{1}{6}(f_{r-1} + 4f_r + f_{r+1})$

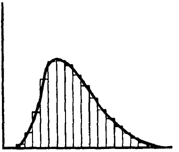

FIG. 13A.

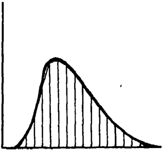

FIG. 13B.

and retaining the g's or by replacing each g_t by $\frac{1}{6}(g_{t-1} + 4g_t + g_{t+1})$ and retaining the f's. The latter is found to lead to less laborious computation.

To justify this process we consider the contribution to the integral due to the trapezium between f_r and f_{r+1} operating on the trapezium between g_p and g_{p+1}. This is clearly

$$\int_0^1 \{f_r + x(f_{r+1} - f_r)\}\{g_{p+1} - x(g_{p+1} - g_p)\}\,dx$$
$$= \tfrac{1}{6}g_{p+1}(f_{r+1} + 2f_r) + \tfrac{1}{6}g_p(2f_{r+1} + f_r)$$
$$= \tfrac{1}{6}f_{r+1}(g_{p+1} + 2g_p) + \tfrac{1}{6}f_r(2g_{p+1} + g_p).$$

Summing for all values of r and p which make $r + p + 1 = s$ we find that $\mathrm{F}(s)$ equals

$$\tfrac{1}{6}[f_s g_1 + f_{s-1}(4g_1 + g_2) + f_{s-2}(g_1 + 4g_2 + g_3) + \dots$$
$$+ f_{s-p}(g_{p-1} + 4g_p + g_{p+1}) + \dots]$$
$$= \tfrac{1}{6}[g_1(f_s + 4f_{s-1} + f_{s-2}) + g_2(f_{s-1} + 4f_{s-2} + f_{s-3})$$
$$+ \dots + g_p(f_{s-p+1} + 4f_{s-p} + f_{s-p-1}) + \dots]$$

And hence, except for the end contributions which are negligible, the substitution proposed suffices to replace the integral corresponding to fig 13A by that corresponding to fig 13B

APPENDIX III

We are indebted to Dr D R. Hartree and Mr E Cunningham for the following proof of the statement made on p. 706, that any agency which affects equally particles falling in straggled and unstraggled traces, disappears from the final result.

As above we have

$$\mathrm{F}(\mathrm{X}) = \int_{-\infty}^{\infty} f(x)\, g(\mathrm{X} - x)\,dx$$

for the ideal case in which there is no spurious broadening of the traces We write F_1 for F and ϕ_1 for f, retaining the symbols F and ϕ for observed functions and using the subscript 1 to denote the ideal case

$$\mathrm{F}_1(\mathrm{X}) = \int_{-\infty}^{\infty} \phi_1(x)\, g(\mathrm{X} - x)\,dx \tag{1}$$

Suppose that when the adventitious broadening occurs, of M particles which would have fallen at a given point, $\mathrm{M}p(w)\,dw$ now fall at a distance w from that point. Then in place of $\mathrm{F}_1(\mathrm{X})$ we observe $\mathrm{F}_2(\mathrm{X})$, which is given by

$$\mathrm{F}_2(\mathrm{X}) = \int_{-\infty}^{\infty} \mathrm{F}_1(w) \, . \, p(\mathrm{X} - w)\,dw$$
$$= \int_{-\infty}^{\infty} dw \int_{-\infty}^{\infty} p(\mathrm{X} - w) \, . \, f(x) \, . \, g(w - x) \, . \, dx, \tag{2}$$

and in place of $\phi_1(x)$, $\phi_2(x)$ which is given by

$$\phi_2(X) = \int_{-\infty}^{\infty} p(x - w) \, . \, f(w) \, dw. \tag{3}$$

We wish to prove that the function g obtained by solution of equation (2) is the same as that obtained from equation (1).

The theorem is simpler to prove in the following, practically equivalent form

If the function g is the same in equations (1) and (2) and if ϕ_1 and ϕ_2 are equal, it is required to show that the functions F_1 and F_2 are equal.

If so, then the same distributions F and ϕ in the straggled and unstraggled lines will give the same g independent of the spurious scattering; if not, then the analysis for g from the observed lines depends on the spurious broadening.

Regarding g as the same in (1) and (2), and putting $\phi_1 = \phi_2$

$$F_1(X) = \int_{-\infty}^{\infty} \int_{-\infty}^{\infty} p(x - w) \quad f(w) \quad g(X - x) \, dx \, dw,$$

$$F_2(X) = \int_{-\infty}^{\infty} \int_{-\infty}^{\infty} p(X - w) \, . \, f(x) \, . \, g(w - x) \, dx \, dw$$

$$= \int_{-\infty}^{\infty} \int_{-\infty}^{\infty} p(X - x) \, . \, f(w) \, . \, g(x - w) \, dx \, dw$$

since x and w are merely variables of integration and take the same limits.

Hence $F_1 = F_2$, if

$$\int_{-\infty}^{\infty} \int_{-\infty}^{\infty} f(w) \left[p(x - w) \, . \, g(X - x) - p(X - x) \, . \, g(x - w) \right] dx \, dw = 0 \tag{4}$$

for all X And since the theorem is to be proved for all forms of the function f, *i.e.*, since f is arbitrary as far as this analysis is concerned, we must have

$$I = \int_{-\infty}^{\infty} \left[p(x - w) \, . \, g(X - x) - g(x - w) \, . \, p(X - x) \right] dx = 0 \tag{5}$$

for all X and all w.

Put $x' = X + w - x$, then

$$I = \int_{-\infty}^{\infty} \left[p(X - x') \, . \, g(x' - w) - p(x' - w) \, . \, g(X - x') \right] dx' = -I,$$

since x and x' are merely variables of integration and can be interchanged.

Hence $I = 0$, and the sufficient condition is always satisfied.

The Distribution of Electrons in a Metal.

By J E. LENNARD-JONES and H. J WOODS, The University, Bristol

(Communicated by R. H Fowler, F.R S —Received July 9, 1928)

1. *The Statistics of a Degenerate Gas*

An interesting application of the new statistics of Fermi* and Dirac† has been made by Thomas‡ (and also independently by Fermi§) to the distribution of electrons in heavy atoms. The basic idea of these researches is that the "electron gas" surrounding a nucleus is "degenerate," so that every cell of extension h^3 of a six dimensional phase space contains two electrons, one electron spinning in one direction and another in the opposite direction An upper limit to the possible translational energies of the electrons is imposed by the condition that electrons shall not have enough energy to escape from the field of the nucleus, viz. .—

$$\varepsilon \leqslant e \,.\, \mathrm{V}, \tag{1}$$

where ε and e represent the energy and charge of the electron and V is the potential field The possible range of momentum co-ordinates (neglecting relativity considerations) is then limited by

$$p \leqslant (2me\mathrm{V})^{1/2} \tag{2}$$

and the total number of cells of extension h^3 in the phase space is given by

$$4\pi\,(2me\mathrm{V})^{3/2}/3h^3 \tag{3}$$

for every unit of ordinary (co-ordinate) space available. If every cell contains two electrons, the density is given by

$$\rho = -\ 8\pi e\,(2me\mathrm{V})^{3/2}/3h^3. \tag{4}$$

Since, however, the potential V is determined by the nuclear charge and the distribution of electrons, we have

$$\nabla^2\mathrm{V} = -\ 4\pi\rho = 32\pi^2 e\,(2me\mathrm{V})^{3/2}/3h^3, \tag{5}$$

an equation to determine V, subject to

$$\left.\begin{array}{l} \mathrm{V} \rightarrow 0 \quad \text{as} \quad r \rightarrow \infty \\ \mathrm{V}r \rightarrow \mathrm{E} \quad \text{as} \quad r \rightarrow 0 \end{array}\right\}, \tag{6}$$

where E is the charge on the nucleus.

---

* 'Z. f. Physik,' vol. 36, p. 902 (1926).

† 'Roy. Soc. Proc.,' A, vol. 112, p. 661 (1926).

‡ 'Proc. Camb. Phil Soc ,' vol. 23, p 542 (1926).

§ 'Z. f. Physik,' vol. 48, p. 73 (1928).

Thomas and Fermi have solved this differential equation by numerical methods, and have found an average distribution which is well confirmed by the recent work of Hartree,* based on the Schrodinger method.

Another application of the statistics has been made by Sommerfeld† to the free electrons of a metal. On the assumption that these electrons obey the Fermi-Dirac statistics instead of the ordinary Maxwellian statistics, Sommerfeld has shown that many well-known difficulties in the electron theory of metals can be resolved, in particular, the electrons make a negligible contribution to the specific heat, as is required by experiment. A defect in Sommerfeld's work is the neglect of the interaction of electrons and the atomic cores No theory of metals can be regarded as adequate which does not include the assembly of electrons and atomic cores as one system to be treated as a whole. Sommerfeld's method is equivalent to considering an assembly of electrons in a closed box of volume V, and even their interaction with each other is neglected, except in so far as the fundamental assumptions of the Fermi-Dirac statistics take this into account The object of this paper is to regard a metal as a whole and to find the average distribution of electrons in the same way that Thomas and Fermi have done for isolated atoms

It is clear that the same differential equation is obtained as above. The essential difference in the problem lies in the boundary conditions. In this case $Vr \rightarrow E$ near every nucleus. If we assume the nuclei to be arranged in a simple cubic lattice array, then, instead of the condition $V \rightarrow 0$ as $r \rightarrow \infty$, we have the condition that V is triply periodic. V is then uniquely determined when it has been evaluated within an elementary cube, surrounding one nucleus. The condition that V shall be triply periodic can be replaced by a simpler one, viz, that the normal component of V shall vanish over the sides of the cube, as is easily seen from conditions of symmetry The solution of the differential equation (5) within a cube subject even to such simple conditions that $Vr \rightarrow E$ at the centre and $\partial V/\partial n = 0$ at the boundary proves, however, to be intractable The problem has, therefore, been modified in the following way to give a kind of two-dimensional metal. The nuclei are replaced by a series of parallel line-charges, arranged so as to intersect a plane perpendicular to them in a square array.‡ A section of the system is made by two parallel planes at a distance d (of atomic dimensions). The charge on each line-charge within the distance d is taken to be Ze, and the number of electrons within the bounding planes (regarded as reflecting) is sufficient to make the system neutral as a whole. Let z be taken along the length of the line-charge and x and y at right angles as shown in the figure. The potential is clearly independent of z, and the problem is to find V as a function of x and y. We suppose that all electrons have the same velocity in the z direction, this being the lowest possible one consistent with a standing de Broglie wave within the bounding planes. The lowest velocity corresponds to a wave-length $2d$, so that

---

* 'Proc. Camb. Phil. Soc.,' vol. 24, p. 89 (1928)

† 'Z. f. Physik,' vol. 47, pp. 1 and 43 (1928)

‡ It is a rough picture of a crystal of hydrocarbons.

$$p_z = \pm h/2d \tag{7}$$

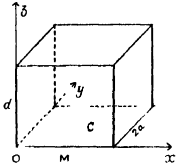

FIG. 1.

In the other directions, p_x and p_y are limited by the condition that the energy shall not be sufficient to take the electron out of the field, so that

$$p_x^2 + p_y^2 \leqslant 2me\mathrm{V}. \tag{8}$$

The total phase space available is then given by

$$\pi\,(2me\mathrm{V})\,.\,2\,.\,(h/2d) \tag{9}$$

per unit of ordinary space, and the maximum number of electrons, being 2 for every cell h^3, is given by

$$4\pi me\mathrm{V}/dh^2, \tag{10}$$

so that the density is given by

$$\rho = -\,4\pi me^2\mathrm{V}/dh^2. \tag{11}$$

Laplace's equation then leads to

$$\nabla^2\mathrm{V} = 16\pi^2 me^2\mathrm{V}/dh^2, \tag{12}$$

and, since V is assumed independent of z,

$$\frac{\partial^2\mathrm{V}}{\partial x^2} + \frac{\partial^2\mathrm{V}}{\partial y^2} = k^2\mathrm{V}, \tag{13}$$

where

$$k^2 = 16\pi^2 me^2/dh^2. \tag{14}$$

Equation (13) is to be solved subject to $\mathrm{V} \sim \log r$ at each line-charge and $\partial\mathrm{V}/\partial n = 0$ over the planes parallel to the axis of x and y midway between the line-charges.

2. *Solution of Differential Equation.*

The problem is therefore reduced to finding the solution of

$$\nabla^2\mathrm{V} = k^2\mathrm{V}$$

within a square of side $2a$, subject to V's being finite and continuous everywhere except at the origin, where $V \sim \log r$, and subject to the condition that the normal component of V vanishes over the sides of the square, $x = \pm a$, $y = \pm a$. Furthermore, from considerations of symmetry, V is symmetrical about both axes, and about the diagonals of the square.

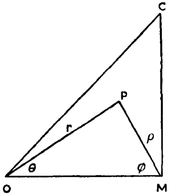

Fig 2.

The last condition restricts possible solutions to the form

$$f_\nu(r)\cos 4\nu\theta,$$

where r, θ are polar co-ordinates referred to the centre of the square as origin, θ being measured from the x-axis. If $f_\nu(r)\cos 4\nu\theta$ is a solution, then

$$\frac{\partial^2 f_\nu}{\partial r^2} + \frac{1}{r}\frac{\partial f_\nu}{\partial r} - \left(k^2 + \frac{16\nu^2}{r^2}\right) f_\nu = 0, \tag{15}$$

which is Bessel's equation of imaginary argument. The solution is, therefore, of the form*

$$V = \sum_\nu \{A_\nu K_{4\nu}(kr) + B_\nu I_{4\nu}(kr)\}\cos 4\nu\theta \tag{16}$$

Since $V \sim \log r$ at the origin, $A_\nu = 0$ except when $\nu = 0$, and so the solution is

$$V = A_0 K_0(kr) + \sum_\nu B_\nu I_{4\nu}(kr)\cos 4\nu\theta \tag{17}$$

This satisfies all the conditions, except the boundary conditions These can best be applied after a transformation of origin to the mid-point of a side of the square (a, o) If ρ, ϕ be the new polar co-ordinates (fig. 2), we have† for $\rho > a$,

$$K_\nu(r)\cos\nu\theta = \sum_{m=-\infty}^{+\infty} K_{\nu+m}(a)\, I_m(\rho)\cos m\phi, \tag{18}$$

$$I_\nu(r)\cos\nu\theta = \sum_{m=-\infty}^{+\infty} (-1)^m I_{\nu+m}(a)\, I_m(\rho)\cos m\phi \tag{19}$$

We then have an expansion of the type

$$\begin{aligned} V &= \sum_{m=-\infty}^{+\infty}\left\{A_0 K_m(ka) + \sum_\nu (-1)^m B_\nu I_{4\nu+m}(ka)\right\} I_m(k\rho)\cos m\phi \\ &= \sum_{m=-\infty}^{+\infty} C_m I_m(k\rho)\cos m\phi, \end{aligned} \tag{20}$$

where

$$C_m = A_0 K_m(ka) + \sum_\nu (-1)^m B_\nu I_{4\nu+m}(ka). \tag{21}$$

---

* Watson, "Bessel Functions," p. 78 (1922); Watson and Whittaker, "Modern Analysis," 3rd Edition, § 17.7.

† Watson, *ibid.*, p 361.

Now since $\partial V/\partial n = 0$ at $x = a$, we have

$$\left[\frac{1}{\rho}\frac{\partial V}{\partial \phi}\right]_{\phi = \pi/2} = 0, \tag{22}$$

and, therefore,

$$\sum_{p=-\infty}^{\infty} C_{2p+1}(2p+1)(-1)^p I_{2p+1}(k\rho) = 0. \tag{23}$$

Using the fact that

$$I_{2p+1}(k\rho) = I_{-2p-1}(k\rho), \tag{24}$$

we have

$$\sum_{p=0}^{\infty} (-)^p (2p+1)\{C_{2p+1} + C_{-2p-1}\} I_{2p+1}(k\rho) = 0, \tag{25}$$

for all values of ρ. We infer that

$$C_{2p+1} + C_{-2p-1} = 0 \tag{26}$$

or

$$2A_0K_{2p+1}(ka) - \sum_{\nu} B_{\nu}\{I_{4\nu+2p+1}(ka) + I_{4\nu-2p-1}(ka)\} = 0 \tag{27}$$

for all values of p. We have, therefore, an infinite series of equations to solve for the ratios $A_0 : B_0 : B_1 : B_2 \ldots$

In this connection the following theorem on determinants is useful* -

Theorem.—If a series of quantities $\beta_0, \beta_1, \ldots \beta_{\nu} \ldots$ are determined by a system of linear equations

$$\sum_{\nu=0}^{\infty} c_{\nu\mu}\beta_{\nu} = a_{\mu}, \quad (\mu = 0, 1, \ldots)$$

then any other linear expression of the same quantities can be expressed in the following way -

$$\sum_{\nu=0}^{\infty} l_{\nu}\beta_{\nu} = \frac{a_0 l_0}{c_{00}} + \frac{\begin{vmatrix} c_{00} & a_0 \\ c_{01} & a_1 \end{vmatrix} \cdot \begin{vmatrix} c_{00} & c_{10} \\ l_0 & l_1 \end{vmatrix}}{c_{00}\begin{vmatrix} c_{00} & c_{10} \\ c_{01} & c_{11} \end{vmatrix}} + \ldots$$

$$+ \frac{\begin{vmatrix} c_{00} & c_{10} & c_{20} \cdots & c_{\nu-1,0}, & a_0 \\ \cdot & \cdot & \cdots & \cdot & \cdot \\ \cdot & \cdot & \cdots & \cdot & \cdot \\ c_{0\nu} & c_{1\nu} & c_{2\nu} \cdots & c_{\nu-1,\nu}, & a_{\nu} \end{vmatrix} \cdot \begin{vmatrix} c_{00} & c_{10} & c_{20} & \cdots & c_{\nu 0} \\ \cdot & \cdot & \cdot & \cdot & \cdot \\ & \cdot & \cdot & \cdots & \cdot \\ l_0 & l_1 & l_2 & \cdot & l_{\nu} \end{vmatrix}}{\begin{vmatrix} c_{00} & c_{10} & c_{20} & \cdots & c_{\nu-1,0} \\ \cdot & \cdot & \cdot & \cdots & \cdot \\ \cdot & \cdot & \cdot & \cdots & \cdot \\ c_{0,\nu-1} & c_{1,\nu-1} & c_{2,\nu-1} & \cdots & c_{\nu-1,\nu-1} \end{vmatrix} \cdot \begin{vmatrix} c_{00} & c_{10} & \cdots & c_{\nu,0} \\ \cdot & \cdot & \cdots & \cdot \\ \cdot & \cdot & \cdot & \cdot \\ c_{0,\nu} & c_{1\nu} & \cdot & c_{\nu,\nu} \end{vmatrix}} + \ldots$$

---

* Enskog, "Kinetische Theorie der Vorgänge in mässig verdünnten Gases." Inaug. Dissertation (Anhang), Uppsala (1917).

If we write

$$\beta_\nu = B_\nu/A_0, \quad c_{\nu\mu} = I_{4\nu+\mu}(ka) + I_{4\nu-\mu}(ka), \quad a_\nu = 2K_\nu(ka),$$
$$l_\nu = I_{4\nu}(kr)\cos 4\nu\theta,$$

we find a formal expression for $\frac{V}{A_0} - K_0(kr)$ given by equation (17), and so a formal solution for V.

The constant A_0 is determined by applying Gauss' Theorem to a small cylinder surrounding the nucleus This gives

$$\operatorname*{Lt}_{r\to 0}\left(r\frac{\partial V}{\partial r}\right) = -\frac{2Ze}{d},$$

whence we deduce that

$$A_0 = -\frac{2Ze}{d}.$$

Since the differential equation (13) is linear in V, the potential can also be calculated by the method of images *

The potential at any point (x, y) is given by

$$V = A_0 K \Sigma_0 \{k^2(x - 2pa)^2 + k^2(y - 2qa)^2\}^{\frac{1}{2}}$$
$$= A_0 \Sigma K_0 [ka \{(\xi - 2p)^2 + (\eta - 2q)^2\}^{\frac{1}{2}}],$$

where the summation includes all integral values of p and q, positive and negative, and $\xi = x/a$, $\eta = y/a$. This expression is a solution of the differential equation, and satisfies all the necessary conditions of the problem. This method is especially convenient in calculating the potential in the neighbourhood of a corner of a square (co-ordinates a, a), owing to the rapid convergence of the series For values of ka of the order of unity, the first four terms of the series ($p = 0, 1$, $q = 0, 1$) give a good approximation near (a, a). It is not so convenient as the other method for calculating the potential at a series of points within the square $x = \pm a$, $y = \pm a$, for that method gives the potential in terms of polar co-ordinates, which is an advantage in some applications of the results

Special Case.

As an illustration, a special case has been worked out, viz, $ka = 2 \cdot 5$ This corresponds to $d = 2a$, $a = 1 \cdot 66$ A°, or an internuclear distance of $3 \cdot 32$ A°. In the tables are given values of $v = (V/A_0) - K_0(kr)$ and V/A_0 for various points in the triangle bounded by $x = y$, $y = 0$, $x = a$. The first table gives the difference (v) between the potential due to the crystal and the potential at the same point due to an isolated system (apart from the constant factor A_0).

---

* This suggestion arose out of a conversation with Prof. Havelock about the above problem.

Table I.—Values of $v = V/A_0 - K_0(kr)$.

r/a \ θ	0	$\frac{1}{16}\pi$	$\frac{1}{8}\pi$	$\frac{3}{16}\pi$	$\frac{1}{4}\pi$
0	$1{\cdot}62 \times 10^{-2}$	$1{\cdot}62 \times 10^{-2}$	$1{\cdot}62 \times 10^{-2}$	$1{\cdot}62 \times 10^{-2}$	$1{\cdot}62 \times 10^{-2}$
0·2	$1{\cdot}726 \times 10^{-2}$	$1{\cdot}725 \times 10^{-2}$	$1{\cdot}724 \times 10^{-2}$	$1{\cdot}723 \times 10^{-2}$	$1{\cdot}722 \times 10^{-2}$
0·4	$2{\cdot}082 \times 10^{-2}$	$2{\cdot}072 \times 10^{-2}$	$2{\cdot}050 \times 10^{-2}$	$2{\cdot}028 \times 10^{-2}$	$2{\cdot}019 \times 10^{-2}$
0·6	$2{\cdot}834 \times 10^{-2}$	$2{\cdot}781 \times 10^{-2}$	$2{\cdot}666 \times 10^{-2}$	$2{\cdot}548 \times 10^{-2}$	$2{\cdot}498 \times 10^{-2}$
0·8	$4{\cdot}228 \times 10^{-2}$	$4{\cdot}102 \times 10^{-2}$	$3{\cdot}678 \times 10^{-2}$	$3{\cdot}286 \times 10^{-2}$	$3{\cdot}132 \times 10^{-2}$
1	$7{\cdot}006 \times 10^{-2}$	$6{\cdot}142 \times 10^{-2}$	$5{\cdot}226 \times 10^{-2}$	$4{\cdot}218 \times 10^{-2}$	$3{\cdot}862 \times 10^{-2}$
$\sqrt{2}$	—	—	—	—	$6{\cdot}243 \times 10^{-2}$

Table II.—Values of $V/A_0 = K_0(kr) + v$.

r/a \ θ	0	$\frac{1}{16}\pi$	$\frac{1}{8}\pi$	$\frac{3}{16}\pi$	$\frac{1}{4}\pi$
0	∞	∞	∞	∞	∞
0·2	0·9417	0·9417	0·9417	0·9416	0·9416
0·4	0·4418	0·4417	0·4415	0·4413	0·4412
0·6	0·2421	0·2416	0·2405	0·2394	0·2388
0·8	0·1562	0·1549	0·1507	0·1468	0·1452
1	0·1321	0·1268	0·1146	0·1045	0·1010
$\sqrt{2}$	—	—			0·0827

The work required to remove an electron from any point in the crystal is given by

$$\begin{aligned}\Phi &= e\;V - A_0 e\,(K_0(kr) + v)\\ &= 2Ze^2\,\{K_0(kr) + v\}/d \text{ ergs},\\ &= (28{\cdot}6)\,Z\,\{K_0(kr) + v\}/\delta \text{ volts}.\end{aligned}$$

where δ is measured in Ångstroms. For example, the work required to remove an electron from a point on an axis midway between two nuclei is Z (1·141) volts, while for a point (a, a) it is $Z\,(0\cdot713)$ volts. We note that the fluctuation of potential in the plane $x = a$ over and above its minimum value is of the order of 60 per cent.

The equipotential lines are plotted in the figure, the nuclei being indicated by crosses Near a nucleus the equipotential lines are approximately circles. These are gradually deformed until a critical curve is reached, shown by the continuous line in the figure This extends throughout the crystal, and encloses

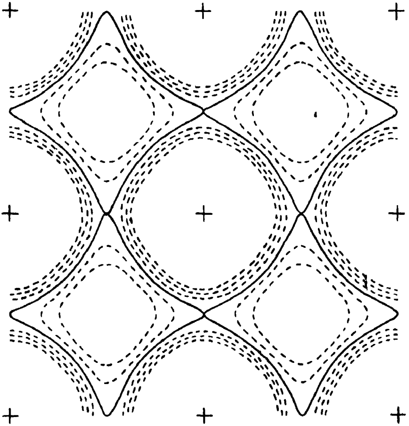

FIG. 3 —Lines of equal potential and equal electron density in a two-dimensional metal.

another system of closed curves which surround the centres of the squares. The electrons in these regions may be regarded as "shared," as they cannot be regarded as belonging to one nucleus more than another. The "shared" electrons form a lattice array which interpenetrates that of the nuclei. This provides some justification for the model of a metal, proposed by Lindemann* and J. J Thomson,† in which the valency electrons form a rigid lattice inter-penetrating that of the atomic cores, though in our case the system is not a static one even at absolute zero. Electrons can have any energy up to but not exceeding that required to take them out of the metal altogether It follows that some electrons cross the critical potential line shown in the figure, and travel from one end of the crystal to the other There is, in fact, a continual interchange of electrons between the various systems It is clear that if an electric field were applied to the system, an electric current would flow without resistance, so that the system would be supra-conducting, just like the static model proposed by Lindemann

---

* Lindemann, 'Phil. Mag,' vol. 29, p. 127 (1915).

† J. J. Thomson 'Phil. Mag,' vol. 44, p. 663 (1922).

INDEX TO VOL. CXX. (A)

Adair (G. S.) A Theory of Partial Osmotic Pressures and Membrane Equilibria, 573

Adam (N. K.) and Jessop (G.) The Structure of Thin Films, XII, 473.

Adsorption of gases, electrical condition of hot surfaces (Finch and Stimson), 235.

Ammonia, decomposition by electrons (McLennan and Greenwood), 283.

Aurora and its spectrum (McLennan), 327.

Bakerian Lecture—McLennan on the Aurora, 327

Bandopadhyaya (G. B.) Photoelectric Effect of Soft X-Rays, 46

Bessel functions and lattice points of ellipsoid (Wilton), 358

Beta-particles, velocity distribution (White and Millington), 701.

Bone (W. A.), Horton (L.), and Tei (L. J.) Researches on the Chemistry of Coal, V, 523.

Bone (W. A.), Townend (D. T. A.), and Scott (G. A.) Gaseous Combustion at High Pressures, XI, 546, **Bone (W. A.), Newitt (D. M.) and Smith (C. M.)** Gaseous Combustion at High Pressures, XII, 563

Bowden (F. P.) and Rideal (E. K.) On the Electrolytic Behaviour of Thin Films, 59, 80.

Brode (W. R.) and Morton (R. A.) The Absorption Spectra of Solutions of Cobalt Halides in Concentrated Hydrochloric, Hydrobromic and Hydriodic Acids, 21

de Bruyne (N. A.) The Action of Strong Electric Fields on the Current from a Thermionic Cathode, 423.

Burton (A. C.) *See* McLennan, Ruedy and Burton

Cæsium, absorption spectrum (Mathews), 650.

Calcium carbonate hexahydrate, kinetics of decomposition (Topley and Hume), 211

Callendar (H. L.) Steam Tables and Equations, 460

Caress (A.) and Rideal (E. K.) The Chemical Reactions of Carbon Monoxide and Hydrogen after Collision with Electrons, 370.

Chemistry of coal, V (Bone, Horton and Tei), 523.

Cobalt halides, absorption spectra (Brode and Morton), 21

Cornish (R. J.) Flow in a Pipe of Rectangular Cross-section, 691.

Curtis (W. E.) and Jevons (W.) The Zeeman Effect in the Band Spectrum of Helium, 110.

Darwin (C. G.) On the Magnetic Moment of the Electron, 621. On the Diffraction of the Magnetic Electron, 631

Detonation in solid explosives (Jones), 603.

Detonation-wave in gaseous mixtures (Payman), 90

Dobson (G. M. B.) *See* Götz and Dobson.

Durnford (A. M. I. A. W.) *See* McLennan and Durnford

Electromagnetic field, action of (Milner), 483

Electromagnetic phenomena in a gravitational field (Whittaker), 1.

Electron, magnetic (Darwin), 621, 631.

Electrons, distribution in metal (Lennard-Jones and Woods), 727.

Electrons in gases, motion (Townsend), 511

Finch (G. I.) and Stimson (J. C.) The Electrical Condition of Hot Surfaces during the Adsorption of Gases, II. 235.

Forsdyke (A. G.) *See* Levy and Forsdyke.

Fowler (A.) and Selwyn (E. W. H.) Further Investigations of the Spectrum, C II, 312.

Fox (J. J.) *See* Robertson and others.

Gaseous combustion at high pressures, XI, XII (Bone and others), 546, 563.

Glauert (H.) The Characteristics of a Karman Vortex Street in a Channel of Finite Breadth, 34.

Götz (F. W. P.) and Dobson (G. M. B.) Observations on the Height of the Ozone, 251.

Gowan (E. H.) The Effect of Ozone on the Temperature of the Upper Atmosphere, 655.

Greenwood (G.) *See* McLennan and Greenwood

Helical vortex, stability (Levy and Forsdyke), 670.

Hiscocks (E. S.) *See* Robertson and others.

Horton (L.) *See* Bone, Horton and Tei.

Hume (J.) *See* Topley and Hume.

Ireton (J. C.) *See* McLennan, Ireton and Samson.

Jack (D.) The Band Spectrum of Water Vapour, III, 222.

Jessop (G.) *See* Adam and Jessop.

Jevons (W.) *See* Curtis and Jevons.

Jones (E.) Photographic Study of Detonation in Solid Explosives, 603

Karman vortex street in a channel of finite breadth (Glauert), 34.

Kichlu (P. K.) The First Spark Spectrum of Krypton, 643

Krypton, first spark spectrum (Kichlu), 643.

Lennard-Jones and Woods (H. J.) The Distribution of Electrons in a Metal, 727

Levy (H.) and Forsdyke (A. G.) The Study Motion and Stability of a Helical Vortex, 670

Long-chain compounds, *n*-Hydrocarbon (Muller), 437.

McLennan (J. C.) The Aurora and its Spectrum, 327

McLennan (J. C.) and Durnford (A. M. I. A. W.) The Zeeman Effect of Tantalum, 502

McLennan (J. C.) and Greenwood (G.) On the Decomposition of Ammonia by High-Speed Electrons, 283

McLennan (J. C.), Ireton (H. J. C.) and Samson (E. W.) On the Luminescence of Solid Nitrogen under Cathode Ray Bombardment, 303.

McLennan (J. C.), Ruedy (R.) and Burton (A. C.) An Investigation of the Absorption Spectra of Water and Ice, with reference to the Spectra of the Major Planets, 296.

Mathews (I. M.) The Absorption Spectrum of Cæsium, 650.

Millington (G.) *See* White and Millington

Milner (S. R.) The Action of an Electromagnetic Field, 483.

Morton (R. A.) *See* Brode and Morton.

Müller (A.) A Further X-Ray Investigation of Long Chain Compounds, 437

Newitt (D. M.) *See* Bone, Newitt and Smith

Nitrogen, solid, luminescence (McLennan, Ireton and Samson), 303.

Osmotic pressures and membrane equilibria (Adair), 573.

Ozone, effect of temperature on upper atmosphere (Gowan), 655.

Ozone, height in upper atmosphere (Götz and Dobson), 251.

Paraffins, chemical equilibrium (Wilson), 247.

Payman (W.) The Detonation-Wave in Gaseous Mixtures and the Pre-Detonation Period, 90.

Phosphine, absorption band (Robertson and others), 161, 189.

Rideal (E. K.) *See* Bowden and Rideal, *and* Caress and Rideal.

Robertson (Sir Robert), Fox (J. J.) and Hiscocks (E. S.) Studies in the Infra-Red Region of the Spectrum, 128, 149, 161, 189.

Rudberg (E.) The Velocity Distribution of Photoelectrons from Soft X-Rays, 385.

Ruedy (R.) *See* McLennan, Ruedy and Burton.

Samson (E. W.) *See* McLennan, Ireton and Samson.

Scott (G. A.) *See* Bone, Townend and Scott.

Selwyn (E. W. H.) *See* Fowler and Selwyn.

Smith (C. M.) *See* Bone, Newitt and Smith.

Spectra, absorption, cobalt halides (Brode and Morton), 21.

Spectra, absorption, of water, ice and major planets (McLennan, and others), 296.

Spectrum, absorption, of cæsium (Mathews), 650.

Spectrum, helium, Zeeman effect (Curtis and Jevons), 110.

Spectrum, infra-red region (Robertson and others), 128, 149, 161, 189.

Spectrum of C H (Fowler and Selwyn), 312.

Spectrum of water vapour (Jack), 222.

Spectrum, spark, of krypton (Kichlu), 643.

Steam Tables and Equations (Callendar), 460.

Stimson (J. C.) *See* Finch and Stimson.

Strong electric fields and thermionic cathode current (de Bruyne), 423.

Taylor (G. I.) The Energy of a Body moving in an Infinite Fluid, with an Application to Airships, 13. The Forces on a Body placed in a Curved or Converging Stream of Fluid, 260.

Tei (L. J.) *See* Bone, Horton and Tei.

Thin films, XII (Adam and Jessop), 473.

Thin films, electrolytic behaviour (Bowden and Rideal), 59, 80.

Topley (B.) and Hume (J.) The Kinetics of the Decomposition of Calcium Carbonate Hexahydrate, 211.

Townend (D. T. A.) *See* Bone, Townend and Scott.

Townsend (J. S.) Motions of Electrons in Gases, 511.

White (P.) and Millington (G.) The Velocity Distribution of β-particles after passing through Thin Foils, 701.

Whittaker (E. T.) On the Potential of Electromagnetic Phenomena in a Gravitational Field, 1.

Wilson (H. A.) Chemical Equilibrium in the Vapour of a Mixture of Paraffins and Unsaturated Hydrocarbons, 247.

Wilton (J. R.) A Series of Bessel Functions connected with the Lattice Points of an n-Dimensional Ellipsoid, 358.

Woods (H. J.) *See* Lennard-Jones and Woods.

X-Rays, soft, distribution of photoelectrons (Rudberg), 385.

X-Rays, soft, photoelectric effect (Bandopadhyaya), 46.

Zeeman effect in band spectrum of helium (Curtis and Jevons), 110.

Zeeman effect of Tantalum (McLennan and Durnford), 502.

END OF THE ONE HUNDRED AND TWENTIETH VOLUME (SERIES A).

I. A. R. I. 75.

IMPERIAL AGRICULTURAL RESEARCH
INSTITUTE LIBRARY
NEW DELHI.

Date of issue.	Date of issue.	Date of issue.
30.4.52		
30.7.52		
30.4.57		